

**DEVELOPMENT OF A COMMERCIAL BUILDING/SITE
EVALUATION FRAMEWORK FOR MINIMIZING ENERGY
CONSUMPTION AND GREENHOUSE GAS EMISSIONS OF
TRANSPORTATION AND BUILDING SYSTEMS**

A Thesis
Presented to
The Academic Faculty

By

Brent A. Weigel

In Partial Fulfillment
of the Requirements for the Degree
Doctor of Philosophy in the
School of Civil and Environmental Engineering

Georgia Institute of Technology
August, 2012

Copyright © Brent Weigel 2012

DEVELOPMENT OF A COMMERCIAL BUILDING/SITE EVALUATION FRAMEWORK FOR MINIMIZING ENERGY CONSUMPTION AND GREENHOUSE GAS EMISSIONS OF TRANSPORTATION AND BUILDING SYSTEMS

Approved by:

Dr. Michael D. Meyer
School of Civil and Environmental Engineering
Georgia Institute of Technology

Dr. Adjo Amekudzi
School of Civil and Environmental Engineering
Georgia Institute of Technology

Dr. Frank Southworth
School of Civil and Environmental Engineering
Georgia Institute of Technology

Dr. Catherine Ross
School of City and Regional Planning
Georgia Institute of Technology

Dr. Marilyn Brown
School of Public Policy
Georgia Institute of Technology

Date Approved: April 20, 2012

PREFACE

Portions of this dissertation consist of text from the author's related conference papers:

Weigel, B., (2012). "Evaluation of the Potential Commute Energy Consumption of Commercial Office Site Alternatives". Presented at the *91st Annual Meeting of the Transportation Research Board (TRB)*. Washington, D.C.

Weigel, B., (2011). "Development of a Commercial Building Site Selection Framework for Minimizing Greenhouse Gas Emissions and Energy Consumption". Presented at the *World Sustainable Building Conference (SB11)*. Helsinki, FI.

ACKNOWLEDGEMENTS

I am extremely grateful to all of those who have inspired, informed, enabled, and supported my work on this dissertation. I am especially grateful for the help of my advisors: Dr. Michael Meyer and Dr. Adjo Amekudzi. From the very start of my graduate studies, Dr. Meyer has created and sustained many opportunities for me to grow as a researcher, an engineer, and a leader in transportation sustainability. I could not have begun nor completed this dissertation without Dr. Meyer's unique combination of intellectual latitude, insight, and encouragement. I am indebted to Dr. Amekudzi's insightful guidance for achieving success in research, relationships, and professional and personal growth. Dr. Amekudzi and Dr. Meyer have shown me what it means to be a great mentor.

I would like to thank Dr. Frank Southworth for our many engaging conversations on transportation research, land-use planning, and professional development. Dr. Southworth's insights on success in research, graduate work, and beyond have been instrumental for translating far-reaching research ideas into both a defensible dissertation and an engaging career path. I would like to thank Dr. Catherine Ross for helping me think through the challenges of connecting research with practice in transportation and land-use planning.

This dissertation would not have been possible without the loving support of my wife Tanya. Through her inspiration and encouragement, Tanya has taught me how to go confidently in the direction of my dreams.

I would also like to thank the leaders of graduate fellowship programs at the National Science Foundation, the U.S. Department of Transportation, and Georgia Power for providing the generous financial support of my graduate studies.

TABLE OF CONTENTS

PREFACE.....	iii
ACKNOWLEDGEMENTS	iv
LIST OF TABLES	xiii
LIST OF FIGURES	xviii
LIST OF SYMBOLS AND ABBREVIATIONS	xxvi
DEFINITIONS	xxx
SUMMARY	xxxi
CHAPTER 1: INTRODUCTION.....	1
1.1. Research objective.....	1
1.2. Significance of work	3
1.3. Background and Motivation.....	4
1.3.1. Energy Conservation and Climate Change Mitigation	4
1.3.2. Efficient Commercial Building Locations / Sites	5
1.3.3. Existing Paradigm of Efficient / Sustainable Commercial Site Evaluation.....	6
1.3.4. Transportation Energy and GHGs in the Context of Commercial Buildings/Sites	8
1.4. Dissertation Organization.....	9
CHAPTER 2: LITERATURE REVIEW	11
2.1. Green Building Rating Systems	14

2.1.1. Site Transportation Impacts	14
2.1.1.1. LEED for Neighborhood Design.....	15
2.1.2. Building Energy and GHGs	16
2.2. Building Design and Operation Energy Standards.....	17
2.2.1. Building Energy Performance.....	17
2.2.1.1. ENERGY STAR Target Finder and Portfolio Manager	17
2.2.2. Energy Use Intensity (EUI)	19
2.2.3. Whole Building Life Cycle Energy and GHGs	20
2.3. Building Energy Modeling.....	20
2.4. Whole Building LCA	22
2.5. Travel Demand Modeling	23
2.5.1. Site or Regional VMT and Land-Use Interactions	23
2.5.1.1. Smart Growth	24
2.5.1.2. Location Efficient Mortgages.....	25
2.5.2. Regional Travel Demand Models	25
2.6. Transportation Impact Analysis	26
2.7. Sustainable Site Development Tools.....	27
2.8. Research Contribution.....	29
CHAPTER 3: RESEARCH METHODOLOGY AND SCOPE	30
3.1. Methodology	30
3.2. Scope	34
3.2.1. Transportation Systems.....	36

3.2.2. Building Systems	37
3.3. Integration of Building and Transportation Systems	37
3.4. Demonstration of Framework	38
3.4.1. Region-Wide Application	39
3.4.2. Scenarios / Case Studies	39
CHAPTER 4: APPLICATION CONTEXT AND CONCEPTUAL FRAMEWORK	43
4.1. Application Context	43
4.1.1. Understanding Commercial Office Building/Site Selection	45
4.1.1.1. Office Firm Location Choice	49
4.2. A Conceptual Framework of Whole-Building Energy Evaluation	50
4.2.1. Relationship Between Building/Site Services and Energy Systems	53
4.2.2. Relationship Between Building/Site Elements and Energy Systems	57
4.2.3. Life Cycle Analysis Perspective	61
4.2.3.1. Analysis boundary	61
4.2.3.2. Functional Units	65
4.2.4. Building/Site Performance Comparisons	67
4.2.4.1. EUI and GEI vs. Total Energy and GHGs	67
4.2.4.2. Comparison between Alternatives vs. Comparison to Baseline	69
4.2.4.3. Reference Frames for New Construction and Major Renovations	71
4.2.5. Accounting for Uncertainty	75
4.2.5.1. Estimation of Uncertainty	77
4.2.5.2. Types of Uncertainty	78
4.2.5.3. Uncertainty of Initial Performance vs. Post-Occupancy Performance	81
CHAPTER 5: ESTIMATION OF BUILDING ENERGY CONSUMPTION AND GHG EMISSIONS	84

5.1. Building Energy Consumption Estimation in Research and Practice	84
5.1.1. Components of Building Energy Consumption	87
5.1.1.1. Variation in Building Energy Consumption between Buildings/Sites	92
5.1.2. Tools for Energy Estimation and Evaluation	99
5.1.2.1. Building Energy Simulation Software	99
5.1.2.2. CBECS	102
5.1.2.3. DOE Benchmark/Reference Buildings	107
5.2. Calculation Procedures for Building Energy Consumption and GHG Emissions	113
5.2.1. Define Building Alternatives Choice Set	114
5.2.1.1. Collect Building Energy System Parameter Data	115
5.2.2. Create Energy Model of Building	116
5.2.2.1. Define Intended Occupancy Schedule	117
5.2.2.2. Allocate Shared Loads for Shared Services	118
5.2.3. Define Range and Distribution of Uncertain Parameters	120
5.2.4. Analyze Sensitivity to Uncertain Parameters	121
5.2.4.1. Example Sensitivity Analysis	123
5.2.5. Monte Carlo Simulation / Propagation of Uncertainty	127
5.2.6. Calculate Upstream Energy and GHG Emissions	129
5.2.6.1. Site Energy vs. Primary Energy	129
5.2.6.2. GHG Emissions	130
CHAPTER 6: ESTIMATION OF TRANSPORTATION ENERGY CONSUMPTION AND GHG EMISSIONS	133
6.1. Site Transportation Energy Consumption Estimation in Research and Practice	133
6.1.1. Tools for Energy Estimation	133
6.1.1.1. Travel Surveys	133
6.1.1.2. Regional Travel Demand Models	137
6.1.1.3. Energy and Emissions Software	139

6.2. Calculation Procedures for Site Transportation Energy Consumption	141
6.2.1. Define Site Alternatives Choice Set	144
6.2.1.1. Collect Site Transportation Data	145
6.2.2. Estimate Building/Site Occupancy	146
6.2.2.1. Estimate Occupant Demographics	148
6.2.3. Estimate Motorized Vehicle Trip Reduction (VTR)	149
6.2.3.1. Bike/Ped Mode Share.....	149
6.2.3.2. Mixed-Use Development and Commute Trips	152
6.2.3.3. Travel Demand Management VTR Programs.....	159
6.2.4. Estimate Annual Motorized Trip Frequency	172
6.2.5. Estimate Trip Origins.....	175
6.2.6. Estimate Mode Choice.....	177
6.2.7. Estimate VMT by Mode	178
6.2.8. Estimate Annualized Trip Energy and GHGs.....	179
6.2.8.1. Estimation of Congestion Effects and Vehicle Efficiency.....	179
6.2.8.2. Upstream Energy vs. Direct Energy.....	186
6.2.8.3. GHG Emissions.....	186
6.2.9. Monte Carlo Simulation / Propagation of Uncertainty	188
6.2.10. Analyze Sensitivity to Uncertain Parameters	189
6.3. Estimating Non-Home Based Trips	190
6.3.1. NHB Mode Choice	193
6.3.2. NHB Trip Frequency	196
CHAPTER 7: APPLICATION OF FRAMEWORK: BUILDING SYSTEMS	202
7.1. Building/Site Selection Scenario.....	202
7.1.1. Alternatives Choice Set.....	203

7.1.1.1.	Intended Occupancy/Operation Schedule	204
7.1.2.	Case Study I: Older Construction, Single-Tenant, Low-Rise Commercial Office Building in Suburban Development Area.....	207
7.1.2.1.	Energy System Parameters and Building Energy Model	208
7.1.2.2.	Sensitivity Analysis of Uncertain Parameters	216
7.1.2.3.	Monte Carlo Analysis.....	222
7.1.2.4.	Site Energy vs. Source Energy / GHG Emissions.....	230
7.1.2.5.	Normalization of Results.....	232
7.1.3.	Case Study II: Recent Construction, Single-Tenant, Low-Rise Commercial Office Building in Suburban Development Area.....	234
7.1.3.1.	Energy System Parameters and Building Energy Model	235
7.1.3.2.	Sensitivity Analysis of Uncertain Parameters	242
7.1.3.3.	Monte Carlo Analysis.....	247
7.1.3.4.	Site Energy vs. Source Energy / GHG Emissions.....	250
7.1.3.5.	Normalization of Results.....	251
7.1.4.	Case Study III: Older Construction, Multi-Tenant, High-Rise Commercial Office Building in Urban Development Area	253
7.1.4.1.	Energy System Parameters and Building Energy Model	254
7.1.4.2.	Sensitivity Analysis of Uncertain Parameters	261
7.1.4.3.	Monte Carlo Analysis.....	269
7.1.4.4.	Site Energy vs. Source Energy / GHG Emissions.....	273
7.1.4.5.	Normalization of Results.....	275
7.1.5.	Case Study IV: Recent Construction, Multi-Tenant, High-Rise Commercial Office Building in Mixed-Use Urban Development Area.....	276
7.1.5.1.	Energy System Parameters and Building Energy Model	277
7.1.5.2.	Sensitivity Analysis of Uncertain Parameters	287
7.1.5.3.	Monte Carlo Analysis.....	293
7.1.5.4.	Site Energy vs. Source Energy / GHG Emissions.....	297
7.1.5.5.	Normalization of Results.....	298
7.1.6.	Comparison of Building Energy Consumption Under Uncertainty.....	299
7.1.6.1.	Summary of Estimated Building Energy Consumption and GHG Emissions 300	
7.1.6.2.	Evaluate Potential Impact of Post-Occupancy Energy Retrofits	309

CHAPTER 8: APPLICATION OF FRAMEWORK: TRANSPORTATION SYSTEMS 312

8.1. Regional Application: Atlanta, GA Metropolitan Region	312
8.1.1. Atlanta, GA Metropolitan Region.....	313
8.1.2. ARC Travel Demand Model	317
8.1.3. Alternatives Choice Set.....	318
8.1.3.1. Building/Site Occupancy.....	320
8.1.3.2. Stratification of Occupant Demographics	320
8.1.4. Motorized Vehicle Trip Reduction	321
8.1.4.1. Bike/Ped Mode Share.....	321
8.1.5. Annual Motorized Trip Frequency	325
8.1.6. Mode Choice	326
8.1.7. VMT.....	335
8.1.8. Energy Consumption	346
8.2. Site Selection Scenario.....	357
8.2.1. Alternatives Choice Set.....	358
8.2.1.1. Site Transportation Data.....	360
8.2.1.2. Building/Site Occupancy.....	361
8.2.2. Motorized Vehicle Trip Reduction	362
8.2.2.1. Bike/Ped Mode Share.....	362
8.2.2.2. Mixed-Use Development Internal Trip Capture	363
8.2.2.3. Travel Demand Management VTR Programs.....	364
8.2.3. Annual Motorized Trip Frequency	367
8.2.3.1. NHB Trip Frequency.....	369
8.2.4. Mode Choice and VMT	370
8.2.4.1. NHB Trips.....	379
8.2.5. Energy Consumption and GHG Emissions.....	381
8.2.5.1. NHB Trips	385
8.2.5.2. Impact of Estimated VTR	389

8.2.6. Combined Transportation and Building Performance	394
8.2.6.1. Probabilities of Relative Performance.....	410
8.2.6.2. Impact of Scale.....	413
CHAPTER 9: CONCLUSION.....	418
9.1. Policy Opportunities for Encouraging the Selection of Efficient Buildings/Sites	420
9.1.1. Development Regulations	421
9.1.2. Financial Incentives/Disincentives	422
9.1.3. Green Building Rating Systems.....	424
9.2. Limitations of the Evaluation Framework	425
9.3. Opportunities for Future Research	427
APPENDIX A: MATLAB Transportation Scripts.....	430
APPENDIX B: Building Energy Simulation Inputs.....	446
APPENDIX C: Morris Method MATLAB Script	478
APPENDIX D: ARC Travel Demand Model Files	480
APPENDIX E: MATLAB Combined Energy Scripts	488
REFERENCES.....	491

LIST OF TABLES

Table 1: Summary of Research and Practice Relevant to Estimation of Site-Specific Energy and GHG Emissions.....	12
Table 2: Summary of Research and Practice Relevant to Estimation of Site-Specific Energy and GHG Emissions (Continued)	13
Table 3: Energy Consumption and GHG Emission Performance Metrics	38
Table 4: Example Building Operation Systems Supporting Rational for Selected Building Operation Elements in Conceptual Framework (Existing Building)	52
Table 5: CBECS Independent Variables Identified by U.S. EPA as Potentially Important for Offices, Bank/Financial Institutions, and Courthouses, Source: (55).....	104
Table 6: CBECS Key Explanatory Variables That Can Be Used to Estimate the Expected Average Source EUI in Offices, Bank/Financial Institutions, and Courthouses, Source: (55).	105
Table 7: Consumption of Electricity for Office Buildings, 2003 CBECS (76)	106
Table 8: ASHRAE/IES Standard 100-2006 Energy Use Intensity Targets, Source: (113)	107
Table 9: DOE Commercial Benchmark/Reference Building Office Dataset. Based on (76, 114)	108
Table 10: Comparison of Annual Building Electrical Energy Consumption for DOE Benchmark/Reference Building Translation from EnergyPlus to eQUEST: Medium Office, Post-1980 Construction, Atlanta, GA	111
Table 11: Comparison of Annual Building Gas Consumption for DOE Benchmark/Reference Building Translation from EnergyPlus to eQUEST: Medium Office, Post-1980 Construction, Atlanta, GA.....	111
Table 12: Example Summary of Building Spaces.	115
Table 13: Default Building Occupancy and Operation Schedules, Source (77).....	118
Table 14: Example Input Variable Uncertainty in DOE Medium Office, Post 1980 Construction, Atlanta, GA	124
Table 15: Example Time of Day Occupancy and Inbound/Outbound Commute Trip Schedule	147
Table 16: Atlanta, GA Non-Motorized Mode Split Estimates from National Surveys.	150

Table 17: Atlantic Station Peak-Period Person Trips and Percent Internal Trip Capture by Land Use, Source: (135).....	154
Table 18: Atlantic Station Percent Distribution of Internal Trip Origins for Entering Trips During A.M Peak-Period, Source: (135).....	155
Table 19: Atlantic Station Percent Distribution of Internal Trip Destinations for Exiting Trips During P.M. Peak-Period, Source: (135)	156
Table 20: Atlantic Station Peak-Period Person-Trips and Percent Internal Trip Capture by Mode of Access, Source: (135)	157
Table 21: Atlantic Station Mode of Access for Entering and Exiting Internal Trips, Based on (135)	157
Table 22: Atlantic Station Mode of Travel for Entering and Exiting Internal Trips, Based on (135)	158
Table 23: Types of TDM Strategies, Based on (127)	160
Table 24: COMMUTER Model Support Strategy Programs, Source: (139).....	169
Table 25: COMMUTER Model Percent Increase in Mode by Support Program Level, Source: (105)	170
Table 26: Non-Home Based Trips to/from Worksites by Trip Purpose Summary (Vehicle Trips), Source: 2009 NHTS	191
Table 27: Mode Choice by General Trip Purpose (Home-Based Purpose Types), Source: 2009 NHTS	194
Table 28: Non-Home Based Bike / Walk Mode Choice by Trip Purpose Summary (Person Trips), Source: 2009 NHTS	195
Table 29: Mean Non-Home Based Vehicle Trip Length by Income and Trip Summary Purpose, Source: 2009 NHTS	198
Table 30: Non-Home Based Daily Trip Rate by Household Income where the Previous Trip Purpose was “Go to Work,” Based on 2009 NHTS.....	199
Table 31: Non-Home Based Daily Trip Rate by Employment Density where the Previous Trip Purpose was “Go to Work,” Based on 2009 NHTS.....	200
Table 32: Trip Attraction Rates for Non-Home Based Trips in the ARC Travel Demand Model, Source: (43).....	201
Table 33: Summary of Building Spaces	203
Table 34: Choice Set of Building Alternatives.....	204

Table 35: Case Study Building Occupancy Schedule and Annual Person-Hours	206
Table 36: Summary of Tenant Spaces (Case Study I)	208
Table 37: Case Study I Building Characteristics	209
Table 38: Input Variables with Absolute Value of Mean Effects Greater Than One Percent of Annual Tenant kWh Consumption (Case Study I)	219
Table 39: Input Variables with Absolute Value of Mean Effects Greater Than One Percent of Annual Tenant MBtu Consumption (Case Study I).....	222
Table 40: Uncertain Input Variables for Monte Carlo Analysis (Case Study I).....	223
Table 41: Estimated GHG Emissions of Purchased Electricity and Natural Gas Combustion (Case Study I).....	232
Table 42: Normalized Building Energy Consumption and GHG Emission Performance (Case Study I).....	233
Table 43: Summary of Tenant Spaces (Case Study II).....	235
Table 44: Case Study II Building Characteristics.....	236
Table 45: Input Variables with an Absolute Value of Mean Effects Greater Than One Percent of Annual Tenant Energy Consumption (Case Study II)	246
Table 46: Uncertain Input Variables for Monte Carlo Analysis (Case Study II).	248
Table 47: Estimated GHG Emissions of Purchased Electricity (Case Study II)	251
Table 48: Normalized Building Energy Consumption and GHG Emission Performance (Case Study II)	253
Table 49: Summary of Tenant Spaces (Case Study III)	254
Table 50: Case Study III Building Characteristics	255
Table 51: Input Variables with Absolute Value of Mean Effects Greater Than One Percent of Annual Tenant kWh Consumption (Case Study III).....	267
Table 52: Input Variables with Absolute Value of Mean Effects Greater Than One Percent of Annual Tenant Btu Consumption (Case Study III).....	269
Table 53: Uncertain Input Variables for Monte Carlo Analysis (Case Study III)	269
Table 54: Estimated GHG Emissions of Purchased Electricity and Natural Gas Combustion (Case Study III)	274

Table 55: Normalized Building Energy Consumption and GHG Emissions Performance (Case Study III)	276
Table 56: Summary of Tenant Spaces (Case Study IV)	277
Table 57: Case Study IV Building Characteristics	279
Table 58: Input Variables with Absolute Value of Mean Effects Greater Than One Percent of Annual Tenant Energy Consumption (Case Study IV).....	291
Table 59: Uncertain Input Variables for Monte Carlo Analysis (Case Study IV).....	293
Table 60: Estimated GHG Emissions of Purchased Electricity (Case Study IV).....	297
Table 61: Normalized Building Energy Consumption and GHG Emission Performance (Case Study IV).....	299
Table 62: Normalized Building Energy Consumption and GHG Emission Performance of Case Study Buildings	301
Table 63: Number of Employees in Each Market Segment of Travel Demand Model.....	320
Table 64: Time of Day Occupancy and Inbound/Outbound Commute Trip Schedule	326
Table 65: Choice Set of Location Alternatives.....	360
Table 66: Non-Motorized Mode Share of HBW Trips Attracted to Case Study TAZs	362
Table 67: Estimated Vehicle Trip Reduction (VTR) for Case Study Locations According to FHWA TDM Guidance Manual and COMMUTER Model	365
Table 68: Estimated Vehicle Trip Reduction (VTR) for Case Study III with \$1 Employee Parking Fee According to FHWA TDM Guidance Manual and COMMUTER Model	367
Table 69: Annual HBW Motorized Vehicle Trips by Direction, Period, and Stratification for Each Case Study TAZ.....	368
Table 70: Annual NHB Motorized Vehicle Trips by Direction, Period, and Stratification for Each Case Study TAZ.....	369
Table 71: Normalized HBW Transportation Energy Consumption and GHG Emission Performance of Case Study Locations	384
Table 72: Comparison of Trip Distance, HOV Mode Share, and Transit Mode Share from Baseline, FHWA TDM Guidance Manual, and EPA COMMUTER Model Estimates.	394

Table 73: Normalized Combined Annual Energy Consumption and GHG Emission Performance 395

LIST OF FIGURES

Figure 1: Elements of whole-building energy consumption and GHG emissions.....	2
Figure 2: Workflow of the research methodology.....	31
Figure 3: Matrix of building scenarios / case studies.	40
Figure 4: Matrix of transportation scenarios / case studies.....	42
Figure 5: Outline of owner/occupant functional considerations for commercial building/site selection alternatives. Source: (78)	47
Figure 6: Elements of whole-building energy consumption and GHG emissions that are potentially variable and constrained by the building site.....	51
Figure 7: Schematic relationship between typical office building/site services and energy systems.	55
Figure 8: Conceptual framework of whole-building energy systems, as they relate to a building site/location, Source: (78).	59
Figure 9: GHG emission scopes and categories included within the life cycle analysis boundary.	64
Figure 10: Example comparisons of building energy consumption via baseline energy, schematic design energy, and energy reductions.	74
Figure 11: Spectrum of Uncertainty in Estimated Building/Site Energy and GHG Performance.	76
Figure 12: Energy flow diagram of net facility energy use, Source: (56).	88
Figure 13: Categorical flow chart of net facility energy use, Source: (56).....	89
Figure 14: 2006 U.S. commercial buildings energy end-use splits, Source: (94).	90
Figure 15: 2003 U.S. commercial office buildings energy end-use splits, Based on (76).....	91
Figure 17: Main factors influencing building energy consumption.....	93
Figure 18: Landsat satellite image of multi-nodal heat island in Atlanta, GA, Source: (97).	95
Figure 19: Building energy consumption components for eQUEST DOE Benchmark/Reference Building: Medium Office, Post-1980 Construction, Atlanta, GA.	113
Figure 20: Process for estimating building energy and GHG performance.....	114

Figure 21: Example mean and standard deviation of elementary effects of uncertain building energy simulation input variables for DOE Medium Office, Post 1980 Construction, Atlanta, GA model using the Morris method.....	125
Figure 22: Example sensitivity analysis of uncertain building energy simulation input variables for DOE Medium Office, Post 1980 Construction, Atlanta, GA model using a central composite design of experiments.	126
Figure 23: Example Monte Carlo analysis of uncertain building energy simulation input variables for DOE Medium Office, Post 1980 Construction, Atlanta, GA model.....	128
Figure 24: Map of Georgia Institute of Technology census tract commute shed, Source: (124).	136
Figure 25: Work trip variables/elements related to fuel consumption and GHG emissions.	142
Figure 26: Process and data diagram for estimating site-specific transportation energy consumption and emissions.	144
Figure 27: Fuel consumption rates as a function of speed, Based on (142).	180
Figure 28: Fuel economy as a function of speed, Based on (142).	183
Figure 29: Fuel economy by speed, 1973, 1984, and 1997 studies, Source: (3).	184
Figure 30: Floor plan for Case Study I.	211
Figure 31: 3-D rendering of building, northwestern perspective (Case Study I).....	212
Figure 32: 3-D rendering of building, southeastern perspective (Case Study I).	213
Figure 33: Components of annual tenant energy consumption (Case Study I).	214
Figure 34: Components of monthly tenant energy consumption (Case Study I).....	215
Figure 35: Mean and standard deviation of elementary effects on annual kWh for Case Study I.	217
Figure 36: Mean and standard deviation of elementary effects on annual kWh for Case Study I.	218
Figure 37: Ordered absolute value of the mean of elementary effects on kWh for Case Study I.	219
Figure 38: Mean and standard deviation of elementary effects on annual natural gas MBtu for Case Study I.	221
Figure 39: Ordered absolute value of the mean of elementary effects on MBtu for Case Study I	222

Figure 40: Monte Carlo analysis of annual energy consumption, kWh (Case Study I).	224
Figure 41: Monte Carlo analysis of annual natural gas energy consumption, MBtu (Case Study I).	225
Figure 42: Monte Carlo analysis of annual building energy consumption, MBtu (Case Study I).	226
Figure 43: Monte Carlo analysis of annual Scope 1 and Scope 2 GHG emissions, kg (Case Study I).	227
Figure 44: Monte Carlo analysis of annual Scope 1, Scope 2, and Scope 3 GHG emissions, kg (Case Study I).	228
Figure 45: Revised Monte Carlo analysis of annual energy consumption, kWh (Case Study I).	230
Figure 46: Floor plan for Case Study II.	237
Figure 47: 3-D rendering of building, northwestern perspective (Case Study II).	238
Figure 48: 3-D rendering of building, southeastern perspective (Case Study II).	239
Figure 49: Components of annual tenant energy consumption (Case Study II).	241
Figure 50: Components of annual tenant energy consumption (Case Study II).	242
Figure 51: Mean and standard deviation of elementary effects on annual kWh for Case Study II.	244
Figure 52: Mean and standard deviation of elementary effects on annual kWh for Case Study II.	245
Figure 53: Ordered absolute value of the mean of elementary effects for Case Study II.	246
Figure 54: Monte Carlo analysis of annual tenant energy consumption, kWh's (Case Study II).	250
Figure 55: Tenant floor plan of core and perimeter zones (Case Study III).	256
Figure 56: Ground floor plan of core and perimeter zones (Case Study III).	257
Figure 57: 3-D rendering of building, western perspective (Case Study III).	258
Figure 58: 3-D rendering of building, eastern perspective (Case Study III).	259
Figure 59: Components of annual tenant energy consumption (Case Study III).	260
Figure 60: Components of annual tenant energy consumption (Case Study III).	261

Figure 61: Mean and standard deviation of elementary effects on annual kWh (Equation 2) for Case Study III.....	263
Figure 62: Mean and standard deviation of elementary effects on annual kWh (Equation 2) for Case Study III.....	264
Figure 63: Mean and standard deviation of elementary effects on annual natural gas MBtu (Equation 2) for Case Study III.....	265
Figure 64: Ordered absolute value of the mean of elementary effects on kWh for Case Study III.....	266
Figure 65: Ordered absolute value of the mean of elementary effects on Btu for Case Study III.....	268
Figure 66: Monte Carlo analysis of annual tenant energy consumption, kWh's (Case Study III).....	271
Figure 67: Revised Monte Carlo analysis of annual tenant energy consumption, kWh's (Case Study III).....	273
Figure 68: Tenant floor plan of core and perimeter zones (Case Study IV).....	280
Figure 69: Ground floor plan of core and perimeter zones (Case Study IV).....	281
Figure 70: 3-D rendering of building floors, southwestern perspective (Case Study IV).	282
Figure 71: 3-D rendering of building floors, northeastern perspective (Case Study IV).	283
Figure 72: Components of annual tenant energy consumption (Case Study IV).	286
Figure 73: Components of annual tenant energy consumption (Case Study IV).	286
Figure 74: Mean and standard deviation of elementary effects on the response variable (Equation 2) for Case Study IV.....	288
Figure 75: Mean and standard deviation of elementary effects on the response variable (Equation 2) for Case Study IV.....	290
Figure 76: Ordered absolute value of the mean of elementary effects for Case Study IV.	291
Figure 77: Monte Carlo analysis of annual tenant energy consumption, kWh's (Case Study IV).....	296
Figure 78: Building annual (site) energy consumption for initial Monte Carlo analyses.....	303
Figure 79: Building annual (site) energy consumption for revised Monte Carlo analyses.	304

Figure 80: Probability distribution functions of estimated annual building energy consumption for Case Study II and Case Study IV.	306
Figure 81: Probability distribution functions of estimated annual building energy saved by Case Study II relative to Case Study IV.	307
Figure 82: Cumulative distribution function of estimated annual building energy saved by Case Study II relative to Case Study IV.	308
Figure 83: Monte Carlo analysis of annual tenant energy consumption, kWh's (Case Study IV, revised office LPD).	311
Figure 84: Map of Atlanta, GA metropolitan region.	314
Figure 85: Map of Atlanta, GA regional population density.	315
Figure 86: Map of Atlanta, GA regional employment density.	316
Figure 87: Map of candidate office site TAZs in Atlanta, GA metropolitan region.	319
Figure 88: Non-motorized mode shares attracted to TAZs in the Atlanta, GA metropolitan region. Based on CTTP Part2, Table2 (123).	322
Figure 89: Walk mode shares attracted to TAZs in the Atlanta, GA metropolitan region. Based on CTTP Part2, Table2 (123).	323
Figure 90: Bike mode shares attracted to TAZs in the Atlanta, GA metropolitan region. Based on CTTP Part2, Table2 (123).	324
Figure 91: Regional average HBW office site mode split for each of the four market segments in the ARC travel demand model.	328
Figure 92: Map of HBW transit mode share for demographic stratification 1.	330
Figure 93: Map of HBW transit mode share for demographic stratification 2.	331
Figure 94: Map of HBW transit mode share for demographic stratification 3.	332
Figure 95: Map of HBW transit mode share for demographic stratification 4.	333
Figure 96: Map of HBW transit mode share for case study demographic profile.	334
Figure 97: SOV annual HBW VMT per 100 employees for candidate TAZs by demographic stratification.	336
Figure 98: SOV average HBW trip distance for candidate TAZs by demographic stratification.	338
Figure 99: Map of SOV average HBW trip distance for demographic stratification 1.	340

Figure 100: Map of SOV average HBW trip distance for demographic stratification 2.	341
Figure 101: Map of SOV average HBW trip distance for demographic stratification 3.	342
Figure 102: Map of SOV average HBW trip distance for demographic stratification 4.	343
Figure 103: Map of SOV average HBW trip distance for case study demographic profile.	344
Figure 104: Average SOV HBW trip distance vs. total TAZ employment.	345
Figure 105: HBW average annual SOV + HOV + drive-to-transit energy consumption per 100 employees for candidate TAZs by demographic stratification.	348
Figure 106: Map of HBW average annual SOV + HOV + drive-to-transit relative energy consumption per 100 employees for demographic stratification 1.	351
Figure 107: Map of HBW average annual SOV + HOV + drive-to-transit relative energy consumption per 100 employees for demographic stratification 2.	352
Figure 108: Map of HBW average annual SOV + HOV + drive-to-transit relative energy consumption per 100 employees for demographic stratification 3.	353
Figure 109: Map of HBW average annual SOV + HOV + drive-to-transit relative energy consumption per 100 employees for demographic stratification 4.	354
Figure 110: Map of HBW average annual SOV + HOV + drive-to-transit relative energy consumption per 100 employees for case study demographic profile.	356
Figure 111: Map of TAZ location choice set (case studies) in the Atlanta, GA metropolitan region.....	359
Figure 112: Average HBW mode choice for case study TAZs.	371
Figure 113: Average annual HBW SOV + D2T VMT for case study TAZs.	372
Figure 114: Average HBW SOV + D2T trip distance for case study TAZs.	374
Figure 115: Average SOV HBW trip distance vs. total TAZ employment (TAZ 521 cluster).	375
Figure 116: Average SOV HBW trip distance vs. total TAZ employment (TAZ 240 cluster).	376
Figure 117: Average SOV HBW trip distance vs. total TAZ employment (TAZ 12 cluster). ..	377
Figure 118: Average SOV HBW trip distance vs. total TAZ employment (TAZ 27 cluster) ...	377
Figure 119: Average HBW SOV + D2T speed for case study TAZs.....	378
Figure 120: Average NHB SOV + D2T trip distance for case study TAZs.	380

Figure 121: HBW average annual SOV + HOV + drive-to-transit energy consumption per 100 employees for case study TAZs.	382
Figure 122: NHB average annual SOV + HOV + drive-to-transit energy consumption per 100 employees for case study TAZs.	386
Figure 123: Proportion of estimated HBW and NHB energy consumption for case study TAZs.	387
Figure 124: Combined HBW and NHB average annual SOV + HOV + drive-to-transit energy consumption per 100 employees for case study TAZs.	388
Figure 125: HBW average annual SOV + HOV + drive-to-transit energy consumption per 100 employees for case study TAZs, with 4.5 percent VTR in TAZ 27.	390
Figure 126: HBW energy consumption with FHWA TDM Guidance Manual trip reduction. .	392
Figure 127: HBW energy consumption with COMMUTER Model mode shift.	393
Figure 128: Relative proportion of direct, metered (site) energy consumption of building and transportation systems.	397
Figure 129: Relative proportion of direct plus upstream (primary) energy consumption of building and transportation systems.	398
Figure 130: Annual building and transportation energy consumption (site and upstream).....	399
Figure 131: Relative proportion of direct GHG emissions of building and transportation systems (Scope 1 and 2).....	401
Figure 132: Relative proportion of direct plus upstream (primary) GHG emissions of building and transportation systems (Scope 1, 2, and 3).....	402
Figure 133: Annual building and transportation GHG emissions (Scope 1, 2, and 3).	403
Figure 134: Combined transportation and building site energy consumption per 100 employees for initial building Monte Carlo analysis.	405
Figure 135: Combined transportation and building site energy consumption per 100 employees for revised building Monte Carlo analysis.	406
Figure 136: Combined transportation and building primary energy consumption per 100 employees for revised building Monte Carlo analysis.	408
Figure 137: Combined transportation and building primary GHG emissions per 100 employees for revised building Monte Carlo analysis.	409
Figure 138: Probability distribution functions of estimated annual combined transportation and building energy consumption for Case Study II and Case Study III.	411

Figure 139: Cumulative distribution function of estimated annual combined transportation and building energy consumption saved for Case Study II relative to Case Study III.	412
Figure 140: HBW average annual SOV + HOV + drive-to-transit energy consumption per 300 employees for case study TAZs.	415

LIST OF SYMBOLS AND ABBREVIATIONS

AC	Air conditioning
ACS	American Community Survey
AE(C)	Architecture, engineering, (and construction)
AFV	Alternative fuel vehicle
ARC	Atlanta Regional Commission
BIM	Building information model
BTU	British thermal unit
CAP	Criteria air pollutant
CBD	Central business district
CBECS	Commercial Building Energy Consumption Survey
CDF	Cumulative distribution function
CFM	Cubic feet per minute
CH ₄	Methane
COMNET	Commercial Energy Services Network
CO ₂	Carbon dioxide
CO ₂ e	Carbon dioxide equivalent
CHW	Chilled water
CHP	Chilled water pump
CT	Cooling tower
CTPP	Census Transportation Planning Products
CW	Condenser water
CWP	Condenser water pump

DOE	U.S. Department of Energy
DOT	Department of Transportation
DHW	Domestic hot water
DRI	Development of regional impact
DX	Direct expansion
D2B	Drive-to-bus
D2R	Drive-to-rail
D2T	Drive-to-transit
EIA	U.S. Energy Information Administration
EUI	Energy use intensity
GEI	Greenhouse gas emissions intensity
GHG	Greenhouse gas
REET	Greenhouse Gases, Regulated Emissions, and Energy Use in Transportation
GRP	General reporting protocol
GWh	Gigawatt-hour
GWP	Global warming potential
HBW	Home based work (trip)
HFC	Hydrofluorocarbon
HOV	High occupancy vehicle
IBC	International Building Code
IECC	International Energy Conservation Code
ICLEI	International Council for Local Environmental Initiatives
IMC	International Mechanical Code

IPCC	Intergovernmental Panel on Climate Change
ISO	International Organization for Standardization
KWh	Kilowatt-hour
LCA	Life cycle analysis (or life cycle assessment)
LEED	Leadership in Energy and Environmental Design
LEHD	Longitudinal Employer-Household Dynamics
N ₂ O	Nitrous oxide
MARTA	Metropolitan Atlanta Rapid Transit Authority
MEP	Mechanical, electrical, and plumbing
NERC	North American Electrical Reliability Council
NHB	Non-home based (trip)
NHBO	Non-home based other (trip)
NHBW	Non-home based work (trip)
NHTS	National Household Travel Survey
NIST	National Institute of Standards and Technology
NREL	National Renewable Energy Laboratory
NTD	National Transit Database
MBtu	10 ⁶ British thermal units
MPO	Metropolitan planning organization
MWh	Megawatt-hour
PDF	Probability distribution function
PMT	Passenger miles travelled (or, passenger miles of travel)
PV	Photovoltaic

SF	Square feet
SHGC	Solar heat gain coefficient
SOV	Single occupancy vehicle
TAZ	Traffic analysis zone
TCR	The Climate Registry
TCRP	Transit Cooperative Research Program
T&D	Transmission & Distribution
TDM	Travel (or transportation) demand management
TIA	Traffic impact analysis
TMY	Typical meteorological year
VAV	Variable air volume
VTR	Vehicle trip reduction (motorized)
W.G.	Water gauge
VMT	Vehicle miles travelled (or, vehicle miles of travel)
WRI	World Resources Institute
W2B	Walk-to-bus
W2R	Walk-to-rail
W2T	Walk-to transit

DEFINITIONS

Direct energy	Energy consumed either through an on-site combustion process or metered end-use.
Primary energy	Total energy consumed by an end-use process: direct energy plus upstream energy.
Site energy	See “direct energy”
Source energy	See “primary energy”
Whole-building	Of or relating to all or most of the building systems affecting a particular domain or measure, typically energy consumption. In professional practice, “whole-building” refers only to systems contained within the building or site boundary, and thus does not include interconnecting systems such as transportation access or energy supply chains. In this dissertation, use of the term “whole-building” is meant to include all onsite building systems as well as the requisite supply chains and transportation systems for occupant access.
Upstream energy	Energy consumed in the preceding processes of the energy supply chain (e.g. extraction, refining, transportation, and distribution). Upstream energy corresponds with Scope 3 of GHG emission inventory protocols.
Uncertainty	“Parameter associated with the result of a measurement, that characterizes the dispersion of the values that could reasonably be attributed to the measurand” ¹

¹ JCGM 100:2008

SUMMARY

In urbanized areas, building and transportation systems generally comprise the majority of energy consumption and greenhouse gas (GHG) emissions. Realization of global environmental sustainability depends upon efficiency improvements of building and transportation systems in the built environment. The selection of efficient buildings and locations can help to improve the efficient utilization of transportation and building systems. Green building design and rating frameworks provide some guidance and incentive for the development of more efficient building and transportation systems. However, current frameworks are based primarily on prescriptive, component standards, rather than performance-based, whole-building evaluations. This research develops a commercial building/site evaluation framework for the minimization of energy consumption and GHG emissions of transportation and building systems through building/site selection.

The framework examines, under uncertainty, multiple dimensions of building/site operation efficiencies: transportation access to/from a building site; heating, ventilation, air conditioning, and domestic hot water; interior and exterior lighting; occupant conveyances; and energy supply. With respect to transportation systems, the framework leverages regional travel demand model data to estimate the activity associated with home-based work and non-home-based work trips. A Monte Carlo simulation approach is used to quantify the dispersion in the estimated trip distances, travel times, and mode choice. The travel activity estimates are linked with a variety of existing calculation resources for quantifying energy consumption and GHG emissions. With respect to building systems, the framework utilizes a building energy simulation approach to estimate energy consumption and GHG emissions. The building system calculation procedures include a sensitivity analysis and Monte Carlo analysis to account for the impacts of

input parameter uncertainty on estimated building performance. The framework incorporates a life cycle approach to performance evaluation, thereby incorporating functional units of building/site performance (e.g energy use intensity).

The evaluation framework is applied to four case studies of commercial office development in the Atlanta, GA metropolitan region that represent a potential range of building/site alternatives for a 100-employee firm in an urbanized area: high transit mode share vs. low transit mode share, high average trip distance vs. low average trip distance, older construction vs. newer construction, and single-tenant vs. multi-tenant. The framework and case studies include estimation of not only the expected baseline performance of unique buildings/sites, but also the potential impact of post-site selection opportunities for improving the energy/emissions performance of buildings/sites, such as travel demand management strategies and building energy retrofits.

The research results indicate that whole-building energy and GHG emissions are sensitive to building/site location, and that site-related transportation is the major determinant of whole-building performance. This research contributes an analytical approach for estimating and comparing, under uncertainty, the energy consumption and GHG emissions of site-related transportation and building systems. The framework and findings may be used to support the development of quantitative performance evaluations for building/site selection in green building rating systems and other efficiency incentive programs designed to encourage more efficient utilization and development of the built environment.

CHAPTER 1

INTRODUCTION

1.1. Research objective

The objective of this research is to develop a commercial building/site selection evaluation framework for evaluating and minimizing the energy consumption and GHG emissions from transportation and building systems. The term “framework” refers to a conceptual approach to and analysis procedures for the evaluation objective. The framework is to include analysis methods for estimating the site-dependent energy consumption and GHG emissions associated with:

- 1) Architectural energy systems:
 - a) Heating, ventilating, and air conditioning (HVAC) & domestic hot water
 - b) Lighting
 - c) Conveyances
 - d) Utility and on-site energy sources
- 2) Transportation energy systems:
 - a) Commuting of tenants
 - b) Non-home based tenant trips

Figure 1 outlines the elements of whole-building energy consumption and GHG emissions that may be considered in a building/site evaluation framework. In essence, Figure 1 represents this dissertation’s boundary of analysis for assessing whole-building energy

consumption and GHG emissions. It should be noted that construction and material elements are not included within the analysis boundary, largely due to time and data constraints. The construction and material impacts likely contribute less than 15 percent of life cycle energy consumption or GHG emissions (1, 2). This research is not designed to test a particular hypotheses; rather, this research is intended to quantify the potential variation in energy consumption and GHG emissions between commercial office sites within a given region.

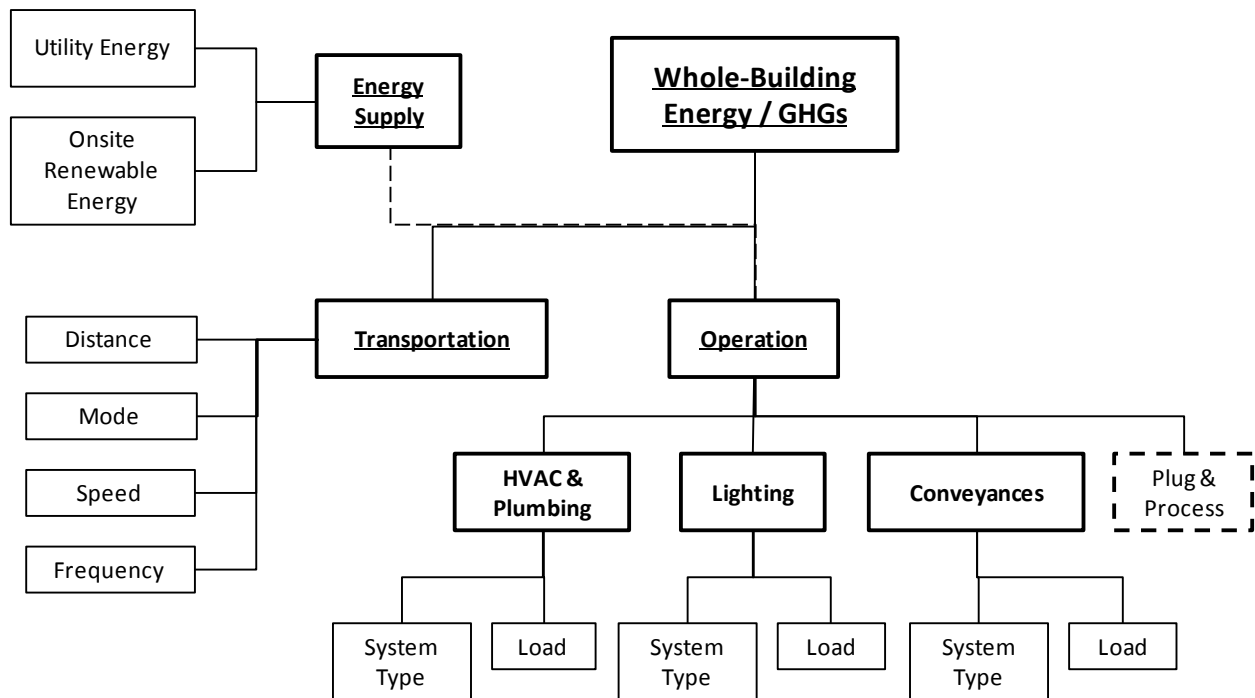


Figure 1: Elements of whole-building energy consumption and GHG emissions.

The calculation framework described here is tailored to the perspective of system users – specifically, office location *decision makers*. The execution of the decision maker’s location choice may be regarded as a marginal increase in demand on the building stock and regional transportation system – a demand that ideally minimizes the marginal increase in energy consumption. The framework is intended to support evaluation of the energy and GHG emissions

of architectural and transportation-related building site aspects, at the key decision point of building/site selection. At this decision point, many uncertainties surround the elements of whole-building energy consumption and GHG emissions. Thus, the framework is intended to account for the propagation of uncertainty from evaluation inputs to evaluation outputs. The framework will be developed through a case study-based research approach. Therefore, to achieve consistency in the case study evaluation, the development and application of the framework will be limited to the context of commercial office buildings.

1.2. Significance of work

This research contributes the first commercial building/site performance evaluation framework for estimating the energy consumption and GHG emissions associated with alternative commercial office sites (see Chapter 2). In doing so, this research pioneers an analytical approach for estimating and comparing, under uncertainty, the energy consumption and GHG emissions of site-related transportation and building systems.

The results of this research can help to inform performance-based standards and rating systems for sustainable building site selections that enable greater whole-building life cycle GHG emission reductions. Application of the evaluation framework can also inform the creation of commercial development incentives (green building certifications and/or financial instruments) aimed at the efficient development and utilization of the built environment through site selection.

1.3. Background and Motivation

1.3.1. Energy Conservation and Climate Change Mitigation

In an increasingly urbanized world, urban transportation and building systems have become an essential component of regional, national, and world economies. To support modern economies these systems require substantial amounts of energy. In the U.S., transportation and commercial buildings represent approximately 28 percent and 20 percent, respectively, of domestic energy consumption (3, 4). The dependence of urban economies on transportation and building energy inputs has given rise to regional, national, and global concerns over energy security, as well as concerns over the negative environmental impacts of both legacy and alternative energy systems. Growing international concerns over climate change and sustainable development have highlighted the need for major reductions in anthropogenic greenhouse gas (GHG) emissions. In 2008, the transportation and buildings sectors in the U.S. accounted for 33 percent and 39 percent, respectively, of direct domestic CO₂ emissions (5). Commercial buildings and passenger / light duty vehicles alone account for 18 percent and 20 percent, respectively, of U.S. GHG emissions (3, 6). For many developed and developing nations, minimizing energy consumption and GHG emissions from transportation and buildings has become an important objective and a challenging task. Although the transportation and commercial building sectors both largely depend on a fossil fuel energy supply, the complexity of energy end-uses and technologies, both within and across these large sectors, necessitates a diverse set of energy conservation and emission reduction strategies that exploit the many unique opportunities for efficiency improvements. One such strategy that lies at the intersection of the transportation and commercial building sectors is the selection/development of commercial building locations that minimize the combined transportation and building energy consumption.

1.3.2. Efficient Commercial Building Locations / Sites

The location or site of a commercial building can place unique constraints on a building's architecture and transportation access, and consequently can impact energy consumption of the building and related transportation system. Urban form (i.e. the spatial arrangement and distribution of building types) influences transportation distances, transportation mode shares, building envelope heat transfer, and building material use/reuse; in turn, each of these factors can impact life cycle energy consumption and GHG emissions of the built environment. It is generally understood among urban planning researchers and practitioners that on a per capita basis, the efficiency of the built environment correlates with the development density and land-use mix (2, 7, 8, 9, 10). Awareness of this relationship may be helpful in planning new urban development that is more energy efficient; however, traditional transportation and land-use planning mechanisms (e.g. land-use regulation and transportation infrastructure programming) are inadequate for capitalizing on improved efficiency opportunities as they currently, and foreseeably, exist in the built environment. Much of the built environment (where populations and economic activities are concentrating) is already built, and much of the new development to come is likely to follow the trend of low-density urban sprawl – the result of enormous economic and institutional inertia (in the case of the developed world, notably the U.S.) and aspiration (in the case of the developing world). Thus, efforts to substantially regulate more compact, mixed-use development or to build large-scale alternative transportation infrastructures face considerable physical, political, and financial obstacles.

To effectively leverage opportunities for improved efficiencies in the built environment, new strategies are needed to complement and/or supplant traditional building and transportation planning strategies. In the U.S., given a large existing building stock where at least half of the existing buildings will still be standing by mid-century (7), and a largely built-out transportation

system where for the last three decades public spending on transportation operations and maintenance has exceeded public spending on transportation capital (11), much of the opportunity for improving the efficiencies of the built environment of today and tomorrow exists in the efficient utilization of transportation and building infrastructures. Efficient utilization of the built environment is basically an exercise in matching system users (user needs) to system infrastructure (system services). In the case of commercial development, the opportunity for matching system users to system infrastructure occurs at the key decision point of building/site selection.

The selection of a building/site can influence the potential for energy and GHG emissions efficiency through site-dependent variables (e.g. transportation distances, transportation mode splits, building envelope heat transfer, and building material use), and through the marginal utilization of the building stock. However, the selection of a building site is a decision constrained by discrete alternatives in the marketplace – the potential for achieving the most efficient utilization of the built environment is limited by the buildings/locations available at the moment of selection. To identify building site locations that maximize the potential for efficiency in the built environment, a performance-based building site selection evaluation framework is needed.

1.3.3. Existing Paradigm of Efficient / Sustainable Commercial Site Evaluation

Sustainable building design and rating systems, such as those found in the United States Green Building Council's LEED (Leadership in Energy and Environmental Design) program, offer a reference framework for evaluating and incentivizing greater efficiency in the built environment. Such rating systems have helped to create a green building market transformation

by informing the design and development of more efficient infrastructure and by working to increase the market value of sustainable buildings. As part of an overarching agenda to transform the building marketplace into one that places greater value on buildings that are designed and operated to reduce energy consumption, green building rating systems award credits to buildings that meet a specific schedule of “green” criteria. Importantly, sustainable building design and rating systems reward both building-related and transportation-related energy efficiency measures in green building projects; however, much of the evaluation of site-dependant energy efficiency measures is *prescriptive* rather than *performance-based*. For example, LEED 2009 for New Construction and Major Renovations encourages urban density/connectivity and alternative transportation in the building site through the use of prescriptive criteria, yet the rating system does not include evaluation of transportation energy savings or GHG emission reduction. Such prescriptive standards may result in site selection decisions that fail to effectively reduce energy consumption and GHG emissions. Although some portions of green building rating systems do employ a performance-based approach (e.g. Energy and Atmosphere Credit 1 of LEED), these performance-based evaluations do not account for the relative energy efficiency performance potential of alternative building sites/locations – each project is evaluated against a site-specific baseline design, after the site has been selected. Considering the many possible variations in existing conditions and design constraints imposed by different building sites (existing envelope construction, adjoining conditioned spaces, solar ground reflection and shading, building footprint limits, available utilities, accommodation of onsite renewable energy infrastructure etc.), it should be expected that different building sites will achieve different levels of baseline performance, and that different sites will support different levels of final design performance. Thus, there exists a research need to develop a quantitative performance evaluation framework of

building site alternatives – a framework that may be used to evaluate and minimize energy consumption and GHG emissions of commercial development.

1.3.4. Transportation Energy and GHGs in the Context of Commercial Buildings/Sites

This dissertation research is inspired in part by literature exploring the magnitude of transportation energy with respect to whole building energy consumption. Currently, the literature offers anecdotal evidence of the proportion of whole building energy consumption related to transportation activity to/from a building site, and the importance of building location and mode choice on reducing transportation energy. Wilson conducted a study of the transportation energy intensity of buildings by comparing “driving energy” to “site energy” (12). Based on national data from DOE and EPA on driver commute distance and vehicle efficiency, and building energy consumption data from DOE, the study found that for an average office building, transportation energy use exceeds building operation energy use by around 30%. For buildings built to meet applicable energy codes, transportation energy use is estimated to exceed building operation energy use by 137%. Wilson advocates for the use of transportation energy intensity metrics and the development of benchmarks of performance.

The location of a commercial building within a regional transportation network and land-use context can influence the mode shares and trip distances of employee journey-to-work and other trips. Commercial office building site selection decision makers (owners or tenants) interested in selecting buildings/sites that minimize transportation energy consumption for necessary employee commute trips need a performance-based evaluation framework for estimating transportation energy consumption. Estimation of commute energy consumption is subject to several significant calculation uncertainties, such as the location of commute origins,

commuter mode choice, and vehicle fuel economy. Thus, such a calculation framework should help the decision maker estimate, *under uncertainty*, the transportation energy efficiency potential of available building site alternatives before selecting a site.

1.4. Dissertation Organization

This dissertation is organized into three major sections. The first section (Chapters 1-3) introduces the research topic and approach. This introductory chapter has explained the objective, significance, background, and motivation of this research effort. Chapter 2 examines the relevant existing literature and defines the contribution of the research in the context of the literature. Chapter 3 describes the research method and scope.

The second section (Chapters 4-6) describes and discusses the development of the building/site evaluation framework. Chapter 4 presents the overall conceptual framework and application context for evaluating commercial building/site energy consumption and GHG emissions. Chapter 5 addresses the estimation and evaluation methods for building (architectural) system energy and GHGs. Similarly, Chapter 6 details the estimation and evaluation methods for transportation systems.

The third section (Chapters 7-9) presents the application of the developed framework and discusses the framework's capabilities and limitations for minimizing energy consumption and GHG emissions. Chapter 7 describes application of the architectural system elements of the evaluation framework to typical commercial office building types. Chapter 8 presents the application of the transportation system elements of the evaluation framework. The framework is applied to locations within the Atlanta, GA metropolitan region. Additionally, Chapter 8 combines the transportation system and building system estimates. Chapter 9 presents the

conclusions from the research, which include discussions on the framework's potential for supporting reductions in energy consumption and GHG emissions, as well as a discussion of the need for future research.

CHAPTER 2

LITERATURE REVIEW

A literature review of academic research and professional practices addressing the energy and GHG performance of building sites indicates that currently no whole-building site selection evaluation framework exists for quantifying, under uncertainty, the energy consumption and GHG emissions from transportation and building systems. However, various existing analysis and calculation methods may be adapted and refined to develop such a framework. Table 1 and Table 2 below summarize the research and practice in the transportation and building design/construction/operation fields relevant to estimation of site-specific energy and GHG emissions. The literature summarized in Table 1 and Table 2 are organized under distinct fields of literature and specific (and in some cases overlapping) sub-fields of focus. Although building material consumption and site land cover impacts are not included in calculation procedures of the developed framework, review of the relevant literature is included to identify the state of practice and research.

Table 1: Summary of Research and Practice Relevant to Estimation of Site-Specific Energy and GHG Emissions

Field of Literature	Sub-Field	State of the Art or Practice	Refs.
Green Building Rating Systems	Site Transportation Impacts	Prescriptive requirements and credits for project location and design, aimed at reducing SOV trips (e.g. bike racks, access to transit service, walk access to trip attractors, accommodation of AFVs, mixed use development, walkable streets, parking limits, etc.). Activity, energy, and emissions impact not quantified.	(13, 14, 15, 16, 17, 18)
		Credits for percent reduction in “conventional” commuting trips.	(19)
		Prescriptive credits for locating project in TAZ with less than average VMT per capita.	(16)
		Transportation energy and emissions benchmarks have been used, but are currently not a part of green building design or rating systems.	(20)
		Methods proposed for estimating traffic generation and mode splits for retail, office, institutional, and multi-use buildings, based on regional survey data and the building location context (mixed/single use, high/low density, and access to transportation facilities).	(21)
	Building Energy Performance	Performance-based credits for improved building energy performance.	(13, 14, 15, 22)
		CO2 emission reductions accounted for in building operation	(17, 22)
	Building Material Consumption	Prescriptive credits for reuse of building materials (renovation), use of recycled materials, regional materials, and rapidly renewable materials, as well as construction waste management	(13, 14, 15, 22)
		CO2 emission reductions accounted for in construction material transport	(17, 22)
	Site Land Cover Impacts	Prescriptive credits for preserving greenfields and including native vegetation.	(13, 14, 15, 22)
Building Design and Operation Energy Standards	Building Energy Performance	ENERGY STAR performance rating systems compare designs and operations to existing building stock. Other standards compare to simulated baseline or specify building component criteria.	(23, 24, 25, 26)
	Energy Use Intensity (EUI)	Site and primary energy use estimated and divided by gross building area.	(23, 27)
		Site energy use estimated and divided by gross building area. Although used by both ASHRAE and DOE, the normalizing metric does not sufficiently reflect the <i>use</i> of a building/site.	(28, 29)
	Whole Building Life Cycle Energy/GHG	Generic frameworks support evaluation of whole building life cycle energy consumption and GHG emissions. No standard accounting system is used in research or in practice.	(30, 31, 32)
Building Energy Modeling	Building Energy Performance	Building energy simulation/modeling is performed during the design process to evaluate the potential energy performance of design alternatives (e.g. parametric runs). Although site weather may deviate substantially throughout a region, current weather data sources do not define local microclimates.	(25, 33, 34)
	Whole Building Life Cycle Energy/GHG	Building construction, operation, and site sequestration estimated. Concepts of “carbon debt” and “payback” are used to account for energy and GHG reductions.	(31, 35)

Table 2: Summary of Research and Practice Relevant to Estimation of Site-Specific Energy and GHG Emissions (Continued)

Field of Literature	Sub-Field	State of the Art or Practice	Refs.
Sustainable Site Development Tools	Site Transportation Impacts	Transportation emissions estimates in URBEMIS are derived from survey-based averages of travel time for either urban or rural developments. TEI Calculator estimates the TEI in kBtu's per day based on the address, the number of employees (stratified across ranges of earnings), and the number of days during the year that the building is in operation.	(36, 37)
	Building Energy Performance	Only onsite combustion is considered. Natural gas is assumed to be the primary source of water and space heating, and consumption (for office space) is based on square footage.	(36)
Traffic Impact Analysis	Trip Generation (Site-Specific)	Trip generation rates provided for various types of commercial buildings/site. Trip purposes are not delineated and published rates are based on small samples.	(38)
	Trip Distribution and Network Assignment (Site-Specific)	Trip distances may be estimated through market analysis, census tract analysis, and a gravity model. Professional/engineering judgment plays a central role in estimating trip distribution and network assignment.	(39, 40, 41)
	Mode Choice (Site-Specific)	Mode choice / mode shift estimated from site strategies, such as walk access and transit access.	(42)
Travel Demand Modeling	Trip Generation (Site-Specific)	Trip generation estimated from household survey data (aggregated to TAZs).	(43, 44)
	Trip Distribution and Network Assignment (Site-Specific)	Trip distances estimated through gravity model and network analysis (aggregated to TAZs).	
	Mode Choice (Site-Specific)	Mode split and multi-modal trip distance estimates of trips attracted by commercial sites are estimated (aggregated to TAZs).	
	Site or Regional VMT/Land-use Interaction	Research literature focuses on relationship between per capita or per household VMT and urban form (residential and employment density and mix, network connectivity, transit service), socioeconomic measures, and demographic measures. Current transportation/land-use research paradigm is centered on residential trip productions rather than commercial trip attraction. Research findings are mixed, due in part to multiple confounding factors.	(2, 10, 45, 46, 47, 48, 49, 50, 51)
Whole-Building LCA	Building Project	Research suggests that transportation energy/emissions is a major portion of whole-building energy/emissions, and that suburban development is more energy intensive.	(2, 12)
	Urban Metabolism	Research provides framework for accounting for energy and material flows. Regional-level of analysis is not sensitive to site-specific factors.	(52, 53)

The following review sections provide additional detail and discussion of the literature review findings summarized in Table 1 and Table 2.

2.1. Green Building Rating Systems

Green building rating systems, such as LEED, are intended to reward building designs or operations that address multiple objectives, such as reduced building energy consumption, reduced water consumption, reduced stormwater runoff, reduced construction waste, reduced light pollution, improved indoor air quality, improved occupant control/comfort, community connectivity, accommodation of alternative modes of transportation, etc. Thus, reducing energy consumption is only one of many complementary or competing objectives of green building rating systems.

2.1.1. Site Transportation Impacts

Currently missing from green building rating systems is a *performance*-based evaluation of the *transportation energy consumption* associated with access to a given building or site. Prescriptive (non-performance-based) requirements and credits exist for project location and design (e.g. bike racks, access to transit service, walk access to trip attractors, accommodation of AFVs, mixed use development, walkable streets, parking limits, etc.) (13, 14, 15, 16, 17, 18). These criteria are broadly intended as strategies for reducing SOV trips and achieving the many associated benefits (reduced emissions, increased physical activity, sense of place, etc.). The transportation activity, energy, and emissions impact of the criteria are not quantified. In the practice of green building rating systems, the most quantitative evaluation of transportation activity is the award of credits for percent reductions in “conventional” commuting trips (19).

However, these are trip reductions through transportation demand management at a continuously occupied site, rather than estimated trips reductions at potential site alternatives.

Transportation energy and emissions performance benchmarks are acknowledged as potentially useful tools for evaluating building site selections (12, 20), but currently they are not part of green building design or rating systems. Methods have been proposed for estimating traffic generation and mode splits for retail, office, institutional, and multi-use buildings, based on regional survey data and the building location context (e.g. mixed/single use, high/low density, and access to transportation facilities) (21). The use of aggregated, region-wide survey data sets to predict zone or location specific estimates of transportation activity can introduce considerable estimation error that is not explicitly accounted for in regression estimates.

2.1.1.1. LEED for Neighborhood Design

The pre-eminent green building rating system that accounts for transportation aspects of building projects is *LEED for Neighborhood Development*. This rating system is unique from all other LEED rating systems (save for the *LEED-NC Application Guide for Multiple Buildings and On-Campus Building Projects*) in that it addresses developments with networks of buildings. Much of the transportation-related criteria is prescriptive and pertains to street network connectivity, proximity and frequency of transit service, and accommodation of non-motorized transportation (16). The only criteria relating to quantified levels of transportation activity is the prescriptive credit option for locating a project in a TAZ with less than average VMT per capita (SSL Credit 3) (16). This credit does not account for the effects of demographics (e.g. household income or automobile ownership) that may significantly impact VMT per capita and may be inconsistent with planned developments. Perhaps the greatest limitation of *LEED for*

Neighborhood Development in the context of this dissertation is that it is a tool designed for evaluating large-scale development decisions, as opposed to office firm location decisions.

2.1.2. Building Energy and GHGs

Green building rating tools include performance-based credits for energy, yet these credits address only improvements in building operation (HVAC, DHW, and lighting), energy performance (13, 14, 15, 22). In the LEED rating systems, energy reductions are measured in units of energy *cost* rather than physical units of energy, as per the invoked “Performance Rating Method” of ASHRAE Standard 90.1 (25). Other ratings systems reward building designs that reduce building operation CO₂ emissions (17, 22).

With respect to the building material consumption, prescriptive credits exist for the reuse of building materials (renovation), use of recycled materials, regional materials, and rapidly renewable materials, as well as construction waste management; however, the energy impacts are not quantified (13, 14, 15, 22). In green building rating systems, consideration of the GHG impacts of materials addresses primarily construction material transportation (17, 22). The Green Building Initiative’s (GBI’s) rating systems for commercial buildings incorporates calculations of life cycle material energy and emission (54). Prescriptive credits exist for preserving greenfields and including native vegetation, but the carbon sequestration effects are not quantified (13, 14, 15, 22).

Although building site elements such as existing construction (building material reuse), building envelope performance, and proximity to public transportation are incorporated into the rating system credits, the energy and GHG emissions performance of site-related elements are not evaluated. GHG emissions are not explicitly accounted for in the LEED evaluation

frameworks, but are an implicit part of prescriptive prerequisites and credits related to energy and material consumption savings. Other rating systems such as BREEAM, SBTool and Green Globes do account for GHG emissions, but only for a limited subset of whole-building aspects (construction materials and building operation energy) (17, 18, 22, 54). Importantly, the energy and emissions tradeoffs of site-related building aspects are not estimated during the site selection process, which may significantly impact life cycle whole-building performance.

2.2. Building Design and Operation Energy Standards

2.2.1. Building Energy Performance

One of the most widely used standards for evaluating commercial building energy performance is ANSI/ASHRAE/IESNA Standard 90.1: *Energy Standard for Buildings Except Low-Rise Residential Buildings* (25). The standard includes prescriptive building component criteria as well as a performance rating method based on building energy simulation (Appendix G). ASHRAE 90.1 is widely referenced in building energy codes. Although ASHRAE 90.1 is intended only as a design standard, the standard used in combination with a building energy model can be helpful for determining the energy performance of buildings designed to meet energy codes.

2.2.1.1. ENERGY STAR Target Finder and Portfolio Manager

The ENERGY STAR program from the U.S. DOE and the U.S. EPA provides ratings of building energy performance for both building designs and existing buildings. The ENERGY STAR Target Finder rating system is intended for commercial building designs and allows users to compare the results of a building energy simulation to similar buildings in the Commercial

Building Energy Consumption Survey (CBECS) database. The ENERGY STAR Portfolio Manager rating system is intended for existing commercial buildings and allows owners to track the energy and water consumption of their building(s) as well as benchmark performance relative to both past performance and similar buildings in the CBECS. Portfolio Manager buildings that perform better than 75 percent of all similar buildings in the CBECS may qualify for the ENERGY STAR label (55). Performance is based on measurement of the EUI, as determined by actual building energy consumption (metered energy) adjusted for actual operation (primarily hours of operation, number of occupants, and weather) (55). It is important to note that evaluation of energy performance is based on measured energy consumption rather than simulated energy consumption. The stated intent of the program is to more accurately account for the impacts of building operation on whole-building energy consumption. Consequently, the ENERGY STAR Portfolio Manager and labeling systems are as much an evaluation of building *use* and *operation* as they are an evaluation of building *design* and *construction*. These rating systems are arguably well-suited for an owner's management of improvements in building energy consumption, but are arguably less suited for a potential owner's selection of a building with the highest energy efficiency potential. Most commercial buildings, including many high-performance buildings, are not registered in the ENERGY STAR performance rating system; thus, energy evaluation between potential buildings (to own/occupy) may not be possible within the framework of the ENERGY STAR performance rating system. Even if a set of building alternatives includes only ENERGY STAR labeled buildings, the whole-building energy performance potential of each of the building alternatives may not be discernible by the ENERGY STAR rating alone – the ENERGY STAR rating system accounts for some, but not all, of the building use/operation variables that impact whole-building energy consumption.

2.2.2. Energy Use Intensity (EUI)

Effective evaluation and comparison of building energy performance requires normalized performance metrics or functional units. Normalized building energy use is typically expressed in terms of the amount of energy consumed per unit of floor area, and is referred to as the energy use intensity (EUI) (27). Several building design and operation energy standards and programs utilize EUIs (22, 23, 27, 28, 54), but the measurement methods vary – different types of energy use are included or omitted (such as plug loads), some standards measure end use energy while others measure primary energy, and some standards vary with respect to the building floor area included (e.g. gross area vs. conditioned floor area) (27). The U.S. DOE is working to standardize the measurement of building energy performance (56). ASHRAE has called upon Congress to foster collaboration between the U.S. DOE, NIST, U.S. EPA, ASHRAE, and other organizations to:

- “Establish a single objective definition of energy use intensity (EUI) for the design of commercial buildings
- Determine a single objective baseline EUI for design of commercial buildings from which to measure relative energy use reductions
- Create a performance environment that will support reduction in energy consumption associated with all loads in commercial buildings
- Identify a single objective set of commercial building types and simulation models for establishment of target design EUIs

- Produce one set of design target EUIs for the commercial building sector to guide the development of future energy codes and standards and building energy codes adopted by state and local government” (57)

Recently, transportation EUI has entered as a measure worth considering for the evaluation of green buildings (12, 37), but so far transportation EUE has not been a part of U.S. DOE or ASHRAE standards development.

2.2.3. Whole Building Life Cycle Energy and GHGs

While the concept of life cycle assessment of building energy consumption and GHG emissions has existed within the building research sphere for several decades, more recently an industry construct of building life cycle assessment has emerged. The American Institute of Architects has outlined procedures and resources for conducting building life cycle assessments, with considerable attention to the complexities of building material systems (31). Currently, only an outline of methods exists and no widely accepted standard calculation method is used in research or in practice. However, whole-building life cycle assessments of energy and GHGs are largely structured on the generic ISO 14040 framework (30, 31, 32).

2.3. Building Energy Modeling

Building energy models/simulations are tools utilized during the design process to evaluate the potential energy or energy cost performance of design alternatives (e.g. parametric runs). Many different types of building energy modeling/simulation tools are available for commercial buildings, ranging from high-level conceptual design models with default definitions

of building systems, to low-level final design models with detailed user-defined inputs of building systems (33). The appropriate level of detail for building energy modeling is a function of the time and expertise available for energy calculations (information costs) and the degree of uncertainty in building system definitions. Despite continual refinements in building energy simulation software tools, a notable paradox persists in the practice of building energy simulation – building energy models are designed to accurately model potential building energy performance; however, building energy models are not regarded as accurate predictors of building energy performance. Due to a multitude of uncertain technological, behavioral, and meteorological variables, simulations of annual whole-building energy consumption are unlikely to predict actual annual energy consumption. Thus, the utility of building energy models lies not in their limited predictive power, but rather in their ability to quantify the relative performance of building system alternatives under typical or expected operating conditions. In practice, this utility is primarily used for evaluating building design alternatives.

Although not specifically intended for such a purpose, building energy models may be used as a means for evaluating the potential relative energy performance of existing buildings. Recognition of this capability is a conceptual starting point for the development of a framework for evaluating the potential building energy performance of building/site alternatives. The building energy research literature indirectly acknowledges the potential utility of evaluating the relative energy performance of site alternatives through building energy simulation – Urban microclimate researchers have utilized building energy simulation to quantify the energy impacts of urban heat islands on urban building sites (58, 59). Although micro climate effects (e.g. urban heat island) may substantially impact the relative building energy performance of site

alternatives, current weather data sources for building energy simulation do not define local microclimates (34, 60).

2.4. Whole Building LCA

The use of building energy models and simulation has expanded into evaluation of whole-building life cycle energy consumption and GHG emissions (31). In whole-building life cycle assessments, the effects of building construction, operation, and site sequestration of carbon are estimated (31, 35). The concepts of “carbon debt” and “payback” are used to evaluate the benefit of building systems that reduce energy consumption and GHG reductions, relative to a baseline, over a building life cycle (31, 35). Within the conventional definition of “whole-building” energy consumption, the dominant category of energy and GHGs is the operation of building mechanical and electrical systems (1). At a regional-level, urban metabolism research has introduced an accounting framework for material and energy flows of both transportation and building systems (52, 53). In the research literature, consideration of transportation systems has entered into the concept of “whole-building.”

Researchers at the University of Toronto found that for low density residential developments, transportation accounted for 61% and 31% of GHG emissions and energy use respectively, whereas for high density development, transportation accounted for 43% and 18% of GHG emissions and energy use respectively (2). Furthermore, the researchers found that “Transportation requirements for low density suburban development are nearly 4x as energy and GHG emissions intensive as high-density urban core development per capita” and “Transportation requirements for low density suburban development are 2x as energy and GHG emissions-intensive as high-density city core development per unit of living space.” It is evident

that urban form and development influence building and transportation GHG emissions (7), yet an evaluation framework targeting site-specific energy efficiencies is lacking in the literature or in professional practice.

2.5. Travel Demand Modeling

2.5.1. Site or Regional VMT and Land-Use Interactions

The relationship between land-use and transportation activity (and by extension GHG emissions) has received considerable attention in transportation research literature. In the travel demand modeling research literature, there have been numerous studies investigating the link between transportation energy (or vehicle miles of travel) and independent transportation network and land-use variables. Newman and Kenworthy (46) are often cited in the literature for their work in identifying the inverse relationship between urban density and per capita VMT. In its Special Report 298, *Driving and the Built Environment*, the Transportation Research Board explored the relationship between vehicle miles of travel (VMT) and land-use, which is measured in terms of different land-use densities, types, and related household demographics (10). The report acknowledges that there are many confounding variables (e.g. socioeconomic factors) related to driving behavior, nonetheless it suggests that employment density is one of the more significant measures of urban form that correlate with commuter selection of alternative modes (10). In their research on the transportation “location efficiency” in residential location choice, Holtzclaw et al., and have identified the significant location variables (residential density and pedestrian and bicycle friendliness) and demographic variables (average income per household and per capita) influencing household VMT (51). Although findings such as these are of interest to transportation and land use researchers and planners, these findings alone are

insufficient for calculating the energy consumption of commute activity for a particular commercial site within a particular region. Much of the research on transportation intensity is focused on household activity and is aggregated at the scale of census blocks or urban regions (45, 46, 48, 51).

It is widely acknowledged in the literature that office location choice can have a significant impact on commute activity, including effects on mode choice and automobile ownership (61, 62). Such impacts on commute activity can translate to significant impacts on commute energy consumption. Office location choice is a decision-making process that includes consideration of multiple location factors, notably proximity to the central business district, zone population size and income, and proximity to transportation infrastructure (61). Although transportation energy consumption is currently not a dominant selection criterion for office location decision makers, sustainable transportation has emerged as a relevant criterion for evaluating the relative sustainability of development sites (13, 16).

2.5.1.1. Smart Growth

The concept of “smart growth” in residential and commercial development has become a popular topic in the research literature (8, 9, 10) and in the practice of planning and development (63, 64, 65, 66). The development of Atlantic Station in Atlanta, GA advanced the formulation and application of a framework for evaluating reductions in site related VMT (47, 64). In selecting the site for the Atlantic Station project, the estimated VMT was compared against VMT estimates for other, more suburban development sites. The Atlantic Station project represents a successful effort to reduce single occupant VMT, for both intra- and inter-site travel, relative to regional averages (67), although not specifically for commute trips.

2.5.1.2. Location Efficient Mortgages

Development of energy efficient locations requires both efficiency evaluation and incentives for efficient development. One of the specialized financial tools for encouraging utilization of location efficient residential properties is the Location Efficient Mortgage®, which allows home mortgage owners in identified transportation efficient locations to borrow one additional dollar per month for every one dollar per month in transportation savings associated with the location (68). According to Burer et al., a Location Efficient Mortgage® “functions analogously to an Energy Efficient Mortgage in which a dollar in utility cost savings entitles the prospective home buyer to spend an additional dollar per month on debt service costs.” This particular financial tool for transportation location efficiency does not translate well to the commercial real market because of the principle agent factor. The costs and costs savings of transportation location efficiency accrue mostly to employees and visitors of an office firm rather than to the firm itself.

2.5.2. Regional Travel Demand Models

Practical region-specific applications of transportation modeling theory are found in regional travel demand models used by metropolitan planning organizations (MPOs) to estimate regional travel activity (e.g. motorized VMT). Designed primarily for the purpose of estimating the regional impact of planned transportation infrastructure and operations projects on air quality conformity, congestion mitigation, and other regional concerns, regional travel demand models are not intended as a tool for estimating sub-regional spatial variations in transportation energy consumption. In fact, regional travel demand models are generally not intended for any sub-

regional analysis of transportation activity, other than the marginal impact of sub-regional changes in land-use or the transportation network. Nevertheless, regional travel demand models explicitly model the production and attraction of multimodal, multi-purpose trips between, in many cases, thousands of unique transportation analysis zones (TAZs). The distribution of trips between zones is typically performed by a doubly constrained gravity model with a trip cost function (normally a travel time function). The cost function can be calibrated to regional surveys of travel times and/or travel distances, but the resulting distribution of trips may or may not be representative of the origin destination patterns of workers. Although the distribution of multimodal, multi-purpose trips between unique pairs of TAZs are not fully calibrated by observed travel behavior, travel demand model trip table outputs indexed by TAZ provide a disaggregate, albeit synthetic, estimate of sub-regional travel activity that is consistent with region-wide, aggregate observations for present years and forecasts for future years. In current modeling practice, site-specific travel activity estimation is limited by aggregation of estimates to TAZs.

2.6. Transportation Impact Analysis

In transportation planning practice, an established framework for estimating travel activity to/from commercial and residential centers exists in the form of transportation (or traffic) impact analysis (TIA). TIA frameworks, such as the review of Developments of Regional Impact (DRI) (69) required by the Georgia Planning Act, include an estimation of the marginal increase in motorized vehicular activity resulting from site development. Typically, TIAs are conducted only for large developments. For example, an office development in Georgia is subject to DRI review if the development is greater than 400,000 gross square feet in a metropolitan region or

greater than 125,000 gross square feet in a nonmetropolitan region (41). For commercial development, the metropolitan and nonmetropolitan thresholds are 300,000 gross SF and 175,000 SF respectively (41). In a DRI analysis, the number of added trips is estimated in accordance with the ITE Trip Generation Handbook. The ITE Trip Generation Handbook provides estimates of trip generation for several different types of office buildings, including general office buildings, corporate headquarters, single tenant offices, and several other types. The trip rates are expressed in terms of the number of employees or the gross floor area, and the trip rates are available for different peak and off-peak travel periods. The trip rates do not distinguish between trip types, such as commute trips, visitor trips, shopping trips, or shipping/receiving trips. For DRI's, number of trips are then distributed to surrounding zones according to a census tract analysis, market analysis, or TRANPLAN-based analysis (41). The main purpose of a TIA is to estimate the potential impact of increased motorized vehicle volume on the level of service of existing or proposed roadway infrastructure. TIA's represent a flexible framework in which available sub-regional travel activity data is used for allocating additional trips to the transportation network. However, TIA's do not provide a detailed framework for quantifying travel distance, energy consumption, or emissions.

2.7. Sustainable Site Development Tools

In recent years, sustainable site development tools have emerged for estimating transportation activity, emissions, and energy consumption for development sites. The URBEMIS software provides an integrative model of construction and transportation emissions from land use development projects (36). With respect to building HVAC and lighting operation (classified under area source emissions), only onsite combustion is considered. Natural gas is

assumed to be the primary source of water and space heating, and consumption (for office space) is based on square footage (36). For transportation estimates, trip generation rates are based on the ITE Trip Generation Manual, with adjustments for site land use and design and for pass-by or diverted-linked trips (36). Transportation emissions estimates in URBEMIS are derived from survey-based averages of travel time for either urban or rural developments (36). This basic estimate of travel time and associated emissions does not account for location- or demographic-specific estimates of VMT or energy within the specific transportation network or land use context.

More recently, the Center for Neighborhood Technology has released a beta version of the Transportation Energy Intensity (TEI) calculator (37), which provides a more location- and demographic-specific estimate of commute energy consumption for commercial developments. The calculator estimates the TEI in kBtu's per day based on the address, the number of employees (stratified across ranges of earnings), and the number of days during the year that the building is in operation. The calculator also includes additional inputs for estimating the TEI of site customers/visitors. The TEI calculator utilizes the Census Transportation Planning Products (CTPP) Part 3 (Worker/Employee Census Tract Matrix) dataset to estimate commute travel origins and mode choice (70). Transportation energy calculations are based on mode-specific energy consumption factors and a straight-line travel distance estimate for origin and destination pairs. By utilizing primarily historical survey data, the calculator's ability to estimate current year and future year trip patterns is significantly limited. As with all calculation methods and frameworks reviews, the TEI calculator does not explicitly account for uncertainty in the estimated travel activity. Currently the literature lacks a commercial office site commute energy calculation framework or method that accounts for the unique land-use and transportation

network performance characteristics of a given site, and that also explicitly accounts for the associated calculation uncertainty.

2.8. Research Contribution

The development of a commercial site evaluation framework should be based on the academic research and professional practices already undertaken to address the energy and GHG performance of building sites. Currently, no whole-building, commercial site selection evaluation framework exists for quantifying energy consumption and GHG emissions from transportation and building systems. However, various existing analysis and calculation methods may be adapted and refined to develop such a framework. Candidate methods may be derived from research and practices in sustainable building rating systems, building design energy standards, building energy modeling, traffic impact analyses, travel demand modeling, transportation and land-use interaction research, and building life cycle analysis studies.

Within the context of the existing literature, this research contributes an integrative framework for estimating, under uncertainty, site-specific energy consumption and GHG emissions from transportation and building systems. The products of this research are intended to enable targeted, performance-based assessment of commercial development sites and will help to inform more efficient and sustainable use of new and existing infrastructures.

The primary product of this research is an integrative framework for evaluating the energy and GHG emissions performance of potential commercial office sites. Assuming that the framework yields significant differences in the energy and GHG emissions performance of commercial buildings/sites, the research results will enable office location decisions that minimize energy consumption and GHG emissions during a building tenant's occupancy.

CHAPTER 3

RESEARCH METHODOLOGY AND SCOPE

3.1. Methodology

The basic methodological structure of this research is as follows. First, the research and practice literature are reviewed (see Chapter 2) to identify the evident gaps in the literature when viewed against the backdrop of the research motivation (see Chapter 1). Based on findings from the literature review, the framework is developed to meet the research objective (see Chapter 1). The term “develop” refers to a process of combining, refining, and augmenting resources and methods in the literature. The concepts and procedures of the framework are then applied to scenarios / case studies that simulate “real-world” application of framework. The results of this demonstration of the framework are analyzed to identify possible improvements and modifications to the framework, and to generate policy recommendations the may help the framework serve as a tool for minimizing energy consumption and GHG emissions.

Figure 2 shows an outline of the workflow of the research methodology. The findings of the literature review inform the development of several elements of the research, with the foremost development being the framework itself. In parallel with the framework development is the development of the application scenarios / case studies. The need for deriving application scenarios / case studies from the literature is two-fold. First, the relevance of the framework demonstration is measured against how well the scenarios / case studies represent typical or prevailing conditions. Second, limited availability of directly observable data necessitate a “hybrid” case-study approach consisting of both observable and notional data. The notional data

values are derived from the literature so that, like the scenarios / case studies as a whole, the data inputs represent typical or prevailing conditions.

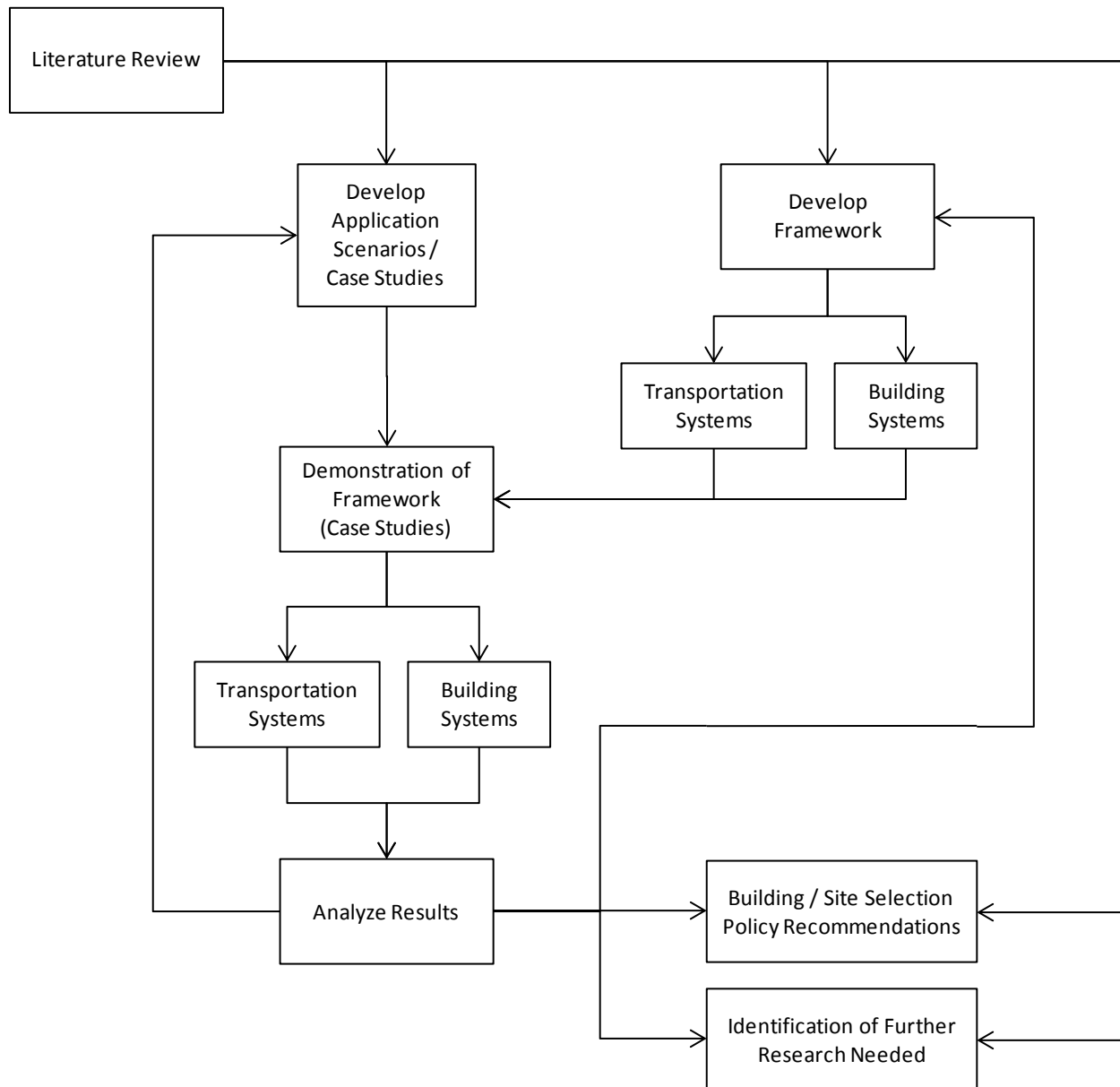


Figure 2: Workflow of the research methodology.

As indicated by Figure 2, the development of the case studies is influenced in part by analysis of the case study results through an iterative process. That is to say, interpretation of the

case study results is part of the process of determining the representativeness of the case studies. This process is a distant departure from more traditional, positivist research methods, in which the selection of research subjects and data is to be performed entirely before and entirely independent of the analysis and interpretation of the results. Acceptance of this elected departure requires, in a general sense, acceptance of qualitative interpretations as a means of determining meaningful and useful research subjects and findings. This critical departure is elected for two important reasons:

1. The primary purpose of demonstrating the evaluation framework is not to test its predictive capability, but rather to gain insight into how it may help to compare, under uncertainty, estimates of potential energy consumption. Thus, part of the process of demonstrating the framework involves modifying input assumptions to observe the impact on estimated outputs.
2. Complete, observable input data are unavailable to conduct a purely empirical study of the transportation and building systems of a commercial development site. Notional data is introduced as a means to simulate applied evaluations of commercial development sites, and the validity of the notional data is determined, in part, by checking the results against expectations expressed in the literature or within the relevant professional community.

Even if complete, observable data were available, it would not be representative of the limited amount of data available to a commercial building / site decision maker. When

evaluating the potential performance of building / site alternatives, decision makers would likely not have access to full or equal specificity of building performance data, especially for elements that pertain to future behaviors (e.g. the commute shed of future employees at a new office site). Furthermore, even if complete observable data were available for some sites, empirical analyses would not produce findings that are generalizable to the larger population of buildings and sites. The energy performance of individual building and transportation systems is the result of many distinct technological and behavioral factors. Specific application results are likely only relevant to the context in which they are applied.

Although it is argued here that the primary purpose of demonstrating the evaluation framework is not to test its predictive capability, there remains the important question of how best to validate the evaluation framework results. Ideally, the framework would be applied to one or several commercial offices, in which the predicted performance could be compared to actual performance. Even if such data were available for this research (and it was not!), it would only be useful for validating the *range* of predicted performance, rather than the *distribution* of predicted performance, which would require many more studies to validate. Validation through comparisons of predicted and actual performance would require a prodigious amount of calibration (calibrating assumed occupancy schedules, occupant behaviors, weather data, etc.). The application of the framework is intended to match the purpose of building energy simulation tools in the parametric design and evaluation of energy saving strategies – the tool does not predict the in-use performance, rather it helps to quantify the potential relative energy savings between alternatives. For the purposes of this dissertation research, the validation of the framework will be pursued through comparisons of the application results to expected ranges of values expressed in the literature.

The original data collection plan of this research involved sourcing office building design and construction data through the USGBC's database of LEED certified buildings, and obtaining additional occupant data (e.g. transportation activity) from the office building owners or employers. Unfortunately, this data collection plan did not come to fruition, largely due to privacy concerns/limitations on behalf of the USGBC and building owners/occupants. Some building geometry data were obtained directly from building owners/occupants, which helped to develop case studies that were representative of actual or typical building designs.

3.2. Scope

This research employs the principles of life cycle assessment to define the scope of systems included within the study. Specifically, the study follows the guidelines of ANSI/ISO 14040 *Environmental management – Life cycle assessment – Principles and framework* (30). The scope of this research is defined by an understanding of both the main elements influencing whole-building energy consumption and the limitations of available building site data. An outline of the systems and elements included within this study is discussed in Chapter 1 (see Research Objective and Figure 1). In general, the scope includes the energy consumption and GHG emissions associated with building operation (onsite or utility energy), and transportation access. With respect to GHG emissions, this dissertation includes Scope 1, Scope 2, and Scope 3 GHG emissions, as defined by GHG emission inventory protocols (71, 72, 73, 74), (see Section 4.2.3). The Scope 3 emissions include only the upstream emissions associated with the fuel/energy supply chain. These emissions are particularly germane to the comparison of onsite or building utility energy systems.

The scope of this research is centered on the occupancy period of a particular office tenant (typically a 10 to 15 year time scale). Thus, the “life cycle” in this study is the period of a building occupant cycle, rather than a complete building service life. From a traditional “cradle-to-grave” perspective on life cycle assessment, it may appear that this revised focus fails to account for important construction (cradle) impacts of building/site decisions, such as the decision to construct a new building vs. renovate an existing building. However, if each building provides approximately 50 years of service life (a period of time extending beyond the typical tenant period), then constructing a new building does not necessarily introduce higher material impacts than renovating an existing building – the service of the new construction likely extends through an average building life cycle.

This research expands upon the literature review findings by investigating and adapting existing methods for quantifying the energy consumption and GHG emissions of commercial buildings and associated transportation access. The evaluation framework consists of two main energy systems: transportation and buildings. This bifurcation of energy systems may seem like a natural, convenient distinction between the main types of activities and technologies that impact the energy consumption and GHG emissions of commercial development sites. Though convenient for the purposes of conceptualizing the basic topology of the energy consumption of commercial sites, the distinction demands two separate research efforts for developing the calculation/evaluation procedures for each system type. These parallel research efforts represent a considerable challenge; and such challenges are to be expected for research of the “problem-solving” type (as opposed to “exploratory” or “testing-out” research) (75). Nevertheless, this research addresses the problem of estimating the potential energy consumption and GHG emissions of commercial office building/site alternatives.

3.2.1. Transportation Systems

The process of developing a site-specific, transportation energy and GHG emissions modeling framework began with a review of the literature to identify both potentially useful resources and the need for expanded capability to meet the research objective. The literature review identified regional travel demand models as a potentially useful resource in estimating transportation activity to/from commercial office sites. Due in large part to established lines of communication with the Atlanta Regional Commission (ARC), the ARC regional travel demand model was selected for closer investigation of its site-specific transportation modeling capabilities. This investigation includes a review of input and output parameters related to home-based work and non-home-based trips. Given that model outputs are aggregated at the TAZ level, additional site transportation activity estimation methods were investigated and incorporated to relate averaged TAZ outputs (e.g. trip frequency, trip distances, mode split, etc.) with site-specific characteristics. This includes a review of resources for estimating the motorized vehicle trip reduction effects of employer-based transportation demand management programs and strategies, such as subsidized transit fare passes, carpool programs, and telecommuting. Additional resources were reviewed and incorporated for translating travel demand model outputs of travel activity into estimates of energy consumption and GHG emissions. The framework for modeling site transportation energy consumption and emissions is applied to case studies of commercial office space, through which the impact of building location on energy consumption and GHG emissions is assessed.

3.2.2. Building Systems

The framework for modeling site-specific building energy consumption and GHG emissions is intended to account for the building heating, ventilating, and air conditioning (HVAC), DHW, lighting, and conveyance systems and loads that vary between potential buildings/sites. These site specific system and load conditions include aspects such as exposed envelope area, microclimate (i.e. localized weather conditions), solar irradiance (orientation and shading), and system technologies. The existing paradigm of building energy assessment and simulation is reviewed to inform the development of an evaluation framework for potential buildings/sites. Building energy modeling resources are reviewed to develop procedures for estimating potential building energy consumption and GHG emissions.

3.3. Integration of Building and Transportation Systems

The analyzed aspects of site-related energy consumption and GHG emissions are integrated through a life cycle assessment framework. Consistent with a life cycle assessment approach is the use of functional units (i.e. performance metrics) to allow normalized comparison of building/site alternatives. Table 3 shows the functional units included in the developed framework. The “inventory units” account for both the direct and upstream energy consumption and GHG emissions. The “normalizing units” represent alternative measures for equating buildings/sites of unequal size or service. The multiple performance metrics help to analyze how different inventory and normalizing units influence performance measurement. Integration of the building site aspects into normalized performance metrics allows comparison of the relative magnitude and variability of each the aspects, which will in turn help to inform rating system recommendations and additional research needs. In the application of the

framework, potential building/site alternatives will be of similar size and will provide similar service.

Table 3: Energy Consumption and GHG Emission Performance Metrics

Inventory Unit		Normalizing Unit	Performance Metric
Annual Energy [kBtu]	Site (end use)	Conditioned floor area [SF]	Annual site energy / conditioned floor area [kBtu/SF]
		Occupant use [person-hrs]	Annual site energy / occupant use [kBtu/person-hrs]
	Primary (end use + upstream)	Conditioned floor area [SF]	Annual primary energy / conditioned floor area [kBtu/SF]
		Occupant use [person-hrs]	Annual primary energy / occupant use [kBtu/person-hrs]
Annual GHGs [lb CO ₂ e]	Site (end use)	Conditioned floor area [SF]	Annual site GHGs / conditioned floor area [lb CO ₂ e /SF]
		Occupant use [person-hrs]	Annual site GHGs / occupant use [lb CO ₂ e /person-hrs]
	Primary (end use + upstream)	Conditioned floor area [SF]	Annual primary GHGs / conditioned floor area [lb CO ₂ e /SF]
		Occupant use [person-hrs]	Annual primary GHGs / occupant use [lb CO ₂ e /person-hrs]

3.4. Demonstration of Framework

The framework developed through this dissertation is intended to be applied to a regional context of location alternatives. Thus a significant portion of this research is focused on applying the framework to location alternatives in the Atlanta metropolitan region, through which the framework's process, procedures, and results are illustrated. By applying/demonstrating the calculation framework, the potential relative differences in energy consumption and GHG emissions between sites may be explored. The important findings of the demonstration are indications of how much regional location “matters” in terms of energy and GHGs.

3.4.1. Region-Wide Application

The calculation framework is applied to the transportation and land-use context of the Atlanta, GA metropolitan region. In this applied context, the calculation results are analyzed for spatial patterns of transportation energy consumption. This “region-wide” application is feasible only for the transportation system calculations – the transportation activity is defined throughout the region by the regional travel demand model, whereas the building energy/emissions are particular to specific building types that are not defined by any regional dataset.. Since transportation is generally the largest component of whole-building energy consumption (12), this single-system, region-wide application provides a good indication of spatial variations in energy/emissions. However, a more meaningful demonstration of the intended application of the framework is an exploration of potential location scenarios / case studies with particular building types.

3.4.2. Scenarios / Case Studies

Meaningful demonstration of the evaluation framework requires the selection of building/site scenarios that both represent realistic location alternatives and that explore expected variations or extremes in energy/emissions. That is to say, the demonstration scenarios / case studies should represent a range of typical building/site characteristics that are suspected to yield different levels of energy and GHG emissions performance. Figure 3 shows the matrix of building scenarios / case studies selected for this research. The building matrix covers two primary distinctions of commercial building types that exist throughout a region: age and configuration. Older buildings are typically designed and built to meet energy codes that are less stringent than contemporary codes, and the efficiencies of building systems have likely degraded

since the original installation (e.g. HVAC equipment and insulation systems) It therefore follows that newer buildings built to contemporary energy codes are expected to consume less energy than older buildings. It is less straightforward how the configuration of a building may impact its energy/emissions performance, although differences in external wall to volume ratios, building conveyance systems, and HVAC system types are factors that may lead to differences in building energy consumption. The single tenant vs. multi tenant dichotomy of the building case study matrix is an approach aimed at revealing significant differences in energy consumption between these two main building types. By “single tenant” it is meant a detached commercial office building serving a single office tenant, and by “multi tenant” it is meant a multi story commercial office building with common areas or spaces and shared floors or partitions.

	“Old”	“New”
Single Tenant --- Suburban	I	II
Multi Tenant --- Urban/ CBD	III	IV

Figure 3: Matrix of building scenarios / case studies.

In this planned matrix of cases studies, the single tenant and multi tenant building types correspond with suburban and urban/CBD development contexts, respectively. This is not to say that these building types exist exclusively in these respective development contexts; Rather,

these are the typical development settings for these building types. Alignment of these two dimensions with each other supports a case study research approach that is both representative of typical location scenarios and efficient in covering a range of development types.

The suburban vs. urban/CBD development contexts of the building case study matrix (Figure 3) correspond with the development contexts included in the matrix of transportation scenarios / case studies (see Figure 4). The matrix of transportation scenarios / case studies defines the location types that are to be included in the demonstration of the calculation framework. In the matrix, urban and CBD locations are divided into separate types so that the performance of non-CBD, urban employment centers may be investigated in the case studies. For each of these development types, locations with “high” and “low” transit mode shares are included so that the energy and emissions impact of transit service may be estimated. The designation of “high” vs. “low” is based on the distribution of transit mode shares within the set of regional TAZs. The suburban location type includes case studies with both “high” and “low” SOV mode trip distance. Since suburban employment centers typically have low transit mode shares (low levels of transit service) and modest levels of ride sharing, the variation in suburban location energy/emissions performance is expected to correlate with variation in SOV trip distances.

		SOV Trip Distance		
		High	Low	
Suburban		I	II	
		III	IV	
Urban / CBD		High	Low	
Transit Mode Share				

Figure 4: Matrix of transportation scenarios / case studies.

A total of four building / site location case studies are used to demonstrate application of the framework. The case studies consist of four main building types (see Figure 3) located in four location types (see Figure 4). The case study buildings each represent uniform levels of service – each commercial office tenant space is of similar floor area and includes similar space types.

CHAPTER 4

APPLICATION CONTEXT AND CONCEPTUAL FRAMEWORK

The commercial building/site evaluation framework developed through this research is intended to serve as a tool for quantifying the potential energy and GHG impacts of commercial building/site selection decisions. Development of a tool for useful application requires conceptualization of the particular conditions of the intended application. This chapter discusses the intended applied context of the evaluation tool and explains the overarching conceptual framework of the tool's functional characteristics.

4.1. Application Context

Development of a useful framework for evaluating the potential energy and GHG emissions performance of building/site alternatives requires definition and consideration of the context in which the framework is to be applied. The evaluation framework is broadly intended for commercial building/site selection. In the building design, construction, finance, and real estate industries, “commercial buildings” are loosely defined as any building that does not meet the definition of “residential,” including but not limited to multiple dwelling buildings over three stories high. Thus, the commercial buildings category includes many different types of buildings with unique services: business offices, retail space, lodging, dining, school buildings, auditoriums, hospitals, etc. The diversity of services from these unique building types impacts commercial building energy assessments of building/site alternatives in two very important ways. First, the unique services provided by each of these building types complicate energy

Commercial building/site energy performance assessments are impacted not only by the particular building type, but also by the building size. Larger sized commercial buildings may have higher efficiencies of scale for both building systems and transportation systems. Increased building system efficiencies may be achieved through larger, more efficient equipment (e.g. central station HVAC systems) and through shared facilities (e.g. shared parking garages and common entry-ways and lobby areas). Increased transportation system efficiencies may be achieved through coordinated transportation demand management programs (e.g. event shuttles, transit station shuttles, vanpools, ridesharing, etc.) which typically achieve higher levels of average vehicle occupancy for larger building developments (e.g. large employers or employment centers).

In light of the aforementioned issues in assessing commercial building/site energy performance, a particular commercial building type and size needed to be selected for this research. As stated in Chapter 1 of this dissertation, the commercial building/site evaluation framework is intended for commercial *office* buildings/sites. This application context may be broadly described as:

- Medium commercial office buildings/sites
 - 100 employees
 - Approximately 25,000 SF of floor space
 - Existing building fit-out or renovation
 - New regional location for owner/occupant

This general application context is applicable to a large number of commercial buildings and locations. In the U.S., offices comprise nearly 20 percent of the total floor space of commercial buildings, and medium office buildings (5,001 to 50,000 SF) comprise approximately 40 percent of all commercial office floor space (76). A 100 employee office roughly equates to a 25,000 to 27,500 SF office space, based on expected occupant densities in ANSI/ASHRAE/IES Standard 90.1 (77). An office in this size range may be a freestanding, one to two story office building, or a floor within a multi-tenant, high-rise, office tower. Thus, this 100 employee test case is applicable to a wide range of suburban, exurban, and central business district development settings. For the selected application context, specification of “existing building fit-out or renovation” and “new regional location for owner/occupant” speaks to particular considerations that play a part in building/site selection. The following section provides additional detail and discussion on how the selected application context fits within the larger decision scenario of building/site selection for office firms.

4.1.1. Understanding Commercial Office Building/Site Selection

Building/site selection is a decision process in which office firms select a space and location that satisfies the selection criteria of the firm. It is understood that the selection of a building/site may significantly impact the energy and GHG emissions performance of the transportation systems and building systems utilized by the owner/occupant (see Chapter 1). For the purpose of developing a commercial office building/site evaluation framework for minimizing energy consumption and GHG emissions, it is necessary to account for the building/site selection criteria that impact potential energy and emissions performance. Figure 5 outlines the owner/occupant’s functional considerations for commercial building/site selection

alternatives that may impact energy and emissions performance. As illustrated in Figure 5, the functional considerations fall under two main categories: the location scenario/considerations and the space requirements/considerations. The location scenario/considerations are defined by answering the question: How does the potential new development relate spatially to the occupant's existing development/operations? The answer to this question may have significant implications for how efficiently the occupant utilizes existing resources (if any). For example, an owner may have existing property and operations within a given urbanized area, and is considering expanding the workforce, either by adding an expansion to an existing facility or by developing another property in the region. If the owner's planned operations require physical correspondence between the existing facility and the new expansion, then the role of transportation energy efficiency is considerably different in this context than if the new facility is completely independent. Similarly, a facility relocation context can present very unique transportation efficiency challenges compared to a new location development, since existing facilities attract trips from an established set of origins (e.g. existing employee commute shed) whereas new locations do not have an established set of origins. In this dissertation, the application context is limited to a "new regional location" scenario.

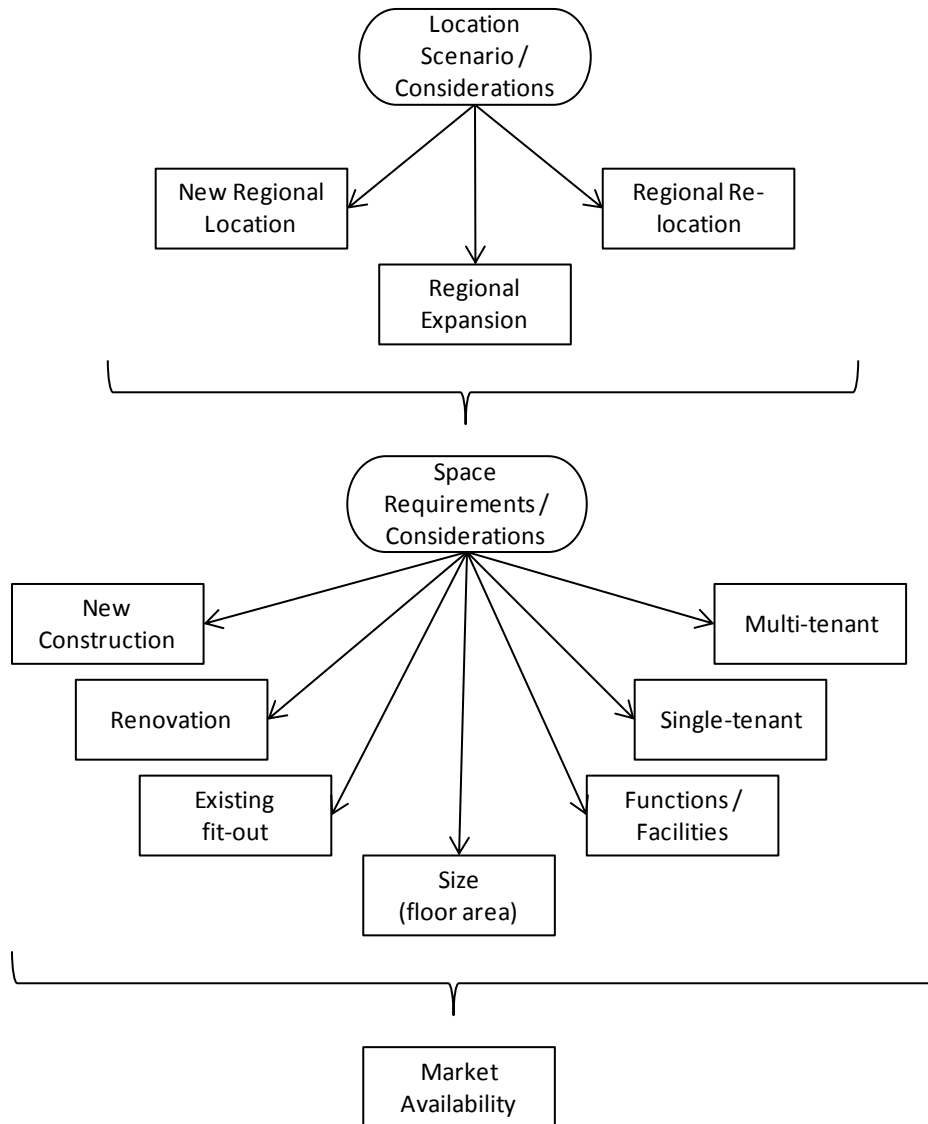


Figure 5: Outline of owner/occupant functional considerations for commercial building/site selection alternatives. Source: (78)

When considering first the space requirements/considerations of the occupant, perhaps the most important criterion is the amount and type of space required. The amount of required space of course dictates the scale of the commercial property and supporting infrastructures. As mentioned previously, developments of different scales will potentially have different economies of scale (e.g. different wall to floor area ratios, centralized vs. de-centralized mechanical

systems, etc.). It should be noted that economies of scale depend upon the normalizing metric of performance (EUI). If the normalizing metric is building floor area (kWh/SF), then a larger building may be the most efficient choice. If, however, the normalizing metric is building occupancy (kWh/person-hrs), then a smaller building may be the most efficient choice. The type of space and structure considered (e.g. multi-tenant high rise vs. single-tenant low rise, renovation vs. new construction) can affect the potential range in energy consumption between potential sites. When considering a renovation, or simply occupation, of an existing building, clearly the performance of the existing building systems will impact the potential for energy efficiency. In the case of constructing a new building on an undeveloped site, it may seem as though the potential for energy efficiency is limited only by available budget, technology, and expertise. However, even an undeveloped site may impose constraints on the potential energy efficiency of a new building design (e.g. available utility energy, onsite power generation feasibility, site boundary and topography constraints on building geometry, zoning laws, transportation mode shares, etc.). Both the location and space requirements must ultimately be matched to the alternatives available in the marketplace – matching user needs to available infrastructure services.

It should be noted that the purpose of this research is not to model building/site selection decision-making of office firms; rather, the purpose is to quantify the potential energy and emission impacts of building/site selection decision alternatives. Therefore, although cost is likely a dominant factor in selecting a preferred building/site, cost is not a direct determinant of building/site energy performance and is thus not a relevant consideration in the development of the evaluation framework. This is not to say that cost is altogether irrelevant to this research. Cost is understood to be an important variable through which policy instruments may help to

influence the selection of building/sites that are identified by the developed framework to potentially minimize energy consumption and GHG emissions. It should also be noted that this research is based on the assumption that office firms are interested in quantifying the potential energy and emissions performance of building/site alternatives; however, the extent to which consideration of energy or emissions performance influences building/site selection is beyond the scope of this research. Although no attempt is made here to model office firm site selection decision-making, the research literature on office location choice is investigated for insights into the office location selection process.

4.1.1.1. Office Firm Location Choice

In the process of selecting a building/site, office firms consider several aspects of location. The research field of integrated land use and transportation modeling has worked toward mathematically modeling the office location choice of employment firms; see (61, 62, 79, 80, 81, 82, 83, 84, 85). It is widely acknowledged in the literature that office location choice has a significant impact on commute activity, including effects on mode choice and automobile ownership. The factors identified in the literature as important to firm location include (61):

- Proximity to the CBD
- Zone population size and income (office firms show a preference for high population and high income)
- Proximity to transportation infrastructure
- Agglomeration factors, with agglomeration perhaps playing only a minor role (62).

Elgar et. al. argue that office firms act as satisficers rather than optimizers or utility maximizers, and thus consider only a small fraction of potential zones or locations within an urban area (61, 62, 79). Based on modeling efforts in the Greater Toronto Area, Elgar et. al. have concluded that the household location of the owner of the office firm is an important anchor point in the location decision process, especially for small office firms (61). Furthermore, small firms that are also new firms exhibit a high preference for locating close to zones in which many workers reside (61). Modeling of firm location decisions is complicated by several dimensions of heterogeneity of firms (79):

- Firm business sector
- Function of the firm
- Size of the firm
- Firm decision processes
- Number of locations.

According to Elgar and Miller, “during location search, a feedback process may occur, in which the availability of ample adequate locations will increase the requirements the firm has from the new location, and inability to find adequate locations will result in lower expectations and a more flexible requirement set” (79).

4.2. A Conceptual Framework of Whole-Building Energy Evaluation

Whole-building energy consumption encompasses multiple building energy systems. In the building AE industry, whole-building energy consumption refers to primarily the building operation energy, which includes building mechanical systems (HVAC and DHW), lighting,

conveyances² (elevators and escalators), and miscellaneous equipment (plug) and process loads. Figure 6 shows the elements of whole-building energy consumption and GHG emissions that are potentially variable and constrained by the building site. The traditional concept of whole-building energy consumption is illustrated in the center of the figure, under the category of “Operation”. The energy consumption of each of the building operation systems is a function of the system type and the load placed on the system. In this conceptual framework of whole building energy evaluation, both the system types and the loads are regarded as elements that are potentially variable and constrained by the building site. The rationale for considering the system type and load for each of these systems is explained through the example building operation systems listed in Table 4.

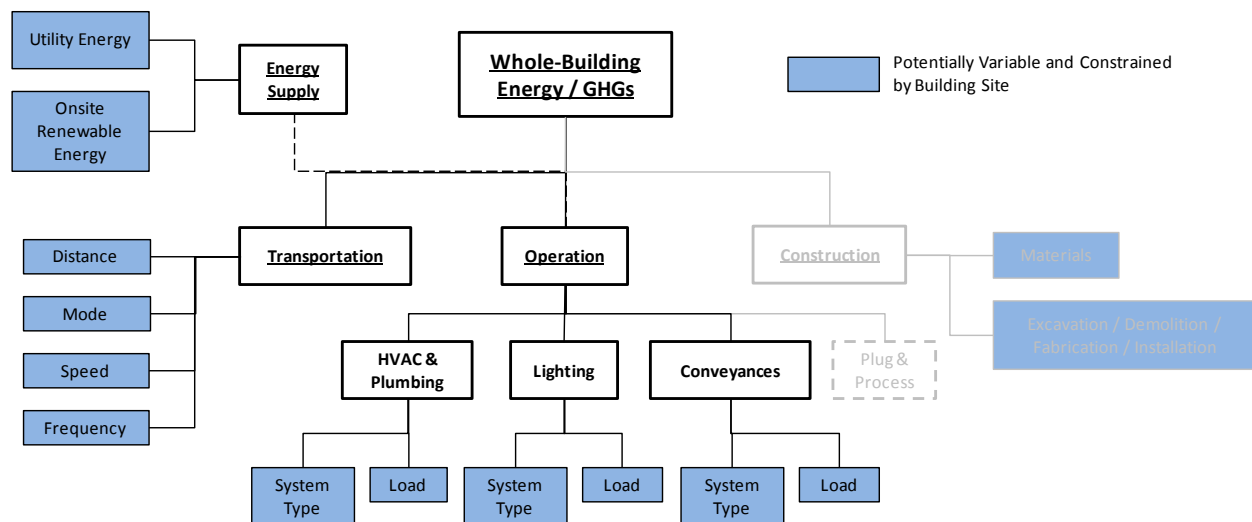


Figure 6: Elements of whole-building energy consumption and GHG emissions that are potentially variable and constrained by the building site.

² In ASHRAE Standard 90.1, conveyances are considered to be miscellaneous equipment loads and are therefore not included in estimated energy reductions.

This research applies a “whole-building” energy consumption analysis boundary that extends beyond the operation of mechanical and electrical services within the building. The analysis boundary includes the transportation necessary to access the building as well as the upstream efficiencies of the energy supply chain. Commercial office site alternatives may have different transportation access distances due to different distances from trip origins/destination (e.g. employee home locations), different mode splits due to relative levels of access to public transportation networks, different access travel speeds (vehicle efficiencies) due to relative levels of transportation network congestion, and different frequencies of trip generation (particularly for non-commute trips such as NHB employee trips). Different sites may have different supplies of utility energy (e.g. natural gas vs. electricity for heating) and may have different site opportunities for onsite renewable energy (e.g. different amounts of surface area available for PV solar panel installation). The grayed-out “Construction” portions of Figure 6 indicate whole-building elements that may be impacted by a site selection decision, but are beyond the scope of this research (see Chapter 1).

Table 4: Example Building Operation Systems Supporting Rational for Selected Building Operation Elements in Conceptual Framework (Existing Building)

Building Operation System		Example
HVAC & DHW	System Type	Water cooled chiller system vs. packaged DX AC system.
	Load	High U-value glazing vs. low U-value glazing.
Lighting	System Type	T8 vs. T12 fluorescent lighting
	Load	Difference in daylighting floor areas.
Conveyances	System Type	Hydraulic vs. gearless traction elevators.
	Load	Low-rise vs. high rise building

4.2.1. Relationship Between Building/Site Services and Energy Systems

Assessment of the energy consumed and GHG emissions produced by building/site alternatives requires consideration of the building/site services provided. Consideration of the building/site services is necessary not only for ensuring the equivalency of alternatives (see Section 4.1), but also for ensuring that all relevant energy systems are accounted for. The schematic relationship between building services (for an office building) and energy systems is illustrated in Figure 7. For an office building, the building/site services may be classified under three functional categories: work space, support space, and access. The work space includes the building services that most directly serve the business functions of the owner/occupant. Thus, the work spaces are typically the building elements for which the owner/occupant will typically have explicit requirements (e.g. minimum floor areas). The support spaces indirectly serve the business needs of the owner/occupant, but are nonetheless essential. Both the work spaces and the support spaces consist of several architectural energy systems: envelope, heating, cooling, ventilation, lighting, and miscellaneous equipment. These architectural systems are supplied energy by one or more energy sources: electric utilities, fossil fuel utilities, district heating, district cooling, and alternative/renewable energy. The “access” services of the building/site are provided by the circulation spaces (hallways, stairways, and elevators), entrances, parking areas, as well as the transportation system. The architectural energy systems related to access spaces are predominately lighting, escalators, and elevators, but may also include envelope, heating, cooling, and ventilation systems. The transportation energy systems are unique in that the energy is, most often, supplied off site. This fact has significant implications for the owner/occupant’s motivation and incentive for minimizing transportation energy consumption, since the potential

cost savings benefits of reduced transportation energy consumption are realized not by the location decision-maker, but by other consumers. Office location decisions that minimize building energy and other costs for the firm, but do not minimize transportation energy costs for employees are an example of what economists refer to as a “principal agent problem” – a problem in which an agent acts on behalf of a consumer but does not fully represent the consumer’s best interest. Although cost calculations are not a part of this research, recognition of this principal agent problem warrants separate accounting for building energy and transportation energy estimates. An opportunity for incentivizing location decisions that minimize transportation energy consumption may exist in the form of either direct financial incentives/disincentives for location decision makers, or indirect incentives such as green building rating system credits that reward transportation efficient site selections.

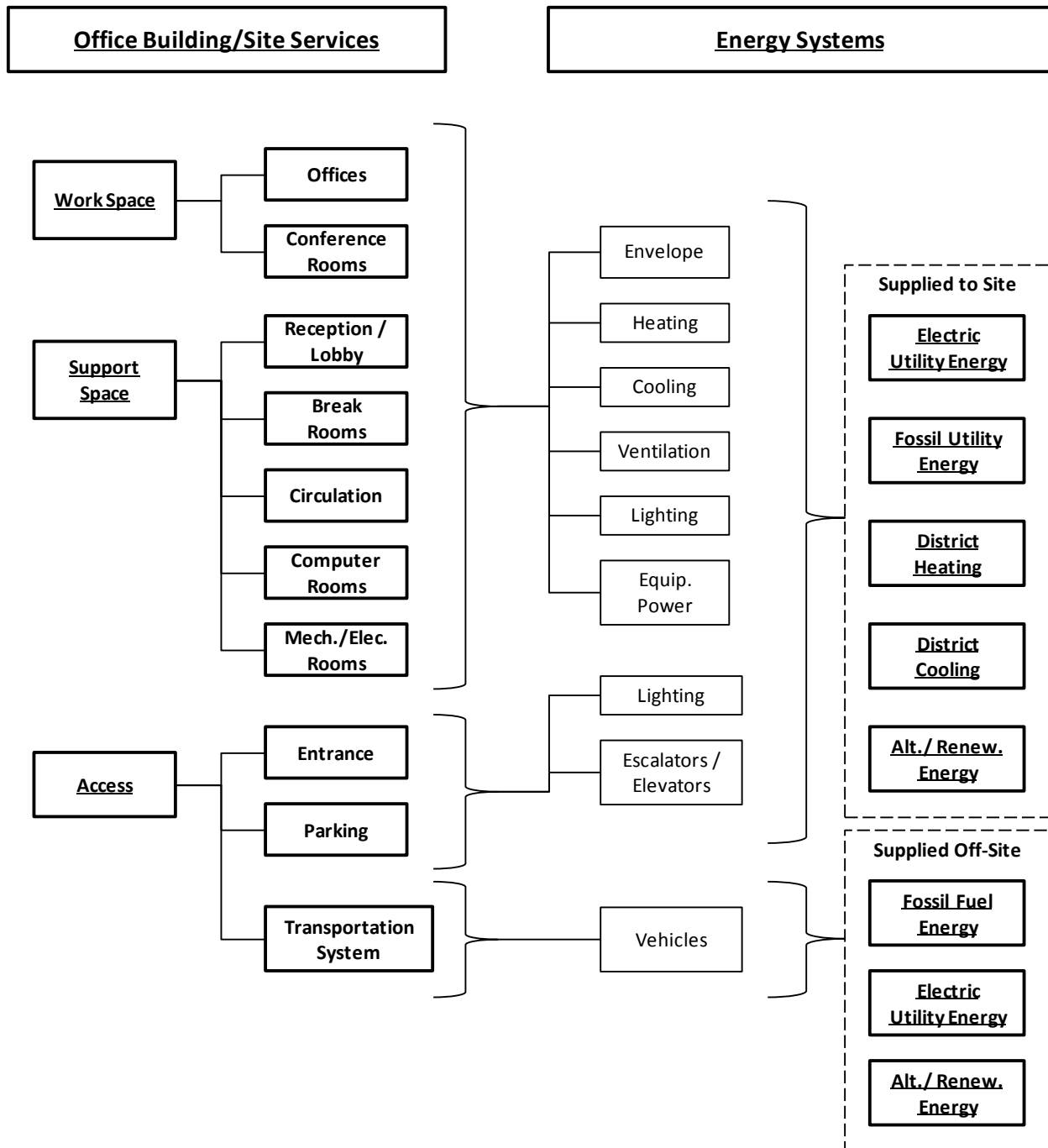


Figure 7: Schematic relationship between typical office building/site services and energy systems.

A robust and categorical accounting of the building services and the supporting energy systems is essential for estimating and *allocating* the building energy consumption associated

with a particular building building/site. This is especially important in multi-tenant office buildings in which building services may be shared between several tenants. For example, a multi-tenant office building may have shared parking facilities, shared lobby/reception areas, and in the case of a multi-story building, shared roof shelter and elevators. The building energy consumption of a mid-floor office tenant should include a proportionate share of the energy consumed in shared building services/facilities. Arguably the most equitable and simplest method for allocating shared energy consumption is by tenant square footage. Although simple in terms of proportionality, this method does require a somewhat sophisticated approach for estimating the energy consumption associated with district heating and cooling systems and shared roof and floor envelope components. District heating and cooling systems may have a known plant efficiency and the consumption of a tenant may be readily estimated, but estimation of the distribution losses for a given tenant versus another requires a considerable amount of data related to the design and performance of the distribution network. Such data is most relevant for distribution systems in which distribution energy losses vary considerably between tenants (e.g. a satellite building served by a district cooling system for a central campus). For the purposes of the evaluation framework developed here, such losses are assumed to be both unlikely and negligible – however, the relative efficiencies of district cooling/heating plants must not be ignored. With respect to shared roof and floor envelope components, the losses through the envelope to/from the spaces incorporating a floor or roof envelope component are to be estimated in the building energy simulation and subsequently allocated to the various tenant spaces. This may be accomplished in a building energy simulation by modeling top and bottom floor spaces both with and without these envelope components and comparing the differences in annual energy consumption (see Section 5.2.2.2).

4.2.2. Relationship Between Building/Site Elements and Energy Systems

In order to calculate the energy and GHG emissions performance of building/site alternatives, it is necessary to identify the relationship between building/site elements and the energy systems they impact. Figure 8 illustrates a conceptual framework of whole-building energy system elements, as they relate to a building site. In the first three columns of the figure, the energy system elements that are potentially constrained by the site and potentially variable between different sites are divided between design, operational, and external elements. The external elements are non-design and non-operational elements that are not managed by the owner occupant, but nevertheless may impact the relative performance of building/site alternatives. Examples include the available utility energy sources that influence fuel-cycle energy efficiency, and environmental factors that influence loading on the building envelope. The environmental factors are considered to be beyond the control of the occupant, although some of these elements (e.g. ground cover and trees) could be within the property boundary and design control of the occupant. The design elements (2nd column) include aspects of the building architecture and mechanical/electrical systems that play a role in several building energy systems: space-cooling, space heating, ventilation, lighting, and materials (embodied energy). The design elements shown in Figure 8 are not an exhaustive list of the relevant variables, but are merely a representative list of potentially relevant elements. The operational elements (3rd column) include site-dependent aspects of using the building – primarily transportation access to/from the building. The location of a building within a given transportation network and land-use context can influence not only trip distances and mode shares for home-based work (HBW), non-home-based work (NHBW), and non-home-based other (NHBO) trips, but also the rate or number of trips taken for NHBO trips (e.g. social and dining trips taken during break times). The exterior lighting schedule has been included in this category since the operation of common area

lighting may not be controlled by the building occupant (e.g. walkway and parking garage lighting for a multi-tenant building). The conceptual framework accounts for energy system elements that are generally not dependent on the building site/location (4th column). The element in this category that has the most extensive impact across whole-building energy systems is the building occupancy. Building occupancy impacts space-cooling, space-heating, ventilation, lighting, and plug/process loads, and transportation activity. Furthermore, building occupancy affects the scale of the development considered in the decision context as well as the per person-hour normalization of building energy performance. It is assumed here that the estimated occupancy demands of the occupant are independent of the available site alternatives.

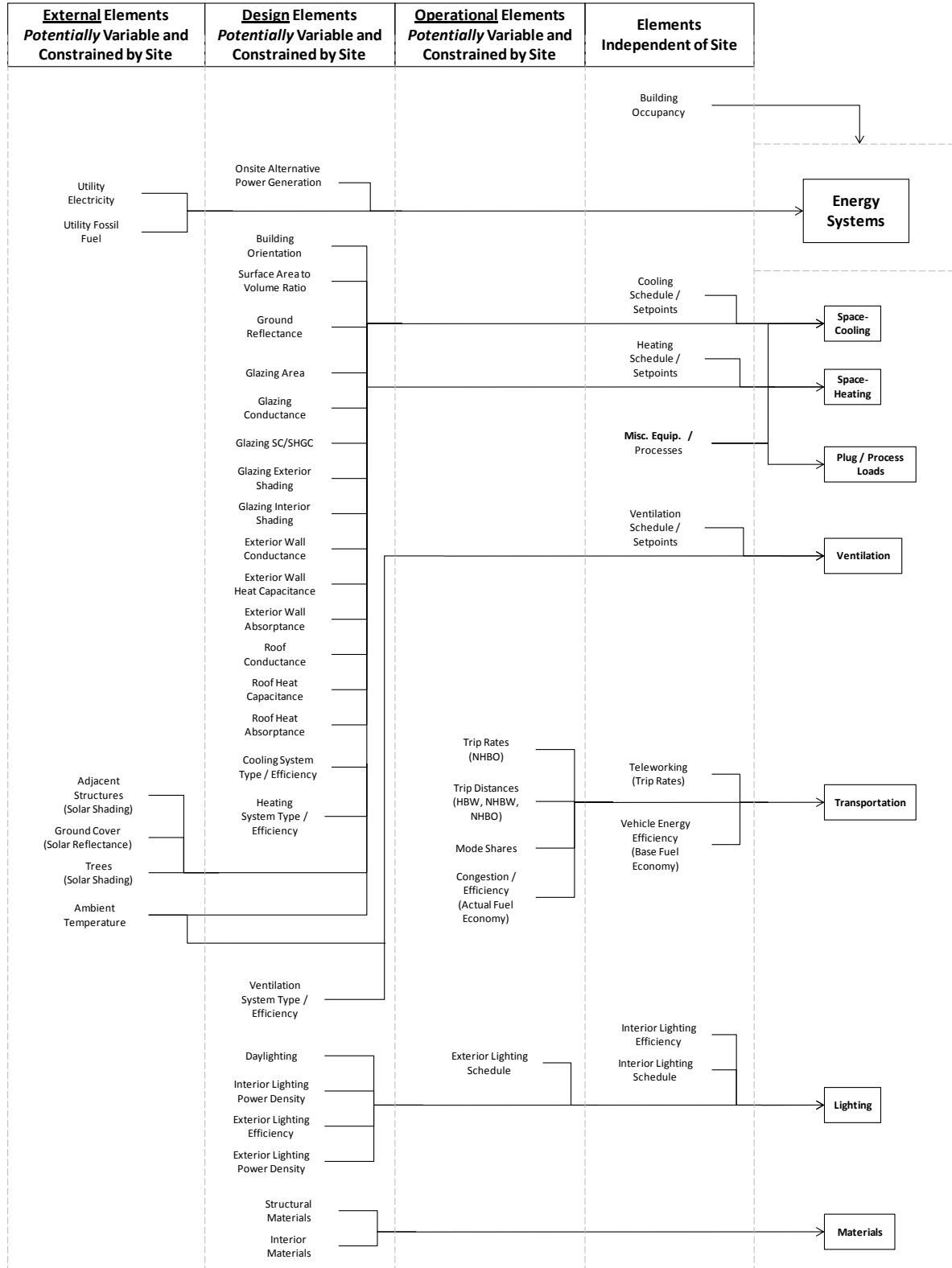


Figure 8: Conceptual framework of whole-building energy systems, as they relate to a building site/location, Source: (78).

This conceptual frame provides a point of departure for analyzing and quantifying the relative performance of building site alternatives. The conceptual framework identifies the energy system variables that may be affected by the building site, and the framework provides a delineation of how these variables may be controlled (by design, by operation, or by external factors beyond the occupant's control – save by site selection). Different site alternatives considered by an occupant will likely be constrained in different ways. For example, an office space in a multi-tenant building may have constrained glazing conductance and shading coefficients (window upgrades are not an option) whereas purchase of a single-tenant building may have unconstrained glazing properties (replacement is an option), but potentially no access to natural gas service for heating.

The “design” elements may be controlled either before occupancy (e.g. energy-saving design features for a new construction building) or post-occupancy (e.g. energy-saving retrofits). Similarly, the operational elements may be controlled before occupancy (e.g. selecting a site with public transit access) or post-occupancy (e.g. teleworking and carpooling programs). The fact that many of the energy system elements may be controlled or adjusted after occupancy does not necessarily eliminate the overall performance variability between sites since post-occupancy measures for energy efficiency may not be capable of achieving the energy efficiency of an alternative site. For example, if an occupant's operations will allow only a maximum of 20% employee teleworking, then an exurban site with 20% employees teleworking and the remainder (80%) commuting primarily by single occupant vehicles may not achieve the same transportation energy efficiency as a central business district site with only 50% of employees commuting by single occupant vehicles and the remainder commuting by public transit, ridesharing, or non-

motorized transportation. The constraints placed on the energy system elements by the site/location can have a lasting impact on the final-design, post-occupancy, efficiency potential. Hence, the purpose of the evaluation framework under development is to quantify and compare these impacts of the site alternatives before an alternative is selected.

4.2.3. Life Cycle Analysis Perspective

As is mentioned in Section 3.2, the framework employs a life cycle analysis perspective for quantifying the energy consumption and GHG emissions of buildings/sites. Consistent with the guidelines of ANSI/ISO 14040 *Environmental management – Life cycle assessment – Principles and framework* (30), the framework is structured on a defined boundary of analysis and the framework measures the performance of buildings/sites based on representative functional units. The following section describes the boundary the energy/emissions estimates included within the framework.

4.2.3.1. Analysis boundary

The analysis or system boundary of a life cycle analysis framework is a specification of the processes to be included within the performance evaluation. Determination of a suitable boundary is dependent upon the performance concerns of the intended audience and the availability of supporting data. This particular framework is designed for building/site selection stakeholders that are concerned with the energy consumption and GHG emission impacts of building/site selection decisions. Such impacts arise both from the direct use of fuel/energy systems and the indirect or “upstream” use of fuel/energy systems in the supply chain. Generally, the largest impacts occur in the direct consumption of fuel/energy systems. This “direct

consumption” includes the combustion of fuels for building or transportation operations, as well as the consumption of purchased electricity for building (or, on a smaller scale, transportation) operations. Not only do these “direct consumption” processes generally represent a greater proportion of the impacts relative to “upstream” processes, but also these “direct consumption” processes typically have a higher quality data set for quantifying the associated energy and emission impacts. This relationship between direct and upstream impacts is reflected in the standard protocols for quantifying and inventorying GHG emissions from organizational activities (71, 72, 73, 74). The GHG emission inventory protocols define three scopes for quantifying GHG emissions. Scope 1 includes all direct GHG emission processes controlled by the organization, notably fossil fuel combustion and refrigerant leaks. Scope 2 includes the GHG emission processes associated with purchased electricity or district heating/cooling. In the language of the protocols, these processes are called “indirect” since the release of GHG emissions occurs through processes that are under the control of an external organization. In this dissertation, the consumption of electricity is referred to as a “direct consumption” process, since electricity is one of the main fuel/energy systems directly supporting building operations, and since electricity consumption is directly proportional to the operational intensity of a building/site. Finally, Scope 3 in the GHG emission inventory protocols includes all of the “upstream” processes in the fuel/energy supply chain, such as extraction, refining, and transportation & distribution (T&D). In the inventory protocols, the Scope 3 emissions are considered to be optional quantifications, since these processes are Scope 1 emissions for the respective controlling organizations. Scope 3 emissions or energy impacts are most relevant for the comparison of fuel/energy system alternatives that have different supply chain processes, such as nuclear power generation vs. natural gas power generation.

The GHG emission scopes and categories included within the life cycle analysis boundary are shown in Figure 9. The scopes and categories shown in Figure 9 represent not only the accounting of GHG emissions, but also the accounting of energy consumption. It is important to note that under “mobile sources,” only the emissions/energy of private automobiles are included. The emissions/energy of public transit modes may impact the total transportation energy consumption of a building/site, but the impact is not relevant to the marginal increase in system energy consumption and GHG emissions. Since public transit modes generally operate on fixed schedules, a marginal increase in travel demand on a public transit route will result in a negligible increase in total energy consumption. In fact, on a Btu (or lb of GHG) per pax-mile basis, the energy efficiency of a transit mode will most likely increase as transit vehicle occupancies increase. Private automobile travel activity to/from building/site alternative comprises the most relevant marginal increase in transportation system energy consumption and GHG emissions.

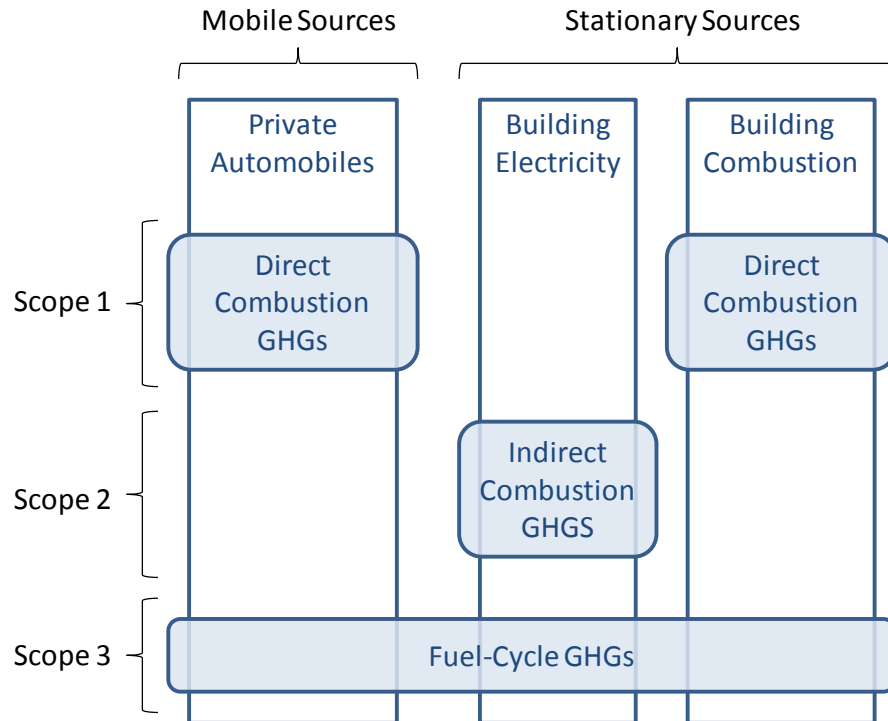


Figure 9: GHG emission scopes and categories included within the life cycle analysis boundary.

The framework accounts for the the six major types of GHG emissions defined by the Kyoto Protocol: carbon dioxide (CO₂), methane (CH₄), nitrous oxide (N₂O), hydrofluorocarbons (HFCs), perfluorocarbons (PFCs), and sulfur hexafluoride (SF₆) (86). The majority of GHG emissions from building and transportation systems arises from fossil fuel combustion and thus consists mainly of CO₂, CH₄, and N₂O emissions. Estimation of fugitive leaks from refrigerants are not included in the framework for two reasons: 1) A modeling framework for estimating potential refrigerant leaks is unavailable; and 2) Refrigerant leaks generally comprise a small (less than 5 percent) fraction of organizational GHG emissions, for which “simplified methods” are typically used for inventorying historical emissions (71, 72).

It should be noted from Figure 9 that GHG emissions from the construction and maintenance of fixed infrastructures such as building architectural/structural systems and MEP

systems are not included in the framework. This omission is due largely to a paucity of infrastructure material inventory data (or material “take-off” data, as it is commonly referred to in the AE industries) for estimating GHG emissions from building materials. The data collection effort necessary for quantifying infrastructure material impacts, either for the case studies of this dissertation or for the application of the framework in professional practice, is considered to be overly onerous for the degree of comparative insight provided. For a given building, the construction and material impacts are understood to contribute less than 15 percent of life cycle energy consumption or GHG emissions (1, 2), and the relative differences between building alternatives is expected to be even less.

As is mentioned in Section 3.2, the “life cycle” of the analysis framework is the occupancy period of a particular office tenant (typically a 10 to 15 year time period). Over this time period, it is expected that the annual energy/emissions of any given year within the occupancy period is representative of the average annual energy/emissions of the building/site. Therefore, the framework is designed to quantify the annual performance of the building/site alternatives to assess the relative potential performance of the alternatives.

4.2.3.2. Functional Units

Meaningful life cycle analysis of energy consumption and GHG emissions from activities requires consideration of the productive output of those activities. In the LCA literature, the productive outputs are related to emission inventories through the use of “functional units” (30). The functional units selected for this framework are the “performance metrics” shown in Table 3 in Section 3.3. GHG estimates are aggregated into carbon dioxide equivalents (CO₂e) based on the global warming potentials (GWPs) published in the IPCC’s 2007 4th Assessment Report: 1

for CO₂, 25 for CH₄, and 298 for N₂O. The role of functional units in this framework is somewhat unusual in that the productive output (or service) of the building/site alternatives are similar to each other. Thus, the functional units are not essential for comparing the energy and emissions performance of building/site alternatives. Rather, the functional units are helpful for comparing the performance of the alternatives relative to regional averages, where available. For a detailed discussion of this issue, see Section 4.2.4.

4.2.3.2.1. *A Note on Inventory vs. Assessment*

It should be noted that, with respect to life cycle analysis, the evaluation framework developed here is an *inventory*-focused analysis rather than an *assessment*-focused analysis. A complete life cycle *assessment* consists of three phases: 1) Goal and scope definition; 2) Inventory analysis; and 3) Impact assessment (30). The last phase, impact assessment, is a process of “evaluating the significance of potential environmental impacts using the results of the life cycle inventory analysis” (30). An example assessment process is the subjective weighting and aggregation of inventory results based on the relative importance/impact of the metrics. In the framework developed in this dissertation, the energy consumption and GHG emissions are inventoried, but no further weighting or aggregation is performed. For this framework it is assumed that energy consumption and GHG emissions are important metrics for the intended audience but there is no further assumption for the relative importance of these metrics.

4.2.4. Building/Site Performance Comparisons

Evaluation of the potential energy and emissions performance of buildings/sites requires a method for expressing the performance of an individual building/site and a method for comparing the relative performance of buildings/sites. The following section discusses appropriate options for expressing the performance of individual buildings/sites in the evaluation framework.

4.2.4.1. EUI and GEI vs. Total Energy and GHGs

The energy and GHG emissions performance of a given building/site may be expressed as either a total quantity or a normalized “intensity.” EUI (energy use intensity) and GEI (greenhouse gas emission intensity) are expressions of the energy consumption and GHG emissions, respectively, normalized by a functional unit (see Table 3 in Section 3.3). ANSI/ASHRAE Standard 105-2007 *Standard Measures of Measuring, Expressing, and Comparing Building Energy Performance* specifies a default energy index measure of kBtu/ft²-yr (28). In practice the most commonly used normalizing unit is conditioned floor area (SF) – the normalizing metric used in the DOE ENERGY Star Portfolio Manager building rating system (24). Normalizing energy consumption by the square footage of building floor area has limited utility for expressing the actual *use* of a building/site. A per SF normalizing unit for buildings/sites is analogous to a per seat normalizing unit for passenger vehicles. If the energy performance of vehicles were expressed merely in terms of the kBtu/seat-yr, the measured efficiency of vehicles would be biased toward vehicles with the greatest number of seats. Thus, for an equal number of miles driven, a 3 mpg, 40 seat bus would have a lower EUI than a 20 mpg 4 seat sedan; for 10,000 miles of travel, the bus would have an EUI of 10,704 kBtu/seat-yr,

whereas the sedan would have a higher EUI of 16,056 kBtu/seat-yr (assuming both vehicles are powered by gasoline with a LHV of 128.45 kBtu/gal). However, if a significant number of seats are empty, as is often the case, then the EUI will not reflect the actual service provided. Vehicle occupancy (analogous to building occupancy) is more representative of the service provided; for 10,000 miles of travel, a bus with an average occupancy of 8 passengers would have an EUI of 53,521 kBtu/pax-yr, whereas a sedan with an average occupancy of 1.6 persons would have a lower EUI of 40,141 kBtu/pax-yr. Consideration of occupancy provides a more direct measure of service than does square footage (or seats), but occupancy expressed simply as the number of persons does not reflect the quantity or duration of service for each person. Employing the building/vehicle analogy once more, the hours of occupancy for a commercial office building are analogous to the miles of travel for a passenger vehicle. In the public transportation industry, energy and GHG emissions performance is expressed by dividing a vehicle's energy consumption and GHG emission by its passenger-miles of service (87, 88). This expression of energy and GHG emissions performance is useful for comparing vehicles of different sizes, weights, and propulsion technologies, both within and across transportation modes. It is rather disappointing that the community of building energy researchers and practitioners have selected a building energy performance metric (kBtu/ft²-yr) that does not account for the quantity or duration of occupancy – the most relevant, generic measures of building service output.

Recognizing that additional building service characteristics may be helpful for expressing the energy performance of a building, ASNI/ASHRAE Standard 105 provides a list of additional “normalizing factors” that may be useful for commercial office buildings, such as number of full-time equivalent workers, number of personal computers, weekly hours of operation, and annual months of operation. Absent from the suggestions listed in ANSI/ASHRAE Standard 105

is the number of person-hrs of building occupancy. This omission does not imply that annual kBtu/person-hrs is not a useful measure of building performance, but rather that annual kBtu/person-hrs is not commonly considered by building energy professionals.

Although it is argued here that a normalizing unit of person-hrs provides a better representation of building/site energy and GHG performance, the utility of this normalizing unit is somewhat limited in the context of a building/site evaluation framework designed for an owner/occupant's site selection. The person-hrs service demand of the owner/occupant should be consistent between the alternatives available in the set of possible buildings/sites. That is to say, the occupancy of the building should not be dependent on the particular building/site selected. In the intended application context of this framework, it is expected that the floor areas of the building/site alternatives will be similar, since floor area size is usually a constant criterion for the available building/sites. Thus, for the intended application context of this framework, total energy consumption and GHG emissions are adequate for comparing energy and emissions performance between building/site alternatives. Normalization of energy and GHG performance becomes pertinent in this evaluation framework when the sizes of the building alternatives vary significantly, or when the buildings/sites are to be compared to average sector baselines.

4.2.4.2. Comparison between Alternatives vs. Comparison to Baseline

Expression of the energy consumption and GHG emissions performance of buildings/sites ultimately serves the task of comparing performance. Evaluation of the most energy efficient building/site among a set of alternatives may be conducted by either one of the following comparisons:

- 1) Comparison between buildings/sites
- 2) Comparison to a building/site regional average (baseline)

The first option, comparison between buildings/sites, allows minimization among the available alternatives. This comparison option effectively supports the objective of the evaluation framework (minimization of energy consumption through site selection), but it does not determine whether the best performing available alternative provides an opportunity for marginal reduction in regional average energy consumption and GHG emissions. The second comparison option, comparison to a building/site regional average baseline, allows such a determination to be made. Building/site decision makers may be concerned with selecting not the best performing alternative, but instead an alternative or collection of alternatives that merely perform(s) better than the regional average. Additionally, comparison to a regional average baseline can be useful for warranting incentives that encourage the use of the most efficient buildings/sites.

The use of building/site regional average baselines requires data on the larger set of developments in the region. For commercial buildings in general, and office buildings in particular, the CBECS database provides data for EUI baselines (76). The CBECS database is the basis for the rank-order ratings in the ENERGY Star Portfolio Manager existing building rating system. Although the CBECS database is *the* national data source for commercial building EUI, the data in CBECS is both highly aggregated and outdated. Regional EUI's are only available at multi-state regional levels, and the data in CBECS has not been updated since 2003. Furthermore, the number of samples in CBECS is not large enough to reliably characterize the EUI of regional building stocks. For example, for all office buildings, built between 1990 and 2003, containing 10,001 to 50,000 SF of floor space, and located in the South Atlantic region

(consisting of Florida, Georgia, South Carolina, North Carolina, Virginia, West Virginia, Maryland, Delaware, and the District of Columbia), the CBECS database contains only 14 samples (89). These 14 samples represent a total of 6,791 buildings meeting the above criteria (89) – less than two per state! The representativeness of this small sample appears even weaker when considering that this 14 building sample includes buildings in 4 different climate zones.

While regional commercial office building EUI data is especially sparse, a dataset for the EUI of transportation access to/from commercial office buildings is non-existent. Thus, comparison of site transportation access EUI and GEI to a regional average baseline would require calculation procedures for estimating the regional average baseline performance.

4.2.4.3. Reference Frames for New Construction and Major Renovations

In addition to the relative vs. absolute evaluation option discussed in the previous section, new construction and major renovation projects involve additional evaluation considerations. These considerations or reference frames stem from the different types of energy estimates that may be performed during the site selection phase of a building project. Evaluations of the building/site performance of new construction or major renovation projects may be conducted within the following three frames of reference:

- 3) Comparison of schematic designs; or
- 4) Comparison of baselines; or
- 5) Comparison of baseline to schematic designs (energy reductions).

Comparison of schematic design performance (reference frame #1) is focused on evaluation of site alternatives in terms of total end-use energy consumption. This comparison accommodates the most explicit evaluation of total energy consumption, but it is highly sensitive to the uncertainty of final building design. Thus, a comparison of schematic design performance between site alternatives may not clearly indicate, under uncertainty, which potential site supports the best energy performance (at least not during the early conceptual or schematic design phases). Alternatively, a comparison of baseline performance between sites (reference frame #2) avoids the uncertainty of design evolution and final design, and may provide a clearer distinction in the relative performance of sites. The second reference frame (comparison of baseline performance) could provide the most targeted identification of the best performing site when utilized in conjunction with the LEED energy performance rating system. Currently, the LEED energy performance rating system (EA Credit 1) measures building energy performance in terms of percent reduction against a baseline design for the given site. Although the LEED rating system rewards improvements made in the energy efficiency of the building stock, the rating system does not necessarily reward development or occupancy of the most energy efficient building/site that meets the occupant's needs. For example, an occupant may select an existing commercial building with an EUI that far exceeds the national average for the building classification. Proposed schematic designs for renovating the building may be estimated to achieve 30 – 40 percent energy reductions against the existing building baseline. Energy reductions of 30 – 40 percent would result in lower levels of final design energy consumption if the baseline design energy consumption were lower. This fact invites consideration of which site alternative provides the lowest baseline performance. If the energy reduction percentage intended by the building owner and designers is independent of the given baseline (percent reduction

predetermined to meet points goal), then selection of the existing building with the lowest baseline energy consumption will result in development of a building with the lowest final design energy consumption. Furthermore, selection of the site with the lowest baseline energy consumption may help to reduce the uncertainty of achieving the best possible energy performance in the final design. If a proposed energy reduction of 40 percent is eventually changed (due to unforeseen cost or technical barriers) to a more modest 25 percent, then selection of the site with the lowest baseline energy consumption would help to preserve or “lock-in” a lower level of final design energy consumption throughout the evolution of the building design/renovation.

The third reference frame (comparison of energy reductions), essentially follows the current paradigm of the LEED rating system, in which more points are awarded for proposed buildings that reduce a higher percentage of energy relative to their own baselines (albeit in terms of energy cost rather than units of energy). Evaluation of the percentage energy reduction against a single site-specific baseline does not properly account for the opportunity to select the most efficient site available. Evaluation of the most efficient site available requires either establishing a baseline from among available site alternatives or deriving one (an average or median performance) from the existing building stock. Whereas the LEED paradigm of building energy performance rating (third reference frame) encourages improvement of the building stock through site/building specific upgrades, the second reference frame encourages utilization of buildings that are currently improved among the building stock.

Figure 10 illustrates example comparisons of building energy consumption via baseline energy, schematic design energy, and energy reductions. According to the LEED paradigm of estimated building energy consumption savings (based on ASHRAE 90.1 Appendix G

Performance Rating Method), the preferred building alternative would be “Building 1” since it offers the greatest reduction in building energy consumption (third reference frame). However, it is evident that “Building 2” offers the lowest level of building energy consumption in absolute terms. Furthermore, the uncertainty range of schematic design energy estimated for “Building 1” overlaps with much of the uncertainty range of baseline energy for “Building 2,” which illustrates the argument for selecting the site with the lowest baseline energy consumption to reduce the uncertainty of achieving the best possible energy performance in the final design.

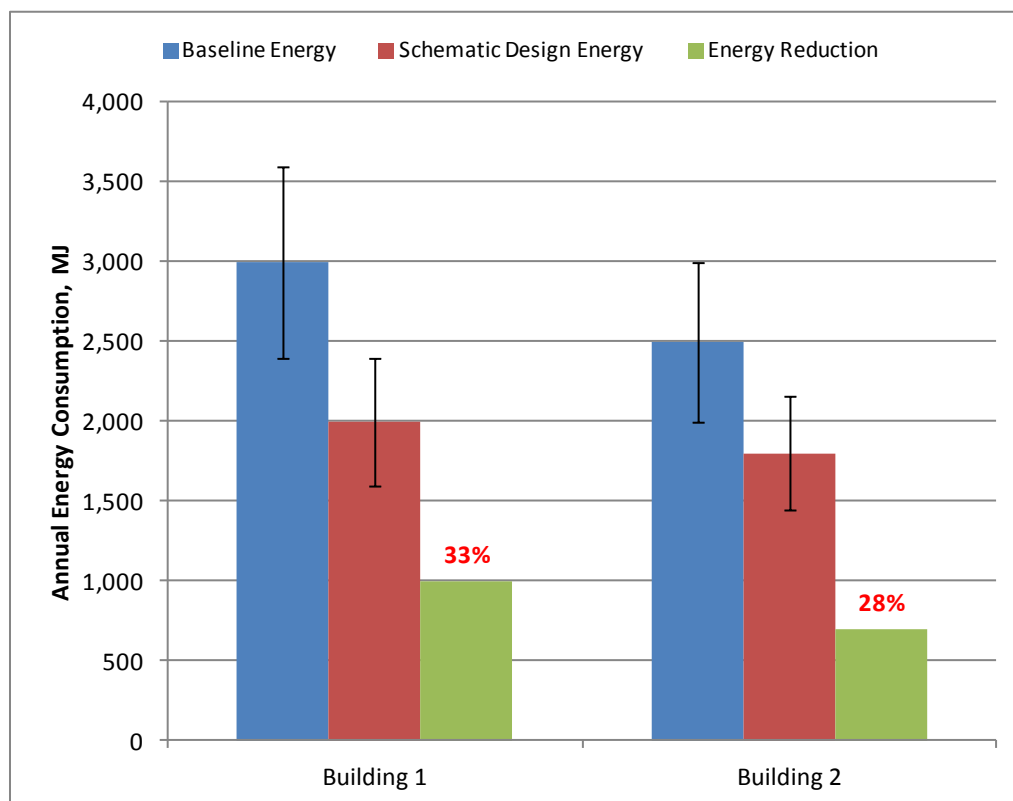


Figure 10: Example comparisons of building energy consumption via baseline energy, schematic design energy, and energy reductions.

4.2.5. Accounting for Uncertainty

The motivation for accounting for uncertainty is based on an understanding that the uncertainty in the whole-building energy performance of a given site alternative may exceed the difference in estimated mean performance between the given site and an alternative site. In other words, the estimated range in performance for some sites may be too wide to determine the relative performance between a pair of potential sites. Whether or not the precision of the estimates are too wide, some capability for visualizing the range or distribution of estimated mean differences in energy consumption between pairs of sites could help the decision maker determine if the degree of uncertainty is acceptable for making a determination of the most energy efficient site. The uncertainty of the estimated whole-building energy performance (or mean difference in energy performance between sites) is a result of the propagation of uncertainty of the calculation inputs. The impact of uncertainty on results calculated in the evaluation framework will be quantified through sensitivity analysis of the propagation of uncertainty.

The analysis framework is designed to explore energy performance within the constraints set by the site/context. The range in energy performance for any one given site is a function of the uncertainty or range of energy system variable values within the constraints of the site and/or within expected limits. For example, the estimated energy performance of a renovated office space in an existing multi-tenant building is a function of many energy system variables, such as opaque wall U-value, glazing SHGC, HVAC compressor and fan efficiencies and control setpoints, lighting power, etc. For an existing building, the values of the existing variables are understood to be uncertain since a complete inventory (energy audit) of these variables will most likely be unavailable to the decision maker at the time of building/site selection. Similarly, the values of variables related to a schematic design of the any building renovations will also be

uncertain since the building renovation design will likely evolve on the way to final design. Figure 11 illustrates the spectrum of uncertainty in estimated building/site energy and GHG performance. The uncertainty in the estimated energy and GHG performance is expected to be less for buildings/sites with completely defined building systems (existing building fit-outs) than for buildings/sites with only a conceptual design of building systems (new construction).

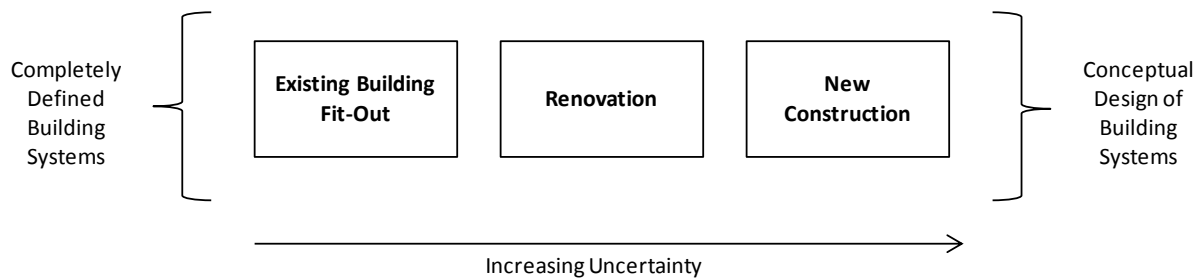


Figure 11: Spectrum of Uncertainty in Estimated Building/Site Energy and GHG Performance.

The framework development and application presented in this dissertation is focused on the lower end of this uncertainty spectrum. At the lower end of the uncertainty spectrum, the number of uncertain input variables and the associated magnitude of uncertainty are lowest. With lower magnitudes of uncertainty in the estimated outputs, the likelihood of estimating significant differences in building/site performance are greatest. Thus, the lower uncertainty of an existing building fit-out application context provides the best starting point for building up a framework for estimating, under uncertainty, potential building/site performance.

4.2.5.1. Estimation of Uncertainty

The development of appropriate uncertainty estimation methods in the building/site evaluation framework is informed by standardized uncertainty expression and estimation methods in the literature. The term “uncertainty” used in this dissertation is taken directly from the literature and is defined as the “parameter, associated with the result of a measurement, that characterizes the dispersion of the values that could reasonably be attributed to the measurand” (90). In energy simulation and modeling, uncertainty and error are important measures of the precision and accuracy, respectively, of numerical estimates. It should be understood that uncertainty and error are two distinctly different terms, for both modeling in general and this evaluation framework in particular. “Error is the difference between the true value, which we do not know, and the measured value; therefore, the error is unknowable. Uncertainty is an estimate of the limits of the error” (56).

4.2.5.1.1. *An Important Note on Error in the Modeling Framework*

In the measurement and modeling literature, error is described as having two components: random and systematic. “The effects of random errors arise from unpredictable temporal or spatial variations in repeated observations of the measurand. All other errors are classified as systematic errors (also called bias errors)” (56). Systematic errors represent the difference between the expected value of a model’s functional output and the expected value of the actual phenomena being modeled. One of the main objectives, stated or inferred, of modeling is to minimize systematic errors. Yet in the case of the estimation framework developed in this dissertation, the systematic error is unknowable. The framework is designed to estimate the expected energy and GHG emissions performance of building/site alternatives, but the estimates

will not be calibrated to actual post selection performance. In fact, for alternatives that are not selected by the site selection decision maker, it is not possible to calibrate the pre-selection estimates. Each particular building/site decision context will likely present unique inputs (i.e. owner/occupant behaviors, building/site requirements, etc.) that forestall repeatable estimates that can be calibrated. Thus, for the framework developed here, minimization of error is pursued through the use of modeling and estimation tools and methods that provide the best available representation of actual phenomena; however, systematic and random error effects will remain largely unknown. This is not to say that there is no possibility of assessing the error of building/site performance estimates. The error of the estimates may be judged through comparison of the estimated outputs to known, comparable values published in the literature. The focus of the framework developed here is not to quantify the error of building/site performance estimates, rather it is to estimate and express the uncertainty of the estimates so that the decision maker may make an informed determination of the potential performance of a given building/site alternative relative to another alternative or a performance baseline.

4.2.5.2. Types of Uncertainty

In this framework, the accounting of uncertainty in model estimates is based on standard guidance in the uncertainty measurement literature. Consistent with the literature, numerical evaluations of uncertainty in model inputs and outputs may be grouped into two main categories (90, 91):

- Type A: Numerical evaluation by statistical methods,
- Type B: Numerical evaluation by other means.

It follows from the definition of Type A uncertainty that in order for this type of evaluation to be performed, a statistical sample of data must be available. Unfortunately, such a dataset set is not always available for some or all model input variables. A lack of a statistical dataset for numerically evaluating input parameter uncertainty does not proscribe a numerical evaluation of uncertainty. Other, non-statistical means are available for quantifying uncertainty for parameters that are known to have at least some (greater than zero) variance. “A Type B evaluation of standard uncertainty is usually based on scientific judgment using all the relevant information available, which may include: previous measurement data, experience with or general knowledge of the behavior and property of relevant materials and instruments, manufacturer’s specifications, data provided in calibration and other reports, and uncertainties assigned to reference data taken from handbooks” (91). For the evaluation framework developed here in this dissertation, the numerical evaluations of uncertainty are predominately of Type B.

Regardless of the type of uncertainty, the generic expression of uncertainty of a measured or estimated quantity is of the following form:

Equation 1

$$U = ku_c(y)$$

Where u_c = the combined standard uncertainty of a measurement result.

k = the coverage factor.

The uncertainty U is referred to as the expanded uncertainty. The combined standard uncertainty, u_c is simply the estimated standard deviation of the measurement or calculation. It is assumed that the probability distribution of the measurement/calculation and its combined

standard deviations is approximately normal. This assumption holds when “the estimate y of the measurand Y is not determined directly but is obtained from the estimated values of a significant number of other quantities . . . describable by well-behaved probability distributions, such as the normal and rectangular distributions; the standard uncertainties of the estimates of these quantities contribute comparable amounts to the combined standard uncertainty $u_c(y)$ of the measurement result y ” (91). The coverage factor, k , represents the desired level of confidence associated with the uncertainty interval. A coverage factor of 2 represents a confidence level of 95 percent for the interval $Y = y \pm U$.

For the building/site evaluation framework developed in this dissertation, most of the estimates of uncertainty are Type B numerical evaluations. Not only are many of the input uncertainties evaluated through non-statistical methods, but also the evaluation of output uncertainty cannot be determined analytically. The complex, non-linear calculations of the building energy simulations do not support an analytical evaluation of the output uncertainty from the uncertainties of the input variables. For this reason, a Monte Carlo simulation approach is selected to evaluate the effect of input uncertainties on output uncertainties. “Given (i) the model relating the input quantities and the output quantity and (ii) the PDFs characterizing the input quantities, there is a unique PDF for the output quantity” (92). For model outputs with a normal distribution, the estimated uncertainty may be expressed either in the form of Equation 1 or in the form of a graphical PDF. In cases where model outputs are not distributed normal, a graphical PDF provides the most appropriate depiction of the estimated uncertainty.

The expression of uncertainty in energy consumption and GHG emissions in this evaluation framework is designed to help location decision makers determine the level of confidence of one site’s performance relative to another. Uncertainty exists in each of the

component estimates of site performance: Both transportation systems and building systems and both initial performance and post-occupancy performance.

4.2.5.3. Uncertainty of Initial Performance vs. Post-Occupancy Performance

It is unreasonable to assume that energy and emissions performance potential of a site will remain constant beyond the instance of site selection. Thus, the uncertainty of a site's estimated performance is expected to change when evaluating over different time scales. That is to say, the uncertainty of the initial site performance is expected to be different from the uncertainty of the post-occupancy site performance. The term "initial" refers to the baseline energy and emissions performance that is expected from the systems that are understood to be in operation at the beginning of the occupancy period. "Post-occupancy" refers to the performance expected later in the occupancy period when potential modifications to the systems may occur. The types of system modifications and the impacts on the uncertainty in whole-building energy consumption are unique to the particular building and transportation systems associated with the site alternatives. Although the evaluation framework is intended to account for multiple uncertainties in evaluation input parameters, not all input parameters will (or necessarily should) include associated uncertainty estimates. The transportation and building systems are defined by hundreds of input parameters, but estimating the uncertainty off all of these parameters can be both impractical and unimportant. The most important input parameter uncertainties are those that have the greatest impact on the *relative* performance of building/site alternatives. Parameters that are not expected to vary between buildings/sites, such as the occupancy schedule and the private automobile fleet fuel efficiencies, will undoubtedly have some associated uncertainty, but the propagation of the uncertainty to the performance estimates should have little or no impact

on the estimated relative performance of building/site alternatives. The details of the uncertainty estimation for building systems and transportation systems are described in Chapter 5 and Chapter 6, respectively. The following sub-sections describe the main uncertainty aspects of initial performance and post-occupancy performance in transportation and building systems.

4.2.5.3.1. Building Systems

For an existing building with defined energy systems, the uncertainty of the initial building/site performance is a function of the uncertainty in the surveyed energy system parameters. Considering that it is likely infeasible to survey, inspect, and verify all building energy system parameters, many of the parameter values may be approximated by uncertainty ranges even though the systems are already physically defined. For example, an existing building envelope, by its very existence, is physically fully defined; however the thermal performance properties of the envelope layers may remain uncertain due to a lack of construction documentation or field survey data on building envelope layers. In some cases, the “initial” performance of the building is the only uncertainty to be evaluated. The need for evaluating the post-occupancy uncertainty of building performance is determined by the possibility for post-occupancy building energy retrofits. For some buildings, the occupant may expect little or no modification of the building energy systems. Furthermore, the set of possible modifications may be defined by the renovation limitations imposed on the occupant by a building/site owner. For example, in a multi-tenant office building in which the occupant is leasing an office space, the occupant may be allowed to replace the lighting systems, but may not be allowed to replace the envelope glazing or insulation. Thus, the post-occupancy, building parameter uncertainties would be a modified subset of the initial occupancy, building parameter uncertainties.

4.2.5.3.2. *Transportation Systems*

The “initial” performance of the transportation systems is the baseline, average performance for a site located within a given TAZ. The performance may deviate from the zone average due to known differences in input parameter values, such as parking costs or transit pass costs. Whereas the post-occupancy uncertainty of building systems is defined by potential building energy retrofit projects, the post-occupancy uncertainty of transportation systems is defined by travel demand management programs. The uncertainty of post-occupancy performance is defined by both the range in program options considered by the occupant (e.g. transit pass subsidy and parking cash-out) and the efficacy of program options in unique location types (e.g. locations with transit service and pay parking vs. locations with no transit service and free parking).

CHAPTER 5

ESTIMATION OF BUILDING ENERGY CONSUMPTION AND GHG EMISSIONS

5.1. Building Energy Consumption Estimation in Research and Practice

Estimation of building energy consumption is a useful exercise in building design, renovation, operation, and research. In building design and renovation, estimates of building energy consumption help to inform the selection of design and retrofit alternatives that minimize energy costs. Often these estimates are an extension of building HVAC load calculations, which are calculations of the peak thermal and electrical power demands on the HVAC systems. For commercial buildings, load calculations and energy estimates are typically produced with the help of building load/energy simulation software (see Section 5.1.2.1). Building energy simulations most often include utility energy cost calculations since the primary goal of energy efficient building design and retrofitting is not to reduce energy consumption per se, but rather the financial cost (either operational or life cycle) of energy consumption. This is the case for the LEED rating system's points for Energy & Atmosphere Credit 1: Optimize Energy Performance – Option 1: Whole Building Energy Simulation (*13*), which references Appendix G of the pre-eminent U.S. commercial building energy standard ASHRAE/IESNA Standard 90.1. Appendix G, also known as the “Performance Rating Method,” provides a standard methodology for quantifying the efficiency of building designs that exceed the prescriptive requirements of the base standard. In this methodology, the energy efficiency of a building design (including alterations) is measured only in terms of operational energy costs; system capital and life cycle costs are ignored, as are energy consumption totals. Despite the fact that the standard practice of

building energy simulation for building design and renovation ignores comparison of energy consumption, the building energy simulation program requirements defined by ASNI/ASHRAE/IESNA Standard 90.1 provide a consistent approach for estimating and comparing building energy consumption. The most salient requirements include simulation program capabilities for explicitly modeling “8,760 hours per year; Hourly variations in occupancy, lighting power, miscellaneous equipment power, thermostat setpoints, and HVAC system operation, defined separately for each day of the week and holidays; Thermal mass effects; ten or more thermal zones; Part-load performance curves for mechanical equipment; capacity and efficiency correction curves for mechanical heating and cooling equipment; and air-side economizers with integrated control” (25). In practice building energy simulation is not intended as a prediction of actual performance – building energy modeling is merely a physically-based method for quantifying the energy (or cost) savings potential of alternative building designs (see Section 2.3).

Determination of the operational energy of commercial buildings is most often achieved through direct measurement. Energy consumption may be measured either through utility meters or building sub-meters that can provide more precise insight into the energy consumption of particular energy-consuming systems (e.g. lighting, heating, cooling, ventilation, etc.). Unfortunately, sub-metered energy consumption data is rarely available to building tenants/stakeholders for two main reasons: 1) Very few commercial buildings have energy sub-meters installed; and 2) Building owners may be reluctant to share energy consumption data with potential leasees. Existing building energy rating programs such as the ENERGY STAR Portfolio Manager program can provide insights into the relative performance of building alternatives, but most commercial buildings are not included in the program (see Section

2.2.1.1). Direct measurement provides the most accurate determination of *actual* energy consumption, but it provides little or no information on the use of energy-consuming systems. The energy consumption of a building is a function of the efficiencies of the installed energy-consuming systems, the occupant usage (duration and intensity) of the energy-consuming systems, and the exterior loads placed on the systems (e.g. incident solar radiation, ambient temperatures, etc.). For the purpose of determining an existing building's EUI, building energy consumption rating systems account for occupant usage and external loads according to aggregated categories of the number of occupants, operating shift hours, and climate zones (24, 76, 93). However, detailed occupant usage and exterior load data is rarely available to potential building tenants interested in estimating the potential energy consumption of their intended usage pattern in building/site alternatives. The framework developed in this dissertation employs a building energy simulation approach to provide a reasonable estimate of the potential energy consumption of building/site alternatives.

In the realm of building energy consumption research, much of the focus is improving the theoretical basis of building energy simulation programs, quantifying the energy efficiency or energy saving potential of building technologies, and quantifying the energy consumption of past, present, and future building stocks. Each of these research fronts is indirectly beneficial to the research objective of this dissertation. High-level, simplified building energy simulation programs can be helpful for estimating the relative energy performance of building/site alternatives for which little data is available. Research on the energy saving potential of building technologies can help building/site selection stakeholders identify the potential retrofit savings of building/site alternatives. Also, research on the energy consumption of building stocks can help building/site decision makers identify the most important data for estimating potential energy

consumption and for subsequently validating energy estimates and identifying the most efficient buildings/sites.

5.1.1. Components of Building Energy Consumption

In research and practice, quantification of building energy consumption is categorized into several main components of consumption: HVAC (heating, ventilating, and air conditioning), lighting, DHW, conveyances, and plug/process loads. These components comprise the elements of “whole-building” energy consumption. For facilities that include on-site energy production (e.g. photovoltaics and wind turbines), the net energy use of a building is the total energy production minus the total energy use. Figure 12 illustrates the energy flow of net facility energy use. The total annual utility energy consumption depends not only on the total annual on-site energy production, but also the coincident supply and demand over time. In order for facility energy production to mitigate total energy consumption it must either be supplied to the coincident loads at the facility or be exported to the utility supply grid for other coincident loads.

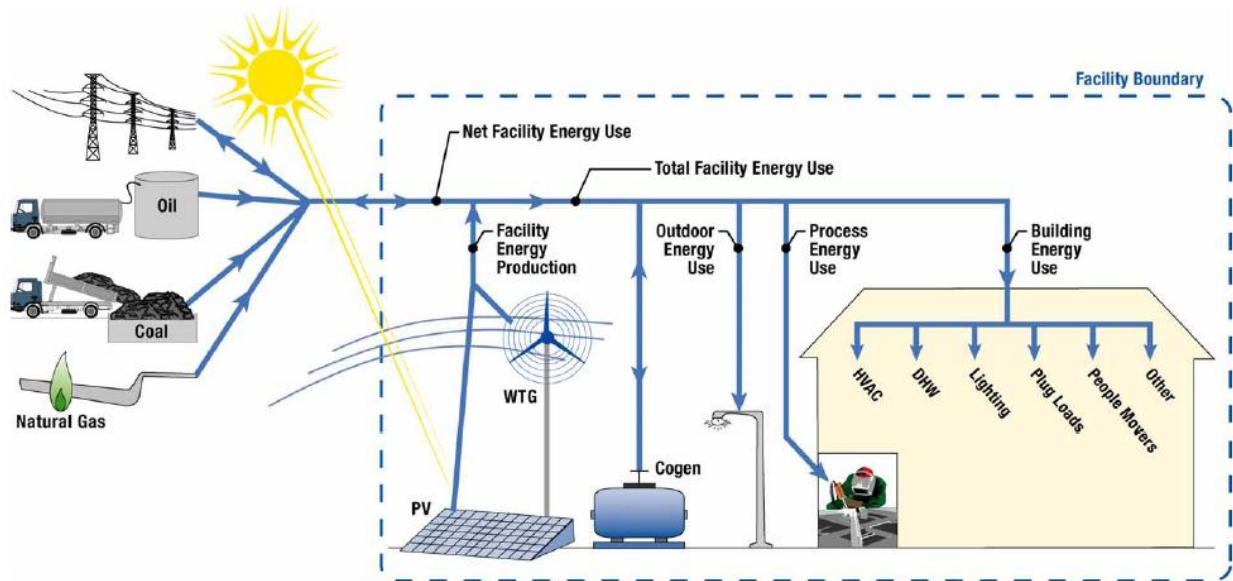


Figure 12: Energy flow diagram of net facility energy use, Source: (56).

The components of both facility energy use and facility energy supply fall under several energy sub-categories. Figure 13 shows the U.S. DOE's categorical flow chart of net facility energy use from its *Procedure for Measuring and Reporting Commercial Building Energy Performance*. Each of the energy use and production categories may be relevant to the energy consumption of a given commercial building, but of course not all energy use and production categories are equal in magnitude. The magnitude of energy use and production in each of the categories for a given set of building/site alternatives, each of which will be subject to the same usage pattern, will depend upon the unique physical/technological attributes of the buildings/sites.

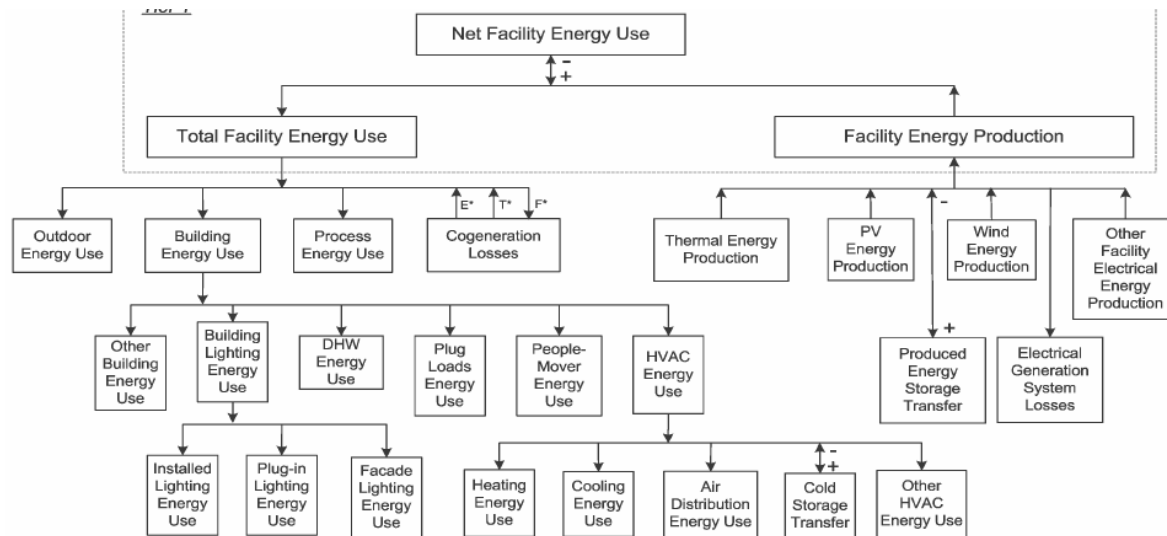


Figure 13: Categorical flow chart of net facility energy use, Source: (56).

Insight into the main components of commercial building energy consumption may be gleaned from data on the U.S. commercial building stock. Figure 14 shows the percentage energy end-use splits for U.S. commercial buildings in 2006. The data in Figure 14 is based on “primary” energy, which is not the metered energy consumption but rather the total amount of energy sourced from production facilities. It is clear from Figure 14 that approximately half of the energy consumption for commercial buildings in the U.S. is used for lighting, cooling, and heating. The relative proportions of space heating and space cooling will vary significantly between heating dominant and cooling dominant climate zones. For the purpose of evaluating the potential energy consumption performance of buildings/sites, it is worth noting that lighting is overall the largest end-use of commercial building energy. This fact is helpful for identifying the most important data for estimating potential energy consumption (see Section 5.2.1.1 Collect Building Energy System Parameter Data).

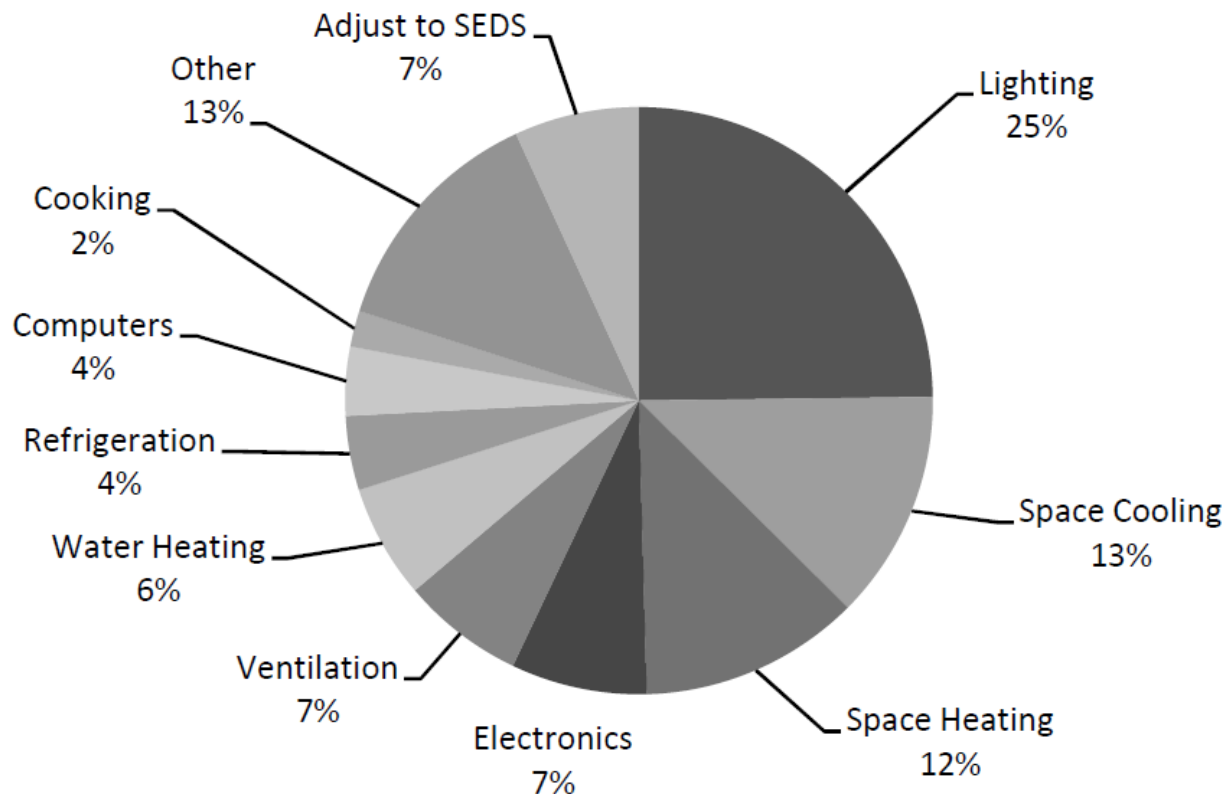


Figure 14: 2006 U.S. commercial buildings energy end-use splits, Source: (94).

Within the stock of commercial buildings, office buildings have a somewhat different end-use split of energy consumption. Figure 15 shows the energy end-use splits for U.S. commercial office buildings in 2003. The end-use splits are based on CBECS Table E1: Major Fuel Consumption by End Use for Non-Mall Buildings, Principal Building Activity: Office. The CBECS contains only “site” energy consumption data. Therefore, to convert the national CBECS data to “primary” energy consumption data the following electricity end-use splits were multiplied by a national source energy factor of 3.365 (95): cooling, ventilation, lighting, refrigeration, office equipment, and computers. For non-mall commercial office buildings, more than half of the space heating energy is supplied by non-electric sources. Figure 15 shows that for commercial office buildings, lighting is on average the most dominant energy end-use.

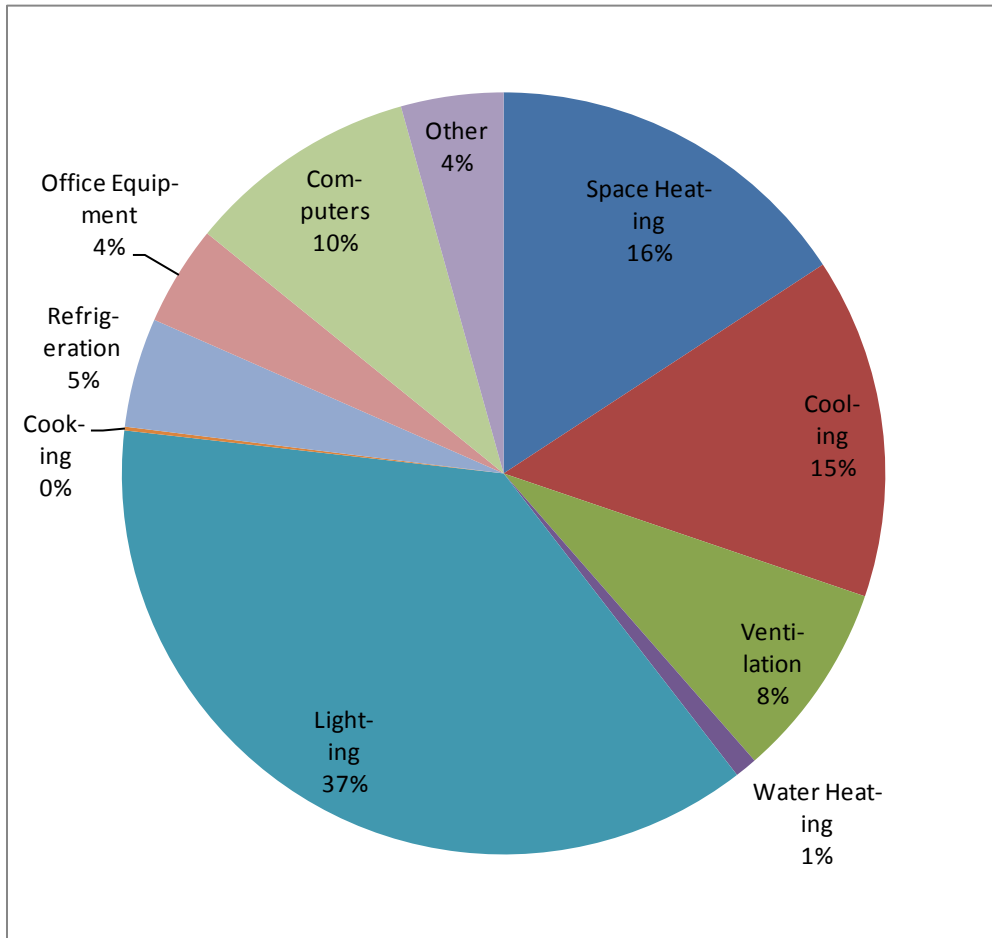


Figure 15: 2003 U.S. commercial office buildings energy end-use splits, Based on (76).

In terms of estimating commercial office building energy consumption, it is convenient that much of the energy is consumed by lighting systems. Conventional commercial office lighting systems are relatively easy to identify and model. That same is true for conventional electrical equipment loads, such as office computers. In contrast, heating, cooling, and ventilation energy consumption is a function of relatively complex thermal energy phenomena and operational sequences. Heating, cooling, and ventilation loads are influenced not only by external, weather-related loads on the building envelope, but also the occupancy of the spaces

and other heat-generating energy end-uses, namely lighting, computers, and other office equipment. Huang and Broderick provide an estimated breakdown of the aggregate component heating and cooling loads for large offices (90,000 – 140,000 SF) (96). According to the DOE estimates by Huang and Broderick, windows, walls, solar irradiance, lighting, and equipment constitute the majority of HVAC loads in large commercial office buildings.

5.1.1.1. Variation in Building Energy Consumption between Buildings/Sites

Effective evaluation of the relative energy performance of buildings/sites requires not only identification of the major categories of energy consumption, but also those categories that are likely to vary between building site alternatives. Variation in building energy consumption between buildings/sites can occur through variation in any of the three main factors influencing whole-building energy consumption (see Section 5.1):

1. Occupant usage (duration and intensity) of the energy-consuming systems.
2. Exterior loads placed on the systems (e.g. incident solar radiation, ambient temperatures, etc.).
3. Efficiencies of the installed energy-consuming systems.

The occupant usage includes the operation of lighting, heating, cooling, and ventilation systems (e.g. light switch operation, window shade operation, heating and cooling setpoints, etc.), as well as the direct heat gain of building occupants and occupant equipment (e.g. computers). The external loads are primarily the climatic conditions that exist at the exterior of the building envelope. The system efficiencies include not only the nameplate efficiencies of

system equipment/components (e.g. air-conditioner COP, insulation R-value, window SHGC, etc.) but also the design efficiency of the systems (e.g. envelope area, percent glazing, lighting power density, etc.). Figure 16 illustrates the influence between the main factors influencing building energy consumption. The occupant usage and external loads influence building energy consumption directly as a demand on the energy consuming systems, and indirectly as determinants of the operating points of systems with part-load efficiencies that deviate from full-load efficiencies (e.g. chiller efficiencies).

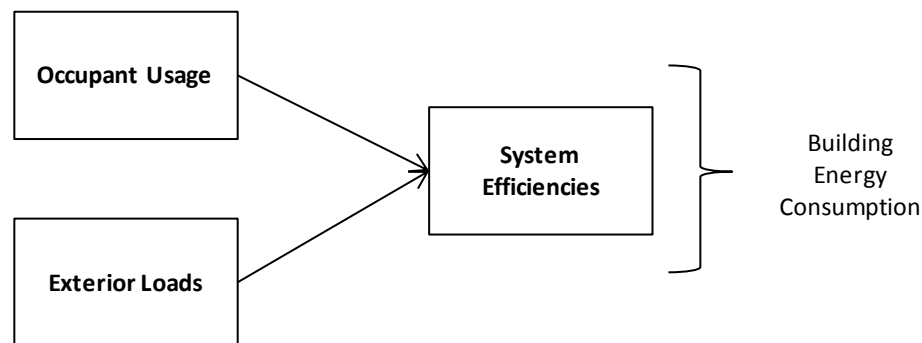


Figure 16: Main factors influencing building energy consumption.

In this building/site evaluation framework, much of occupant usage of the building is assumed to be independent of the building site characteristics. In particular, the building occupancy schedule, computer density and usage, and heating and cooling setpoints are assumed to be consistent between building/site alternatives. However, heating and cooling setpoints, as well as exterior lighting schedules may be controlled by building property managers and may vary between building/site alternatives. The evaluation framework is intended to account for such variations where they are known to exist.

5.1.1.1.1. Exterior Loads: A Note on Building/Site Microclimate

The exterior loads on building energy consumption are the result of both natural weather and built environment conditions. Research on variations in building exterior loads has proceeded within the sphere of urban microclimate research. Observational data has established the existence of urban heat islands in which surface and air temperatures within urban environments are several degrees above the temperatures in surrounding rural areas (97). Figure 17 shows an example Landsat satellite image of the surface temperature variations of a multi-nodal heat island in Atlanta, GA. Urban heat islands like the one illustrated in Figure 17 are the result of higher incident solar radiation absorption and thermal heat capacitance in urban infrastructure materials, as well as higher rates of heat rejection from combustion processes. According to Williamson and Erell, differences between urban and rural climates may be explained by five phenomena: “the radiation budget, sub-surface (storage) heat flux, advection, anthropogenic heat release, and turbulent heat transfer including the effects of vegetation” (60). In the U.S., the urban heat island effect is estimated to be responsible for 5 to 10 percent of urban peak electricity demand for air conditioning (59). During the heating season, the heat island can actually help to lower heating energy; In a heat island study of Athens, Greece, researchers have estimated that the heating load of urban buildings may be 30 to 50 percent lower than the heating load of buildings located in the suburbs (98).

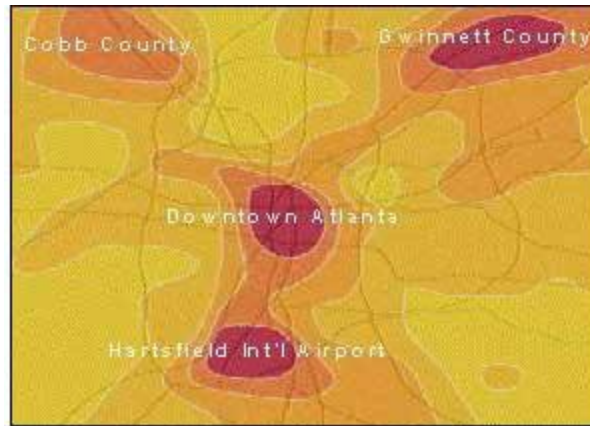


Figure 17: Landsat satellite image of multi-nodal heat island in Atlanta, GA, Source: (97).

The microclimate affecting the exterior load on a building/site is defined not only by the urban heat island, but also by the geometric and material conditions immediately adjacent to the building/site. Adjacent building structures and vegetation can provide shading that may influence both the incident solar radiation and the ambient (shade) temperatures. In developed areas, building heights and urban canyons produce variations in how heat is absorbed and by how much (99). The work of Williamson et. al suggests that not accounting for urban microclimate in computer simulations of building energy performance may result in estimates of heating and cooling energy consumption that deviate by as much as 10 percent (58).

Although urban microclimates are known to exist and are estimated to have a measureable impact on building energy consumption, building energy simulation practices in the AE industry have yet to incorporate the effects of microclimates. The main reason for this is a lack of microclimate datasets that sufficiently define regional variations in exterior loads. In building energy simulations of design alternatives, exterior loads are defined by weather data input files that represent a local typical meteorological year (TMY). TMY data “provides designers and other users with a reasonably sized annual data set that holds hourly

meteorological values that typify conditions at a specific location over a longer period of time, such as 30 years” (100). Unfortunately, TMY data is available for, at most, only a few locations within or surrounding a metropolitan region. In most cases, the weather data is based on observations from airport weather stations. The large, paved tarmacs of airports may influence both the temperature and wind readings at airport weather stations, and thus TMY data derived from such readings may not be representative of development areas within the region that have different geometric and material characteristics. Building energy simulation researchers and software developers have been exploring methods for enhancing the resolution of regional weather datasets. So far, these efforts have centered on creating synthetic weather datasets for an array of regional locations based on reference weather stations and land-use characteristics (34, 101, 102). For the majority of building design and selection contexts, the use of synthetic weather datasets is highly unlikely. Most building energy simulation professionals remain reliant on publicly provided TMY datasets.

Incorporation of microclimate effects in building energy simulation practices may be limited by the availability of high resolution weather data, but most all building energy simulation programs are capable of incorporating some of the effects of shading from adjacent structures and vegetation. The theoretical foundations of surface shading vary between different simulation engines; different programs often include different effects within their respective calculations (i.e. some programs consider surface reflection for only daylighting calculations whereas other programs consider surface reflection for both daylighting and thermal calculations). The importance of building shading modeling capabilities depends upon the degree to which incident solar radiation affects building energy consumption. For many modern

commercial office buildings, building energy consumption is dominated by internal loads such as lighting and equipment (see Section 5.1.1).

5.1.1.1.2. System Efficiencies: A Note on Air Infiltration / Exfiltration

Building outdoor air infiltration is one of the main heating and cooling loads for commercial buildings and yet outdoor air infiltration is one of the least documented or standardized variables in building energy simulation. Outdoor air infiltrates building spaces through two main pathways: 1) building envelope design openings (e.g. operable windows and doorways) and 2) leakage through less-than-airtight envelope surfaces. Infiltration by this second pathway is a function of the design and construction of the envelope – both the airtightness of the design/construction and the amount of envelope area. Infiltration by the first pathway is a function of both design/construction and the use of the building (e.g. use of doorways and operable windows). In building energy modeling, infiltration resulting from operable windows and doorways is typically based on conservative rule of thumb estimates. For commercial office buildings in North America, most all windows are inoperable – if any windows are operable, the infiltration associated with their operation is likely part of a natural ventilation analysis. The case studies in this dissertation do not involve natural ventilation designs/analyses. Thus, the main pathways for infiltration in the case studies are doorways and leakage through envelope surfaces. Outdoor air infiltration creates significant heating and cooling loads and energy consumption for buildings and thus management of outdoor infiltration is a common strategy for managing building energy consumption. The impact of infiltration on energy consumption is dependent upon the amount of building pressurization. With sufficient positive pressurization, air exchange across the building envelope will shift from wind-driven infiltration to building pressurization-

driven exfiltration. If all air leakage occurs by exfiltration, and if the total amount of exfiltration is less than the total requirement for outdoor air ventilation, then the exfiltration will pose no direct additional heating or cooling load – building air that would otherwise be exhausted as relief air at the air handler is instead exfiltrated through the building envelope. Thus, the infiltration load experienced in commercial office buildings is a function of the envelope design/construction and the ventilation design. The infiltration rate of the building envelope may be estimated either from a bottom-up inventory of building envelope components with known or estimated component infiltration rates or from average infiltration rates for wall or space types. The bottom-up component approach is more meticulous, but not necessarily more accurate since accurate infiltration data for envelope components is rarely available for building designers, let alone potential building tenants. The wall area or space type approach offers a level of calculation detail that is arguably more consistent with the low-level of data precision and accuracy. The building energy simulation practice literature provides very little guidance for modeling outdoor air infiltration rates, although some guidance is available from DOE, NIST, and COMNET (*103, 104, 105*).

Building envelope fan pressurization tests indicate that in the southern U.S., the average airtightness values for commercial buildings three stories or less is 2.3 CFM per SF of above grade envelope area (at 0.3 in w.g.) (*104*). Based on building envelope test data, the average airtightness for envelopes built according to “good construction practices” is 0.24 CFM/SF, and the “best achievable” airtightness is 0.04 CFM/SF (*104*). An airtightness is not representative of the rate of infiltration under normal commercial building pressurization (actual infiltration would be less). DOE’s Infiltration Modeling Guidelines for Commercial Building Energy Analysis provides tabulated data on airtightness/leakage rates (CFM/SF at 0.3 in. w.g.)

for both envelope components and a total building leakage (103). The DOE Guidelines also provide a methodology for converting airtightness/leakage values to building infiltration rates. According to the example conversion provided in the Guideline, the conversion factor is approximately $0.2016/1.8 = 0.122$ CFM/SF of above grade envelope area (103). ± According to the Commercial Buildings Energy Modeling Guidelines and Procedures from COMNET, the infiltration rate appropriate for the purpose of federal tax credit calculations is 0.038 CFM/SF (105).

5.1.2. Tools for Energy Estimation and Evaluation

The evaluation framework utilizes existing tools for building energy estimation and evaluation. The following sub-sections describe the utility of the existing energy estimation and evaluation tools and the rationale for utilizing the tools in the framework calculation procedures.

5.1.2.1. Building Energy Simulation Software

Building energy simulation software provides the capability for estimating the potential energy consumption of building designs, as well as existing buildings. Many different types of building energy modeling/simulation tools are available for commercial buildings, ranging from high-level conceptual design models with default definitions of building systems, to low-level final design models with detailed user-defined inputs of building systems (33). In general, high-level conceptual design energy models require less time to develop than do more detailed design models. Such simulation programs are attractive for modeling the performance of several different buildings for which less than complete specification data are available. The integration of building energy simulation programs with building information models (BIM) has helped to

streamline integrative design processes that account for building energy consumption. In both building research and design, interest has been growing in building energy simulation tools that provide energy performance estimates early in the design process. One such popular development is Autodesk's Project Vasari, which supports energy "performance-based design via integrated energy modeling and analysis features," using both geometric and parametric modeling (106). Although integrated programs like Project Vasari provide rapid development and feedback on building design concepts, invariably user input specification is sacrificed for development speed. This means that model users are either limited to the default system specifications or must manually adjust the default system specifications. A high-level simulation program may support the fastest development of multiple building alternatives, but the time required to modify model inputs so that they are consistent with actual building/site alternatives will in many cases offset the original savings in time and effort. For the building/site evaluation framework developed in this dissertation, the simulation program should strike a balance between ease and precision of model input specification.

The selection of a simulation program for the development and demonstration of the building/site evaluation framework was based on several criteria. First and foremost, the simulation program must allow user control of input specifications that define the similarities and differences between building/site alternatives (see Section 4.2.2). This requirement includes specification of building occupancy, building geometry, internal and external miscellaneous thermal loads, HVAC system type and control setpoints/schedules, lighting system type and schedules (including daylighting), and building envelope physical properties. Additionally, the program should allow for the definition of input parameter uncertainty for the purpose of analyzing the sensitivity of energy estimates to input uncertainty (see Sections 5.2.3 and 5.2.4).

In the interest of developing a framework that may be applied beyond the realm of this dissertation research, the simulation program should be one that is widely accepted/utilized and meets the requirements of ANSI/ASHRAE/IESNA Standard 90.1. The pre-eminent simulation programs that satisfy all of these criteria (save for uncertainty analysis) are eQUEST/DOE2.2 (107) and EnergyPlus (108). EnergyPlus is the U.S. DOE's official whole building energy simulation program designed for use by engineers, architects, and researchers. Unfortunately, the poor user interface, complex input specification requirements, and slower runtime of EnergyPlus have resulted in minimal adoption by industry engineers and architects. In industry practice, eQUEST/DOE2.2 has been the preferred, freely available building energy simulation software. eQUEST serves as a graphical user interface for the simulation engine DOE2.2 – the former official U.S. DOE simulation program. Despite continual advances in the calculation capabilities and recent industry collaborations to make EnergyPlus the preferred and standard whole-building simulation program for architects and engineers (109), the promise of EnergyPlus remains a promise.

Based on the aforementioned relative benefits, eQUEST/DOE2.2 was selected as the preferred simulation program for applying the energy evaluation framework. As was previously mentioned, eQUEST/DOE2.2 does not include genetic functionality for uncertainty analysis. However, it is possible to perform uncertainty analysis with eQUEST/DOE2.2 by integrating it with other programs that allow scripted iterations/variations of simulation runs. One such program is ModelCenter by Phoenix Integration, Inc. (110). ModelCenter provides a graphical user interface for scripting trade studies in programs that utilize text input and output files and command line execution. The trade study functions include sensitivity analysis and Monte Carlo analysis of input variable uncertainty. With licenses priced around \$10,000, ModelCenter is an

expensive program that is likely beyond the financial reach or interest of many AE firms. However, ModelCenter was available for this research through a College of Engineering software license at Georgia Tech. In the absence of ModelCenter, it is possible, albeit more time consuming, to script sensitivity analysis and Monte Carlo analysis simulations using the Perl programming language.

The use of building energy simulation software for estimating the potential performance of buildings/site presents introduces several issues related to accuracy and uncertainty (see Section 4.2.5.1.1). Even if calibrated building energy simulation models were available for each of the building alternatives, several accuracy and uncertainty difficulties would remain. According to Huang & Franconi, calibration of simulated energy consumption to measured data is difficult for the following reasons: “(1) the scarcity of detailed measured data - typical surveys provide only yearly or monthly aggregate totals, while detailed hourly data, particularly end-use data, exists only for very few buildings; (2) the large variations of energy use among any collection of buildings - surveys often show differences by factors of 5 or more, making it difficult to perform a meaningful calibration; (3) the multiple degrees of freedom in the calibration – there are so many building inputs that can be modified that the end result might be completely serendipitous” (111).

5.1.2.2. CBECS

In the U.S., the CBECS (Commercial Building Energy Consumption Survey) is the primary inventory of measured commercial building energy consumption. The first CBECS survey was conducted in 1979 and the latest available survey was conducted in 2003. A 2007 survey was conducted but failed to yield statistically significant estimates of building counts,

energy characteristics, consumption, and expenditures (76). The 2003 CBECS contains over 4,800 commercial buildings with a total floorspace of over 71.6 billion SF. The CBECS database serves as a resource for estimating building energy consumption characteristics and trends for various building types and U.S. regions. CBECS provides estimates of average building EUI for commercial buildings including offices. However, the survey sample size is too small to represent the average EUI of a particular metropolitan region or even a particular state (see Section 4.2.4.2).

In cooperation with the U.S. DOE, the U.S. EPA explored measures of building service (i.e. normalizing units) in the CBECS database that may be helpful for expressing the EUI or predicting the energy consumption of commercial office buildings. Table 5 shows the CBECS independent variables identified by the U.S. EPA as potentially important for offices, bank/financial institutions, and courthouses.

Table 5: CBECS Independent Variables Identified by U.S. EPA as Potentially Important for Offices, Bank/Financial Institutions, and Courthouses, Source: (55).

Variable	Description
SQFT8	Square footage
WKHRS8	Weekly hours of operation
NWKER8	Number of employees during the main shift
PCNUM8	Number of personal computers
SRVNUM8	Number of servers
PRNTRN8	Number of printers
MNFRM8	Mainframe computer room (yes/no)
SRVFRM8	Server farm (yes/no)
TRNGRM8	Computer-based training room (yes/no)
COPRN8	Number of photocopiers
RFGWIN8	Number of walk-in refrigeration units
RFGOPN8	Number of open refrigerated cases
RFGRSN8	Number of residential refrigerators
RFGCLN8	Number of closed refrigerated cases
RFGVNN8	Number of refrigerated vending machines
COOK8	Energy used for cooking (yes/no)
FDRM8	Commercial food preparation area (yes/no)
SNACK8	Snack bar (yes/no)
FASTFD8	Fast food or small restaurant (yes/no)
CAF8	Cafeteria or large refrigerator (yes/no)
ELEVTR8	Elevators (yes/no)
LABEQP8	Laboratory equipment used (yes/no)
SKYLT8	Skylights/atriums designed for lighting (yes/no)
HEATP8	Percent heated
COOLP8	Percent cooled
HDD658	Heating degree days

The variables accounted for in the normalization of building energy performance include only those that are included in the CBECS data fields and that are statistically correlated to building EUI. Only a handful of the variables shown in Table 5 were found to be statistically

correlated to building EUI. Table 6 shows the CBECS key explanatory variables that can be used to estimate the expected average source EUI in offices, bank/financial institutions, and courthouses.

Table 6: CBECS Key Explanatory Variables That Can Be Used to Estimate the Expected Average Source EUI in Offices, Bank/Financial Institutions, and Courthouses, Source: (55).

Characteristics
Natural log of gross square feet
Number of personal computers (PCs) per 1,000 square feet
Natural log of weekly operating hours
Natural log of number of workers per 1,000 square feet
Heating degree days times Percent of the building that is heated
Cooling degree days times Percent of the building that is cooled

It is interesting to note the absence of building design variables, save for the natural log of the gross square footage. Several design or operation normalization variables not included in the above tables may impact whole-building energy consumption, such as lighting operation schedules, and HVAC operation schedules and setpoints. Explicitly including and modeling such additional variables in a building energy simulation may help to better characterize the potential whole-building energy consumption in relation to a particular building design and a particular occupants use/operation. The identified CBECS explanatory variables may be useful for highly aggregate estimates of building energy consumption, but are not promising for a building/site specific estimate.

Despite its limited value for estimating the potential energy performance of a particular building/site, the CBECS database can be helpful for verifying and/or benchmarking the energy estimates produced from building energy simulations. In particular the EUI data in CBECS can

serve as a reference for determining the reasonableness of energy simulation outputs. Table 7 shows data on the consumption of electricity for office buildings in the 2003 CBECS. The electricity EUI's in Table 7 provide an approximate indication of the expected range of performance for office buildings in the national building stock. When using this aggregate data, one must keep in mind that the values are averaged across climate zones.

Table 7: Consumption of Electricity for Office Buildings, 2003 CBECS (76)

	Electricity Consumption			Distribution of Building-Level Intensities (kWh/SF)		
	per Building (MWh)	per SF (kWh)	per Worker (MWh)	25th Percentile	Median	75th Percentile
All Buildings	226	14.9	*	3.8	8.8	18.1
All Office Buildings	256	17.3	7.5	6.5		
Type of Office Building:						
Admin. / Professional	254	17.0	7.3	6.7	11.0	15.0
Bank / Financial	217	20.4	9.7	14.5	22.2	29.5
Government	325	17.7	6.8	8.1	10.7	19.3
Other Office	249	16.5	7.5	4.9	10.1	15.5

For referencing the energy performance of newer, higher performing buildings, ASHRAE/IES Standard 100-2006, *Energy Efficiency in Existing Buildings* provides a useful alternative to the CBECS database (112). Along with guidance for analyzing and improving the energy efficiency of existing buildings, ASHRAE Standard 100 contains EUI targets for various types of commercial buildings (see Table 8).

Table 8: ASHRAE/IES Standard 100-2006 Energy Use Intensity Targets, Source: (113)

	EUIs by Building Type by Climate Zone (kBTU/SF-yr)														
	ASHRAE Climate Zone														
Commercial Building Type	1A	2A	2B	3A	3B	3C	4A	4B	4C	5A	5B	6A	6B	7	8
Admin. / Professional Office	39	40	39	42	33	33	46	40	40	48	42	54	47	58	81
Bank / Other Financial	55	57	56	59	46	47	65	56	57	68	59	76	67	82	115
Government Office	49	50	49	52	41	42	57	49	50	60	52	67	59	72	101
Medical Office (non-diag.)	33	34	33	35	28	28	39	34	34	41	36	46	40	49	69
Mixed-Use Office	45	46	45	48	38	39	53	46	47	56	48	62	55	67	94
Other Office	38	39	38	40	32	32	44	38	39	47	40	52	46	56	78

5.1.2.3. DOE Benchmark/Reference Buildings

One way of benchmarking the energy performance of commercial buildings in the U.S. is through the use of benchmark building models that represent the average performance characteristics of commercial buildings in the U.S. building stock. The U.S. National Renewable Energy Laboratory (NREL) of the U.S. DOE has developed a set of commercial benchmark/reference building models that “directly characterize more than 60% of the commercial building stock and are very similar to other commercial building types” (114). The building models are based on the distribution and performance of buildings in the Commercial Building Energy Consumption Survey (CBECS) database. The reference building model set includes fifteen commercial building types, and for each building type three vintages and sixteen U.S. locations, including Atlanta, GA. Included in the model set are three commercial office types, shown in Table 9 below.

Table 9: DOE Commercial Benchmark/Reference Building Office Dataset. Based on (76, 114)

Building Type	Size (SF)	No. of Floors	Nearest CBECS Size Classification (SF)
Small Office	5,500	12	1,001 – 5,000
Medium Office	53,630	3	5,001 – 50,000
Large Office	498,590	1	> 50,000

Although the characteristics of the DOE benchmark/reference buildings are derived from the CBECS, the “small, medium,” and “large” sizes of the building models do not entirely correspond with the building sizes in the CBECS (see 2nd and 4th columns in Table 9). For each of the three office types, there are models for three building vintages: Pre-1980 construction, post-1980 construction, and new construction. For each building type, the different vintages have the same building form and area and the same operation schedules, but have different envelope insulation, lighting levels, and HVAC equipment types and efficiencies (114). The new construction models comply with the minimum requirements of ANSI/ASHRAE/IESNA Standard 90.1-2004 (114). The benchmark/reference building models are available as EnergyPlus building energy simulation input files.

The DOE benchmark/reference building models of commercial office buildings offer a meaningful and representative baseline of average building energy performance. The developers of the benchmark/reference building models stress that the “reference building model definitions are not intended to act as targets to rate the energy performance of single existing or proposed buildings” (114). For the purpose of this research, the DOE benchmark/reference buildings are

not employed as targets, but rather to serve as case studies of older building energy performance and input variable sensitivity analysis.

The DOE benchmark/reference office buildings strike a balance between simplicity and robustness in modeling building energy consumption. The most significant simplifications/approximations of the model files may be found in the envelope construction (no doors are included and infiltration is modeled evenly across the building exterior), the building ventilation (no bathroom exhaust fans), the building space allocation and associated people, lighting, and equipment heat gains (the entire space allocation is assumed to be of the open office type, with even distribution of internal heat gains), and the HVAC zoning (building core and perimeter zoning). The benchmark/reference building model files otherwise provide a detailed model of building geometry, building envelope thermal properties, building use schedules, internal heat gains, and HVAC systems components and operation.

5.1.2.3.1. Conversion of DOE Benchmark/Reference Buildings from EnergyPlus to eQUEST

The availability of the DOE benchmark/reference buildings in only the EnergyPlus format presents a challenge for using the benchmark/reference buildings in eQUEST (the software format selected for this research effort). Utilization of the DOE benchmark/reference buildings models in this research effort required a manual translation of the EnergyPlus files to eQUEST files. Translation of the files began with the post-1980 construction, medium office model files. To translate the model inputs, the EnergyPlus input file (.idf file) was inspected through the EnergyPlus IDFEditor tool. Additionally, the model input and output summary spreadsheets accompanying the DOE files were used to both interpret the model inputs and to calibrate the new eQUEST model outputs to the given EnergyPlus model outputs. The

calculation input variables and algorithms of the EnergyPlus and eQUEST softwares are not congruent; thus many translation iterations were necessary to calibrate the eQUEST model outputs to the EnergyPlus model outputs. Some of the most significant differences between the programs that produce discrepancies in the model outputs include differences in the variables defining vapor compression efficiency curves, differences in the accounting of radiant fraction heat gain from equipment, differences in the calculation of heat transfer from ceiling plenums, differences in the estimation of air infiltration, differences in outdoor air damper control, and differences in heating and cooling coil temperature resets. The manual translation of the models from EnergyPlus to eQUEST required some modification of the inputs related to the aforementioned discrepancies so that the total energy outputs from the eQUEST energy simulation converged to the outputs from the EnergyPlus energy simulation, and so that the differences in the building energy components were minimized. Table 10 and Table 11 show comparisons of building electrical energy and gas consumption for the DOE benchmark/reference building translation from EnergyPlus to eQUEST.

Table 10: Comparison of Annual Building Electrical Energy Consumption for DOE Benchmark/Reference Building Translation from EnergyPlus to eQUEST: Medium Office, Post-1980 Construction, Atlanta, GA

Building Energy Component	EnergyPlus (kWh x 1000)	eQUEST (kWh x 1000)	Difference (kWh x 1000)	Difference (percent)
Space Cooling	158.98	172.66	13.68	9%
Space Heating	108.01	98.63	-9.38	-9%
Ventilation Fans	21.7	32.19	10.49	48%
Pumps & Auxiliaries	0.08	0.30	0.22	275%
External Usage (Lighting)	77.79	77.81	0.02	0%
Miscellaneous Equipment	296.26	300.08	3.82	1%
Area Lights	264.34	268.81	4.47	2%
Total	927.15	950.49	23.34	3%

Table 11: Comparison of Annual Building Gas Consumption for DOE Benchmark/Reference Building Translation from EnergyPlus to eQUEST: Medium Office, Post-1980 Construction, Atlanta, GA

Building Energy Component	EnergyPlus (MBtu's)	eQUEST (MBtu's)	Difference (MBtu's)	Difference (percent)
Space Heating	47.28	45.73	-1.55	-3%
Hot Water	29.58	26.57	-3.01	-10%
Total	76.86	72.30	-4.56	-6%

The translation and calibration effort yielded a convergence of total building energy consumption; however, considerable differences in estimated building energy component consumption could not be further mitigated without sacrificing the convergence to total building energy consumption. The remaining differences in energy consumption indicate the sensitivity of calculation outputs to discrepancies in input variables and calculation algorithms. Incidentally, it

is generally understood in the field of building energy simulation that large discrepancies in simulation outputs between different simulation software packages are common and difficult to resolve. For example, in the California Energy Commission's effort to transition from DOE2.1 to EnergyPlus for the non-residential Title-24 (building energy standard) compliance calculations, heating energy output discrepancies of 30 to 60 percent and cooling energy output discrepancies of 15 to 20 percent were encountered (115). The impact of such discrepancies on this doctoral research effort is not all that severe, since the central purpose of this research is to develop a framework of internally consistent calculations of energy consumption. Although the use of different building energy simulation software will yield different calculation results, the focus here is the comparison of results within a common simulation program.

The overall reasonableness of the eQUEST DOE benchmark/reference building results may be understood by comparing the energy consumption categories to national building energy consumption data. Figure 18 shows the building energy consumption components for the eQUEST DOE Benchmark/Reference Building: Medium Office, Post-1980 Construction, Atlanta, GA. The relative proportions of energy end-uses are similar to those shown in Section 5.1.1 Components of Building Energy Consumption. The main difference is the larger proportion of energy consumed for miscellaneous office equipment. This difference is not a concern for the building case studies since the amount of energy-consuming, miscellaneous office equipment will be a consistent, user-specified input for each of the building/site alternatives.

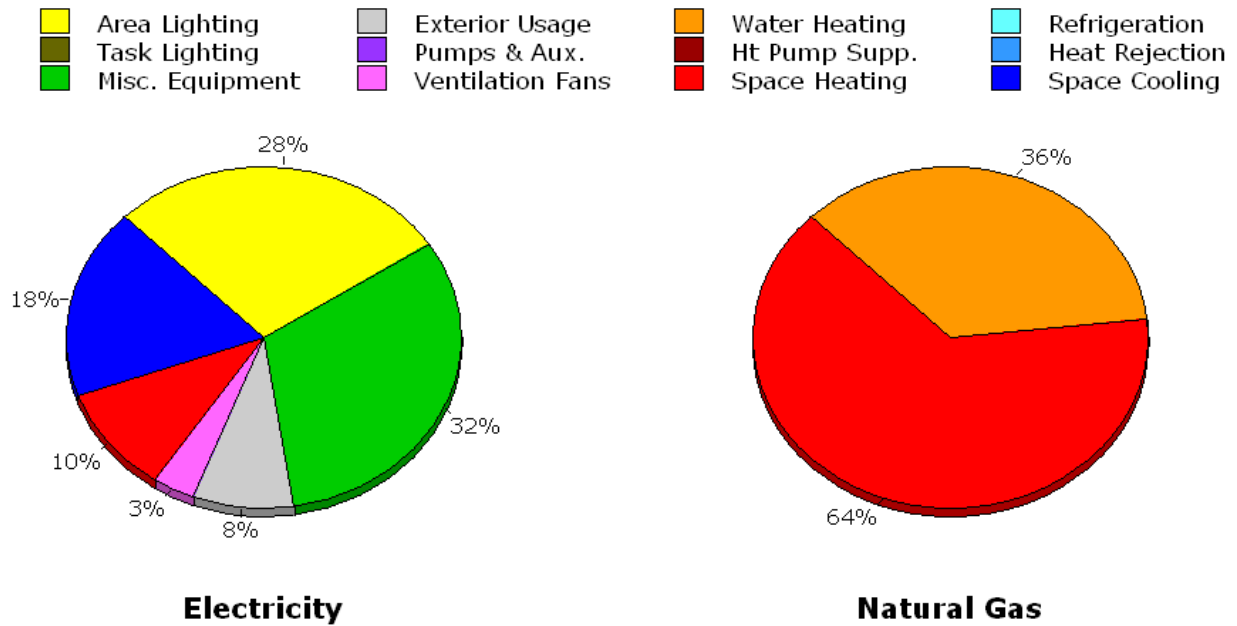


Figure 18: Building energy consumption components for eQUEST DOE Benchmark/Reference Building: Medium Office, Post-1980 Construction, Atlanta, GA.

5.2. Calculation Procedures for Building Energy Consumption and GHG Emissions

The core of the building evaluation framework is the calculation procedures for estimating the building energy consumption and GHG emissions performance. The calculation procedures were developed to operationalize the conceptual framework of building performance evaluation in Chapter 4. Figure 19 outlines the overall process for estimating building energy and GHG performance. For the most part, the calculation procedures follow a linear process, save for the handling of parameter uncertainty.

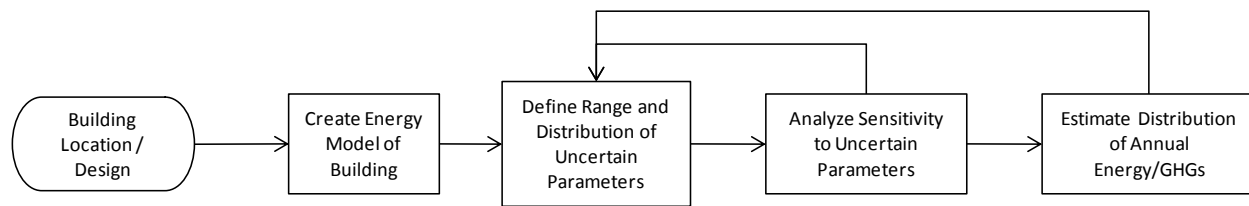


Figure 19: Process for estimating building energy and GHG performance.

The following sections detail and describe the calculation procedures for estimating the building energy consumption and GHG emissions performance.

5.2.1. Define Building Alternatives Choice Set

The first step in the series of evaluations procedures is to define the building alternatives choice set. The building alternatives choice set is the subset of buildings in the building stock that the firm is considering for occupancy. This building evaluation framework is not designed to model the building alternatives selection process, but rather to quantify the performance of the alternatives choice set. The productive performance of the building alternatives choice set is related to the building services provided by each of the building alternatives (see Section 4.2.1). The building services may be summarized by the square footage of the space types in the architectural program, as shown Table 12. The ranges in building space size represent the ranges present within the alternatives choice set – the range in service that is understood to be acceptable or desirable for the occupant. The spaces in Table 12 without a “min – max” range are spaces that may be non-essential for satisfying the needs of the occupant.

Table 12: Example Summary of Building Spaces.

Space Category	Space Type	Size (SF)
Total	Total	min - max
Work Space	Office	min - max
	Conference	min - max
Support Space	Break Areas	min - max
	Mech. / Elect.	--
	Lobby (shared)	min - max
Circulation	Stairs (on floor)	--
	Elevator (on floor)	--

The building services afforded by the alternatives choice set are a product of the physical building sub-systems (e.g. building envelope, lighting, heating, cooling, ventilation, etc.). In order to quantify the energy consumed by each of these sub-systems, it is necessary to define the building energy system parameters. Thus, in addition to determining the space sizes of the building alternatives, building energy system parameter data must either be collected or assumed.

5.2.1.1. Collect Building Energy System Parameter Data

The goal of collecting building energy system parameter data is to sufficiently define the building design and operation elements so that the building energy consumption can be estimated within an acceptable range of uncertainty. The collection of building energy system parameter data is subject to practical constraints on the quantity and precision of data that may feasibly be collected. Some energy system parameter data may be entirely inaccessible, due to physical barriers to observation (e.g. building envelope insulation) or due to privacy barriers (e.g. building owner's reluctance to allow field inspection). In the interest of minimizing uncertainty, a building energy system data collection effort should include collection of data that is readily

observable from a public perspective. The most readily observable data are the geometry and material properties of the building exterior. Resources like Google® Earth and Google® Maps with Street View effectively enable observation of building exterior geometry and material properties without any need for visiting the building/site. Admittedly, some exterior details such as exterior lighting and glazing thermal properties cannot be determined by aerial and elevation imagery alone. In light of national average data on commercial office building energy consumption (see Section 5.1.1), one of the most essential building energy system design parameters to be included in a data collection effort is the installed lighting power density (or total installed lighting power). Interior lighting very often comprises a significant portion of whole-building energy consumption, and the installed lighting power density can be ascertained through a simple field inspection. The energy system elements to include in the data collection effort should mirror what would be included in a building energy audit (116). Building design drawings and specifications may help to supplement data collection by field inspection.

5.2.2. Create Energy Model of Building

In this evaluation framework, a building energy modeling approach is taken to estimate the annual building energy consumption. In particular, a detailed modeling approach is utilized so that the energy consumption of the unique design and operation characteristics of the energy systems in each of the building alternatives may be sufficiently accounted for. Both time and data constraints limit the feasible (or reasonable) degree of precision for the energy model inputs and estimates. In instances where building-specific data are unavailable or where time does not permit incorporation of building-specific data, parameter assumptions can be helpful for completing the building energy models as long as either the assumption are consistent between

the alternatives or the parameter uncertainty is defined (see Section 5.2.3). One aspect of the building energy models that shall remain consistent between the alternatives is the building occupancy.

5.2.2.1. Define Intended Occupancy Schedule

Pre-occupancy definition of the intended use of an office building is a familiar exercise to building design and energy simulation professionals. In building energy simulations which model heating, ventilating, air conditioning, lighting, and conveyance energy consumption associated with time variant building occupancy, the building occupancy must be defined over time, as required by the Energy Cost Budget method and Performance Rating method of ANSI/ASHRAE/IES Standard 90.1 (25). Such simulations require definition of hourly levels of occupancy for each of the types of expected daily operations, typically a day schedule for Monday through Friday, a day schedule for Saturday, and a day schedule for Sunday/Holidays. These schedules are assigned to a seven-day weekly schedule and an annual calendar. The result is a simple hourly definition/estimation of the building occupancy throughout an entire calendar year.

The building occupancy and operation schedules shall be defined for each hour of the day (workday, Saturday, Sunday/Holiday). It is quite unlikely that a firm can accurately predict the hourly, weekly, and seasonal occupancy patterns for a future occupancy. Fortunately, modeling guidance on the definition of building schedules for energy simulation is available in the User's Manual for ASHRAE Standard 90.1 (see Table 13). Since each of the building alternatives would serve the same potential group of building occupants, the building occupancy schedule shall remain consistent in each of the building energy models.

Table 13: Default Building Occupancy and Operation Schedules, Source (77)

Hour of Day (Time)	Schedule for Occupancy Percent of Maximum Load			Schedule for Lighting Receptacle Percent of Maximum Load			Schedule for HVAC System			Schedule for Service Hot Water Percent of Maximum Load			Schedule for Elevator Percent of Maximum Load		
	Wk	Sat	Sun	Wk	Sat	Sun	Wk	Sat	Sun	Wk	Sat	Sun	Wk	Sat	Sun
1 (12-1 am)	0	0	0	5	5	5	Off	Off	Off	5	5	4	0	0	0
2 (1-2 am)	0	0	0	5	5	5	Off	Off	Off	5	5	4	0	0	0
3 (2-3 am)	0	0	0	5	5	5	Off	Off	Off	5	5	4	0	0	0
4 (3-4 am)	0	0	0	5	5	5	Off	Off	Off	5	5	4	0	0	0
5 (4-5 am)	0	0	0	5	5	5	Off	Off	Off	5	5	4	0	0	0
6 (5-6 am)	0	0	0	10	5	5	Off	Off	Off	8	8	7	0	0	0
7 (6-7 am)	10	10	5	10	10	5	On	On	Off	7	7	4	0	0	0
8 (7-8 am)	20	10	5	30	10	5	On	On	Off	19	11	4	35	16	0
9 (8-9 am)	95	30	5	90	30	5	On	On	Off	35	15	4	69	14	0
10 (9-10 am)	95	30	5	90	30	5	On	On	Off	38	21	4	43	21	0
11 (10-11 am)	95	30	5	90	30	5	On	On	Off	39	19	4	37	18	0
12 (11-12 pm)	95	30	5	90	30	5	On	On	Off	47	23	6	43	25	0
13 (12-1 pm)	50	10	5	80	15	5	On	On	Off	57	20	6	58	21	0
14 (1-2 pm)	95	10	5	90	15	5	On	On	Off	54	19	9	48	13	0
15 (2-3 pm)	95	10	5	90	15	5	On	On	Off	34	15	6	37	8	0
16 (3-4 pm)	95	10	5	90	15	5	On	On	Off	33	12	4	37	4	0
17 (4-5 pm)	95	10	5	90	15	5	On	On	Off	44	14	4	46	5	0
18 (5-6 pm)	30	5	5	50	5	5	On	On	Off	26	7	4	62	6	0
19 (6-7 pm)	10	5	0	30	5	5	On	Off	Off	21	7	4	20	0	0
20 (7-8 pm)	10	0	0	30	5	5	On	Off	Off	15	7	4	12	0	0
21 (8-9 pm)	10	0	0	20	5	5	On	Off	Off	17	7	4	4	0	0
22 (9-10 pm)	10	0	0	20	5	5	On	Off	Off	8	9	7	4	0	0
23 (10-11 pm)	5	0	0	10	5	5	Off	Off	Off	5	5	4	0	0	0
24 (11-12 am)	5	0	0	5	5	5	Off	Off	Off	5	5	4	0	0	0
Total/Day	920	200	60	1040	280	120	1600	1200	0	537	256	113	555	151	0
Total/Week	48.60 hours			56.00 hours			92.00 hours			30.54 hours			29.26 hours		
Total/Year	2534 hours			2920 hours			4797 hours			1592 hours			1526 hours		

Wk = Weekday

The one schedule in Table 13 that is most likely to be defined by observable building energy system data is the HVAC system operating schedule. HVAC systems serving multiple office tenant spaces in a multi-tenant office building may have operating schedules that are defined and controlled by a building manager.

5.2.2.2. Allocate Shared Loads for Shared Services

One of the unique building energy modeling challenges of this evaluation framework is the need to allocate shared energy loads in proportion to the shared services of the respective building systems (see Section 4.2.1). Considering that some of the energy-intensive building

services are shared between multiple tenant spaces (e.g. parking lighting, lobby space, roof shelter, floor slab insulation, etc.), and that a portion of these services are utilized by the selected tenant space, a formula is needed to appropriately allocate the energy consumption of shared services to the selected tenant space. Equation 2 provides a means for allocating energy estimates in the building energy simulation model to the selected tenant space.

Equation 2

$$E_{Total_t} = E_{floor_t} + [(E_{top_hypo} - E_{floor_t}) + (E_{bot} - E_{bot_hypo}) + E_{misc_load} + E_{comm}]/N_f + E_{dhw_t}$$

where: E_{Total_t} = Total energy consumption allocated to tenant space.

E_{floor_t} = Energy consumption of lighting, HVAC, and miscellaneous equipment for tenant floor.

E_{top_hypo} = Energy consumption of lighting, HVAC, and miscellaneous equipment on hypothetical top floor.

E_{bot} = Energy consumption of lighting, HVAC, and miscellaneous equipment on bottom floor (excluding common lobby area).

E_{bot_hypo} = Energy consumption of lighting, HVAC, and miscellaneous equipment on hypothetical bottom floor (excluding common lobby area).

E_{misc_load} = Energy consumption of miscellaneous, shared loads (elevators, parking lighting, entryway lighting, and signage lighting).

E_{comm}	= Energy consumption of lighting, HVAC, and miscellaneous equipment in common lobby area.
N_f	= Number of floors in building.
E_{dhw_t}	= Domestic hot water energy consumption for tenant floor.

Equation 2 includes variables referring to “hypothetical” top and bottom floors. The hypothetical top floor is a floor space that is identical to the tenant space (mid-floor) except that a roof surfaces is included in its envelope. By taking the difference in energy consumption between this hypothetical top floor and the actual tenant space, and then dividing by the number floors (each with the same square footage), the added envelope load of the roof is added to the selected tenant space. The hypothetical bottom floor is a space that is identical to the actual bottom floor (lobby and banking area) except that the hypothetical bottom floor does not include a bottom floor slab exposed to the parking garage space. Thus, by taking the difference in energy consumption between the actual bottom floor and the hypothetical bottom floor, and then dividing by the number of floors, the added envelope load of the floor slab is added to the selected tenant space.

5.2.3. Define Range and Distribution of Uncertain Parameters

The challenge of collecting data for a large number of building energy system parameters will likely result in remaining uncertainty in many, if not most, of the building energy system parameters. Quantification of the input parameter uncertainty can help to determine if a best performing building alternative can be ascertained from the available data, or if further data collection is necessary to reduce the uncertainty in the estimated building performance. For most

all building energy system parameters, evaluation of the uncertainty will be by non-statistical methods (i.e. “Type B”, see Section 4.2.5.2). To define the uncertainty of a design or operation parameter, a range and distribution of values must be defined. According to the NIST’s *Guidance for Evaluating and Expressing Uncertainty of NIST Measurement Results*, “the rectangular distribution is a reasonable default model in the absence of any other information. But if it is known that values of the quantity in question near the center of the limits are more likely than values close to the limits, a triangular or a normal distribution may be a better model” (91). Industry literature, such as ASHRAE Standard 90.1 and ASHRAE Handbooks can be helpful for defining reasonable ranges in parameter values.

It is important to note that the geometry can be defined/modeled within a very narrow range of uncertainty. Furthermore, lighting, which is generally the most impactful single parameter in commercial building energy consumption, can generally be defined/modeled within a narrow range of uncertainty (relative to HVAC efficiency and controls, and building envelope construction and integrity). The building occupant and equipment heat gains are undoubtedly essential parameters in building energy simulation, but they are not inherent to the performance of an existing building. The occupants and equipment will in essence be supplied by the decision maker, and as such, any uncertainty associated with these parameters should be consistent between each of the existing building alternatives under evaluation. Therefore, it is not necessary to explicitly define the uncertainty of these parameters in each of the building alternative models.

5.2.4. Analyze Sensitivity to Uncertain Parameters

Upon defining the input parameter uncertainty and incorporating the uncertainty into the building energy model, the next logical step is to analyze the impact of the uncertainty on the

estimated annual building energy consumption. In fields of engineering design, a sensitivity analyses of multiple design variables is commonly conducted as a “design of experiments.” A design of experiments allows investigation of the joint effects of changes in multiple input factors. A design of experiments and sensitivity analysis helps to identify which variables, if any, have an outsized influence on the uncertainty in the estimated energy consumption, and for which it may be beneficial to reduce the parameter uncertainty through further data collection. Additionally, a sensitivity analysis for the first of several building energy models can help to simplify the definition of input parameter uncertainty in subsequent energy models by helping to identify which uncertain parameters have negligible impact on the estimated annual energy consumption (sometimes referred to as “factor screening”).

In the first pass of modeling the annual building energy consumption of a building alternative, it is most prudent to define the range and distribution for any parameter that is expected to significantly impact the estimated annual energy consumption. In a detailed building energy simulation program like eQUEST/DOE2.2 or EnergyPlus, this may apply to hundreds of input parameters. In a sensitivity analysis trade study, increasing the number of uncertainty specifications will not only slow down the model development process, but will also increase the time required for running the sensitivity analysis simulations. In a full factorial design of experiments the number of runs required for a 2 level definition of input variation (min value and max value) is equal to 2^k runs, where k is equal to the number of input factors. If a building energy simulation takes 30 seconds to run and there are 100 uncertain input parameters, then the amount of computation time required for full factorial design of experiment would be 1.21×10^{24} years! Clearly an alternative sampling procedure is necessary to reduce the number of runs and total computation time. Two sampling options frequently used in the design of experiments

literature are Latin hypercube sampling and the Morris Method for global sensitivity analysis. Latin hypercube sampling ensures representation of the distribution of all of the input variables and results in more precise estimation of the output mean and standard deviation than do random or stratified sampling methods (117). The Morris Method allows an even more efficient sensitivity analysis (reduced number of runs) and allows direct observation of the elementary effects of the inputs (mean and standard deviation) (118). Direct observation of the elementary effects is made possible by a “one at a time” sampling for input parameter values. The Morris Method was selected for sensitivity analysis in the application of this building evaluation framework, due to the efficiency of the computation and the insights gained into the elementary effects.

5.2.4.1. Example Sensitivity Analysis

The DOE Reference Building for a Post 1980 Construction Medium Office building is used here to illustrate exploration of the sensitivity of the total annual energy consumption to the uncertainty of simulation input variables. The input variables and their associated uncertainty are listed below in Table 14. These variables represent the parameters that are suspected to have the most impact on total annual energy consumption and that would be uncertain from the perspective of an existing building inspection. The values of the variables are defined by a mean value “Ref”, and min and max values. It should be noted that in the building evaluation framework presented in this dissertation, the occupant heat gain (variable 1 in Table 14) and equipment power density (variable 3 in Table 14) would *not* be included as uncertain variables (see Section 5.2.3). Also, the number of variables in Table 14 is much less than the number of variables that would potentially be investigated in a building alternative. Only fifteen variables

are shown here for the purpose of providing a simplified, illustrative example of the sensitivity analysis process.

Table 14: Example Input Variable Uncertainty in DOE Medium Office, Post 1980 Construction, Atlanta, GA

Variable			Units	Ref	Min	Max
1	Occupant heat gain	total heat gain	Btu/h-person	409.00	350.00	450.00
2	Lighting	LPD	W/SF	1.57	1.00	2.00
3	Equipment	EPD	W/SF	1.00	0.75	1.50
4	Slab on Grade	Floor U-Value	But/h-SF-deg F	0.33	0.25	0.50
5	Construction	wall insul conductivity	But/h-ft-deg F	0.03	0.02	0.04
6	Construction	wall insul thickness	ft	0.17	0.08	0.25
7	Construction	roof insul conductivity	But/h-ft-deg F	0.03	0.02	0.04
8	Construction	roof insul thickness	ft	0.35	0.25	0.50
9	Window	Conductance	Btu/h-degF	0.72	0.60	0.85
10	Window	Shading Coefficient	NA	0.29	0.25	0.35
11	DHWH	Heat Input Ratio	Btu/Btu	1.28	1.20	1.35
12	DHWH	Peak load	gpm	0.50	0.40	0.60
13	Cooling	Electric Input Ratio	Btu/Btu	0.36	0.30	0.50
14	Heating (gas)	Heat Input Ratio	Btu/Btu	1.24	1.20	1.30
15	Infiltration	Air Changes	Multiplier	1.00	0.50	1.50
	Infiltration	Air Chg P NS	AC/Hr	0.98	0.49	1.47
	Infiltration	Air Chg P EW	AC/Hr	1.03	0.52	1.55
	Infiltration	Air Chg Plnm GM	AC/Hr	0.41	0.21	0.62
	Infiltration	Air Chg Plnm T	AC/Hr	3.76	1.88	5.64

For each of the numbered variables listed in Table 14, the Morris Method was used to generate a matrix of input variable values that may be used to test the sensitivity of total building energy consumption. A copy of the MATLAB script used to generate the matrix is shown in Appendix C. From the generated matrix, a sensitivity analysis was run in ModelCenter and the

results were imported into MATLAB to plot the mean and standard deviation of the elementary effects. The mean and standard deviation of elementary effects of the uncertain building energy simulation input variables for the DOE Medium Office, Post 1980 Construction model using the Morris Method are shown in Figure 20.

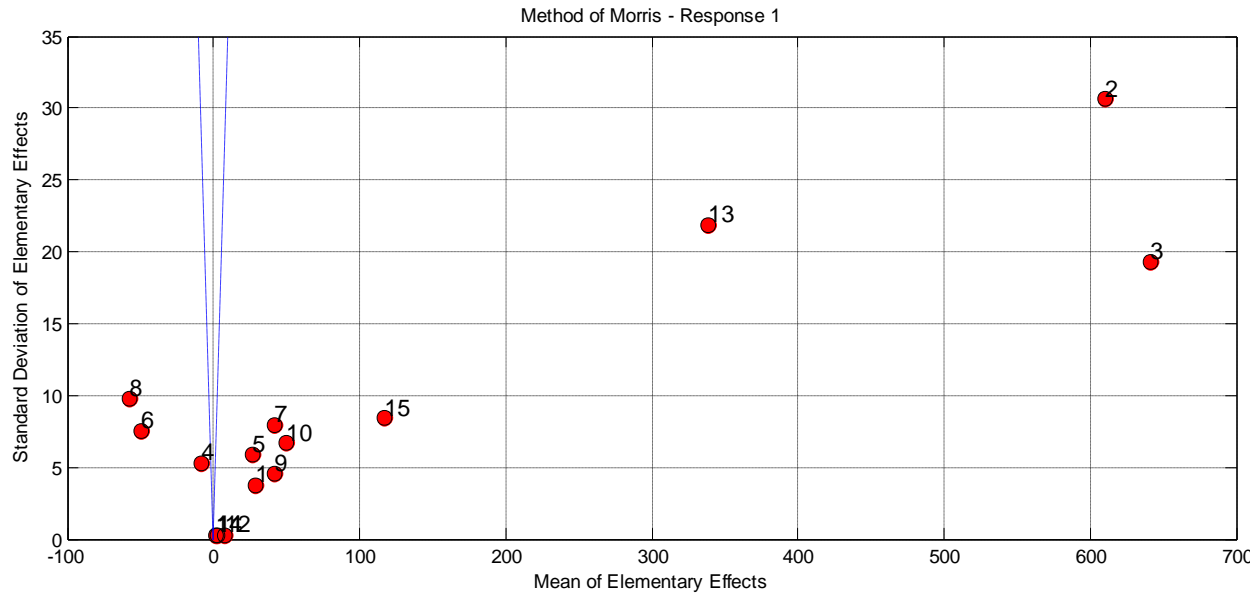


Figure 20: Example mean and standard deviation of elementary effects of uncertain building energy simulation input variables for DOE Medium Office, Post 1980 Construction, Atlanta, GA model using the Morris method.

Figure 20 indicates that three variables (lighting power density, equipment power density, and cooling electric input ratio) dominate the mean effect on total annual energy consumption. Furthermore, the relatively high standard deviation of elementary effects of these variables indicates that the effects of these parameters are dependent upon other input variables. The domestic hot water heating variables had a negligible effect on total annual energy consumption. In the interest of limiting the sensitivity analysis to only those variables that have the most significant elementary effects (and simplifying subsequent calculations), the uncertainty of the

domestic hot water parameters, the slab-on-grade U-Value, the wall insulation conductivity, and the occupant heat were eliminated.

With a reduced subset of uncertain variables, it becomes more feasible to conduct a central composite design of experiments for sensitivity analysis. Figure 21 shows an example sensitivity analysis of uncertain building energy simulation input variables for the DOE Medium Office Post 1980 Construction model using a central composite design of experiments.

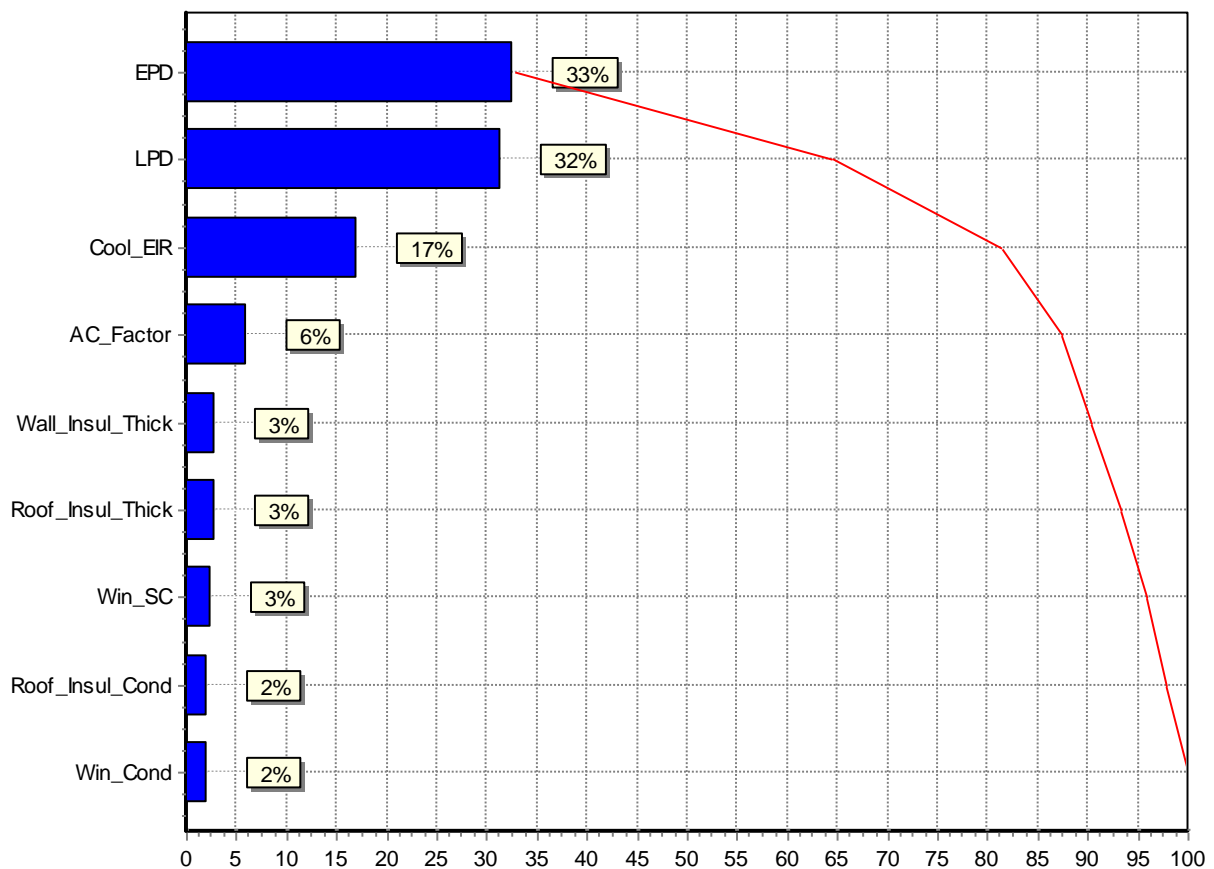


Figure 21: Example sensitivity analysis of uncertain building energy simulation input variables for DOE Medium Office, Post 1980 Construction, Atlanta, GA model using a central composite design of experiments.

Again it should be noted that the equipment power density would *not* be included as an uncertain variable in each of the models of building energy consumption in the building energy performance evaluation framework. Removing “EPD” from the sensitivity analysis shown in Figure 21 would result in an increased percent sensitivity for each of the remaining variables. The results shown in Figure 20 and Figure 21 should not be interpreted as a generalization of the input variables having the greatest effect on estimated building energy consumption. The sensitivity of a particular building alternative will depend upon the unique variables and uncertainty ranges present in the building design/operation.

5.2.5. Monte Carlo Simulation / Propagation of Uncertainty

The input variables with the greatest impact on output uncertainty shall retain their uncertainty definitions so that the distribution of probable output values may be estimated. Ideally the uncertainty definitions of all of the input variables would be retained; however, doing so can be unnecessarily cumbersome. In this evaluation framework, uncertain input variables with a mean effect of less than one percent of the output mean are regarded as having a negligible impact on the output uncertainty. Input variables with a mean effect of one percent or greater will retain their uncertainty definitions and the uncertainty will be propagated to the output distribution.

The propagation of uncertainty in the estimated annual building energy consumption is accomplished through a Monte Carlo simulation approach (see Section 4.2.5.2). In a Monte Carlo simulation the input parameter values are randomly selected for each annual building energy simulation run. The building energy simulation runs are iterated for each of the randomly selected combinations of input variable values. After many simulation runs (e.g. 1000) a PDF

may be generated from the histogram of simulation outputs. Figure 22 shows an example Monte Carlo analysis of uncertain building energy simulation input variables for the DOE Medium Office, Post 1980 Construction, Atlanta, GA model. The output values are approximately distributed normal, which should be expected from inputs with rectangular uncertainty distributions (evidence of the Central Limit Theorem).

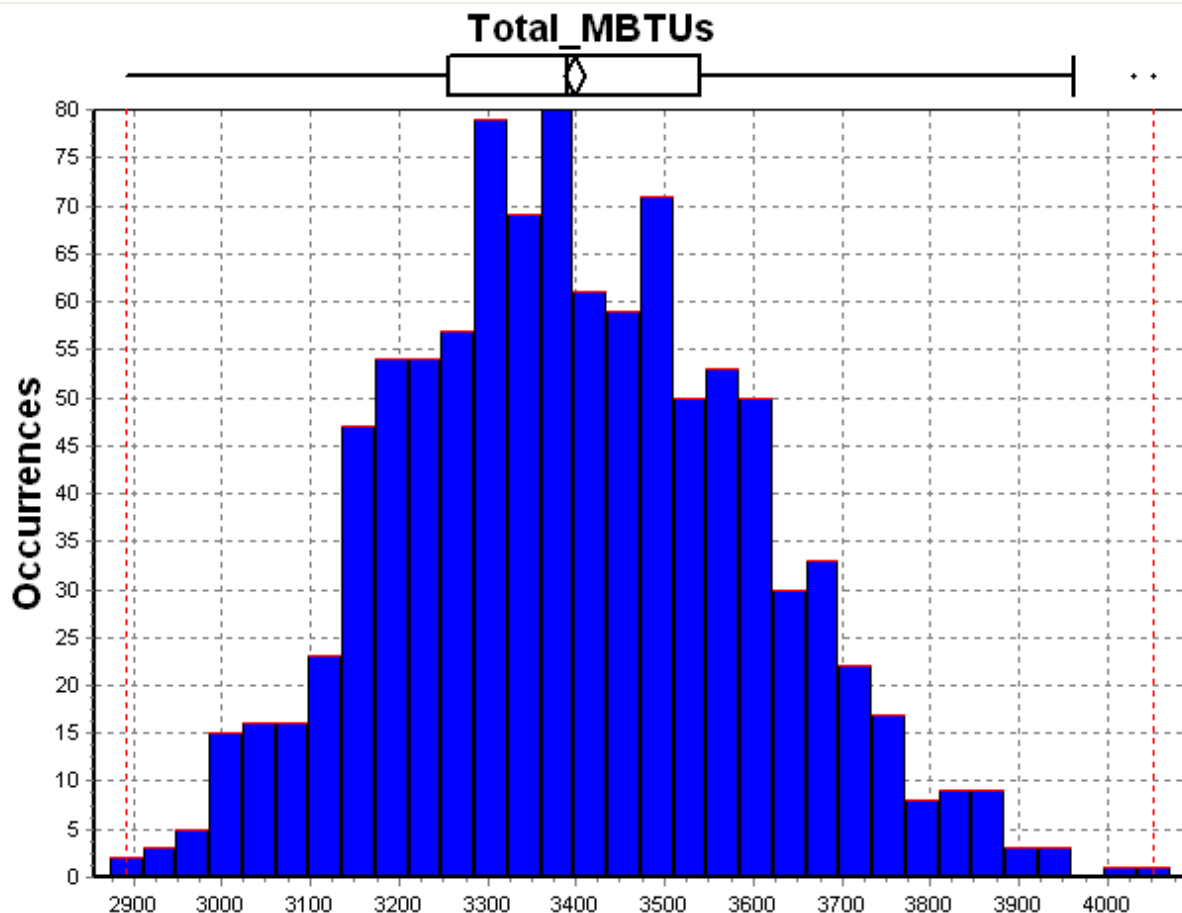


Figure 22: Example Monte Carlo analysis of uncertain building energy simulation input variables for DOE Medium Office, Post 1980 Construction, Atlanta, GA model.

The propagation of uncertainty through Monte Carlo simulation allows the decision-maker to see if the relative energy performance of the building alternatives can be ascertained

from the available design/operation data. It may be that the PDFs of the building alternatives overlap so much that the best performing site cannot be determined. If it is possible to obtain more precise input parameter data from the building/site, then the uncertainty definition and Monte Carlo simulation processes may be repeated to see if a high performing building alternative emerges with a degree of uncertainty that is acceptable to the decision maker.

5.2.6. Calculate Upstream Energy and GHG Emissions

Upon estimating the direct annual utility energy consumption, the next step is to estimate the upstream energy consumption and the direct and upstream GHG emissions. The basic method used for estimating upstream energy and GHG emissions is to apply energy/emission factors from the literature to the estimated quantities of energy consumption. Emission factor data from the literature is entirely deterministic, not because the emission factors have no associated uncertainty, but because no uncertainty data is provided. Regardless, the uncertainty associated with emission factors for utility energy supplied to building alternatives located within the same region would be the same for each alternative. The following sections describe the data and calculation methods for estimating the primary energy consumption, as well as the direct and upstream GHG emissions.

5.2.6.1. Site Energy vs. Primary Energy

In the life cycle energy perspective of this evaluation framework, the energy consumed both at the building/site and in the energy supply chain is taken into account. In the literature, the energy consumed directly on site is called “site energy” and the total energy consumed both on site and upstream in the supply chain is called “primary energy” or “source energy.” The U.S.

DOE has compiled and published source energy factors for each of the NERC (North American Electrical Reliability Council) grid regions (interconnections) and each state in the U.S. (95). These energy factors incorporate the transmission and distribution (T&D) losses, as well as the “precombustion effects” (i.e. extraction, processing, and transportation of fuels). These factors are arguably the most frequently used, as they are embedded within the eQUEST/DOE2.2 output reports (107).

5.2.6.2. GHG Emissions

The main, national source of GHG emission factor data for electric utility energy in the U.S. is the U.S. EPA’s eGRID (119). eGRID contains purchased electricity emission factors for all of the NERC grid regions and states in the U.S. In the GHG emission inventory protocols, these emission factors are applicable to Scope 2 emissions. The direct combustion GHG emissions from purchased electricity are calculated from Equation 3 and Equation 4 below:

Equation 3

$$E_{(CO_2)fac} = q_{fac} \times F_{(CO_2)grid}$$

$$\text{where } E_{(CO_2)fac} = \text{CO}_2 \text{ emissions [lbs CO}_2\text{]}$$

$$q_{fac} = \text{electricity consumed [MWh]}$$

$$F_{(CO_2)grid} = \text{CO}_2 \text{ emission factor [lbs CO}_2\text{/MWh]}$$

Equation 4

$$E_{fac} = q_{fac} \times F_{grid}$$

$$\text{where } E_{fac} = \text{CH}_4 \text{ (or N}_2\text{O) emissions [lbs CH}_4 \text{ (or N}_2\text{O)}\text{]}$$

$$q_{fac} = \text{electricity consumed [GWh]}$$

$$F_{grid} = \text{CH}_4 \text{ (or N}_2\text{O) emission factor [lbs CO}_2\text{/GWh]}$$

The emission factors for CH₄ and N₂O used in Equation 4 are expressed in larger units of energy than are the emission factors for CO₂ used in Equation 3 (GWh vs. MWh) since electrical power generation generally produces much less CH₄ and N₂O per unit of energy generated. Multiplying the estimates of CO₂, CH₄, and N₂O by the respective 2007 IPCC global warming potentials yields the direct combustion GHG emissions in CO₂e.

For fossil fuel combustion on-site, CO₂ emissions are estimate from Equation 5 below:

Equation 5

$$F_{(CO_2)fuel} = H_{(v)fuel} \times C_{(H)fuel} \times \theta \times K$$

$$\text{where } F_{(CO_2)fuel} = \text{CO}_2 \text{ emission factor [kg CO}_2\text{/gallon]}$$

$$H_{(v)fuel} = \text{heat content [Btu/gallon]}$$

$$C_{(H)fuel} = \text{carbon content [kg C/Btu]}$$

$$\theta = \% \text{ oxidized (assumed to be 100\%)}$$

$$K = 44/12 \text{ [mol. wt. of CO}_2\text{/mol. wt. of C]}$$

Once the CO₂ emissions are calculated, the next step is to calculate the CH₄ and N₂O emissions. The CH₄ and N₂O emissions from stationary combustion utilize technology specific default emission factors. These default emission factors are given on per unit of energy basis (g/MBtu) in the GHG emission inventory protocols. The following equation is used to calculate CH₄ and N₂O emissions:

Equation 6

$$E_{fuel} = Q_{(h)fuel} \times F_{fuel}$$

where E_{fuel} = CH₄ (or N₂O) emissions [g CH₄ (or g N₂O)]

$Q_{(h)fuel}$ = fuel combusted [MBtu]

F_{fuel} = CH₄ (or N₂O) emission factor [g CH₄/MBtu (or g N₂O /MBtu)]

In keeping with the life cycle analysis perspective of this research, the GHG emissions associated with the upstream fuel-energy supply chain are to be estimated as well. It should be noted that the eGRID emission factors (Scope 2 emissions) do *not* account for T&D losses, nor do they account for precombustion effects (Scope 3 emissions). Upstream emission factor data for purchased electricity or fossil fuel combustion may be sourced from the U.S. DOE (95), or from the author's previous research into estimation of life cycle GHG emissions (120, 121).

CHAPTER 6

ESTIMATION OF TRANSPORTATION ENERGY CONSUMPTION AND GHG EMISSIONS

6.1. Site Transportation Energy Consumption Estimation in Research and Practice

Estimation of site transportation energy consumption has yet to become a standard or common activity within the fields of infrastructure planning and engineering. Site transportation energy consumption has received some attention in life cycle analysis and built environment research literature (2, 12, 48), and somewhat indirectly in building rating systems (16, 20, 21), but a process for estimating, comparing, and evaluating site transportation energy consumption for location alternatives has yet to emerge. Estimation of site transportation energy consumption (and GHG emissions) has yet to be formalized into planning activities, but this is not to say that resources are entirely lacking for such an endeavor. In the field of transportation planning, there are several existing tools that may be utilized for estimating the potential energy consumption associated with commercial office site alternatives. The following sub-section describes the capabilities of these tools and their application to the evaluation framework presented in this dissertation.

6.1.1. Tools for Energy Estimation

6.1.1.1. Travel Surveys

The primary information source for regional travel behavior is regional travel surveys. The basic purpose of regional travel surveys is to sample individual and household travel activity (i.e. revealed travel preferences). The most common and pertinent travel activity variables

captured by regional travel surveys include trip purposes, mode choice, trip time (and/or distance), and origin/destination locations. The three largest surveys of regional passenger travel are the U.S. Census long form (decennial), the U.S. American Community Survey (1, 3 and 5 year), and the National Household Travel Survey (NHTS). Designed primarily for characterizing travel activity trends of and between regions, states, or metropolitan statistical areas (MSAs), these surveys provide very limited data for estimating travel activity *within* an urbanized area. The decennial U.S. Census long form and the 5 year American Community Survey (ACS) provide travel activity data for the smallest geographic divisions of national surveys: U.S. Census block groups. There are several notable limitations of available travel survey data:

“For the 2000 Census the Census Bureau data disclosure rules limited the availability of JTW data, particularly at detailed geography. More importantly for future analyses, the American Community Survey (ACS) has replaced the Decennial Census Long Form. With the advent of the ACS, both the quality and level of detail of the JTW flow data may be further diminished. The ACS is a continuous survey with a smaller sample with margins of error that are higher than the Decennial Census Long Form and small area data will be available only for multiyear periods. Further, recent rulings by the Census Bureau’s Disclosure Review Board (DRB) keeping a threshold of 3 unweighted records per category of means of transportation to work makes it very difficult for the transportation community to get the required data that will help arrive at informed decisions regarding transportation policy” (122).

Recognizing the need to summarize census transportation data for state and regional transportation planning activities, the Federal Highway Administration has created the Census

Transportation Planning Products (*123*), which provide tabulated data up to the 2000 decennial U.S. Census. Additionally, the U.S. Census Bureau has created the Longitudinal Employer-Household Dynamics (LEHD) program, which combines federal and state employment data with U.S. Census data to help characterize place of work and journey to work activities. The LEHD program is particularly helpful for identifying and visualizing worker commute sheds in urbanized areas. Figure 23 below shows an example labor commute shed map for the Georgia Institute of Technology census tract.

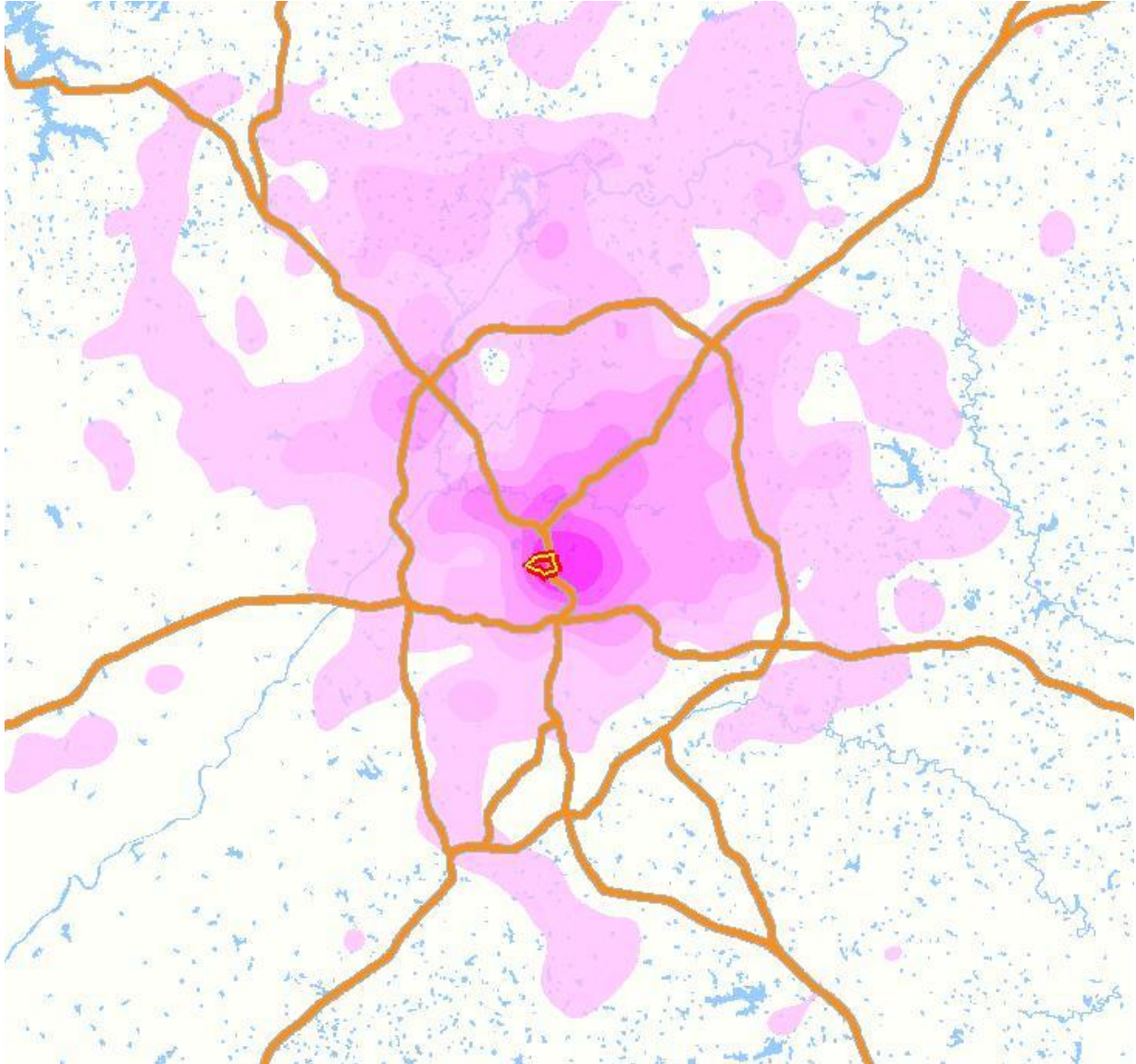


Figure 23: Map of Georgia Institute of Technology census tract commute shed, Source: (124).

Travel survey resources like the LEHD and the CTPP provide useful information on the origin-destination flows for (primarily) journey-to-work trips, but these survey resources are insufficient for estimating the associated energy consumption. The main piece of information lacking in these resources is the network travel time and distance between origins and

destinations. This data is essential for estimating the physical work/energy required for accessing locations within a region.

6.1.1.2. Regional Travel Demand Models

The need for regional transportation network travel data (e.g. motorized VMT) between origins and destinations for current and future years has been addressed by the development of regional travel demand models. Used by metropolitan planning organizations (MPOs), travel demand models have been developed to estimate the regional impact of planned transportation infrastructure and operations projects on air quality conformity, congestion mitigation, and other regional planning concerns. Most regional travel demand models employ a 4-step modeling structure for estimating travel activity: 1) Trip generation; 2) Trip distribution; 3) Mode choice; and 4) Network assignment. These 4-steps represent an iterative process that is calibrated and validated with data from both regional travel surveys and transportation network vehicle counts. The first step, trip generation, is based largely on the individual and household trip frequency data from regional travel surveys. The distribution of trips incorporates a travel cost function and transportation network data to generate a synthetic origin-destination table of person trips for a variety of trip types. The most common method used for trip distribution is the gravity model, represented by Equation 7:

Equation 7

$$T_{ij} = T_i \frac{A_j f(C_{ij}) K_{ij}}{\sum_{j=1}^n A_j (C_{ij}) K_{ij}}$$

where T_{ij} = trips from zone i to zone j

T_i = trips from zone i

A_j = trips attracted to zone j

$f(C_{ij})$ = travel cost function (friction factor, typically travel time)

K_{ij} = calibration (socioeconomic) factor

The gravity model is so called because it matches the mathematical form of Newton's law of gravity. The travel cost function is based on iterations of the estimated network performance resulting from the network assignment (step 4). The gravity model of trip distribution is based on the assumption that persons select trip destinations that satisfy their activity demands while minimizing travel cost (e.g. travel time). This assumption plays a significant role in the resulting estimates of trip distance between origins and destinations. For estimates of journey to work trip attractions, a gravity model may select trip producers (household origins) that are closer than those in reality.

The estimated mode choice is typically based on a logit model of mode choice probability. A logit model represents the discrete choice of alternatives based on the estimated utility of the alternatives. The estimated utility of the alternatives is in turn based on tangible attributes, such as out of pocket cost, in-vehicle travel time, and out-of-vehicle travel time. The final modeling step, network assignment, incorporates a shortest path algorithm (e.g. Dijkstra's algorithm) to determine the network links used to complete a trip.

There are many identified shortcomings in the 4-step travel demand modeling process which deserve some attention. One fundamental critique is that "the process is not behavioral in nature; that is, it is not based on a coherent theory of travel behavior and is not well suited to representing travelers' responses to the complex range of policies typically of interest to today's

planners” (44). The development of agent-based models has attempted to improve the underlying travel behavior theory and internal consistency of the 4-step models, but agent-based models face enormous challenges in calibrating and validating the travel behavior of the hour-by-hour travel behavior of a disaggregate population of agents. Additionally, “conventional travel demand models make use of networks, both highway and transit, in which impedances are averages over an extended period, reflect no uncertainty or unreliability, and are not representative of the conditions that would be expected or found by an individual traveler at the time a trip choice is made” (44). Another major critique of travel demand models is their poor representation of uncertainty. “Most travel forecasting models produce a single answer, although the model is estimated, calibrated, and validated on the basis of data sets subject to sampling and other errors. There are many sources of error and uncertainty in travel demand forecasting, but end users of most travel forecasts would not be aware of these limitations” (44).

Despite their many limitations, regional travel demand models are very often the exclusive resource for disaggregate, sub-regional travel activity data (albeit synthetic). Regional travel demand models are not intended for estimating sub-regional travel patterns, but offer the best available resource for comparing the potential trip activity for various sites within a region (see Section 2.5.2).

6.1.1.3. Energy and Emissions Software

A common activity for transportation engineers and planners is to quantify the criteria air pollutant (CAP) emissions of transportation infrastructure or operations projects. Whether performed at a regional scale for air quality conformity analysis, or at a project/corridor scale for environmental impact assessment, transportation emissions have typically been quantified using

the U.S. EPA's mobile source emissions software: MOBILE6 and MOVES. MOVES has become the new standard tool for estimating energy consumption and emissions production associated with on-road vehicle emissions (mobile sources). Replacing MOBILE6, the program is increasingly being used by air quality regulators, MPO's, and their consultants for on-road emission inventories for state implementation plans (SIPs) and regional air quality conformity analyses. Some of the improvements in MOVES relating to energy and emissions estimation include the incorporation of new emissions test data, representation of changes in vehicle technology and regulations, and the incorporation of more sophisticated algorithms that account for more of the factors affecting in-use vehicle emissions (125). With respect to GHG emissions estimation, MOVES provides a more robust calculation that includes CH₄ and N₂O in addition to CO₂, and that accounts for variations in vehicle efficiency according to vehicle speed. Unfortunately, MOVES functions as a "black box" and does not allow the user to view the vehicle efficiency curves used in the calculations. To account for variations in vehicle speed, MOVES uses a time-based distribution of speeds, whereas MOBILE6.2 uses a VMT-based speed distribution; although, MOVES may be used to create emission rate output tables on a "rate per distance" basis (126). This distinction makes MOBILE6 a more convenient tool for estimating energy consumption and GHG emissions from travel demand model outputs (e.g. O/D tables for number of trips, travel distance, and travel time) that enable estimation of motorized VMT and *average* speed for trips attracted to an office location TAZ. It should be noted that the use of average speed data to estimate vehicle emissions per VMT may not be representative of the actual efficiency across variations in vehicle speed (see Section 6.2.8.1 for a discussion of estimating vehicle efficiency and using travel demand model distance and speed data). MOVES is recognized as the pre-eminent software for estimating energy consumption and GHG

emissions from passenger vehicles on regional transportation networks; however the utility of MOVES as a tool for directly estimating the energy consumption and GHG emissions of trips to/from commercial office locations is not on par with its complexity. In an energy consumption and GHG emission estimation framework utilizing travel demand O/D table outputs, the best use of tools like MOBILE6 and MOVES is to estimate /derive vehicle energy efficiency curves that may be applied to estimates of average trip speed and VMT.

6.2. Calculation Procedures for Site Transportation Energy Consumption

Estimation of the potential commute energy consumption of commercial office site alternatives requires a framework for calculating sub-regional variations in home-based work trip activity and efficiency. Such a framework should allow the decision maker (office owner / tenant) to apply known activity variables (e.g. number of employees, employee demographics, home-based work trip rates, etc.) to a set of calculations that evince which office site among available alternatives best enables the lowest level of transportation energy consumption.

A calculation framework for estimating the commute energy consumption of commercial office site alternatives should identify the relevant calculation variables and data sources. Work trip fuel/energy consumption is primarily a function of trip frequency, mode shares, trip distances, and vehicle efficiencies. Figure 24 outlines the connections between parameters related to work trip fuel/energy consumption, including the resources available for quantifying the parameters. The items with a bold outline are understood to be the site-dependent elements – the parameters that are potentially variable between and constrained by the building/site. The other parameters are either consistent between the building/site alternatives or are simply not a function of location.

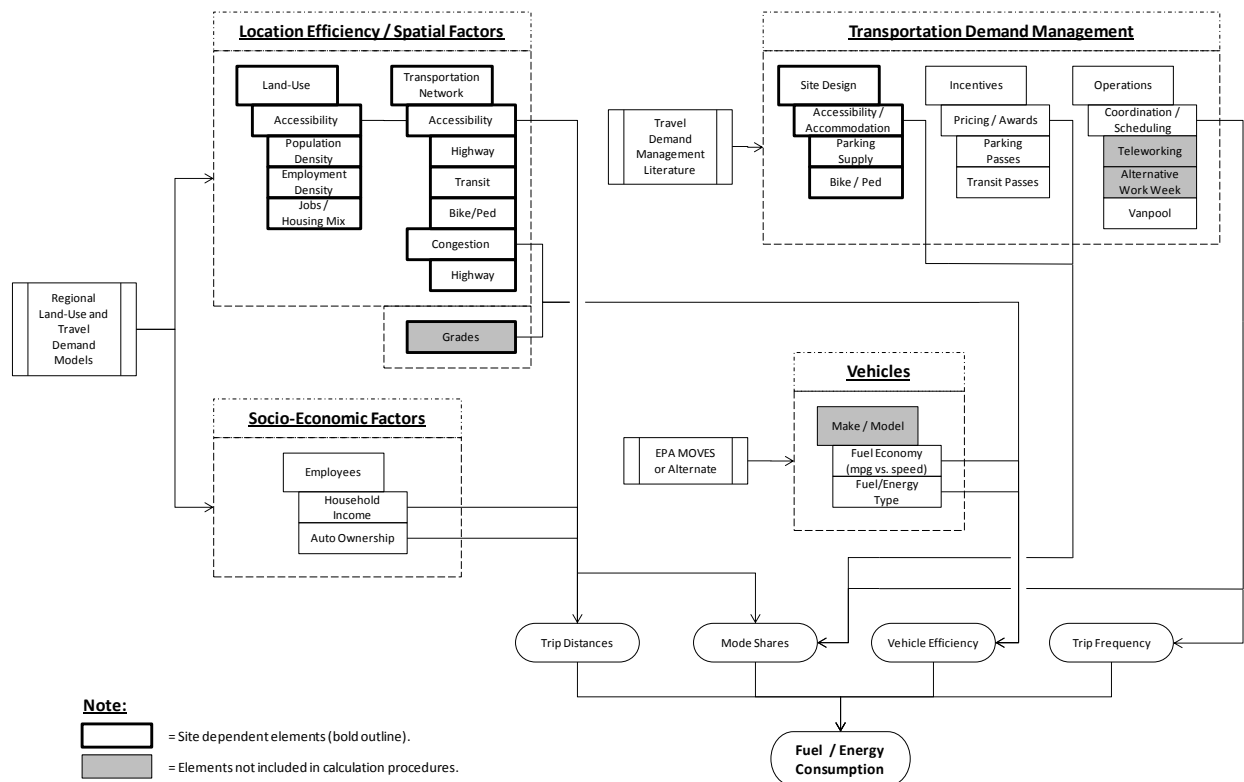


Figure 24: Work trip variables/elements related to fuel consumption and GHG emissions.

The primary resources selected for quantifying the spatial and socio-economic factors are the regional land-use and travel demand models. The land-use model contains a current inventory of the spatial distribution of population and employment in the region, and provides an estimate of forecasted land use development influencing transportation activity. The multimodal home-based work trip tables of the travel demand model provide an estimate of the origin TAZs of trips attracted to employment TAZs, along with the associated network distance, time, and mode split. Stratification of the trip table outputs into disjoint socio-economic categories of household income and automobile ownership (generally the two strongest explanatory socio-economic factors in household transportation activity) supports an investigation of the spatial

variation in commute trip energy consumption. The variables/elements shown in Figure 24 are applicable to non-home based trips, save for the transportation demand management incentive and operation parameters which are designed for journey to work trips.

The transportation demand management parameters may either be defined by the site (e.g. “Site Design”) or limited by the site (e.g. “Incentives” and “Operations”). It is understood that the impact of transportation demand management measures is limited by, or is synergistic with, baseline location factors such as public transit accessibility (127). Thus, the transportation energy savings potential of transportation demand management incentives, like subsidized transit passes, will depend upon the transit accessibility to a given location.

Additional detail on the process and data for estimating site-specific transportation energy consumption and emissions are shown in Figure 25 below. The building firm defines several important inputs, including the building location, square footage, occupancy, and occupant demographics. This information is combined with data from the travel demand model to determine travel activity and to normalize the building/site performance metrics. The specific vehicle fleet of the building occupants are assumed to be unknown to the location decision-maker, thus average fleet efficiency characteristics are applied. Estimation of the transit energy consumption and GHG emissions are included in the calculation procedures so that a true whole-building estimate may be produced; however, only the SOV energy and emissions are considered to be relevant to the relative performance/impacts of the site alternatives (see Section 4.2.3.1).

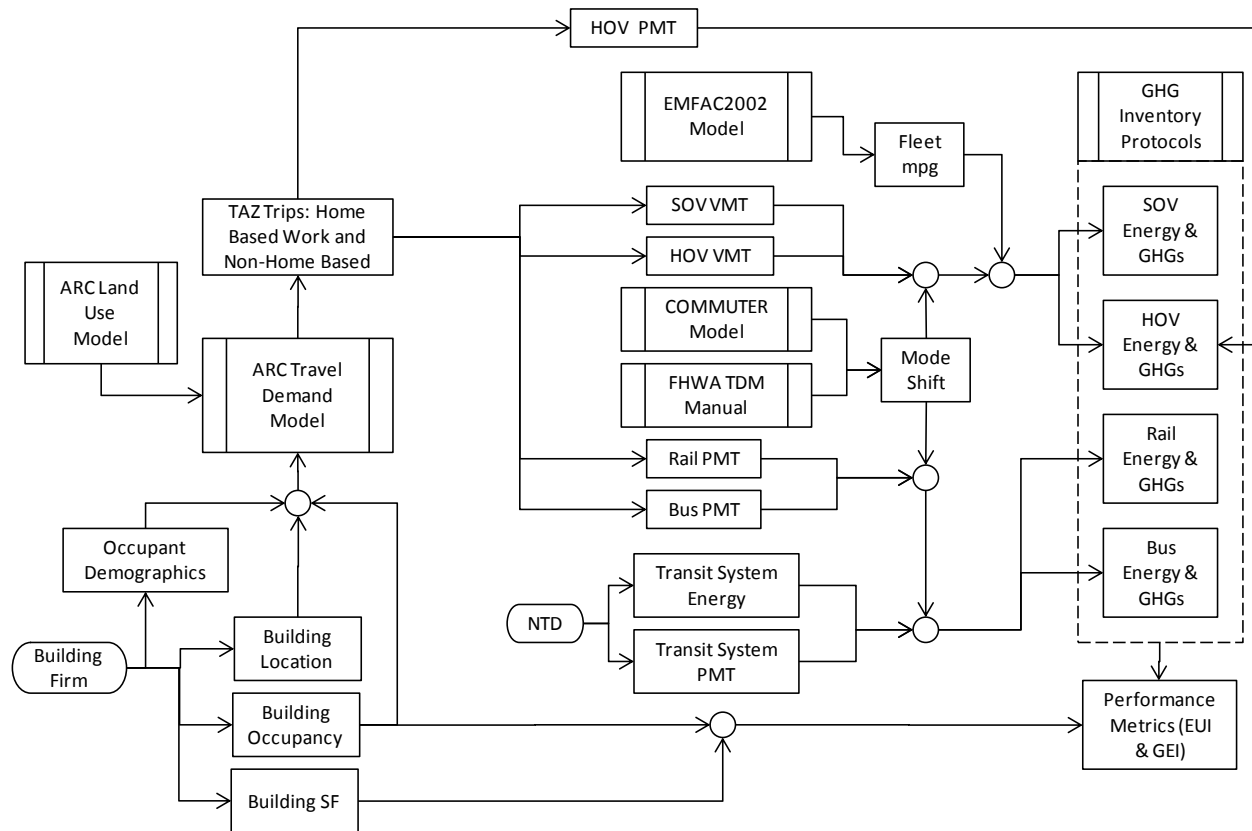


Figure 25: Process and data diagram for estimating site-specific transportation energy consumption and emissions.

The following sections detail the calculation procedures for estimating site transportation energy consumption and GHG emissions. The calculation procedure descriptions make frequent reference to the MATLAB code developed for estimating site transportation energy consumption and GHG emissions (see Appendix A).

6.2.1. Define Site Alternatives Choice Set

The first and most basic step in the calculation procedures is to define the site alternatives choice set. The choice set is determined by whatever building and location criteria are established by the building/site decision maker (see Section 4.1.1 and Section 5.2.1). Once these

locations are defined, the locations are overlaid on a map of the regional travel demand model traffic analysis zones (TAZs) to determine the corresponding TAZs. The TAZs represent a spatial aggregation of land-use and travel activity characteristics which are assumed to be representative of each of the sites contained within their boundaries.

6.2.1.1. Collect Site Transportation Data

It is certainly possible that the average model input values for the TAZ may not represent the particular characteristics of a potential site. Therefore it may be necessary to collect some site-specific transportation data to compare the site characteristics to the model inputs. The one variable that is likely to both have a significant impact on travel behavior and be misrepresented by aggregated TAZ attributes is parking cost. In the transportation research literature, parking cost and supply are recognized as some of the more important variables influencing traveler mode choice (128, 129, 130, 131). In regional travel demand models, parking costs are very often estimated rather than directly observed. For example, in the ARC travel demand model parking costs are calculated from a formula, in which the zone parking cost is proportional to the zone employment density with a minimum density threshold of 20 employees per acre (below which parking is assumed to be free). If a discrepancy is found between the travel demand model inputs and the actual parking costs for a site, the discrepancy may be corrected either by rerunning the model with the actual parking costs, or applying a parking incentive (or disincentive) to mode shift estimates (See Section 6.2.3.3). Collecting data on parking costs, as well as transit service, is important for determining the feasibility of potential transportation demand management strategies. For example, in locations where parking is supplied for free and public transportation service is non-existent, parking and transit-focused mode shift strategies

will be ineffective. Site data on mixed-use development at or adjacent to a potential site can be helpful for estimating vehicle trips reductions through non-motorized access (see Section 6.2.3)

6.2.2. Estimate Building/Site Occupancy

Consistent with the building energy and GHG emission calculation procedure, the hourly building/site occupancy schedule should be defined in accordance with the intended use of the building/site (see Section 5.2.2.1). By defining the occupancy level at each hour, the schedules indicate the number of commute trips that are taken during and between peak periods of congested travel. Trips to the office site are equal to the hourly increase in building/site occupancy, and trips from the site are equal to the hourly decrease in occupancy. The building occupancy schedule should be consistent with any travel demand management measures that may reduce the hourly occupancy of the office space (e.g. telecommuting and alternative work week schedules). The intended occupancy of a building/site is uncertain, but the degree of uncertainty should be consistent between building/site alternatives. Table 15 shows an example time of day occupancy and inbound/outbound commute trip schedule.

Table 15: Example Time of Day Occupancy and Inbound/Outbound Commute Trip Schedule

Peak / Non-Peak	Weekday Period	Hour of Day		Occupancy (%)			Trips Wrk Wk	Direct.	Trips Sat	Direct.	Trips Sun/Hol	Direct.
		Begin	End	Wrk Wk	Sat	Sun/Hol						
NP	Nighttime	12:00 AM	1:00 AM	0	0	0	5	OB	0		0	
NP	Nighttime	1:00 AM	2:00 AM	0	0	0	0		0		0	
NP	Nighttime	2:00 AM	3:00 AM	0	0	0	0		0		0	
NP	Nighttime	3:00 AM	4:00 AM	0	0	0	0		0		0	
NP	Nighttime	4:00 AM	5:00 AM	0	0	0	0		0		0	
NP	Nighttime	5:00 AM	6:00 AM	0	0	0	0		0		0	
P	AM	6:00 AM	7:00 AM	10	10	5	10	IB	10	IB	5	IB
P	AM	7:00 AM	8:00 AM	20	10	5	10	IB	0		0	
P	AM	8:00 AM	9:00 AM	95	30	5	75	IB	20	IB	0	
P	AM	9:00 AM	10:00 AM	95	30	5	0		0		0	
NP	Midday	10:00 AM	11:00 AM	95	30	5	0		0		0	
NP	Midday	11:00 AM	12:00 PM	95	30	5	0		0		0	
NP	Midday	12:00 PM	1:00 PM	50	10	5	-45	OB (NHB)	20	OB	0	
NP	Midday	1:00 PM	2:00 PM	95	10	5	45	IB (NHB)	0		0	
NP	Midday	2:00 PM	3:00 PM	95	10	5	0		0		0	
P	PM	3:00 PM	4:00 PM	95	10	5	0		0		0	
P	PM	4:00 PM	5:00 PM	95	10	5	0		0		0	
P	PM	5:00 PM	6:00 PM	30	5	5	65	OB	5	OB	0	
P	PM	6:00 PM	7:00 PM	10	5	0	20	OB	0		5	OB
NP	Nighttime	7:00 PM	8:00 PM	10	0	0	0	OB	5	OB	0	
NP	Nighttime	8:00 PM	9:00 PM	10	0	0	0		0		0	
NP	Nighttime	9:00 PM	10:00 PM	10	0	0	0		0		0	
NP	Nighttime	10:00 PM	11:00 PM	5	0	0	5	OB	0		0	
NP	Nighttime	11:00 PM	12:00 AM	5	0	0	0		0		0	
Inbound Peak							95		0		0	
Inbound Non-Peak							0		30		5	
Outbound Peak							85		30		0	
Outbound Non-Peak							10		0		5	
# of Times per Year Trip Pattern Occurs (2010)							253		52		60	

The portion of the table framed by the bold outline is based on the default office occupancy schedule from ANSI/ASHRAE/IES Standard 90.1 (77). The number of inbound and outbound commute trips taken at each hour of the day (Weekday, Saturday, or Sunday/Holiday) is calculated from the hourly changes in occupancy. The midday weekday trips shown in grey are interpreted as non-commute trips, and are thus not included in the commute trip accounting. The peak/non-peak designation of each hour is defined by the travel demand model, save for the Saturday trips taken during midday, PM, and nighttime – these are conservatively classified as

peak period trips. At the bottom of the table, the number of IB/OB, peak/non-peak trips are summarized for each day type. Referring to a 2010 work calendar,, the annual number of work weekdays, work Saturdays, and Sundays/Holidays are 253, 52, and 60, respectively. The building occupancy estimate is used to calculate the number of trips attracted for each of the trip types (see Section 6.2.5) and the annual motorized trip frequency for inbound peak, inbound non-peak, outbound peak, and outbound non-peak trips (see Section 6.2.4).

6.2.2.1. Estimate Occupant Demographics

Another essential aspect of the building/site occupancy is the estimated occupant demographics. The socio-economic characteristics of individuals and households, particularly household income and automobile ownership, are strong indicators of travel behaviors. Regional travel demand model data are very often stratified by socioeconomic groups. In the case of the ARC travel demand model, outputs are stratified into four household “market segments:” 1) No automobiles; 2) Number of automobiles is less than number of workers; 3) Number of autos is greater than or equal to number of workers and income is less than \$50,000; and 4) Number of autos is greater than or equal to number of workers and income is greater than \$50,000. Based on knowledge of the intended positions to be filled for a new office, office firms should have at least an approximate estimate of the number of employees within different income groups. Office firms will have little or no information on the automobile ownership of its future (or current) employees, but it is safe to assume in auto-centric areas like the Atlanta, GA metropolitan region that most office employees will have at least as many automobiles as workers.

In the MATLAB code for loading travel demand model data, “Load_Var_HBW,” the number of stratifications are defined by the user (lines 6 – 12). Based on the stratification(s)

defined by the user, the corresponding stratified trip tables (by mode) are loaded (lines 125 – 139 and script “Load_Var_HBW_S1”). In the calculation code “Transp_Calcs_HBW,” the user enters the number of employees in each of the included stratifications (lines 17 – 24). The calculations are looped for each of the stratifications and the results for each of the stratifications are combined into an aggregated output.

6.2.3. Estimate Motorized Vehicle Trip Reduction (VTR)

In order to determine the number of motorized trips taken to/from a given office location, it is necessary to estimate any potential reductions in motorized vehicle trips that are not accounted for in the travel demand model data. The following sub-sections describe methods for estimating potential vehicle trip reductions (VTR) from bike/ped mode share survey data, mixed-use development, and travel demand management VTR programs.

6.2.3.1. Bike/Ped Mode Share

In the ARC travel demand model, non-motorized trips are not explicitly modeled to the same degree as motorized vehicle trips. Non-motorized trip productions are estimated, and the occurrence of non-motorized trips is embedded within motorized vehicle trip production (particularly in densely developed areas of the region), but non-motorized trips are not distributed between TAZs (save for non-motorized access to transit trips). This lack of non-motorized trip estimation for regional commute trips is typical of MPO travel demand modeling practices in the U.S (44). A novel estimation method is needed to determine how many (or what fraction) of trips attracted to a given office location are non-motorized.

Non-motorized commute trips are a function of commuter demographics, land-use (spatial distribution of housing and jobs), and the transportation network. Data linking these three categories are inadequate to sufficiently simulate the non-motorized commute activity within the Atlanta metropolitan region. In terms of the transportation network, the performance characteristics of the bicycle and pedestrian network (e.g. connectivity, traffic volumes, and level of service) is generally unknown. Some bicycle counts and bicyclist surveys have been conducted by the Atlanta Bicycle Coalition, the local bicycle advocacy group, at intersections with concentrated bicycle traffic; however, this data does not reveal the network activity of bicycle commuting. Similarly, no data has been collected on pedestrian network activity, and very little data has been amassed on the walkability of Atlanta's transportation network. For many metropolitan areas, the most current data on non-motorized commute activity is survey data on the regional average mode share for bike and walk home-based work trips. Table 16 below summarizes the Atlanta, GA non-motorized mode split estimates from national surveys.

Table 16: Atlanta, GA Non-Motorized Mode Split Estimates from National Surveys.

Non-Motorized Mode	2000 U.S. Census, AFF (1)	2000 U.S. Census, CTPP (2)	2009 U.S. ACS, AFF (3)	2009 U.S. NHTS (4)
Bike	0.01%	0.08%	0.20%	0%
Walk	1.30%	0.95%	1.40%	3.8%
Source: (1) American Fact Finder 2000 U.S. Census Journey to Work Survey, Atlanta MSA, Means of Transportation to Work for Workers 16 Years and Over (P030). (2) Census Transportation Planning Products 2000, U.S. Census Tracts within ARC travel demand model, Sex by Means of Transportation to Work, All Workers (Part 2, Table 2). (3) American Fact Finder 2009 American Community Survey, 1-Year Estimates, Atlanta MSA, Means of Transportation to Work for Workers 16 Years and Over (B08301) (4) National Household Travel Survey 2009, Atlanta MSA.				

Unfortunately, a regional average cannot effectively represent the spatial variations in non-motorized commute mode shares that may exist across a region. It is widely acknowledged

in transportation planning research and practice that non-motorized travel can vary significantly across land-use and transportation network types. Some land-use and transportation network types can effectively proscribe any measurable level of safe non-motorized commute travel (e.g. suburban commercial development parcels located several miles from housing and safely accessible only by personal automobile or taxi). The regional average mode share of non-motorized home-based work trips may actually exceed the practical limit of non-motorized commute trips to a particular site.

One of the most spatially detailed data sources for non-motorized work trip attractions in U.S. urbanized areas is the Census Transportation Planning Products (CTPP) 2000 dataset (123). This dataset contains a sample of bike and walk journey-to-work mode shares for employer census tracts. Within the CTPP, the most complete tabulation of non-motorized mode shares attracted to employer TAZs exists in Part 2, Table 2, Sex by Means of Transportation to Work (132). The use of this dataset is discussed in the regional application of the calculation framework (see Section 8.1.4.1).

Utilizing a given mode share for attracted non-motorized trips, the number of motorized work trip can estimated from the following equation:

Equation 8

$$T_{x,s} = Emp_{x,s} \times (1 - NM_x)$$

Where $T_{x,s}$ = the number of attracted motorized trips.

$Emp_{x,s}$ = the number of employees.

x = the site TAZ index.

s = the stratification index.

NM_x = the percent non-motorized trips.

This calculation is applied in the MATLAB “Transp_Calcs_HBW” script (lines 114 – 121). The non-motorized mode share is applied evenly across all stratifications since stratification-specific data is currently unavailable. The impact of non-motorized work trips on VTR is expected to be small – most TAZs in the Atlanta, GA metropolitan area have a non-motorized work trip mode share of only a few percentage points.

6.2.3.2. Mixed-Use Development and Commute Trips

In the field of transportation planning, the impact of land-use on single occupant vehicle travel demand is generally conceptualized in three land-use characteristics: The “3 Ds” – Density, Diversity, and Design (*133*). Regional travel demand models explicitly account for land-use density and diversity in their estimates of VMT between TAZs; the amount and density of employment and population are explicit inputs used for estimating the distribution of trips. On the other hand, “design” factors within a TAZ and the associated impact on VMT are not explicitly modeled. Design factors are taken to be any development features that promote a pedestrian or non-private automobile travel environment, such as the design philosophies of new urbanism, transit-oriented development, and traditional town planning (*133*). Broadly speaking, these design philosophies may be represented by the design features of mixed-use developments: building arrangements that are accessible by non-motorized transportation and include multiple origin/destination types.

Mixed-use commercial office sites typically include a combination of office space, retail space, and housing. The close proximity of these origin/destination types may help to reduce

motorized vehicle trips, particularly for non-commute trips. In a study of suburban activity centers, Cervero found that for every 10 percent addition of retail (or other commercial use) floor space was associated with a 3 percent increase in non-SOV commutes (49). Interestingly, this figure does not adjust for differences in employee household income that may occur between office workers and retail workers, which may explain the differences in commute mode choice. In the “Travel Model Improvement Program (TMIP) study by Cambridge Systematics, researchers found that urban design elements such as land use mix, accessibility to services, availability of convenience stores, perception of safety, and aesthetic setting increased work trip transit mode share by 3 to 4 percent (134).

6.2.3.2.1. *Internal Trip Capture*

Mixed-use sites are recognized within the transportation planning community as developments that offer opportunities for reduced trip generation through internal trip capture. Internal trip capture results in transportation energy-savings by reducing the number of motorized trips taken to/from the development site. In order for savings to be realized, the captured trips must be either non-motorized, or of shorter distance than would otherwise occur to/from the site. Depending on the boundary drawn for analyzing internal trip capture, “captured” trips may not result in relative reductions in transportation energy. For example, if the internal trip activity may be satisfied by an adjacent development providing non-motorized accessibility for trips that may also be served internally, no relative reduction in transportation energy would occur. Thus, the spatial boundary of analysis is crucial to determining the amount of transportation energy saved through internal trip capture.

The Transportation Research Board’s NCHRP Report 684, Enhancing Internal Trip Capture Estimation for Mixed-Use Developments, provides some insight into quantifying internal trip capture for mixed-use developments (135). The research effort for NCHRP Report 684 involved field data collection of mixed-use development trips, by mode, by origin/destination land use, and by time of day. One of the mixed-use development sites used for the data collection effort is Atlantic Station, the location of TAZ 27 (see Section 8.2.1). Table 17 shows the peak-period person trips and percent internal trip capture by land use and time of day for Atlantic Station. The data show that for trips entering offices at the start of normal business hours, 8 percent of the trips are internal. Similarly, for trips exiting offices at the end of normal business hours, 9 percent of the trips are internal. Thus, for the Atlantic Station mixed-use development the percentage of commute trips captured by the land-uses within the development boundary is, on average, no more than 10 percent.

Table 17: Atlantic Station Peak-Period Person Trips and Percent Internal Trip Capture by Land Use, Source: (135)

Land Use	A.M. Peak Period				P.M. Peak Period			
	Entering		Exiting		Entering		Exiting	
	Trips	Percent Internal	Trips	Percent Internal	Trips	Percent Internal	Trips	Percent Internal
Office	990	8%	152	33%	124	45%	668	9%
Retail ¹	135	44%	136	42%	1,431	38%	1,867	39%
Restaurant	34	77%	29	48%	1,218	39%	967	60%
Residential	200	0%	591	2%	543	57%	350	13%
Cinema ²	—	—	—	—	315	52%	281	42%
Hotel	25	4%	36	95%	95	92%	94	86%
Total All Trips	1,384	12%	944	17%	3,726	44%	4,227	38%

¹ Retail open during A.M. peak period was primarily grocery store.

² Cinema not open to customers during morning peak period.

In order to determine how many commute trips originate/terminate to/from residences within the mixed-use development, data is needed on the origins/destinations of internally captured office trips. Table 18 shows the percent distribution of internal trip origins for entering trips during the A.M peak-period. According to the data in Table 18, none of the internal trips entering offices during the A.M peak-period originate from residential land uses. This means that either no morning commute trips originate from within the mixed-use development, or that the internally captured morning commute trips involve a commute tour with a stop at either a retail or restaurant establishment. Therefore, the average internally captured commute trips to offices in the Atlantic Station development is approximately 0 to 8 percent of morning commute trips.

Table 18: Atlantic Station Percent Distribution of Internal Trip Origins for Entering Trips During A.M Peak-Period, Source: (I35)

Destination Land Use	Origin Land Use						Summary			
	Office	Retail ²	Restaurant	Residential	Cinema ³	Hotel	Internal	External	Total	Total Trips
Office	— ¹	4	1	0	—	3	8	92	100	990
Retail ²	32	— ¹	3	5	—	4	44	56	100	135
Restaurant	21	50	— ¹	0	—	6	77	23	100	34
Residential	0	0	0	— ¹	—	0	0	100	100	200
Cinema ³	—	—	—	—	— ¹	—	—	—	—	—
Hotel	0	0	4	0	—	— ¹	4	96	100	25
All Destinations	4	4	1	1	—	2	12	88	100	1,384

¹ Internal trips within a land use are not included in internal trip capture methodology.

² Retail open during A.M. peak period was primarily grocery store.

³ Cinema not open to customer during morning peak period.

The data on internally captured office trips occurring at the end of business hours indicates behavior similar to what is shown in Table 18. Table 19 shows the percent distribution

of internal trip destinations for exiting trips during the P.M. peak-period. The data show that for Atlantic Station none of the office commute trips are destined for residential land uses within the mixed-use development. Internally captured trips from offices are destined for either retail or restaurant establishments. Thus, either no internally captured evening commute trips from offices terminate at residential land uses within the mixed-use development, or the internally captured evening commute trips involve a commute tour with a stop at either a retail or restaurant establishment. Therefore, the average internally captured commute trips from offices in the Atlantic Station development is approximately 0 to 9 percent of evening commute trips. This range is consistent with the range of trip reduction (up to 9 percent) for either residential or non-residential land-uses in mixed use developments in the URBEMIS model (36, 135).

Table 19: Atlantic Station Percent Distribution of Internal Trip Destinations for Exiting Trips During P.M. Peak-Period, Source: (135)

Origin Land Use	Destination Land Use						Summary			
	Office	Retail	Restaurant	Residential	Cinema	Hotel	Internal	External	Total	Total Trips
Office	— ¹	6	3	0	0	0	9	91	100	668
Retail	2	— ¹	19	13	4	1	39	61	100	1,867
Restaurant	1	41	— ¹	3	8	7	60	40	100	967
Residential	0	9	3	— ¹	0	1	13	87	100	350
Cinema	2	21	11	8	— ¹	0	42	58	100	281
Hotel	0	16	68	2	0	— ¹	86	14	100	94
All Origins	1	13	11	7	4	2	38	62	100	4,227

¹ Internal trips within a land use are not included in internal trip capture methodology.

An important variable for estimating the energy reduction of internally captured trips is the mode of access. Table 20 shows the peak-period person-trips and percent internal trip capture by mode of access for Atlantic Station.

Table 20: Atlantic Station Peak-Period Person-Trips and Percent Internal Trip Capture by Mode of Access, Source: (I35)

Mode of Access	A.M. Peak Period ¹				P.M. Peak Period ²			
	Entering		Exiting		Entering		Exiting	
	Trips	Percent Internal	Trips	Percent Internal	Trips	Percent Internal	Trips	Percent Internal
Vehicle Driver	1,141	6%	283	26%	2,552	32%	2,645	31%
Vehicle Passenger	70	7%	31	16%	277	43%	409	29%
Taxi/Car Service	1	100%	1	100%	22	100%	22	100%
Transit (Bus)	36	100%	56	64%	40	100%	152	26%
Transit (Circulating Shuttle)	89	3%	4	75%	468	59%	331	84%
Walk/Bicycle	11	100%	18	61%	86	100%	129	68%

¹ Access mode not reported for 36 entering trips and 551 exiting trips.

² Access mode not reported for 281 entering trips and 539 exiting trips.

The data allows estimation of the mode split of internally captured trips. The mode split is simply the number of reported trips by mode, multiplied by the percent internal by mode, and divided by the total number of internal trips. The estimated shares of mode of access are shown in Table 21. The “mode of access” refers to the first (or last) trip to (or from) Atlantic Station.

Table 21: Atlantic Station Mode of Access for Entering and Exiting Internal Trips, Based on (I35)

Mode of Access	Entering A.M. Peak-Period	Exiting P.M. Peak-Period
Vehicle Driver	55%	60%
Vehicle Passenger	4%	9%
Taxi/Car Service	1%	2%
Transit (Bus)	29%	3%
Transit (Circulating Shuttle)	2%	20%
Walk/Bicycle	9%	6%

It can be seen from Table 21 that more than half of the access trips are by personal automobile. This fact suggests that the mode shares of the internally captured trips to/from offices shown in Table 17 are likely not all non-motorized trips. Table 22 shows the estimated shares of mode of travel, which are the mode shares for all of the trips surveyed at Atlantic Station. Table 22 indicates that overall more than half of the internally captured trips are bike/walk trips, yet approximately 25 percent of all internally captured trips are taken by private automobile.

Table 22: Atlantic Station Mode of Travel for Entering and Exiting Internal Trips, Based on (135)

Mode of Travel	Entering A.M. Peak-Period	Exiting P.M. Peak-Period
Vehicle Driver	26%	22%
Vehicle Passenger	4%	3%
Taxi/Car Service	0%	1%
Transit (Bus)	0%	1%
Transit (Circulating Shuttle)	0%	14%
Walk/Bicycle	69%	58%

The high mode shares of private automobile travel in the internal trip capture data from Atlantic Station suggest that the VTR from mixed-use developments is likely on the order of 4 to 5 percent for HBW trips. Considering the uncertainty of the internal trip capture of mixed-use developments, as well as the time consuming data collection and analysis procedures in NCHRP Report 684 to account for the different commercial and residential properties in, it is reasoned

here that the best method for incorporating mixed-use development internal trip capture estimates into the calculation procedures of this framework is to define the percent VTR as a range of values that are consistent with the findings of NCHRP Report 684. The percent VTR can be applied as an additional non-motorized mode share in Equation 8.

6.2.3.3. Travel Demand Management VTR Programs

Transportation demand management (TDM) programs and incentives exist to reduce congestion on roadways and improve productivity and quality of life, not necessarily to reduce energy consumption. The common measure by which TDM strategies are evaluated is vehicle trip reduction (VTR), which is the percentage of vehicles removed from a site's commute traffic load (127). For the purposes of this site selection evaluation framework, the potential energy and emissions impact of TDM strategies should be taken into consideration, particularly if the strategies may have a significant impact on energy and emissions performance, and if different site alternatives enable or limit particular TDM strategies. Clearly, the presence of transit service at a site is necessary to enable mode shift to transit modes. Importantly, "the combination of financial incentive TDM programs with better land-use is almost always synergistic, i.e., it produces a higher net effect on both mode share and AVR than the two measures independently" (127).

Various types of TDM strategies are used for reducing total and peak period SOV trips. Table 23 lists various types of common TDM strategies.

Table 23: Types of TDM Strategies, Based on (127)

Employer or Institutional Support Actions	Provision of Transportation Services	Financial Incentives or Disincentives	Alternative Work Arrangements
Transportation Coordinators	Shuttle Bus Services	Transit Subsidies	Flexible Work Hours
Transportation Management Association (TMA)	Vanpool Formation Assistance / Cost Sharing	Vanpool Subsidies	Staggered Work Hours
On-Site Information and Pass Sales	Use of Company Vehicles	In-Kind Incentives	Compressed Work Week
Rideshare Matching Services	Bicycle Loan Programs	Parking Supply and Pricing	Telecommuting
Guaranteed Ride Home	--	--	--
Preferential Parking	--	--	--
Bicycle Storage, Lockers, and Changing Facilities	--	--	--

Transportation demand management measures have historically had very limited success in reducing commuter VMT and emissions (136). Though modest in their effectiveness, two of the most effective employer-based strategies for reducing SOV VMT (primarily through ridesharing) have been: 1) use of parking incentives/disincentives coupled with transit pass or commute subsidies; and 2) management commitment coupled with the presence of an on-site transportation coordinator (131). In the FHWA’s review of 330 employment sites in Los Angeles County that were participating in California’s Regulation XV TDM program, the average drive alone share decreased from 76.2 percent to 71.4 percent, and average VTR was 2.5 percent (127).

Quantification of the VTR and VMT impacts of TDM strategies is hampered by several analytical limitations. TDM strategies are most often implemented in packages, rather than individually, making it “statistically very challenging” to ascertain the effectiveness of an individual TDM strategy (127). In the aforementioned FHWA study of 330 employment sites, only financial incentive strategies were found to be statistically significant (127). The considerably small datasets for VTR associated with TDM strategies, particularly strategies employed in combination, suggest that there is a high degree of uncertainty in VTR for proposed TDM strategies for a given employment site. The statistical challenges are compounded by the fact that pre-implementation performance data is rarely available for comparison (127). Also, the context in which a strategy is applied (e.g. the quality of transit service and parking supply and pricing) can influence a strategy’s impact (127). Finally, data on implemented TDM strategies rarely contains information on the magnitude, quality, and/or time period of the implementation (127).

The high degree of uncertainty in estimates of TDM VTR presents a challenge for estimating the potential energy and emissions performance of commercial office site alternatives. For the evaluation framework presented in this dissertation, TDM VTR estimation capability is needed to assess the potential energy and emissions performance of sites for the set of intended TDM strategies. The set of intended TDM strategies are expected to be fairly consistent between site alternatives since, at least in terms of cost and convenience. Unique site characteristics, such as pay-parking and public transit service, may support the selection of unique TDM strategies for a subset of site alternatives. The TDM VTR calculation procedures for this framework attempt to leverage calculation resources that are based on the largest available TDM strategy datasets.

Multiple calculation resources are incorporated in the framework to estimate potential ranges in the expected impact of TDM strategies.

One resource available for estimating the impact of TDM strategies is the Center for Urban Transportation Research (CUTR) Worksite Trip Reduction Model. The CUTR was developed from TDM program data from California's Regulation IV/Rule 2202 program, as well as data from Washington State's Commute Trip Reduction Law, and the Pima Association of Governments in Tucson, AZ (127). In working with this data the CUTR researchers recognized significant challenges, "namely problems of aggregation, missing or incomplete employer plan records, and insufficient information on the nature or monetary value of key incentive programs" (127). The researchers used an artificial neural network (ANN) modeling approach to estimate the impact of individual strategies and strategies in combination (137). Unfortunately, the CUTR model has very poor bin accuracies (slightly above random selection) and very low R-squares (less than 0.2) (137). The CUTR researchers identified the need for better data; especially disaggregate data that allows for testing of the impact of TDM incentives on individual behavior, particularly individuals in different demographic or workforce groups (137). The researchers also identify a need for better understanding of the impacts of TDM incentives over time, e.g. are the impacts constant, increasing, or decreasing, or even exponential (137). Due to the aforementioned limitations of the CUTR model, additional TDM VTR estimation resources were explored for incorporation into the calculation procedures of the site evaluation framework.

According to the review of TDM estimation resources in TCRP 95, "perhaps the most comprehensive set of research and guidance materials on employee-focused TDM is still the report series titled *Implementing Effective Travel Demand Management Measures*" (127). Included in this FHWA series is *Implementing Effective Employer-Based Travel Demand*

Management Programs, A Guidance Manual, which contains calculation steps for ascertaining the VTR impact of TDM strategies (138). An alternative calculation resource, derived from the FHWA TDM Guidance Manual and its underlying dataset, is the U.S. EPA's COMMUTER Model (42). One major difference between the outputs of the COMMUTER Model and the FHWA TDM Guidance Manual is the COMMUTER Model provides estimates of the adjusted mode shares, vehicle trip reduction, and VMT reduction (based on average trip lengths by mode), whereas the FHWA TDM report method provides only estimates of the trip reduction and average vehicle ridership (AVR). Thus, the VTR estimates may be compared between the two methods, but the adjusted mode shares associated with the trip reduction are only available in the COMMUTER Model.

Although the VTR estimates are based on the same underlying dataset of TDM programs, the COMMUTER Model methodology and the FHWA TDM Guidance Manual methodology differ in several important ways. First of all, the FHWA TDM Guidance Manual accounts for the initial average vehicle ridership (AVR) of the site in its estimates of potential mode shift to alternative commute modes, whereas the COMMUTER Model does not. In light of the potentially synergistic effect between TDM strategies and land-use/site characteristics, it is reasonable to expect that the baseline average vehicle ridership may impact the incremental change in modes shares in response to TDM strategies. From an intuitive standpoint, the degree of mode shift in response to a TDM strategy should be inversely proportional to the initial AVR, which is an indicator of the mode share of alternative modes. Sites with a low AVR are dominated by drive alone trips, and such sites may be less favorable to alternative commute trips than are sites with a high AVR. However, a similar argument may be made for sites with relatively high AVR, based on the law of diminishing returns. This dissertation does not

investigate the relationship between initial AVR and potential mode shift, but it is recognized here that different estimates are to be expected from each of the methodologies and that a comparison of mode shift estimates from each methodology should be explored in the application of the framework.

Another difference between the mode shift methodology of the FHWA TDM Guidance Manual and the COMMUTER Model exists in the consideration of the modal bias (transit favorable, rideshare favorable, or neutral) of the sites. The FHWA TDM Guidance Manual accounts for the modal bias of the site in its estimates of potential mode shift to alternative commute modes, both for financial incentives and non-financial programs, whereas the COMMUTER Model does not. One may expect this difference to yield notably different mode shift estimates in cases where ridesharing program strategies are applied to transit favorable sites and where transit program strategies are applied to ridesharing favorable sites. Yet another difference in methodology between the COMMUTER Model and the FHWA TDM Guidance Manual exists in the estimation of mode shift in response to financial incentives or disincentives. The FHWA TDM report method considers only tabulated increments of combined incentive totals for alternative modes (or drive-alone disincentives), whereas the COMMUTER Model utilizes a pivot logit model of mode shift for each alternative mode, based on the unique incentives/disincentives for parking, transit fares, or other direct subsidies, and the region-specific demand model coefficients for parking and transit fares. Additionally, the pivot logit model includes variables and coefficients for in-vehicle travel time, out-of-vehicle walk time, and out-of-vehicle transit wait time, which are utilized for modeling strategies that improve walk access (e.g. preferential parking for carpools) and improvements in transit service.

The following sub-sections describe the calculation procedures of the FHWA TDM Guidance Manual and the EPA COMMUTER Model that are adopted into the calculation framework.

6.2.3.3.1. *FHWA TDM Guidance Manual*

The FHWA Guidance Manual contains a series of calculation steps for estimating the VTR impact of financial and non-financial employer-based TDM strategies. For an office location, the first step in estimating the VTR impact is to determine the baseline AVR. The AVR is basically the total number of person trips divided by the total number of private automobile vehicle-trips, and is calculated according to Equation 9:

Equation 9

$$AVR = \frac{\sum_{m=1}^M PT_m}{PT_{SOV} + (\sum_{n=2}^4 PT_{HOVn})/n}$$

where: AVR = Average vehicle ridership.

PT_{SOV} = SOV person-trips.

PT_{HOVn} = HOV person-trips with n riders.

PT_m = Person-trips for mode m (total of M modes).

The next step is to determine the “modal bias” of the office site, which is a measure of the alternative commute mode dominance of either ridesharing modes or transit modes. The modal bias is determined from Equation 10 and Equation 11:

Equation 10

$$TB = \frac{TR}{AM}$$

where: TB = Transit bias, %.

TR = Transit mode share, %.

AM = Alternative mode share, %.

Equation 11

$$RB = \frac{RS}{AM}$$

where: RB = Rideshare bias, %.

RS = HOV mode share, %.

If TB is greater than 50 percent then the site is categorized as “transit favorable,” and if RB is greater than 50 percent then the site is “rideshare favorable.” Otherwise, the site is categorized as “mode neutral.” With the modal bias defined, the next steps are to either determine the desired percent trip reduction or to specify the intended TDM program options. The available program options include alternative work schedules, carpool & vanpool programs, transit programs, and incentives/disincentives. The alternative work schedule options include compressed work weeks (e.g. 3 days of 36 hours, 4 days of 40 hours, and 9 days of 80 hours) and telecommuting (percent of employees telecommuting for each of 1 to 5 days per week). The carpool & vanpool programs consist of 4 program levels and are a combination of the separate carpool and vanpool program levels described in the COMMUTER Model (see sub-section 6.2.3.3.2). Similarly, the 4 transit program levels match those included in the COMMUTER Model. Financial incentives/disincentives are in 1 dollar increments from 0 to 3 dollars, and

include the total of all multi-modal incentives aimed at reducing drive alone mode share. The combined VTR impact of the program levels and financial incentives/disincentives are tabulated for different ranges of baseline AVR (1 – 1.2, 1.21 – 1.5, and 1.51+) and different modal biases.

In the MATLAB calculation code, the estimated VTR and the associated rideshare and transit program levels from the FHWA TDM Guidance Manual are entered by the user (see “Load_Var_HBW” lines 19 – 24 and 32 – 41). After running through the calculation script once, the baseline number of vehicle trips is stored (see “Transp_Calcs_HBW” line 574). The target number of vehicle trips is equal to the baseline vehicle trips less the percent VTR estimated from the FHWA TDM Guidance Manual (see “Transp_Calcs_HBW” line 577). A calculation procedure was created to translate the VTR from the FHWA TDM Guidance Manual into an estimated mode shift of SOV trips to HOV and transit. The relative magnitude of mode shift to either HOV or transit trips is based on the ratio of the TDM program levels (see “Transp_Calcs_HBW” lines 598 – 614). The rideshare and transit mode choice probabilities are scaled-up (see “Transp_Calcs_HBW” lines 285 – 295) according to the ratio of the TDM program levels and in proportion to the difference between the target number of vehicle trips and the estimated number of vehicle trips (see “Transp_Calcs_HBW” lines 595 - 596). The calculations are repeated until the percent difference between the estimated number of vehicle trips and the target number of vehicle trips is within ± 0.5 percent (see “Transp_Calcs_HBW” lines 272 – 283, and 594).

6.2.3.3.2. *EPA COMMUTER Model*

The EPA’s COMMUTER Model is a spreadsheet-based software model for estimating reductions in employee commute travel and emissions in response to site walk access

improvements, transit service improvements, financial incentives, employer support programs, and alternative work schedules. The estimates are based on mode shares, average trip lengths, vehicle fleet mix, average vehicle speed, VMT by highway facility type, etc. A mode choice model with adjustable coefficients is used to estimate the mode shift and associated travel and emissions reductions. Since only reductions are provided, a total inventory of commute travel emissions is unavailable (VMT and emissions from transit modes are unavailable). Energy consumption (reduction) is not included in the results. The Model includes MOBILE 6.2 elements, and custom emission factors from MOBILE 6.2 can be imported.

The first step in estimating the mode shift and associated VTR from TDM strategies is to determine the “soft” program support levels, which are shown below in Table 24.

Table 24: COMMUTER Model Support Strategy Programs, Source: (139)

Mode	Level	Strategies Included in Program
Carpool	1	Carpool information activities (tied in with areawide matching) Quarter-time transportation coordinator
	2	All the above, PLUS: In-house carpool matching service and/or personalized carpool candidate get-togethers
	3	All the above, PLUS: Preferential parking (reserved, indoor, and/or close-in) Flexible work schedule policy to accommodate carpool schedules. Half-time transportation coordinator
	4	All the above, PLUS: Full-time transportation coordinator
Vanpool	1	Vanpool information activities (tied in with areawide vanpool matching and/or third party vanpool programs) Quarter-time transportation coordinator
	2	All the above, PLUS: In-house vanpool matching services and/or personalized vanpool candidate get-togethers Non-monetary vanpool development assistance Policy of flexible work schedules to accommodate vanpool schedule
	3	All the above, PLUS: Vanpool development and operating assistance, including financial assistance such as vanpool purchase loan guarantees, consolidate purchase of insurance, and a startup subsidy. Supporting services such as van washing and fueling Half-time transportation coordinator
	4	All the above, PLUS: Major financial assistance for development and operations, such as employer purchase of vans with favorable leaseback, continuing subsidy, free maintenance, free insurance. Full-time transportation coordinator
Transit	1	Transit information center Quarter-time transportation coordinator
	2	All the above, PLUS: Policy of work hours flexibility to accommodate transit schedules/delays
	3	All the above, PLUS: On-site transit pass sales Half-time transportation coordinator
	4	All the above, PLUS: Guaranteed ride home Full-time transportation coordinator
Bicycle	1	Provision of on-site bicycle parking (racks or lockers)
	2	All the above, PLUS: Shower and change facilities
	3	All the above, PLUS: Provision of secure bicycle parking (storage lockers or indoor storage) Development of local bike-friendly infrastructure
	4	All the above, PLUS: Workplace information and promotional activities

The corresponding percent increases in mode by support program level are shown in Table 25 below. The “increments of change are associated with particular types of programs, reflecting different application assumptions, levels of intensity, and setting” (140).

Table 25: COMMUTER Model Percent Increase in Mode by Support Program Level, Source: (105)

		Program Level			
Program	Type of Workplace	1	2	3	4
Carpool	Office	0.4%	1.0%	2.0%	4.0%
	Non-Office	0.2%	0.4%	1.4%	2.0%
Vanpool	Office	0.4%	1.0%	2.0%	4.0%
	Non-Office	0.2%	0.4%	1.4%	2.0%
Transit	Office	0.2%	0.5%	1.5%	2.0%
	Non-Office	0.2%	0.5%	1.5%	2.0%
Bicycle	Office	0.2%	0.5%	1.5%	2.0%
	Non-Office	0.1%	0.25%	0.75%	1.0%

The mode shift percentages shown in Table 25 are based on the FHWA TDM Model, 1993 (carpool, vanpool, and transit) and Cambridge Systematics, Inc. for COMMUTER v1.0 (139). “The Level 3 and Level 4 carpool and vanpool support impacts have been reduced to reflect current professional opinion that support measures are less effective than direct financial incentives and disincentives to commuters, all else being equal” (139).

Once the individual mode shift percentages are added together, each mode shift must be scaled down so that the mode share for each mode totals to 100 percent. The mode shifts are scaled down by an “adjustment factor,” which is the baseline total of the mode shares (100 percent) divided by the sum of the revised mode shares (< 100 percent). The adjustment factor is then multiplied by each of the revised mode shares to calculate the adjusted mode shares.

Estimation of the VTR of alternative work schedules follows the structure of the FHWA TDM Guidance Manual.

For travel time and cost (financial incentives/disincentives) measures, the COMMUTER Model utilizes a multimodal logit pivot-point model. Changes in mode share are based on the change in the relative utility of each of the modes. The change in utility of mode m in response to a change in cost in category n is estimated according to Equation 12 below:

Equation 12

$$\Delta U_m = B_n \times \Delta C_{m,n}$$

where: ΔU_m = change in utility for mode m .

B_n = model coefficient for cost category n .

$\Delta C_{m,n}$ = change in cost (time or money) for mode m , cost category n .

The new mode share of mode m in response to a change in the mode's utility is estimated according to Equation 13 (139):

Equation 13

$$p'(m) = \frac{p(m) \times e^{-\Delta U(m)}}{[(e^{-\Delta U(m)} - 1) \times p(m)] + 1}$$

where: $p'(m)$ = new share of mode m .

$p(m)$ = original share of mode m .

$\Delta U(m)$ = change in utility of mode m .

The revised mode shares resulting from Equation 13 are adjusted using the previously described “adjustment factor” process.

The energy and emissions impacts of the COMMUTER Model rideshare and transit mode shifts are estimated in the MATLAB calculation script. First, the estimated mode shift is entered by the user (see “Load_Var_HBW” lines 25 – 26, and 42 – 47). In the first run of the calculations, the baseline mode shares for transit and ridesharing are stored (see “Transp_Calcs_HBW” line 580) and the target mode shares are set (see lines 582 – 585). In subsequent loops of the calculations, the percent difference between the target and actual mode shares are calculated (see “Transp_Calcs_HBW” lines 620 and 628) and the mode shift multipliers are determined (see lines 622 – 626, 630 – 634). The mode shift multipliers are proportional to the difference between the target and actual mode shares. As with the FHWA TDM Guidance Manual VTR calculations (see Section 6.2.3.3.1), the mode shift multipliers are used to scale-up the rideshare and transit mode choice probabilities (see “Transp_Calcs_HBW” lines 285 – 295). The calculations are repeated until the percent difference between the estimated alternative modes shares and the target alternative mode shares are within ± 0.5 percent (see “Transp_Calcs_HBW” lines 272 – 283, and 636 – 640).

The calculation procedures described in the following sections of this chapter translate the estimated mode shifts and VTR to transportation energy and GHG emission reductions.

6.2.4. Estimate Annual Motorized Trip Frequency

In this calculation framework, the annual transportation energy consumption and GHG emissions are estimated from the daily trip patterns defined by the intended building occupancy schedule (see Section 6.2.2). These daily trip patterns by day type (e.g. weekday, Saturday, and

Sunday/Holiday) must be applied to the trip data available in the travel demand model trip tables and must be scaled-up to represent annual totals. In travel demand model trip tables, the flow characteristics (i.e. travel time and travel distance) of trips between O-D pairs for all modes and all socio-economic stratifications is subject to two main distinctions: 1) The direction of travel; and 2) the time of day (TOD). The direction of travel simply defines a trip's O-D pairs and the unique network path. The time of day defines whether a trip occurs during a congested (peak) or un-congested (non-peak) travel period and thereby determines the loaded network performance characteristics for the trip's network links. Both the direction of travel and the time of day affect the travel distance, travel time, and consequently the estimated energy consumption and GHG emissions. Therefore, for all modes, socio-economic stratifications, and trip types, the transportation and emissions calculations are performed for the following four combinations of direction and time:

- Inbound, peak (IB/P)
- Inbound, non-peak (IB/NP)
- Outbound, peak (OB/P)
- Outbound, non-peak (OB/NP)

The time peak vs. non-peak distinction determines which travel time and travel distance tables are used for the calculations (see MATLAB script "Load_Var_HBW" lines 66 – 89 and MATLAB script "Transp_Calcs_HBW" lines 351, 356, 361, and 366). The inbound vs. outbound distinction determines whether the trips is attracted to the office location (office TAZ # identifies table column) or whether the trips is returning to a home location (office TAZ # identifies table row) (see MATLAB script "Transp_Calcs_HBW" lines 349 – 350, 354 – 355, 359 – 360, and 364 – 365).

In order to estimate the annual energy consumption and GHG emissions, each of these daily trip occurrences must be scaled-up to an annual total. This is accomplished by calculating a trip frequency multiplier. The frequency multiplier represents the number of times that the sampled trip is taken during the entire year, according to its trip category (e.g. IB/P, IB/NP, OB/P, or OB/NP). The number of times that each inbound, peak trip attracted to the office occurs annually is approximated by Equation 14:

Equation 14

$$Freq_{TAZ,IB,P} = \frac{freq_{Wk} \times Trips_{TAZ,Wk,IB,P} + freq_{Sat} \times Trips_{TAZ,Sat,IB,P}}{Trips_{TAZ,Wk,IB,P} + Trips_{TAZ,Sat,IB,P}}$$

where $freq_{Wk}$ = Annual number of work weekdays

$freq_{Sat}$ = Annual number of work Saturdays

$Trips_{TAZ,Wk,IB,P}$ = Number of inbound, peak motorized trips attracted to the TAZ on a weekday.

$Trips_{TAZ,Sat,IB,P}$ = Number of inbound, peak motorized trips attracted to the TAZ on a Saturday.

The equation for the annual number of times that an *outbound*, peak trip returns from the office is of the same form as Equation 14. This equation is utilized in the MATLAB script “Trans_Calcs_HBW” lines 146 – 153. The annual number of times that each inbound, non-peak trip attracted to the office occurs annually is approximated by Equation 15:

Equation 15

$$Freq_{TAZ,IB,NP} = \frac{freq_{Wk} \times Trips_{TAZ,Wk,IB,NP} + freq_{Sat} \times Trips_{TAZ,Sat,IB,NP} + freq_{Sun/Hol} \times Trips_{TAZ,SH,IB,NP}}{Trips_{TAZ,Wk,IB,NP} + Trips_{TAZ,Sat,IB,NP} + Trips_{TAZ,SH,IB,NP}}$$

where $freq_{SH}$ = Annual number of Sundays/Holidays

$Trips_{TAZ,SH,IB,NP}$ = Number of inbound, non-peak motorized trips attracted to the TAZ on a Sunday/Holiday.

The equation for the annual number of times that an *outbound*, non-peak trip returns from the office is of the same form as Equation 15. This equation appears in the MATLAB script “Transp_Calcs_HBW” lines 154 – 161. Recall that *Trips* is equal to the total number of trips adjusted for non-motorized access (see Equation 8). In the MATLAB code, the number of motorized trips for each of the trip categories in Table 15 are calculated by multiplying the total number of motorized trips in stratification *s* by the percentage of occupants taking trips in the category (see lines 124 – 138).

6.2.5. Estimate Trip Origins

Estimation of the home-based work trip distances, times, and mode shares requires determination of the commute trip origins. It may be the case for a given decision maker that the commute trip origins are known, as in the case of a regional office relocation. The calculation framework presented here is designed for unknown commute trip origins, as in the case of a new regional office location. Given that the commute origins are unknown, the calculation procedure

should account for the uncertainty in trip origins and the associated dispersion in trip distances, travel times, energy consumption, and GHG emissions. Toward this end, a Monte Carlo simulation approach is utilized; whereby random samples of $T_{x,s}$ trips are iterated 1000 times (see “Transp_Calcs_HBW” lines 15 and 297).

For a selected office site TAZ, x , the commute trip origins are randomly sampled from the stratified person trip tables. The total number of origins sampled is equal to the number of employees commuting by motorized modes, and the probability for each random sample is weighted by the percentage of person-trips attracted from the origin TAZs (see “Transp_Calcs_HBW” line 312). The weighting of the attracted person trips is based on a probability distribution function (PDF) vector created from the column of attracted person-trips:

Equation 16

$$(PT_PDF_i)_{x,s} = \frac{PT_{i,x,s}}{\sum_{i=1}^n PT_{i,x,s}}$$

where: $(PT_PDF_j)_{x,s}$ = Person-trip PDF vector x,s of percentage of trips attracted from origin i to destination TAZ x .

$PT_{i,x,s}$ = Number of person-trips in stratification table s attracted from origin i to destination TAZ x .

n = Total number of possible origins i .

For each office location, x , and for each stratification, s , of person-trips, a trip attraction PDF vector is created (see “Transp_Calcs_HBW” lines 165 – 178). From the weighted random sample of commute trip origins (home locations) an un-weighted random sub-sample of home

locations are taken each of the following inbound/outbound, peak/non-peak, and day-type, combinations (see “Transp_Calcs_HBW” lines 315 – 326):

- Weekday, inbound, peak
- Weekday, inbound, non-peak
- Weekday, outbound, peak
- Weekday, outbound, non-peak
- Saturday, inbound, peak
- Saturday, inbound, non-peak
- Saturday, outbound, peak
- Saturday, outbound, non-peak
- Sunday/holiday, inbound, non-peak
- Sunday/holiday, outbound, non-peak

These sub-samples are taken for each stratification s of office TAZ x . The sub-samples of home locations for each of these trip categories are aggregated into the four basic trip categories: inbound peak (IB/P), inbound non-peak (IB/NP), outbound peak (OB/P), and outbound non-peak (OB/NP). The result is four concatenated vectors of home location TAZ #s by trip category for each stratification s of office TAZ x (see “Transp_Calcs_HBW” lines 331 – 336). As per the four-step modeling process used to produce the travel demand model output tables, the next step after determining the trip origins (i.e. trips distribution) is to estimate the mode choice for the trips.

6.2.6. Estimate Mode Choice

The mode choice for a trip to/from an office TAZ is estimated from the travel demand model vehicle trip tables for each mode. For each of the sampled home-based work person-trips (commute origin-destination pairs contained in the four trip type vectors), a random sample of mode choice is taken, weighted by the percentage of trips taken by each mode to/from the home location (see “Transp_Calcs_HBW” lines 371 – 377). The weighting of the attracted person trips

is based on PDF vectors for each stratification s created from the trips taken to/from each OD pair in each modal vehicle trip table (see “Transp_Calcs_HBW” lines 187 – 224).

Equation 17

$$(MC_PDF_{m,i})_{x,s} = \frac{VT_{m,i,x,s}}{\sum_{m=1}^n VT_{m,i,x,s}}$$

where: $(MC_PDF_{m,i})_{x,s}$ = Mode choice PDF vector x,s of percentage of trips taken by mode m from origin i .

$VT_{mi,x,s}$ = Number of vehicle-trips in stratification s attracted from origin i to destination TAZ x by mode m .

n = Total number of motorized modes.

If a person-trip is found in the trip tables, but no vehicle trips are found, then the trip is assumed to be an HOV trip and the random sample of mode choice is weighted by the PDF of HOV2, HOV3, and HOV4 trips (see “Transp_Calcs_HBW” lines 227 – 262).

6.2.7. Estimate VMT by Mode

One of the determinants of transportation energy consumption and GHG emissions is the amount of travel activity, which is commonly measured in terms of VMT. The VMT of individual trips is represented in travel demand models by the trip distance tables. This data is loaded for both highway and transit trips (see “Load_Var_HBW” lines 66 – 67, 70 – 73, and 79 – 83).

In the MATLAB calculation script, the VMT of each mode is calculated by multiplying the trip table distance for each O-D pair by a count of the number of trips taken from/to a given

home location and the number of times that trip occurs annually (see “Transp_Calcs_HBW” line 398 for SOV VMT). For HOV trips, the effective VMT is the trip distance divided by the number of occupants (see lines 407 – 408). Walk access transit trip VMT is calculated in the same manner as SOV trips (see lines 418 and 427). For heavy rail and commuter rail HBW trips, it is common for commuters to access rail service by driving to a station. Therefore, when estimating the VMT of commute trips it is important to account for the transit vehicle trip distance separately from the drive to transit trip distance. In the calculation script, the transit vehicle VMT is calculated for bus and heavy rail trips (see lines 436 and 445), and the drive to transit VMT for both bus and heavy rail trips is also calculated (see line 454). The drive to transit VMT is combined with the SOV VMT in a separate mode category (see line 466). This combined driving VMT estimate helps to compare the incremental private automobile impact of trips to/from each of the office location alternatives.

For each of the VMT calculations by mode, travel time data from the travel demand model trip tables are used to determine the annual travel time (see lines 399, 409, 419, 428, 437, 446, 456, and 467). The average distance data is divided by the average time data to calculate the average speed for each mode (see lines 400, 410, 420, 429, 438, 447, 458, and 468).

6.2.8. Estimate Annualized Trip Energy and GHGs

6.2.8.1. Estimation of Congestion Effects and Vehicle Efficiency

Once a mode is selected for a particular commute trip to/from the office TAZ, trip distance and time information from the travel demand model trip tables is utilized to estimate the energy consumption of the trip. For single occupant vehicle (SOV) trips, the energy consumption is a function of the trip distance divided by the average fuel economy. The average fuel economy

is calculated from the California Department of Transportation's (CALTRANS) automobile fuel consumption vs. vehicle speed curve (see Figure 26) utilized in the CALTRANS Life-Cycle Benefit-Cost Analysis Model (CAL-B/C) (141). The curve was created from the California Air Resources Board's (CARB) EMFAC2002 v2.2 model by dividing total automobile (passenger car through medium duty truck) daily fuel consumption by VMT for each speed bin for years 2003 and 2023 (141).

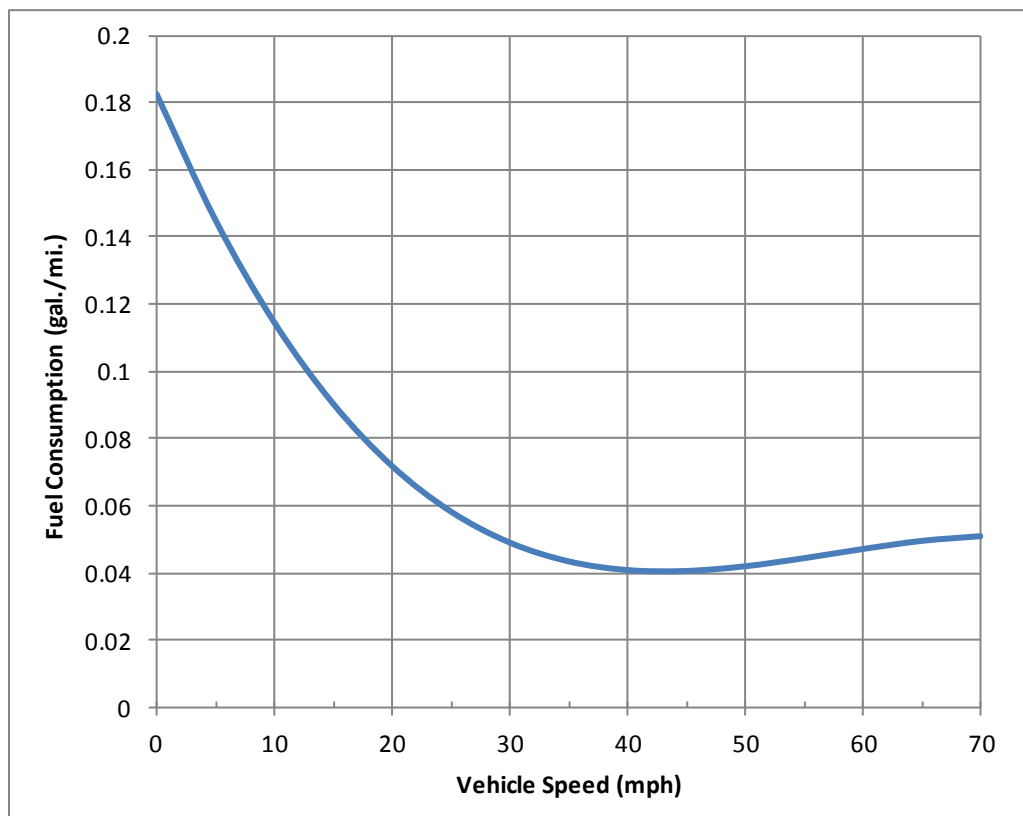


Figure 26: Fuel consumption rates as a function of speed, Based on (142).

Use of this fuel economy curve introduces several sources of unspecified error in estimating SOV fuel consumption. As an average curve for a multitude of different vehicle makes/models, the estimated fuel economy is likely not representative of any one particular

vehicle used for any one particular trip. The accounting of the uncertainty of estimated fuel economy might be improved if region-specific fuel consumption curves were derived in MOVES for each of the possible vehicle types on each of the roadway network link types, and if the vehicle types were sampled from a population of registered vehicles at the home locations. The average fuel economy curve from CALTRANS/CARB was selected for this calculation framework due to data availability constraints: 1) Regional vehicle population data for a MOVES analysis; and 2) TAZ-specific vehicle registration data for commute vehicle selection. Vehicles used for commuting represent a unique sub-population of the total passenger car LDV fleet, and may be newer and more fuel efficient than the fleet average (*143*). For the purposes of the site evaluation framework presented in this dissertation, it is reasonable to assume that vehicle efficiency is not site dependent, particularly for the same population of building/site occupants.

Another source of unspecified error in the selected calculation method is the use of an average trip speed derived from the distance and time data from the trip tables. Two trips with the same distance and same average speed may have different levels of fuel consumption and fuel economy due to different speed profiles over the time span of the trip. For example, one trip may occur in stop-and-go traffic with frequent energy consuming accelerations, whereas the other trip may occur in a more free-flowing traffic stream supporting better overall fuel economy. Additional network link-by-link performance data for each individual trip would be needed. Many regional travel demand models, like the one used by ARC, approximate link speeds with the use of assumed volume speed curves / look-up tables. For most all links, the relationship between volume and speed is uncalibrated and therefore the reported travel times in the trip tables may not be representative of actual travel times. Nevertheless, an average fuel

economy function dependent upon average trip speed was incorporated into the calculation framework to provide at least some approximate, physically-based measure of location-specific effects of congestion on SOV and HOV commute trip energy consumption.

Figure 26 provides a notably conservative estimate of vehicle fuel consumption. The peak efficiency shown at a speed of 42 mph is approximately 25 mpg (see Figure 27 below). This estimate is likely more representative of the stop and go “city” fuel economy that vehicles would achieve during journey to work trips. The U.S. EPA’s “city” driving cycle includes 23 stops in 11 miles and 31 minutes, with a top speed of 56 mph and an average speed of 20 mph (3). In 2009, the average fuel efficiency of U.S. light duty vehicles (LDV) was 23.8 mpg for short wheel base LDVs and 17.4 mpg for long wheel base LDVs (144). Considering that these estimates combine both city and highway driving cycles, the fuel economy shown in Figure 27 appears to be a reasonable estimate of city-weighted driving cycles.

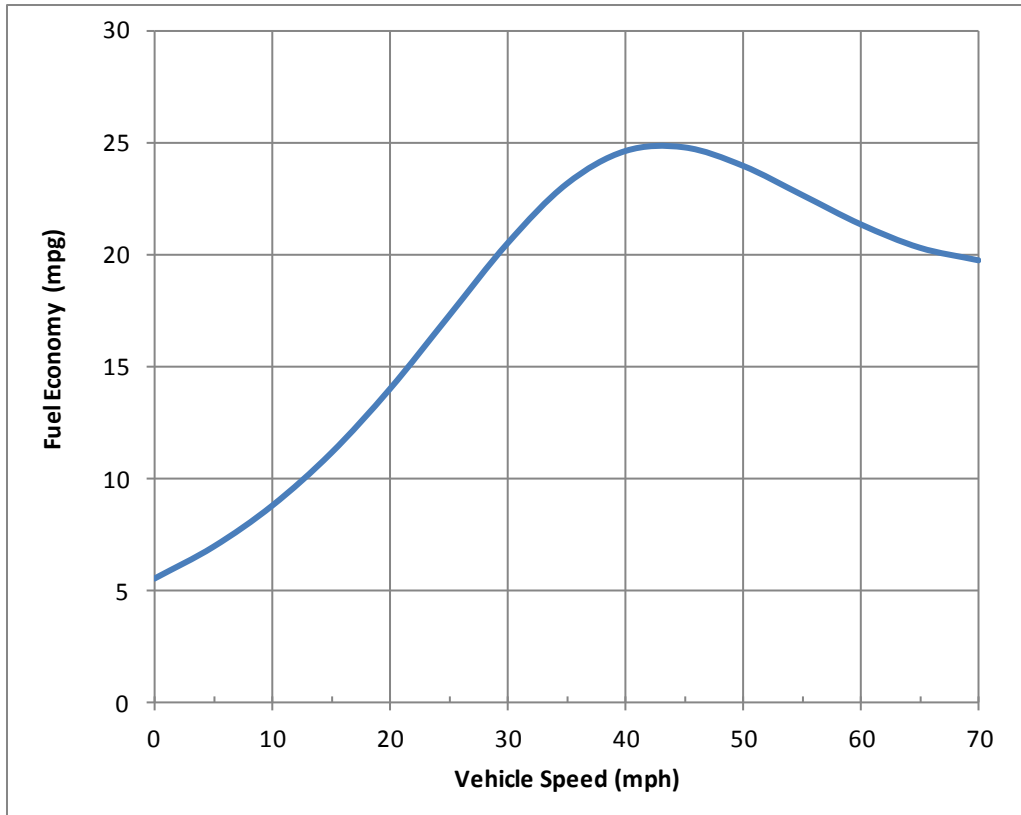


Figure 27: Fuel economy as a function of speed, Based on (142).

For comparison with highway fuel economy, Figure 28 shows fuel economy by speed according to studies performed in the last few decades of the 20th Century. The curves exhibit a similar shape and a higher overall fuel economy.

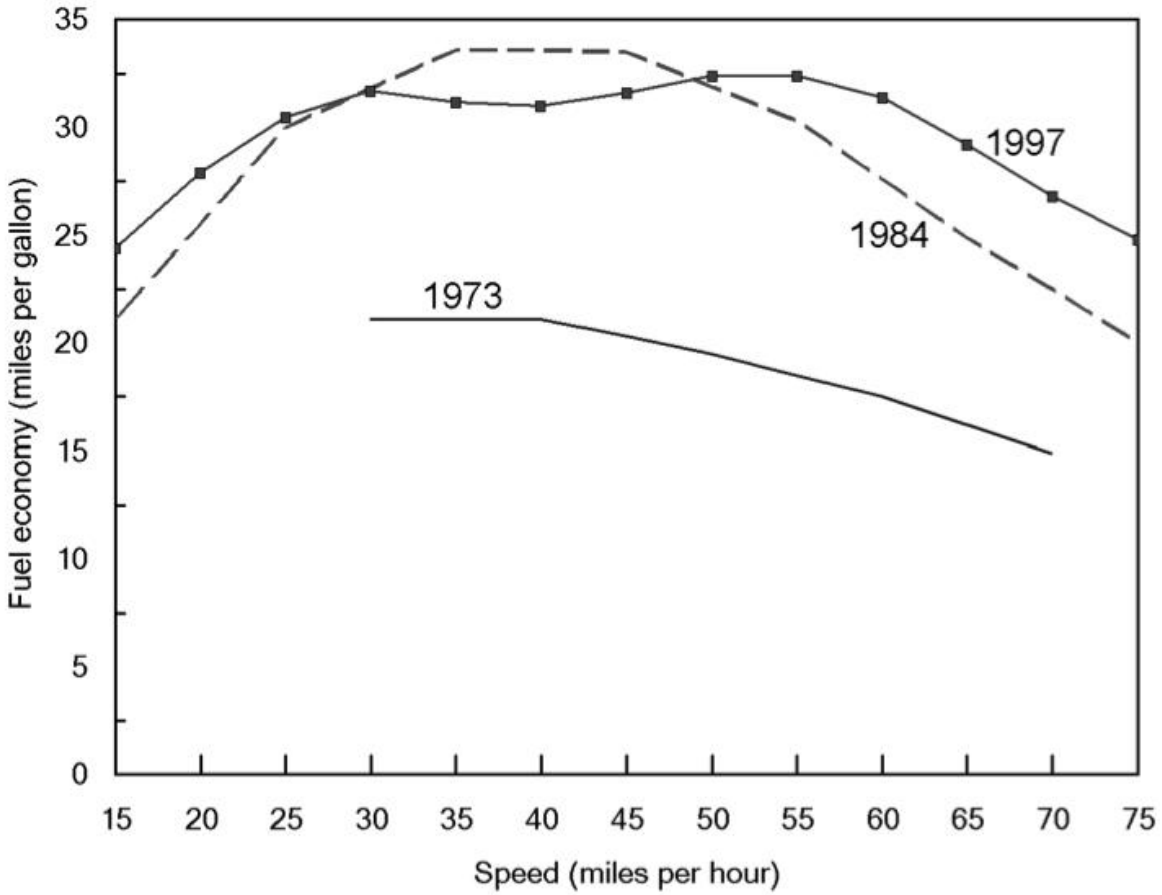


Figure 28: Fuel economy by speed, 1973, 1984, and 1997 studies, Source: (3).

The fuel consumption vs. speed curve shown in Figure 26 is defined by Equation 18 below (142):

Equation 18

$$g = a_0 + (a_1S) + (a_2S^2) + (a_3S^3)$$

Where g = fuel consumption rate (gal./mi.)

S = speed (mph)

a_0 = regression coefficients (1.823381×10^{-1})

a_1 = regression coefficients (-8.2321×10^{-3})

a_2 = regression coefficients (1.5265×10^{-4})

a_3 = regression coefficients (-8.8419×10^{-7})

The equation is utilized in the MATLAB calculation script to estimate the total fuel consumption for private automobile trips (see “Transp_Calcs_HBW” lines 404, 414, and 462). The commute trip energy consumption of HOV trips follows the same procedure used for SOV trips, except that the energy (specifically the VMT) is normalized by the occupancy of the vehicle. For all modes, the unit of measure of energy consumption for each trip is Btu’s per person. For transit trips the ridership of the transit mode impacts the energy efficiency of the trip. Due to a lack of data on the vehicle- or route-specific energy efficiency of transit serving the TAZs, the rail and bus energy consumption for each trip is estimated from modal energy consumption per passenger mile, based on aggregate agency data for MARTA in Tables 17 and 19 the National Transit Database (*145*) The transit energy calculations are shown in the script “Transp_Calcs_HBW,” lines 424, 433, 442, and 451.

One of the work trip variables that may influence fuel consumption and GHG emissions but is not included in the calculation procedures of the framework is the grade/slope of network links (see Figure 24). The difference in fuel economy for flat vs. hilly routes on roadways may be on the order of 15 – 20 percent (*146*). Commercial sites that are at a different elevation than the attracted home locations or sites that are accessed by roadways with “sawtooth” profiles may require more transportation energy to access than sites accessible by flat roadways. Incorporation of roadway grades into the calculation framework would require additional vehicle and network modeling resources that are not readily available, but are potential opportunities for future research.

6.2.8.2. Upstream Energy vs. Direct Energy

The direct energy consumed by private automobile trips is equal to the fuel combusted on-board each vehicle. For the most part, the fuel consumed for commute trips to/from commercial office sites is gasoline, either conventional, reformulated, or low-level ethanol blend. The extraction, refining, and transportation of gasoline inevitably requires additional upstream energy to supply the fuel to the tanks of private automobiles. Argonne National Laboratory's GREET fuel-cycle model of life cycle transportation sector fuel energy consumption and GHG emissions reports a well-to-pump (WTP) efficiency of 80% for conventional and reformulated gasoline and a 76.6% WTP efficiency for low-level ethanol blend gasoline (147). For the calculation framework of this dissertation, an approximate WTP efficiency of 80% is assumed. Thus, for each Btu of gasoline consumed, an additional 0.25 Btu's are consumed in upstream processes.

6.2.8.3. GHG Emissions

The following equation is used to calculate CO₂ emissions from fuel use and a default emission factor from GHG emission inventory protocols:

Equation 19

$$E_{(CO_2)fuel} = Q_{(v)fuel} \times F_{(CO_2)fuel}$$

where $E_{(CO_2)fuel}$ = CO₂ emissions [kg CO₂]

$Q_{(v)fuel}$ = fuel combusted [gal]

$F_{(CO_2)fuel}$ = CO₂ emission factor [kg CO₂/gallon]

Unlike CO₂ emissions, which are simply the result of the degree of combustion and the carbon content of fuels, CH₄ and N₂O emissions are a complex function of combustion dynamics that vary between vehicle and fuel-types. CH₄ and N₂O emissions may be estimated by multiplying VMT by vehicle/fuel technology-specific, distance-based emission factors. The following equations are used to calculate CH₄ and N₂O emissions from driving distance vehicle activity data and default emission factors:

Equation 20

$$E_{(CH_4)veh} = D_{veh} \times F_{(CH_4)veh}$$

where $E_{(CH_4)veh}$ = CH₄ emissions [g CH₄]

D_{veh} = vehicle driving distance [miles]

$F_{(CH_4)veh}$ = CH₄ emission factor [g CH₄/mile]

Equation 21

$$E_{(N_2O)veh} = D_{veh} \times F_{(N_2O)veh}$$

where $E_{(N_2O)veh}$ = N₂O emissions [g N₂O]

D_{veh} = vehicle driving distance [miles]

$F_{(N_2O)veh}$ = N₂O emission factor [g N₂O/mile]

The equations shown above are combined into a single expression for GHG emissions (see “Transp_Calcs_HBW” lines 406, 416, and 464). The CH₄ and N₂O emissions are weighted according to their IPCC GWPs. For public transit bus and heavy rail modes, the GHG emissions

are calculated from weighted pax-mile emission factors calculated for MARTA (120) (see “Transp_Calcs_HBW” lines 425, 434, 443, and 452). Upstream GHG emission factors are available from the author’s previous work on public transportation GHG emissions (120, 121).

6.2.9. Monte Carlo Simulation / Propagation of Uncertainty

The uncertainty in the transportation energy consumption and GHG emissions for each of the commercial office site alternatives is quantified by propagating the input uncertainties through a Monte Carlo simulation process. The main input uncertainties accounted for in the calculation procedures are the home locations of commute trips (and associated travel times and distances) and the trip mode choice. The calculation procedures described in the preceding sections, beginning with random sampling of home locations, are iterated 1,000 times to generate a distribution of results that reflect the uncertainty explicitly accounted for in the calculation framework. The distributions of the output variables are stored in the MATLAB program as matrices indexed by the Monte Carlo simulation run and TAZ (see “Transp_Calcs_HBW” lines 33, 36, 38 – 39, 41 – 45). The average, standard deviation, and covariance of the output variables are calculated for the complete set of simulation runs (see lines 46 – 85). The total energy consumption results are reported as X Btu’s per N employees per year. Similarly, the GHG emission results are reported as Y kg’s of CO₂e per N employees per year.

The uncertainty in the estimated energy consumption and GHG is sensitive the number of employees for which the calculations are run. This fact is based on the mathematical definitions of standard deviation and the coefficient of variation. Based on the estimated energy’s sensitivity to the dispersion of the calculation inputs (notably the commute origins and associated variance in trip distance), the difference in energy consumption between two different sites will depend

upon the number of commute origins considered. In other words, the variance in the estimated energy consumption of a TAZ is a function of the number of samples (commute origins / employees) taken; thus, as more employees are considered the estimated probability associated with a given percent difference in energy consumption will increase. Based on this relationship between sample size (number of employees) and dispersion of estimated energy consumption, at some minimum number of employees the overlapping area of a pair of estimated energy probability distribution functions would become large enough to preclude a sufficiently confident determination of the relative energy performance.

Upon running the Monte Carlo simulations of transportation energy consumption and GHG emissions, a histogram of the results for each site can be produced. From these histograms, a probability distribution function (PDF) and cumulative distribution function (CDF) can also be produced. The PDFs and CDFs can provide an illustration of the overlap in estimated outputs for each site. Using the overlapping areas of the PDFs, it is possible to calculate the probability of saving at least more than 0 Btu's of annual private automobile transportation energy for one site versus another.

6.2.10. Analyze Sensitivity to Uncertain Parameters

The results calculated from the Monte Carlo simulation are not necessarily the final estimation of the output distributions. In the calculation procedures presented in this framework, the uncertainty of the impact of TDM programs is not propagated to the output distributions. The location decision makers may wish to test the potential impact of various levels of TDM program support across each of the location alternatives. Therefore, additional parametric runs, each employing a Monte Carlo simulation of trip origin and mode choice, may be conducted to

compare the relative energy consumption and GHG emissions performance of location alternatives with intended TDM strategies. For each set of intended strategies, the calculations may be run for the range in VTR and/or mode shift estimated from TDM quantification resources (see Section 6.2.3.3).

6.3. Estimating Non-Home Based Trips

Transportation activity to/from commercial office sites includes not only the home-based commute trips of employees occupying the office space, but also several other types of non-home based trips. Potential types of non-home based trips to/from commercial offices include work-based trips taken by employees as part of the discharge of work duties (e.g. trips to/from other office locations within the region and trips to/from locations external to the region), trips taken by visitors of the office, commercial vehicle trips for office deliveries, and social/shopping/lunch trips taken by employees during break times. Table 26 shows national percentages of non-home based trips by purpose, where the previous trip was either a commute trip (“go to work”) or a completed trip tour from work (“return to work”). These previous trip purposes were extracted from the 2009 NHTS to gain insight into employee non-home based trips to/from work sites.

Table 26: Non-Home Based Trips to/from Worksites by Trip Purpose Summary (Vehicle Trips), Source: 2009 NHTS

Trip Purpose Summary	Trip Purpose for Previous Trip	
	Go to Work	Return to Work
Refused	0.0%	0.0%
Don't know	0.0%	0.0%
Not ascertained	--	--
Work	21.2%	16.8%
School/Daycare/ Religious Activity	1.5%	1.3%
Medical/Dental Services	3.0%	4.2%
Shopping/Errands	30.0%	32.4%
Social/Recreational	8.2%	12.3%
Family Personal Business / Obligations	4.8%	4.7%
Transport Someone	12.7%	17.7%
Meals	17.9%	10.3%
Other Reason	0.6%	0.1%
All	100%	100%

The data in Table 26 indicate that most of the non-home based trips to/from worksites serve personal or household purposes rather than work purposes, which represent only approximately one sixth to one fifth of the non-home based trips. Nearly half of the non-home based trips to/from worksites are destined for retail or dining establishments. Each of these types of non-home based trips may influence the relative transportation energy performance of office location alternatives. Unfortunately, accurate estimation of the transportation energy impact of non-home based trips is significantly hampered by a paucity of TAZ level survey or modeling data for non-home based trips. Unlike home based journey-to-work trips which have been the

primary focus of national and regional transportation survey (e.g. NHTS, LEHD, and SMARTRAQ) and modeling programs, non-home based trips have received considerably less attention. The dominant focus on journey-to-work trips is largely the result of a legacy of concern with peak-period congestion, which corresponds with journey-to-work commute periods. It is interesting to note that although commute periods correspond with the periods of peak travel and congestion, non-work travel now constitutes more than half of the peak period travel on an average weekday (148). Nevertheless, the level of detail of travel survey and modeling data for non-home based trips is considerably less than that for home-based journey-to-work trips.

The relative paucity of non-home based travel data is not only a function of a dominant focus on journey-to-work trips, but also a function of the unique characteristics of non-home based trips – notably the mode choice and trip frequency. The trip frequencies of weekday, non-home based trips are considerably less consistent than those of home-based work trips. This disparity in trip frequency consistency can be explained by the unique demands that these different types of trips satisfy. Commute trips satisfy the demand for a worker's presence at a designated worksite, and despite opportunities for telecommuting, most employment arrangements require a commute trip from home to the employment site (and a return trip home). Thus, the trip frequency of most jobs in most locations is nearly equal to 2 trips per employee. The frequency of non-home based trips is an entirely different matter. Non-home based trips satisfy many different types of demands (e.g. shopping, dining, recreation, childcare, medical, etc.) that are altogether less consistent than the demand for an employee's physical presence at a worksite. These different types of demands can be satisfied by trips other than non-home based trips (e.g. home-based shopping trips) as well as by trip tours for which there are considerably

less survey data. Not only can the demands necessitating non-home based trips be satisfied by other types of trips and trip tours, but also these demands may be sensitive to the land-use at the worksite. For example, a worksite with more convenient access to lunch destinations may create more demand for lunch trips.

6.3.1. NHB Mode Choice

For a set of trip makers (e.g. office occupants), the mode choice of non-home based trips may be more variable than the mode choice of home-based work trips, since non-home based trips serve a greater diversity of purposes, access a greater diversity of destinations, and are less habitual than home-based work trips. This issue of mode choice consistency presents a considerable challenge for accurately estimating non-home based trip activity to/from commercial office sites. Furthermore, non-home-based trips have a higher mode share of non-motorized modes than to journey to work trips. Table 27 shows average mode shares by general trip purpose types according to the 2009 NHTS. The table shows that not only are non-motorized mode shares higher for non-home based than for home based work trips, but also home based work trips have the lowest non-motorized mode share out of all general trip purpose types.

**Table 27: Mode Choice by General Trip Purpose (Home-Based Purpose Types),
Source: 2009 NHTS**

Trip Purpose	Mode Choice		
	Walk	Bike	Non-Motorized
Not ascertained	18.5%	1.0%	19.5%
Other home-based	11.0%	0.5%	11.5%
Home-based shopping	7.7%	0.6%	8.3%
Home-based social/recreational	24.1%	3.5%	27.6%
Home based work	2.9%	0.9%	3.8%
Non-home-based	8.6%	0.5%	9.1%
All	10.4%	1.0%	11.4%

Table 28 shows 2009 NHTS data for non-home based bike and walk mode choice by trip purpose summary. It is evident from Table 28 that the non-motorized mode share for non-home based trips is sensitive to the particular trip purpose.

Table 28: Non-Home Based Bike / Walk Mode Choice by Trip Purpose Summary (Person Trips), Source: 2009 NHTS

Trip Purpose Summary	Mode Choice		
	Walk	Bike	Non-Motorized
Refused	--	--	--
Don't know	2.4%	0.0%	2.4%
Not ascertained	5.6%	--	5.6%
Work	9.6%	0.4%	10.0%
School/Daycare/Religious Activity	8.1%	0.3%	8.4%
Medical/Dental Services	3.7%	0.1%	3.8%
Shopping/Errands	4.8%	0.2%	5.0%
Social/Recreational	15.8%	1.7%	17.5%
Family Personal Business / Obligations	9.5%	0.3%	9.8%
Transport Someone	1.6%	0.2%	1.8%
Meals	11.4%	0.1%	11.5%
Other Reason	17.3%	0.0%	17.3%
All	8.6%	0.5%	9.1%

A higher non-motorized mode share for non-home based trips and the diversity of non-home based trip purposes presents a challenge for estimating the non-home based trip activity from commercial office sites. Regional travel data resources for estimating regional patterns of trip-taking activity (e.g. regional travel demand models) provide little or no estimation of the distribution and subsequent mode choice (in the four-step process) of non-motorized trips. The lack of non-motorized trip distribution data is largely a function of the aforementioned focus on peak period journey to work trips in regional travel demand modeling. Although the data and accuracy for mode choice estimates are relatively weak for non-home based trips, it is reasonable

to assume that the SOV mode share for non-home based trips taken to/from employment sites is likely less than or equal to the SOV mode share for journey to work trips; the availability of a personal automobile for non-home based trips is conditional upon the morning commute mode choice.

6.3.2. NHB Trip Frequency

The practical impact of a relative paucity of data for estimating non-home based trip activity to/from commercial office sites may be better understood by comparing the intensity of trip activity between non-home based trips and home-based work trips. The intensity of such trips can be defined by the trip frequency, average trip length, and the subsequent VMT. As discussed previously, the trip frequency of non-home based trips to/from worksites is likely more variable than the trip frequency of home-based work trips. National survey data do not describe typical worksite trip tour patterns, but some insights are available on the types of non-home based trips taken. According to the 2009 NHTS, $10,463 \times 10^6$ non-home based trips were taken where the previous trip purpose was “go to work.” Assuming that these trips are paired with a return trip to the worksite, $20,926 \times 10^6$ non-home based trips were taken to/from worksites. Of course, non-home based trip tours may be taken more than once in a day. The 2009 NHTS indicates that $1,904 \times 10^6$ non-home based trips were taken where the previous trip purpose was “return to work.” If these trips are doubled (assuming a simple trip tour) and added to the previous estimate, then $24,734 \times 10^6$ non-home based vehicle trips were taken to/from worksites. The total of these trips are less than the total number of home based work vehicle trips for which there were $38,051 \times 10^6$ (2009 NHTS). These trip totals represent a national aggregate of non-home based and home based journey-to-work vehicle trip frequencies. Based on the

aforementioned numbers, the frequency of non-home based vehicle trips to/from worksites is approximately two-thirds of the frequency of home based work vehicle trips.

In total, non-home based trips taken to/from a worksite occur less frequently than home-based work trips, yet a more relevant measure of travel intensity as it relates to energy consumption is VMT. According to the 2009 NHTS, the total VMT for the aforementioned non-home based trips to/from worksites were $255,332 \times 10^6$ vehicle-miles, whereas the total VMT for home-based work trips were $483,370 \times 10^6$ vehicle-miles (nearly twice as much). Considering the relatively higher travel intensity of home based work trips, the relative focus of regional travel demand modeling resources on home-based work trips is fortunately consistent with the main effects of worksite passenger travel activity associated with commercial office sites.

Household and individual demographics (particularly income) play a role in the types and intensity of travel activity, so it is worth a look at the correlation between household income and the vehicle trip length of non-home based trips. Table 29 shows data from the 2009 NHTS on the mean non-home based vehicle trip length by income and trip summary purpose. The data indicate that for all of the different types of non-home based trips, there is little or no correlation between household income and average vehicle trip length.

Table 29: Mean Non-Home Based Vehicle Trip Length by Income and Trip Summary Purpose, Source: 2009 NHTS

Derived total HH income	Vehicle Trip Length (Mean), Miles									
	Trip Summary Purpose									
	Work	School/ Daycare/ Religious Activity	Medical/ Dental Services	Shopping/ Errands	Social/ Recreational	Family Personal Business / Obligations	Transport Someone	Meals	Other Reason	All
< \$5,000	20.22	4.61	6.14	5.51	18.68	6.21	10.10	8.30	33.07	9.74
\$5,000 - \$9,999	11.50	5.16	10.71	8.28	17.95	13.74	5.28	5.67	3.65	9.74
\$10,000 - \$14,999	9.83	3.77	7.77	6.06	13.94	9.37	6.93	5.25	46.24	7.85
\$15,000 - \$19,999	9.72	4.73	6.41	4.14	18.76	6.07	5.38	4.56	9.23	6.70
\$20,000 - \$24,999	12.60	9.08	9.71	6.57	15.65	16.55	7.89	6.47	7.21	9.36
\$25,000 - \$29,999	12.34	10.01	10.89	4.98	12.55	10.80	9.15	6.24	29.77	8.25
\$30,000 - \$34,999	9.79	8.68	5.31	8.94	11.01	14.89	8.07	7.84	10.03	9.25
\$35,000 - \$39,999	12.31	12.46	7.87	5.84	13.17	6.12	7.69	5.49	12.93	8.16
\$40,000 - \$44,999	12.61	146.62	12.52	5.34	11.40	10.94	8.61	6.90	27.72	11.10
\$45,000 - \$49,999	14.32	9.37	22.10	5.86	15.74	8.99	7.71	6.52	15.48	9.70
\$50,000 - \$54,999	19.27	8.22	12.95	4.72	20.79	13.27	7.41	4.84	12.75	10.68
\$55,000 - \$59,999	11.25	18.32	7.40	6.67	14.72	7.72	8.14	6.00	131.71	9.35
\$60,000 - \$64,999	15.33	9.63	8.11	5.85	11.15	18.54	7.72	6.78	197.83	10.00
\$65,000 - \$69,999	11.27	9.83	8.46	7.24	14.53	10.27	8.30	4.75	33.74	9.08
\$70,000 - \$74,999	11.48	7.76	8.67	6.41	18.14	19.55	7.57	5.46	6.85	9.69
\$75,000 - \$79,999	12.40	9.15	8.64	6.84	22.01	9.58	9.08	6.96	18.60	10.54
\$80,000 - \$99,999	13.72	9.08	12.62	7.07	13.35	10.79	8.16	5.80	24.80	9.65
> = \$100,000	12.09	8.20	8.96	6.27	18.98	15.49	9.00	7.74	33.05	10.34
All	13.16	13.25	9.48	6.25	16.35	11.80	8.35	6.70	29.88	9.70

The relationship between household income and non-home based trip frequency at worksites is another potentially important parameter for estimating commercial office non-home based trip energy consumption. Table 30 shows survey data and estimates of the non-home based daily trip rate by household income where the previous trip purpose was “got to work.” The annual number of person trips and vehicle trips and the number of workers are taken from the 2009 NHTS. The daily trip rates shown in the last two columns are based on an assumed five-day work week and fifty work weeks per year. Both the person trip and vehicle trip rates increase somewhat as household income increases (mostly for the very lowest ranges of household income).

Table 30: Non-Home Based Daily Trip Rate by Household Income where the Previous Trip Purpose was “Go to Work,” Based on 2009 NHTS

Derived total HH income	Annual Person Trips (Millions)	Annual Vehicle Trips (Millions)	Number of Workers (Thousands)	Daily Person Trips per Worker	Daily Vehicle Trips per Worker
Refused	427	318	5,274	0.32	0.24
Don't know	69	46	1,482	0.19	0.12
Not ascertained	4	4	53	0.30	0.30
< \$5,000	99	67	1,921	0.21	0.14
\$5,000 - \$9,999	173	99	3,060	0.23	0.13
\$10,000 - \$14,999	343	252	4,755	0.29	0.21
\$15,000 - \$19,999	406	319	6,001	0.27	0.21
\$20,000 - \$24,999	393	309	5,130	0.31	0.24
\$25,000 - \$29,999	641	502	7,851	0.33	0.26
\$30,000 - \$34,999	423	345	5,159	0.33	0.27
\$35,000 - \$39,999	687	550	8,694	0.32	0.25
\$40,000 - \$44,999	410	315	4,881	0.34	0.26
\$45,000 - \$49,999	784	653	8,378	0.37	0.31
\$50,000 - \$54,999	464	386	4,565	0.41	0.34
\$55,000 - \$59,999	719	612	8,391	0.34	0.29
\$60,000 - \$64,999	324	248	3,996	0.32	0.25
\$65,000 - \$69,999	764	603	7,870	0.39	0.31
\$70,000 - \$74,999	336	265	3,692	0.36	0.29
\$75,000 - \$79,999	837	684	8,410	0.40	0.33
\$80,000 - \$99,999	1,563	1,228	16,765	0.37	0.29
> = \$100,000	3,498	2,658	35,046	0.40	0.30
All	13,365	10,463	151,373	0.35	0.28

At a national level, the impact of land-use on the frequency of non-home based work trips is considerably small. Table 31 shows the non-home based daily trip rates by employment density where the previous trip purpose was “go to work” in the 2009 NHTS. The trips rates shown in the last two columns of Table 31 are based on the same assumptions used for the trip

rates in Table 30. The daily person-trip rate is approximately constant across employment densities, and the vehicle trip rate decreases approximately 25 percent as the employment density increases from approximately 400 to 4,000 workers per square mile.

Table 31: Non-Home Based Daily Trip Rate by Employment Density where the Previous Trip Purpose was “Go to Work,” Based on 2009 NHTS

Workers per Square Mile Living in Tract	Annual Person Trips (Millions)	Annual Vehicle Trips (Millions)	Number of Workers (Thousands)	Daily Person Trips per Worker	Daily Vehicle Trips per Worker
N/A	.	--	12	--	--
0-49	2,672	2,249	29,634	0.25	0.21
50-99	768	667	8,849	0.24	0.21
100-249	1,495	1,222	15,901	0.26	0.21
250-499	1,656	1,367	19,032	0.24	0.20
500-999	1,966	1,569	23,593	0.23	0.18
1,000-1,999	2,069	1,591	23,638	0.24	0.18
2,000-3,999	1,442	1,055	17,246	0.23	0.17
4,000-999,999	1,298	743	13,468	0.26	0.15
All	13,365	10,463	151,373	0.24	0.19

The national level data provides some insight into the frequency and modes of non-home based trips taken to/from employment sites, but the data is insufficient for estimating the motorized trip activity of NHB trips within an urbanized area. Regional travel demand models like the one used by ARC in Atlanta, GA, include estimation of NHB trip activity. Since most regional travel demand models consider only motorized trips in their estimation of travel activity, the trip rates included in travel demand models are typically only for motorized NHB trips. Table 32 shows the trip attraction rates for NHB trips in the ARC travel demand model. The area types listed across the columns are based on population and employment density. The variation in trip rates between area types is intuitively a function of the type of development within the areas and

the probability of accessing destinations by motorized modes. According to the ARC Model Documentation, “the reduced trip rates . . . for the CBD areas, may simply be a reflection that many of the CBD trips are made by workers during the lunch hour and after work by walking and are therefore not identified as motorized trips” (43).

Table 32: Trip Attraction Rates for Non-Home Based Trips in the ARC Travel Demand Model, Source: (43)

Variable	Measured as	Trip Rate By Area Type						
		CBD	Urban Commercial	Urban Residential	Suburban Commercial	Suburban Residential	Exurban	Rural
Households	Household	0.1711	0.1711	0.1711	0.1711	0.1711	0.1711	0.1711
Population	Person	0.0134	0.0134	0.0134	0.0134	0.0134	0.0134	0.0134
Construction	Employee	0.3640	0.4393	0.4393	0.4351	0.4351	0.4351	0.4351
Manufacturing	Employee	0.3640	0.4393	0.4393	0.4351	0.4351	0.4351	0.4351
Retail	Employee	4.7113	3.2971	3.2971	6.9456	6.9456	5.6967	5.6967
TCU	Employee	0.3640	0.4393	0.4393	0.4351	0.4351	0.4351	0.4351
Wholesale	Employee	0.3640	0.4393	0.4393	0.4351	0.4351	0.4351	0.4351
F.I.R.E.	Employee	0.6339	0.8180	0.8180	0.4519	0.4519	0.4519	0.4519
Service	Employee	0.6339	0.8180	0.8180	0.4519	0.4519	0.4519	0.4519
Government	Employee	0.6339	0.8180	0.8180	0.4519	0.4519	0.4519	0.4519

The ARC travel demand model contains estimates of non-motorized trip productions and attractions for each trip type, but these trips are not distributed between productions and attractions. Furthermore, conversion of these non-motorized trips to trip rates results in unrealistic trips NHB trip rates (e.g. greater than 4 trips per employee) for many TAZs in the region. Absent additional travel model or survey data, the best approach available for estimating the number of energy consuming NHB trips for unique TAZs is to apply the estimated NHB trip attraction rates for the respective area type designation of each office location. The design characteristics (e.g. walkability and development diversity) of each of the zones may result in motorized NHB trip rates that deviate from those listed in the travel demand model.

CHAPTER 7

APPLICATION OF FRAMEWORK: BUILDING SYSTEMS

7.1. Building/Site Selection Scenario

This chapter presents a demonstration of the evaluation framework as it applies to building systems. The framework is demonstrated by applying the evaluation procedures to four building types (see Figure 3 in Section 3.4.2). The four building types represent a range of building energy systems that may be available to an office firm looking to locate 100 employees within a metropolitan region. In the application of the evaluation framework, only existing building fit-outs are considered.

Table 33 shows a summary of spaces included in the office building case studies used to demonstrate application of the evaluation framework. The summary represents a simplified building program expressed in terms of functional space requirements. The “space categories” relate to the conceptualization of building services illustrated in Figure 7 in Section 4.2.1. The “space type” of “office” is inclusive of both open and private office space. Most of the listed “space types” exist within the tenant space, including the enclosed portions of stairways and elevator shafts on the tenant floor. In the case of multi-tenant office buildings, lobby space may exist outside of the tenant space and may be shared between several building tenants.

Table 33: Summary of Building Spaces

Space Category	Space Type	Size (SF)
Total	Total	24,000 - 26,000
Work Space	Office	20,000 - 22,000
	Conference	700 - 1,000
Support Space	Break Areas / Toilets	750 - 1,250
	Mech. / Elect.	0 - 100
	Lobby (shared)	0 - 11,000
Circulation	Stairs (on floor)	1,100 - 1,600
	Elevator (on floor)	750 - 900

Table 33 defines the approximate limits of functional spaces that satisfy building program requirements at the “medium” building scale. In addition to the spaces specified in Table 33 are essential building services that are satisfied by spaces or facilities outside of the tenant space or even outside of the building. These services include entryway circulation and parking. The sizes of these spaces/facilities are not specified as they are considered to be flexible requirements that may vary in accordance with the building context (urban vs. suburban).

7.1.1. Alternatives Choice Set

The program of building spaces/facilities may be satisfied by a variety of building types. The application of the evaluation framework in this chapter is designed to explore the potential performance of building types that are representative of the building stock (see Section 3.4.2). Four representative case study buildings are included in the building alternatives choice set. Table 34 shows the choice set of building alternatives, which includes combinations of old and new buildings, and buildings with single- and multi-tenant occupancy. Each of the buildings in the choice set provides a very similar amount of office work space and total conditioned floor

area. The similarity in floor areas not only helps to maintain consistency in the amount of service supplied by the building alternatives, but also helps to mitigate the effect of building size on the estimated EUI's.

Table 34: Choice Set of Building Alternatives.

Case Study		Work Space Area, (SF)	Total Conditioned Area, (SF)
I	Single Tenant, Old (Post 1980 Construction)	22,200	24,934
II	Single Tenant, New (LEED Certified)	22,200	24,934
III	Multi-Tenant, Old (Post 1980 Construction)	20,757	24,336
IV	Multi Tenant, New (LEED Certified)	21,292	24,871

More detail on the characteristics of each of the building alternatives is available in the sections of this chapter dedicated to each of the building case studies.

7.1.1.1. Intended Occupancy/Operation Schedule

The intended building occupancy schedule is an important factor in the estimated building operation energy consumption. The hourly occupancy schedules define the duration and intensity of building use. Prediction of building occupancy rarely matches actually building use, and furthermore hourly building occupancy is rarely ever validated or measured. The purpose of defining the intended building occupancy schedule for the alternative choice set is to establish a consistent pattern of use for each of the building alternatives. Table 35 shows the case study building occupancy schedule and annual person-hours. The percent occupancy for the work

week, Saturday, and Sunday/Holiday are taken from the suggested default values in the User Manual for ASHRAE Standard 90.1. The occupancy percentages indicate that less than 100 percent of the building occupants will use the building during any given hour. These default percentages attempt to capture the effect of employee absenteeism, teleworking, business travel, and variations in working hours. The total number of person-hours is calculated for a population of 100 office employees during the 2010 calendar year. The person-hours are a measure of building use/service and can be used to normalize the building operation energy consumption (see Section 3.3).

Table 35: Case Study Building Occupancy Schedule and Annual Person-Hours.

Hour of Day		Occupancy (%)		
Begin	End	Wrk Wk	Sat	Sun/Hol
12:00 AM	1:00 AM	0	0	0
1:00 AM	2:00 AM	0	0	0
2:00 AM	3:00 AM	0	0	0
3:00 AM	4:00 AM	0	0	0
4:00 AM	5:00 AM	0	0	0
5:00 AM	6:00 AM	0	0	0
6:00 AM	7:00 AM	10	10	5
7:00 AM	8:00 AM	20	10	5
8:00 AM	9:00 AM	95	30	5
9:00 AM	10:00 AM	95	30	5
10:00 AM	11:00 AM	95	30	5
11:00 AM	12:00 PM	95	30	5
12:00 PM	1:00 PM	50	10	5
1:00 PM	2:00 PM	95	10	5
2:00 PM	3:00 PM	95	10	5
3:00 PM	4:00 PM	95	10	5
4:00 PM	5:00 PM	95	10	5
5:00 PM	6:00 PM	30	5	5
6:00 PM	7:00 PM	10	5	0
7:00 PM	8:00 PM	10	0	0
8:00 PM	9:00 PM	10	0	0
9:00 PM	10:00 PM	10	0	0
10:00 PM	11:00 PM	5	0	0
11:00 PM	12:00 AM	5	0	0
Person-hours / day		920	200	60
Days / year (2010)		253	52	60
Person-hours		232,760	10,400	3,600
Person-hours		246,760		

For the case studies derived from the DOE Benchmark/Reference building models, the system operation schedules (HVAC fans, OA damper operation, interior lighting, exterior lighting, miscellaneous equipment operation, cooling setpoints, heating setpoints, elevator operation) follow the schedules of the Benchmark/Reference models. For all of the case studies, the system operation schedules for systems not included in or defined by the DOE

Benchmark/Reference building models (e.g. window shading), a uniform schedule is applied across all building models.

The following sections describe the case study buildings used to apply the building system calculation procedures of the evaluation framework. The case studies incorporate a combination of building-specific data, industry average data, and engineering judgment to estimate the potential performance of four office building alternatives.

7.1.2. Case Study I: Older Construction, Single-Tenant, Low-Rise Commercial Office Building in Suburban Development Area

This case study represents a building type that is commonly found in suburban development areas: an older (post-1980 construction), single-tenant, low-rise commercial office buildings. A summary of the tenant spaces are shown below in Table 36. Like all of the case studies in this chapter, the building includes approximately 25,000 SF of conditioned floor area. The majority of its square footage is dedicated work space, which includes open office area and conference space. The remainder of the floor plan contains support and circulation spaces. The office work space includes non-partitioned circulation spaces (walkways).

Table 36: Summary of Tenant Spaces (Case Study I)

Building Size	Space Category	Space Type	Size (SF)
Medium	Total	Total	24,934
	Work Space	Office	21,450
		Conference	750
	Support Space	Toilet	800
		Mech. / Elect.	0
		Lobby	450
	Circulation	Stairs	1,200
		Elevator	288

The space types and space sizes in Table 36 indicate the type and quantity of services provided by the building. The following section describes the building characteristics/parameters related to the building's energy systems and performance.

7.1.2.1. Energy System Parameters and Building Energy Model

The energy system parameters for the Case Study I building are derived primarily from the U.S. DOE Commercial Benchmark/Reference Building for a “medium,” post-1980 construction office building in Atlanta, GA. The case study buildings are within the “medium” size range of office buildings in the CBECS; however, the case study buildings (single-tenant space) are one-half the size of the “medium” benchmark/reference buildings (see Section 5.1.2.3). Therefore, it was necessary to scale the benchmark/reference building square footage down to the square footage of the case study. This scale-down was performed so that the 1.5 aspect ratio (length to width) was maintained, and the height was reduced from three to two stories. Nearly all of the building load inputs scaled directly with the reduction in size, save for the number of elevators (reduced from two to one) – the façade was reduced according to the

new building form and the parking lot (and associated parking lighting) was reduced in proportion to the reduction in the building floor plan. Table 37 below summarizes the main characteristics of the Case Study I building. The envelope to floor area ratio is the ratio of the walls and roof to the conditioned floor area. As a scaled-down building, this ratio is slightly higher than the ratio for the original “medium” DOE Benchmark/Reference Building. The envelope, lighting systems, HVAC systems, and conveyances are each defined by the Benchmark/Reference Building parameters. All energy is supplied by electric utility service, save for natural gas heating for the domestic hot water and the air handler pre-heat coil.

Table 37: Case Study I Building Characteristics

Tenant Space Occupancy	Single Tenant
Total Number of Floors	2
Length to Width Ratio	0.66
Orientation	West
Envelope to Floor Area Ratio	0.98
Percent Glazing (wall area)	33%
Floor Condition	Slab on grade
Lighting System Type	Suspended fluorescent, not vented
HVAC System Type	VAV with natural gas preheat, DX cooling, non-powered terminal units, electric reheat, plenum return
Conveyances	1 elevator

One significant difference between Case Study I and the DOE Benchmark/Reference Building is the definition of specific space types (see Table 36). The DOE Benchmark/Reference Building interior spaces are all of the same type, with an open floor plan and uniform internal

loads. The office areas of Case Study I are modeled on the properties of the DOE Benchmark/Reference Building, but support and circulation spaces are defined/zoned separately to represent a more realistic building system (e.g. different lighting power densities by space type, toilet room exhaust fans, different occupancy levels, different types of miscellaneous equipment, etc.). Another important aspect of the building model for Case Study I (and the other case studies as well) is the use of perimeter and core thermal zoning. Consistent with the DOE Benchmark/Reference Buildings, the thermal zones in the building energy model are divided into 15 ft wide perimeter zones (one for each exterior face) and core zones that cover the remainder of the interior space. Perimeter and core zoning is a modeling approximation that is not only employed in the DOE Benchmark/Reference Building models, but is also used extensively in the early phases of HVAC system design for a building. This zoning method is designed to capture the main effects of the envelope thermal loads and interior heat gains, which are typically served by separate HVAC units or thermal zones of a VAV system. Perimeter and core zoning is a simplified alternative to defining the exact thermal zones for a particular HVAC layout design in an actual building. – an approximation that introduces unspecified error in HVAC system energy consumption. This approximation is utilized in the case studies to reduce the complexity and development time of the building energy model, and to maintain a consistent approach to evaluating the efficiencies of the building alternatives (thermal performance of envelopes, internal heat gains, etc.). Another approximation used in the building HVAC modeling is the assignment of a single VAV air handler to each of the floors. This air handler is sized according to the estimated load in the building energy simulation and a unit sizing ratio (factor of safety sizing ratio with a range of uncertainty). The equipment part load efficiencies are based on the defaults in eQUEST/DOE2.2.

Figure 29 below shows the floor plan of the spaces/zones of Case Study I. The perimeter zones consist of office areas, a lobby space, and stairwells. The core zones consist of office areas, conference space, toilet rooms, and an elevator. The office zones, conference space, and lobby space are each served by terminal units with electric reheat. The stairwells are served by unit heaters and the toilet rooms have exhaust fans that draw transfer air from the adjacent, core office zones.

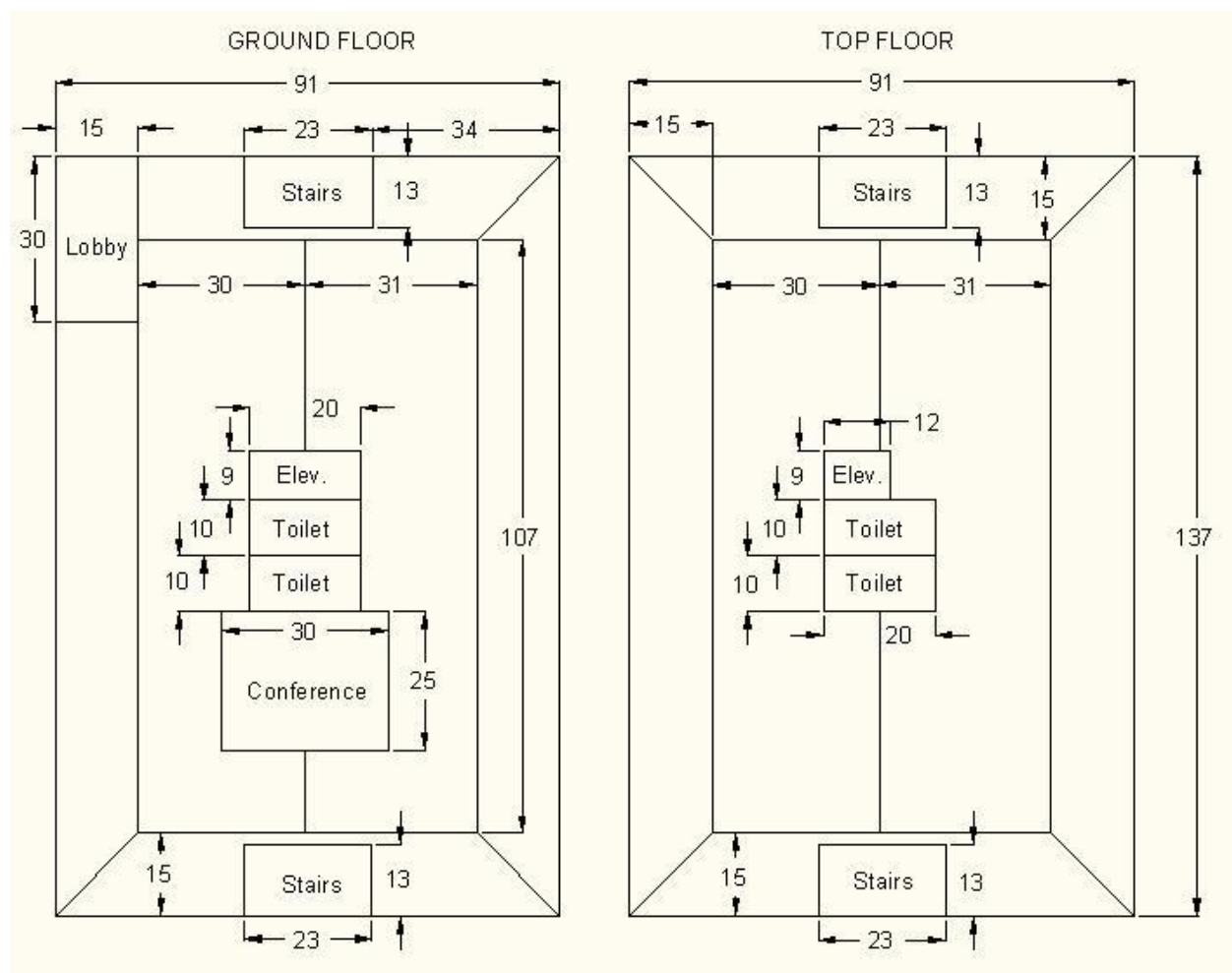


Figure 29: Floor plan for Case Study I.

Three dimensional renderings of the building energy model are shown below in Figure 30 and Figure 31. The renderings show the extensive glazing around all four faces of the building exterior – a notable feature of the DOE Benchmark/Reference Building. The nearly continuous glazing is interrupted by added doorways for the lobby entrance and stairwells. The floor to floor (or floor to roof) height is 13 ft, with a floor to ceiling height of 9 ft. The building geometry does not include any uncertainty, since the dimensions of the floor plans and elevations may be clearly discerned from basic floor plans, elevations, and photography (including satellite images available through Google).

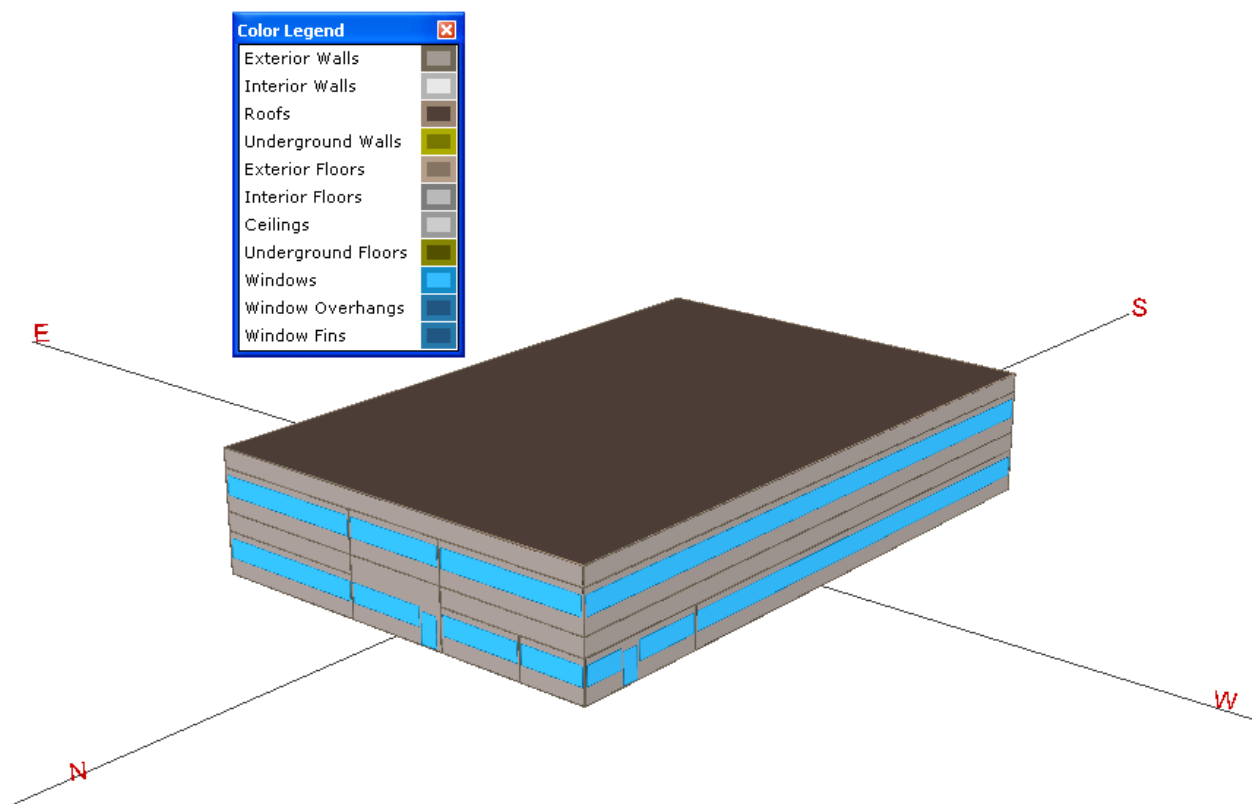


Figure 30: 3-D rendering of building, northwestern perspective (Case Study I).

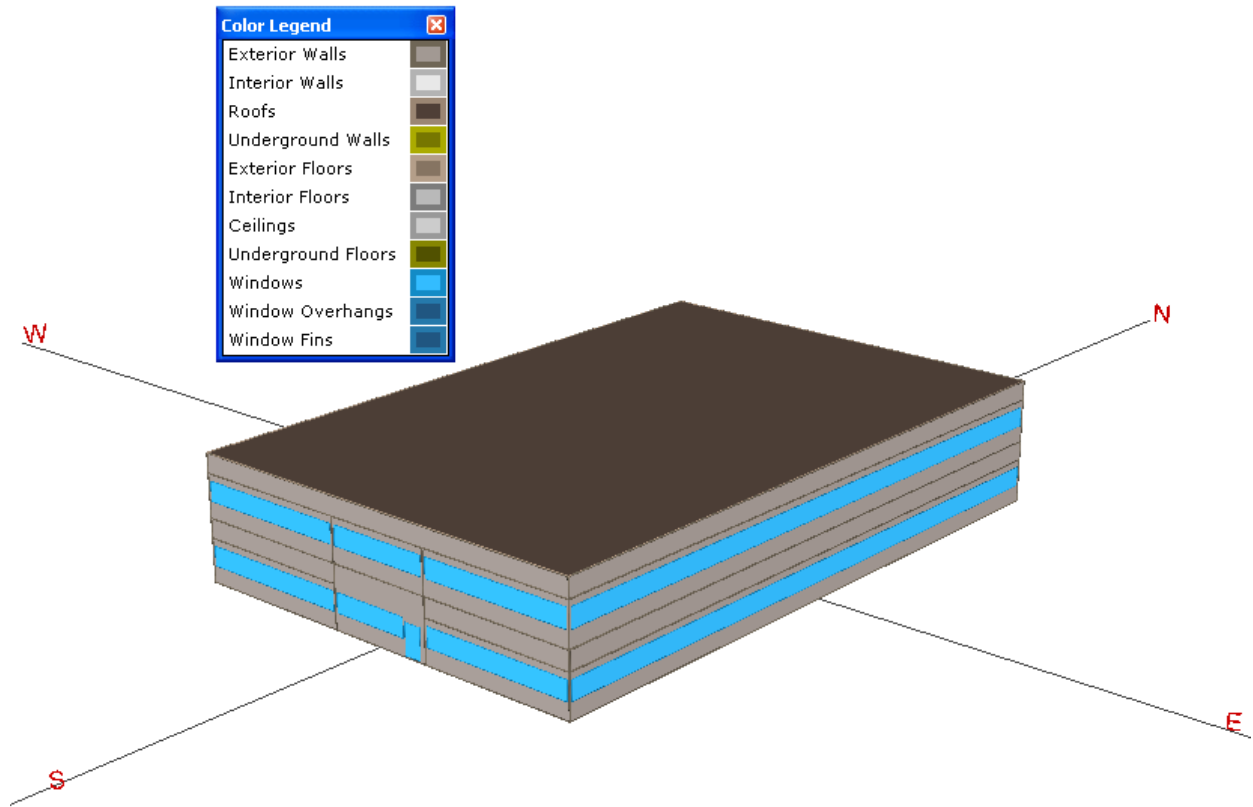


Figure 31: 3-D rendering of building, southeastern perspective (Case Study I).

The colors shown in Figure 30 and Figure 31 correspond to the legend of building features, and do not represent the actual exterior finish of the building. The details of the building energy simulation input parameters are listed in Table B-1 (see Appendix B). Several of the parameter values shown in Table B-1 are consistent with the other case studies, such as the estimated heat gain per person. These parameters are marked with the note “COMMON.” The remainder of the parameter values and ranges in values are derived from either the DOE Benchmark/Reference model, HVAC modeling literature, or from engineering judgment. In actual practice, the parameter values would be defined by a combination of field survey estimates, literature values, and engineering judgment.

The parameter values listed in Table B-1 (without uncertainty) and the operation schedules from the DOE Benchmark/Reference Building models were entered into an eQUEST/DOE2.2 energy model to estimate the building energy consumption. Figure 32 shows the components of annual tenant energy consumption for Case Study I. The results indicate that the largest single category of building energy consumption is the interior lighting systems. The miscellaneous equipment is the second-highest consumer of energy, but this category is not specific to the case study building/site (miscellaneous equipment power density is consistent between each of the case studies). Most of the remaining energy consumption is due to space heating and cooling. The results appear to be in agreement with the average results in the CBECS data (see Figure 15), although the miscellaneous equipment energy consumption is considerably higher for the energy model.

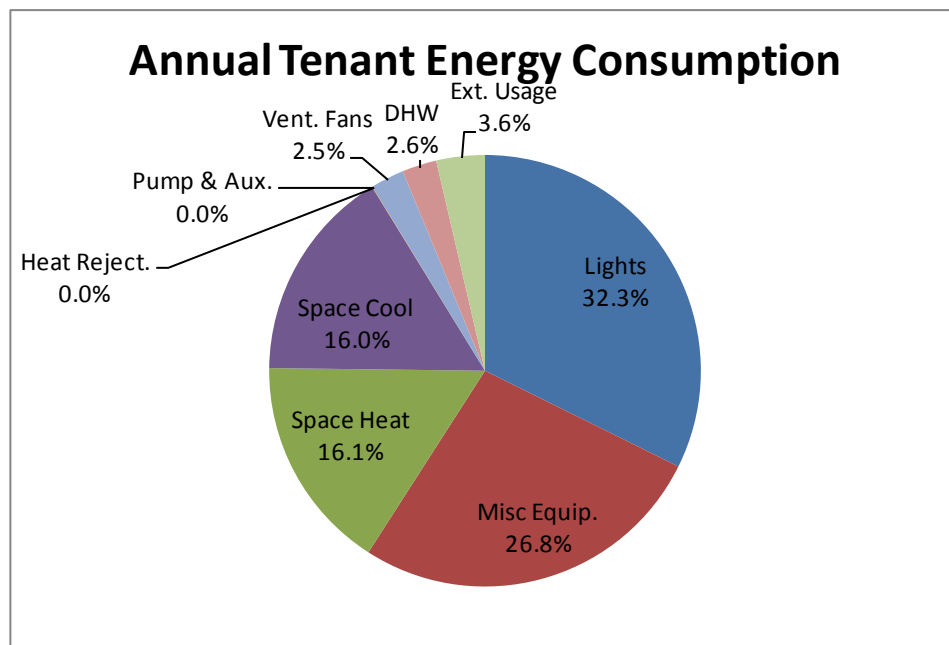


Figure 32: Components of annual tenant energy consumption (Case Study I).

To assess the reasonableness of the simulation results, it is helpful to check the monthly energy consumption for each of the component energy systems. Figure 33 shows the components of monthly tenant energy consumption for Case Study I. The results show the use of the natural gas preheat coil during the winter months, electric heating during the winter months, and cooling in mostly the summer months, but also throughout the year (no air-side economizer operation). The lighting and other weather-independent components experience only slight variations throughout the year, depending upon building occupancy.

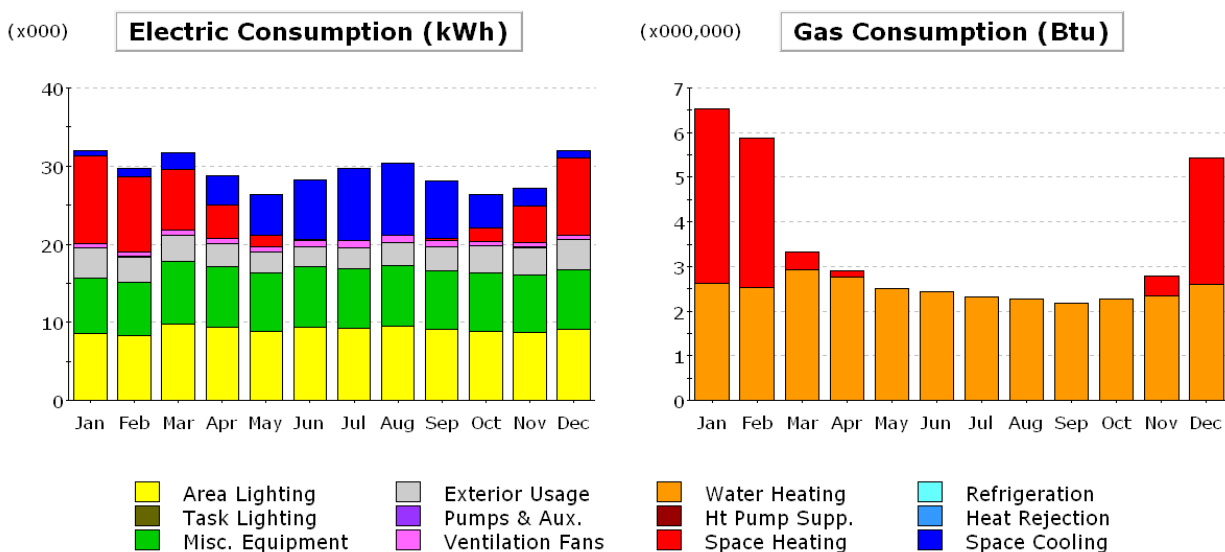


Figure 33: Components of monthly tenant energy consumption (Case Study I).

The annual energy consumption per SF is approximately 25 percent less than the energy consumption of the DOE Benchmark/Reference Building model. This reduction is due to a reduced “office space” square footage and the associated reductions in lighting and miscellaneous equipment, and a lower density of office occupancy (100 total persons vs. 125

total persons). The following section explores the sensitivity of the estimated energy consumption to the uncertainty of the input parameters.

7.1.2.2. Sensitivity Analysis of Uncertain Parameters

An important part of the case study building energy modeling is the estimation of the impact of input parameter uncertainty on building energy consumption. This section presents the sensitivity analysis of the building energy consumption for Case Study I. A Morris Method sensitivity analysis was performed, using the ranges of uncertain parameter values in Table B-1. Figure 34 below shows a plot of the mean and standard deviation of elementary effects on annual kWh for Case Study I. The dashed blue line indicates the division between effects dominated by the plotted variable and effects dominated by other variables. For variables plotted below the dashed blue line, the effect of the variable is less dependent on the other variables, and for variables plotted above the dashed blue line, the effect of the variable is more dependent on the other variables. The figure shows that two variables have an outsized impact on the annual energy consumption: The minimum air handler flow ratio (Variable #45) and the terminal unit reheat delta T limit (Variable #52). Thus, more precise data on the HVAC control settings presents an opportunity to significantly reduce the uncertainty in the annual energy consumption estimates.

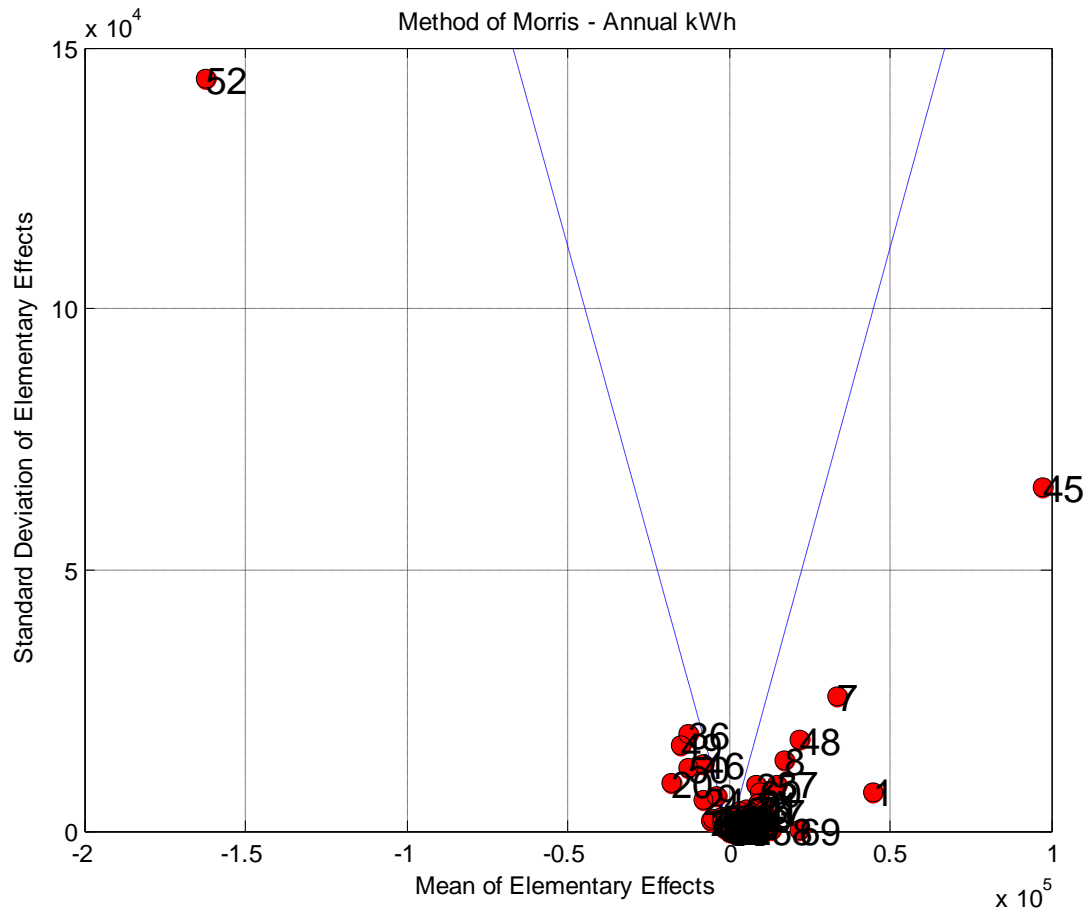


Figure 34: Mean and standard deviation of elementary effects on annual kWh for Case Study I.

A focused view of the clustered data points in Figure 34 is shown in Figure 35. Figure 35 shows that many, but not all, of the energy model input variables have a notable impact on the energy consumption uncertainty. Most of these variables have interactive effects with the other input variables, which means that they have some impact on the heating and cooling system energy consumption. The parking lighting (Variable # 68) and the elevator (Variable #69) have a noticeable impact on energy consumption, but since they are not coupled with the heating and cooling systems they have zero standard deviation of elementary effects.

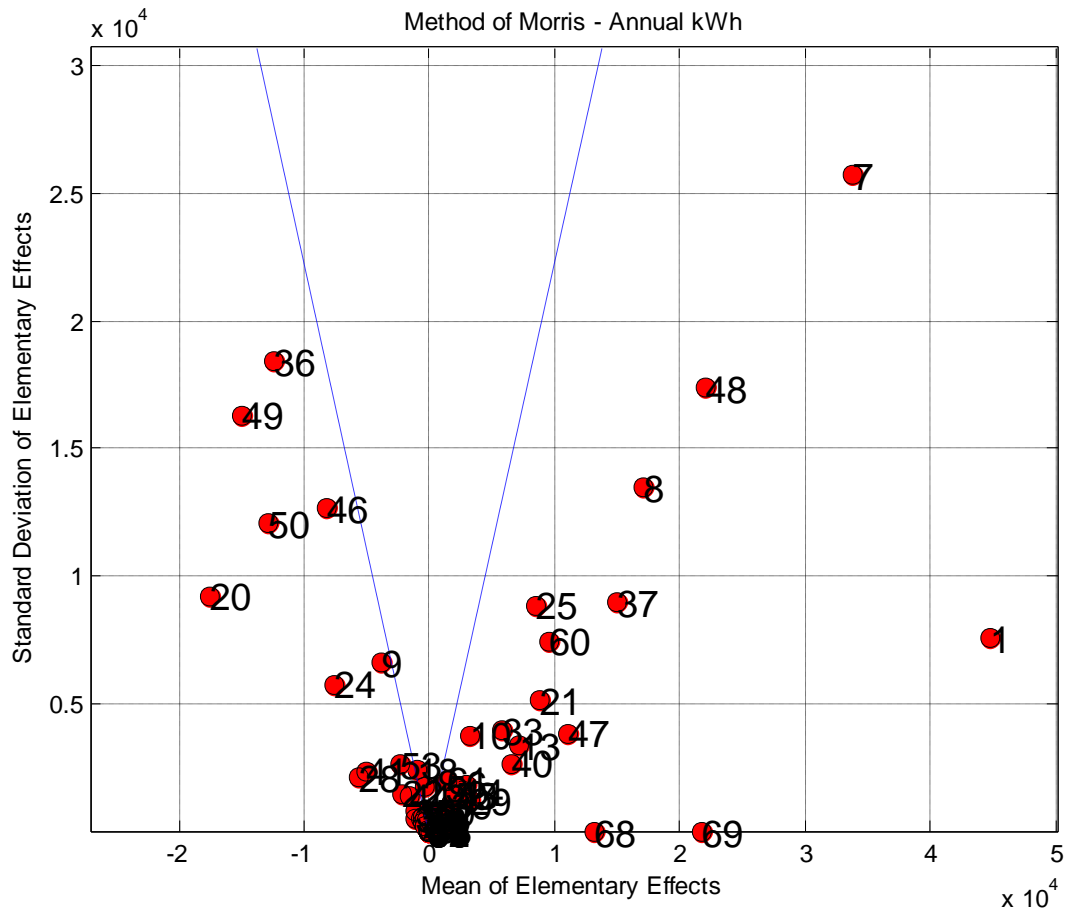


Figure 35: Mean and standard deviation of elementary effects on annual kWh for Case Study I.

Figure 36 shows the ordered absolute value of the mean of elementary effects on kWh for Case Study I. The figure shows a steep and then gradual decline in the kWh impact of the uncertain variables. The horizontal black line crossed by the data points represents a one percent impact on the annual kWh.

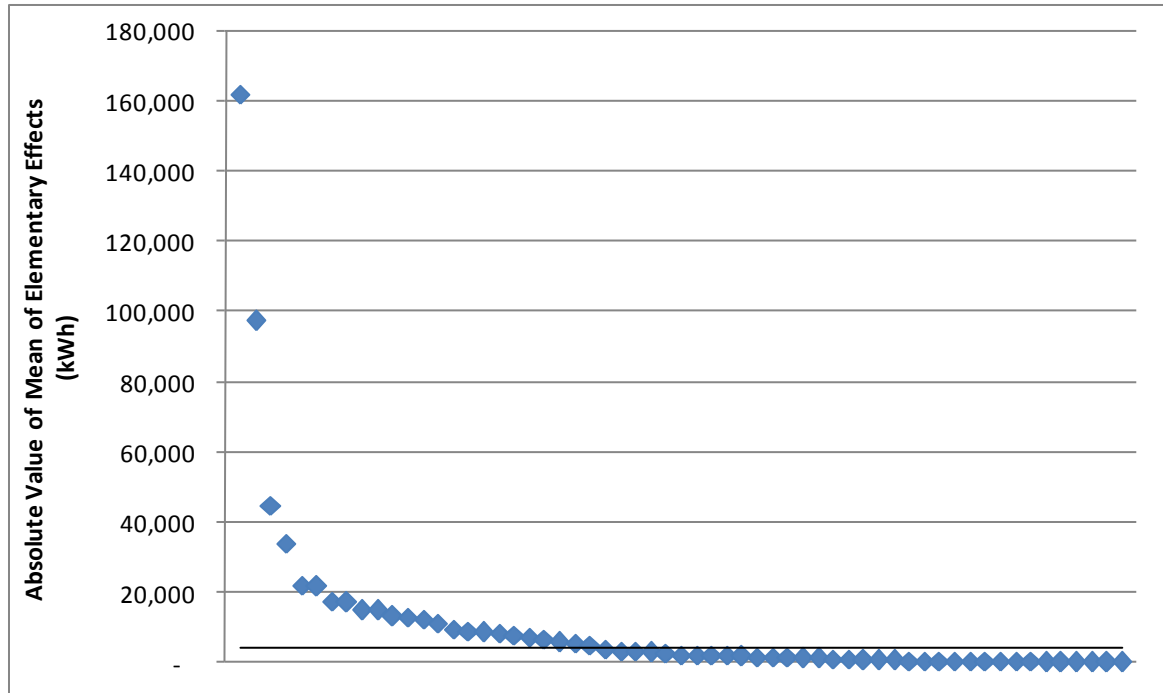


Figure 36: Ordered absolute value of the mean of elementary effects on kWh for Case Study I.

All of the variables above the black line in Figure 36 are listed below in Table 38. The variables listed in Table 38 represent many different elements of the building design, including HVAC control settings, lighting power, envelope air infiltration rates, envelope construction layer properties, and HVAC equipment efficiencies.

Table 38: Input Variables with Absolute Value of Mean Effects Greater Than One Percent of Annual Tenant kWh Consumption (Case Study I)

Var. #	Variable	Mean	Std. Dev.	Abs(Mean)
52	Heat_DT	-162,107	143,882	162,107
45	Fan_MinFlow	97,409	65,746	97,409
1	LPD_Off	44,817	7,557	44,817
7	Infil_EW	33,800	25,686	33,800
48	AHU_Cap_R	22,018	17,365	22,018
69	Elev	21,751	1	21,751

Var. #	Variable	Mean	Std. Dev.	Abs(Mean)
20	Face1_Thk	-17,564	9,235	17,564
8	Infil_NS	17,096	13,485	17,096
49	CRS_Sup_at_Low	-14,930	16,321	14,930
37	Glaz1_Cond	14,907	8,991	14,907
68	Park_Light	13,108	0	13,108
50	CRS_MinFlow	-12,802	12,083	12,802
36	Glaz1_SC	-12,448	18,392	12,448
47	Cool_EIR	11,079	3,855	11,079
60	Tstat_ThRng	9,627	7,460	9,627
21	Face1_Cond	8,847	5,150	8,847
25	Wall_Insul1_Cond	8,577	8,866	8,577
46	Cool_Cntl_Rng	-8,169	12,640	8,169
24	Wall_Insul1_Thk	-7,627	5,777	7,627
13	Frm_Width	7,196	3,370	7,196
40	SFan_Sp	6,600	2,686	6,600
33	Gflr_Conc_Cond	5,771	3,987	5,771
28	Roof_Blt_Thk	-5,602	2,127	5,602
41	SFan_Tot_Eff	-5,040	2,379	5,040

The building energy consumption consists of not only the kWh of electric utility energy, but also the utility natural gas for heating. Figure 37 shows the mean and standard deviation of elementary effects on annual natural gas MBtu for Case Study I. A handful of variables have a distinct impact on the natural gas energy consumption, yet the impact on total building energy consumption is considerably low.

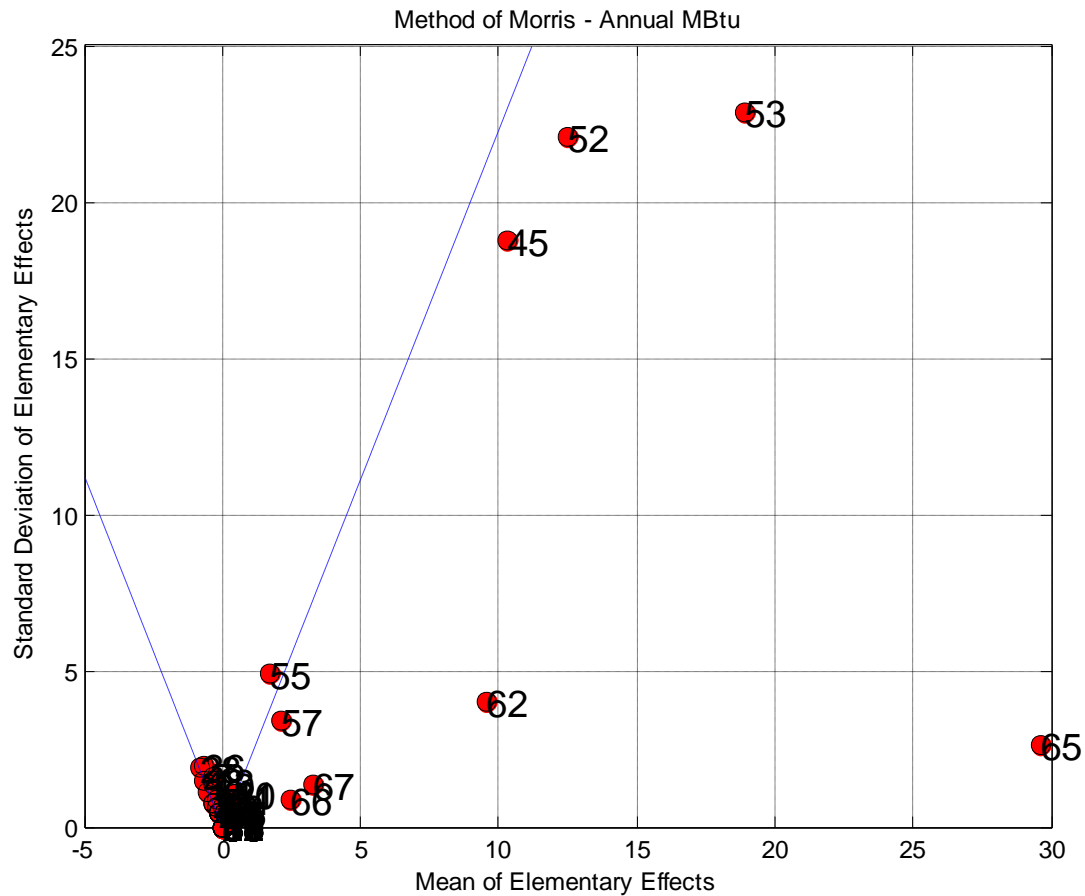


Figure 37: Mean and standard deviation of elementary effects on annual natural gas MBtu for Case Study I.

Figure 38 shows the ordered absolute value of the mean of elementary effects on MBtu for Case Study I. Only two variables have a mean of elementary effects greater than one percent of the total annual building energy consumption (data points shown above the horizontal black line). These variables are listed in Table 39. It is not surprising that very few input parameters have a notable effect on the building energy consumption. Only a subset of all input parameters influence the heating energy consumption, and the natural gas energy satisfies only a portion of the total heating load.

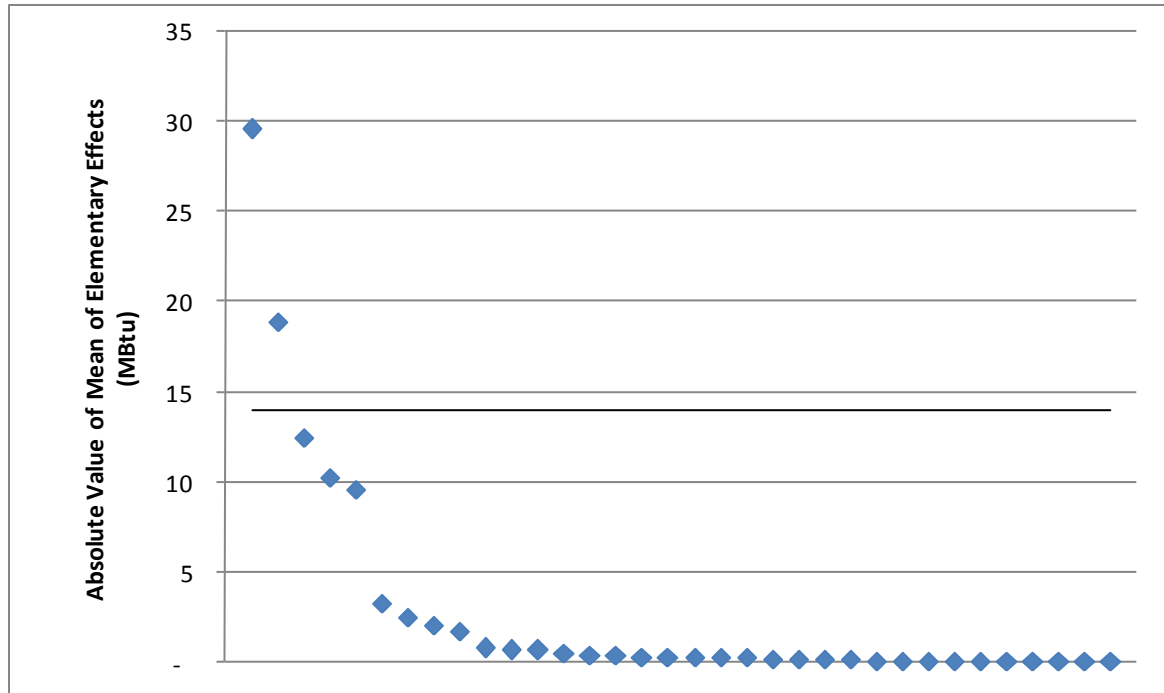


Figure 38: Ordered absolute value of the mean of elementary effects on MBtu for Case Study I

Table 39: Input Variables with Absolute Value of Mean Effects Greater Than One Percent of Annual Tenant MBtu Consumption (Case Study I)

Var. #	Variable	Mean	Std. Dev.	Abs(Mean)
65	DHW_Load_single	30	3	30
53	Heat_Pre_T	19	23	19

The following section describes the Monte Carlo analysis of the building energy simulation uncertainty.

7.1.2.3. Monte Carlo Analysis

For the Monte Carlo analysis of the building energy simulation uncertainty, each of the input variables having a mean of elementary effects greater than one percent is included. These

input variables and their ranges of uncertainty are shown below in Table 40. The ranges of uncertainty are taken directly from Table B-1. Thus, an initial Monte Carlo simulation is performed without mitigating the effects of the variables having the greatest impact on estimated energy consumption.

Table 40: Uncertain Input Variables for Monte Carlo Analysis (Case Study I)

Var. #	Variable	Min	Max	Units
52	Heat_DT	20	40	degF
45	Fan_MinFlow	0.2	0.5	NA
1	LPD_Off	1	1.8	W/SF
7	Infil_EW	0.49	1.47	AC/hr
48	AHU_Cap_R	1	1.2	NA
69	Elev	7.305	21.92	kW
20	Face1_Thk	0.083	0.333	ft
8	Infil_NS	0.515	1.545	AC/hr
49	CRS_Sup_at_Low	60	65	degF
37	Glaz1_Cond	0.5	0.8	Btu/h-SF-degF
68	Park_Light	7	10	kW
50	CRS_MinFlow	0.3	0.66	NA
36	Glaz1_SC	0.2	0.6	NA
47	Cool_EIR	0.3346	0.379	NA
60	Tstat_ThRng	1	3	degF
21	Face1_Cond	0.04	0.1	Btu/h-ft-degF
25	Wall_Insul1_Cond	0.017	0.417	Btu/h-ft-degF
46	Cool_Cntl_Rng	3	6	degF
24	Wall_Insul1_Thk	0.066	0.333	ft
13	Frm_Width	0.0833	0.208	ft
40	SFan_Sp	2.5	4.5	in. wg
33	Gflr_Conc_Cond	0.275	1.667	Btu/h-ft-degF
28	Roof_Blt_Thk	0.25	0.417	ft
41	SFan_Tot_Eff	0.5	0.75	NA
65	DHW_Load_single	0.15	0.5	gpm
53	Heat_Pre_T	40	65	degF

Upon iterating the Monte Carlo simulation 1,000 times, histograms of estimated energy consumption and GHG emissions may be reviewed. Figure 39 shows the Monte Carlo analysis of annual electric energy consumption for Case Study I. The high degree of impact from the variables in the sensitivity analysis (see previous section) is evident in the skew shown in Figure 39. Specifically, this skew is the result of a high-end value for Variable #45, and a low-end value for Variable #52.

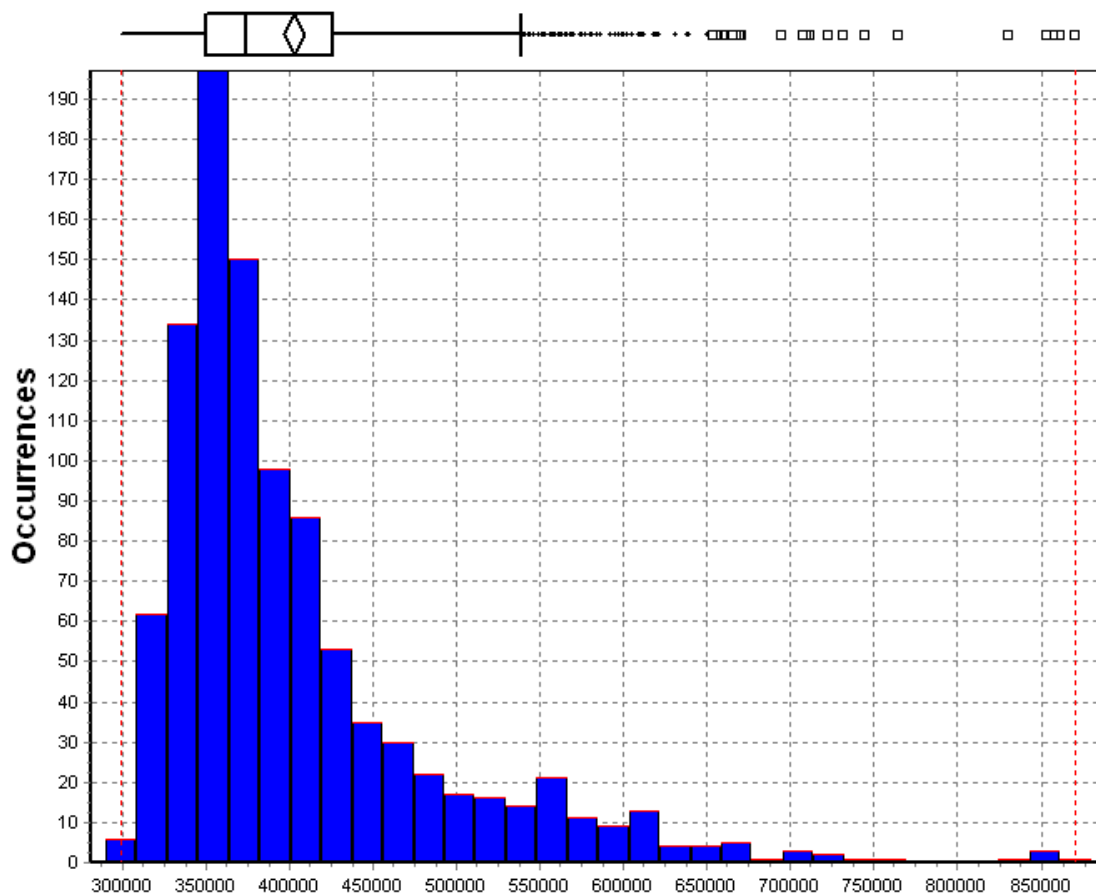


Figure 39: Monte Carlo analysis of annual energy consumption, kWh (Case Study I).

For the annual natural gas energy consumption, some skew exists as well. The skew is influenced mostly by high values of the variables listed in Table 39.

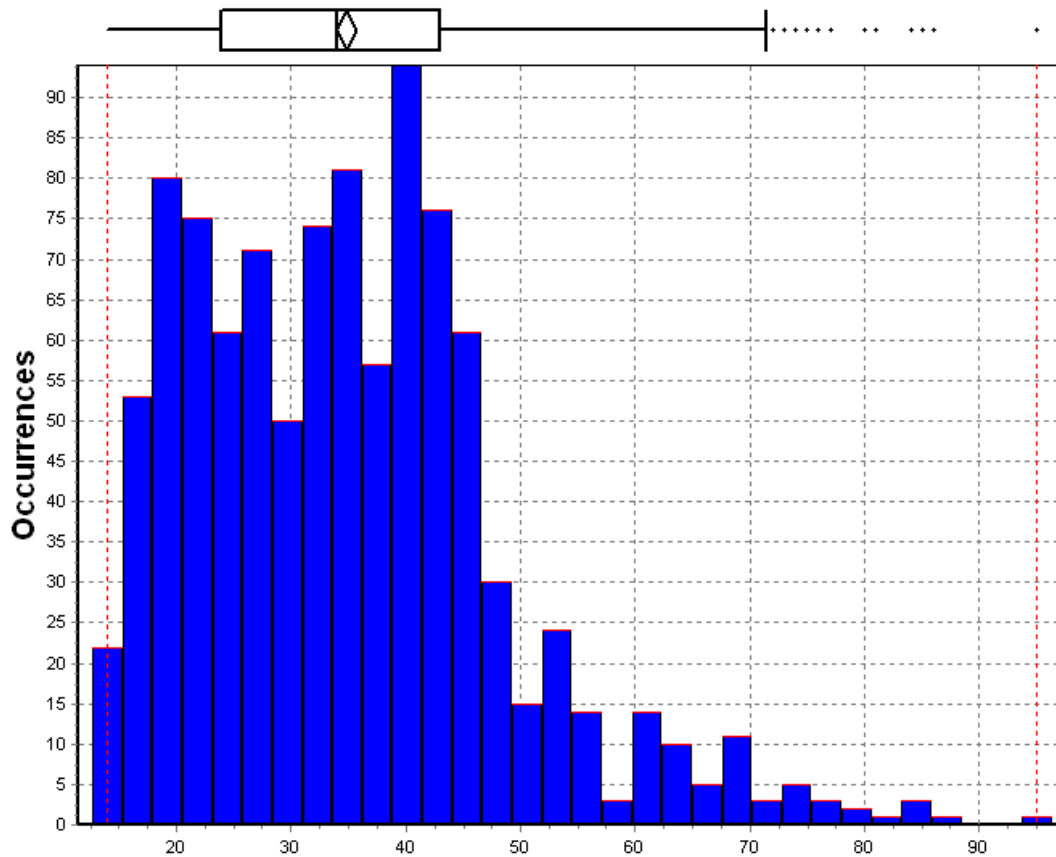


Figure 40: Monte Carlo analysis of annual natural gas energy consumption, MBtu (Case Study I).

The histogram of total building energy consumption (electricity plus natural gas) is shown below in Figure 41. The shape of Figure 41 is most similar to Figure 39 since the electric utility energy consumption represents most of the building energy consumption. It comes as no surprise then that the Scope 1 plus Scope 2 (direct combustion plus purchased electricity) GHG emissions histogram shown in Figure 42 is very similar to Figure 41.

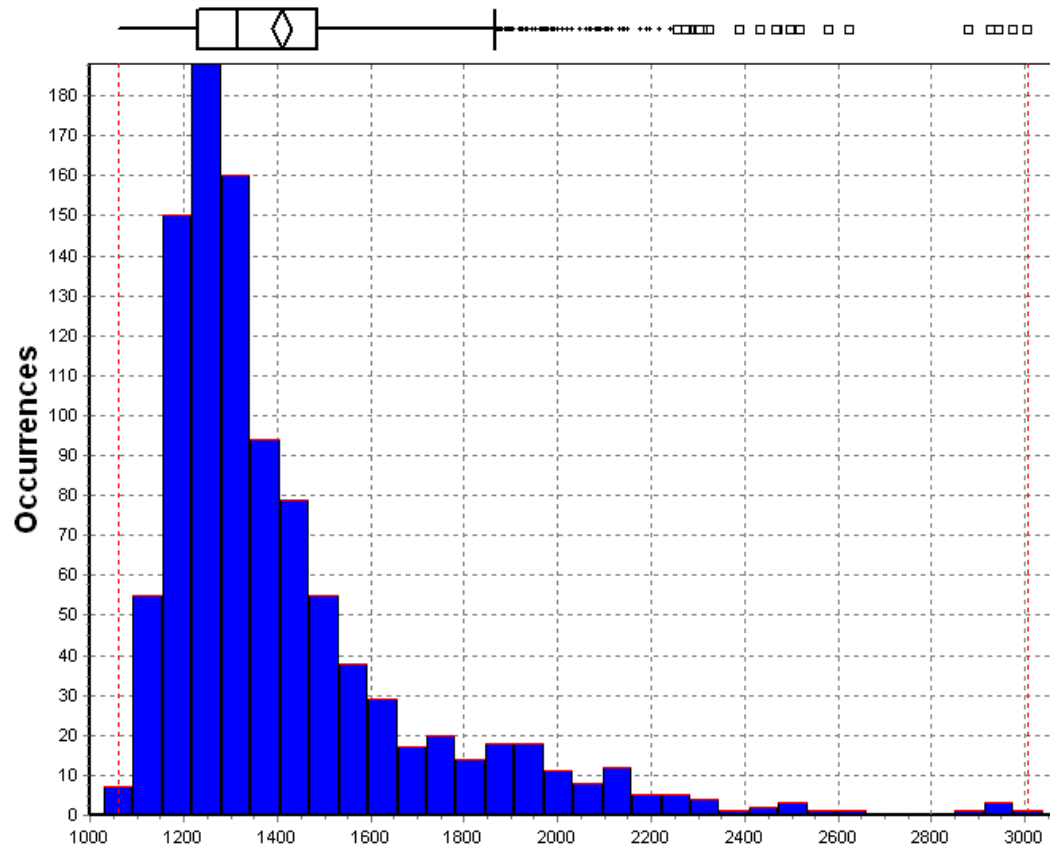


Figure 41: Monte Carlo analysis of annual building energy consumption, MBtu (Case Study I).

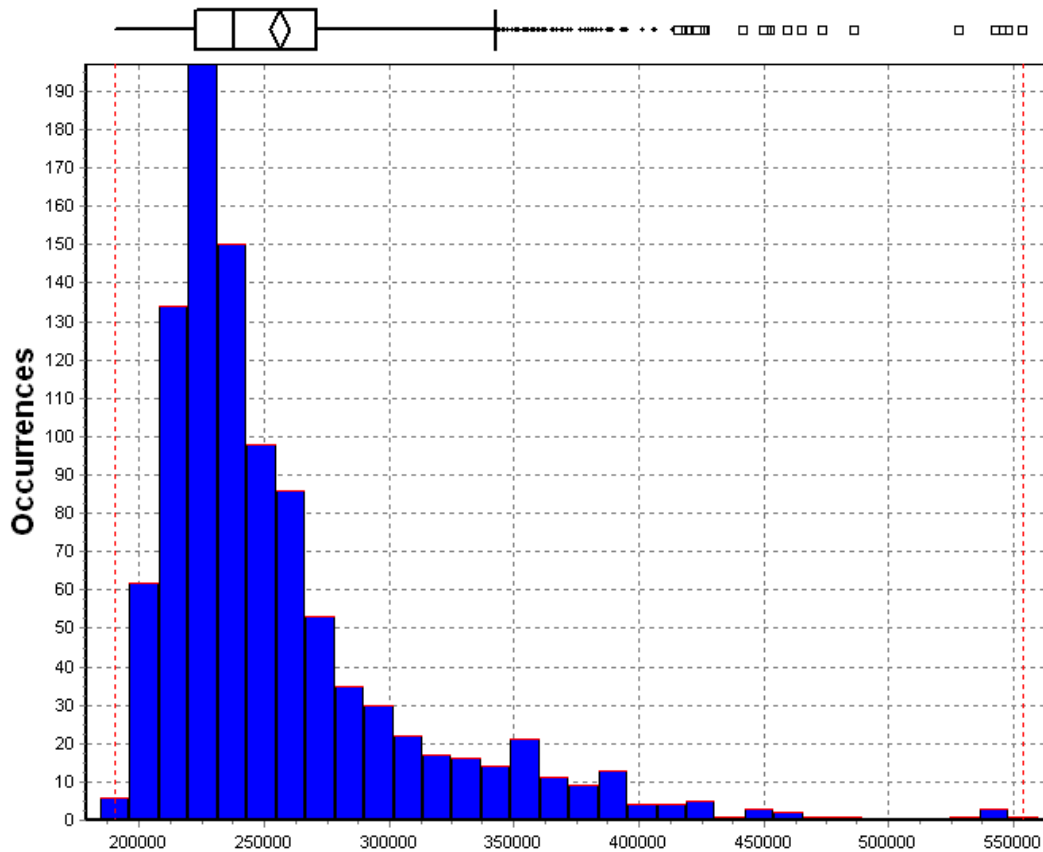


Figure 42: Monte Carlo analysis of annual Scope 1 and Scope 2 GHG emissions, kg (Case Study I).

The combined Scope 1, 2, and 3 GHG emissions for the building energy consumption are shown below in Figure 43. The shape of the skewed output distribution remains the same, but the total GHG emissions are greater. A description of the data used to calculate the direct and upstream GHG emissions is provided in the following section (7.1.3.4). The GHG Monte Carlo analysis includes uncertainty in the energy consumption, but does not include uncertainty in the GHG emission factors.

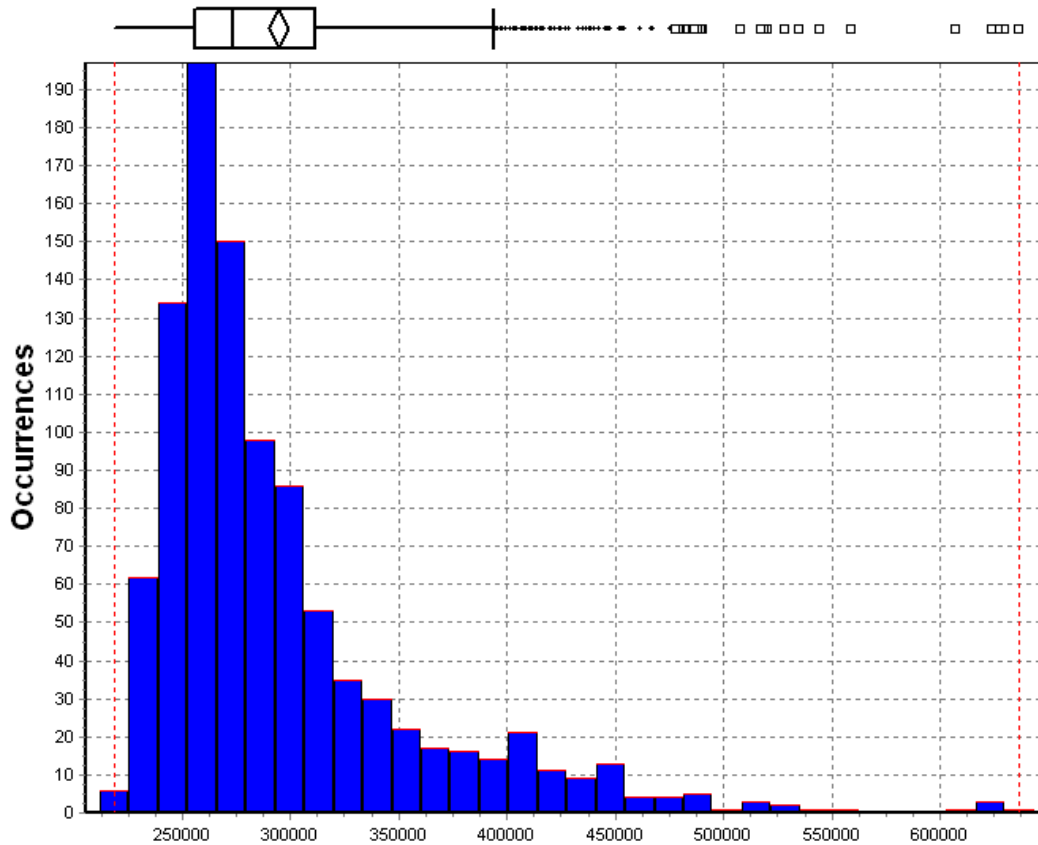


Figure 43: Monte Carlo analysis of annual Scope 1, Scope 2, and Scope 3 GHG emissions, kg (Case Study I).

The high degree of skew in this initial Monte Carlo analysis for Case Study I results in a large range of energy consumption and GHG emission estimates. The skew and range of energy consumption could be significantly reduced by reducing the input variable uncertainty for the parameters having the greatest impact on the simulation output. In the sensitivity analysis in the previous section (7.1.2.2), many input variables have a mean of elementary effects that is greater than one percent of the building energy consumption. As can be seen in Figure 34 and Figure 36, the minimum air handler flow ratio (Variable #45), the terminal unit reheat delta T limit (Variable #52), and the office lighting power density (Variable #1) have a large impact on the annual energy consumption. These variables are prime candidates for additional building data

collection that can help to reduce estimation uncertainty. Reflecting a focused data collection effort to reduce the simulation uncertainty, the min-max range of these variables are redefined as follows: Variable #1 is 1.6 to 1.7 W/SF, Variable #45 is 0.3 to 0.35, and Variable #52 is 50 to 60 deg F. With these revised ranges of uncertainty, the Monte Carlo energy simulation was rerun. Figure 44 below shows the revised Monte Carlo analysis of annual electric energy consumption in kWh's. For the revised Monte Carlo analysis, the skew and range of the estimated energy consumption is significantly reduced, and the histogram of estimates takes the form of a normal distribution.

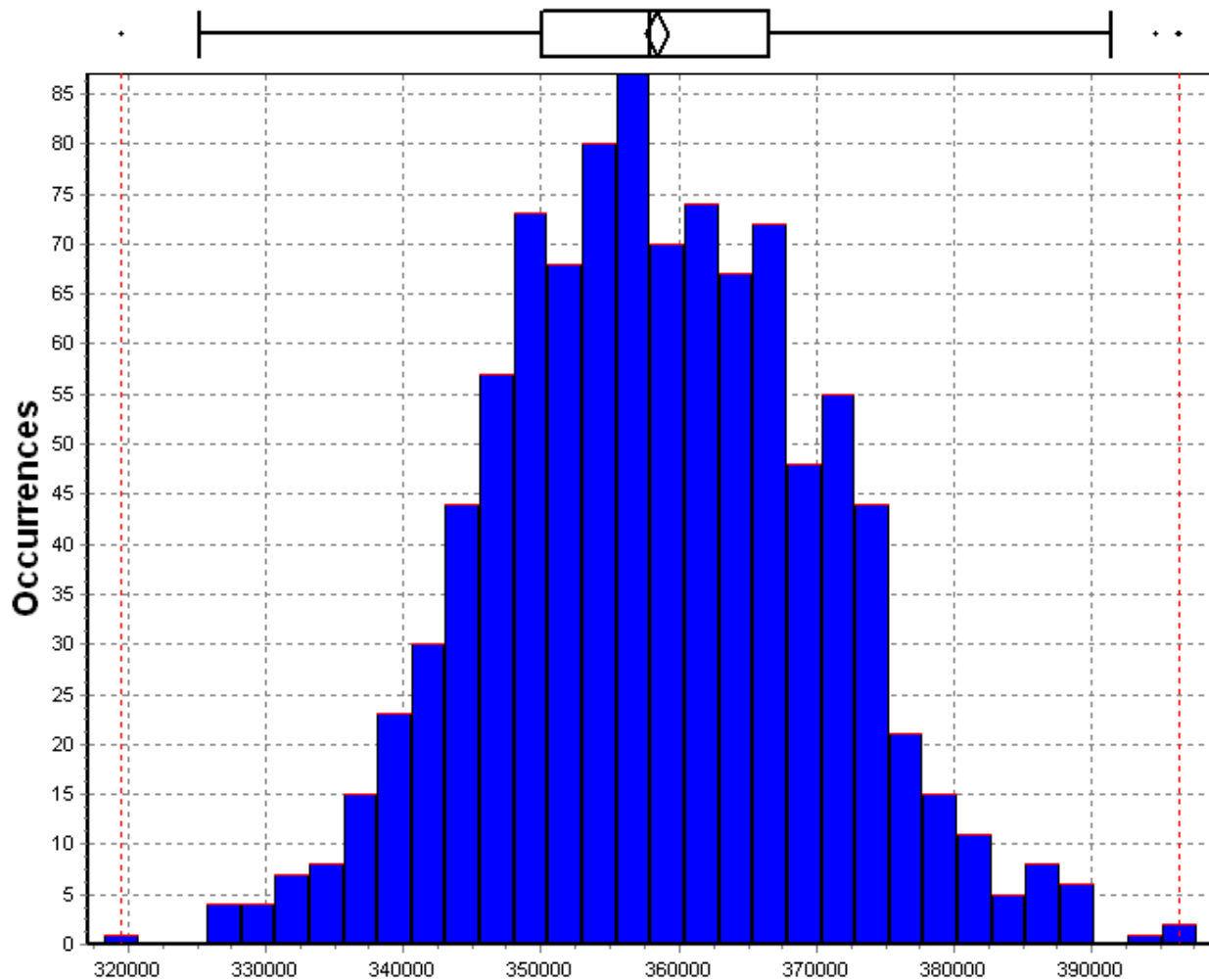


Figure 44: Revised Monte Carlo analysis of annual energy consumption, kWh (Case Study I).

The following section presents the estimation of source energy consumption and GHG emissions.

7.1.2.4. Site Energy vs. Source Energy / GHG Emissions

The above estimated annual energy consumption is specifically the direct energy consumed on site (referred to as the “site energy” by DOE) (56, 95). Alternatively, the “source

energy” is the “sum of the energy consumed at a facility plus the energy required for extraction, conversion, and transmission of that energy to the facility” (56). Based on energy consumption/loss data for the energy supply chain, a “source energy factor” may be estimated and multiplied by the site energy to obtain the estimated source energy consumption. According to DOE, the source energy factor for electrical energy consumed at a facility located in Georgia is 3.364 kWh of source energy consumed per kWh of delivered electricity (see (95), Table B-9). Thus, the average source energy consumption of electric utility energy for Case Study I is approximately 1,206,000 kWh or 1,222 MBtu. With respect to natural gas energy consumption, the national average source energy factor is 1.092 MBtu of source energy consumed per MBtu of delivered natural gas (see (95), Table 5). This means that for the mean of 38.24 MBtu of natural gas consumed for Case Study I (site energy), approximately 41.75 MBtu of source energy is consumed. Comparison of source energy (instead of site energy) between building alternatives becomes relevant if the building alternatives have different sources of energy, such as gas-fired heating vs. electric heating or onsite solar power generation vs. purchased electric utility energy. In this case study, like many commercial buildings in Climate Zone 3A, the natural gas energy consumption is only a fraction of the total building energy consumption.

The results of both the direct and upstream GHG emission estimates for electricity purchased in the state of Georgia are shown in Table 41. Consistent with GHG emission inventory protocols (71, 72, 73, 74), the natural gas combustion emissions are counted as “Scope 1,” the purchased electricity emissions are counted as “Scope 2,” and the upstream fuel-energy supply chain emissions are counted as “Scope 3.”

Table 41: Estimated GHG Emissions of Purchased Electricity and Natural Gas Combustion (Case Study I)

kWh Electricity	kBtu Natural Gas	CO ₂ e (Scope 1), tonnes	CO ₂ e (Scope 2), tonnes	CO ₂ e (Scope 3), tonnes	CO ₂ e (Total), tonnes	Calc. Source
358,399	38,240	2.03	228.0	34.3	264.4	(121)
					263.8	(95)

The source energy estimation guidance of DOE provides an estimation method and emission factors for total (direct and upstream) electricity GHG emissions (95). Using the DOE electric utility emission factor for the State of Georgia (1.62 lb CO₂e per kWh) and the national natural gas emission factor of 27.8 CO₂e per 1,000 SCF, the estimated total CO₂e emissions are 263.8 tonnes, which nearly matches the piecewise estimate of Scope 1, Scope 2, and Scope 3 emissions from the author's GHG emission calculator.

7.1.2.5. Normalization of Results

The estimates of total energy consumption and GHG emissions are normalized by building square footage and person-hours of occupancy to calculate the building's performance metric values. Table 42 shows the normalized energy consumption and GHG emission performance of Case Study I. The square-footage of the conditioned floor area is the total tenant square footage shown in Table 36. The person-hours of occupancy are based on the amount shown in Table 35. Each value is expressed as a mean \pm 2 standard deviations. Based on the comparative data shown from the CBECS database, the building is more energy efficient than the average office building in the South Atlantic region. Some caution should be taken when comparing the case study's EUI with the CBECS data (see Section 5.1.2.2). The CBECS sample sizes are very small and the region extends across multiple climate zones. Furthermore, the usage

pattern (occupancy schedule, lighting schedule, HVAC schedule) of the case studies in this chapter may be substantially different from the usage pattern of buildings in the CBECS database. Compared to ASHRAE/IES Standard 100-2006, Case Study I does not meet the desired EUI target (see Climate Zone 3A in Table 8).

Table 42: Normalized Building Energy Consumption and GHG Emission Performance (Case Study I)

Inventory Unit		Normalizing Unit	Performance Metric	Value
Annual Energy [kBtu]	Site (end use)	Conditioned floor area [SF]	Annual site energy / conditioned floor area [kBtu/SF]	50.6 ± 3.3
		Occupant use [person-hrs]	Annual site energy / occupant use [kBtu/person-hrs]	5.1 ± 0.3
	Primary (end use + upstream)	Conditioned floor area [SF]	Annual primary energy / conditioned floor area [kBtu/SF]	166.7 ± 10.9
		Occupant use [person-hrs]	Annual primary energy / occupant use [kBtu/person-hrs]	16.8 ± 1.1
CBECS annual site energy / conditioned floor area [kBtu/SF] *				75.7
CBECS annual source energy / conditioned floor area [kBtu/SF] ^				217.7
Annual GHGs [lb CO2e]	Site (end use)	Conditioned floor area [SF]	Annual site GHGs / conditioned floor area [lb CO2e /SF]	3,661.0 ± 240.1
		Occupant use [person-hrs]	Annual site GHGs / occupant use [lb CO2e /person-hrs]	369.9 ± 24.3
	Primary (end use + upstream)	Conditioned floor area [SF]	Annual primary GHGs / conditioned floor area [lb CO2e /SF]	4,206.7 ± 275.9
		Occupant use [person-hrs]	Annual primary GHGs / occupant use [lb CO2e /person-hrs]	425.1 ± 27.9
Source: * CBECS: South Atlantic, office, constructed 1980 - 1999, 10,001 - 50,000 SF ^ CBECS and Deru & Torcellini				

7.1.3. Case Study II: Recent Construction, Single-Tenant, Low-Rise Commercial Office Building in Suburban Development Area

The second building case study represents a more recently constructed, single-tenant, low-rise commercial office building in a suburban development area. The building is adapted from an actual, LEED Certified, two-story office building in a suburban office park. The building is actually not a new construction, but rather a recent major renovation of an older building. The renovation includes extensive upgrades to the building envelope, lighting, and HVAC system. The overall size of the building, as well as the sizes of the constituent spaces, were adjusted to be consistent with the program of spaces for all of the case studies (see Table 33 and Table 43). The actual building contains 30,000 SF of interior space, of which over 4,000 SF is a data center. The first floor of the actual building is partially below grade (including the data center). Adjustments to the program of spaces and geometry of the actual building include replacement of the data center space with office space, exposure of below grade walls to atmosphere, adjustment of glazing areas, and adjustment of work space, support space, and circulation space sizes and locations. The building footprint length to width ratio of 1.5 was preserved (150 ft x 100 ft adjusted to 137 ft x 91 ft). The building spaces are summarized in Table 43, and the building system characteristics are summarized in Table 44 of the following section.

Table 43: Summary of Tenant Spaces (Case Study II)

Building Size	Space Category	Space Type	Size (SF)
Medium	Total	Total	24,934
	Work Space	Office	21,450
		Conference	750
	Support Space	Toilet	800
		Mech. / Elect.	0
		Lobby	450
	Circulation	Stairs	1,200
		Elevator	288

7.1.3.1. Energy System Parameters and Building Energy Model

The building energy system parameters represent a substantially more modern and efficient building than is represented by Case Study I. The building has recently undergone a major renovation and has achieved LEED certification. LEED submittal data was utilized to define several important building design parameters for this case study, including the HVAC system, the interior and exterior lighting, the building envelope, and the elevator. The building HVAC system consists of a rooftop air handler with DX cooling, and VAV terminal unit reheat. Dedicated exhaust fans provide ventilation of the restrooms with no energy recovery. Domestic hot water is heated by an electric hot water heater tank. The window to wall area ratio is 0.17. Table 44 below summarizes the main building characteristics of Case Study II. The equipment part load efficiencies are based on the defaults in eQUEST/DOE2.2. Utility service is all electric and there is no on-site power generation. The detailed energy system parameter values are shown in Table B-2 in Appendix B. Similar to the other case studies, these energy system parameters are entered into an eQUEST/DOE2.2 building energy model.

Table 44: Case Study II Building Characteristics

Tenant Space Occupancy	Single Tenant
Number of Tenant Floors	2
Total Number of Floors	2
Width to Length Ratio	0.66
Orientation	West
Envelope to Floor Area Ratio	0.94
Percent Glazing	17%
Floor Condition	Slab on grade
Lighting System Type	Suspended fluorescent, not vented
HVAC System Type	VAV with air-side economizer, DCV, DX cooling, non-powered terminal units, electric reheat, ducted return
Conveyances	1 elevator

The floor plan of the spaces/zones in the building energy model is shown below in Figure 45. The floor plan, adjusted from the actual building data, matches the floor plan of Case Study I. As such, the energy model for Case Study II contains the same perimeter and core zoning of HVAC thermal zones. Any space/zone not labeled in Figure 45 is an open office area (either perimeter or core).

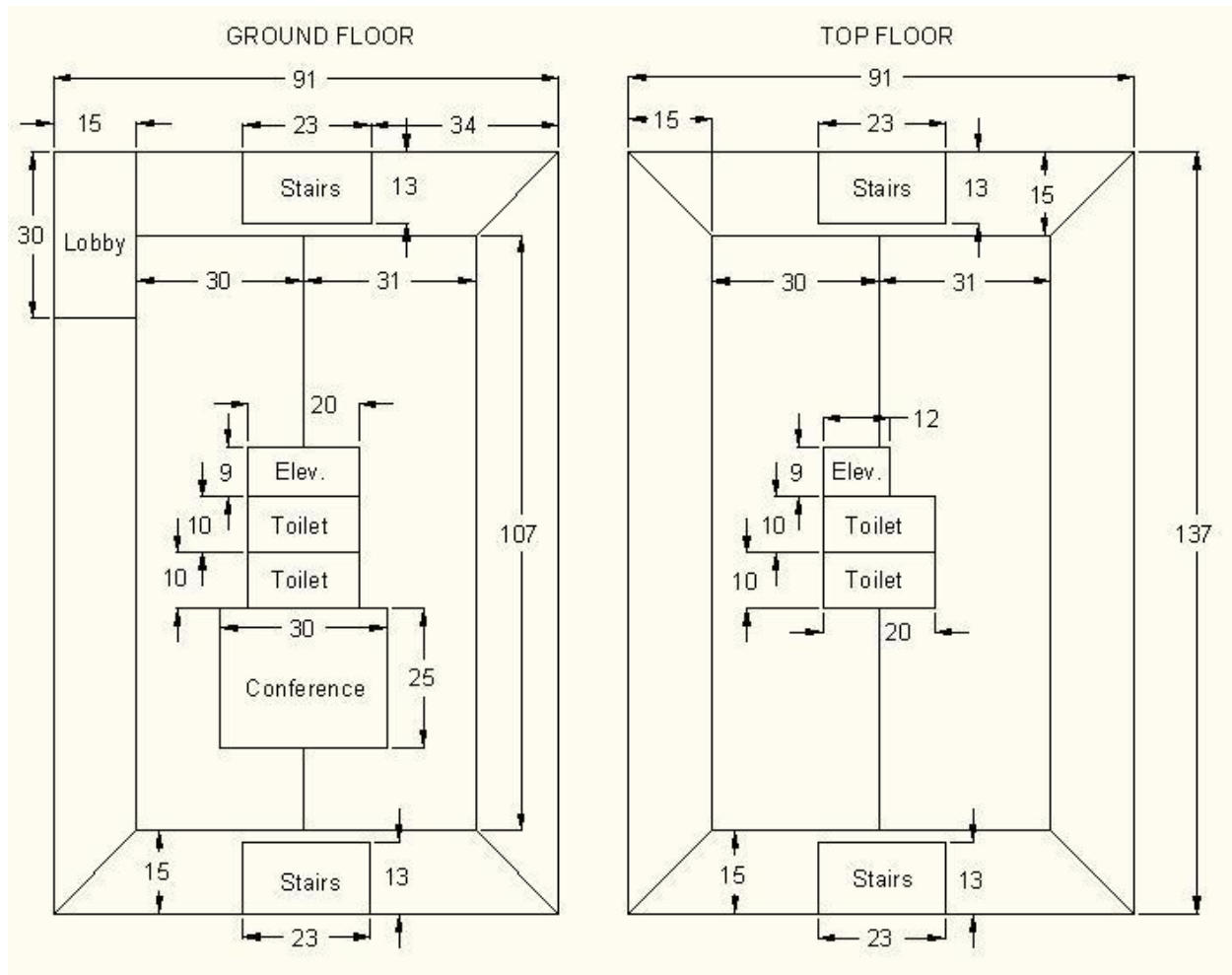


Figure 45: Floor plan for Case Study II.

Three-dimensional views of the building geometry are shown in Figure 46 and Figure 47. As is indicated in Table 44, the building envelope includes much less glazing area than does the building envelope of Case Study I. The model includes the shading effect of two deciduous trees adjacent to the building, whose transmittance is modified between the winter and summer season (shown as vertical shading surfaces in the figures below).

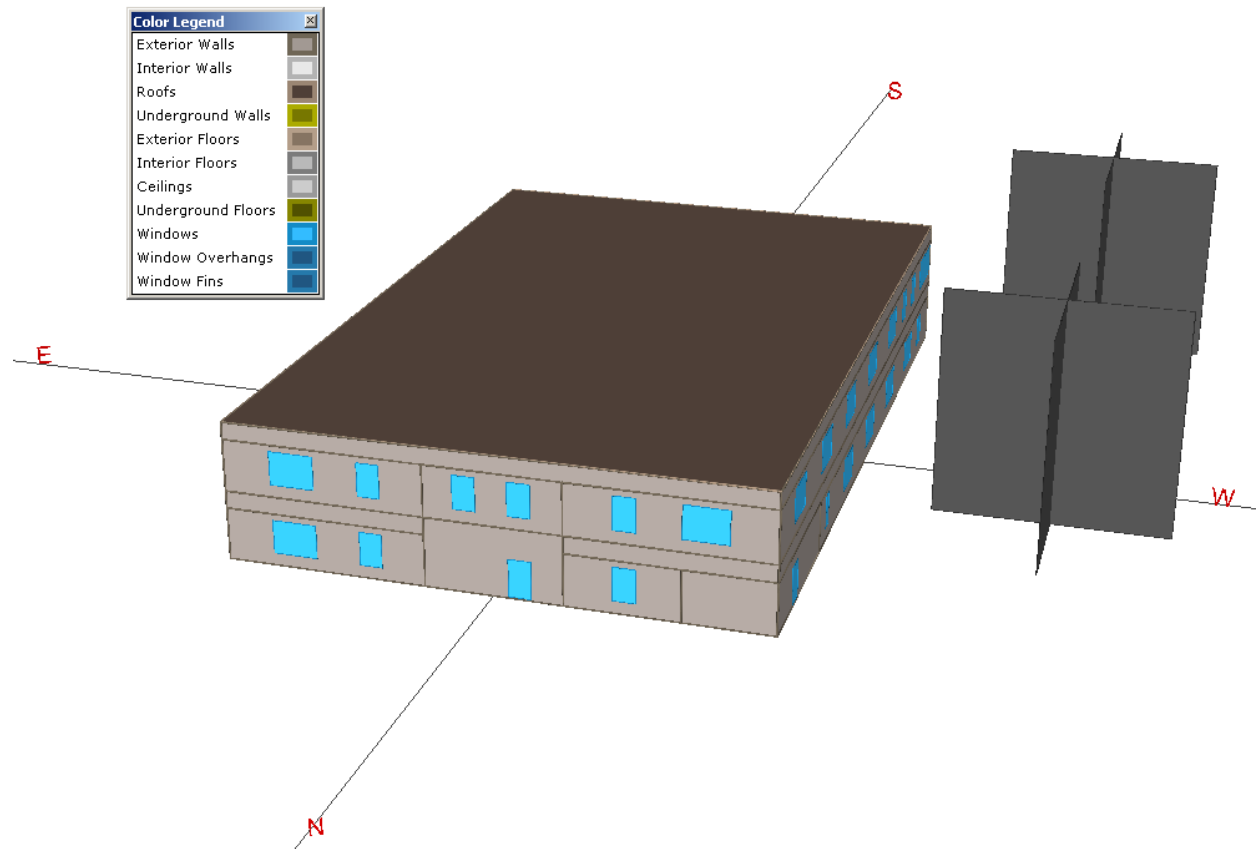


Figure 46: 3-D rendering of building, northwestern perspective (Case Study II).

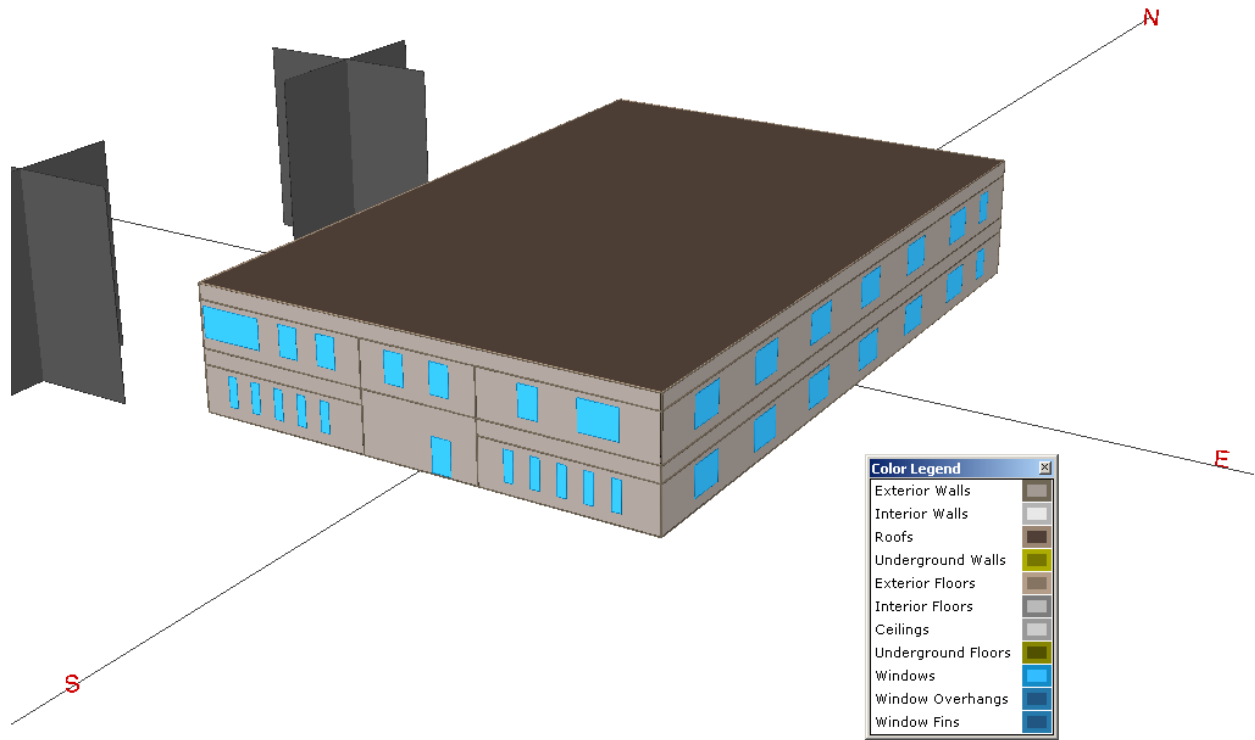


Figure 47: 3-D rendering of building, southeastern perspective (Case Study II).

One of the more difficult to define energy system parameters in a building energy model is the building air infiltration (see Section 5.1.1.1.2). For the purposes of the case studies, the infiltration rate is defined as a range of values, rather than a single value (see Appendix B). The range of values encompass the eQUEST defaults as well as values from NIST, DOE, and COMNET. The eQUEST building energy simulation software contains default infiltration rates in units of CFM per SF of floor area. The default infiltration rates vary by type of space: perimeter spaces facing North, South, or West, perimeter spaces facing East, and core spaces (see Table B-2). Assuming constant infiltration rates and applying these eQUEST rates to the space geometry of this case study, the infiltration rate is approximately 340 CFM. Alternatively, using the COMNET infiltration rate (constant) yields approximately 415 CFM. Considering the

low-level of precision in building air infiltration estimation, these values are in close agreement with one another (20 percent difference). It should be noted that infiltration rates are in fact not constant over time. Infiltration rates vary throughout the day in response to changes in building pressurization (operation of supply fans), changes in wind speed, and occurrences of building ingress and egress. Hourly building energy models typically utilize hourly schedules to reflect building fan operation as well as building ingress and egress. These schedules apply hourly multipliers to the constant infiltration rates. The COMNET standard references the California 2005 Building Energy Efficiency Standards and thereby provides an infiltration schedule with zero infiltration during fan operation (149). In order to achieve zero outdoor air infiltration during fan operation, the building HVAC would need to be perfectly balanced and provide uniform pressurization in all enveloped spaces. This condition is highly unlikely, especially since occupant ingress and egress would very likely occur during fan operation. The default eQUEST infiltration schedules provide hourly values that apparently account for reduced infiltration during fan operation and increase infiltration during peak ingress/egress periods. Although no documentation is available for the eQUEST default schedules, the schedules provide a reasonable values for modeling outdoor air infiltration.

Upon defining the building energy model, the model was run using the Atlanta Hartsfield-Jackson International Airport TMY weather data. Figure 48 shows the estimated monthly components of annual tenant energy consumption for Case Study II. The results indicate a load pattern very similar to Case Study I. The area (interior) lighting and the exterior (lighting) usage are noticeably lower for Case Study II, which is the result of lower installed interior and exterior lighting power.

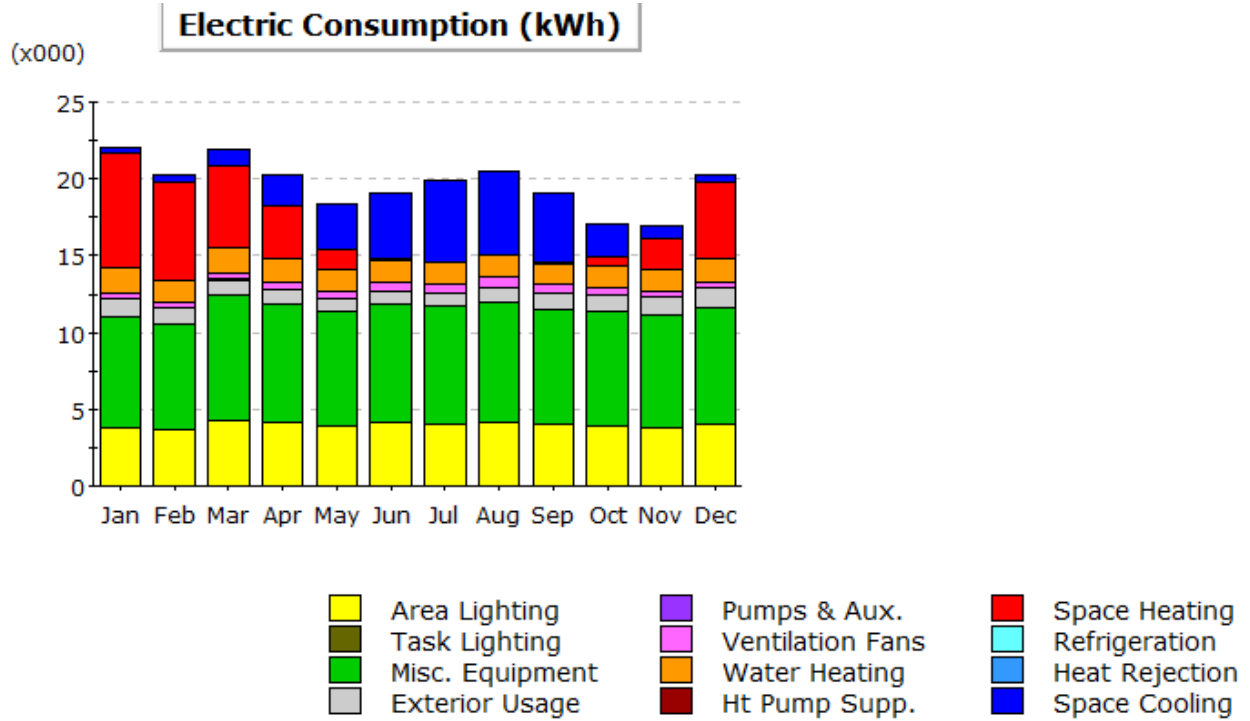


Figure 48: Components of annual tenant energy consumption (Case Study II).

The percentage break-down in annual building energy consumption for Case Study II is shown below in Figure 49. The more efficient lighting systems of this case study appear to dominate the energy efficiency/effects of the relatively newer systems – the lighting energy constitutes a much smaller percentage of building energy relative to the lighting energy of Case Study I. The percentage of energy consumption for DHW heating is higher relative to Case Study I and the CBECS database (see Figure 15). This is not to say that the DHW system is less efficient in Case Study II, rather the reduction in energy consumption across the other end-use categories increases the relative contribution of DHW heating energy.

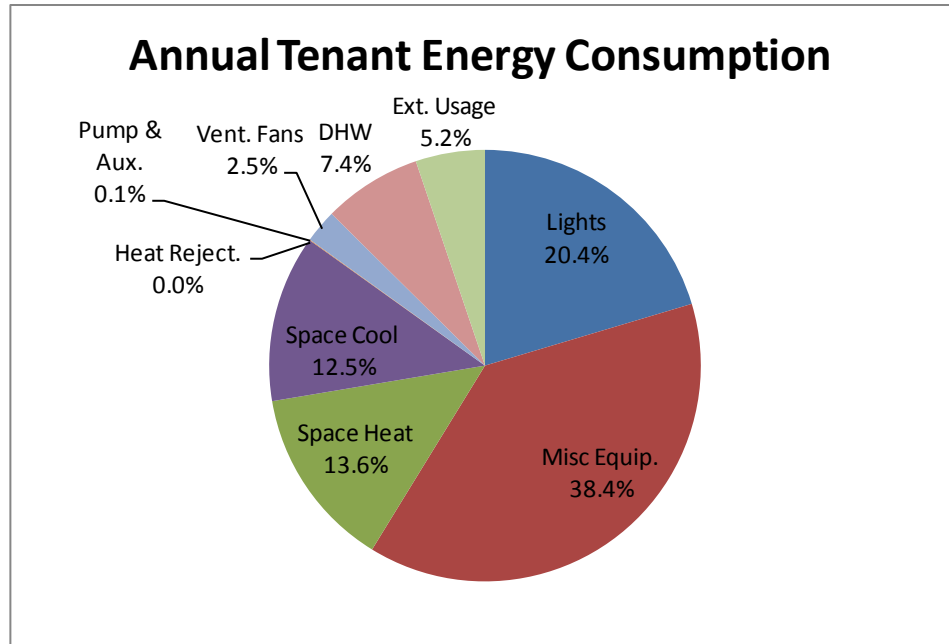


Figure 49: Components of annual tenant energy consumption (Case Study II).

The above energy consumption estimates are based on the single parameters values shown in Table B-2 in Appendix B. The following section presents the impact of input parameter uncertainty on the estimated building energy consumption.

7.1.3.2. Sensitivity Analysis of Uncertain Parameters

Many of the building energy model input parameters have a range of uncertainty defined by minimum and maximum values (see Table-B2). The estimated minimum and maximum values are based on a combination of building design data, LEED certification submittal data, building science literature, and engineering judgment. The impact of each of the uncertain parameters on estimated building energy consumption is explored through a sensitivity analysis. Consistent with the other case studies, the Morris Method of sensitivity analysis is utilized.

Using the MATLAB script in Appendix C and for $m = 20$ random observations, the 73 uncertain variables result in 1,480 simulation runs.

The results of the mean and standard deviation of elementary effects on estimated annual energy consumption are shown in Figure 50 and Figure 51. Figure 50 shows that a handful of the 73 uncertain variables appear to dominate the mean response of the estimated annual energy consumption. The dominant variables include the minimum supply fan airflow (Variable #50), the office lighting power density (Variable #1), the infiltration rate (Variable #8), the elevator power (Variable #73), the DHW load (Variable #68), the air conditioning vapor compression efficiency (Variable #53), the air handler sizing ratio (Variable #54), the DHW temperature setpoint (Variable #65), the ground slab conductance (Variable #42), and the cooling air reset setpoints (Variables #55 and #56).

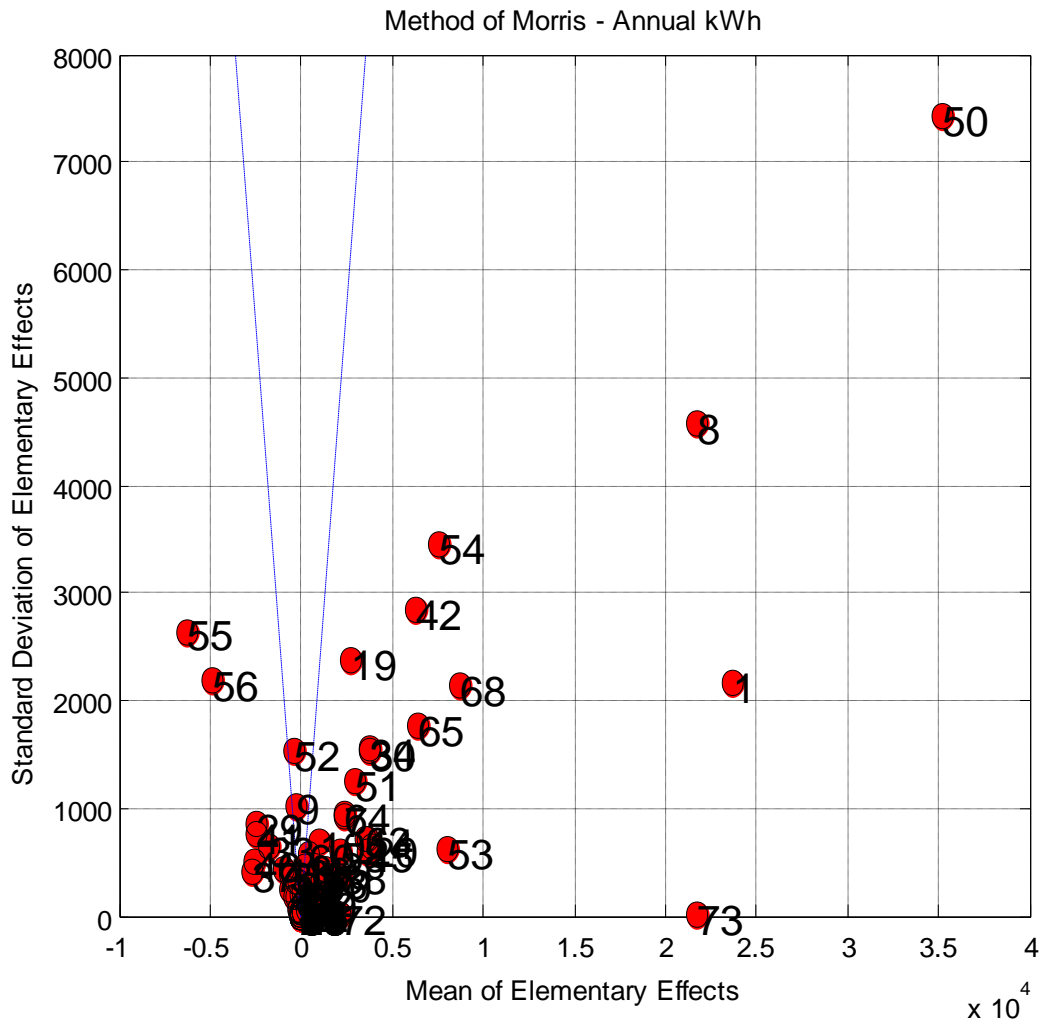


Figure 50: Mean and standard deviation of elementary effects on annual kWh for Case Study II.

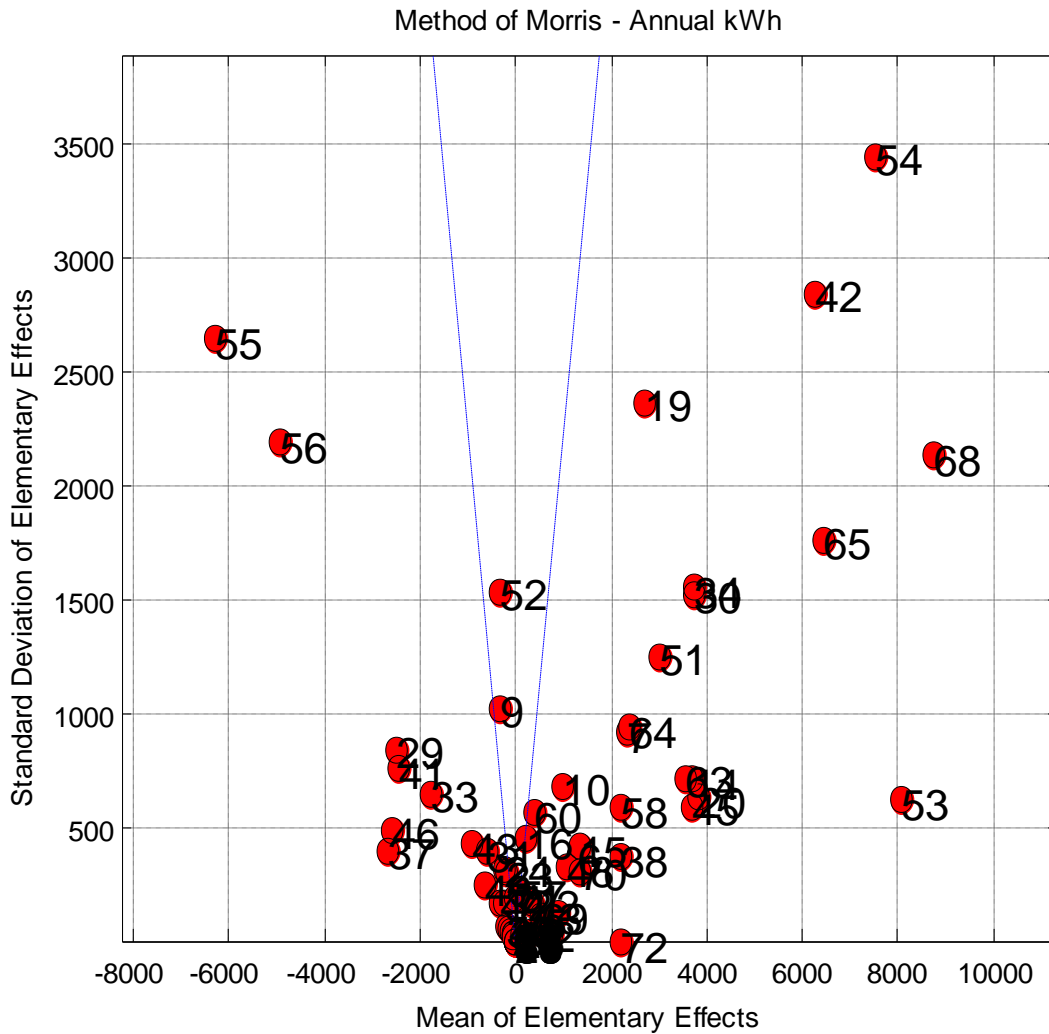


Figure 51: Mean and standard deviation of elementary effects on annual kWh for Case Study II.

Figure 51 provides a closer view of the data points clustered in Figure 50. It is evident from Figure 51 that the majority of uncertain input variables have a negligible (near zero mean) effect on the estimated annual energy consumption. The relative mean effect of the input variables are further illustrated in Figure 52, which shows the ordered absolute value of the mean of elementary effects. Less than half of the 73 uncertain parameters have a mean effect greater than one percent of the estimated annual energy consumption (data points above the black line).

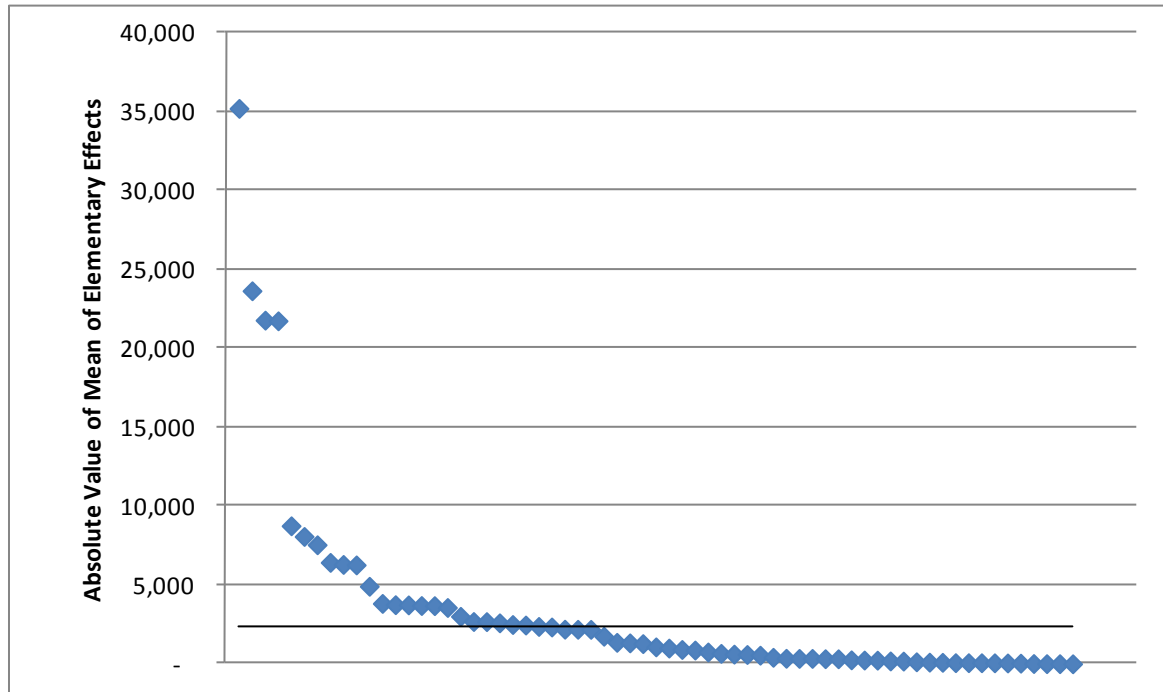


Figure 52: Ordered absolute value of the mean of elementary effects for Case Study II.

Table 45 below lists the input variables with an absolute value of mean effects greater than one-percent of annual tenant energy consumption.

Table 45: Input Variables with an Absolute Value of Mean Effects Greater Than One Percent of Annual Tenant Energy Consumption (Case Study II)

Var. #	Variable	Mean	Std. Dev.	Abs(Mean)
50	Fan_MinFlow	35,221	7,418	35,221
1	LPD_Off	23,655	2,154	23,655
8	Infil_NSW	21,793	4,576	21,793
73	Elev	21,751	1	21,751
68	DHW_Load_single	8,752	2,130	8,752
53	Cool_EIR	8,076	625	8,076
54	AHU_Cap_R	7,549	3,446	7,549
65	DHW_Temp	6,431	1,762	6,431

Table 45 (continued)

Var. #	Variable	Mean	Std. Dev.	Abs(Mean)
55	CRS_Sup_at_Low	-6,302	2,643	6,302
42	Gflr_Conc_Cond	6,272	2,843	6,272
56	CRS_MinFlow	-4,916	2,189	4,916
20	Glaz1_Cond	3,830	632	3,830
34	Wall_Insul1_Cond	3,749	1,556	3,749
30	Insul_Bd1_Cond	3,736	1,527	3,736
45	SFan_Sp	3,696	595	3,696
14	Frm_Width	3,688	714	3,688
63	Tstat_ThRng	3,571	721	3,571
51	Econ_Enthalpy	3,010	1,252	3,010
19	Glaz1_SC	2,682	2,365	2,682
37	Roof_Insul1_Thk	-2,675	404	2,675
46	SFan_Tot_Eff	-2,598	493	2,598
29	Insul_Bd1_Thk	-2,492	842	2,492
41	Gflr_Conc_Thk	-2,459	757	2,459
64	Hmax_Flow	2,370	938	2,370
7	Infil_E	2,335	920	2,335

7.1.3.3. Monte Carlo Analysis

In a process of additional data collection, several of the variables in Table 45 are candidates for refined ranges of uncertainty. The main candidates for refined/reduced ranges of uncertainty are variables that either have the greatest mean effect on the estimated annual energy consumption and/or variables for which data is relatively easy to collect. For this case study the defined range of values for Variable #50 will be replaced by a smaller range (0.25 to 0.35) representing detailed data collected from an air handler design schedule – a range of uncertain values is maintained to reflect uncertainty in the VFD performance of the actual air handler. The office lighting power density has a relatively high degree of impact on the estimated energy consumption, and lighting audits are one of the easier energy data collection efforts that may be

performed onsite. Thus, the defined range of values for Variable #1 is reduced to a minimum of 0.6 W/SF and a maximum of 0.7 W/SF. The range of values for the remainder of the variables in Table 45 will remain the same, meaning that more precise data for the variables was either unattainable or considered not worth the additional informational cost. The minimum and maximum values set for the uncertain variables are shown in Table 46.

Table 46: Uncertain Input Variables for Monte Carlo Analysis (Case Study II).

Var. #	Variable	Min	Max	Units
1	LPD_Off	0.6	0.7	W/SF
7	Infil_E	0.0168	0.067	CFM/SF
8	Infil_NSW	0.0145	0.058	CFM/SF
14	Frm_Width	0.0833	0.208	ft
19	Glaz1_SC	0.28	0.6	NA
20	Glaz1_Cond	0.29	0.5	Btu/h-SF-degF
29	Insul_Bd1_Thk	0.0833	0.25	ft
30	Insul_Bd1_Cond	0.0083	0.048	Btu/h-ft-degF
34	Wall_Insul1_Cond	0.01	0.025	Btu/h-ft-degF
37	Roof_Insul1_Thk	0.25	0.417	ft
41	Gflr_Conc_Thk	0.333	0.5	ft
42	Gflr_Conc_Cond	0.275	1.667	Btu/h-ft-degF
45	SFan_Sp	2.5	4.5	in.
46	SFan_Tot_Eff	0.5	0.75	NA
50	Fan_MinFlow	0.25	0.35	NA
51	Econ_Enthalpy	28	32	Btu/lb
53	Cool_EIR	0.3103	0.379	NA
54	AHU_Cap_R	1	1.2	NA
55	CRS_Sup_at_Low	60	65	deg F
56	CRS_MinFlow	0.3	0.66	NA
63	Tstat_ThRng	1	3	deg F
64	Hmax_Flow	0.4	0.6	NA
65	DHW_Temp	110	140	deg F
68	DHW_Load_single	0.15	0.5	gpm
73	Elev	7.305	21.92	kW

Figure 53 shows the results of the Monte Carlo analysis (consisting of 1000 simulation runs) of annual tenant energy consumption (kWh's) for Case Study II. The histogram shows an approximately normal distribution of energy consumption. The range of estimated energy consumption is about 30 percent of the estimated mean energy consumption. This range could be reduced by further reducing the ranges of the input parameter values. The benefit of additional uncertainty mitigation should be based on an assessment of the energy consumption uncertainty, relative to the other case study estimates. In other words, further reduction in the range of estimated energy consumption is worthwhile if and only if the case study energy consumption histogram/pdf overlaps considerably with the energy consumption histogram/pdf of another case study.

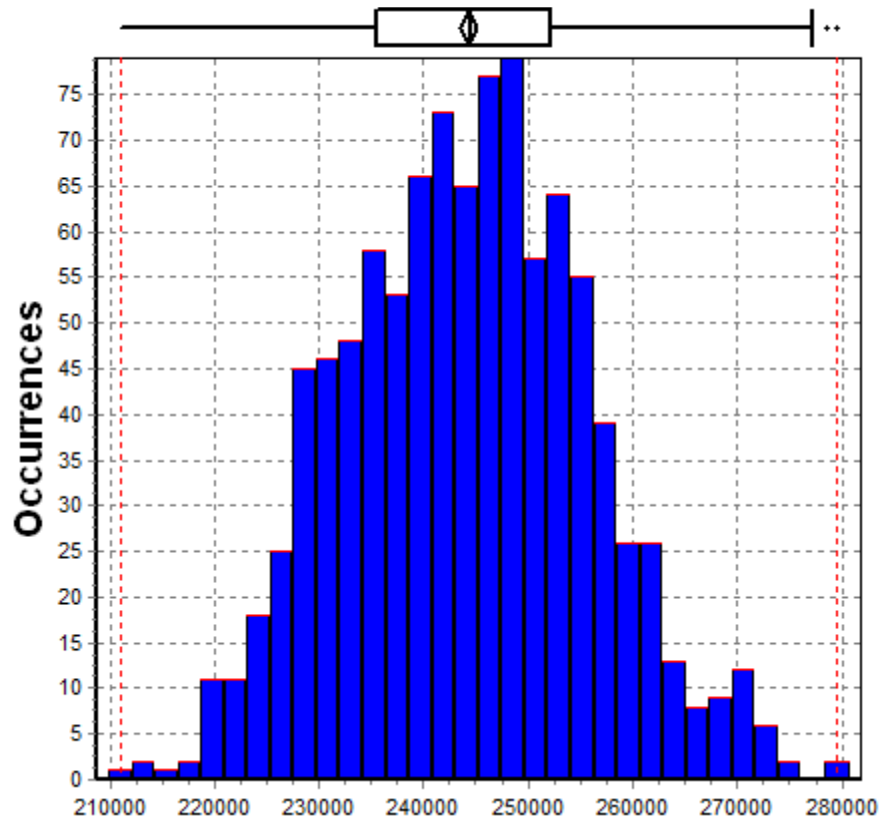


Figure 53: Monte Carlo analysis of annual tenant energy consumption, kWh's (Case Study II).

The following section presents the estimation of source energy consumption and GHG emissions.

7.1.3.4. Site Energy vs. Source Energy / GHG Emissions

The building energy is supplied entirely by electric utility power. Based on energy consumption/loss data for the energy supply chain, a “source energy factor” may be estimated and multiplied by the site energy to obtain the estimated source energy consumption. According to DOE, the source energy factor for electrical energy consumed at a facility located in Georgia

is 3.364 kWh of source energy consumed per kWh of delivered electricity (see (95), Table B-9). Thus the average source energy consumption for Case Study II is approximately 821,700 kWh.

The results of both the direct and upstream GHG emission estimates for electricity purchased in the state of Georgia are shown in Table 47. Consistent with GHG emission inventory protocols (71, 72, 73, 74), the purchased electricity emissions are counted as “Scope 2,” and the upstream fuel-energy supply chain emissions are counted as “Scope 3.”

Table 47: Estimated GHG Emissions of Purchased Electricity (Case Study II)

kWh	CO ₂ e (Scope 2), tonnes	CO ₂ e (Scope 3), tonnes	CO ₂ e (Total), tonnes	Calc. Source
244,248	155.4	23.1	178.5	(121)
			179.3	(95)

The source energy estimation guidance of DOE provides an estimation method and emission factors for total (direct and upstream) electricity GHG emissions (95). Using the DOE emission factor for the State of Georgia (1.62 lb CO₂e per kWh), the estimated total CO₂e emissions nearly matches the piecewise estimate of Scope 2 and Scope 3 emissions from the author’s GHG calculator.

7.1.3.5. Normalization of Results

Comparison of the energy performance of the case studies to other alternatives in the building stock requires normalization of the modeling results. Table 48 shows the normalized energy consumption and GHG emission performance of Case Study II. The square-footage of the conditioned floor area is the total tenant square footage shown in Table 43. The person-hours of

occupancy are based on the amount shown in Table 35. In this research, the annual person-hours are to remain consistent between building/site alternatives. Each of the values below is expressed as a mean \pm 2 standard deviations. Based on the comparative data shown from the CBECS database, the building is much more energy efficient than the average office building in the South Atlantic region. Compared to ASHRAE/IES Standard 100-2006, Case Study II performs better than the desired EUI target for an administrative/professional office (see Climate Zone 3A in Table 8).

Table 48: Normalized Building Energy Consumption and GHG Emission Performance (Case Study II)

Inventory Unit		Normalizing Unit	Performance Metric	Value
Annual Energy [kBtu]	Site (end use)	Conditioned floor area [SF]	Annual site energy / conditioned floor area [kBtu/SF]	33.4 ± 3.2
		Occupant use [person-hrs]	Annual site energy / occupant use [kBtu/person-hrs]	3.4 ± 0.3
	Primary (end use + upstream)	Conditioned floor area [SF]	Annual primary energy / conditioned floor area [kBtu/SF]	112.4 ± 10.7
		Occupant use [person-hrs]	Annual primary energy / occupant use [kBtu/person-hrs]	11.4 ± 1.1
CBECS annual site energy / conditioned floor area [kBtu/SF] *				56.9
CBECS annual source energy / conditioned floor area [kBtu/SF] ^				191.5
Annual GHGs [lb CO2e]	Site (end use)	Conditioned floor area [SF]	Annual site GHGs / conditioned floor area [lb CO2e /SF]	2,473.2 ± 234.7
		Occupant use [person-hrs]	Annual site GHGs / occupant use [lb CO2e /person-hrs]	249.9 ± 23.7
	Primary (end use + upstream)	Conditioned floor area [SF]	Annual primary GHGs / conditioned floor area [lb CO2e /SF]	2,840.9 ± 269.6
		Occupant use [person-hrs]	Annual primary GHGs / occupant use [lb CO2e /person-hrs]	287.1 ± 27.2
Source: * CBECS: South Atlantic, office, constructed 2000 - 2003, 10,001 - 50,000 SF ^ CBECS and Deru & Torcellini				

7.1.4. Case Study III: Older Construction, Multi-Tenant, High-Rise Commercial Office Building in Urban Development Area

This building case study examines the energy and GHG performance of an existing multi-tenant, high-rise commercial office building in a mixed-use, urban development. This case study represents an actual, post-1980 construction building intended to be occupied as-is

(existing building fit-out with no renovation save for interior finishes, furniture, and equipment). The building component data for this case study is sourced primarily from the U.S. DOE Commercial Benchmark/Reference Building for a “large,” post-1980 construction building in Atlanta, GA. The remainder of the building component data is based on building design references (e.g. ASHRAE handbooks) and engineering judgment. The building geometry (number and layout of floors) is based loosely on buildings found in the Atlanta, GA CBD. The tenant space is a mid-level floor within a 15 story office building, with a lobby (shared space) and bank on the ground floor. Table 49 shows the summary of spaces for this case study. The approximately 25,000 SF of tenant floor space includes all of the work space, the circulation space and toilet rooms (part of the support space).

Table 49: Summary of Tenant Spaces (Case Study III)

Space Category	Space Type	Size (SF)
Total	Total	24,336
Work Space	Office	20,009
	Conference	748
Support Space	Toilet	1,176
	Mech. / Elect.	0
	Lobby (shared)	10,156
Circulation	Stairs (on floor)	1,568
	Elevator (on floor)	840

The following section describes the energy system parameters comprising the case study building energy model.

7.1.4.1. Energy System Parameters and Building Energy Model

The building energy model and associated energy system parameters are derived from the U.S. DOE Commercial Benchmark/Reference Building for a “large,” post-1980 construction building in Atlanta, GA. The geometry of the benchmark/referencing building model is substantially modified to represent a smaller building footprint of the type found in the Atlanta, GA CBD. Table 50 below shows the main Case Study III building characteristics. The building is rectangular in its layout and has a considerable amount of glazing on each of its 15 floors. The lighting and HVAC systems are similar to those in the previous case studies. The HVAC system consists of VAV roof-mounted air handler and chiller systems. All power is supplied by electric utility energy, except for the natural gas preheat of outdoor air and the domestic hot water heating. The floors of the building are served by six high-rise elevators.

Table 50: Case Study III Building Characteristics

Tenant Space Occupancy	Multi Tenant
Number of Tenant Floors	1
Total Number of Floors	15
Width to Length Ratio	0.56
Orientation	Southwest
Envelope to Floor Area Ratio	0.35
Percent Glazing	31%
Floor Condition	Slab on grade
Lighting System Type	Suspended fluorescent, not vented
HVAC System Type	VAV with natural gas preheat, water-cooled chillers, non-powered terminal units, electric reheat, ducted return
Conveyances	6 high-rise elevators

The floor plan of the tenant space is shown in Figure 54 below. This floor plan is very similar to the one shown in Case Study IV. As with all of the case studies in this chapter, a perimeter and core thermal zoning is used to model the HVAC system loads (see discussion in Section 7.1.2.1 of Case Study I and Section 7.1.5.1 of Case Study IV). In Figure 54, the open office area encompasses all of the un-named interior spaces.

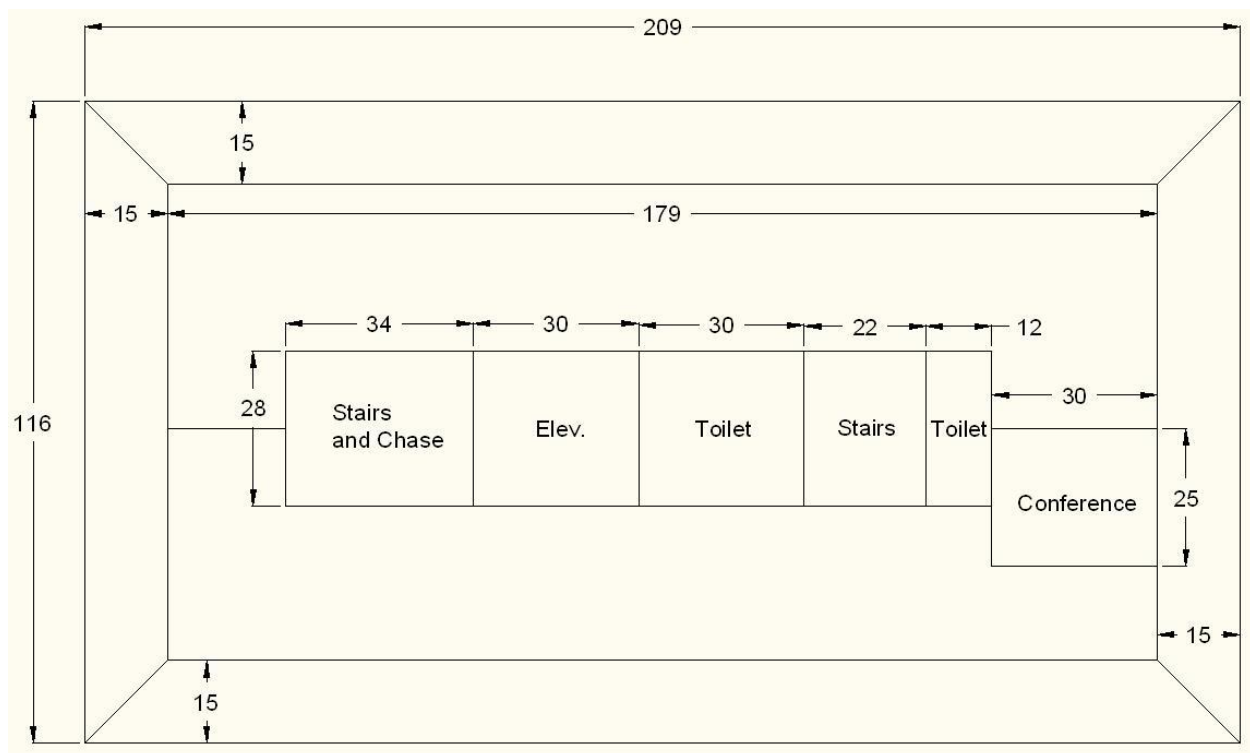


Figure 54: Tenant floor plan of core and perimeter zones (Case Study III).

The shared lobby space is not part of the total tenant space, but the energy consumption associated with this space is allocated to the tenant space in proportion to the tenant's floor space relative to the total building floor space. Figure 55 shows the building ground floor plan with the lobby located below the phantom line. The "tenant" space represents the first floor bank branch.

In addition to the shared lobby space, the building occupants utilize approximately 39,500 SF of garage parking space. The garage spaces are located in a structure near the building. Also, exterior lighting is installed near the building entry-ways.

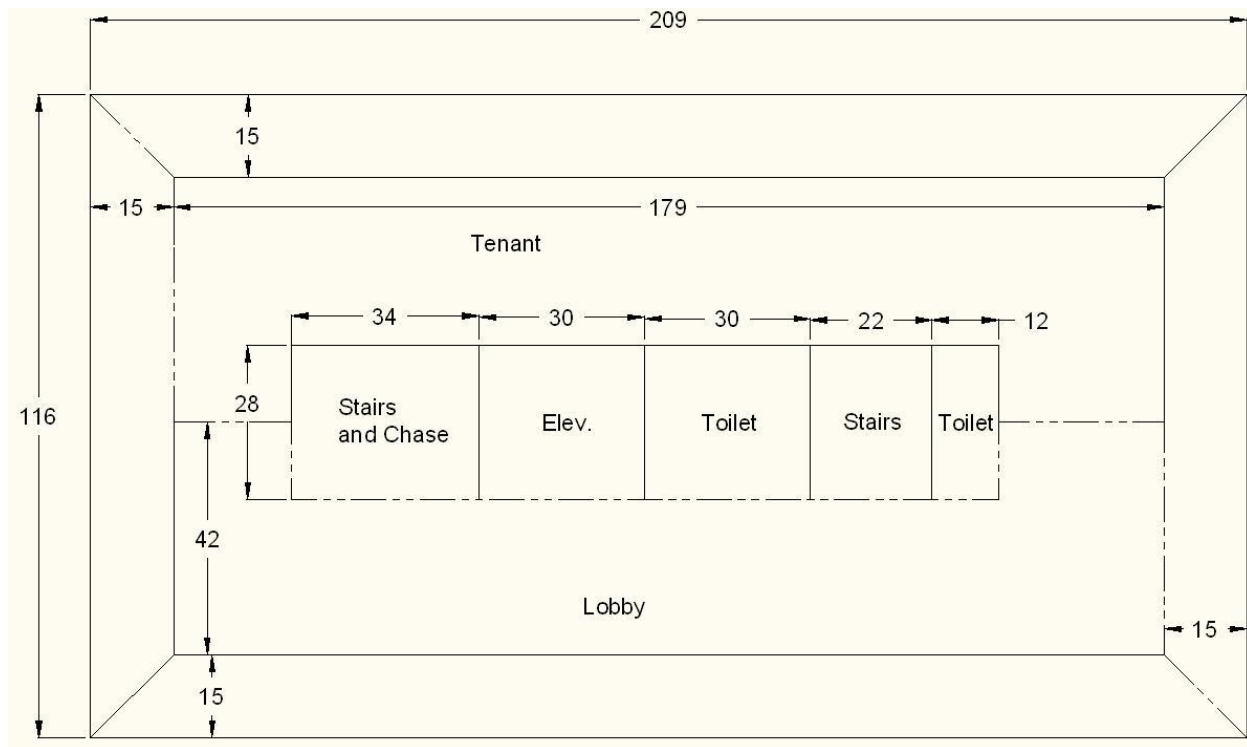


Figure 55: Ground floor plan of core and perimeter zones (Case Study III).

The building geometry, construction, and energy consuming systems were entered into an eQUEST building energy simulation model. Figure 56 and Figure 57 show 3-dimensional renderings of the case study building from two perspectives. The three floors shown represent the three main floor types in the model: ground floor, mid floor (typical and tenant floor), and top floor. The un-enclosed objects near the building floors represent the surfaces of adjacent structures (included to model shading effects).

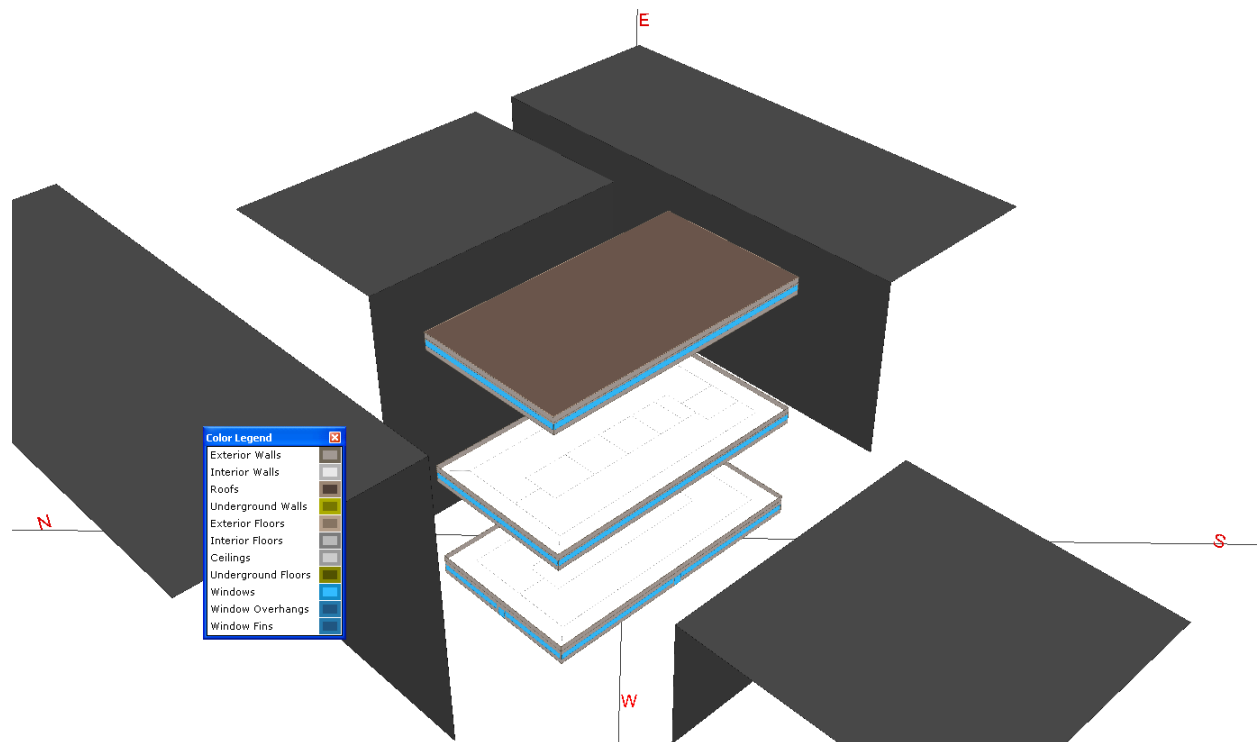


Figure 56: 3-D rendering of building, western perspective (Case Study III).

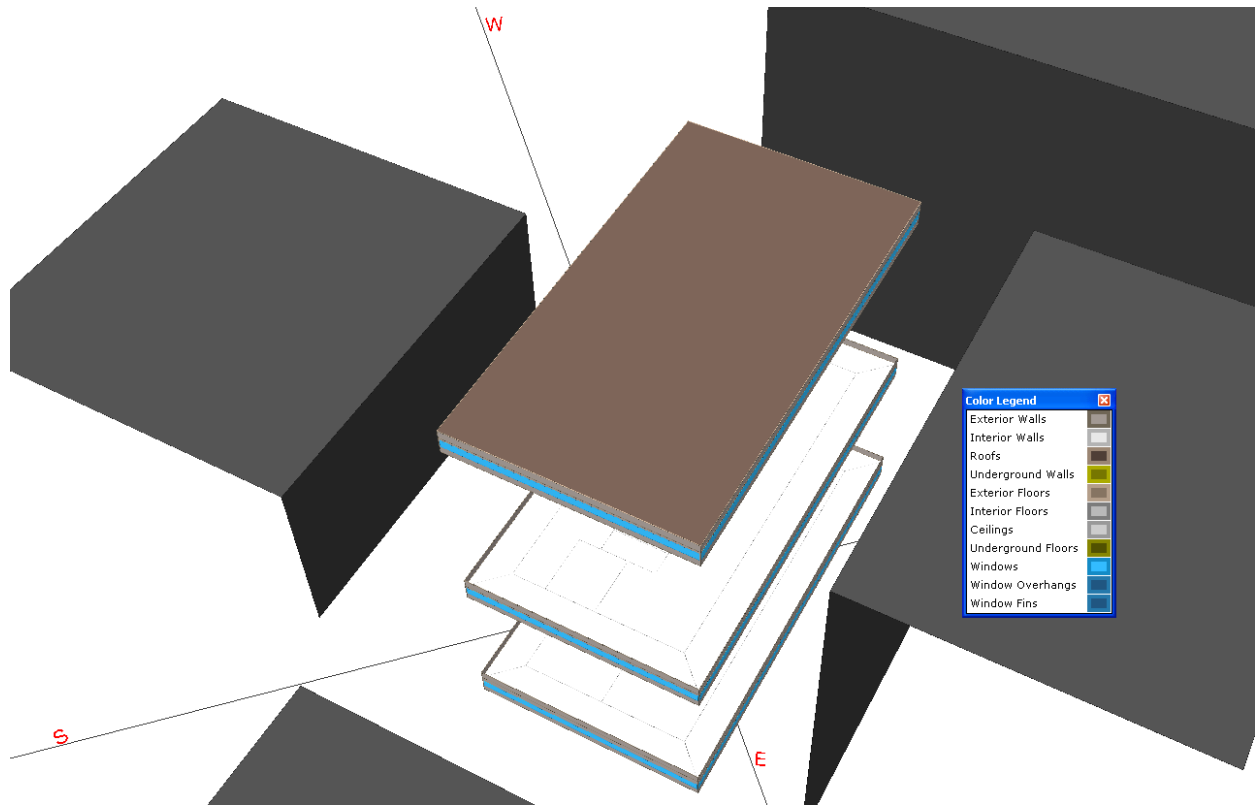


Figure 57: 3-D rendering of building, eastern perspective (Case Study III).

The details of the building energy simulation input parameters are shown in Table B - 3 in Appendix B. The building operation schedules are based on the benchmark/reference building and are not included in Table B - 3. The most precisely defined aspect of the building in the building energy simulation model is the building geometry – building height, footprint, space floor plans, and exterior envelope design. Information on the building geometry is typically available from leasing literature and from building aerial photographs and thus little or no quantification of geometry uncertainty is warranted.

The components of the estimated annual tenant energy consumption are shown in Figure 58 and Figure 59. The estimated total annual tenant energy consumption includes both electric and natural gas utility energy and is based on Equation 2. Similar to the other case studies, the

figures show that a majority of the energy is consumed by the interior lighting and miscellaneous equipment. Approximately one-quarter of the estimated miscellaneous energy is consumed by the elevator (the only site-dependent energy consumption in the miscellaneous category). The percent energy consumption for space heating and space cooling is similar to the percentage for the other post-1980 building, Case Study I.

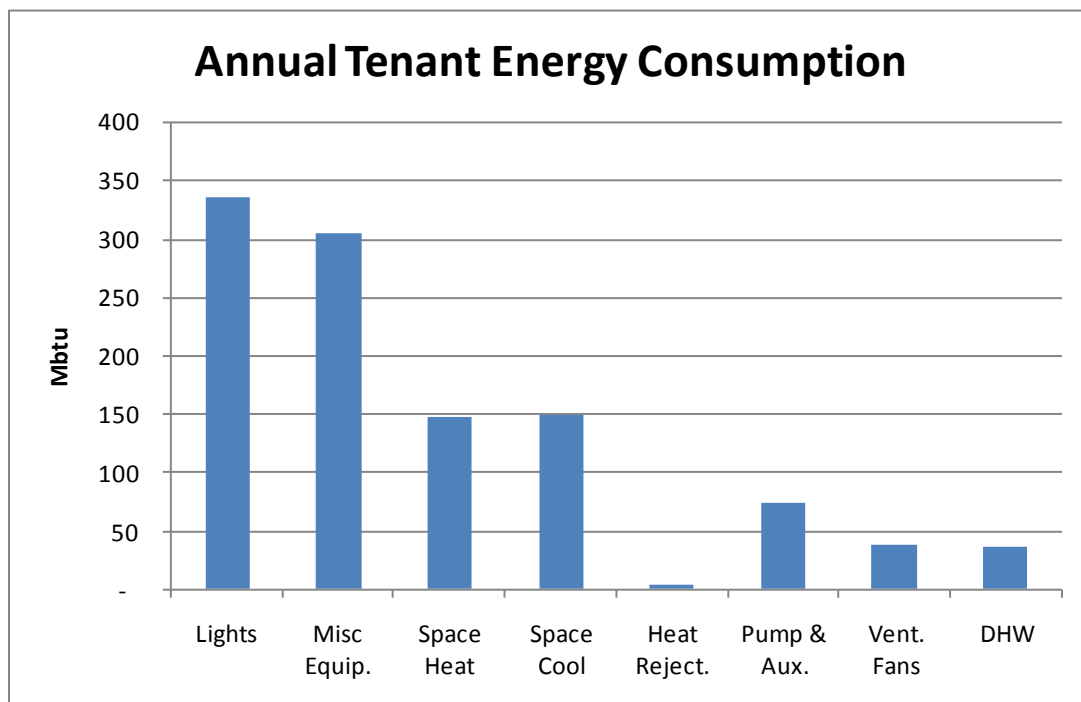


Figure 58: Components of annual tenant energy consumption (Case Study III).

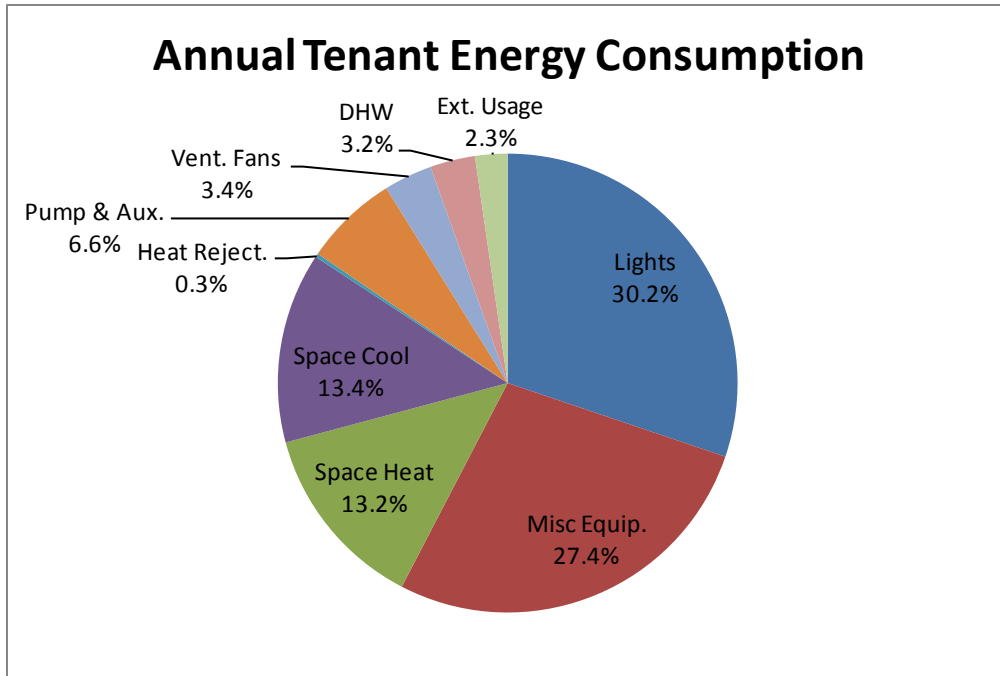


Figure 59: Components of annual tenant energy consumption (Case Study III).

Upon defining the building in the building energy simulation model, a sensitivity analysis was performed for Case Study III.

7.1.4.2. Sensitivity Analysis of Uncertain Parameters

The variables included in the sensitivity analysis of this case study are shown in Table B - 3 in Appendix B. The variables span across all major categories of building systems (e.g. HVAC, lighting, envelope, etc.) except for building geometry. Table B - 3 includes 113 numbered variables with defined ranges of probable values. The ranges of probable values are determined either from design references (e.g. ASHRAE Handbooks) or from engineering judgment. The un-numbered variables noted as “COMMON” are variables whose values are expected to be consistent between case studies. It should be noted that none of the part-load curve coefficients

for the equipment (pumps, fans, compressors, etc.) were modified – only the total (full load) efficiencies were modified.

The MATLAB script in Appendix C was executed to generate a Morris Method matrix of simulation input values. The generated matrix of values was then imported into a ModelCenter trade study of the eQUEST building energy simulation. The trade study was setup to estimate the response of the tenant space energy consumption (see Equation 2) to the uncertain input variables. The results of the ModelCenter trade study were exported to MATLAB to plot the effect of the input variables on the response variable. Figure 60 and Figure 61 show the mean and standard deviation of elementary effects on the response variable for Case Study IV. The plot labels correspond to the variable numbers in Table B - 3.

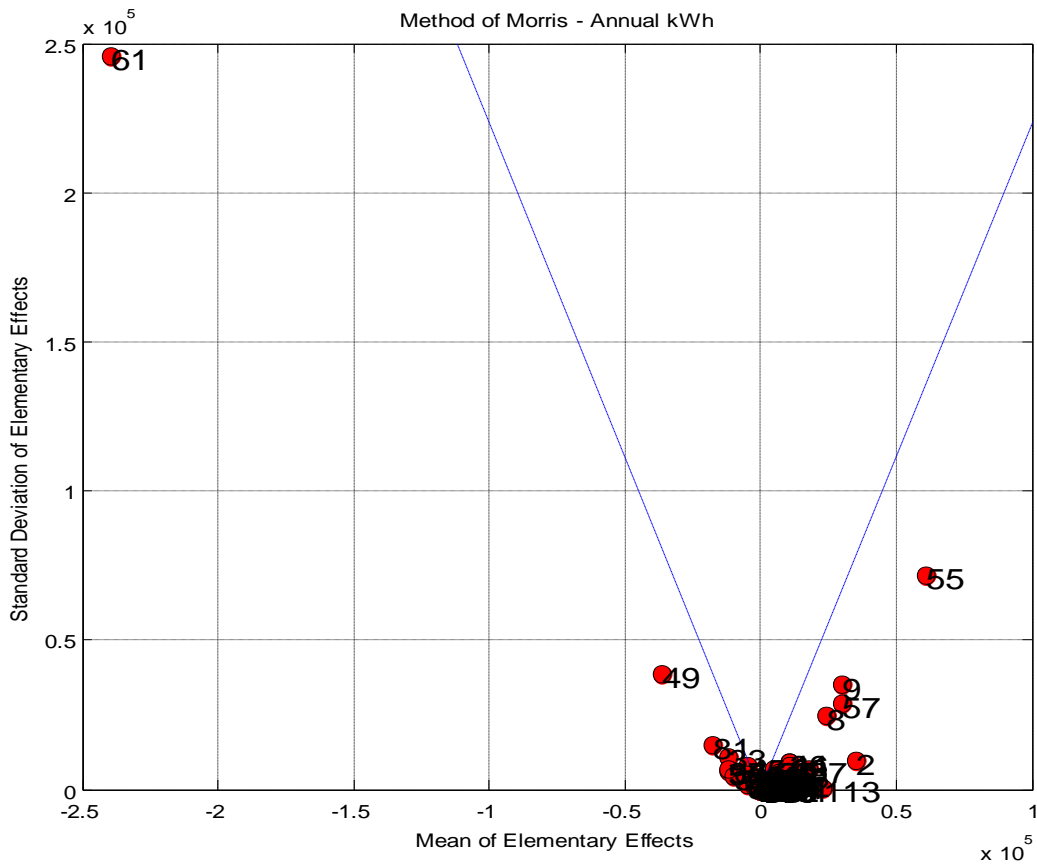


Figure 60: Mean and standard deviation of elementary effects on annual kWh (Equation 2) for Case Study III.

Similar to the sensitivity analysis results in the other case studies, it is evident that two variables have a relatively large impact on the annual space energy consumption: The terminal unit reheat ΔT (Variable #61) and the supply fan minimum flow ratio (Variable #55). Based on the apparent sensitivity of the estimated energy consumption to these control setpoints, the uncertainty may be significantly reduced by targeting a detailed building data collection effort on these two HVAC setpoints.

The mean and standard deviation of the elementary effects of the remaining variables are shown in more detail in Figure 61. Evidently, many of the variables have relatively little effect

on the annual energy consumption. Several input variables having a notable mean effect on the response variable: the air infiltration (Variables # 8 and 9), the office lighting power density (Variable #2), equipment capacities (Variables # 57 and 87), chiller setpoints (Variable #81), the wall insulation thickness (Variable #33) and the elevator (Variable # 113). The elevator power consumption is typically not a variable that is considered for reducing energy consumption through site selection or building design. (see discussion in Section 7.1.5.2).

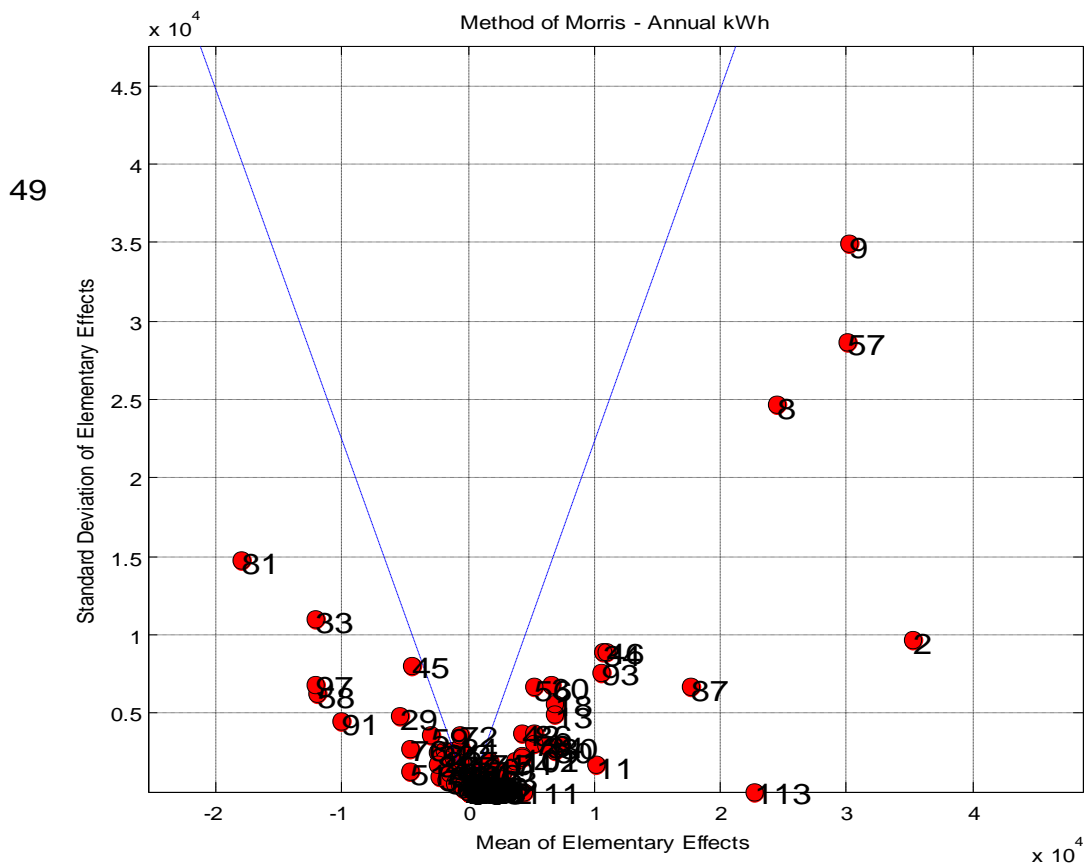


Figure 61: Mean and standard deviation of elementary effects on annual kWh (Equation 2) for Case Study III.

The Morris Method sensitivity analysis includes an analysis of the natural gas consumption sensitivity to the input parameters. Figure 62 below shows the mean and standard deviation of elementary effects on annual natural gas consumption for Case Study III. As one should expect, the variables with the largest mean effect on natural gas consumption are those pertaining to the natural gas systems, the domestic hot water load (Variable #109), the domestic hot water temperature (Variable # 105), and the domestic hot water heat input ratio (Variable #104).

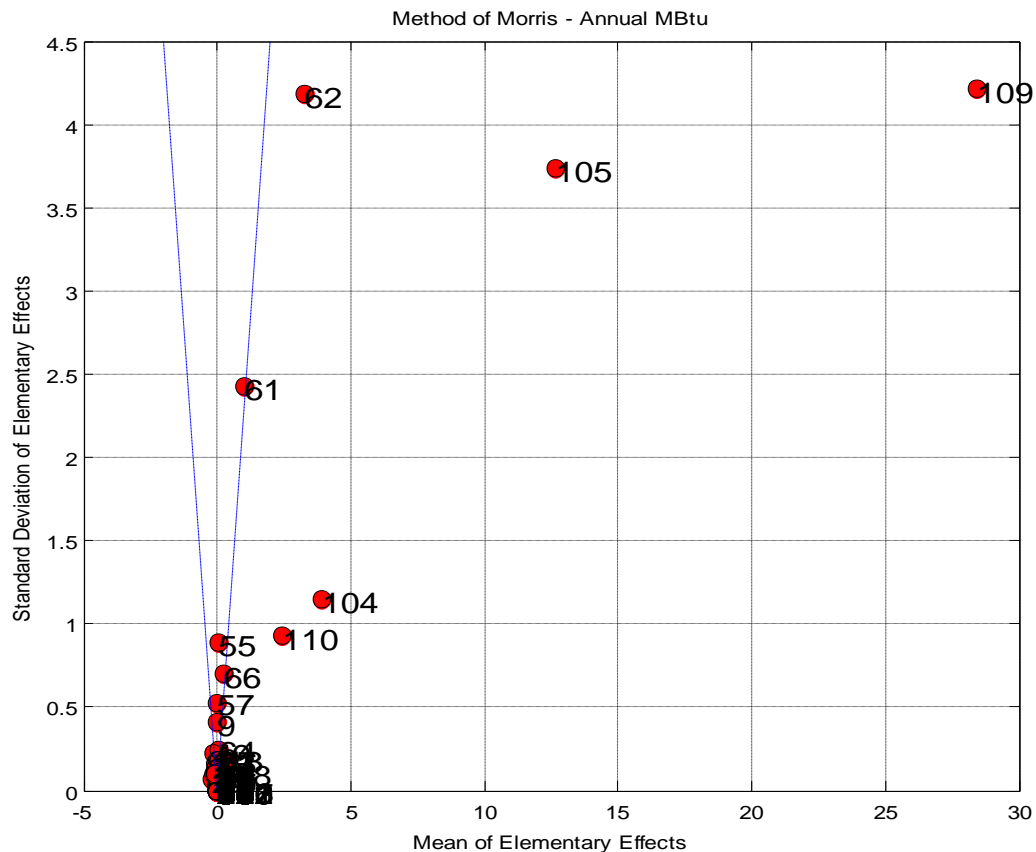


Figure 62: Mean and standard deviation of elementary effects on annual natural gas MBtu (Equation 2) for Case Study III.

With respect to electric utility energy consumption, Figure 63 shows the Ordered absolute value of the mean of elementary effects for the variables included in the sensitivity analysis. The black horizontal line near the bottom of the figure represents a one percent effect on the average annual electrical energy consumption. It appears that many of the 113 variables have at least a one percent impact on the estimated kWh's of energy consumption and that among these variables a few variables have a dominant effect.

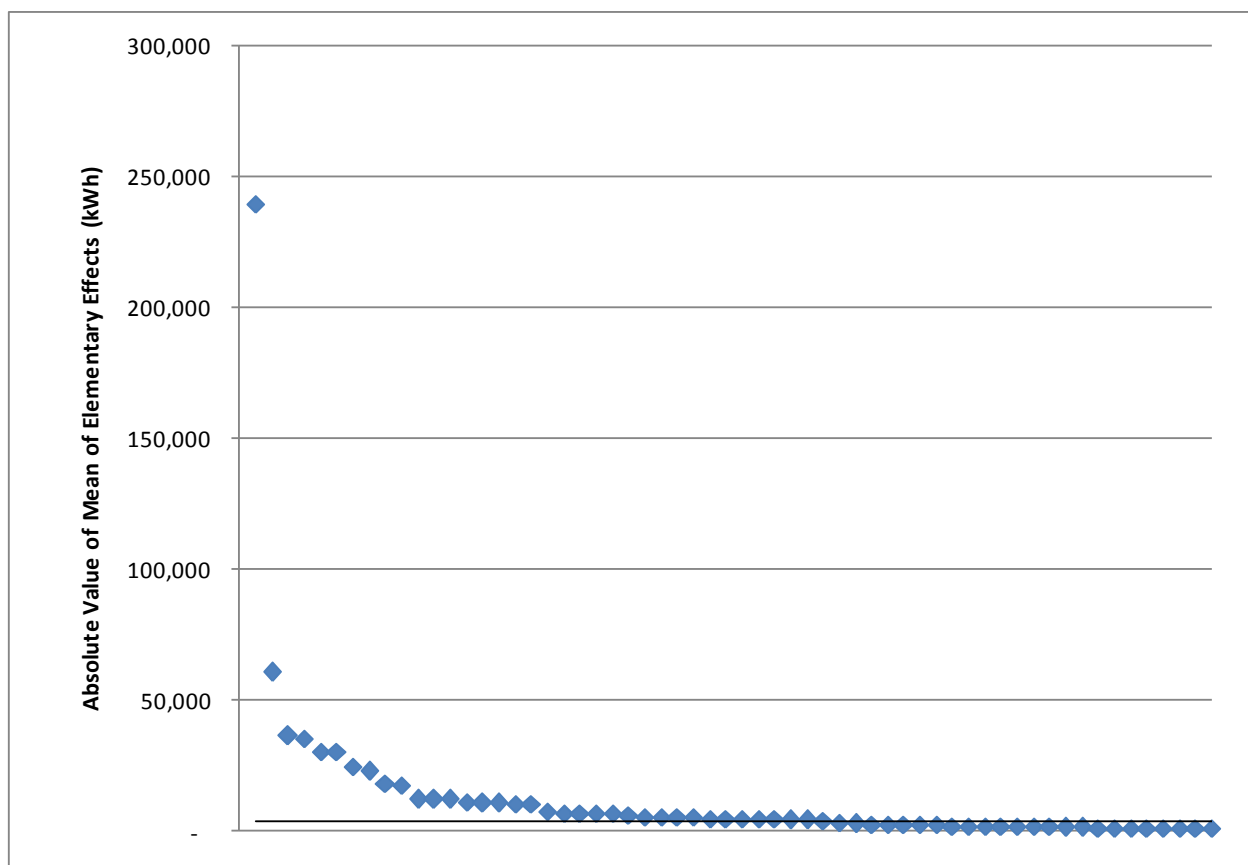


Figure 63: Ordered absolute value of the mean of elementary effects on kWh for Case Study III.

Table 51 below lists the input variables with an absolute value of mean effects greater than one percent of annual tenant electrical energy consumption. In total, 36 of the 113 variables have a mean effect greater than one percent of the annual electrical energy consumption.

Table 51: Input Variables with Absolute Value of Mean Effects Greater Than One Percent of Annual Tenant kWh Consumption (Case Study III)

Var. #	Variable	Mean	Std. Dev.	Abs(Mean)
61	Heat_DT	-239,632	245,647	239,632
55	Fan_MinFlow	60,698	71,611	60,698
49	Max_Humid	-36,416	38,498	36,416
2	LPD_Off	35,282	9,654	35,282
9	Infil_NS	30,187	34,956	30,187
57	AHU_Cap_R	30,108	28,695	30,108
8	Infil_EW	24,462	24,656	24,462
113	Elev	22,749	0	22,749
81	Chill_MinR	-17,917	14,696	17,917
87	Chill_Cap_R	17,640	6,700	17,640
33	Wall_Insul1_Thk	-12,088	11,005	12,088
97	CWP_Mot_Eff	-12,028	6,823	12,028
58	CRS_Sup_at_Low	-11,987	6,230	11,987
46	Glaz1_Cond	10,932	8,945	10,932
34	Wall_Insul1_Cond	10,674	8,866	10,674
93	CW_PipeHead	10,600	7,600	10,600
11	Infil_PT	10,155	1,679	10,155
91	CW_DT	-10,081	4,501	10,081
80	Chill_EIR	7,306	2,922	7,306
18	Frm_Width	6,909	5,638	6,909
13	Out_Emiss	6,879	4,870	6,879
50	SFan_Sp	6,869	2,636	6,869
30	Wall_Conc_Cond	6,671	6,770	6,671
84	Chill_ConHead	6,130	2,973	6,130
29	Wall_Conc_Thk	-5,418	4,783	5,418
70	Tstat_ThRng	5,272	3,082	5,272
56	Cool_Cntl_Rng	5,244	6,665	5,244
86	Chill_Standby_t	5,231	3,748	5,231

Table 51 (continued)

Var. #	Variable	Mean	Std. Dev.	Abs(Mean)
51	SFan_Tot_Eff	-4,533	1,250	4,533
76	CHW_FlowRes	-4,532	2,742	4,532
45	Glaz1_SC	-4,434	8,043	4,434
111	Park_Light	4,380	0	4,380
102	CT_StatHead	4,339	2,168	4,339
42	Gflr_Conc_Cond	4,307	3,757	4,307
101	CT_Head	4,233	2,224	4,233
74	CHW_PipeHead	3,713	1,913	3,713

In terms of natural gas energy consumption, only two of the input parameters have an absolute value of mean elementary effects on building energy consumption greater than one percent of the total energy consumption. These two variables are shown below in Figure 64 and Table 52.

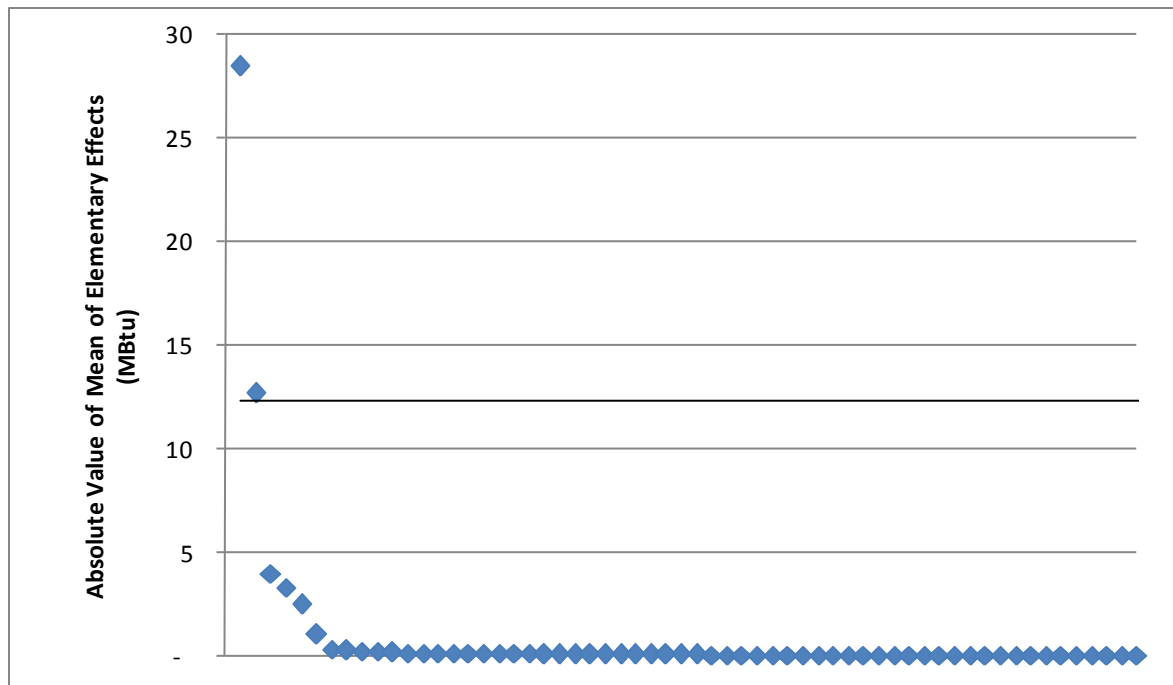


Figure 64: Ordered absolute value of the mean of elementary effects on Btu for Case Study III.

Table 52: Input Variables with Absolute Value of Mean Effects Greater Than One Percent of Annual Tenant Btu Consumption (Case Study III)

Var. #	Variable	Mean	Std. Dev.	Abs(Mean)
109	DHW_Load_single	28	4	28
105	DHW_Temp	13	4	13

The 38 variables found to have mean effects greater than one percent of the annual tenant energy consumption retain their individual uncertainty distributions for the Monte Carlo analysis presented in the following section.

7.1.4.3. Monte Carlo Analysis

The minimum and maximum values set for the uncertain variables retaining their uncertainty distributions in the Monte Carlo analysis are shown in Table 53 below. For the rest of the 113 variables included in the sensitivity analysis, each with a mean effect less than one percent of the annual tenant energy consumption, the defined range of uncertain values is reduced to a single value (see values in Table B - 3 in Appendix B). The reduction in the number of variables with a defined range of uncertain values helps to simplify the computation intensity of the building energy simulation.

Table 53: Uncertain Input Variables for Monte Carlo Analysis (Case Study III)

Var. #	Variable	Min	Max	Units
61	Heat_DT	20	50	degF
55	Fan_MinFlow	0.2	0.5	NA
49	Max_Humid	40	60	%
2	LPD_Off	1	1.8	W/SF
9	Infil_NS	0.49	1.47	AC/hr

Table 53 (continued)

Var. #	Variable	Min	Max	Units
57	AHU_Cap_R	1	1.2	NA
8	Infil_EW	0.475	1.425	AC/hr
113	Elev	55.6	166.8	kW
81	Chill_MinR	0.1	0.3	NA
87	Chill_Cap_R	1	1.5	NA
33	Wall_Insul1_Thk	0.066	0.333	ft
97	CWP_Mot_Eff	0.6	0.95	NA
58	CRS_Sup_at_Low	60	65	degF
46	Glaz1_Cond	0.5	0.8	Btu/h-SF-degF
34	Wall_Insul1_Cond	0.017	0.417	Btu/h-ft-degF
93	CW_PipeHead	15	50	ft
11	Infil_PT	1.815	5.445	AC/hr
91	CW_DT	8	14	degF
80	Chill_EIR	0.17	0.2	NA
18	Frm_Width	0.08333	0.2083	ft
13	Out_Emiss	0.1	0.9	NA
50	SFan_Sp	2.5	4.5	in. wg
30	Wall_Conc_Cond	0.5833	1.667	Btu/h-ft-degF
84	Chill_ConHead	10	30	ft
29	Wall_Conc_Thk	0.50025	0.83375	ft
70	Tstat_ThRng	1	3	degF
56	Cool_Cntl_Rng	3	6	degF
86	Chill_Standby_t	0.0167	0.0833	h
51	SFan_Tot_Eff	0.5	0.75	NA
76	CHW_FlowRes	0.5	0.8	NA
45	Glaz1_SC	0.2	0.6	NA
111	Park_Light	7.5	15	kW
102	CT_StatHead	5	20	ft
42	Gflr_Conc_Cond	0.275	1.667	Btu/h-ft-degF
101	CT_Head	5	20	ft
74	CHW_PipeHead	15	50	ft
109	DHW_Load_single	0.15	0.5	gpm
105	DHW_Temp	110	140	degF

After reducing the number of variables with defined ranges of uncertainty, the building energy simulation was run through a Monte Carlo analysis. For each of the variables with a defined range of uncertainty, a uniform distribution was assumed (see Section 5.2.3). Figure 76 shows the results of the 1000-run Monte Carlo analysis of annual tenant energy consumption (kWh's) for Case Study IV. The large degree of skew in the histogram can be attributed to the high sensitivity to variables identified in the sensitivity analysis. Reduction of this skew requires a reduction in the range of uncertainty in the input parameters.

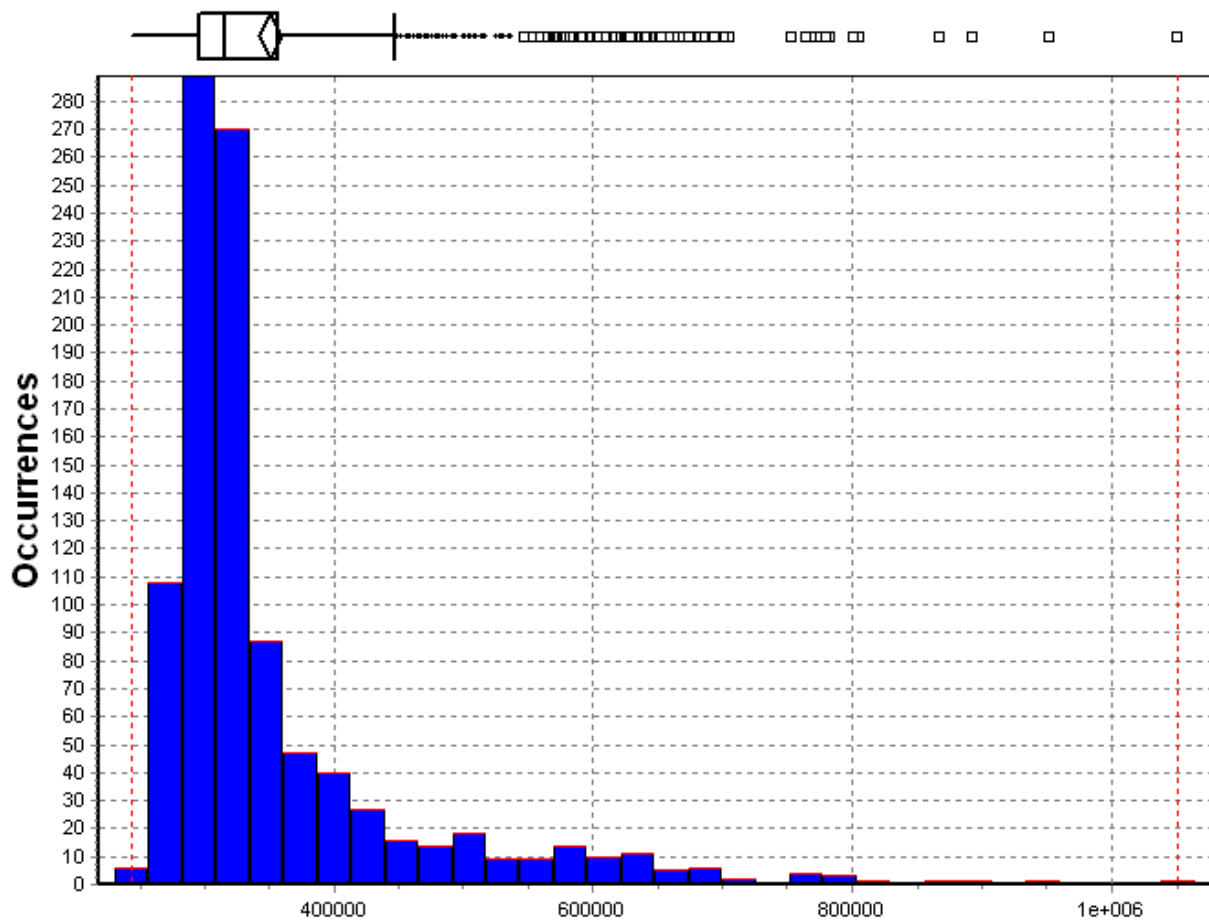


Figure 65: Monte Carlo analysis of annual tenant energy consumption, kWh's (Case Study III).

The Monte Carlo analysis is revised to reflect data collection aimed at reducing the uncertainty in the estimated tenant space annual energy consumption. The terminal unit reheat limit (Variable #61) is redefined to 50 – 60 deg F ΔT (the heating system is undersized below a terminal unit reheat ΔT of 30 deg F). The air handler fan minimum turndown ratio (Variable #55) is replaced by a smaller range (0.3 to 0.35) representing detailed data collected from an air handler design schedule – a range of uncertain values is maintained to reflect uncertainty in the current damper settings of the actual air handler. The maximum return air relative humidity (Variable #49) is redefined to 50 – 55 percent, reflecting an inspection of the HVAC control setpoints and possible humidity sensor drift. Also, the lighting power density (Variable #2) is redefined to 1.4 – 1.5 W/SF, according to an audit of the installed lighting power density. The range of values for the remainder of the variables in Table 53 are to remain the same, meaning that more precise data for the variables was either unattainable or considered not worth the additional informational cost.

The building energy simulation results of the revised Monte Carlo analysis are shown below in Figure 66. The reduction in the input parameter uncertainties has helped to reduce the skew in the Monte Carlo histogram, producing an approximately normal distribution of estimated energy consumption.

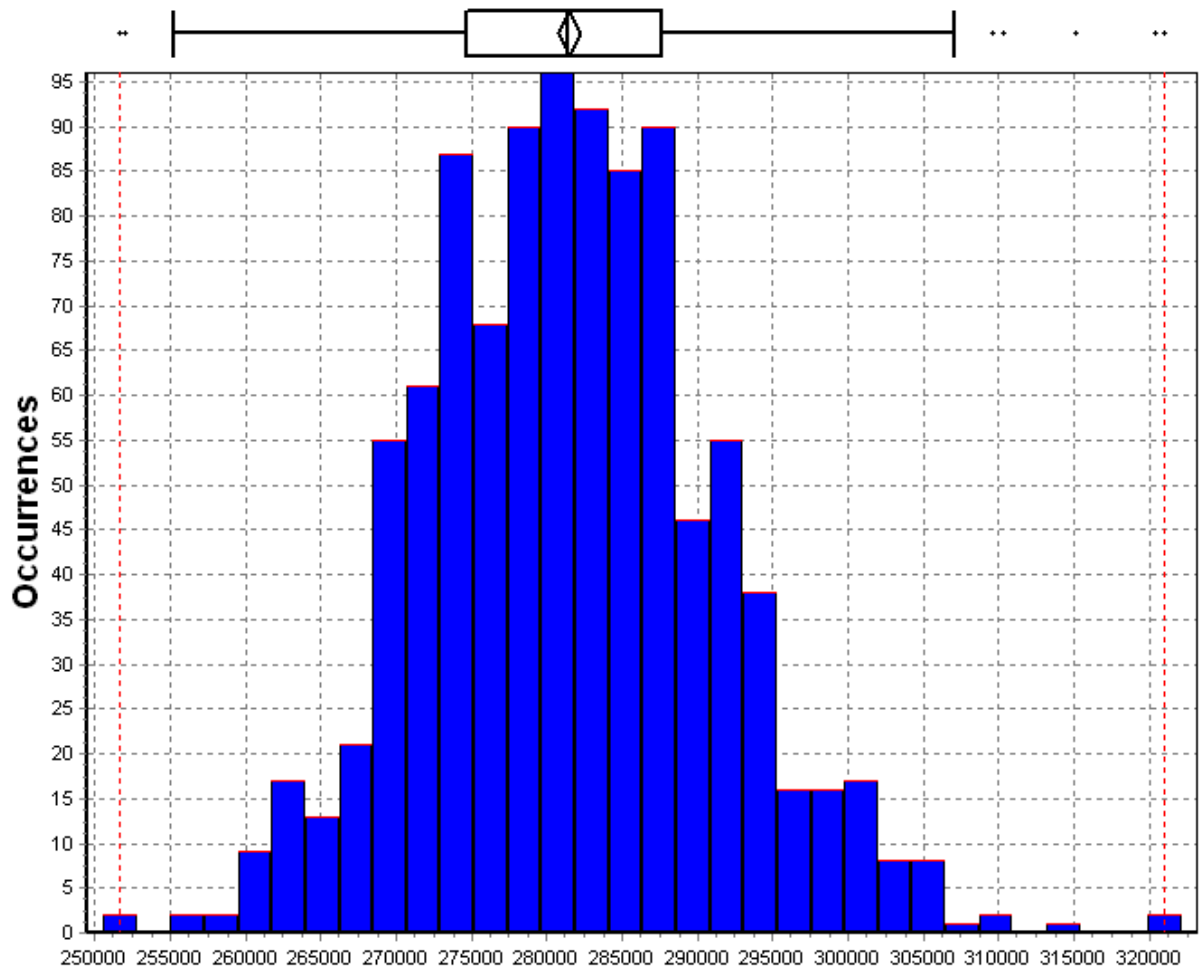


Figure 66: Revised Monte Carlo analysis of annual tenant energy consumption, kWh's (Case Study III).

7.1.4.4. Site Energy vs. Source Energy / GHG Emissions

This section presents the estimated site vs. source energy consumption and GHG emissions for Case Study III. According to DOE, the source energy factor for electrical energy consumed at a facility located in Georgia is 3.364 kWh of source energy consumed per kWh of delivered electricity (see (95) Table B-9). Thus, the average source energy consumption for Case Study III is approximately 948,700 kWh or 3,237 MBtu. With respect to natural gas energy

consumption, the national average source energy factor is 1.092 MBtu of source energy consumed per MBtu of delivered natural gas (see (95), Table 5). Hence, for the mean of 34.18 MBtu of natural gas consumed for Case Study III (site energy), approximately 37.32 MBtu of source energy is consumed. Similar to Case Study I, the natural gas energy consumption is only a fraction of the total building energy consumption.

The results of both the direct and upstream GHG emission estimates for electricity purchased in the state of Georgia are shown in Table 54. The purchased electricity emissions are counted as “Scope 2,” and the upstream fuel-energy supply chain emissions are counted as “Scope 3.”

Table 54: Estimated GHG Emissions of Purchased Electricity and Natural Gas Combustion (Case Study III)

kWh Electricity	kBtu Natural Gas	CO ₂ e (Scope 1), tonnes	CO ₂ e (Scope 2), tonnes	CO ₂ e (Scope 3), tonnes	CO ₂ e (Total), tonnes	Calc. Source
282,010	34,200	1.82	179.4	27.1	208.3	(121)
					207.6	(95)

The U.S. DOE provides an estimation method and emission factors for total (direct and upstream) electricity GHG emissions (95). Using the DOE electric utility emission factor for the State of Georgia (1.62 lb CO₂e per kWh) and the national natural gas emission factor of 27.8 CO₂e per 1,000 SCF, the estimated total CO₂e emissions are 207.6 tonnes, which very nearly matches the piecewise estimate of Scope 1, Scope 2, and Scope 3 emissions.

7.1.4.5. Normalization of Results

Table 55 shows the normalized energy consumption and GHG emission performance of Case Study III. The square-footage of the conditioned floor area is the total tenant square footage shown in Table 49. The person-hours of occupancy are based on the amount shown in Table 35. The normalized energy results for Case Study III are lower than for Case Study I – the other “post-1980” construction building. This means that Case Study III is estimated to perform better than the average CBECS building in the respective building category. However, comparison to the CBECS data should take into account the limitations of the CBECS database (see discussion in Section 7.1.2.5). The Case Study III building is estimated to meet the desired EUI target of ASHRAE/IES Standard 100-2006 (see Climate Zone 3A in Table 8).

Table 55: Normalized Building Energy Consumption and GHG Emissions Performance (Case Study III)

Inventory Unit		Normalizing Unit	Performance Metric	Value
Annual Energy [kBtu]	Site (end use)	Conditioned floor area [SF]	Annual site energy / conditioned floor area [kBtu/SF]	40.9 ± 3.1
		Occupant use [person-hrs]	Annual site energy / occupant use [kBtu/person-hrs]	4.0 ± 0.3
	Primary (end use + upstream)	Conditioned floor area [SF]	Annual primary energy / conditioned floor area [kBtu/SF]	134.5 ± 10.1
		Occupant use [person-hrs]	Annual primary energy / occupant use [kBtu/person-hrs]	13.3 ± 1.0
CBECS annual site energy / conditioned floor area [kBtu/SF] *				75.7
CBECS annual source energy / conditioned floor area [kBtu/SF] ^				217.7
Annual GHGs [lb CO2e]	Site (end use)	Conditioned floor area [SF]	Annual site GHGs / conditioned floor area [lb CO2e /SF]	2,955.3 ± 221.1
		Occupant use [person-hrs]	Annual site GHGs / occupant use [lb CO2e /person-hrs]	291.5 ± 21.8
	Primary (end use + upstream)	Conditioned floor area [SF]	Annual primary GHGs / conditioned floor area [lb CO2e /SF]	3,396.3 ± 254.1
		Occupant use [person-hrs]	Annual primary GHGs / occupant use [lb CO2e /person-hrs]	335.0 ± 25.1
Source:				
* CBECS: South Atlantic, office, constructed 1980 - 1999, 10,001 - 50,000 SF				
^ CBECS and Deru & Torcellini				

7.1.5. Case Study IV: Recent Construction, Multi-Tenant, High-Rise Commercial Office Building in Mixed-Use Urban Development Area

This building case study presents the energy and GHG performance of an existing multi-tenant, high-rise commercial office building in a mixed-use development. This case study represents a recently LEED certified office space that is to be occupied as-is (existing building

fit-out with no renovation, save for interior finishes, furniture, and equipment). The building data for this case study is sourced partly from the owner and designer (under a confidentiality agreement) and partly from assumed characteristics based on building design references (e.g. ASHRAE Standard 90.1, International Building Code, ASHRAE handbooks, etc). The tenant space is a mid-level floor within a 22 story office building, with a lobby (shared space among tenants) and bank on the ground floor. Table 56 shows the summary of spaces for this case study. The approximately 25,000 SF of tenant floor space includes all of the work space, the circulation space and toilet rooms (part of the support space).

Table 56: Summary of Tenant Spaces (Case Study IV)

Space Category	Space Type	Size (SF)
Total	Total	24,871
Work Space	Office	20,544
	Conference	748
Support Space	Toilet	1,176
	Mech. / Elect.	0
	Lobby (shared)	10,156
Circulation	Stairs (on floor)	1,568
	Elevator (on floor)	840

The following section describes the energy system parameters comprising the case study building energy model.

7.1.5.1. Energy System Parameters and Building Energy Model

The building is LEED certified and thus incorporates several energy saving design features. The building envelope is a curtain wall system with low-e glazing, spandrel, face

granite, and board insulation, and the roof is colored with a reflective white finish. The building HVAC system (air-side) consists of two rooftop, dedicated outdoor air handlers (with demand control ventilation), each with energy recovery enthalpy wheels and serving space cooling and heating VAV systems on each floor. Cooling is provided by air handler cooling coils served by a campus chilled water system. The campus chilled water system consists of staged centrifugal chillers that reject heat to axial fan forced draft cooling towers. Heating is provided by electric reheat coils in un-powered VAV terminal units. Interior lighting consists of suspended fluorescent fixtures with daylighting offsetting part of the electrical lighting load. The building envelope, mechanical, and lighting systems are assumed to meet the prescriptive requirements of the 2003 International Build Code (IBC 2003) and all applicable reference codes, notably ASHRAE 90.1-2001. Table 57 below shows the main Case Study IV building characteristics.

Table 57: Case Study IV Building Characteristics

Tenant Space Occupancy	Multi Tenant
Number of Tenant Floors	1
Total Number of Floors	22
Width to Length Ratio	0.56
Orientation	South
Envelope to Floor Area Ratio	0.37
Percent Glazing	45%
Floor Condition	Exposed to garage space
Lighting System Type	Suspended fluorescent, not vented, with daylighting
HVAC System Type	VAV with air-side economizer, DCV, OA total enthalpy energy recovery, water-cooled chillers with economizer, non-powered terminal units, electric reheat, ducted return
Conveyances	10 high-rise elevators, 4 low-rise elevators, 3 parking elevators

The floor plan of the tenant space is shown in Figure 67 below. The floor plan is very similar to the one shown in Case Study III. Similar to all of the case studies in this chapter, a perimeter and core thermal zoning is used to model the HVAC system loads (see discussion in Section 7.1.2.1 of Case Study I and further discussion in this section). In Figure 67, the open office area encompasses all of the un-named interior spaces.

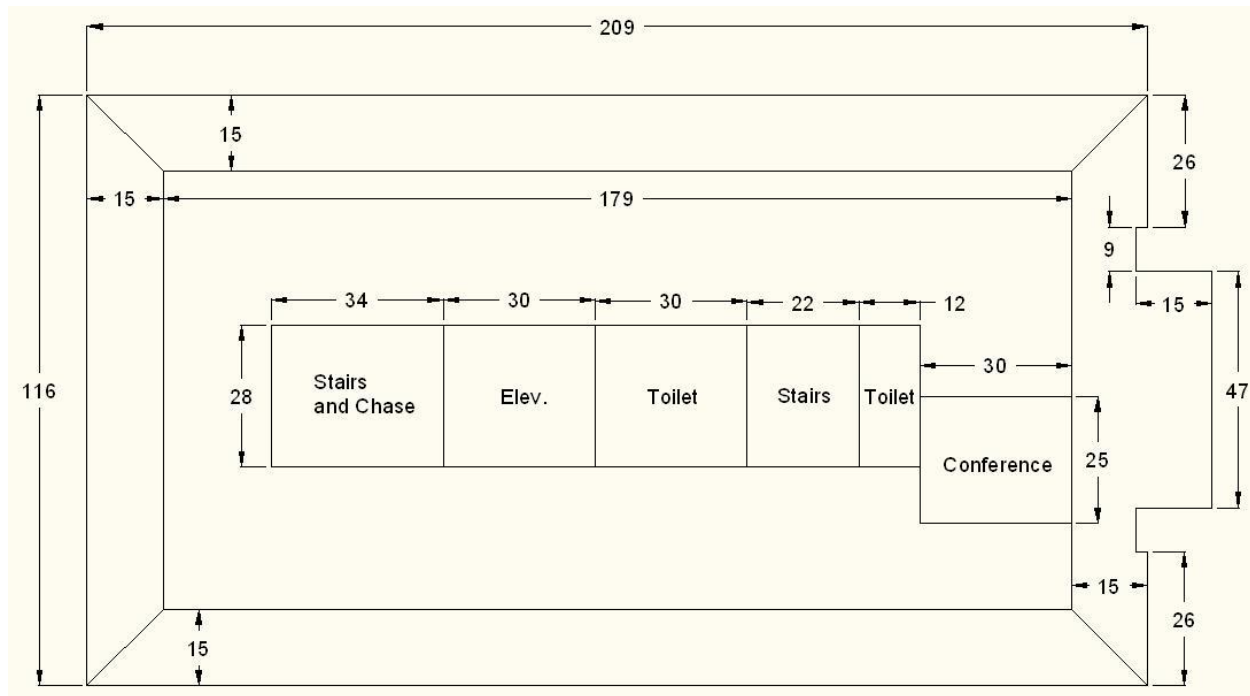


Figure 67: Tenant floor plan of core and perimeter zones (Case Study IV).

In this case study, the shared lobby space is not part of the total tenant space, but the energy consumption associated with this space is allocated to the tenant space in proportion to the tenant's floor space relative to the total building floor space. Figure 68 shows the building ground floor plan with the lobby located below the phantom line. The "tenant" space represents the first floor bank branch. In addition to the shared lobby space, the building occupants utilize approximately 39,500 SF of garage parking space. The garage space is located below the ground floor of the building; it is served by three elevators and it is lighted 24 hours a day. Exterior lighting is also installed near the building entry-ways and within a large marketing sign at the top of the building. The floors of the building are served by four low-rise elevators (floors 1 – 12) and six high-rise elevators (floors 13 – 22).

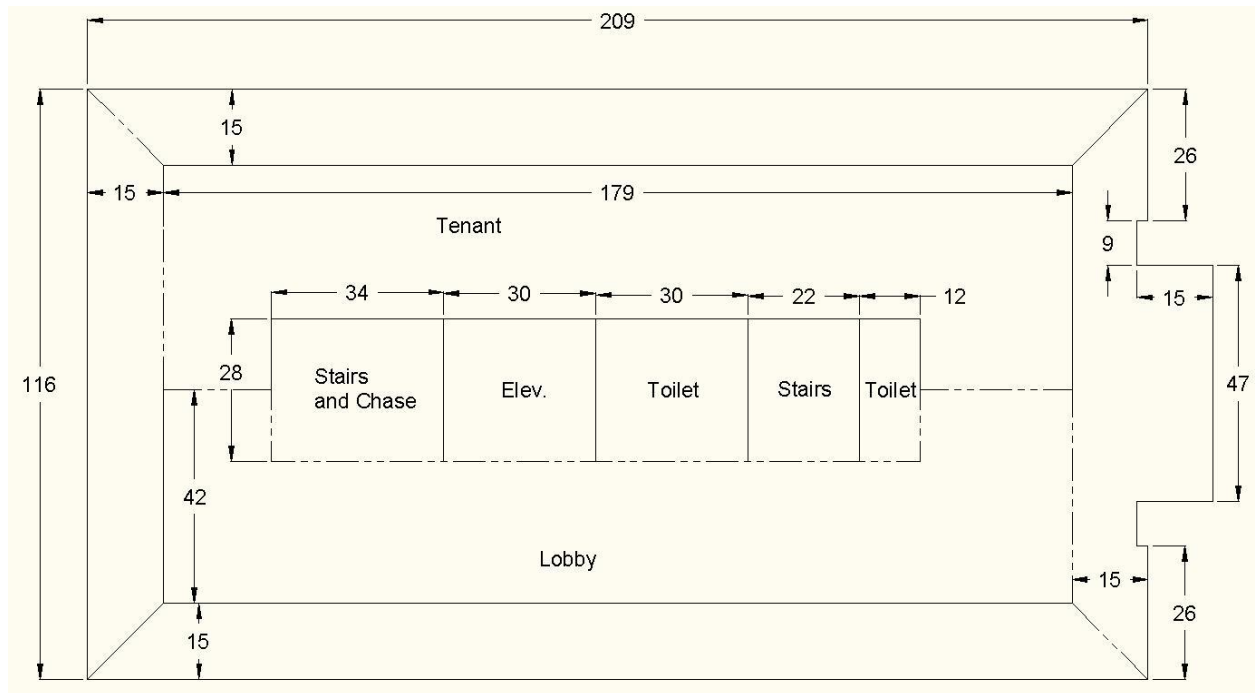


Figure 68: Ground floor plan of core and perimeter zones (Case Study IV).

The details of the building geometry, construction, and energy consuming systems were entered into an eQUEST/DOE2.2 building energy simulation model. Figure 69 and Figure 70 show 3-dimensional renderings of the case study building from two perspectives. The three floors shown represent the three main floor types in the model: ground floor, mid floor (typical), and top floor. The un-enclosed objects near the building floors represent the surfaces of adjacent structures (included to model the effects of shading).

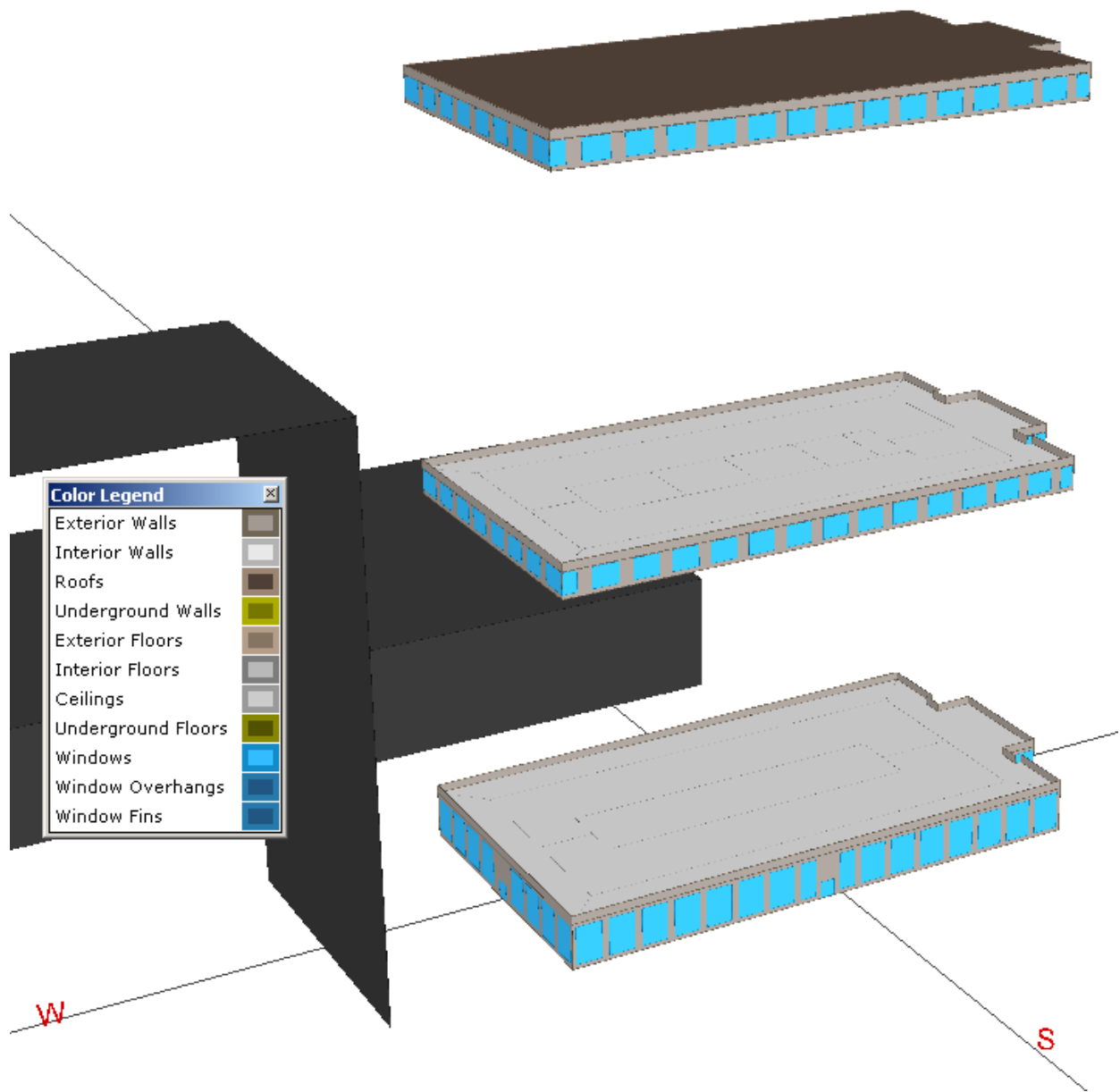


Figure 69: 3-D rendering of building floors, southwestern perspective (Case Study IV).

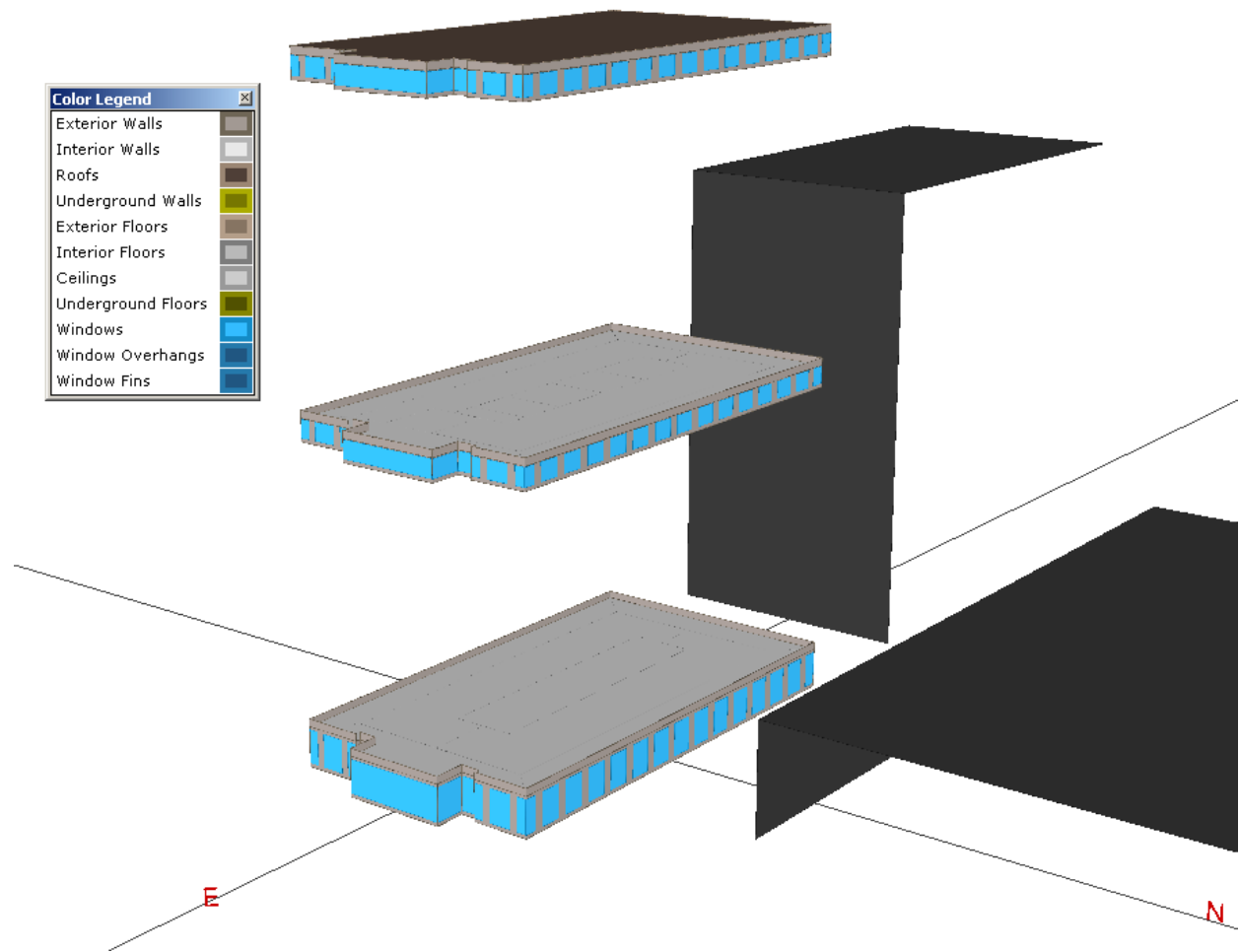


Figure 70: 3-D rendering of building floors, northeastern perspective (Case Study IV).

A list of the building energy model input parameters is shown in Table B - 4 in Appendix B. The building operation schedules are consistent with those of the other case studies. The most precisely defined aspect of the building in the building energy simulation model is the building geometry – building height, footprint, space floor plans, and exterior envelope design. Information on the building geometry is readily available from the leasing literature and from several building aerial photographs found in the Google Building Maker / SketchUp file in Google Earth.

Although the building is an existing building, precise data was not available for all building design parameters. For example, the basic system type and configuration of the HVAC was known, however precise system zoning and the nameplate capacities and power requirements of the air handlers, chillers, and cooling towers were unknown. Thus, HVAC equipment capacities and efficiencies are modeled with a range of possible values that represent the uncertainty of the system parameters. This modeling approach is reflective of not only the limitations of available data in this particular case study, but also of the amount of data that may be available to a potential building owner/occupant investigating a building/site alternative. Building leasing and sales professionals are very likely unable or unwilling to furnish complete details on the building energy system parameters needed to define a building energy simulation model. Furthermore, the time and effort required on behalf of a building energy simulation professional to collect enough data to fully and precisely define a building energy simulation model may exceed available resources (i.e. excessive informational cost).

One of the more significant approximations in the building energy model is the zoning of the HVAC systems (see Figure 67). An existing tenant space will contain heating/cooling zones across the floor plan, with multiple zones serving core and perimeter areas. HVAC design data is necessary to exactly match the number and location of zones and the associated design airflows and heating/cooling capacities. In the absence of such data, a perimeter core zoning configuration may be employed, in which a 15 foot wide perimeter zone is assigned to each space/area adjacent to an exterior wall whose plan orientation differs by more than 45 degrees from the nearest connected exterior wall (e.g. four perimeter zones for a rectangular floor plan), and a core zone is assigned to each space with a unique functional characteristic (e.g. office vs. conference space). The perimeter-core zoning strategy is consistent with professional HVAC

design practice for preliminary load and energy calculations in early design phases of a building project.

Another significant approximation related to the HVAC systems is the modeling of the campus chiller plant. In order to accurately estimate the energy consumption of a chiller plant, the load, equipment capacities, and equipment efficiencies must be defined. Without data on the chilled water load for the rest of the campus, the chiller plant had to be modeled for only the loads related to the case study building. Furthermore, in order to separate the chiller plant loads for individual floors (e.g. the selected tenant floor) separate “sub-plants” needed to be defined (to which each unique floor could be assigned). The result of this modeling approach is many, smaller chilled water plants/loops (with associated smaller condenser water loops) rather than one large chilled water plant with larger, staged chillers and cooling towers. To account for the increased uncertainty in the estimated energy consumption of the chilled water plant (at least for the portion of energy serving the case study building) a wide range of equipment efficiencies and sizing ratios were used for the input variables in the sensitivity analysis (see Section 7.1.5.2).

The components of the estimated annual tenant energy consumption are shown in Figure 71 and Figure 72. The figures show that a majority of the energy is consumed by the interior lighting and miscellaneous equipment. Nearly one-quarter of the estimated miscellaneous energy is consumed by the elevator (the only site-dependent energy consumption in the miscellaneous category). The space heating and space cooling energy consumptions are very low, owing to the heating and cooling energy saving technologies incorporated into the building design: enthalpy wheel energy recovery, air-side economizer, water-side economizer, district cooling, and high-performance envelope.

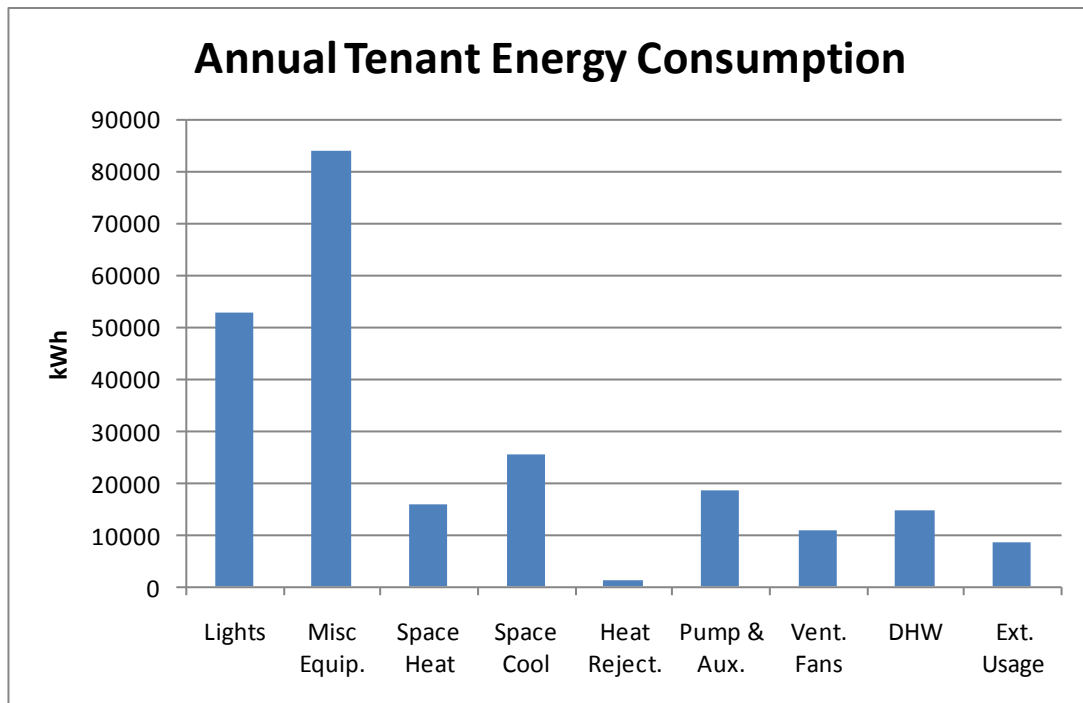


Figure 71: Components of annual tenant energy consumption (Case Study IV).

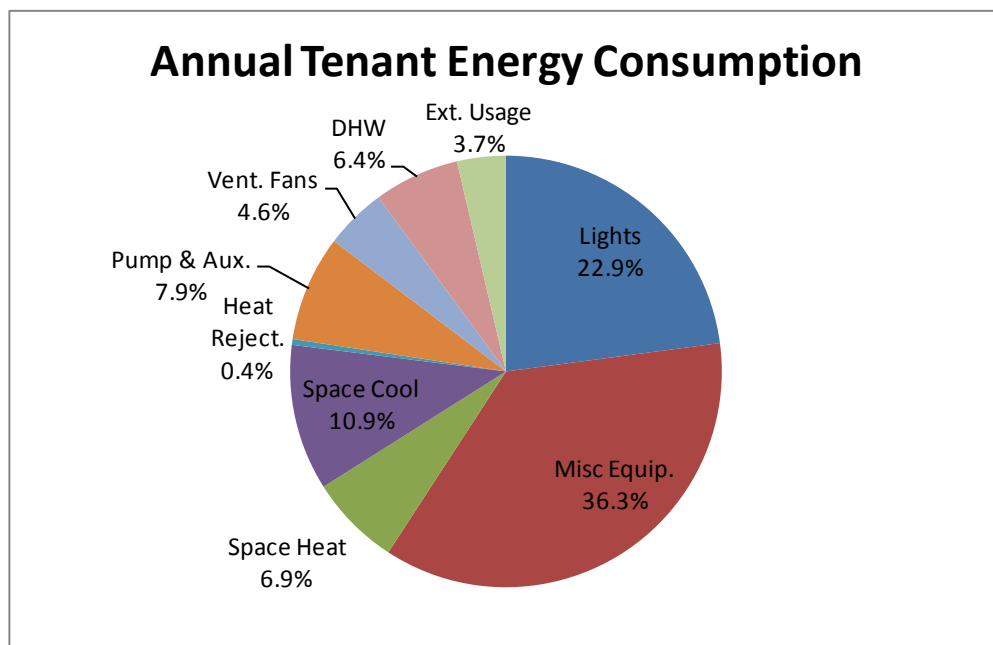


Figure 72: Components of annual tenant energy consumption (Case Study IV).

Upon defining the building in the building energy simulation model and allocating the energy consumption to the selected tenant space, a sensitivity analysis was performed.

7.1.5.2. Sensitivity Analysis of Uncertain Parameters

The variables included in the sensitivity analysis of this case study are shown in Table B - 4 in Appendix B. The variables span across all major categories of building systems (e.g. HVAC, lighting, envelope, etc.) except for building geometry, which is discernible from the building leasing literature, Google BuildingMaker files, and designer CAD files of architectural floor plans, sections, and elevations. Table B - 4 includes 138 numbered variables with defined ranges of probable values. The ranges of probable values are determined either from design references (e.g. ASHRAE 90.1 or ASHRAE Handbooks) or from engineering judgment. The un-numbered variables noted as “COMMON” are variables whose values are expected to be consistent between case studies. For example, the tenant space occupancy schedule is expected to be the same for all potential building/site alternatives. The other un-numbered, un-labeled variables are those that are recognized as relevant model inputs that were not assigned a range of values (see associated table notes). It should be noted that none of the part-load curve coefficients for the equipment (pumps, fans, compressors, etc.) were modified – only the total (full load) efficiencies were modified.

For the numbered variables with defined value ranges, the MATLAB script in Appendix C was executed to generate a Morris Method matrix of simulation input values. The generated matrix of values was then imported into a ModelCenter trade study of the eQUEST building energy simulation. The trade study was setup to estimate the response of the tenant space energy

consumption (see Equation 2) to the uncertain input variables. The results of the ModelCenter trade study were exported to MATLAB to plot the effect of the input variables on the response variable. Figure 73 and Figure 74 show the mean and standard deviation of elementary effects on the response variable (Equation 2) for Case Study IV. The plot labels correspond to the variable numbers in Table B - 4. In each of the plots, the dashed blue line indicates the division between effects dominated by the plotted variable and effects dominated by other variables. For variables plotted below the dashed blue line, the effect of the variable is less dependent on the other variables, and for variables plotted above the dashed blue line, the effect of the variable is more dependent on the other variables.

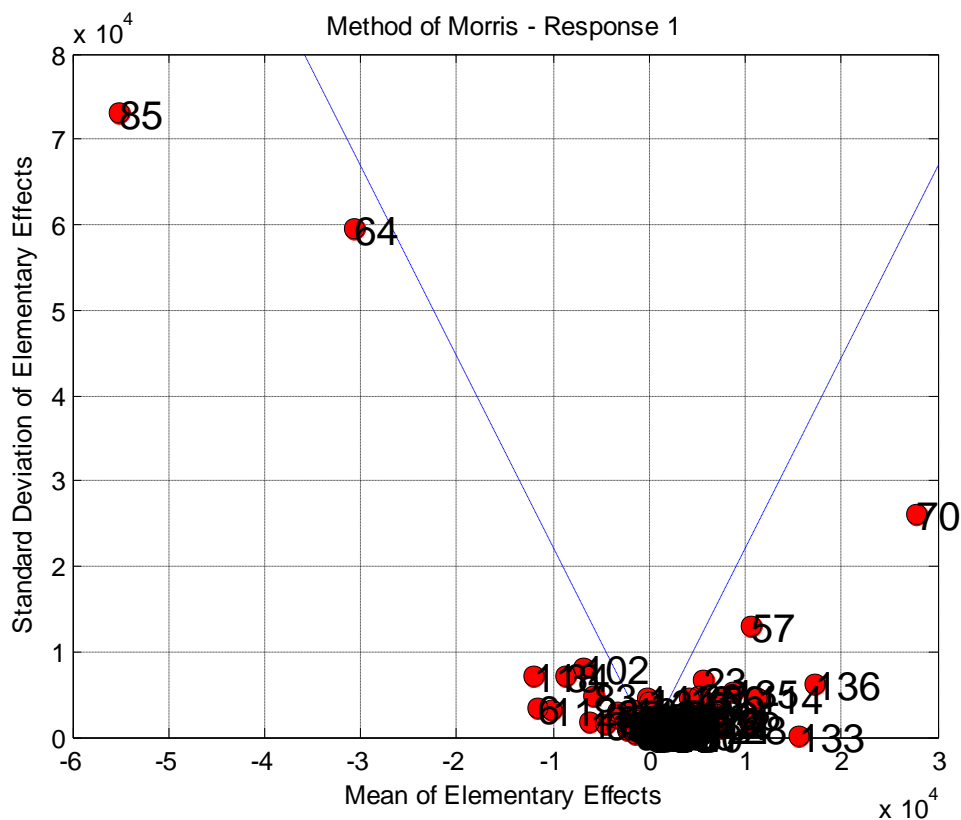


Figure 73: Mean and standard deviation of elementary effects on the response variable (Equation 2) for Case Study IV.

It is evident from Figure 73 that three variables have a relatively large impact on the annual space energy consumption: The terminal unit reheat ΔT (Variable #85), the supply fan minimum flow ratio (Variable #70), and the maximum space relative humidity (Variable #64). It is notable that all of these three variables are HVAC control setpoints, which are evidence of the large impact of HVAC system control parameters in estimated building energy consumption. Based on the apparent sensitivity of the estimated energy consumption to these control setpoints, the uncertainty may be significantly reduced by targeting a detailed building data collection effort on these three HVAC setpoints.

The mean and standard deviation of the elementary effects of the remaining variables are shown in more detail in Figure 74. It is apparent that many of the variables have very little effect on the annual energy consumption. Nonetheless, the salient variables at the left and right of Figure 74 are variables for which further refinement (or at least inclusion) of the value ranges is likely warranted. Many of the salient variables are none too surprising to a building energy modeler: glazing conductance (Variable #57), condenser water pump motor efficiency (Variable #118), the condenser water pump mechanical efficiency (Variable # 119), chiller capacity ratio (Variable #136), the condenser water ΔT (Variable #112), the chiller minimum ratio (Variable #102), the daylighting minimum power fraction (Variable #6), the office lighting power density (Variable #2), and the exterior wall insulation (Variable #34). However, some of the salient variables are typically not identified as important elements for minimizing building energy consumption: the total elevator power (Variable #133), and the condenser water pipe head, (Variable #114). In conventional building design practice, the elevator power consumption is typically an afterthought for reducing whole-building energy consumption. In fact, very little

guidance is available to building design and energy simulation professionals on the energy consumption of conveyance systems, or the relative energy consumption performance of various conveyance technologies.

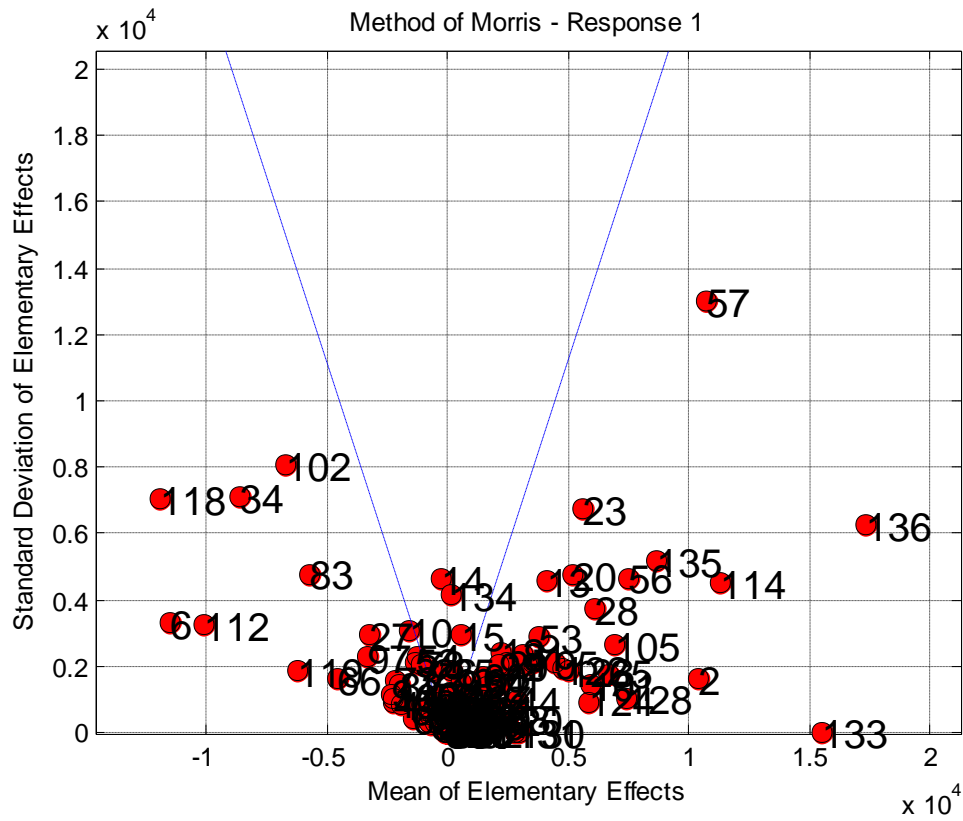


Figure 74: Mean and standard deviation of elementary effects on the response variable (Equation 2) for Case Study IV.

Figure 75 shows the ordered absolute value of the mean of elementary effects for the variables included in the sensitivity analysis. The figure shows that a minority of variables in this robust sensitivity analysis represent most of the impact on the response variable (annual tenant energy consumption). Only 44 of the 138 input variables have an absolute value of mean of

elementary effects that are greater than one percent of the average response variable value (see Table 58).

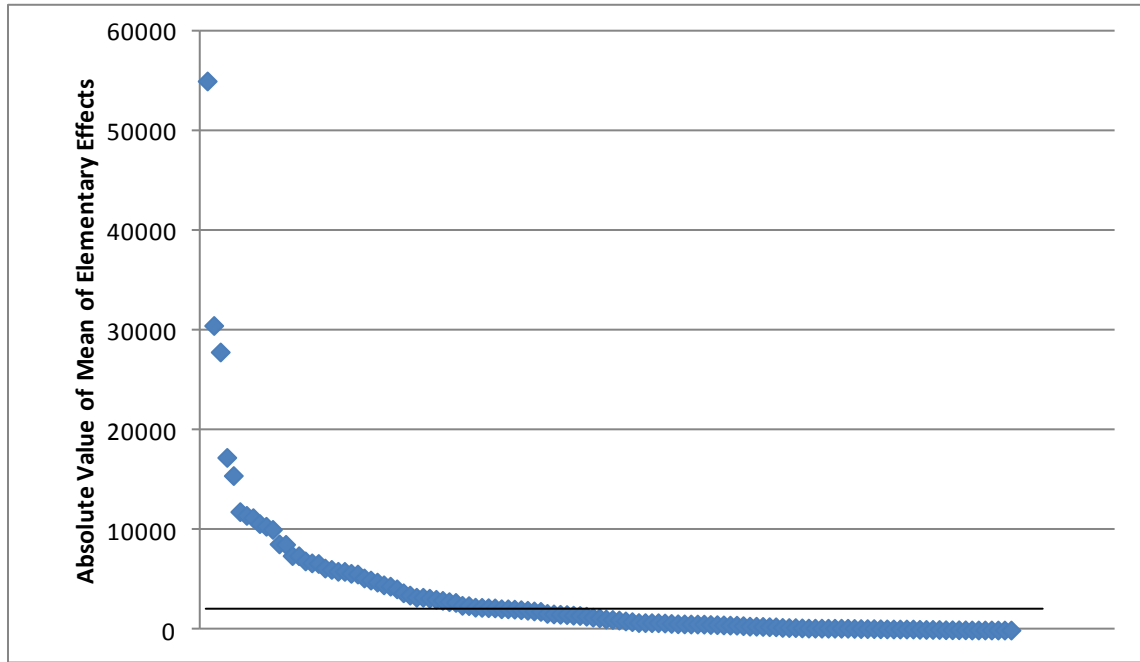


Figure 75: Ordered absolute value of the mean of elementary effects for Case Study IV.

Table 58: Input Variables with Absolute Value of Mean Effects Greater Than One Percent of Annual Tenant Energy Consumption (Case Study IV)

Var. #	Variable	Mean	Std. Dev.	Abs(Mean)
85	Heat_DT	-55,102	73,156	55,102
64	Max_Humid	-30,569	59,527	30,569
70	Fan_MinFlow	27,912	26,023	27,912
136	Chill_Cap_R	17,331	6,280	17,331
133	Elev	15,511	0	15,511
118	CWP_Mot_Eff	-11,891	7,049	11,891
6	DL_kW_F	-11,515	3,332	11,515
114	CW_PipeHead	11,285	4,493	11,285
57	Glaz1_Cond	10,691	13,024	10,691
2	LPD_Off	10,423	1,641	10,423

Table 58 (continued)

Var. #	Variable	Mean	Std. Dev.	Abs(Mean)
112	CW_DT	-10,108	3,232	10,108
135	OA_PerPers_Conf	8,653	5,180	8,653
34	Ewall_M2_Rval	-8,608	7,094	8,608
56	Glaz1_SC	7,480	4,668	7,480
128	DHW_Load_single	7,463	1,004	7,463
105	Chill_ConHead	6,943	2,653	6,943
102	Chill_MinR	-6,748	8,054	6,748
65	SFan_Sp	6,685	1,775	6,685
119	CWP_Mech_Eff	-6,230	1,853	6,230
28	Insul_Bd1_Cond	6,093	3,741	6,093
101	Chill_EIR	5,902	1,428	5,902
124	DHW_Temp	5,895	933	5,895
83	CRS_MinFlow	-5,698	4,783	5,698
23	Shade_Sch	5,627	6,757	5,627
20	Frm_Width	5,233	4,782	5,233
123	CT_StatHead	5,022	1,868	5,022
122	CT_Head	4,816	1,919	4,816
66	SFan_Tot_Eff	-4,544	1,610	4,544
95	CHW_PipeHead	4,410	2,103	4,410
13	Infil_NSW	4,144	4,575	4,144
53	Gflr_Conc_Cond	3,748	2,900	3,748
7	DL_MinP_F	3,514	2,143	3,514
9	DL_Setpoint	3,300	2,058	3,300
97	CHW_FlowRes	-3,298	2,311	3,298
27	Insul_Bd1_Thk	-3,201	2,944	3,201
81	Cool_Cntl_Rng	3,092	2,340	3,092
130	Park_Light	2,986	0	2,986
44	Roof_Insul_Cond	2,857	959	2,857
131	Sign_Light	2,781	0	2,781
21	Frm_Cond	2,486	2,098	2,486
68	RFan_Sp	2,458	394	2,458
94	CHW_CircTime	-2,300	1,172	2,300
109	CHWP_Mot_Eff	-2,285	1,053	2,285
43	Roof_Insul_Thk	-2,251	908	2,251
12	Infil_E	2,231	2,435	2,231

The 44 variables with mean effects greater than one percent of the annual tenant energy consumption retain their uncertainty distributions for the Monte Carlo analysis presented in the following section.

7.1.5.3. Monte Carlo Analysis

For the Monte Carlo analysis of the tenant space annual energy consumption, each of the variables in Table 58 will either retain their uncertainty, or will have their range in values reduced (representing a targeted data collection effort to reduce uncertainty). For this case study, the range of values for Variable #85 will be redefined to 30 – 50 deg F ΔT , since the heating system is undersized below a terminal unit reheat ΔT of 30 deg F. The defined range of values for Variable #70 will be replaced by a smaller range (0.25 to 0.35) representing detailed data collected from an air handler design schedule – a range of uncertain values is maintained to reflect uncertainty in the current damper settings of the actual air handler. The maximum return air relative humidity (Variable #64) will be fixed at 50 percent. The range of values for the remainder of the variables in Table 58 will remain the same, meaning that more precise data for the variables was either unattainable or considered not worth the additional informational cost. The minimum and maximum values set for the uncertain variables are shown in Table 59.

Table 59: Uncertain Input Variables for Monte Carlo Analysis (Case Study IV)

Var. #	Variable	Min	Max	Units
2	LPD_Off	0.9	1.1	W/SF
6	DL_kW_F	0	1	NA
7	DL_MinP_F	0.1	0.5	NA
9	DL_Setpoint	20	500	fc
12	Infil_E	0.01675	0.05025	cfm/SF

Table 59 (continued)

Var. #	Variable	Min	Max	Units
13	Infil_NSW	0.0145	0.0435	cfm/SF
20	Frm_Width	0.08333	0.2083	ft
21	Frm_Cond	1.63	3.01	Btu/h-SF-degF
23	Shade_Sch	0.4	0.9	NA
27	Insul_Bd1_Thk	0.0417	0.0833	ft
28	Insul_Bd1_Cond	0.0083	0.0475	Btu/h-ft-degF
34	Ewall_M2_Rval	0	5	h-SF-degF/Btu
43	Roof_Insul_Thk	0.25	0.5	ft
44	Roof_Insul_Cond	0.01	0.025	Btu/h-ft-degF
53	Gflr_Conc_Cond	0.275	1.667	Btu/h-ft-degF
56	Glaz1_SC	0.28	0.6	NA
57	Glaz1_Cond	0.3	0.5	Btu/h-SF-degF
65	SFan_Sp	2.5	4.5	in. wg
66	SFan_Tot_Eff	0.5	0.75	NA
68	RFan_Sp	1	2	in. wg
70	Fan_MinFlow	0.25	0.35	NA
81	Cool_Cntl_Rng	3	6	degF
83	CRS_MinFlow	0.3	0.66	NA
85	Heat_DT	30	50	degF
94	CHW_CircTime	1.5	15	minutes
95	CHW_PipeHead	15	50	ft
97	CHW_FlowRes	0.5	0.8	NA
101	Chill_EIR	0.15	0.18	NA
102	Chill_MinR	0.1	0.3	NA
105	Chill_ConHead	10	30	ft
109	CHWP_Mot_Eff	0.6	0.95	NA
112	CW_DT	8	14	degF
114	CW_PipeHead	15	50	ft
118	CWP_Mot_Eff	0.6	0.95	NA
119	CWP_Mech_Eff	0.6	0.8	NA
122	CT_Head	5	20	ft
123	CT_StatHead	5	20	ft
124	DHW_Temp	110	140	degF
128	DHW_Load_single	0.15	0.5	gpm
130	Park_Light	7.5	15	kW
131	Sign_Light	8	22	kW

Table 59 (continued)

Var. #	Variable	Min	Max	Units
133	Elev	114.6	343.8	kW
135	OA_PerPers_Conf	5	15	cfm/pers.
136	Chill_Cap_R	1	1.5	NA

For the rest of the 138 variables included in the sensitivity analysis, each with a mean effect less than one percent of the annual tenant energy consumption, the defined range of uncertain values is reduced to a single value (see values in Table B - 4 in Appendix B). The reduction in the number of variables with a defined range of uncertain values helps to simplify the building energy model simulation.

After reducing the number of variables with defined ranges of uncertainty, the building energy simulation was run through a Monte Carlo analysis. For each of the variables with a defined range of uncertainty, a uniform distribution was assumed. A uniform distribution was chosen since, in the case of building design variable uncertainty, there is no “tailed” distribution that is known to represent the uncertainty. Furthermore, assumption of a uniform distribution increases the dispersion of the response variable that would otherwise be estimated from an assumed normal or triangular distribution, thereby producing a conservative estimate of uncertainty in estimated annual energy consumption.

Figure 76 shows the results of the Monte Carlo analysis of annual tenant energy consumption (kWh's) for Case Study IV. The Monte Carlo analysis consists of 1000 simulation runs. The estimated energy consumption results appear to form a triangular or approximately normal distribution.

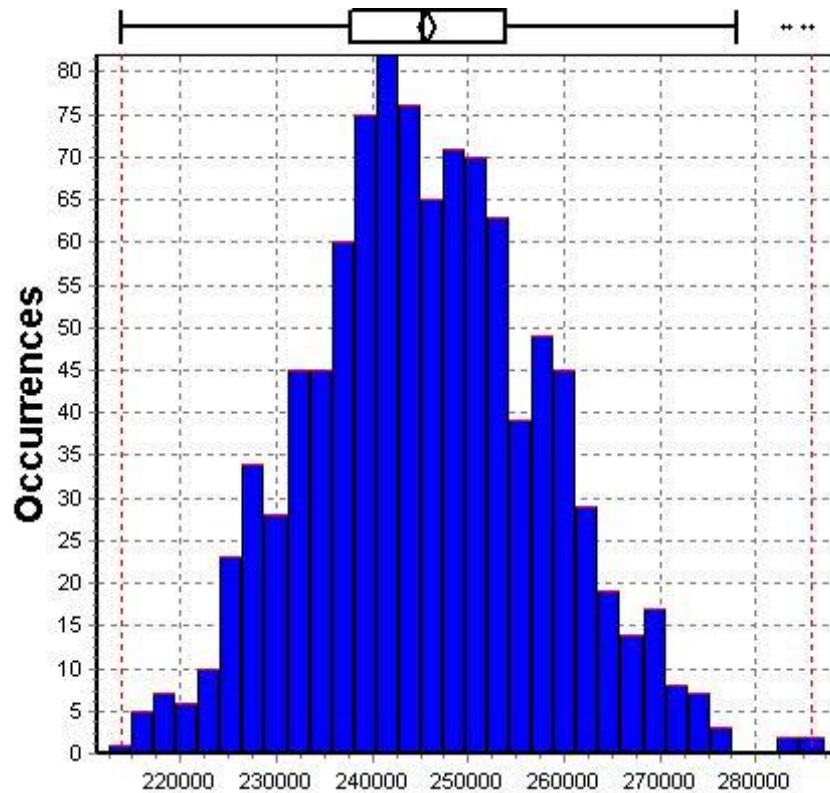


Figure 76: Monte Carlo analysis of annual tenant energy consumption, kWh's (Case Study IV).

It should be noted that the estimated average energy consumption is greater than the amount estimated without uncertainty. Intuitively, one would expect that an estimate from approximately median input values should produce a result close to the median of the output distribution. However, it is to be expected that some, if not many, of the input variables have non-linear effects on response variable, and certainly the mean effect of some variables are greater than others. Thus, the results shown in Figure 76 highlight the importance of estimating annual tenant energy consumption under uncertainty – estimated outputs based on median inputs may not be representative of median outputs.

7.1.5.4. Site Energy vs. Source Energy / GHG Emissions

Based on energy consumption/loss data for the energy supply chain, a “source energy factor” may be estimated and multiplied by the site energy to obtain the estimated source energy consumption. According to DOE, the source energy factor for electrical energy consumed at a facility located in Georgia is 3.364 kWh of source energy consumed per kWh of delivered electricity (see (95) Table B-9). Thus the average source energy consumption for Case Study IV is approximately 827,000 kWh or 2,822 MBtu.

The results of both the direct and upstream GHG emission estimates for electricity purchased in the state of Georgia are shown in Table 60. Consistent with GHG emission inventory protocols (71, 72, 73, 74), the purchased electricity emissions are counted as “Scope 2,” and the upstream fuel-energy supply chain emissions are counted as “Scope 3.”

Table 60: Estimated GHG Emissions of Purchased Electricity (Case Study IV)

kWh	CO ₂ e (Scope 2), tonnes	CO ₂ e (Scope 3), tonnes	CO ₂ e (Total), tonnes	Calc. Source
245,831	156.4	23.3	179.7	(121)
			180.6	(95)

The source energy estimation guidance of DOE provides an estimation method and emission factors for total (direct and upstream) electricity GHG emissions (95). Using the DOE emission factor for the State of Georgia (1.62 lb CO₂e per kWh), the estimated total CO₂e emissions nearly matches the piecewise estimate of Scope 2 and Scope 3 emissions. Since all of the building energy is supplied from utility energy sources, the dispersion of GHG emission estimates matches the dispersion in energy consumption estimates.

7.1.5.5. Normalization of Results

Table 61 shows the normalized energy consumption and GHG emission performance of Case Study IV. The square-footage of the conditioned floor area is the total tenant square footage shown in Table 56. The person-hours of occupancy are based on the amount shown in Table 35. In this research, the annual person-hours are to remain consistent between building/site alternatives. The values are expressed as a mean plus or minus 2 standard deviations (see Section 4.2.5.2). According to the data shown from the CBECS database, the Case Study IV building is much more energy efficient than the average office building in the South Atlantic region, which should be expected for a high-performance LEED certified building. The building also performs better than the ASHRAE/IES Standard 100-2006 EUI target for an administrative/professional office (see Climate Zone 3A in Table 8).

Table 61: Normalized Building Energy Consumption and GHG Emission Performance (Case Study IV)

Inventory Unit		Normalizing Unit	Performance Metric	Value
Annual Energy [kBtu]	Site (end use)	Conditioned floor area [SF]	Annual site energy / conditioned floor area [kBtu/SF]	33.7 ± 3.3
		Occupant use [person-hrs]	Annual site energy / occupant use [kBtu/person-hrs]	3.4 ± 0.3
	Primary (end use + upstream)	Conditioned floor area [SF]	Annual primary energy / conditioned floor area [kBtu/SF]	113.5 ± 11.2
		Occupant use [person-hrs]	Annual primary energy / occupant use [kBtu/person-hrs]	11.4 ± 1.1
CBECS annual site energy / conditioned floor area [kBtu/SF] *				56.9
CBECS annual source energy / conditioned floor area [kBtu/SF] ^				191.5
Annual GHGs [lb CO2e]	Site (end use)	Conditioned floor area [SF]	Annual site GHGs / conditioned floor area [lb CO2e /SF]	2,489.1 ± 245.3
		Occupant use [person-hrs]	Annual site GHGs / occupant use [lb CO2e /person-hrs]	250.9 ± 24.7
	Primary (end use + upstream)	Conditioned floor area [SF]	Annual primary GHGs / conditioned floor area [lb CO2e /SF]	2,860.8 ± 281.9
		Occupant use [person-hrs]	Annual primary GHGs / occupant use [lb CO2e /person-hrs]	288.3 ± 28.4
Source: * CBECS: South Atlantic, office, constructed 2000 - 2003, 10,001 - 50,000 SF ^ CBECS and Deru & Torcellini				

7.1.6. Comparison of Building Energy Consumption Under Uncertainty

The quantification of uncertainty in building energy consumption and GHG emissions can support a more robust comparison of the relative performance of building alternatives. This section compares the estimated performance of the case study buildings under uncertainty.

Included is an estimate of the probability of energy savings for one building relative to another and the capabilities for estimating the impact of post-occupancy energy retrofits.

7.1.6.1. Summary of Estimated Building Energy Consumption and GHG Emissions

This section summarizes the estimated building energy consumption and GHG emissions from each of the building cases studies included in this chapter. Table 62 shows the normalized building energy consumption and GHG emission performance of the case study buildings. The values shown in Table 62 are the same as those shown separately in Table 42, Table 48, Table 55, and Table 61. According to the average values shown in Table 62, Case Study II is the best performing site, but the uncertainty in the estimates suggests that the superiority of Case Study II relative to Case Study IV is very slight. The value ranges defined by the plus/minus 2 standard deviations provide a sense of the overlap between the performance estimates, but it is difficult to visually discern from the table data how much overlap exists, or more importantly how the uncertainty may impact determination of a “best” alternative. While expression of uncertainty consistent with NIST guidelines is helpful for consistent uncertainty quantification, it is arguably better to compare the performance estimates in graphical form.

Table 62: Normalized Building Energy Consumption and GHG Emission Performance of Case Study Buildings

Performance Metric	Case Study			
	I	II	III	IV
Annual site energy / conditioned floor area [kBtu/SF]	50.6 ± 3.3	33.4 ± 3.2	40.9 ± 3.1	33.7 ± 3.3
Annual site energy / occupant use [kBtu/person-hrs]	5.1 ± 0.3	3.4 ± 0.3	4.0 ± 0.3	3.4 ± 0.3
Annual primary energy / conditioned floor area [kBtu/SF]	166.7 ± 10.9	112.4 ± 10.7	134.5 ± 10.1	113.5 ± 11.2
Annual primary energy / occupant use [kBtu/person-hrs]	16.8 ± 1.1	11.4 ± 1.1	13.3 ± 1.0	11.4 ± 1.1
CBECS annual site energy / conditioned floor area [kBtu/SF]	75.7 *	56.9 ^	75.7 *	56.9 ^
CBECS annual source energy / conditioned floor area [kBtu/SF]	217.7 #	191.5 #	217.7 #	191.5 #
Annual site GHGs / conditioned floor area [lb CO ₂ e /SF]	3,661 ± 240.1	2,473 ± 234.7	2,955 ± 221.1	2,489 ± 245.3
Annual site GHGs / occupant use [lb CO ₂ e /person-hrs]	369.9 ± 24.3	249.9 ± 23.7	291.5 ± 21.8	250.9 ± 24.7
Annual primary GHGs / conditioned floor area [lb CO ₂ e /SF]	4,207 ± 275.9	2,841 ± 269.6	3,396 ± 254.1	2,861 ± 281.9
Annual primary GHGs / occupant use [lb CO ₂ e /person-hrs]	425.1 ± 27.9	287.1 ± 27.2	335.0 ± 25.1	288.3 ± 28.4
Source: * CBECS: South Atlantic, office, constructed 1980 - 1999, 10,001 - 50,000 SF ^ CBECS: South Atlantic, office, constructed 2000 - 2003, 10,001 - 50,000 SF # CBECS and Deru & Torcellini				

Figure 77 shows the annual building (site) energy consumption for the initial Monte Carlo analyses. The histograms in Figure 77 offer a visual representation of the dispersion in the

energy consumption estimates. It should be noted that the average values of energy consumption in Figure 77 do not match the averages in Table 62; Table 62 presents the average values from each of the final/revised Monte Carlo analyses. The initial Monte Carlo analyses include high degrees of skew in Case Study I and Case Study III. In both of these case studies, the results of a sensitivity analysis were used to refine the input parameter uncertainty and to reduce the dispersion in the energy consumption estimates. The results of the revised Monte Carlo analyses of building energy consumption are shown in Figure 78. With the reduced skew, Figure 78 shows a much clearer illustration of the overlap in estimated building energy consumption for each of the case studies. The figures below offer a lesson in minimizing the amount of time spent collecting building data and performing uncertainty analyses. The lesson lies in the fact that even though the uncertainty was reduced for Case Studies I and III, the extra effort to reduce the uncertainty did not impact the determination of the most energy efficient building. Thus, in practical application of the building evaluation framework, it is best to attempt uncertainty reductions after viewing the relative performance of each of the building alternatives.

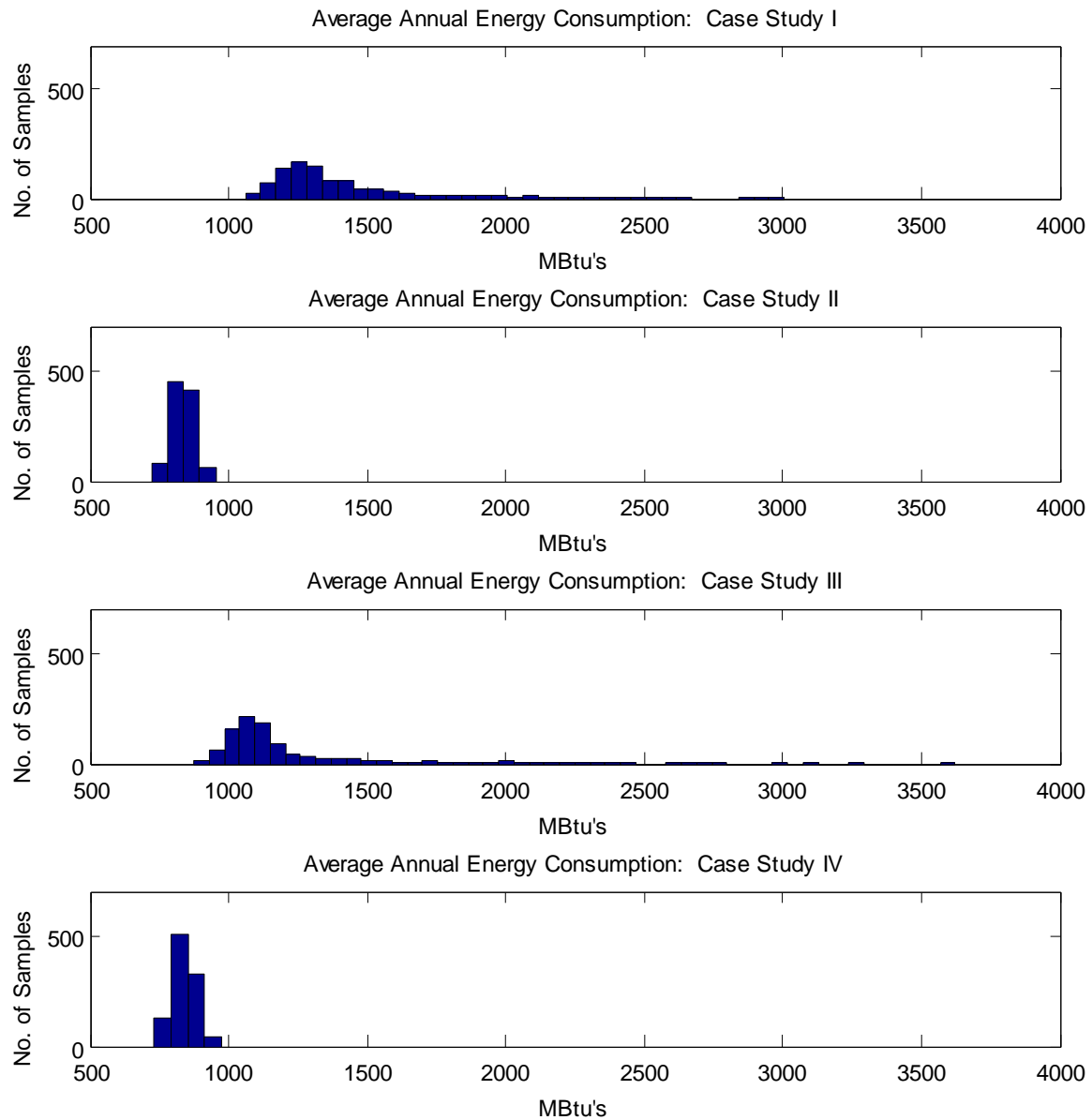


Figure 77: Building annual (site) energy consumption for initial Monte Carlo analyses.

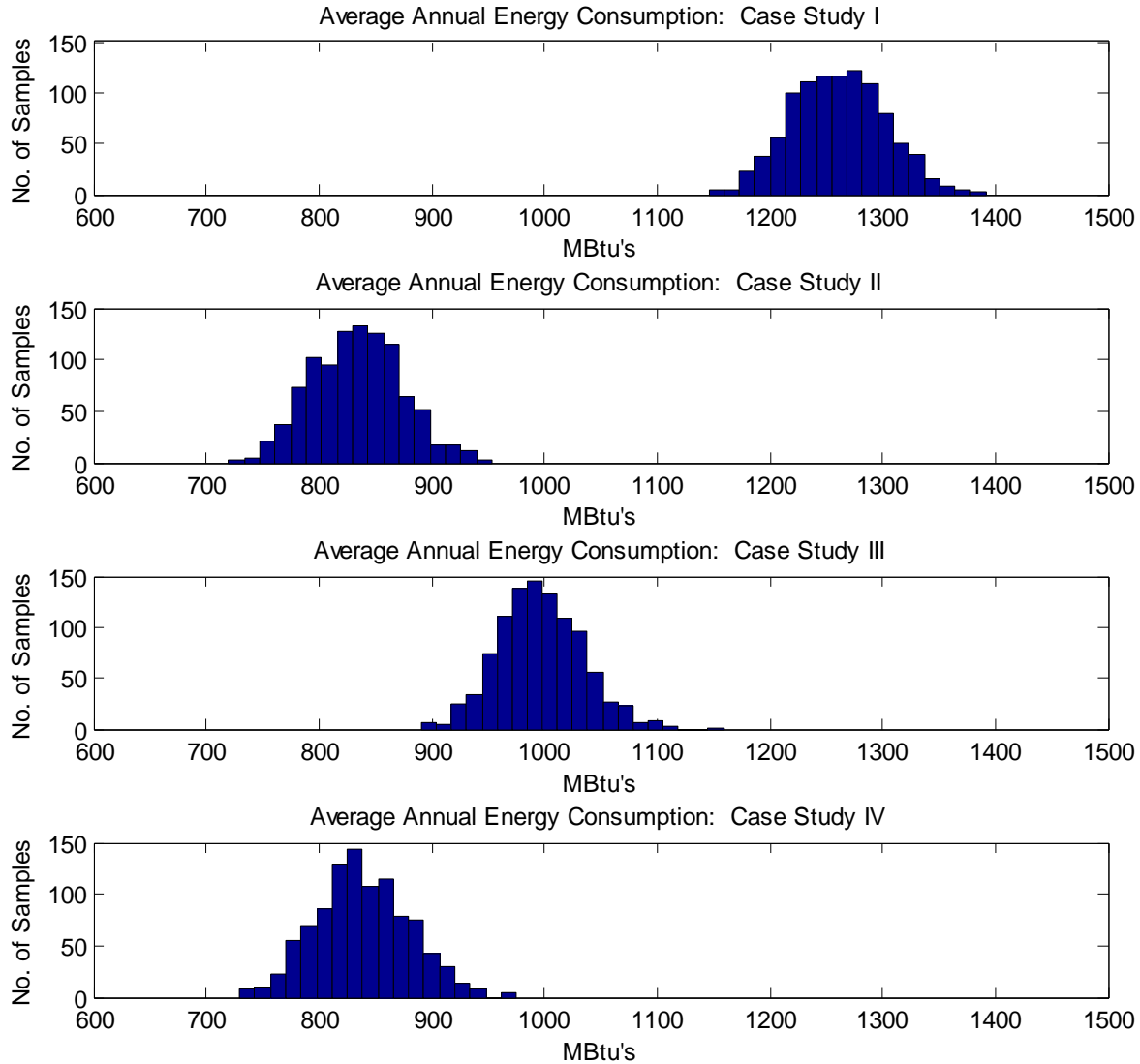


Figure 78: Building annual (site) energy consumption for revised Monte Carlo analyses.

The dispersion in the estimated building energy consumption is such that the results for Case Study II and Case Study IV appear to completely overlap. Recall that both of these buildings are recently constructed LEED certified buildings with high performance building systems. While it may be expected that the two LEED certified buildings may be the best performing buildings and have similar levels of performance, it is interesting how similar the estimates are given that each of the buildings have very different mechanical systems, lighting

systems, and glazing (see Table 44 and Table 57). The similarity of the results serves as a testimony to the value of building energy simulation in evaluating whole-building operation energy consumption. If the relative performance was judged merely by a prescriptive or component-based assessment of the installed technologies, then Case Study IV would arguably be the top choice, with its ventilation air energy recovery, daylighting, and high performance glazing. Yet, the higher percent glazing area, the greater number of floors and elevators, the greater amount of exterior lighting, and the higher LPD have the effect of mitigating the energy conservation impact of the high performance building technologies.

7.1.6.1.1. Probabilities of Relative Performance

Based on the Monte Carlo simulation outputs of building energy consumption, it is possible to calculate the probabilities of relative performance. The Monte Carlo output histograms may be converted to probability distribution functions (PDFs) through a mathematical process known as kernel density estimation or kernel smoothing. The kernel density function in MATLAB was used to convert the combined energy consumption histograms into a smooth PDF. Figure 79 shows the PDFs of the estimated annual building energy consumption for Case Studies II and IV. The overlap of the PDFs indicates that it is nearly equally likely that Case Study II or Case Study IV is the lowest energy consuming building. Nevertheless, a decision-maker may wish to know the probability of achieving energy savings from one building alternative relative to another.

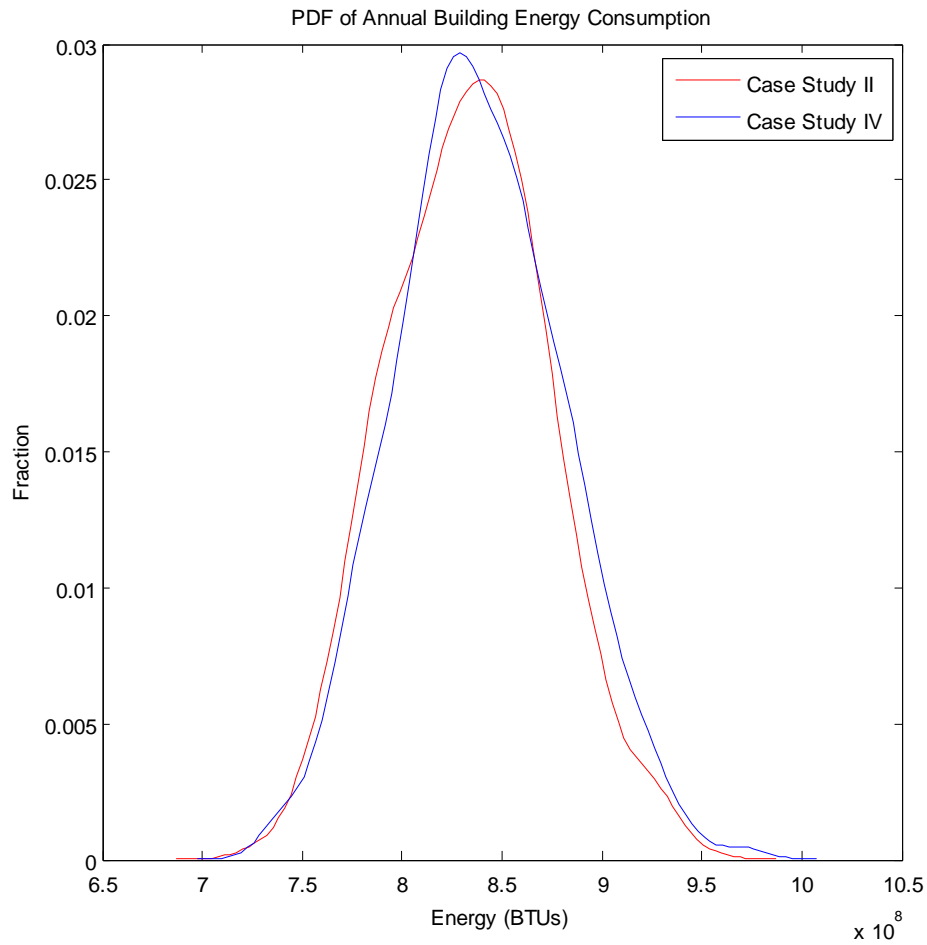


Figure 79: Probability distribution functions of estimated annual building energy consumption for Case Study II and Case Study IV.

The probability of Case Study II saving energy relative to Case Study IV may be calculated from the PDFs of estimated annual energy consumption. Appendix E contains the MATLAB code used to calculate the probability of energy savings (starting at the line containing the “ksdensity” function). Each of the PDFs are discretized into 100 intervals by the kernel smoothing function. In the nested loops following the use of the kernel smoothing function, the discrete differences in energy consumption between the two curves are taken, with the probability of each difference calculated as the product of the independent probabilities. The

probabilities are then added together for each of 100 bins of estimated energy savings (negative energy consumption). The result is a PDF of energy savings between two building alternatives, which is shown below in Figure 80.

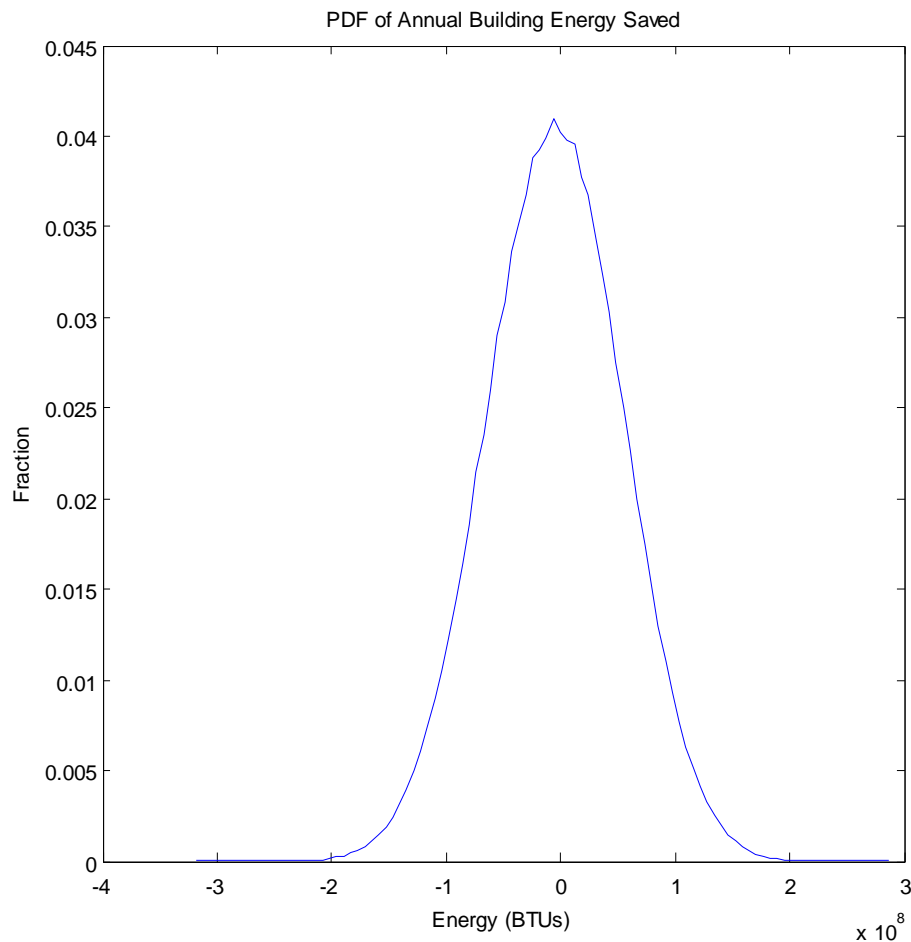


Figure 80: Probability distribution functions of estimated annual building energy saved by Case Study II relative to Case Study IV.

Figure 81 below shows the cumulative distribution function (CDF) of estimated annual building energy saved for Case Study II relative to Case Study IV. The probability of saving 0 or more Btu's of energy is 55 percent. The probability of saving at least the mean difference in

combined energy consumption (5,400,000 Btu's) is 52 percent. These probabilities confirm what has already been discerned by comparison of the Case Studies in Table 62 and Figure 78 – that it is nearly equally likely that Case Study II or Case Study IV is the lowest energy consuming building.

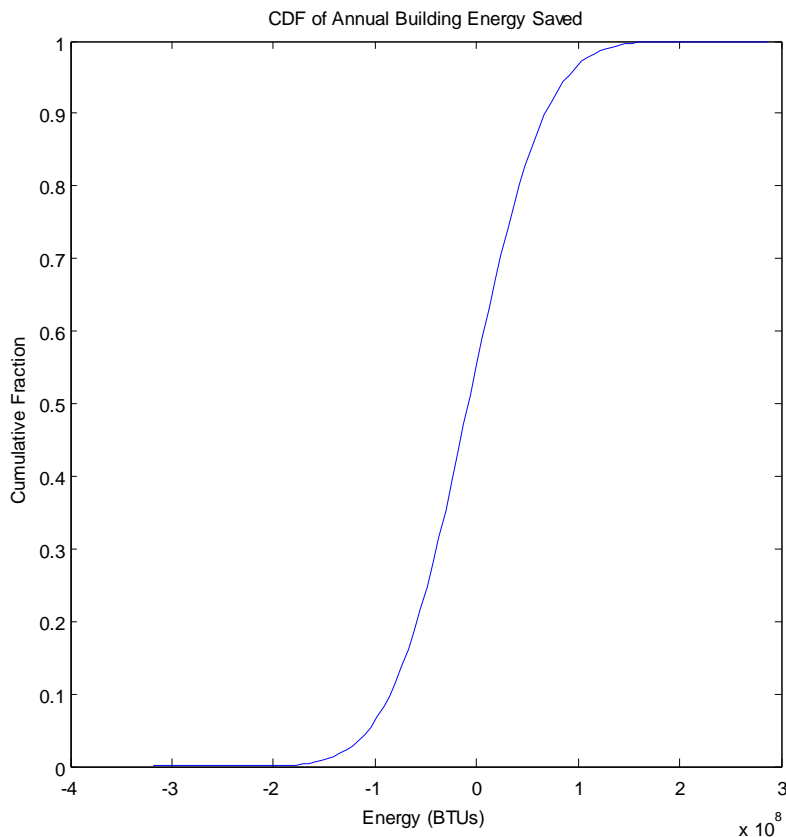


Figure 81: Cumulative distribution function of estimated annual building energy saved by Case Study II relative to Case Study IV.

A more precise estimate of the energy savings of Case Study II relative to Case Study IV (or vice versa) would require additional data collection and modeling to refine the dispersion in the energy estimates for either one or both of the case studies. The probability of energy savings could then be recalculated from the Monte Carlo analysis histograms. However, the need for this

additional effort may be forestalled by the energy consumption estimates of the transportation systems (see Chapter 8). In other words, in a whole building evaluation framework that includes building system energy consumption and transportation system energy consumption, the transportation system energy performance may be the deciding factor for two case studies with similar building system energy performance, which is the case shown in Chapter 8.

7.1.6.2. Evaluate Potential Impact of Post-Occupancy Energy Retrofits

The application of the evaluation framework in this chapter is focused on the quantification of existing building performance. However, it should be recognized that most existing buildings will have some opportunity for improving energy performance through post-occupancy actions such as energy retrofits; the opportunity for energy retrofits will be dependent upon any limitations on modifying the building systems (see Section 4.2.5.3.1). One of the strengths of the framework's calculation procedures is that they enable estimation of the impact of post-occupancy energy and emission management strategies. Specifically, the building energy models created to estimate existing energy and emissions performance can be rather easily adapted to include potential energy retrofits.

One of the most commonly implemented building energy retrofits is efficient lighting replacements, such as replacing T12 fluorescent lamps with T8 fluorescent lamps, or replacing fluorescent fixtures with LED fixtures. Lighting efficiency upgrades are a popular energy retrofit strategy since they typically involve relatively low capital costs and have relatively short payback periods. The impact of a lighting efficiency upgrade on whole-building operation energy consumption can be easily estimated in a building energy simulation model by modifying the input parameter(s) for the lighting system(s) (i.e. parametric analysis). In the evaluation

framework of this dissertation, the impact is estimated with the effects of uncertainty in the input parameters.

To illustrate the evaluation of post-occupancy energy retrofits, an example calculation is presented here for a lighting efficiency upgrade of Case Study IV. The Case Study IV building is a high-performance, LEED certified building with efficient lighting: 0.9 – 1.1 W/SF office lighting power density and daylighting controls. The lighting power density meets ASHRAE Standard 90.1-2007, but it is possible to reduce the lighting power density (increase lighting efficiency) with T5 fluorescent or LED lighting. The building energy Monte Carlo analysis for Case Study IV was reran for a revised lighting power density of 0.6 – 0.7 W/SF. The results of this revised analysis for an aggressive lighting efficiency upgrade are shown in Figure 82. The original estimated energy performance is shown in blue, and the revised performance is shown in red. The approximately 35 percent reduction in office lighting power density results in a tenant energy consumption reduction of approximately 8 percent.

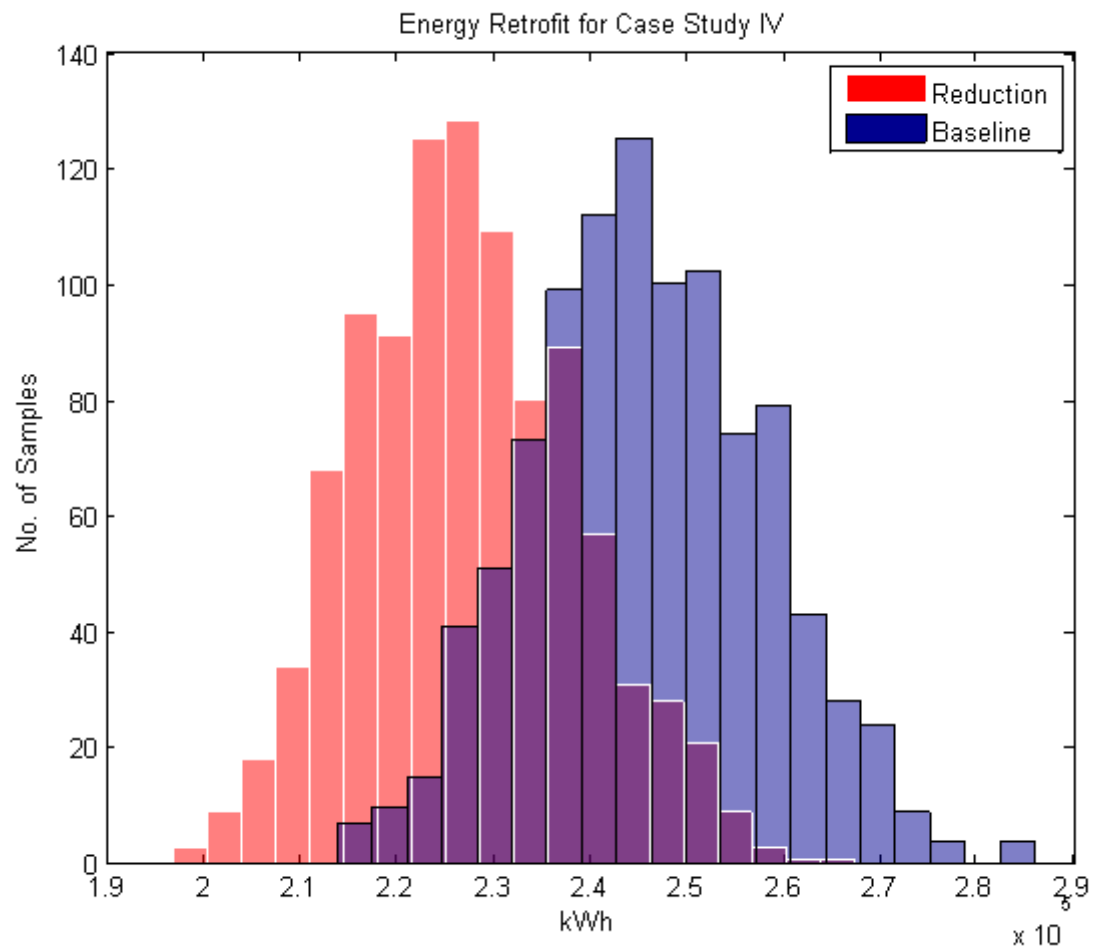


Figure 82: Monte Carlo analysis of annual tenant energy consumption, kWh's (Case Study IV, revised office LPD).

CHAPTER 8

APPLICATION OF FRAMEWORK: TRANSPORTATION SYSTEMS

This chapter presents the application of the evaluation framework for transportation system energy consumption and GHG emissions. The intent of the framework application is to explore the potential variation in transportation system energy consumption and GHG emissions for commercial office site alternatives within a metropolitan area. The framework application yields an estimate of baseline transportation energy/emissions performance based on TAZ travel activity parameters, as well as estimated energy/emissions reductions resulting from employer-based travel demand management strategies. The evaluation framework is applied to 4 unique location types within a regional transportation network (see Chapter 3, Section 3.4).

8.1. Regional Application: Atlanta, GA Metropolitan Region

The developed calculation framework of location-specific, transportation energy consumption is applied to the context of the Atlanta, GA metropolitan region. The intended real-world application of the framework is evaluation of only a few potential office sites that meet the location decision-maker's selection criteria. However, broad regional application of the framework to all TAZs containing employment that is similar to the employment of the proposed office may offer insights into spatial patterns of efficiency and enable estimation of a regional baseline of average consumption.

8.1.1. Atlanta, GA Metropolitan Region

The Atlanta, GA metropolitan region is one of the largest urbanized areas in North America in terms of both land area and population. The region is spatially defined in several different ways. The largest spatial definition that is most commonly used for the Atlanta, GA region is the 28-county metropolitan statistical area (MSA). The extent of this 28-county area is shown in Figure 83. This area represents the spatial definition of the Atlanta region in the U.S. Census. Another spatial definition of the Atlanta region is the U.S. EPA's 20-county PM2.5 nonattainment area. The extent of this 20-county area is also shown in Figure 83. Transportation planning in the Atlanta region is closely tied to air quality conformity analysis, thus the regional travel demand model covers this 20-county area. In the 2010 ARC land use and travel demand models, the 20-county area contains a population of 5,171,685 over an area of 6,403 square miles. The population densities in the travel demand model TAZs are shown in Figure 84. It is evident from Figure 83 and Figure 84 that the higher population density areas correspond approximately with the public transit network. The employment densities in the travel demand model TAZs are shown in Figure 85, which indicates a polycentric pattern of employment centers.

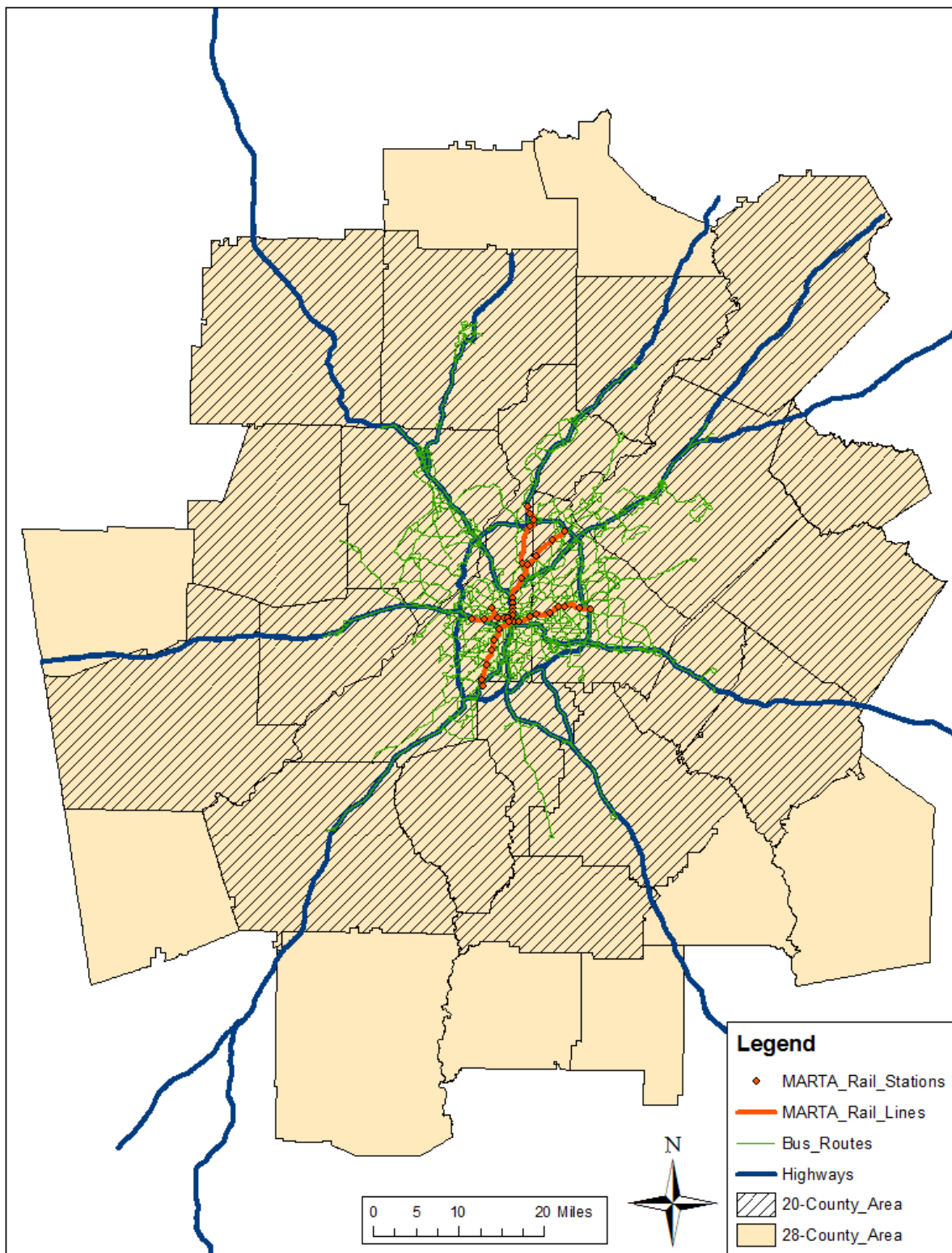


Figure 83: Map of Atlanta, GA metropolitan region.

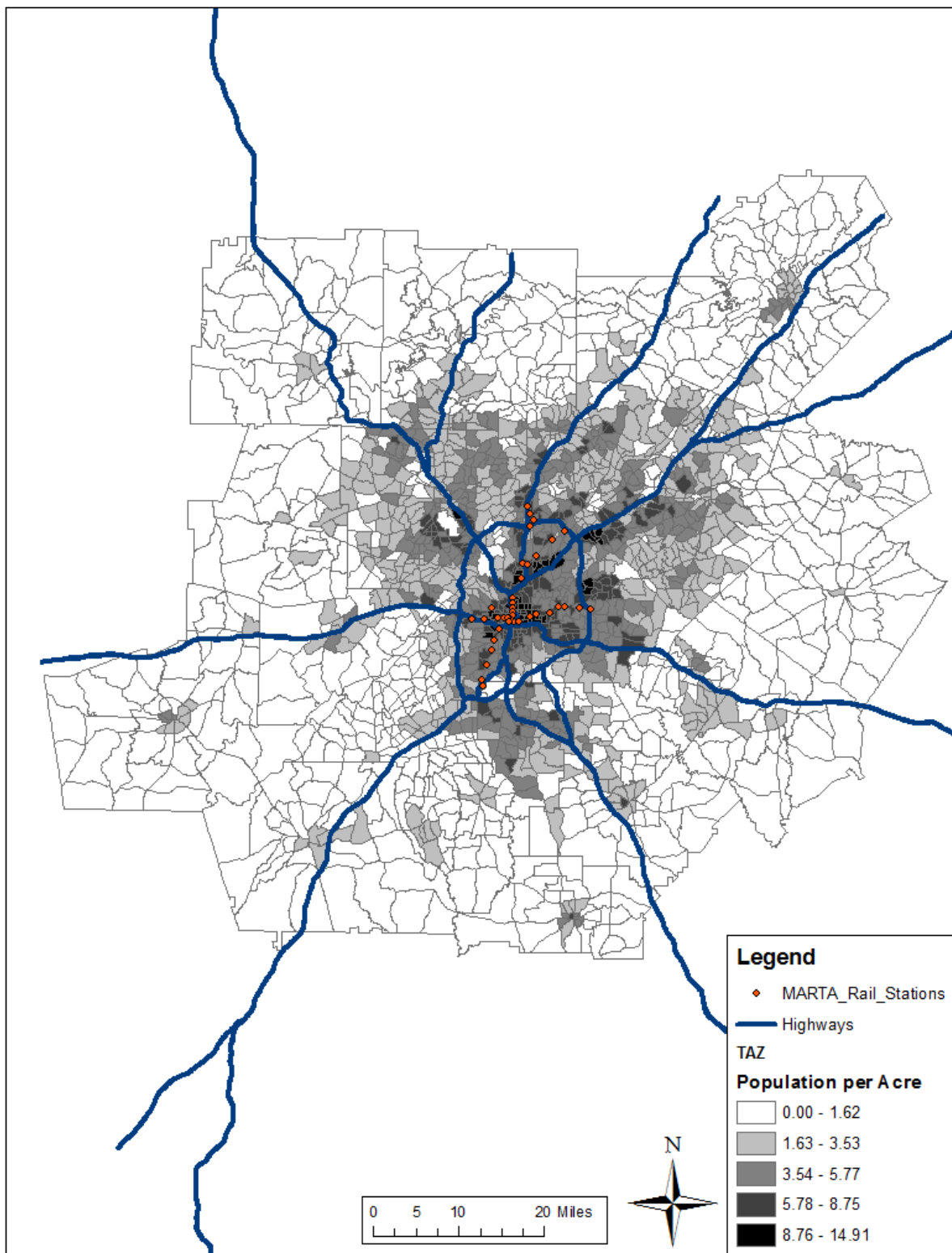


Figure 84: Map of Atlanta, GA regional population density.

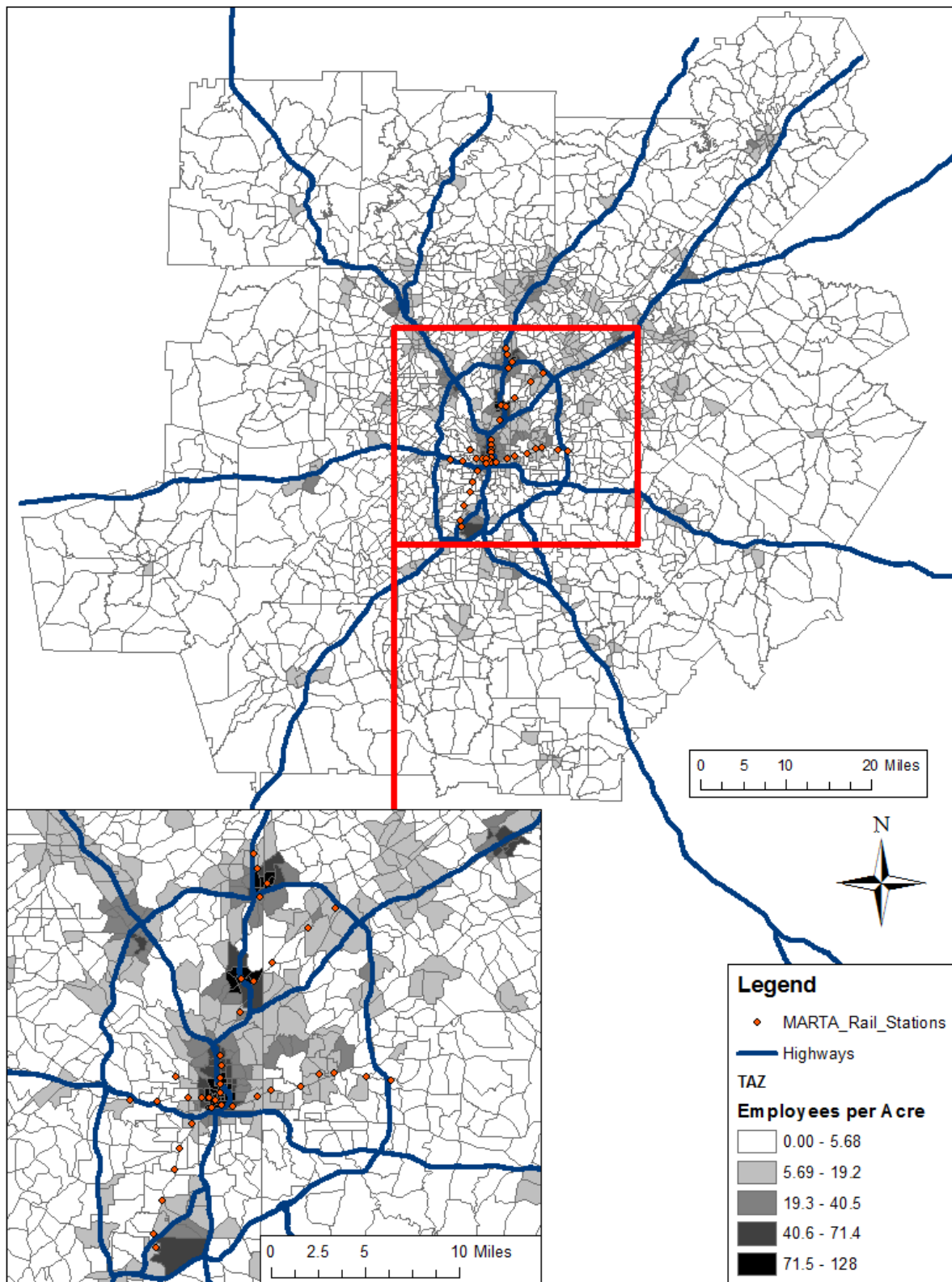


Figure 85: Map of Atlanta, GA regional employment density.

8.1.2. ARC Travel Demand Model

The application presented in this chapter utilizes model outputs from the ARC travel demand model. The ARC travel demand model is a multi-trip purpose, multi-modal, 4-step model of regional passenger travel (43). As a 4-step model it does not estimate trip tours to/from work, but rather HBW trips and NHB trips. The modes include SOV, HOV2, HOV3, HOV4, walk to local transit (W2B), walk to premium transit (W2R), drive to local transit (D2B), and drive to premium transit (D2R). Travel activity is estimated for motorized modes only – non-motorized trip productions are estimated, but are not distributed. The model utilizes a tabulated cost function for distributing trips between 2,027 TAZs in the region, and mode choice is based on a nested logit structure. The model trips are divided into 4 demographic stratifications, or market segments, of traveler types: 1) Zero automobiles in the household; 2) Number of household automobiles is less than the number of household workers; 3) Number of household automobiles is greater than or equal to the number of household workers, and household income is less than or equal to \$50,000; and 4) Number of household automobiles is greater than or equal to the number of household workers, and household income is greater than or equal to \$50,000.

The ARC travel demand model is programmed within the CUBE software environment, with additional Fortran sub-routines. The ARC travel demand model was run for the 2010 inventory of regional land use. The stratified output tables of trips, mode choice, trip distance, and travel time were converted to MATLAB mat file for use in the MATLAB script calculations of travel activity, energy consumption, and GHG emissions (see Appendix A and Appendix D).

8.1.3. Alternatives Choice Set

In this region-wide application of the calculation framework, a TAZ was included as a candidate site if it met two criteria: 1) The number of jobs in the ARC's employment categories of "Information," "Finance, Real Estate, Rental and Leasing," "Professional, Scientific and Technical," "Management of Companies," "Administrative/Waste Management," and "Public Administration" is greater than or equal to 25 (employment typically located within an office); and 2) The percentage of employment in these categories represents greater than or equal to 25 percent of total employment in the TAZ. Under these criteria, 635 out of 2027 TAZs in the model are selected as office employment locations. Figure 86 shows a map of the candidate office site TAZs in the Atlanta, GA metropolitan region. If a site were to be considered where representative employment does not exist in the model, then the employment would need to be added to the model inputs to generate new output trip tables.

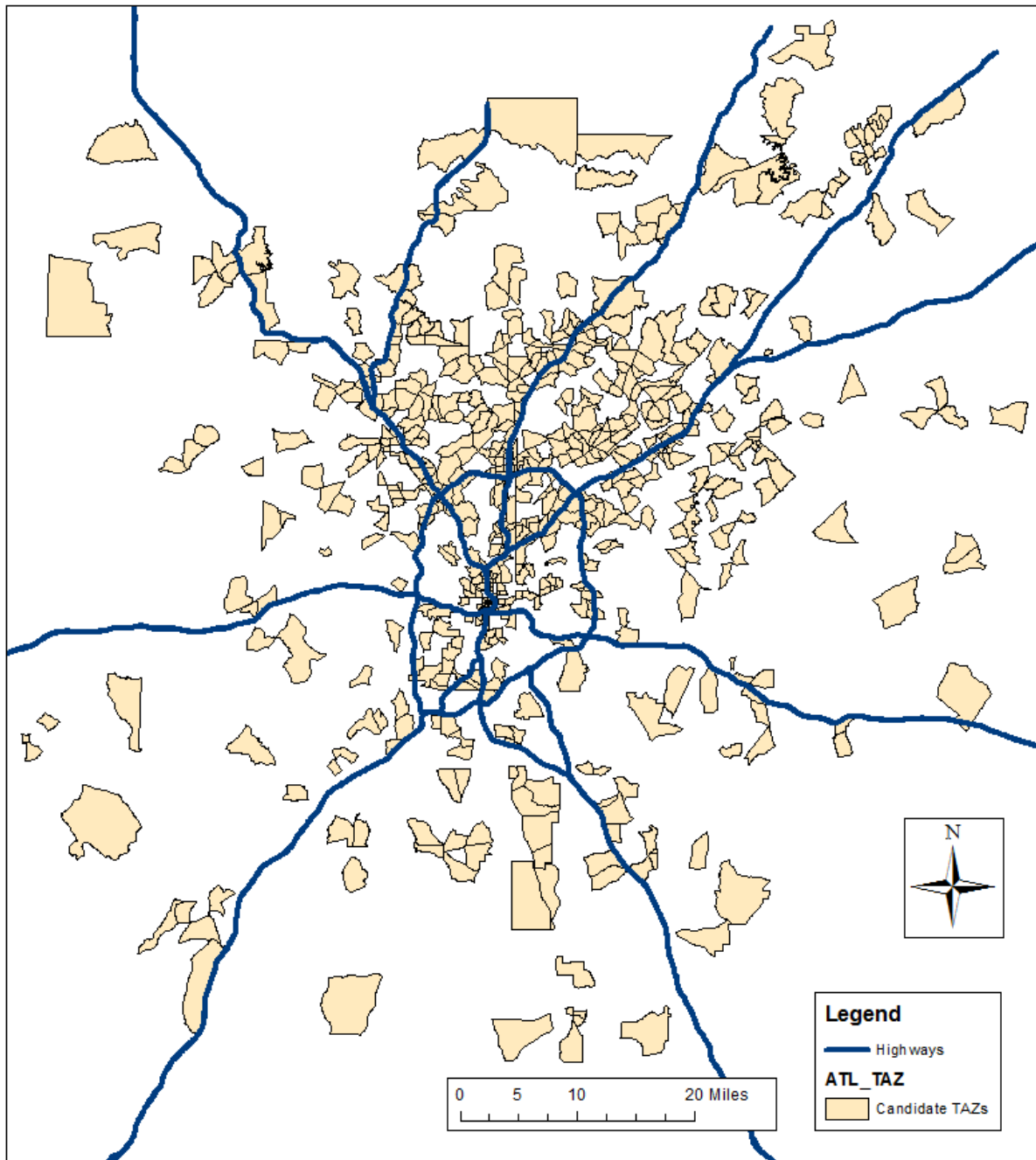


Figure 86: Map of candidate office site TAZs in Atlanta, GA metropolitan region.

8.1.3.1. Building/Site Occupancy

The estimated hourly site occupancy is assumed to be consistent between all sites and consistent with the building occupancy schedule (see Chapter 7, Table 35). The site occupancy translates into the frequency of trips taken to/from the site (see Section 8.1.5).

8.1.3.2. Stratification of Occupant Demographics

Estimation of the demographic characteristics of workers that will occupy an office site is an important step in estimating travel activity. In the application of the framework presented here, the employees are to be allocated to the demographic stratifications or market segments of the ARC travel demand model. Although office firms utilizing this framework would realistically have little or no information on the automobile ownership or household income of their employees, an approximate and consistent allocation of the site employees can be developed from the intended payroll. Table 63 below shows the estimated number of employees in each market segment of the ARC travel demand model. The subsequent travel activity calculations are performed for each stratification and aggregated for the total of 100 employees.

Table 63: Number of Employees in Each Market Segment of Travel Demand Model

Market Segment		# of Employees
1	no autos	2
2	# autos < # workers (for all income groups)	10
3	# autos >= # workers and household income < 50K	20
4	# autos >= # workers and household income >= 50K	68
Total		100

8.1.4. Motorized Vehicle Trip Reduction

Although the ARC travel demand model does not distribute non-motorized trips, there is still an opportunity to investigate the impact of non-motorized mode share for office trips. Non-motorized mode share for trips to/from the office sites represents simply a percent reduction in the motorized trips. In this application, data from the Census Transportation Planning Products (CTPP) was utilized to determine the motorized vehicle trip reduction for each TAZ.

8.1.4.1. Bike/Ped Mode Share

For some MPOs, including the Atlanta Regional Commission, the CTPP (derived from the American Community Survey) contains journey to work data down to the TAZ-level. Unfortunately, upon investigating the TAZ-level data in the CTPP, it was found that the TAZ numbers included in the CTPP for Atlanta do not match the ARC's 2010 TAZ numbering system. An attempt was made to match the CTPP's TAZ numbers to the ARC's TAZ numbers by performing a spatial join in ArcGIS between the ARC's TAZ shape file and the CTPP's TAZ shape file. However, the CTPP's TAZ shape file lacks any TAZ names in its attribute table to link the TAZ polygons with the TAZs listed in the CTPP data tables. The most fine-scale, spatial units common to both the CTPP data tables and the ARCs TAZ documentation are U.S. census tract numbers. The CTPP non-motorized trip data by census block number (Part 2, Table 2) were joined to the ARC TAZ attribute data to map the attracted non-motorized journey to work mode shares for each of the TAZs in the Atlanta, GA metropolitan region. Figure 87 through Figure 89 show the non-motorized (bike and walk) mode shares for work trips attracted to TAZs. The non-motorized mode share percentages in Figure 87 are used to reduce the total number of motorized

trips across the stratifications (TAZ-specific non-motorized mode share data from CTPP is not stratified for different demographic groups).

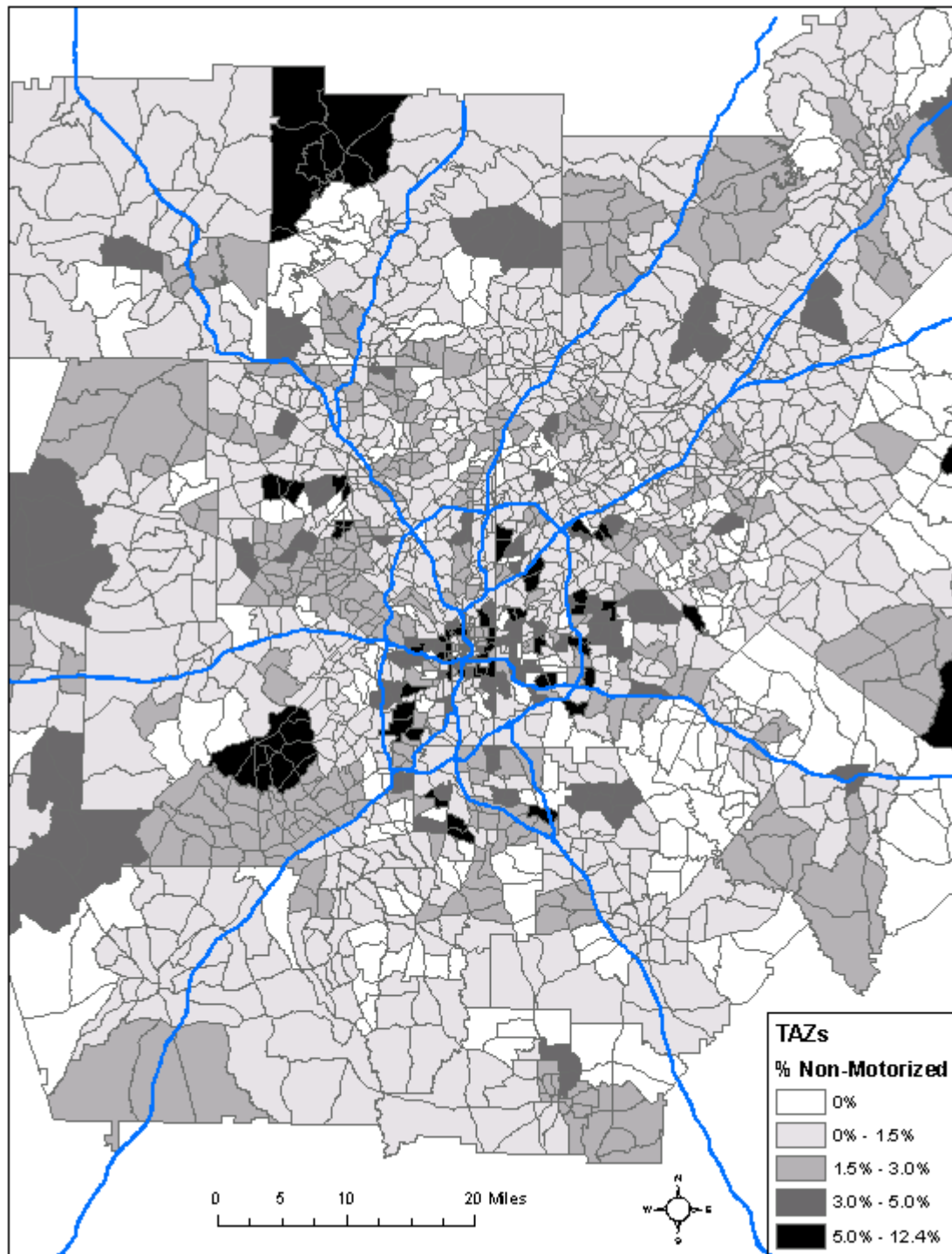


Figure 87: Non-motorized mode shares attracted to TAZs in the Atlanta, GA metropolitan region. Based on CTPP Part2, Table2 (123).

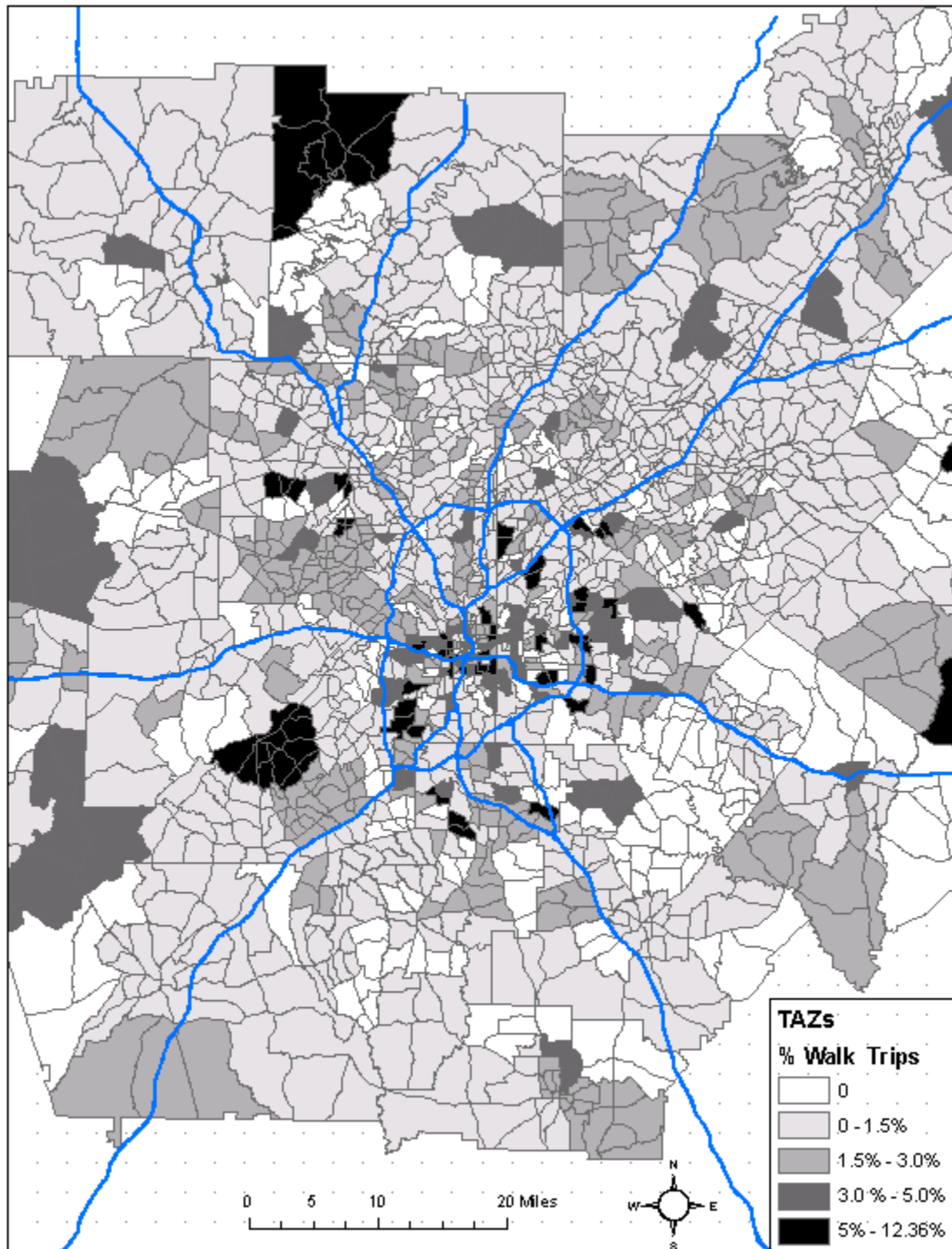


Figure 88: Walk mode shares attracted to TAZs in the Atlanta, GA metropolitan region. Based on CTTTP Part2, Table2 (I23).

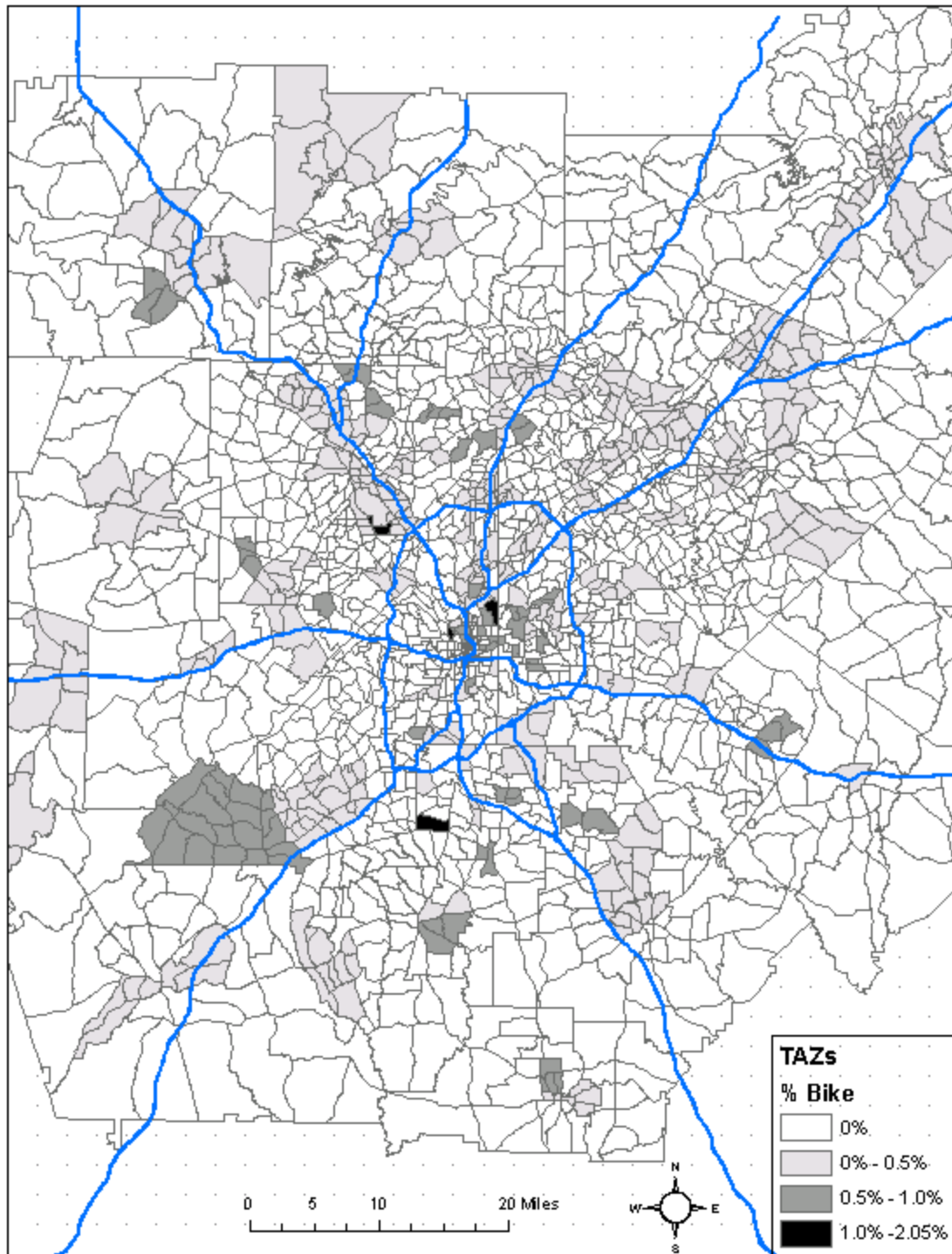


Figure 89: Bike mode shares attracted to TAZs in the Atlanta, GA metropolitan region. Based on CTP Part2, Table2 (123).

8.1.5. Annual Motorized Trip Frequency

The annual motorized trip frequency is derived from an estimate of the intended occupancy of the building/site (see Chapter 7, Table 35). Table 64 shows the time of day occupancy and the corresponding inbound/outbound commute trip schedule. The baseline trip schedule does not include any travel demand management strategies that might reduce occupancy, such as teleworking or alternative work weeks. The “Trips” columns define the number of trips taken for each day type, by time of day (peak vs. non-peak) and by direction (inbound vs. outbound). For each TAZ, the number of trips are reduced by the estimated non-motorized mode (see previous section).

Table 64: Time of Day Occupancy and Inbound/Outbound Commute Trip Schedule

Peak / Non- Peak	Period	Hour of Day		Occupancy (%)			Trips	IB/OB	Trips	IB/OB.	Trips	IB/OB
		Begin	End	Wk	Sat	Sun/ Hol						
NP	NT	12:00 AM	1:00 AM	0	0	0	5	OB	0		0	
NP	NT	1:00 AM	2:00 AM	0	0	0	0		0		0	
NP	NT	2:00 AM	3:00 AM	0	0	0	0		0		0	
NP	NT	3:00 AM	4:00 AM	0	0	0	0		0		0	
NP	NT	4:00 AM	5:00 AM	0	0	0	0		0		0	
NP	NT	5:00 AM	6:00 AM	0	0	0	0		0		0	
P	AM	6:00 AM	7:00 AM	10	10	5	10	IB	10	IB	5	IB
P	AM	7:00 AM	8:00 AM	20	10	5	10	IB	0		0	
P	AM	8:00 AM	9:00 AM	95	30	5	75	IB	20	IB	0	
P	AM	9:00 AM	10:00 AM	95	30	5	0		0		0	
NP	MD	10:00 AM	11:00 AM	95	30	5	0		0		0	
NP	MD	11:00 AM	12:00 PM	95	30	5	0		0		0	
NP	MD	12:00 PM	1:00 PM	50	10	5	-45	OB (NHB)	20	OB	0	
NP	MD	1:00 PM	2:00 PM	95	10	5	45	IB (NHB)	0		0	
NP	MD	2:00 PM	3:00 PM	95	10	5	0		0		0	
P	PM	3:00 PM	4:00 PM	95	10	5	0		0		0	
P	PM	4:00 PM	5:00 PM	95	10	5	0		0		0	
P	PM	5:00 PM	6:00 PM	30	5	5	65	OB	5	OB	0	
P	PM	6:00 PM	7:00 PM	10	5	0	20	OB	0		5	OB
NP	NT	7:00 PM	8:00 PM	10	0	0	0	OB	5	OB	0	
NP	NT	8:00 PM	9:00 PM	10	0	0	0		0		0	
NP	NT	9:00 PM	10:00 PM	10	0	0	0		0		0	
NP	NT	10:00 PM	11:00 PM	5	0	0	5	OB	0		0	
NP	NT	11:00 PM	12:00 AM	5	0	0	0		0		0	
Inbound Peak							95		0		0	
Inbound Non-Peak							0		30		5	
Outbound Peak							85		30		0	
Outbound Non-Peak							10		0		5	
# of Times per Year Trip Pattern Occurs (2010)							253		52		60	

8.1.6. Mode Choice

The mode choice of trips is determined by the stratified mode choice tables in the travel demand model (see Table D - 1 in Appendix D). For the region as a whole, the mode choice can vary significantly between demographic stratifications. Figure 90 below shows the regional

average HBW office site mode split for each of the four market segments in the ARC travel demand model. The mode splits were estimated by running the MATLAB script for each of the demographic stratifications (all 100 employees in one stratification) and for all of the 635 candidate TAZ locations. Figure 90 clearly indicates that on average across the set of candidate TAZs, SOV trips dominate the mode choice for HBW work trips in stratifications 3 and 4. This result should not be surprising, since many of the candidate TAZs are not serviced by a transit network. For the first stratification (zero household automobiles), less than half of the HBW trips are by transit modes.

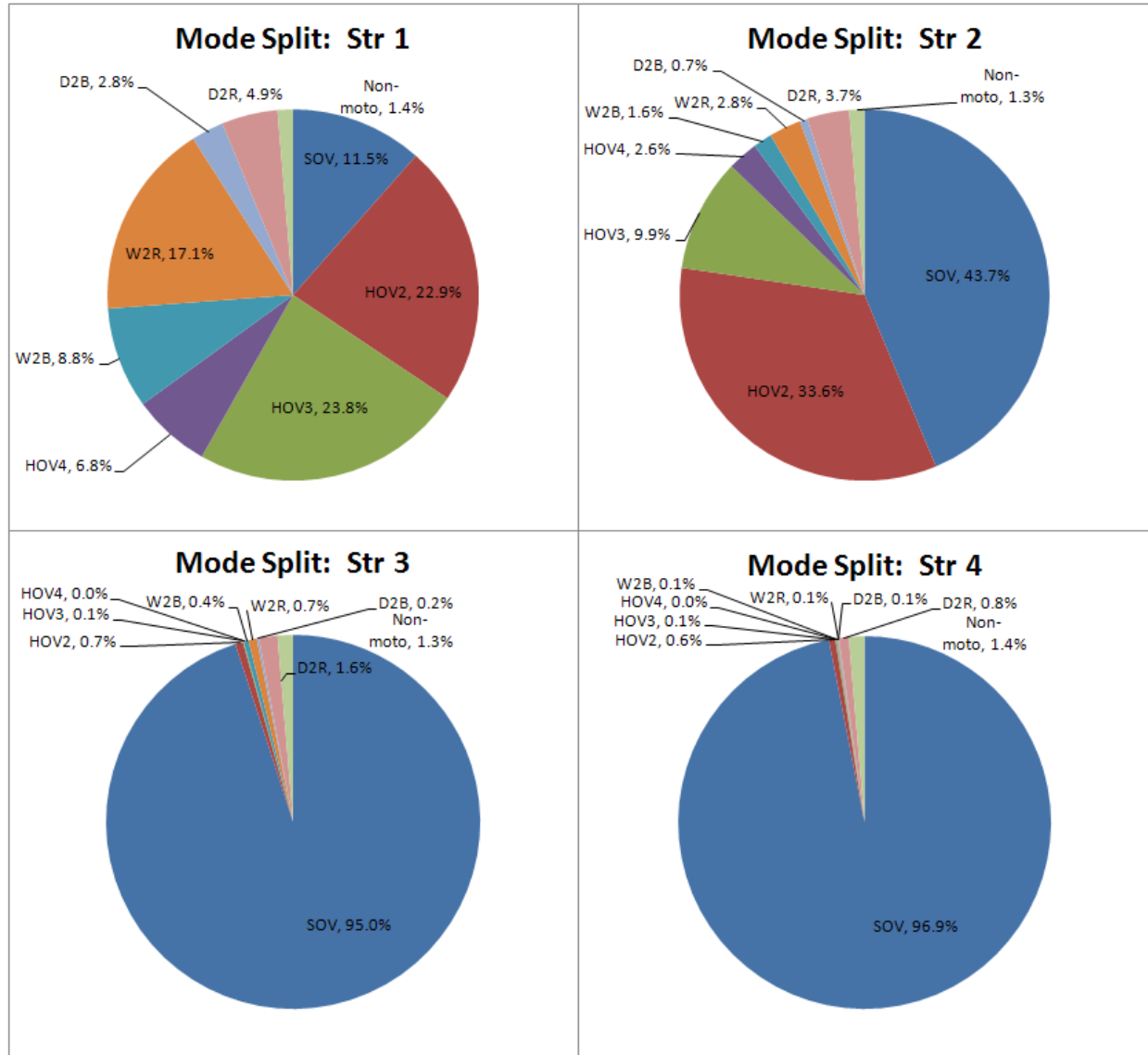


Figure 90: Regional average HBW office site mode split for each of the four market segments in the ARC travel demand model.

The regional average mode splits shown in Figure 90 are an aggregate measure of the mode splits estimated for each of the candidate TAZs. Figure 91 through Figure 94 show the HBW transit mode shares across all of the candidate TAZ locations, for each demographic stratification. In Figure 91, transit mode shares approaching or greater than 50 percent are distributed throughout much of the transit network shown in Figure 83. For many of the TAZs in

the CBD, the transit mode share is greater than 80 percent. The figures for the other three demographic stratifications show a retreat of transit mode shares to the CBD and a reduction in total CBD transit mode share as automobile ownership and household income increase. For the highest income group, the only sites that offer significant transit mode splits are in the center of the region, with transit mode splits around 30 percent. Figure 95 shows the HBW transit mode share in the candidate TAZ locations for the case study demographic profile. The concentration of significant transit mode shares (around 30 percent) in the CBD is a reflection of the case study demographic profile has 68 percent of its employees in stratification 4.

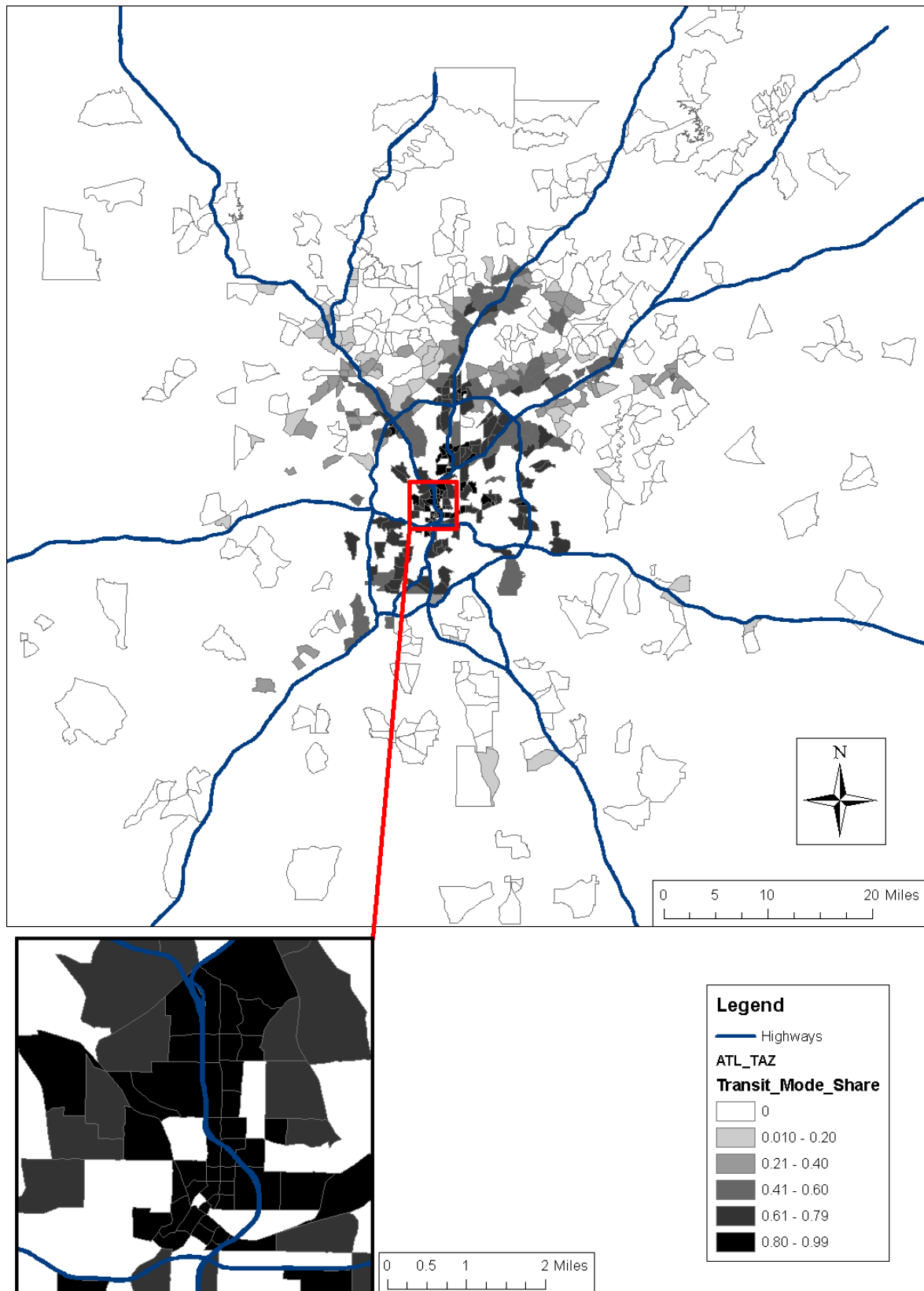


Figure 91: Map of HBW transit mode share for demographic stratification 1.

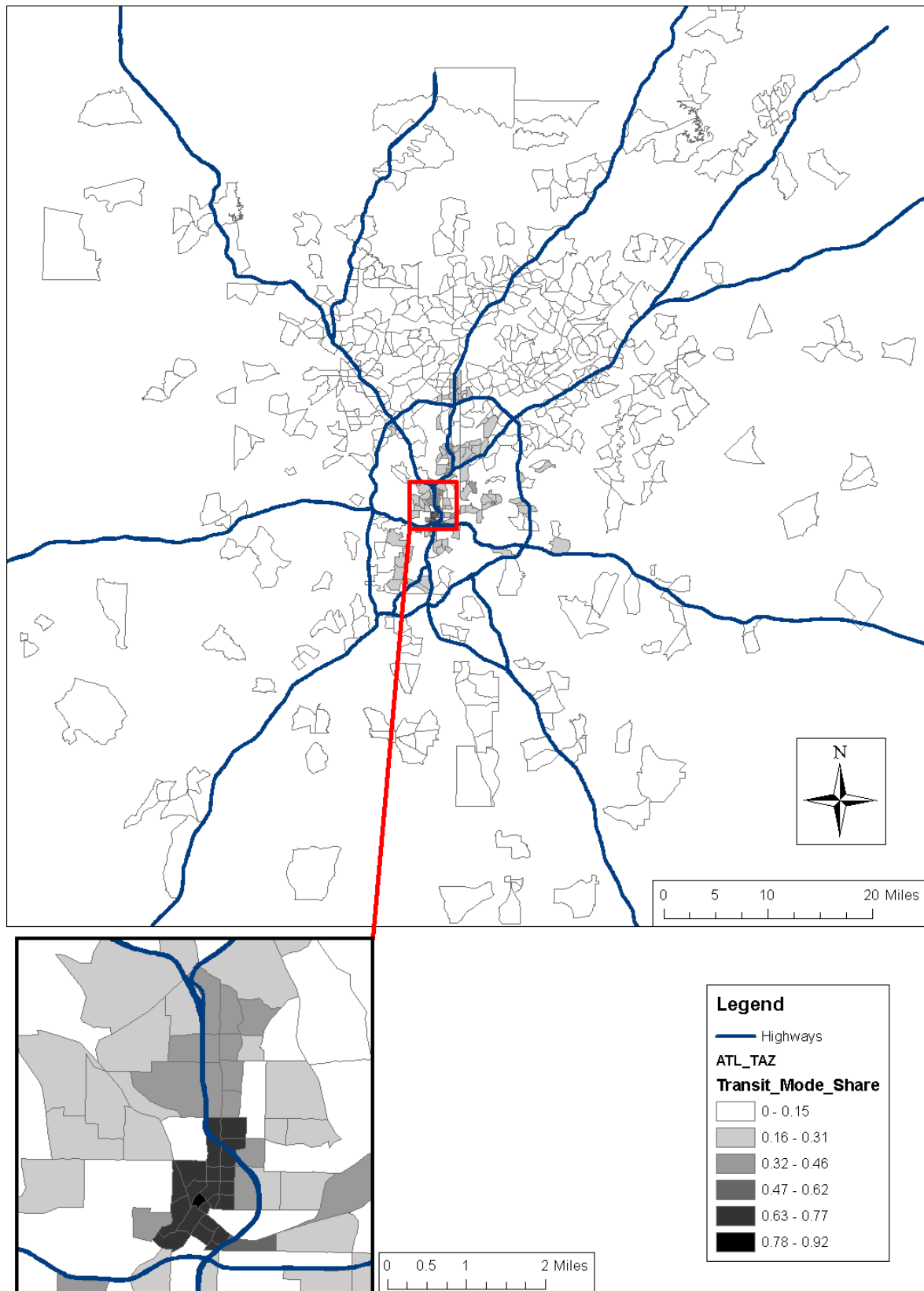


Figure 92: Map of HBW transit mode share for demographic stratification 2.

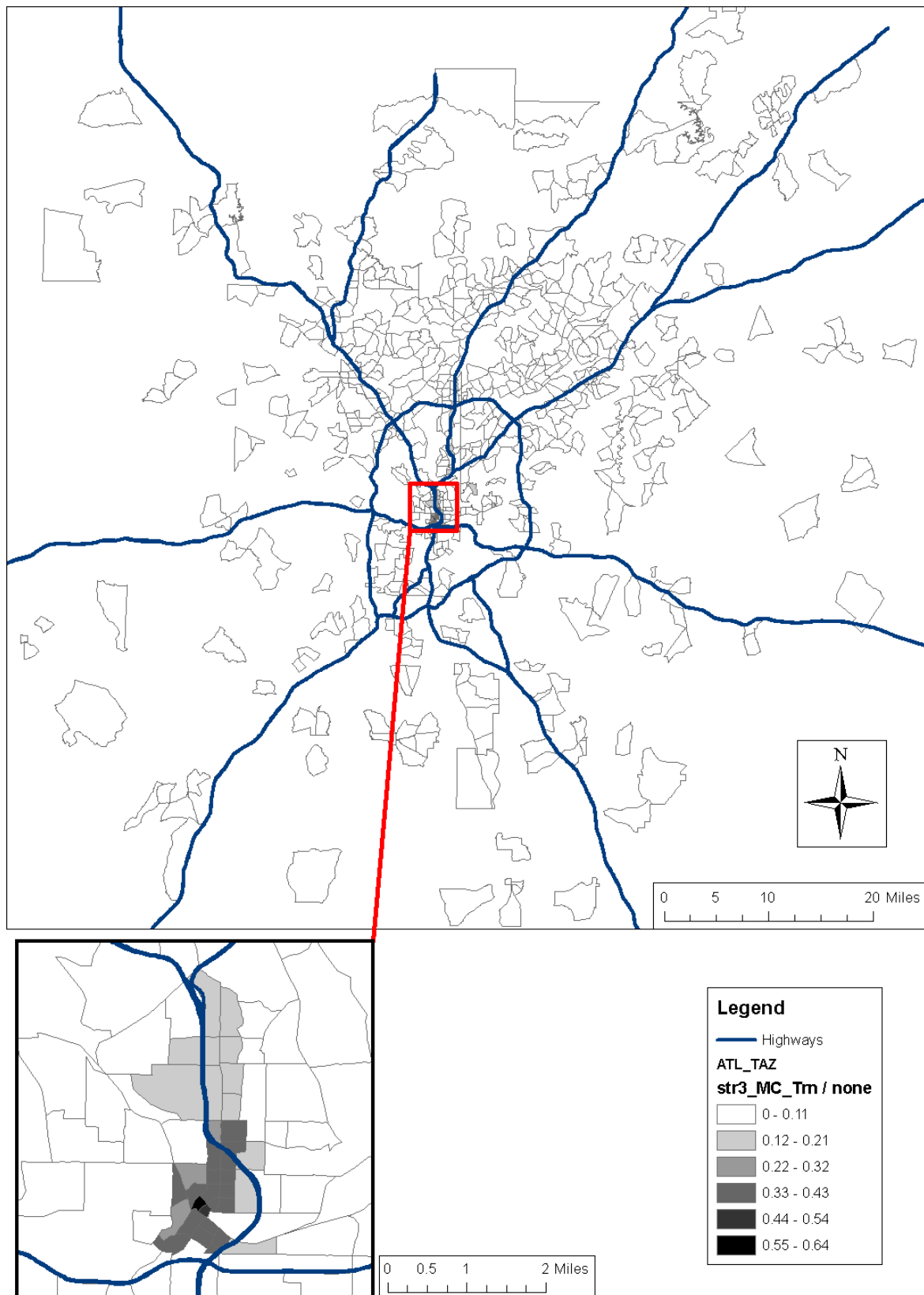


Figure 93: Map of HBW transit mode share for demographic stratification 3.

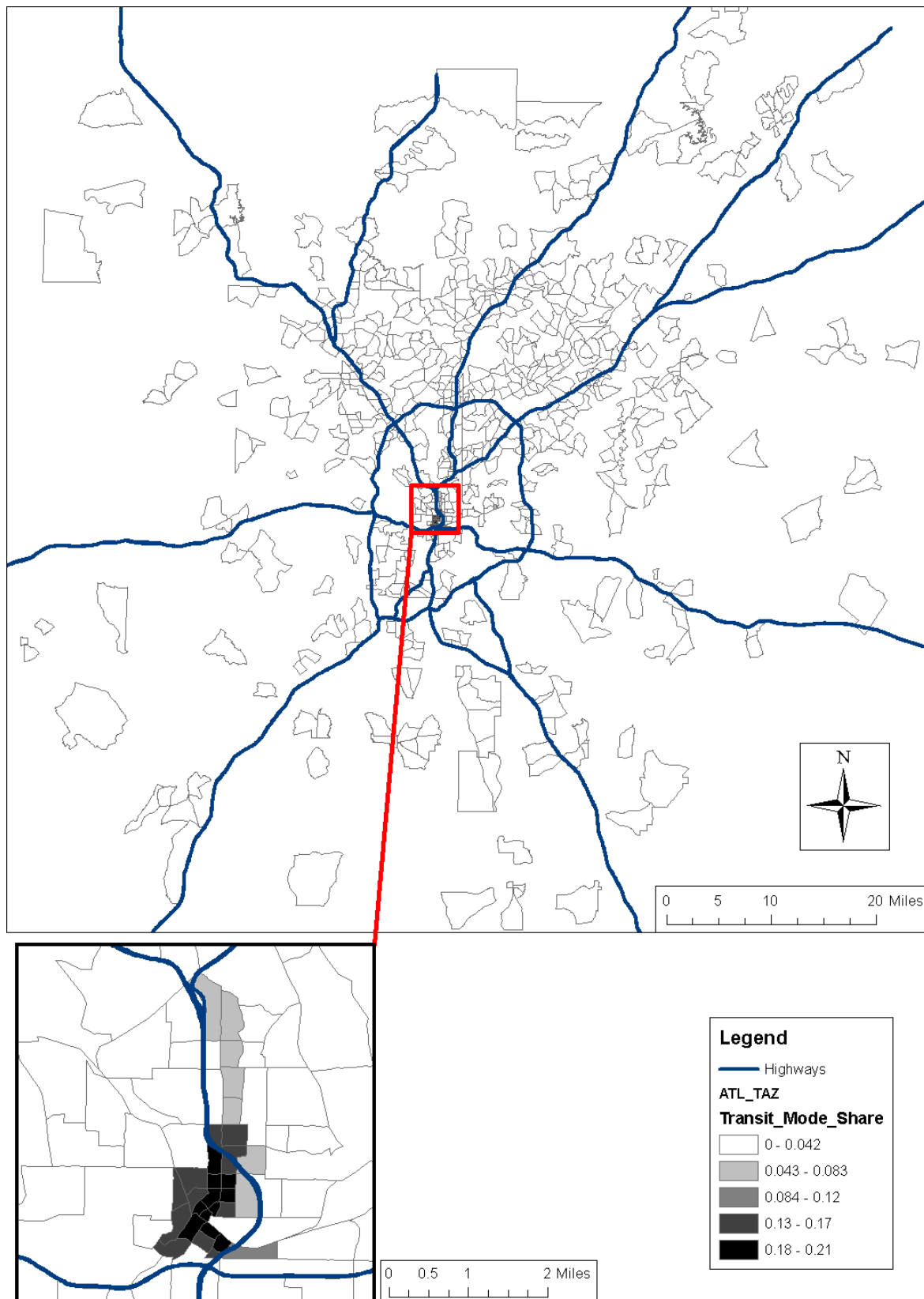


Figure 94: Map of HBW transit mode share for demographic stratification 4.

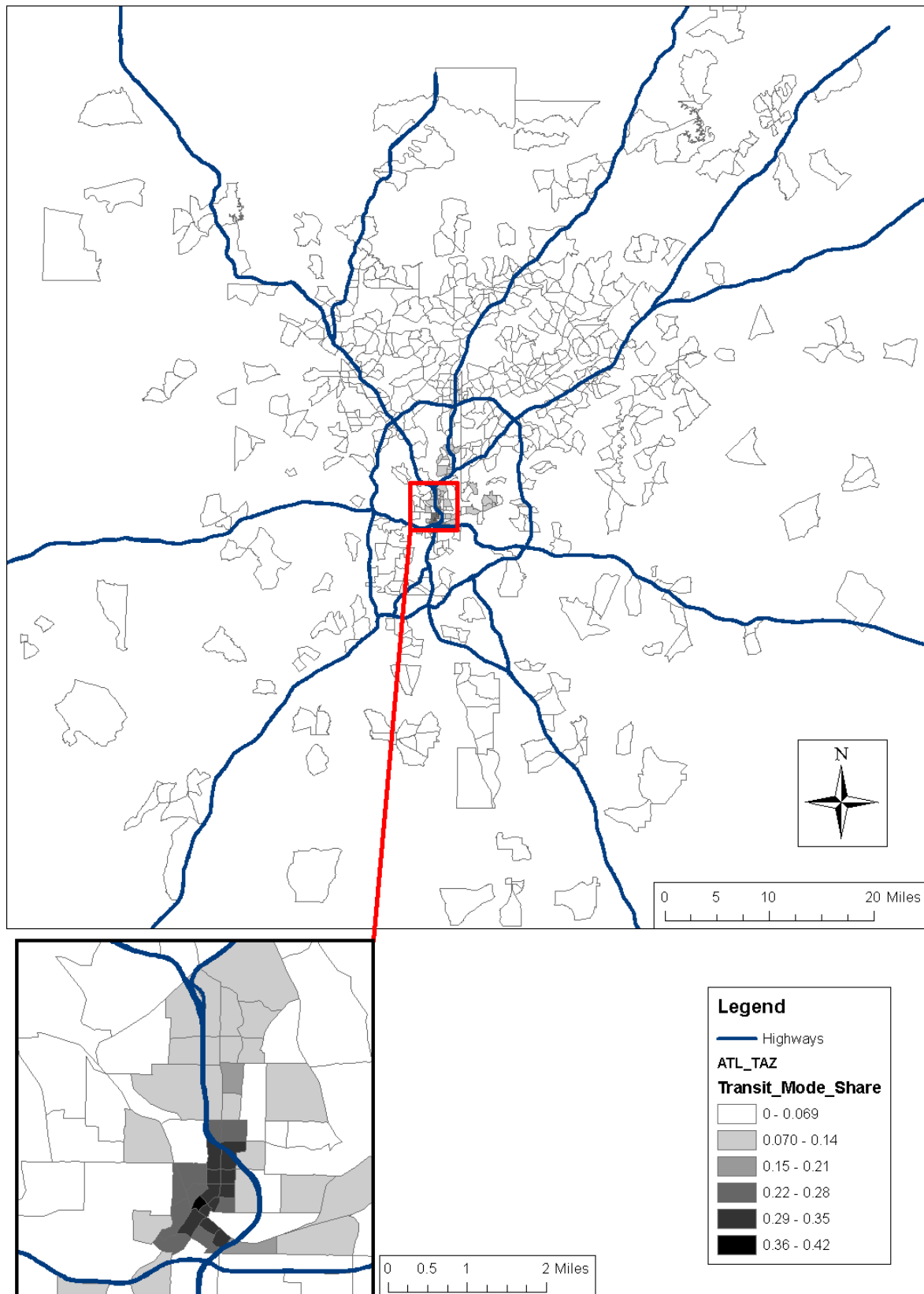


Figure 95: Map of HBW transit mode share for case study demographic profile.

8.1.7. VMT

The VMT (vehicle miles travelled) for HBW trips accessing the candidate TAZ sites is a function of the mode splits and the average trip distances; trip frequency is consistent between the candidate TAZs, save for the reduction in motorized trips by non-motorized mode access. Figure 96 shows the SOV annual HBW VMT per 100 employees for the candidate TAZs by demographic stratification (str). The very low VMT for stratification 1 is largely a reflection of the low SOV mode share within this demographic group. As one might expect, the VMT increases as automobile ownership and household income increase. The dispersion of VMT is quite considerable within stratifications 2, 3, and 4, which indicates that significant regional variations exist.

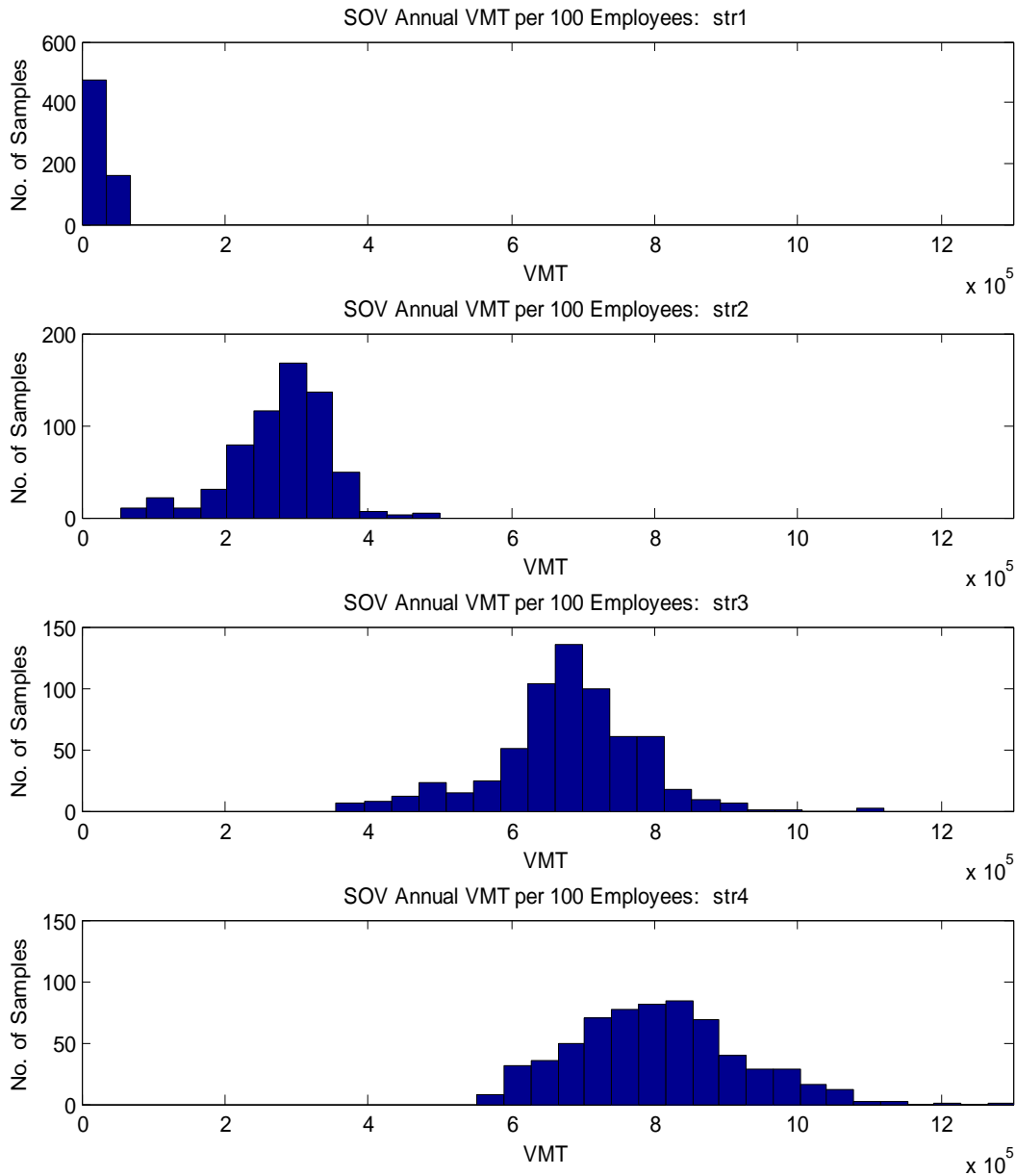


Figure 96: SOV annual HBW VMT per 100 employees for candidate TAZs by demographic stratification.

As was mentioned previously, average trip distance is the other important factor influencing estimated annual VMT. Figure 97 shows the average SOV HBW trip distance for

candidate TAZs by demographic stratification. The figure indicates that the average trip distance for stratification 1 is less than 30 percent of the average trip distance for each of the other stratifications. For the other stratifications, the average trip distance increases slightly with automobile ownership and income.

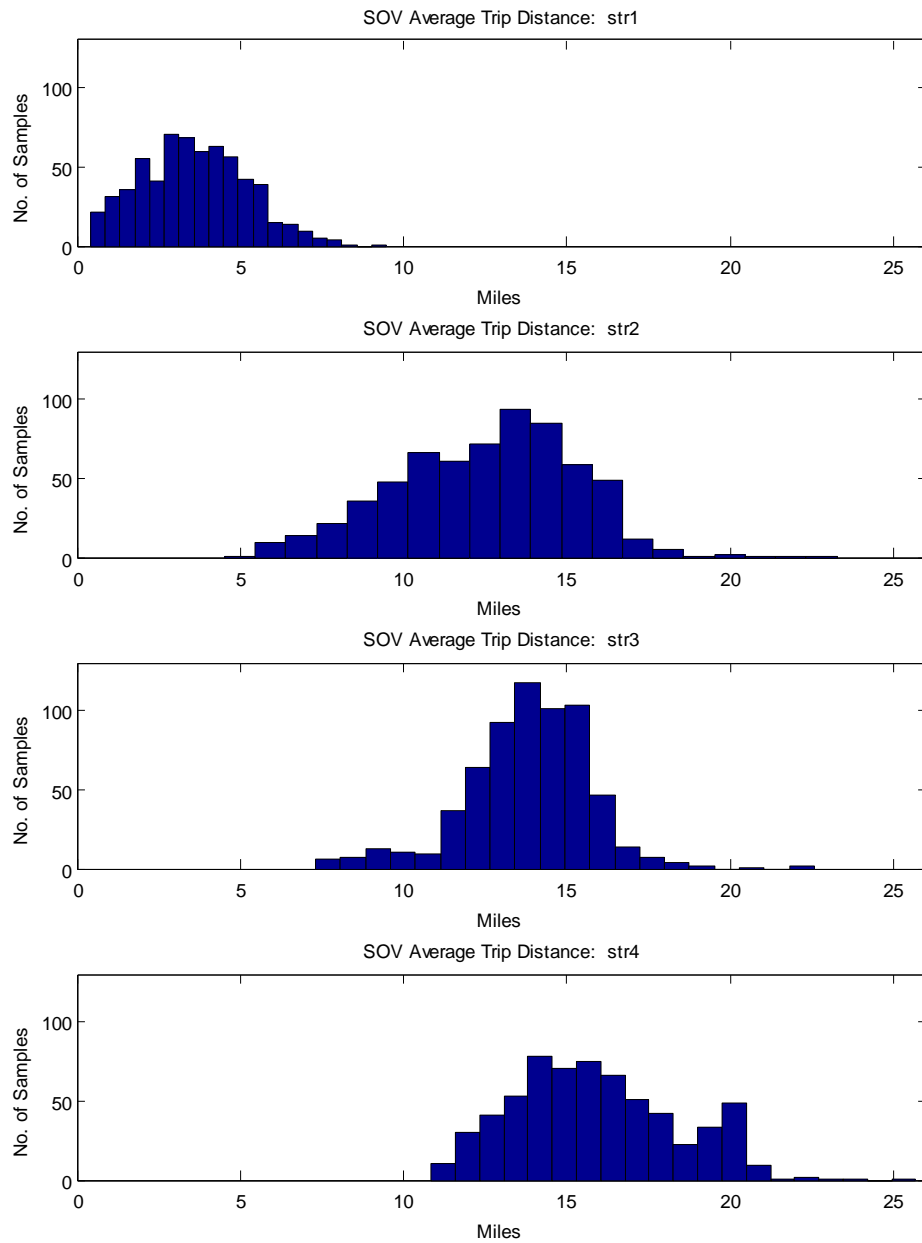


Figure 97: SOV average HBW trip distance for candidate TAZs by demographic stratification.

The spatial variation in SOV average HBW trip distance is shown for each of the demographic stratifications in Figure 98 through Figure 101. For stratification 1, many of the TAZs with the shortest average HBW trip length are within the perimeter highway (I-285). Outside of this perimeter, high and low trip lengths are scattered across the TAZs. In stratifications 1 through 3, many of the TAZs with the shortest average HBW trip length are located outside of the perimeter. It is interesting to note that for stratification 3 the northern suburbs of the region have higher trip lengths, whereas for stratification 4 the northern suburbs have lower trip lengths. The HBW trip distances are defined by the TAZs' network proximity to the residential locations (trip origins). Thus, the difference in trip lengths for stratifications 3 and 4 in the northern suburbs is a reflection of the difference in residential location for employees in these stratifications. Figure 102 shows the SOV average HBW trip distance for the case study demographic profile. Given the dominance of stratification 4 employees in the profile, the spatial variation in trip distance shown in Figure 102 is similar to that shown in Figure 101.

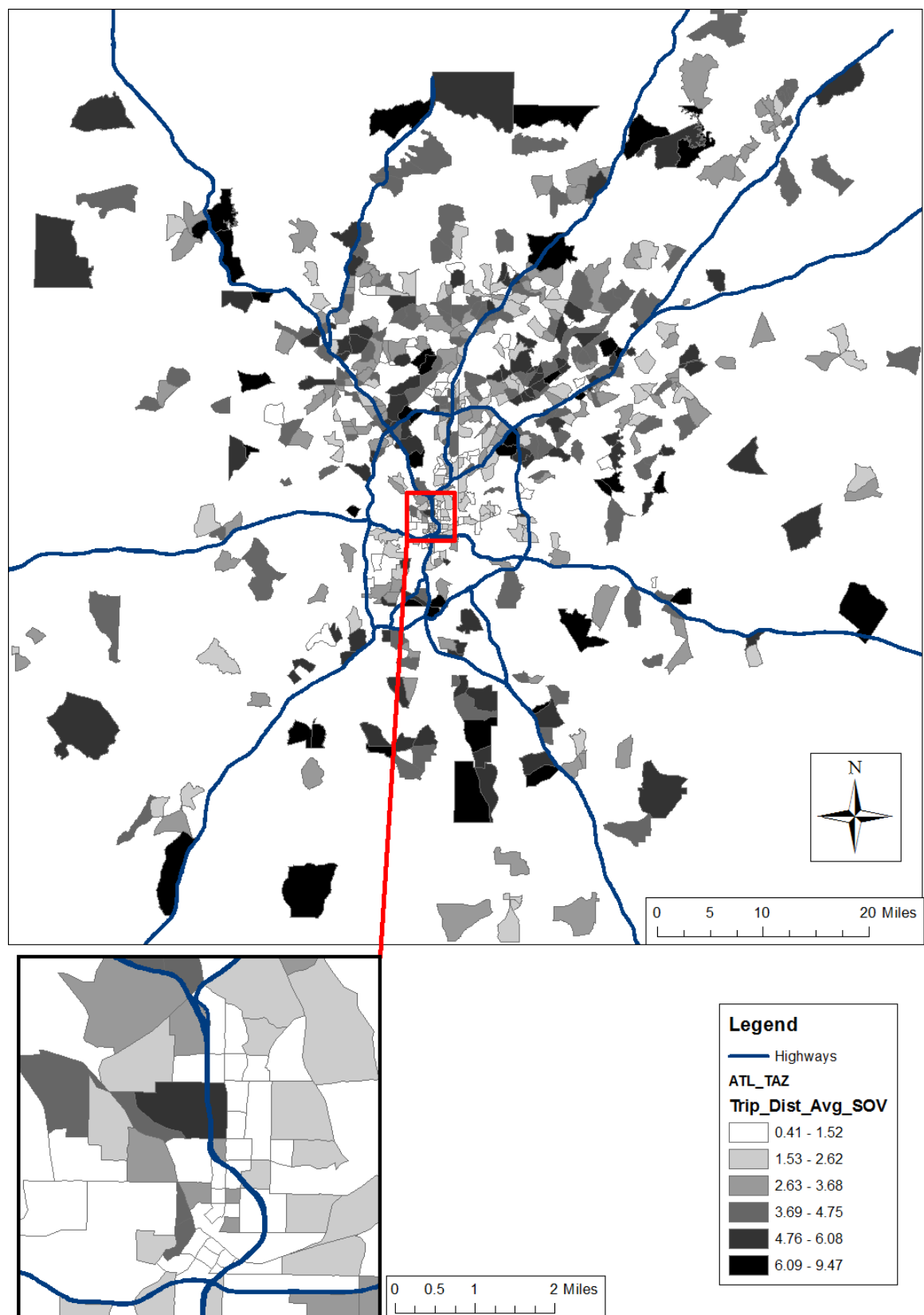


Figure 98: Map of SOV average HBW trip distance for demographic stratification 1.

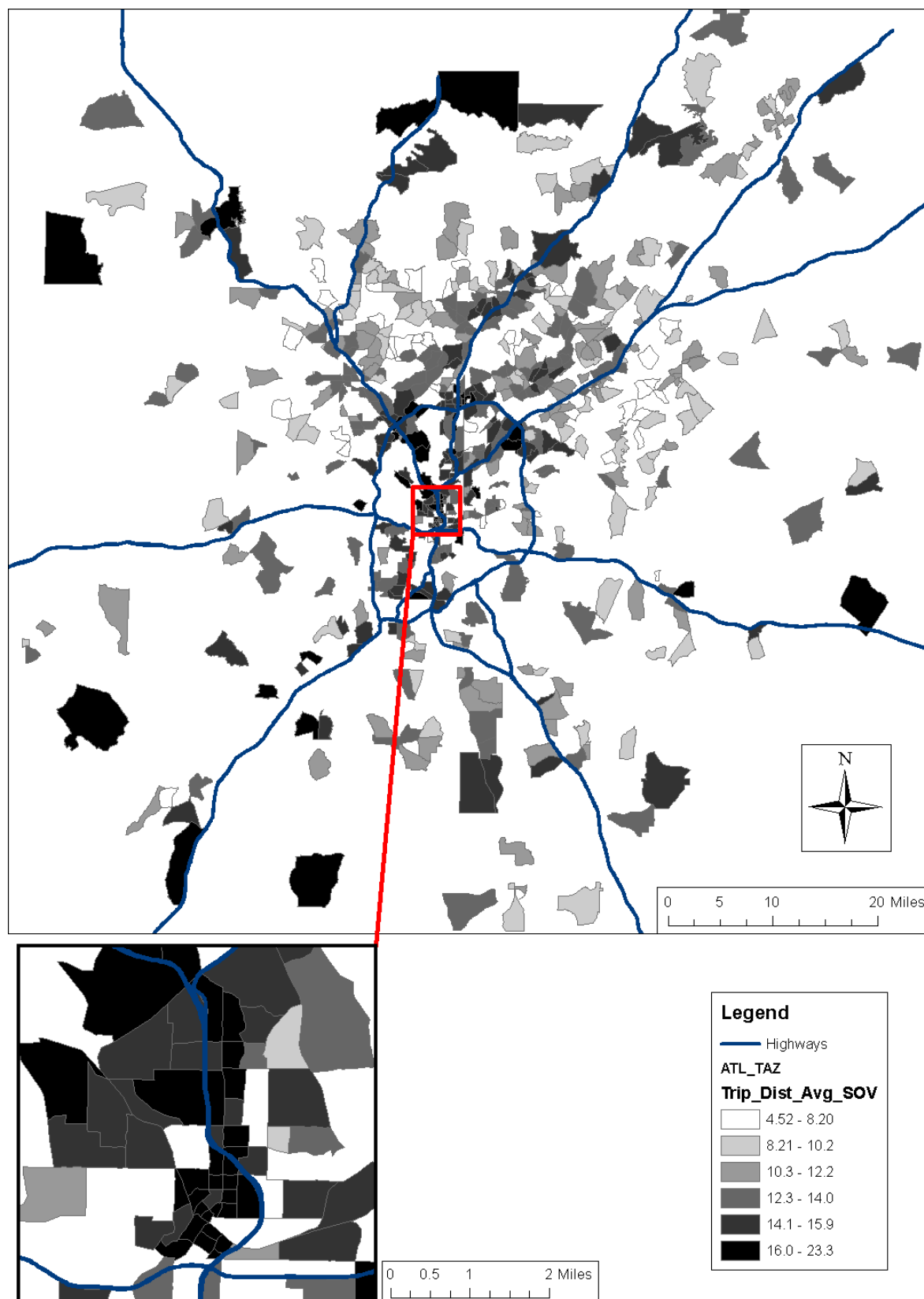


Figure 99: Map of SOV average HBW trip distance for demographic stratification 2.

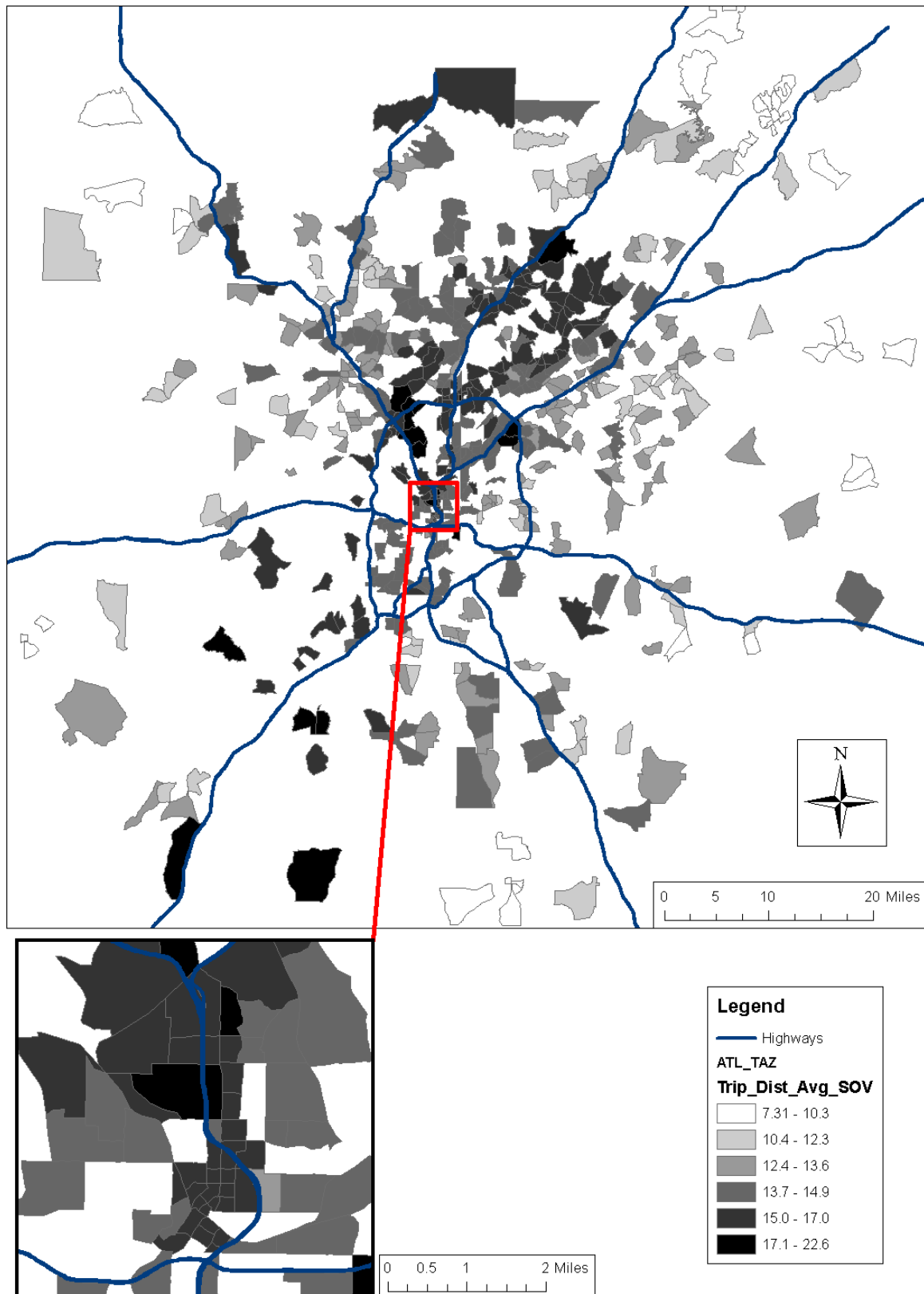


Figure 100: Map of SOV average HBW trip distance for demographic stratification 3.

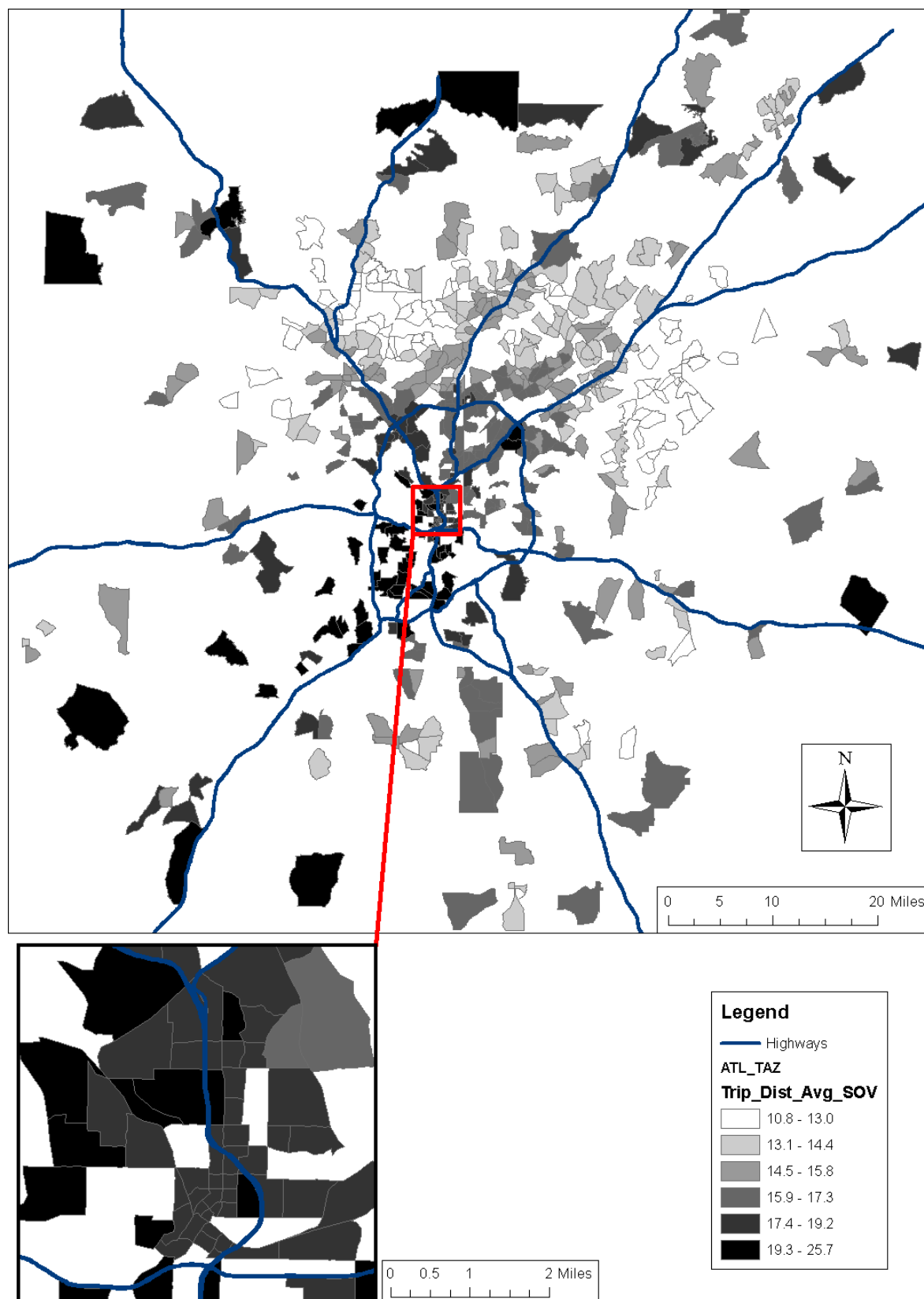


Figure 101: Map of SOV average HBW trip distance for demographic stratification 4.

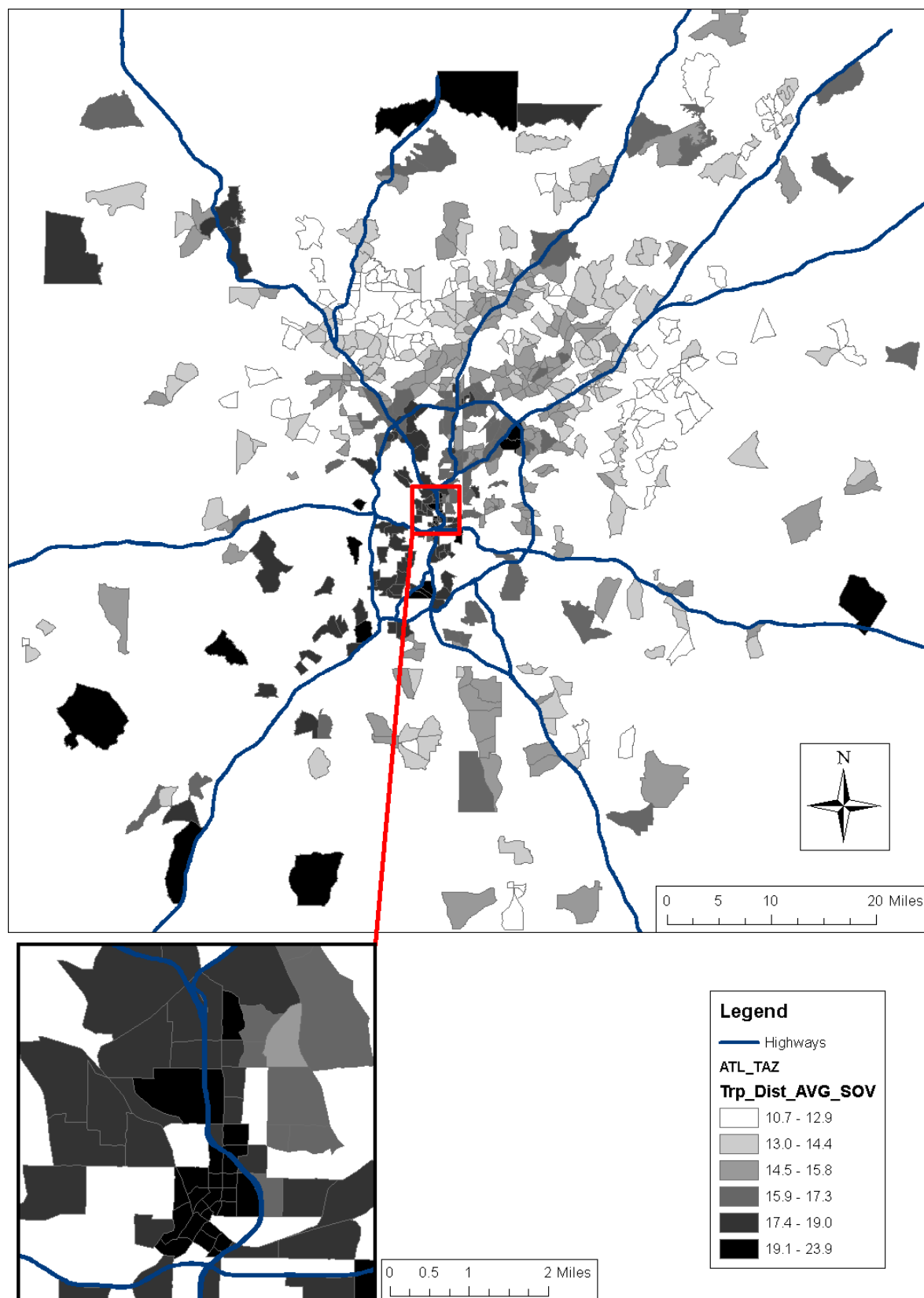


Figure 102: Map of SOV average HBW trip distance for case study demographic profile.

According to the basic formulation of the gravity model for trip attraction and distribution (see Equation 7), employment sites with higher levels of employment may attract trips from a greater distance away. If the average trip distance increases according to employment size, then it would be considerably more difficult to estimate the average trip distance for N employees located in TAZs with different levels of employment. Figure 103 shows a plot and linear regression trendline of average SOV HBW trip distance vs. total TAZ employment. The trendline indicates that the average SOV HBW trip distance is generally greater for TAZs with higher levels of employment; However, the very low coefficient of determination indicates that this relationship is considerably weak. In fact the plot shows that the TAZs with the highest average trip distance actually have some of the lowest levels of employment.



Figure 103: Average SOV HBW trip distance vs. total TAZ employment.

It is possible that the relationship between average trip distance and employment may be stronger for clusters of TAZs rather than for the region as a whole. Clusters of adjacent TAZs will likely have collectively more similar mode shares and household accessibilities than the set of all TAZs within a region. A cluster analysis is provided for the case study sites in Section 8.2.4.

8.1.8. Energy Consumption

Although the framework includes calculations of energy consumption for all modes used to access the office location, only private automobile energy consumption (SOV, HOV, and D2T) is presented here for comparison of spatial patterns in commute energy consumption. The energy consumption is expressed in Btu's per 100 employees per year. A focus on SOV + HOV + D2T energy consumption is chosen for several reasons. For a given marginal trip attractor (new employment site), SOV, HOV, and D2T commute trips represent the single largest marginal increase in transportation energy consumption among all modes. Transit commute modes generally operate on fixed schedules, thus a marginal increase in travel demand on a transit route will likely result in a negligible increase in total energy consumption. On a Btu per pax-mile basis, the energy efficiency of a transit mode will most likely increase as vehicle occupancies increase. Quantification of the SOV + HOV + D2T Btu's per 100 employees enables comparison of the relative marginal addition of commute trip energy consumption. Based on the underlying energy calculation procedure, the relative difference in SOV + HOV + D2T Btu's per 100 employees (between different office locations) is largely a function of the mode shares, the average trip distances, and the average trip speeds.

Figure 104 shows the HBW average annual SOV + HOV + D2T energy consumption per 100 employees for the candidate TAZs by demographic stratification. The figure indicates both a significant amount of dispersion within the stratifications and a progressive increase in energy consumption across the stratifications, as automobile ownership and household income increase.

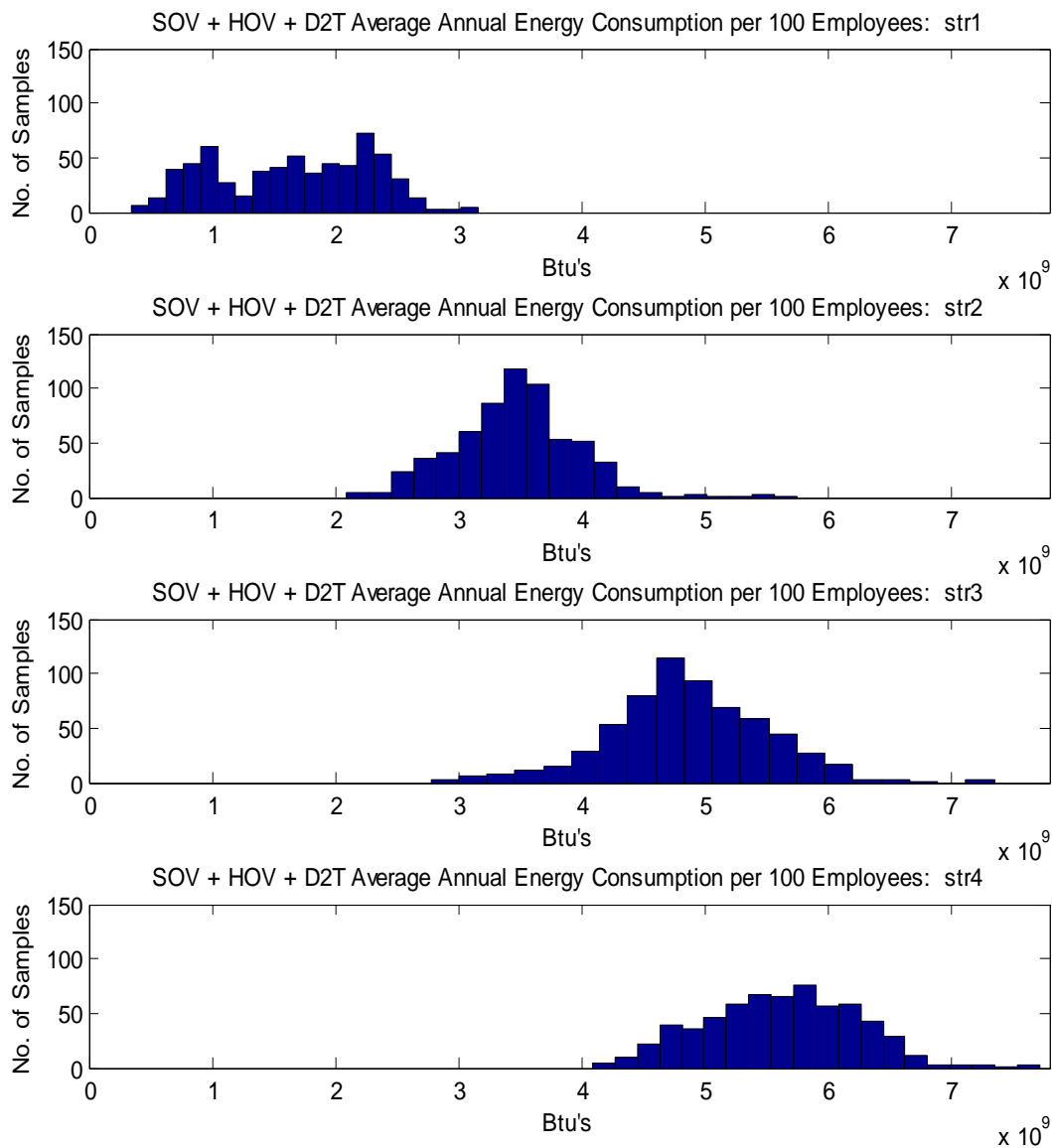


Figure 104: HBW average annual SOV + HOV + drive-to-transit energy consumption per 100 employees for candidate TAZs by demographic stratification.

The spatial variation of HBW average annual SOV + HOV + D2T energy consumption is mapped for each of the demographic stratifications in Figure 105 through Figure 108. Each of the selected TAZs in the maps display graduated shadings representing the energy consumption

relative to the regional average Btu's per 100 employees per year. Some subtle patterns of estimated annual commute energy consumption are discernable within the defined demographic stratifications. In Figure 105 it is evident that the zones with the least transportation energy consumption are located in the service area of the public transportation network (see Figure 83 and Figure 91). For stratification 1, the energy consumption increases with increasing distance from the center of the region. For stratification 2 (see Figure 106), the CBD is one of the areas supporting a relatively low level of transportation energy consumption, yet many other locations throughout the region also accommodate HBW trip efficiency. The exurban areas of the region, as well as the suburban commercial centers on the northern section of I-285 where it intersects I-75 and I-85, are shown to consume more transportation energy. Figure 107 indicates that the lowest energy consumption for HBW trips in stratification 3 are estimated for the CBD and the exurban areas. The northern suburban commercial centers and northern suburbs are associated with the highest levels of transportation energy consumption. Figure 108 shows a nearly inverse pattern of transportation energy efficiency for stratification 4. The areas appearing to have the most extensive clusters of average to below average energy consumption are the northern and eastern portions of the Atlanta suburbs. These areas contain a large proportion of the regional household population within this demographic stratification – an area where sprawl development outside of the city has occurred for several decades. Many of the TAZ's with above average commute energy consumption are found both in the exurban and central portions of the region. The occurrence of above average commute energy consumption in the exurban areas is consistent with the preeminent observations in the literature of higher transportation energy consumption in areas of low density, low land-use mix, and few alternative modes of transportation. In apparent contrast with this concept of transportation efficiency are the

estimated above average levels of energy consumption found in the CBD of the region. In the CBD, alternative mode shares are relatively higher than those in exurban and suburban areas, but many of the alternative mode commute trips are drive to transit trips that include private automobile VMT. Furthermore, the CBD TAZs are located further from the main bedroom communities of the region than are many of the suburban TAZs. Thus, the average commute distances for suburban TAZs are less than the average SOV commute distances for CBD TAZs. From a land-use planning perspective, Figure 108 indicates an opportunity for marginal improvement in commute energy consumption performance by locating new office employment for a particular socio-demographic market segment closer to residential development, thereby increasing land-use diversity and improving jobs/housing balance.

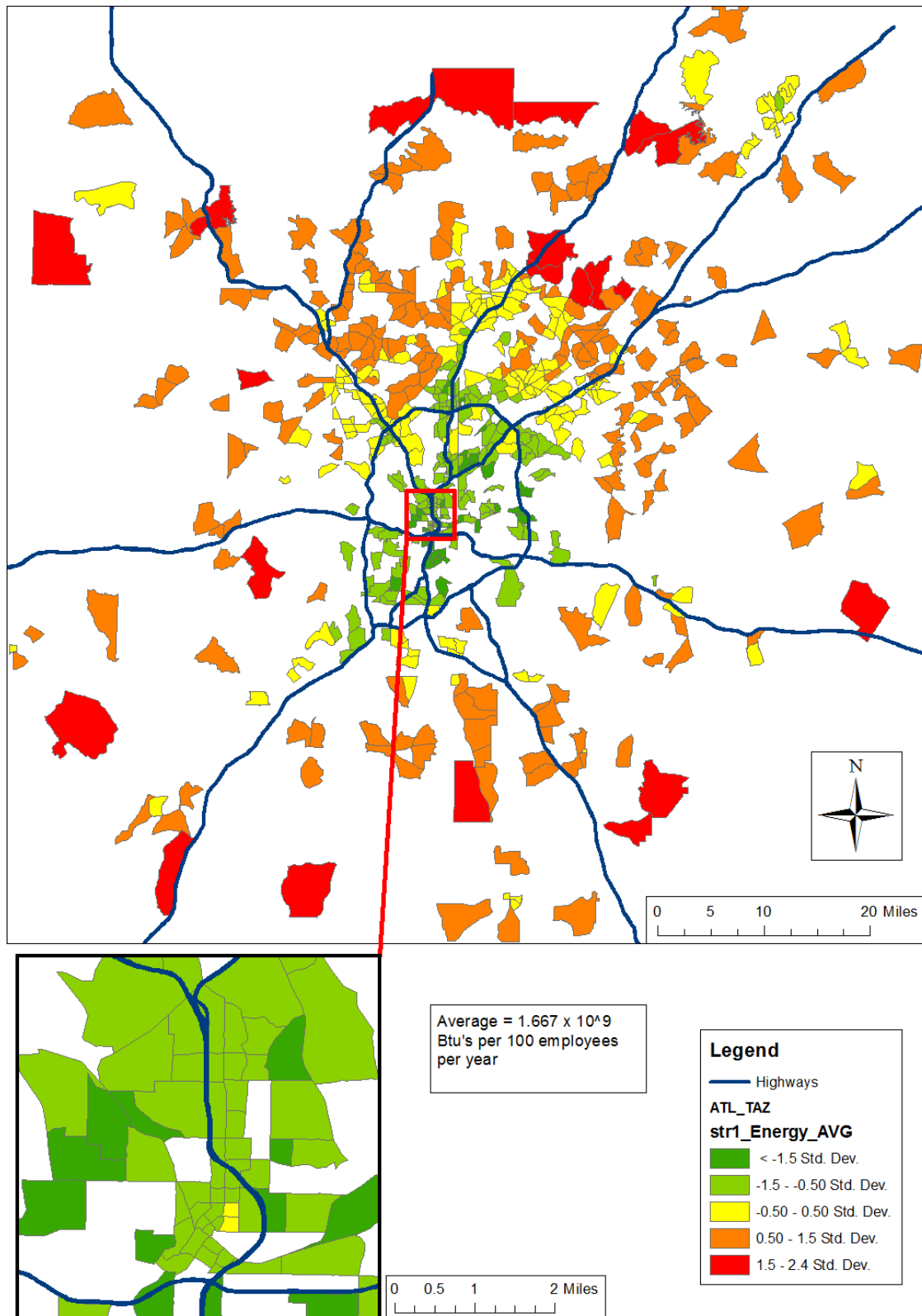


Figure 105: Map of HBW average annual SOV + HOV + drive-to-transit relative energy consumption per 100 employees for demographic stratification 1.

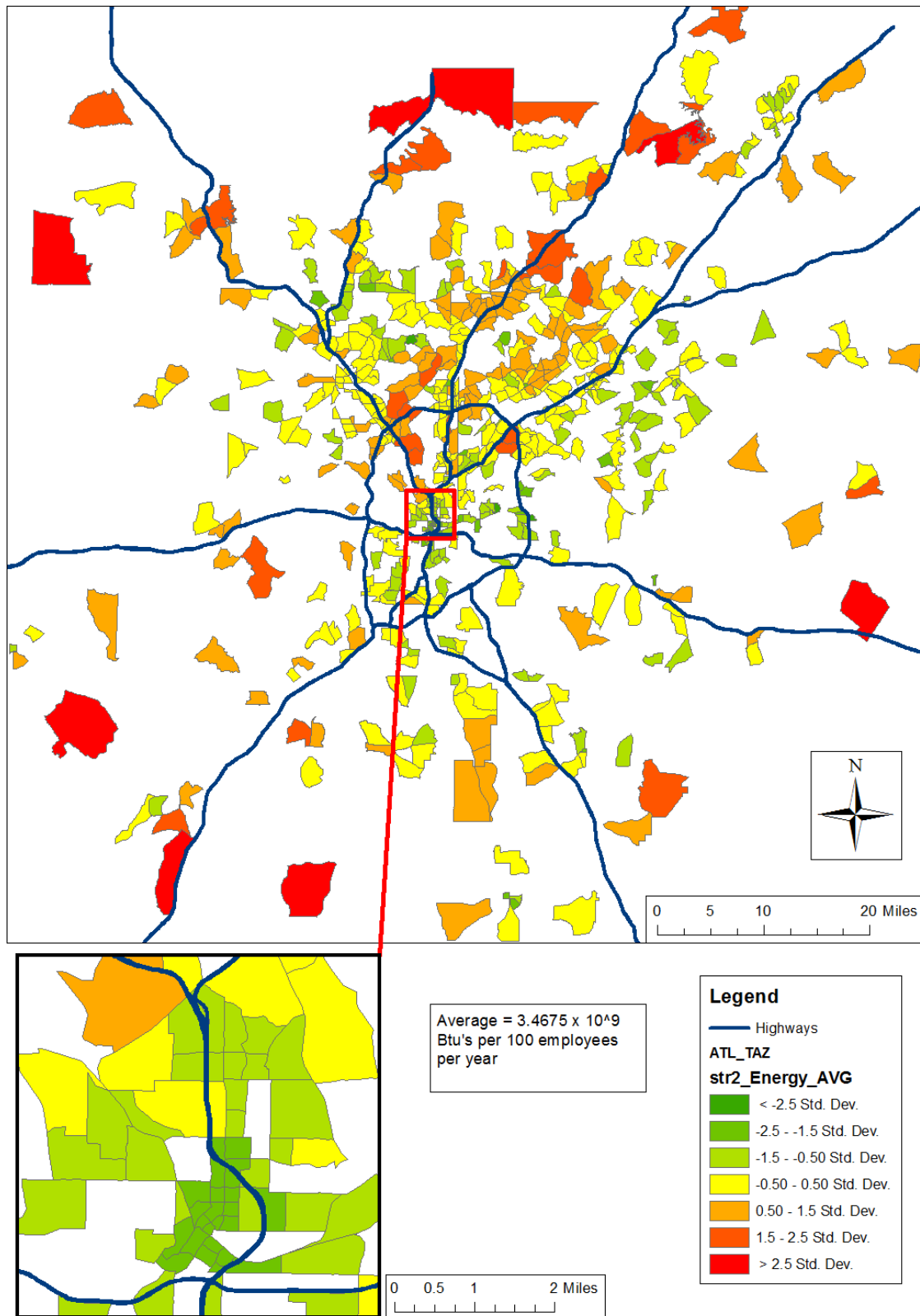


Figure 106: Map of HBW average annual SOV + HOV + drive-to-transit relative energy consumption per 100 employees for demographic stratification 2.

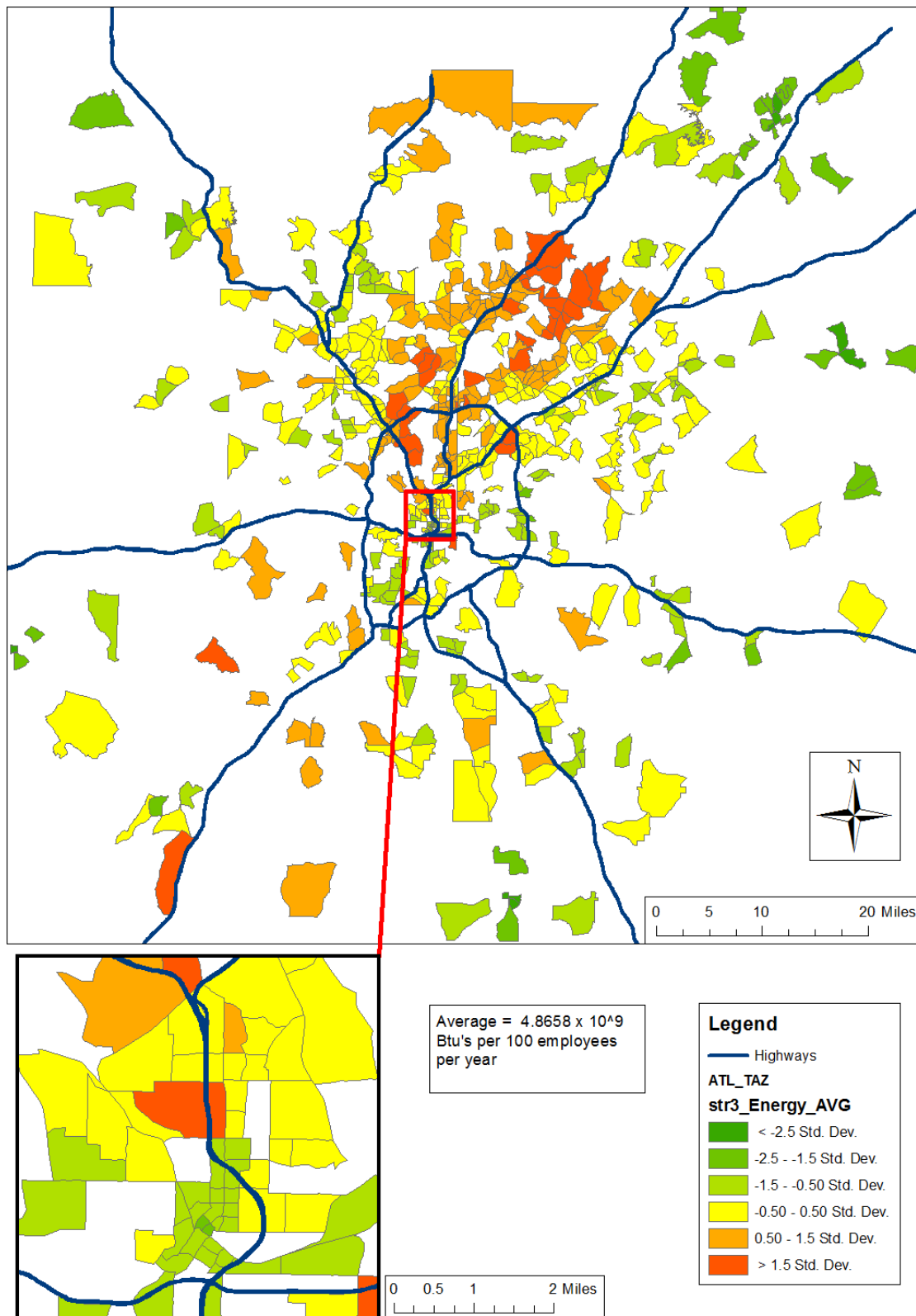


Figure 107: Map of HBW average annual SOV + HOV + drive-to-transit relative energy consumption per 100 employees for demographic stratification 3.

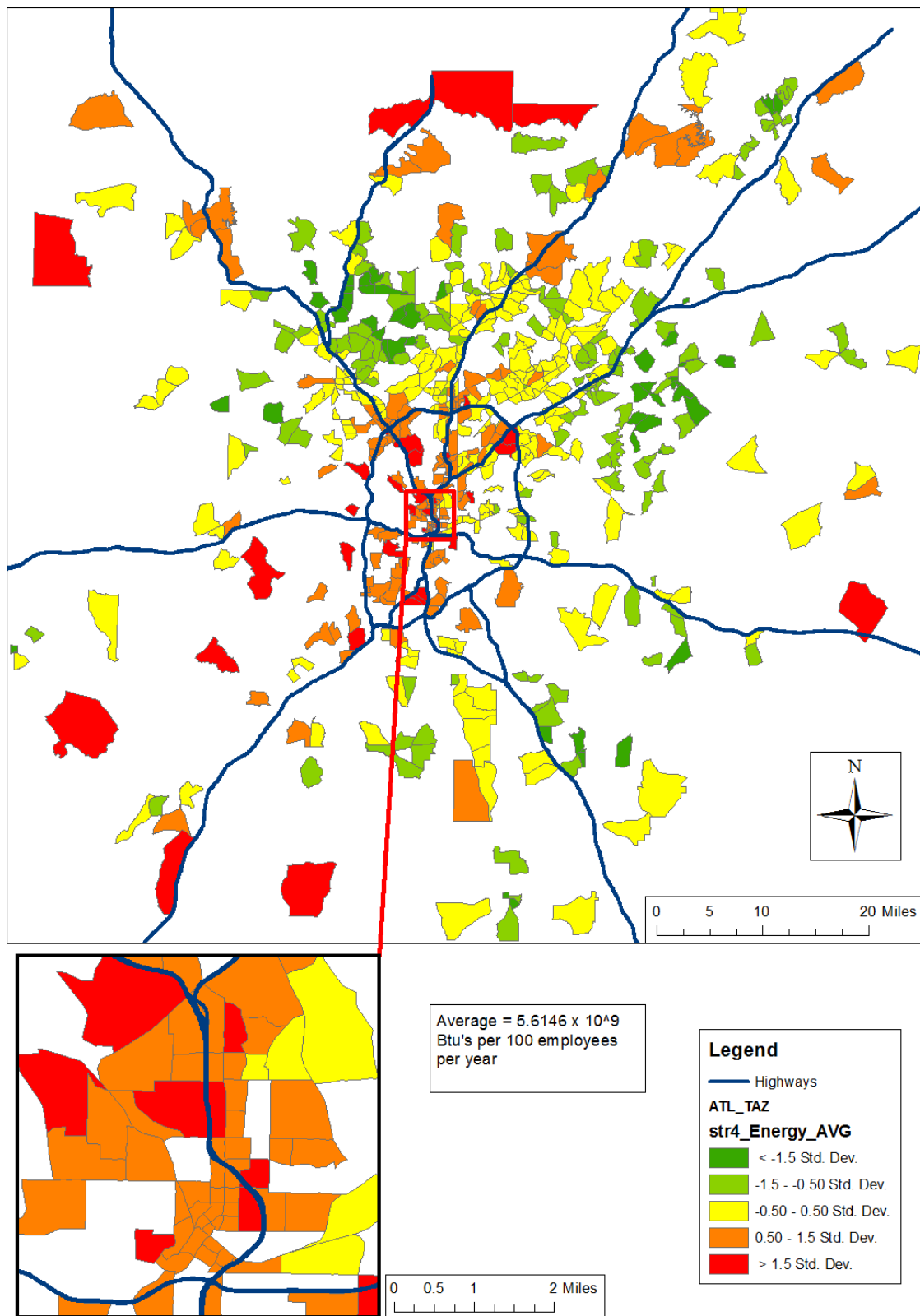


Figure 108: Map of HBW average annual SOV + HOV + drive-to-transit relative energy consumption per 100 employees for demographic stratification 4.

The spatial variation in HBW transportation energy consumption among the candidate TAZs for the case study demographic profile is shown in Figure 109. The results shown in the figure are similar to those shown for stratification 4. As with the results shown in the previous sections, this similarity is not surprising given the dominance of stratification 4 in the case study demographic profile. The results shown in Figure 109 can serve as a useful survey of potential sites that offer the best transportation energy efficiency. The results show spatial variation in estimated average transportation energy consumption for a large number of potential sites, but they do not indicate the dispersion of estimated energy consumption for each site. The application of the framework to case study sites in Section 8.2 includes quantification of the dispersion in estimated transportation energy consumption for each site.

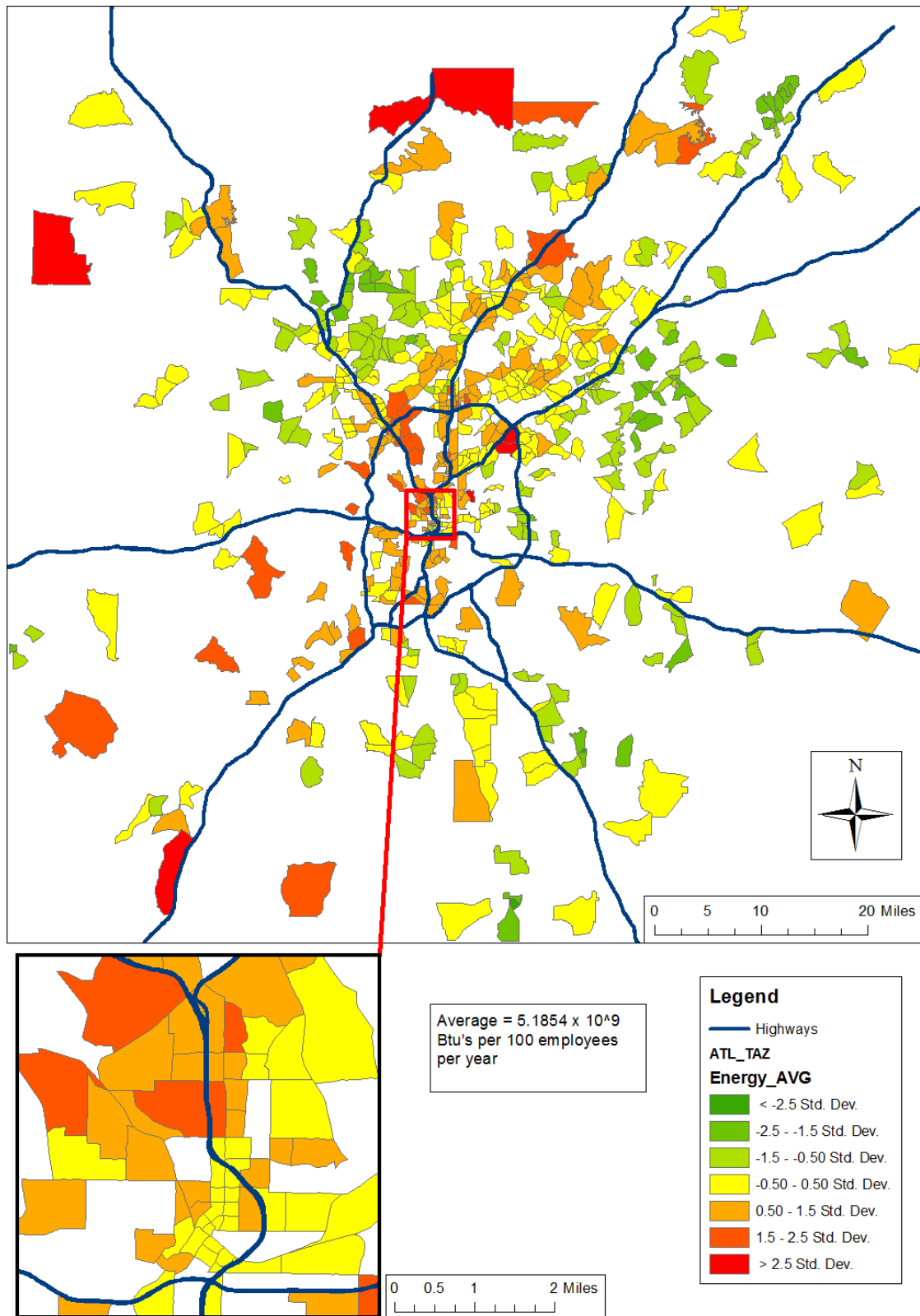


Figure 109: Map of HBW average annual SOV + HOV + drive-to-transit relative energy consumption per 100 employees for case study demographic profile.

The GHG emissions produced from the HBW trips is proportional to the energy consumption indicated in the preceding figures. The type of energy (motor vehicle gasoline) consumed for private automobile HBW trips is assumed to be consistent for each of the TAZs in the region. Therefore, the dispersion and pattern of transportation GHG emissions across the different TAZs follows the same dispersion and pattern shown for the estimated transportation energy consumption.

8.2. Site Selection Scenario

This section presents and discusses the application of the transportation evaluation framework to an office tenant site selection scenario. The selection scenario is a particular example of the general conditions outlined in Sections 3.4.2 and 6.2.1, and the scenario is consistent with the building case studies described in Section 7.1.1. The site selection scenario consists of four potential new regional locations (case studies) for an office firm. The energy consumption and GHG emission calculation procedures are applied to the four locations to determine the relative performance of the sites under uncertainty in travel behavior. The transportation calculations are performed for both HBW and NHB trips, and the energy and emissions are estimated for both direct fuel consumption and upstream fuel-energy processes. The estimated effect of employer-based travel demand management strategies are included to help determine how the relative performance of the sites may change. The energy calculations presented in this section are based on the baseline calculations presented in Section 8.1

8.2.1. Alternatives Choice Set

The choice set of location alternatives consists of four sites selected from among the “candidate” sites presented in Section 8.1.3. The locations of these sites are shown in Figure 110 below. Each of the locations shown in Figure 110 corresponds with a TAZ in the ARC regional travel demand model. These four sites were chosen to explore differences in performance between sites with unique transportation network and land-use contexts. The choice set of four location alternatives and their associated contexts/characteristics are shown in Table 65. Case Studies I and II are located in a suburban land-use context and represent sites with high and low average HBW SOV trip distance. Case Studies III and IV are located in a more urban land-use context and represent sites with high and low public transit mode shares. The mode shares and trip distances shown in Table 65 are based on the ARC travel demand model calculations presented in Section 8.1. Thus, the demographics for this set of office location case studies are based on the demographic profile shown in Table 63.

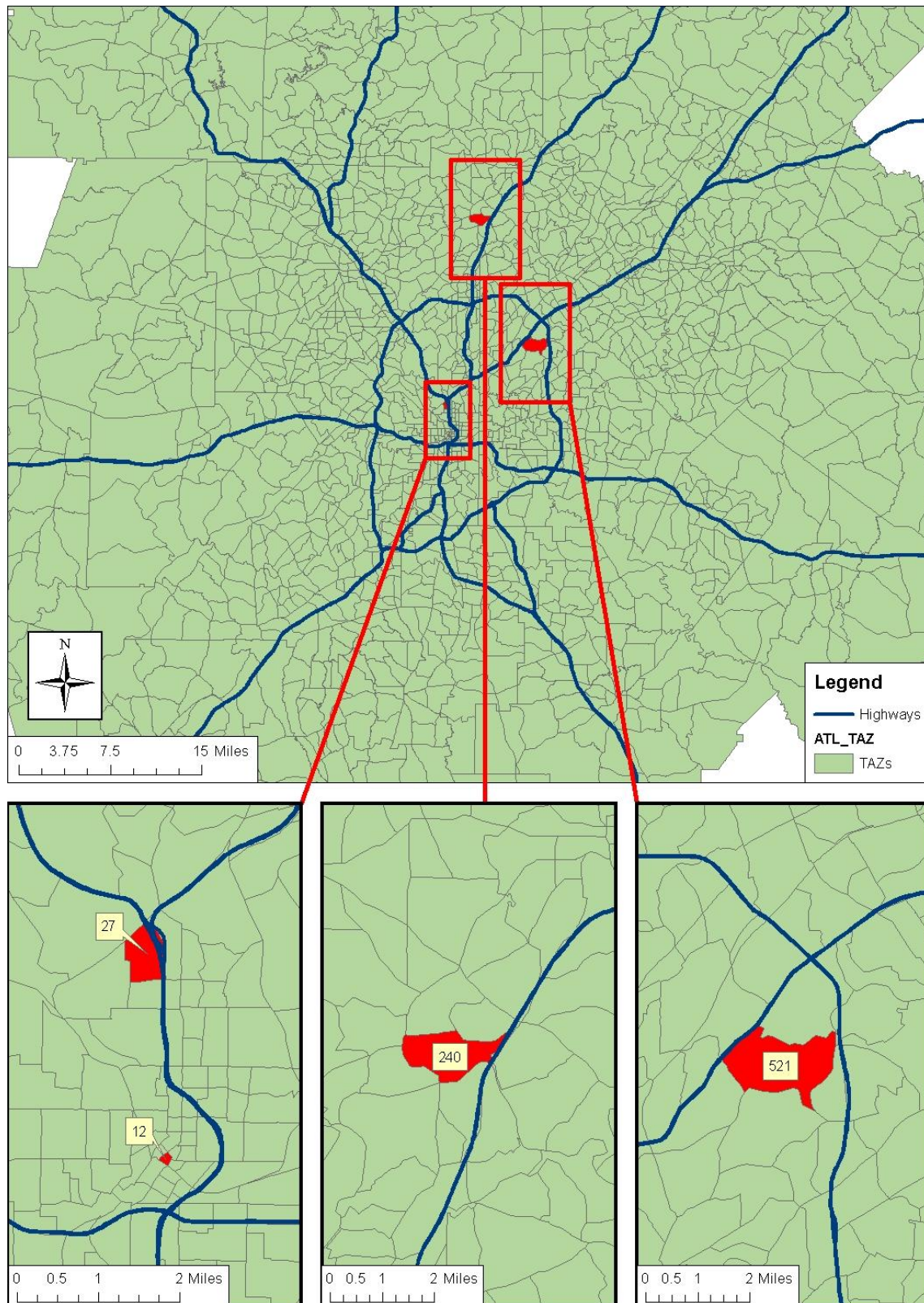


Figure 110: Map of TAZ location choice set (case studies) in the Atlanta, GA metropolitan region.

Table 65: Choice Set of Location Alternatives

Case Study		TAZ #	Average SOV Trip Distance (mi.)	Average Transit Mode Share
I	Suburban, High SOV Trip Distance	521	20.9	2.3%
II	Suburban, Low SOV Trip Distance	240	13.5	2.3%
III	Urban, High Transit Mode Share	12	19.7	33.3%
IV	Urban, Low Transit Mode Share	27	17.9	8.8%

8.2.1.1. Site Transportation Data

Additional site transportation data, beyond what is shown in Table 65, are needed to capture the impact of site characteristics that either may not be fully captured by the TAZ characteristics in the travel demand model, or that may be relevant to potential transportation demand management strategies (see Section 6.2.1.1). One of the most important site characteristics for evaluating potential travel demand management strategies is the presence of pay parking. Although most visitors to TAZ 27 are charged a parking fee for visits over two hours, employees at TAZ 27 park for free – employee parking costs are included in lease rents. TAZ 12 is the only site where parking costs are charged for employee parking.

In the ARC travel demand model, parking costs are estimated from zone employee density. For employee densities below 20 employees per acre, the parking costs are assumed to be zero. This assumption is consistent with the no-cost employee parking in TAZ 27. In the ARC travel demand model, the parking costs for TAZ 12 are \$4.90 per day. Any actual or planned

deviation in parking cost can be accounted for in a vehicle trip reduction (VTR) impact evaluation for travel demand management incentive/disincentive programs (see Section 8.2.2.3).

Another important characteristic of a given site that may not be fully captured by the zone characteristics in a travel demand model is the presence of mixed-use development. TAZ 27 contains the Atlantic Station infill development, one of the largest mixed-use residential and commercial development sites in the Atlanta, GA metropolitan region. Consideration of the development diversity within TAZ 27 can help to quantify the potential vehicle trip reduction impact of the mixed-use development (see Section 8.2.2.2).

8.2.1.2. Building/Site Occupancy

The building/site occupancy schedule that defines the time of day and frequency of inbound and outbound trips for each of the case studies is consistent with the occupancy schedule utilized for the building energy calculations and the regional application of the transportation framework (see Sections 7.1.1.1, 8.1.3.1, and 8.1.5). The midday occupancy of the site may vary between sites that have unique NHB trip frequencies (see Section 8.2.3.1). Even though the occupancy schedule is for the most part consistent between the case study sites, the number of motorized trips required to satisfy the inbound/outbound flows to/from each site may differ. The following section presents the quantification of motorized vehicle trip reductions resulting from site characteristics and transportation demand management strategies.

8.2.2. Motorized Vehicle Trip Reduction

The motorized vehicle trip reduction (VTR) estimated in this section includes bicycle/pedestrian mode share for HBW trips, mixed-use development internal trip capture, and travel demand management VTR programs.

8.2.2.1. Bike/Ped Mode Share

As has been discussed previously in Section 6.2.3.1, the best available data source for site-specific HBW non-motorized mode shares in the Atlanta, GA metropolitan region is the CTPP 2000 dataset. The dataset predates the case studies by ten years, however the spatial extent and resolution of the dataset surpasses all other known sources of non-motorized mode share data. Table 66 shows the non-motorized mode share of HBW trips attracted to the case study TAZs. Overall, the HBW trip non-motorized mode shares are very low, and the variation between any two case studies is at most 1.5 percent. Only a minority of zones in the region are known to have a HBW trip non-motorized mode share above 3 percent (see Figure 87).

Table 66: Non-Motorized Mode Share of HBW Trips Attracted to Case Study TAZs

Case Study	TAZ	Bike	Walk	Total Non-Moto.
I	521	0.00%	1.09%	1.09%
II	240	0.31%	1.98%	2.29%
III	12	0.14%	0.58%	0.72%
IV	27	0.00%	0.83%	0.83%
Source: CTPP 2000 Part 2, Table2, Sex by Means of Transportation to Work				

The VTR is simply equal to the total non-motorized mode share shown in Table 66. For each case study TAZ, the number of attracted motorized trips is calculated from Equation 8. Additional motorized VTR can be accounted for by estimating the impact of mixed-use development internal trip capture.

8.2.2.2. Mixed-Use Development Internal Trip Capture

The internal trip capture of mixed-use developments is effectively an increase in the baseline non-motorized mode share which results in motorized VTR. Like many other 4-step travel demand models, the ARC travel demand model accounts for the VTR effect of densely-developed, mixed-use TAZs through motorized vehicle trip attraction rates. In the ARC travel demand model, trip attraction rates vary across different “area types,” such as “CBD” and “Suburban Commercial” (see Section 6.3.2, Table 32 for trip attraction rates for NHB trips). Such trip attraction rates are insufficient for quantifying the VTR for HBW trips, since the calculation framework presented in this dissertation makes use of a tenant-supplied, building occupancy schedule, rather than a model-based HBW trip rate. The HBW internal trip capture calculation methods discussed in Section 6.2.3.2.1 provide additional capability for quantifying the VTR impacts of mixed-use developments.

Each case study TAZ represents a unique area type in the ARC travel demand model: TAZ 12 is of type “CBD,” TAZ 27 is of type “Urban Commercial,” TAZ 240 is of type “Suburban Commercial,” and TAZ 521 is of type “Suburban Residential.” TAZ 27 is unique among the other case study TAZs in that it contains a large mixed-use development with a considerable number of residential units (Atlantic Station). Conveniently, the studies underlying NCHRP Report 684 included the Atlantic Station mixed-use development. The analysis

presented in Section 6.2.3.2.1 indicates that the HBW trip mode shift and subsequent motorized VTR associated with the mixed-use development at Atlantic station is approximately 4 – 5 percent. In the subsequent energy and GHG emission calculations in this chapter, the relative transportation system performance of TAZ 27 is estimated with and without the 4 – 5 percent internal trip capture.

8.2.2.3. Travel Demand Management VTR Programs

In order to estimate the VTR impact of travel demand management programs, it is first necessary to establish the planned level of program support. For the case study sites, the maximum level of program support considered is “Level 3” (see definitions of program levels in Section 6.2.3.3.2, Table 24). “Level 3” ridesharing support is programmed consistently across all case study sites, but “Level 3” transit support is only programmed for sites that have a significant transit mode share, or transit “modal bias” in the language of the FHWA TDM Guidance Manual. Table 67 below shows the estimated VTR for case study locations according to the FHWA TDM Guidance Manual and the U.S. EPA COMMUTER Model. The table shows the calculation results from Equation 9 through Equation 11, and indicates that only TAZs 12 and 27 have a transit modal bias. Given the low baseline non-motorized mode shares of the TAZs and the low potential mode shift for non-motorized program support (see Table 25), no bicycle program support is included in these case studies. The VTR percentages shown Table 67 indicate a range in estimated impacts from the selected travel demand management programs, with the COMMUTER Model providing much more conservative estimates relative to the FHWA TDM Guidance Manual. Interestingly, for both the COMMUTER Model and FHWA TDM Guidance Manual results, the relative degree of impact between the case study sites is consistent.

Table 67: Estimated Vehicle Trip Reduction (VTR) for Case Study Locations According to FHWA TDM Guidance Manual and COMMUTER Model

Case Study	I	II	III	IV
TAZ	521	240	12	27
Drive Alone (SOV) Mode Share	89.0%	89.0%	63.1%	85.2%
Rideshare (HOV) Mode Share	7.6%	6.3%	2.9%	5.1%
Transit Mode Share	2.3%	2.3%	33.3%	8.8%
Bike / Walk Mode Share	1.1%	2.3%	0.7%	0.8%
Average Vehicle Ridership (AVR)	1.08	1.09	1.55	1.14
Vehicle Trips (VT)	92.3	91.9	64.3	87.5
% of Trips by Alternative Modes (AM)	11.0%	11.0%	36.9%	14.8%
% of Trips by Rideshare Modes (RS)	7.6%	6.3%	2.9%	5.1%
% of Trips by Public Transit (TR)	2.3%	2.3%	33.3%	8.8%
RS/AM	69.2%	57.7%	7.8%	34.7%
TR/AM	20.8%	21.3%	90.2%	59.7%
Modal Bias	Rideshare	Rideshare	Transit	Transit
FHWA TDM CP & VP Program Level	3	3	3	3
FHWA TDM Transit Program Level	0	0	3	3
FHWA TDM Vehicle Trip Reduction (VTR)	6.9%	6.9%	7.9%	8.4%
COMMUTER Model CP Program Level	3	3	3	3
COMMUTER Model VP Program Level	3	3	3	3
COMMUTER Model Transit Program Level	0	0	3	3
COMMUTER Model Bicycle Program Level	0	0	0	0
COMMUTER Model Rideshare Mode Shift	4.0%	4.0%	4.0%	4.0%
COMMUTER Model Transit Mode Shift	0.0%	0.0%	1.5%	1.5%
COMMUTER Model Adjusted SOV Mode Share	85.6%	85.6%	59.8%	80.8%
COMMUTER Model Adjusted HOV Mode Share	11.1%	9.9%	6.5%	8.7%
COMMUTER Model Adjusted Transit Mode Share	2.2%	2.2%	33.0%	9.8%
COMMUTER Model Adjusted HOV Mode Shift	3.6%	3.6%	3.6%	3.5%
COMMUTER Model Adjusted Transit Mode Shift	-0.1%	-0.1%	-0.3%	1.0%
COMMUTER Model Vehicle Trip Reduction (VTR)	2.1%	2.0%	2.7%	3.3%

Parking pricing can be a powerful mechanism for encouraging mode shift from SOV or private automobile trips. Only Case Study III is located in an area with employee parking fees.

An employer would likely be unwillingly to impose a high parking fee for its employees at a candidate location if the other location alternatives provide free employee parking. The impact of a nominal parking fee increase, limited to \$1 per day, is explored here for Case Study III. Table 68 below shows the estimated VTR for Case Study III with a \$1 parking fee increase according to the FHWA TDM Guidance Manual and the U.S. EPA COMMUTER Model. The VTR from the FHWA TDM Guidance Manual jumps considerably relative to a \$0 financial incentive/disincentive differential – an increase of 19.3 percent. The unique estimation methodology of the U.S. EPA COMMUTER MODEL (described in Section 6.2.3.3.2) produces a very different result. The \$1 parking fee is applied to Equation 12, which yields a change in SOV utility of -0.31. The revised SOV mode share is estimated according to Equation 13. After adjusting the mode shares so that the total of all modes is 100 percent, the resulting SOV mode share is 56.2 percent. Considering the increase in HOV and transit mode shares, the estimated VTR is 7.4 percent, a far more conservative estimate than the 27.2 percent from the FHWA TDM Guidance Manual.

Table 68: Estimated Vehicle Trip Reduction (VTR) for Case Study III with \$1 Employee Parking Fee According to FHWA TDM Guidance Manual and COMMUTER Model

Case Study	III
TAZ	12
FHWA TDM CP & VP Program Level	3
FHWA TDM Transit Program Level	3
FHWA TDM Financial Incentive Differential	\$1.00
FHWA TDM Vehicle Trip Reduction (VTR)	27.2%
COMMUTER Model CP Program Level	3
COMMUTER Model VP Program Level	3
COMMUTER Model Transit Program Level	3
COMMUTER Model Bicycle Program Level	0
COMMUTER Model Parking Fee	\$1.00
COMMUTER Model dU SOV	-0.310
COMMUTER Model SOV Mode Share	52.2%
COMMUTER Model Adjusted SOV Mode Share	56.5%
COMMUTER Model Adjusted HOV Mode Share	7.1%
COMMUTER Model Adjusted Transit Mode Share	35.7%
COMMUTER Model Adjusted HOV Mode Shift	4.2%
COMMUTER Model Adjusted Transit Mode Shift	2.4%
COMMUTER Model Vehicle Trip Reduction (VTR)	7.4%

8.2.3. Annual Motorized Trip Frequency

The annual motorized trip frequency is calculated based on the occupancy schedule (see Table 64), the demographic profile of the building/site occupants (see Table 63), and adjusting from any motorized VTR. The number of annual motorized vehicle trips is equal to the number of inbound/outbound, peak/non-peak trips taken during each day type (weekday, Saturday, Sunday/Holiday) multiplied by the frequency of the trip patterns estimated from Equation 14 and Equation 15. The number of trips can be estimated for each demographic stratification in the employee population by applying the occupancy percentages in the occupancy schedule to each

stratification separately. Table 69 shows the Annual HBW motorized vehicle trips by direction, period, and stratification for each case study TAZ. Clearly, more trips are taken by stratification 4 since this stratification comprises the largest group within the case study population. Across the time periods, most of the HBW commute trips are taken during the peak period. In Table 69, the total motorized vehicle trips are similar for each TAZ since the values reflect only the differences in baseline non-motorized mode shares, each of which are no more than 2.3%.

Table 69: Annual HBW Motorized Vehicle Trips by Direction, Period, and Stratification for Each Case Study TAZ

Case Study	TAZ	Trip Direction and Period	Stratification			
			1	2	3	4
I	521	Inbound Peak	506	2,530	4,807	16,192
		Outbound Peak	558	2,433	4,613	15,461
		Inbound Non-Peak	52	216	372	1,220
		Outbound Non-Peak	-	313	566	1,951
II	240	Inbound Peak	506	2,530	4,807	15,939
		Outbound Peak	558	2,433	4,613	15,208
		Inbound Non-Peak	52	216	372	1,220
		Outbound Non-Peak	-	313	566	1,951
III	12	Inbound Peak	506	2,530	4,807	16,445
		Outbound Peak	558	2,433	4,613	15,714
		Inbound Non-Peak	52	216	372	1,220
		Outbound Non-Peak	-	313	566	1,951
IV	27	Inbound Peak	506	2,530	4,807	16,192
		Outbound Peak	558	2,433	4,613	15,461
		Inbound Non-Peak	52	216	372	1,220
		Outbound Non-Peak	-	313	566	1,951

8.2.3.1. NHB Trip Frequency

The NHB trip frequency is sourced from the NHB trip attraction rates estimated in the ARC travel demand model. The trip rates are expressed as trips per employee and are estimated for each zone “area type.” Table 70 below shows the Annual NHB motorized vehicle trips by direction, period, and stratification for each case study TAZ. The annual number of NHB trips is equal to the NHB trip rate multiplied by the number of workdays in the year multiplied by the number of employees in the stratification. The NHB trips vary by as much as a factor of 2 between TAZs, yet overall the number of NHB trips is less than the number of HBW trips (NHB trips are between 45 and 80 percent of HBW trips).

Table 70: Annual NHB Motorized Vehicle Trips by Direction, Period, and Stratification for Each Case Study TAZ

Case Study	TAZ	Trip Direction and Period	Trips per Employee	Stratification			
				1	2	3	4
I	521	Inbound Non-Peak	0.4519	253	1,265	2,277	7,843
		Outbound Non-Peak	0.4519	253	1,265	2,277	7,843
II	240	Inbound Non-Peak	0.4519	253	1,265	2,277	7,843
		Outbound Non-Peak	0.4519	253	1,265	2,277	7,843
III	12	Inbound Non-Peak	0.6339	253	1,518	3,289	10,879
		Outbound Non-Peak	0.6339	253	1,518	3,289	10,879
IV	27	Inbound Non-Peak	0.818	506	2,024	4,048	14,168
		Outbound Non-Peak	0.818	506	2,024	4,048	14,168

Utilization of NHB trip rates to estimate motorized NHB trip activity presents a challenge for estimating the potential VTR from site-specific factors such as mixed-used development. Intuitively, walk access to dining, retail, and other amenities from an employment site can help to reduce motorized NHB trips. For a given motorized NHB trip rate, it is difficult to determine

whether the rate in any way reflects the effect of mixed-use development at the site. As was mentioned in Section 6.3.2, relatively lower NHB trip rates in the ARC travel demand model may reflect relatively higher non-motorized mode choice. However, lower NHB trip rates may also reflect lower access to NHB trip ends. Without knowing the total or non-motorized NHB trip rate in addition to the motorized NHB trip rate, the baseline non-motorized mode share for NHB trips in a given zone remain unknown. Case Study IV is located in the mixed-use development of Atlantic Station, yet it has the highest motorized NHB trip rate of all of the case studies (see Table 70). It is reasonable to suspect that this trip rate should be lower than the average “urban commercial” area type NHB trip rate, but in the absence of data on the NHB non-motorized trip rate or mode share, the VTR effect of the mixed-use development remains indeterminate.

8.2.4. Mode Choice and VMT

Upon estimating the non-motorized mode shares and the annual trip frequencies, the MATLAB script (see “Transp_Calcs_HBW” in Appendix A) was run for the four case study TAZs. The iterations of the MATLAB script yield average mode shares for the motorized modes. Figure 111 shows the estimated average HBW mode choice for each of the case study TAZs. The mode shares indicate that SOV trips dominate the mode choice for all of the TAZs. For the suburban TAZs, HOV comprises the largest share of non-SOV modes. The CBD case study located in TAZ 12 has by far the largest non-SOV mode share. Interestingly, most of the non-SOV mode share for TAZ 12 is D2R (drive-to-rail or drive-to-premium transit). So, even though TAZ has a significant alternative mode share, most of the mode share includes private automobile trips to transit stations. Thus, much of the alternative mode share for HBW trips

attracted to TAZ 12 does not eliminate SOV trips, but rather reduces SOV trip distance. In effect, the park and ride transit stations provide an extension of the parking facilities serving the office site.

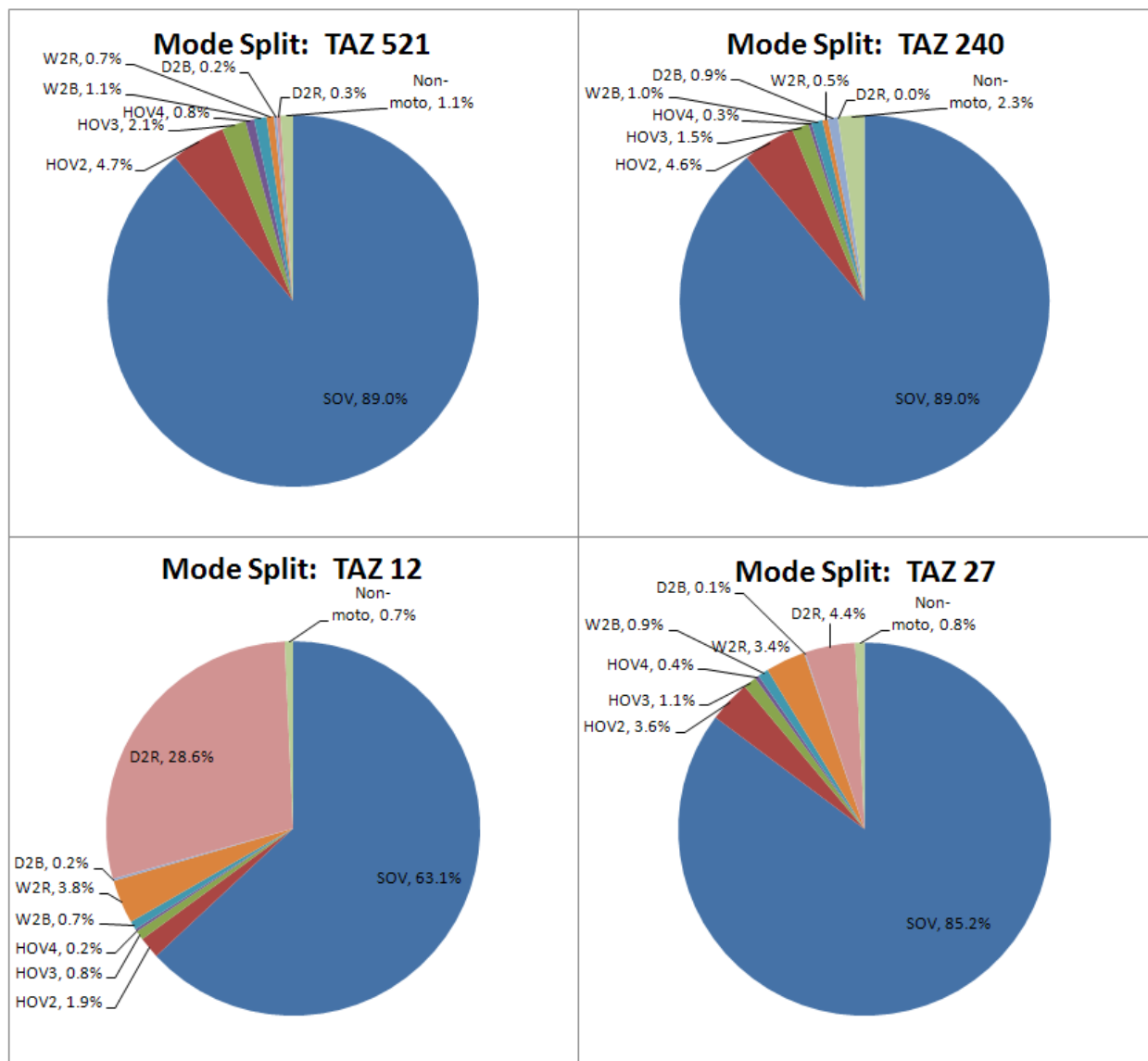


Figure 111: Average HBW mode choice for case study TAZs.

The VMT impact of D2T trips for TAZ 12 is not insignificant. Figure 112 shows the average annual HBW SOV + D2T VMT for each of the case study TAZs. The red error bars represent one standard deviation above and below the mean. Even though TAZ 12 has more than twice the alternative mode share of TAZ 27, the SOV + D2T VMT for these TAZs are quite similar. This similarity is due in part to the high percentage of D2T mode share in TAZ 12's alternative mode share.

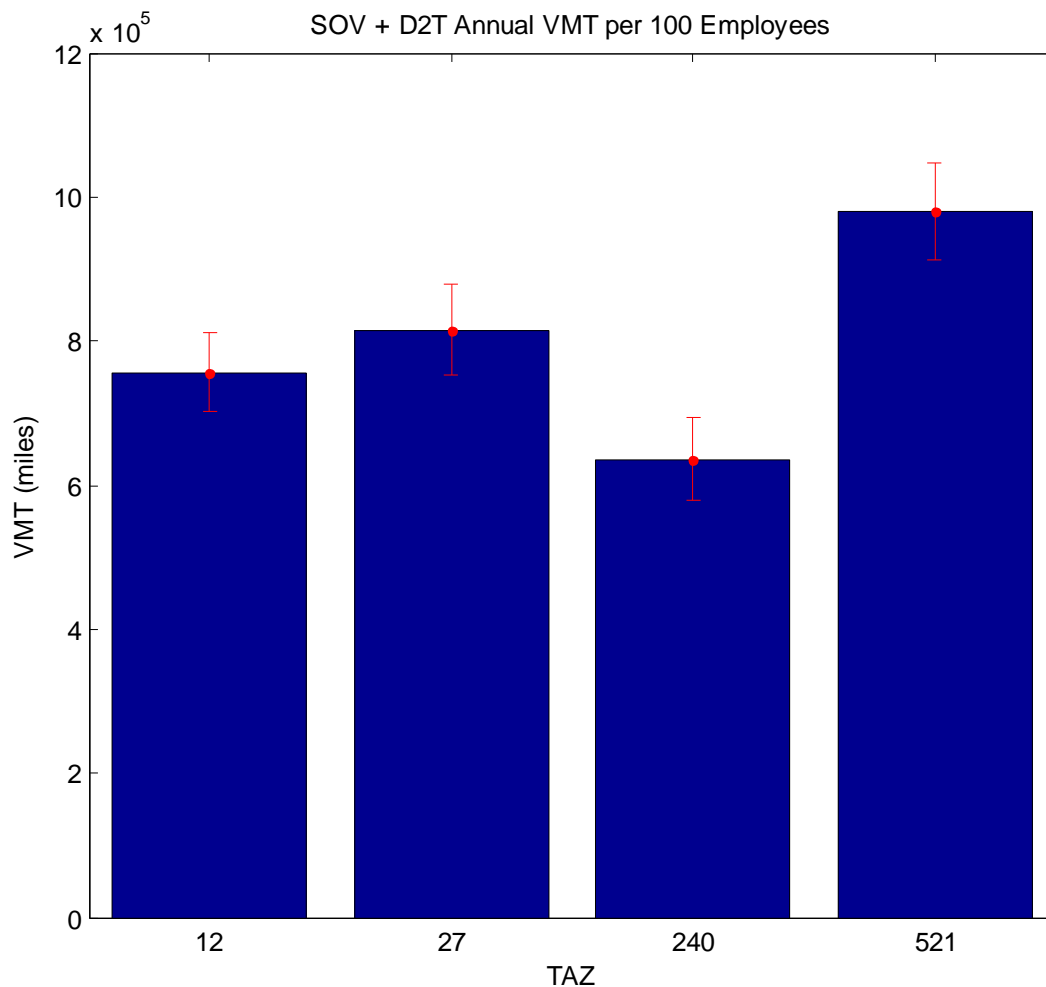


Figure 112: Average annual HBW SOV + D2T VMT for case study TAZs.

The VMT for each TAZ is a function of not only the mode share, but also the average trip distance. Figure 113 shows the average HBW SOV + D2T trip distance for each of the case study TAZs. The D2T mode share of TAZ 12 contributes to a relatively low average trip distance, but the lowest average trip distance is found in the suburban TAZ 240. Given the high SOV mode share for TAZ 240, the low VMT shown for TAZ 240 in Figure 112 is due to its low average trip distance. The average trip distance is a product of the ARC travel demand model's trip distribution/attraction model. TAZ 240 happens to be surrounded by residential development, thereby making it highly accessible from potential commute origins. The assumptions and theoretical basis of the trip distribution/attraction model (see Section 6.1.1.2) may not reflect the actual HBW commute shed of the TAZs. Nevertheless, the modeled trip attractions provide the best available estimate of HBW trip origins and network trip distance.

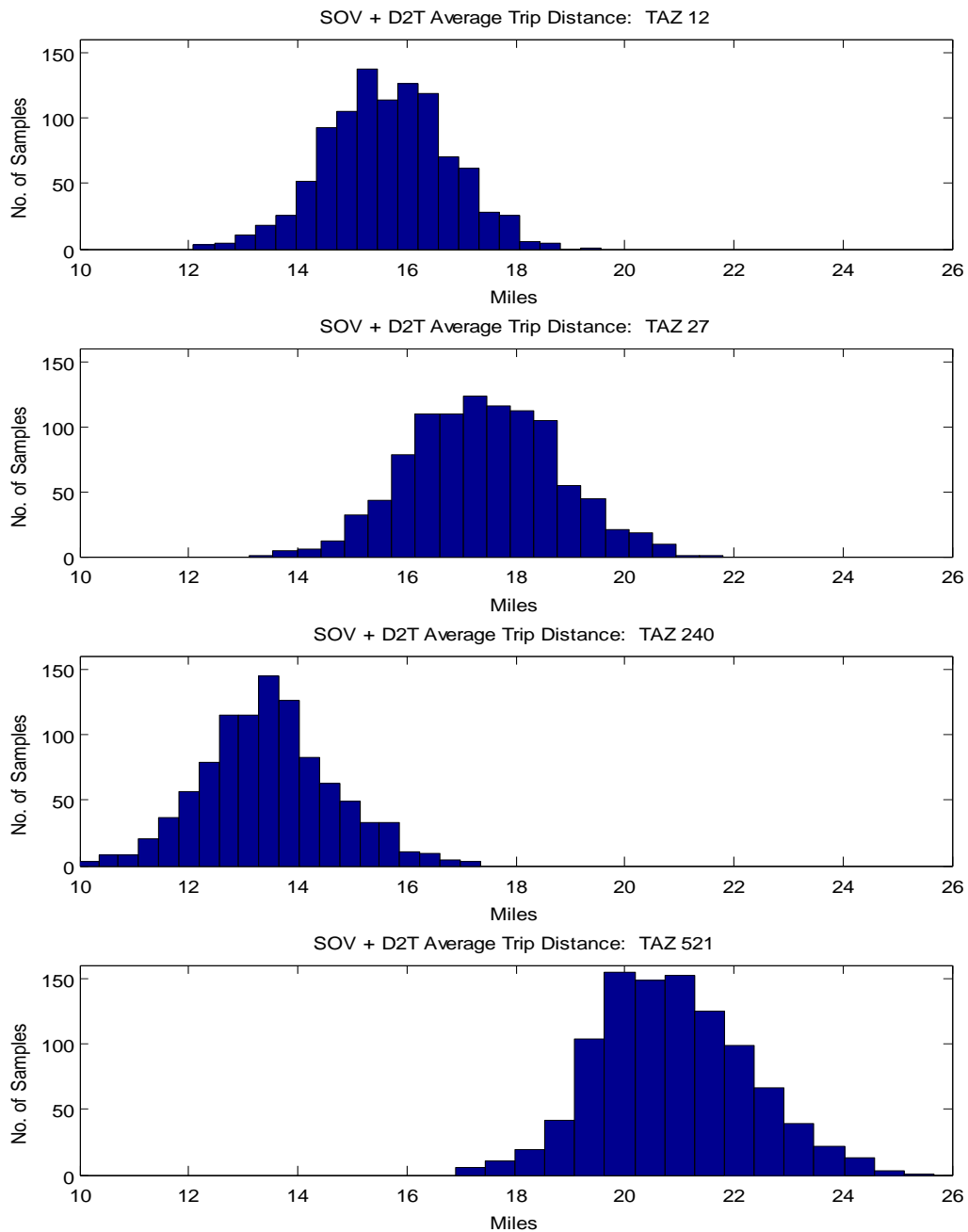


Figure 113: Average HBW SOV + D2T trip distance for case study TAZs.

The results shown in Figure 113 may be skewed by the number of employees within each of the TAZs (see discussion of Figure 103 in Section 8.1.7). A regression analysis was conducted

to explore the influence of employment size on average trip distance. Figure 114 shows a plot and linear regression of average SOV HBW trip distance vs. total TAZ employment for TAZ 521 and the cluster of adjacent TAZs. The trendline and the coefficient of determination indicate that there is very little correlation between the average SOV HBW trip distance and the number of jobs in the TAZs. This finding suggests that the level of employment within a TAZ containing a potential building/site likely does not bias an estimate of average trips distance for a sample of *N* employees.



Figure 114: Average SOV HBW trip distance vs. total TAZ employment (TAZ 521 cluster).

For the other suburban site (located in TAZ 240), the relationship between the number of jobs and the average trips distance is also quite weak. Figure 115 shows a plot and linear regression of average SOV HBW trip distance vs. total TAZ employment for TAZ 240 and the cluster of adjacent TAZs. Although the coefficient of determination is greater for this cluster, the

number of adjacent TAZs is less (5 vs. 10); more samples may have resulted in more regression error. For both of the TAZ clusters, the linear regression variable coefficient is the same and it is equal to the variable coefficient for the region as a whole (see Section 8.1.7).

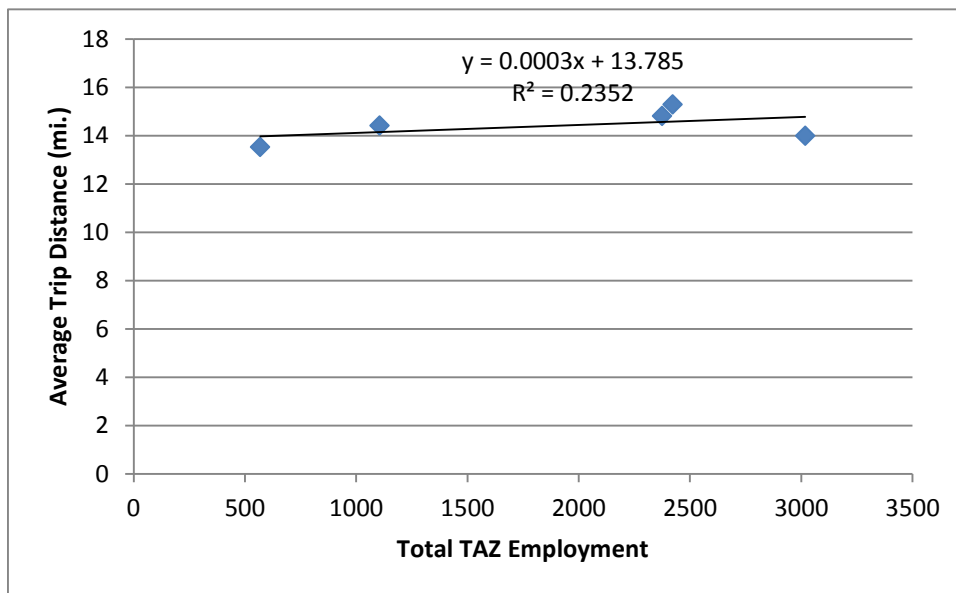


Figure 115: Average SOV HBW trip distance vs. total TAZ employment (TAZ 240 cluster).

At the CBD site (TAZ 12), correlation between average trip distance and TAZ employment size is even weaker. Figure 116 shows a plot and linear regression of average SOV HBW trip distance vs. total TAZ employment for TAZ 12 and the cluster of adjacent TAZs. The coefficient of determination is much higher, but the linear regression variable coefficient is much lower (and this for a much greater range of TAZ employment levels). Altogether, the level of employment within a TAZ appears to have minimal impact on the estimated trip distance and associated energy consumption and GHG emissions for N employees sampled.

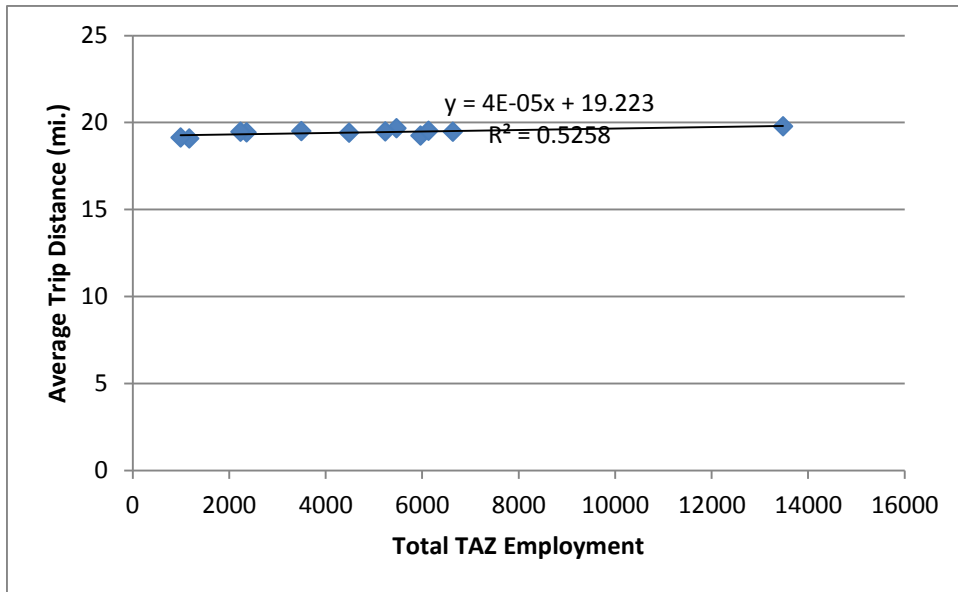


Figure 116: Average SOV HBW trip distance vs. total TAZ employment (TAZ 12 cluster).

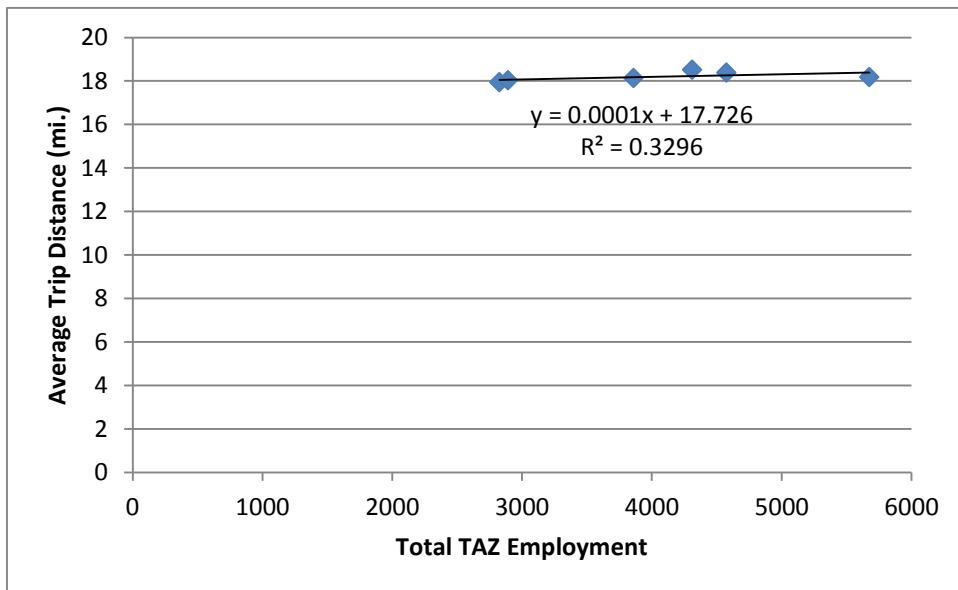


Figure 117: Average SOV HBW trip distance vs. total TAZ employment (TAZ 27 cluster)

An additional factor affecting the estimated energy consumption of trips attracted to the case study TAZs is the average vehicle speed and efficiency. Figure 118 below shows the average HBW SOV + D2T speed for the case study TAZs, with error bars indicating 1 standard

deviation above and below the means. It is interesting to note that the TAZ with the lowest SOV + D2T VMT also has the lowest average SOV + D2T speed. Based on the fuel economy curve shown in Figure 27, the variation in average speeds between the case study TAZs equates to only a few miles per gallon in fuel efficiency.

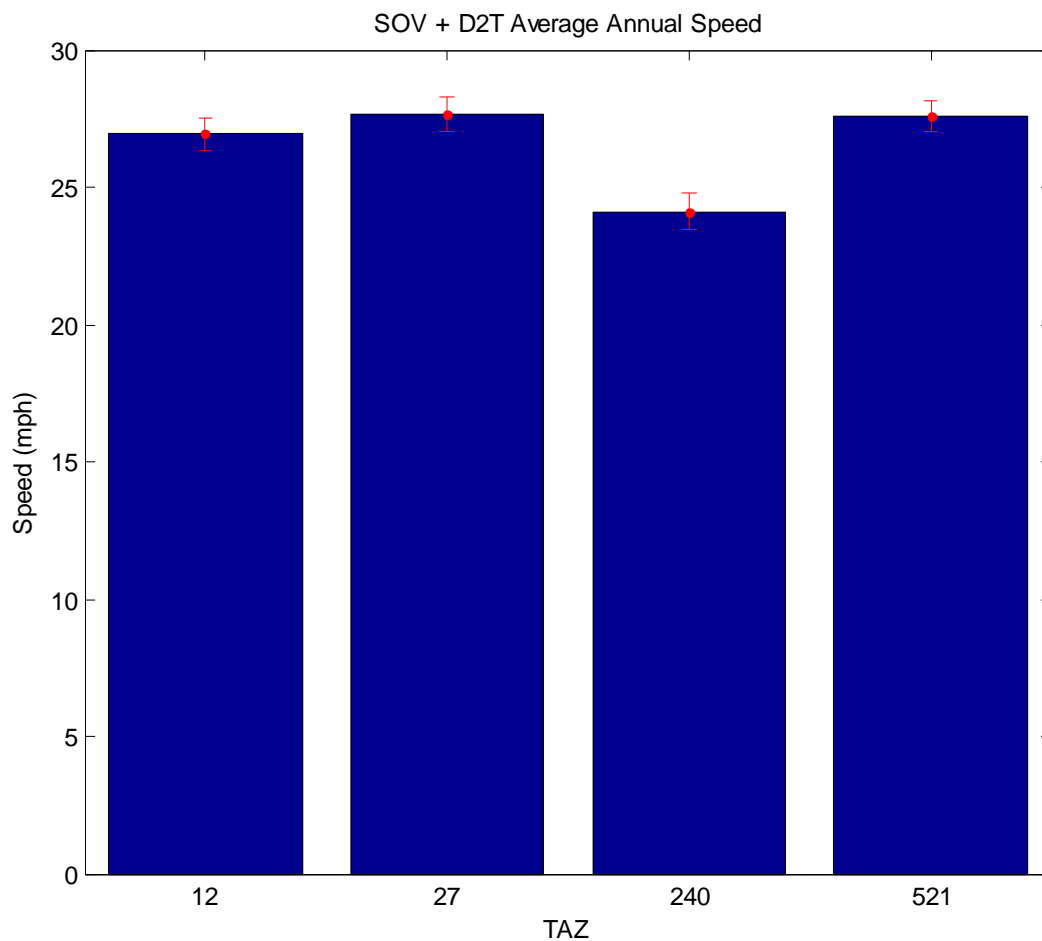


Figure 118: Average HBW SOV + D2T speed for case study TAZs.

8.2.4.1. NHB Trips

The average trip distances for NHB trips are estimated to be less than the average trip distances for HBW trips. Figure 119 shows the average NHB SOV + D2T trip distance for each of the case study TAZs. The average NHB trip distances are lowest for the CBD TAZ and highest for the “suburban residential” TAZ. This result appears reasonable, since the CBD TAZ has greater access to NHB trip destinations (offices, retail, dining) than does the more suburban TAZs.

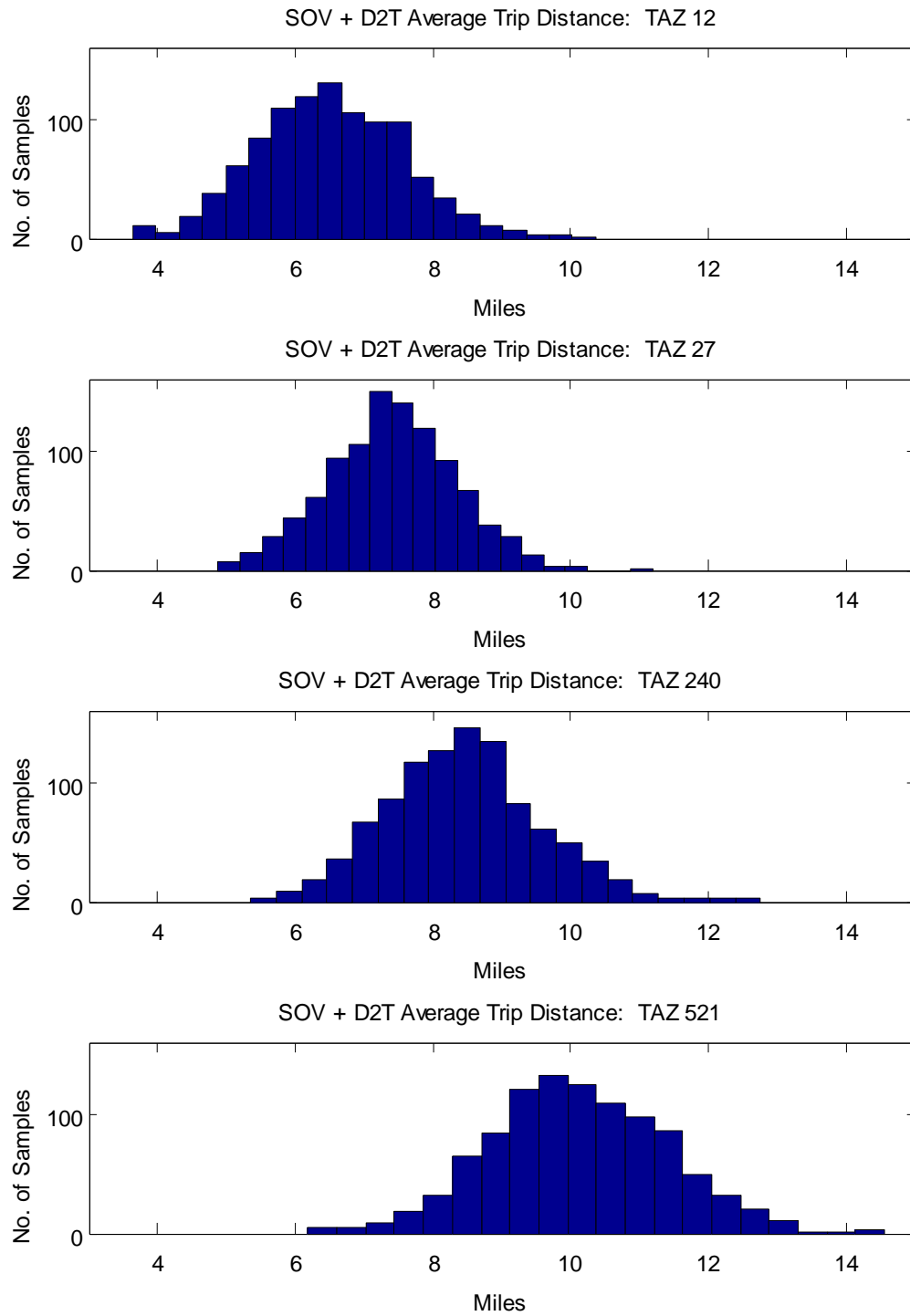


Figure 119: Average NHB SOV + D2T trip distance for case study TAZs.

8.2.5. Energy Consumption and GHG Emissions

The estimated transportation energy consumption and GHG emissions are the ultimate measure of performance in the transportation evaluation framework. The results discussed in the previous sections provide insight into the contributing factors for transportation energy and emissions, but the calculated energy consumption and GHG emissions serve as the definitive measures of performance. Figure 120 below shows the HBW average annual SOV + HOV + D2T energy consumption per 100 employees for the case study TAZs. Given the results shown in the previous sections, the results shown in Figure 120 are not all that surprising. The relative energy performance of the TAZs matches the relative levels of VMT shown in Figure 112. Thus, the estimated impact of travel speed and vehicle efficiency on the relative energy performance of the case study sites appears to be insignificant (see Figure 118). In light of the limitations discussed in the calculation methodology (see Section 6.2.8.1), the impact of vehicle speed on the estimated relative energy performance of the case study locations may increase with more detailed data on time-variant vehicle speeds.

It is interesting to note that the site with the best energy performance is one located in a suburban development area with the lowest public transportation access and with an unconstrained supply of parking. According to LEED NC 2009, locations in TAZ 12 and 27 could achieve SS Credit 2: Development Density and Community Connectivity (5 points), and SS Credit 4.1: Alternative Transportation – Public Transportation Access (6 points), whereas a location in TAZ 240 would not.

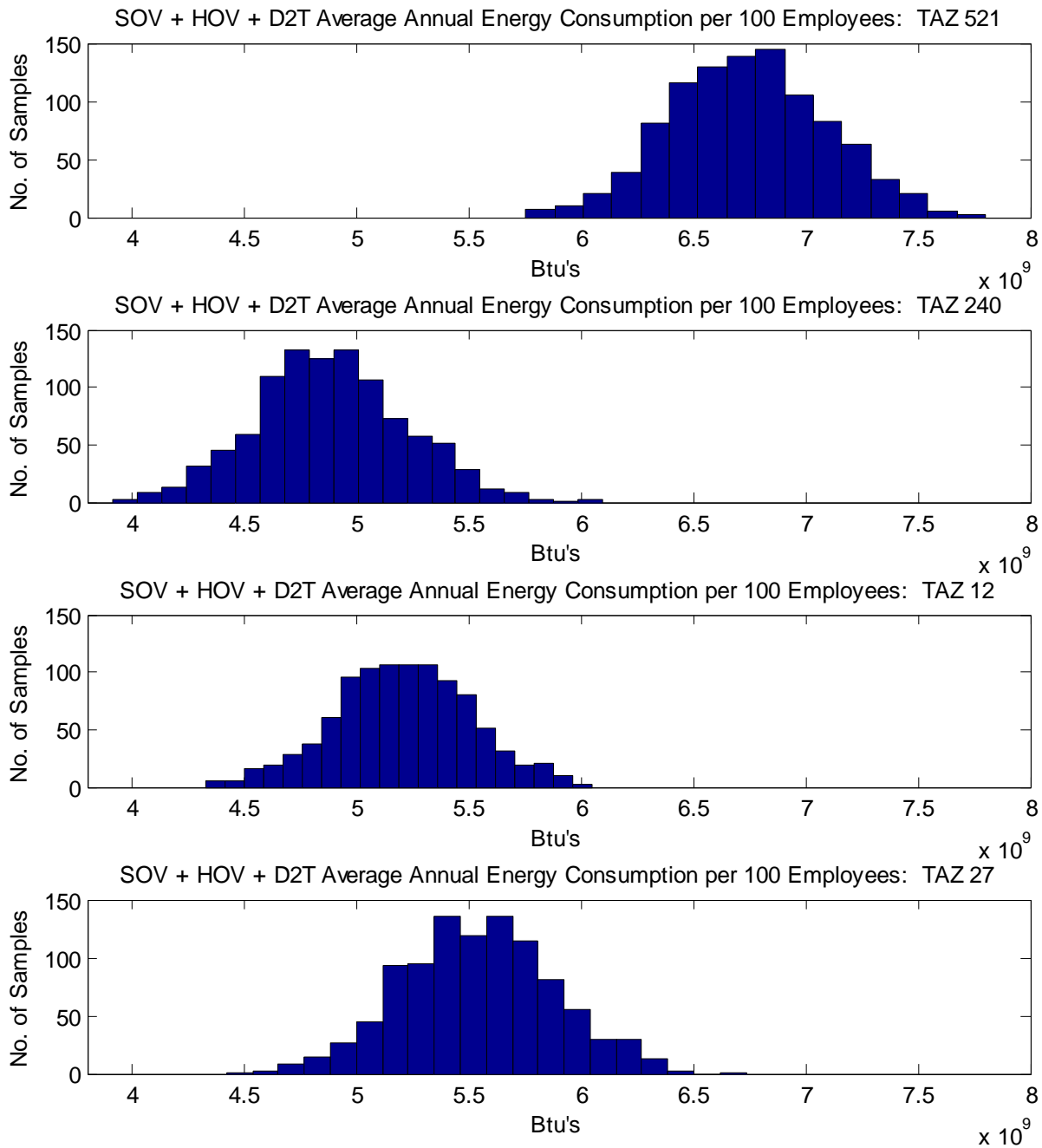


Figure 120: HBW average annual SOV + HOV + drive-to-transit energy consumption per 100 employees for case study TAZs.

The dispersion in the estimated annual transportation energy consumption associated with HBW trips to/from the case study TAZs is such that there is notable overlap in the case study estimates. Very little overlap is estimated between the best and worst performing site, but considerable overlap is present for the other two sites. The degree of overlap between the case study estimates and the resulting probability of relative performance levels are discussed later in Section 8.2.6.1. As with the energy results calculated for regional application of calculation procedures, the SOV + HOV + D2T GHG emissions are proportional to the energy consumption and thus the GHG dispersion and relative performance of the sites matches the energy performance.

The transportation performance of the case study locations is measured not only by the total energy consumption and GHG emissions, but also by normalized performance metrics that account for building service (square footage or person-hours) as well as upstream energy and emission processes. Table 71 below shows the normalized transportation energy consumption and GHG emissions performance of the case study locations. The performance metrics are expressed as a mean \pm 2 standard deviations (coverage factor of 2). Table 71 includes an estimate of the regional average transportation energy consumption per conditioned floor area. The average regional transportation energy consumption is based on the regional application of the framework (see Section 8.1). Interestingly, three of the four case study sites exceed the regional average. An exceedance of the estimated regional average does not necessarily mean a location is a poor performing choice. Case Study's III and IV have an estimated transportation energy consumption that exceeds the regional average, but are also within 2 standard deviations of the regional mean.

Table 71: Normalized HBW Transportation Energy Consumption and GHG Emission Performance of Case Study Locations

Performance Metric	Case Study			
	I	II	III	IV
Annual site energy / conditioned floor area [kBtu/SF]	270.6 ± 28.3	195.9 ± 26.5	214.0 ± 24.8	222.8 ± 26.3
Annual site energy / occupant use [kBtu/person-hrs]	27.3 ± 2.9	19.8 ± 2.7	21.1 ± 2.4	22.5 ± 2.7
Annual primary energy / conditioned floor area [kBtu/SF]	351.8 ± 36.8	254.7 ± 34.5	278.2 ± 32.3	289.7 ± 34.2
Annual primary energy / occupant use [kBtu/person-hrs]	35.5 ± 3.7	25.7 ± 3.5	27.4 ± 3.2	29.2 ± 3.5
Regional average site energy / conditioned floor area [kBtu/SF] *	207.4 ± 20.3			
Annual site GHGs / conditioned floor area [lb CO ₂ e /SF]	7,691 ± 807.0	5,564 ± 754.7	6,082 ± 707.3	6,334 ± 750.8
Annual site GHGs / occupant use [lb CO ₂ e /person-hrs]	777.1 ± 81.5	562.2 ± 76.3	599.8 ± 69.8	638.4 ± 75.7
Annual primary GHGs / conditioned floor area [lb CO ₂ e /SF]	9,826 ± 1,031	7,110 ± 964.4	7,771 ± 904	8,093 ± 959.2
Annual primary GHGs / occupant use [lb CO ₂ e /person-hrs]	992.9 ± 104.2	718.4 ± 97.5	766.4 ± 89.1	815.7 ± 96.7
Source: * Based on regional application of transportation energy calculation procedures and 25,000 SF				

The GHG emissions are estimated according to the formulae and procedures described in Section 6.2.8.3. The emission factors are indicated in the MATLAB script “Transp_Calc_HBW” in Appendix A. The upstream GHG emissions associated with the gasoline supply-chain add approximately an additional 28% to the “site” or “direct” combustion GHG emissions.

8.2.5.1. NHB Trips

The NHB trip activity constitutes an additional source of energy consumption and GHG emissions. Figure 121 shows the NHB average annual SOV + HOV + D2T energy consumption per 100 employees for the case study TAZs. The estimated NHB energy consumption dispersion accounts for modeled uncertainty in trip destinations and mode choice, but does not account for uncertainty in the location-specific NHB trip rates. The impact of this limitation on the overall modeling capability of the evaluation framework is moderated by the fact that the NHB energy consumption is comparatively only a fraction of the HBW energy consumption. Figure 122 shows the proportion of estimated HBW and NHB energy consumption for each of the case study TAZs.

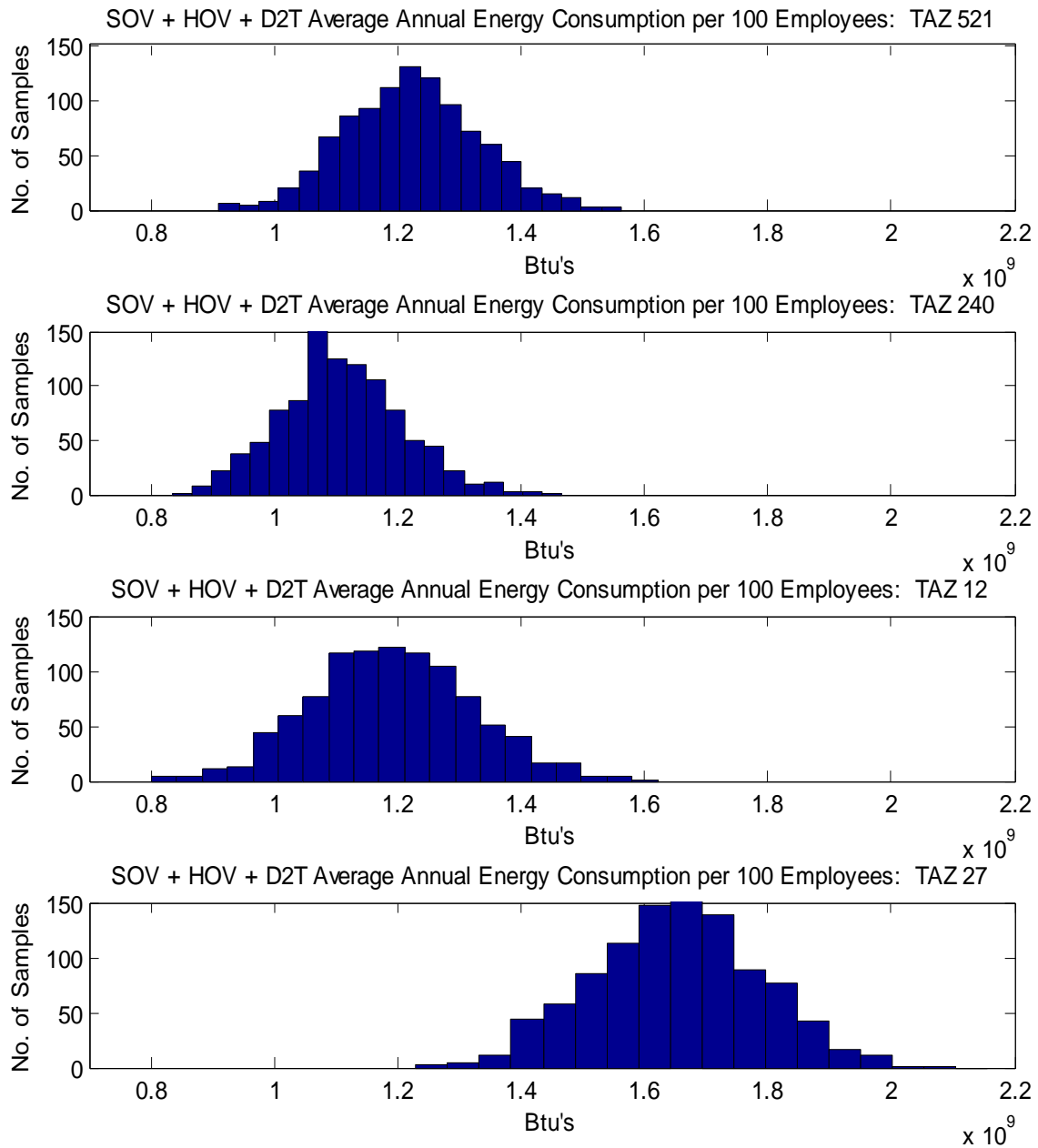


Figure 121: NHB average annual SOV + HOV + drive-to-transit energy consumption per 100 employees for case study TAZs.

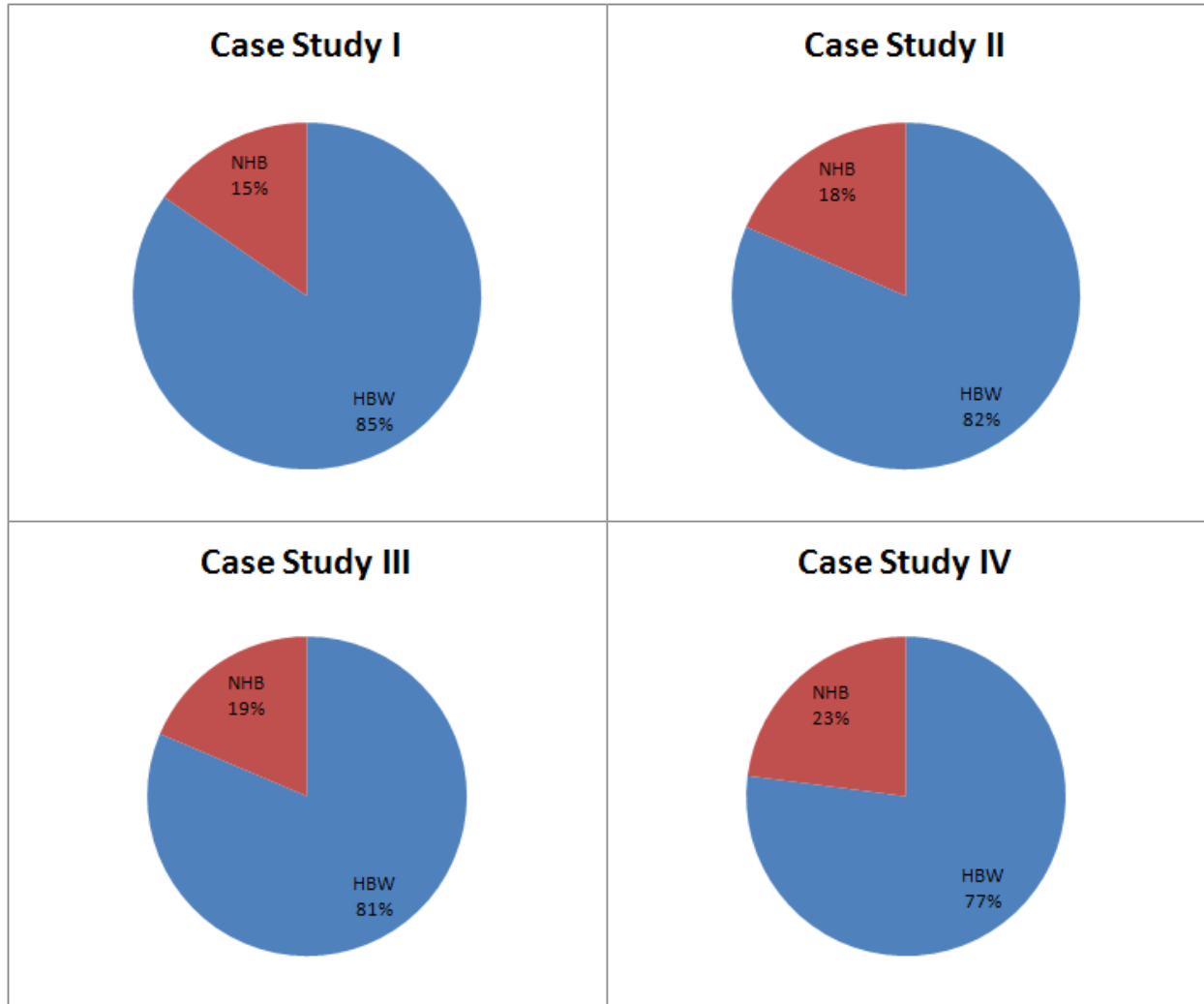
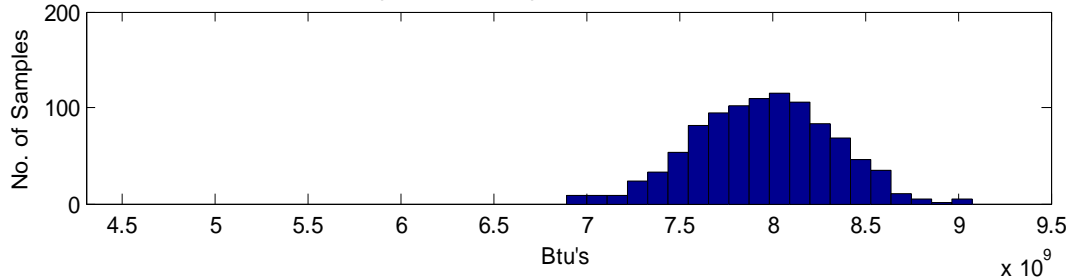


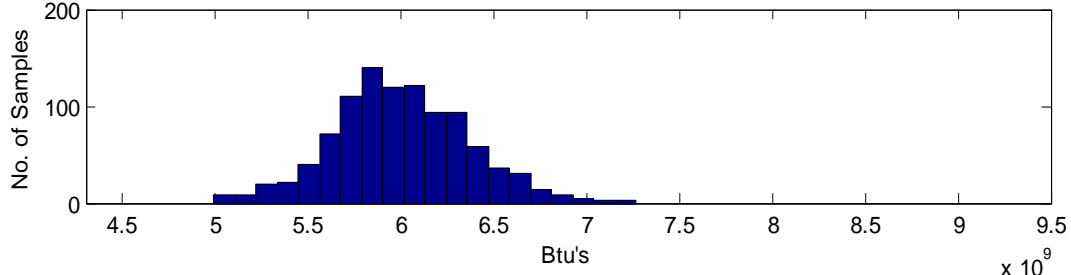
Figure 122: Proportion of estimated HBW and NHB energy consumption for case study TAZs.

Even though the relative proportion of HBW energy consumption varies between the cases study sites, the impact on the relative performance of the sites is not significant. Figure 123 shows the combined HBW and NHB average annual SOV + HOV + drive-to-transit energy consumption per 100 employees for case study TAZs. The NHB results in Figure 123 show the same relative rank in energy consumption shown by the HBW results in Figure 120

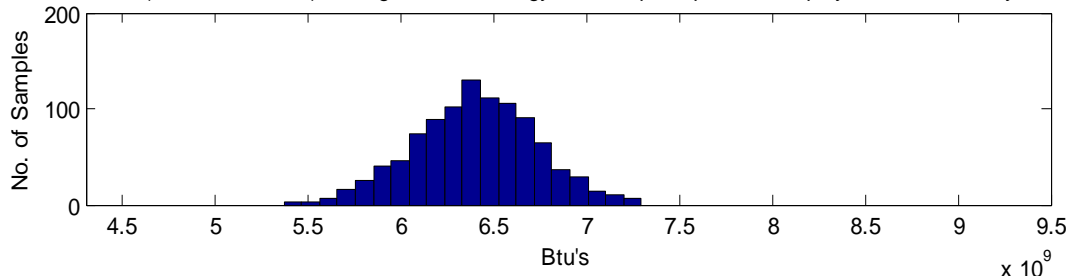
HBW + NHB (SOV+HOV+D2T) Average Annual Energy Consumption per 100 Employees: Case Study I, TAZ 521



HBW + NHB (SOV+HOV+D2T) Average Annual Energy Consumption per 100 Employees: Case Study II, TAZ 240



HBW + NHB (SOV+HOV+D2T) Average Annual Energy Consumption per 100 Employees: Case Study III, TAZ 12



HBW + NHB (SOV+HOV+D2T) Average Annual Energy Consumption per 100 Employees: Case Study IV, TAZ 27

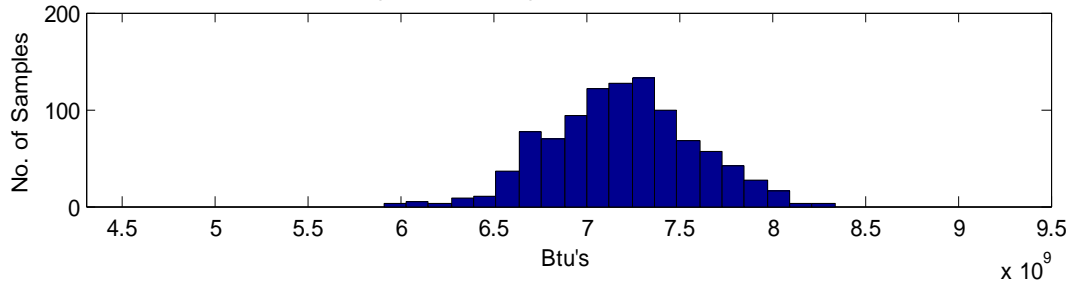


Figure 123: Combined HBW and NHB average annual SOV + HOV + drive-to-transit energy consumption per 100 employees for case study TAZs.

8.2.5.2. Impact of Estimated VTR

One of the important considerations of the site evaluation framework is the potential energy/emissions impact of travel demand management strategies. The framework is designed to account for the motorized VTR potential of unique sites and how this potential may impact the relative energy/emissions performance of the site alternatives. The following sub-sections present the estimated energy impacts of travel demand management programs and mixed-use development. It should be noted that the baseline HBW estimates already account for the TAZ-specific data for non-motorized mode share.

8.2.5.2.1. *Mixed-Use Development*

As was mentioned previously in Section 8.2.2.2, TAZ 27 contains the Atlantic Station mixed-use development. For this development, the estimated motorized VTR relative to the ARC travel demand model or CTTTP estimates of non-motorized mode share is 4 - 5 percent. The impact of this motorized VTR is presented below in Figure 124, which shows the HBW average annual SOV + HOV + D2T energy consumption per 100 employees for each of the case study TAZs, with a 4.5 percent motorized VTR in TAZ 27. The estimated motorized VTR in TAZ 27 shifts the estimated distribution of energy consumption lower, but the relative HBW transportation energy consumption performance of the sites remains unchanged (refer back to Figure 120).

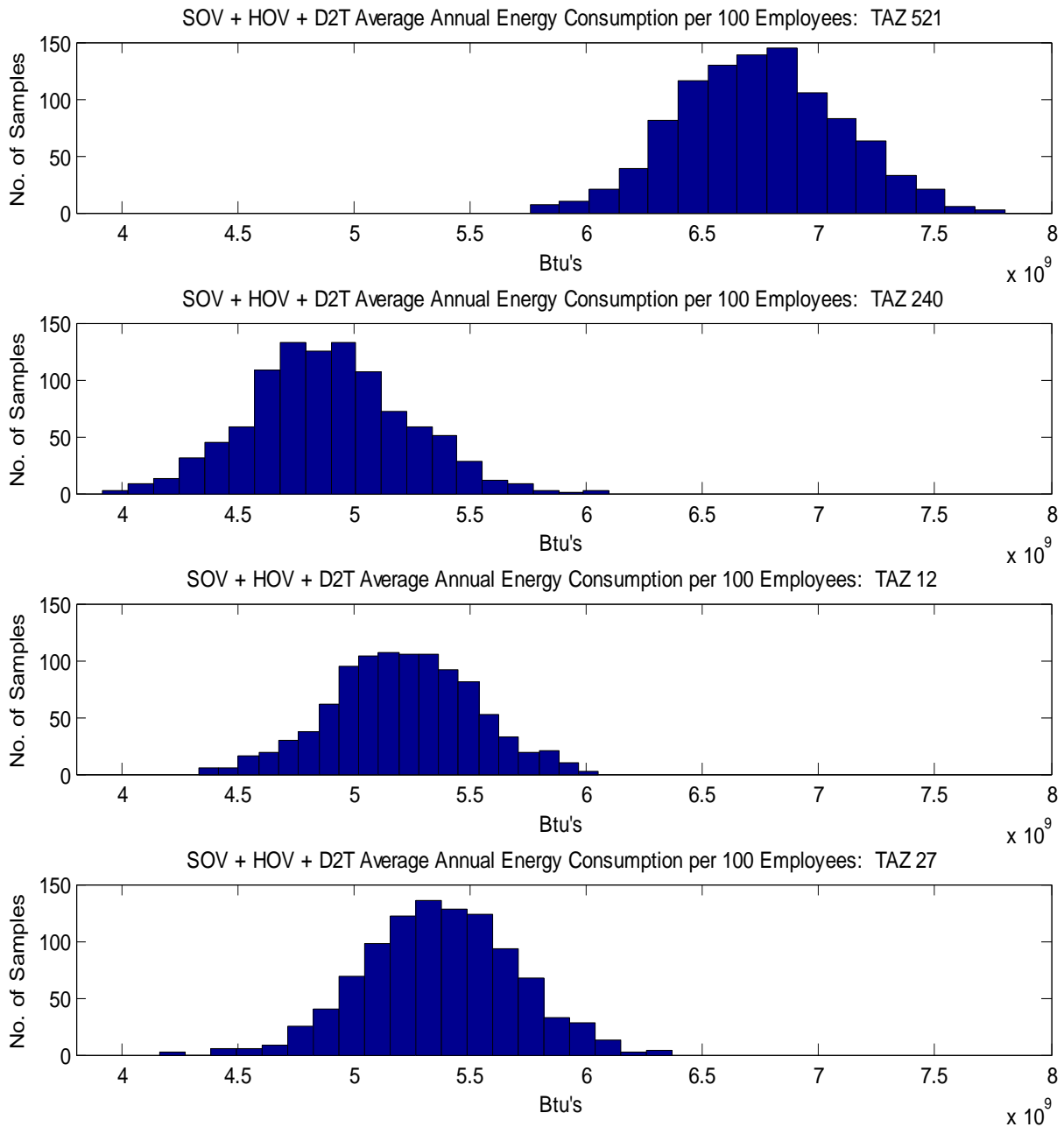


Figure 124: HBW average annual SOV + HOV + drive-to-transit energy consumption per 100 employees for case study TAZs, with 4.5 percent VTR in TAZ 27.

The following section presents the estimated energy impact of the intended travel demand management strategies.

8.2.5.2.2. *Travel Demand Management Programs*

The site-specific energy reduction potential of the selected travel demand management programs (see Section 8.2.2.3) are explored here to see if the estimated VTR of the programs influence the relative energy/emissions performance of the location alternatives. Figure 125 shows the HBW energy consumption with and without the trip reduction estimated from the FHWA TDM Guidance Manual. Each of the TAZs exhibit significant reductions in HBW transportation energy consumption as a result of the estimated VTR. However, the relative energy impacts of the estimated VTRs do not alter the relative performance estimated from the baseline energy estimates.

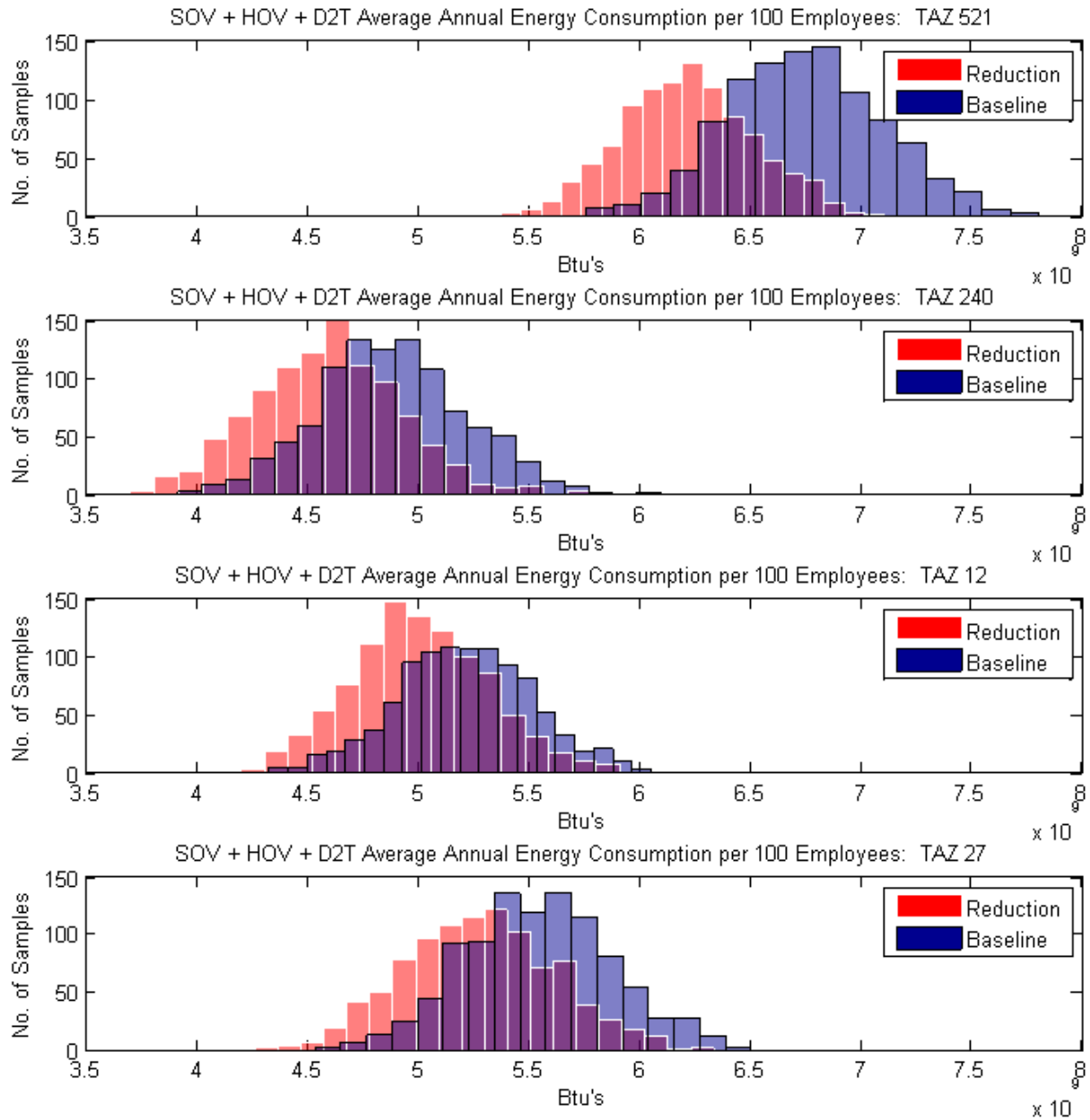


Figure 125: HBW energy consumption with FHWA TDM Guidance Manual trip reduction.

Figure 126 shows comparable results from the COMMUTER Model mode shift estimates. The estimated reduction in energy consumption is noticeably less in Figure 126 than

in Figure 125. Recall that the U.S. EPA COMMUTER Model yields a far more conservative estimate of mode shift and VTR than does the FHWA TDM Guidance Manual.

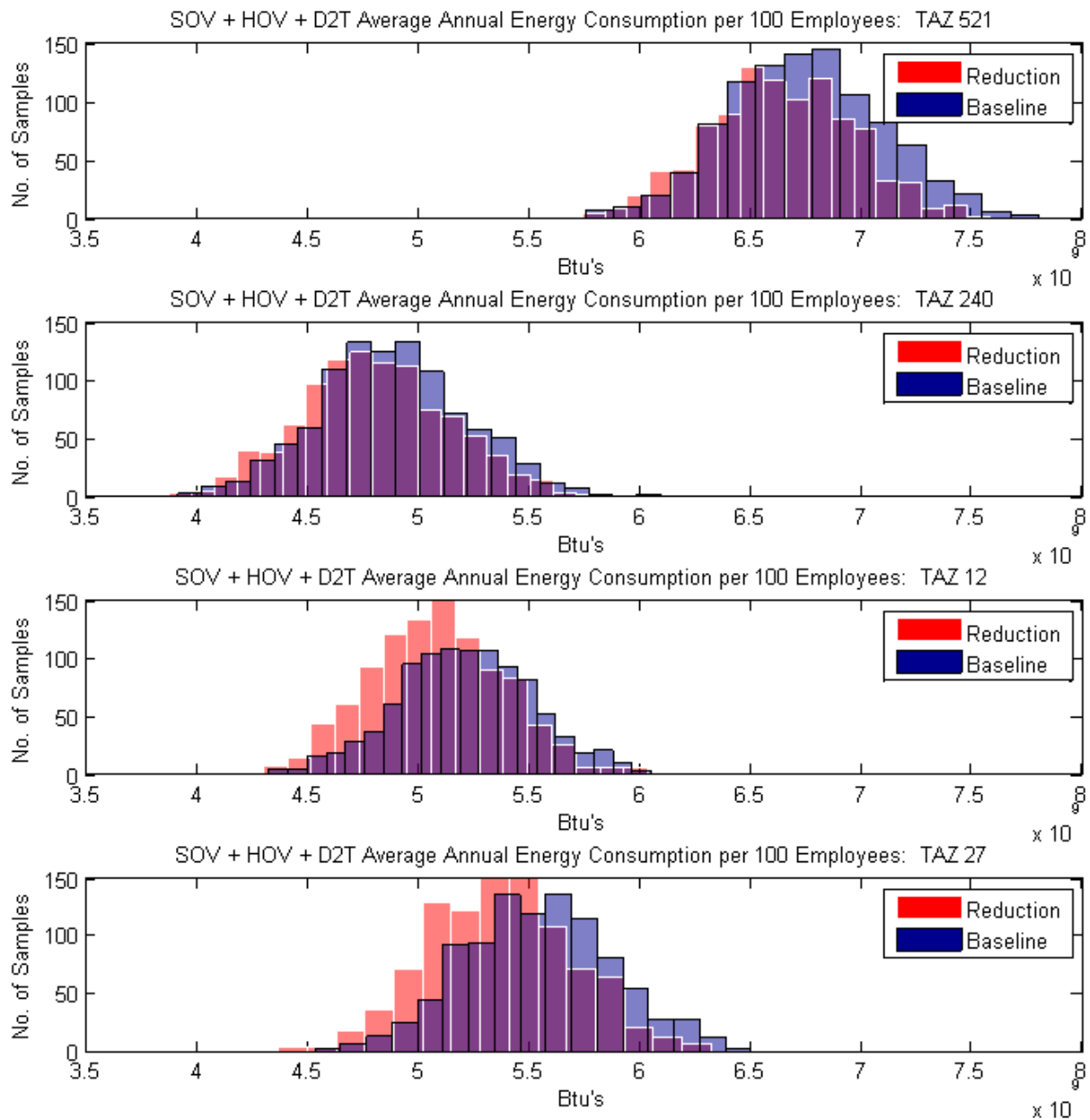


Figure 126: HBW energy consumption with COMMUTER Model mode shift.

In the MATLAB calculation script (see Appendix A), the VTR estimates from the FHWA TDM Guidance Manual are effectively translated into shifts in mode choice. Table 72 shows a comparison of trip distance, HOV mode share, and transit mode share from the baseline, FHWA Guidance Manual, and EPA COMMUTER Model estimates. The results indicate that the average trip distances remain fairly constant between the model runs and that the main differences are found in HOV and transit mode shares.

Table 72: Comparison of Trip Distance, HOV Mode Share, and Transit Mode Share from Baseline, FHWA TDM Guidance Manual, and EPA COMMUTER Model Estimates.

Case Study	I	II	III	IV
TAZ	521	240	12	27
Average SOV Trip Distance (mi.), Baseline	20.9	13.5	19.7	17.9
Average SOV Trip Distance (mi.), FHWA TDM	20.7	14.2	19.9	18.2
Average SOV Trip Distance (mi.), COMMUTER Model	20.9	13.6	19.7	18.0
Average HOV Mode Share, Baseline	7.6%	6.3%	2.9%	5.1%
Average HOV Mode Share, FHWA TDM	22.3%	21.3%	3.1%	7.3%
Average HOV Mode Share, COMMUTER Model	11.2%	9.8%	6.3%	9.0%
Average Transit Mode Share, Baseline	2.3%	2.3%	33.3%	8.8%
Average Transit Mode Share, FHWA TDM	0.9%	1.1%	38.1%	14.6%
Average Transit Mode Share, COMMUTER Model	1.7%	2.0%	33.1%	9.8%

8.2.6. Combined Transportation and Building Performance

In this evaluation framework, the energy consumption and GHG emission estimates of the transportation systems and building systems are ultimately combined into whole-building measures of performance. Table 73 below shows the normalized, combined, annual energy consumption and GHG emission performance of the case studies. The transportation component of the combined estimates does not include NHB trips nor the impact of the proposed travel

demand management strategies. The performance metrics correspond to the measures discussed in Section 3.3. The values are expressed as a mean \pm 2 standard deviations (see Equation 1). For all measures of performance the best performing alternative is Case Study II, although a considerable amount of uncertainty exists in the results.

Table 73: Normalized Combined Annual Energy Consumption and GHG Emission Performance

Performance Metric	Case Study			
	I	II	III	IV
Annual site energy / conditioned floor area [kBtu/SF]	321.2 \pm 14.7	229.4 \pm 14.4	255.0 \pm 13.2	256.6 \pm 14.9
Annual site energy / occupant use [kBtu/person-hrs]	32.5 \pm 1.5	23.2 \pm 1.5	25.1 \pm 1.3	25.9 \pm 1.5
Annual primary energy / conditioned floor area [kBtu/SF]	518.4 \pm 18.9	367.2 \pm 18.3	412.8 \pm 16.8	403.1 \pm 18.5
Annual primary energy / occupant use [kBtu/person-hrs]	52.4 \pm 1.9	37.1 \pm 1.9	40.7 \pm 1.7	40.6 \pm 1.9
Annual site GHGs / conditioned floor area [lb CO ₂ e /SF]	11,352 \pm 428.8	8,037 \pm 429.0	9,037 \pm 399.8	8,823 \pm 439.4
Annual site GHGs / occupant use [lb CO ₂ e /person-hrs]	1,147 \pm 43.3	812 \pm 43.4	891 \pm 39.4	889 \pm 44.3
Annual primary GHGs / conditioned floor area [lb CO ₂ e /SF]	14,033 \pm 529.4	9,951 \pm 486.0	11,167 \pm 452.8	10,953 \pm 502.2
Annual primary GHGs / occupant use [lb CO ₂ e /person-hrs]	1,418 \pm 53.5	1,005 \pm 49.1	1,101 \pm 44.7	1,104 \pm 50.6

In terms of site (direct) energy consumption, the majority of the combined energy consumption is contributed by the transportation systems. Figure 127 shows the relative proportion of direct, metered (site) energy consumption of the building and transportation

systems for each of the case studies. For all of the case studies, the direct energy consumption of the transportation systems is approximately five and a half times the energy consumption of the building systems. These relative results are more than twice as transportation energy-intensive as the results estimated by Wilson in his discussion of the potential transportation energy intensity of commercial office buildings (12). The difference between Wilson's results and the results presented here may be traced to differences in several important parameters. In this application of the evaluation framework, the buildings are estimated to be more energy efficient than the "code-compliant" building in Wilson's estimates. The difference in energy intensity can be partly explained by the fact that the national-level data used by Wilson includes other, heating-dominant climate zones that have higher building envelope loads. On the transportation side, the calculations presented in this chapter involve higher average trip distances, higher SOV mode shares, lower average fuel economy, and a higher frequency of annual trips. Each of these deviations from Wilson's assumptions contribute to a substantially higher proportion of transportation energy consumption.

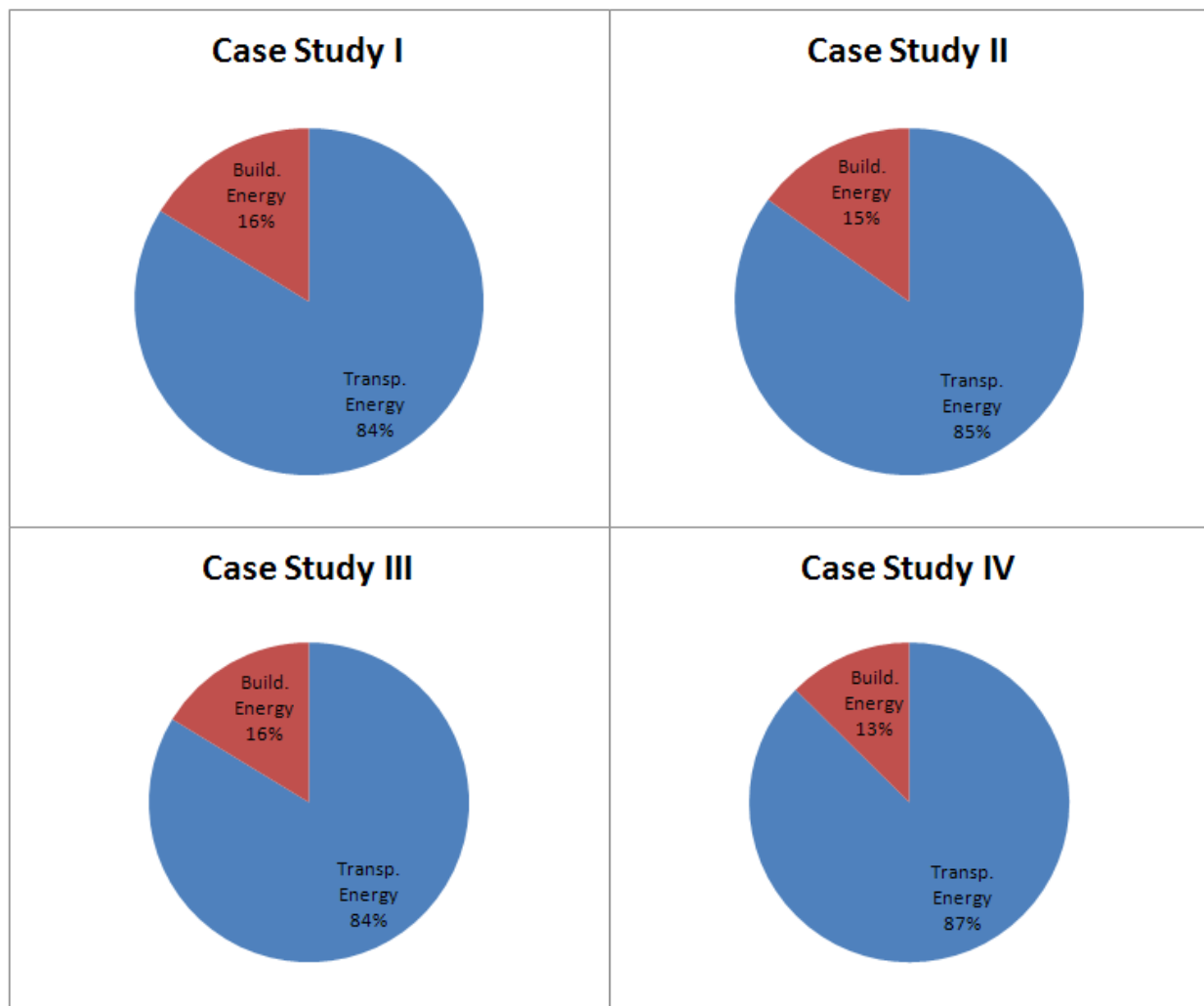


Figure 127: Relative proportion of direct, metered (site) energy consumption of building and transportation systems.

The proportion of transportation energy consumption to building energy consumption reduces significantly when measured in terms of primary energy consumption. Figure 128 below shows the relative proportion of direct plus upstream (primary) energy consumption of building and transportation systems for each of the case studies. The increase in the relative proportion of building energy consumption is due to the substantially higher losses in the electric energy supply chain. With power plant efficiencies of approximately 33 percent and transmission &

distribution (T&D) losses of approximately 8 percent, the ratio of primary to site energy consumption is much higher for electric utility energy use than for gasoline use (in this case 3.364 vs. 1.3).

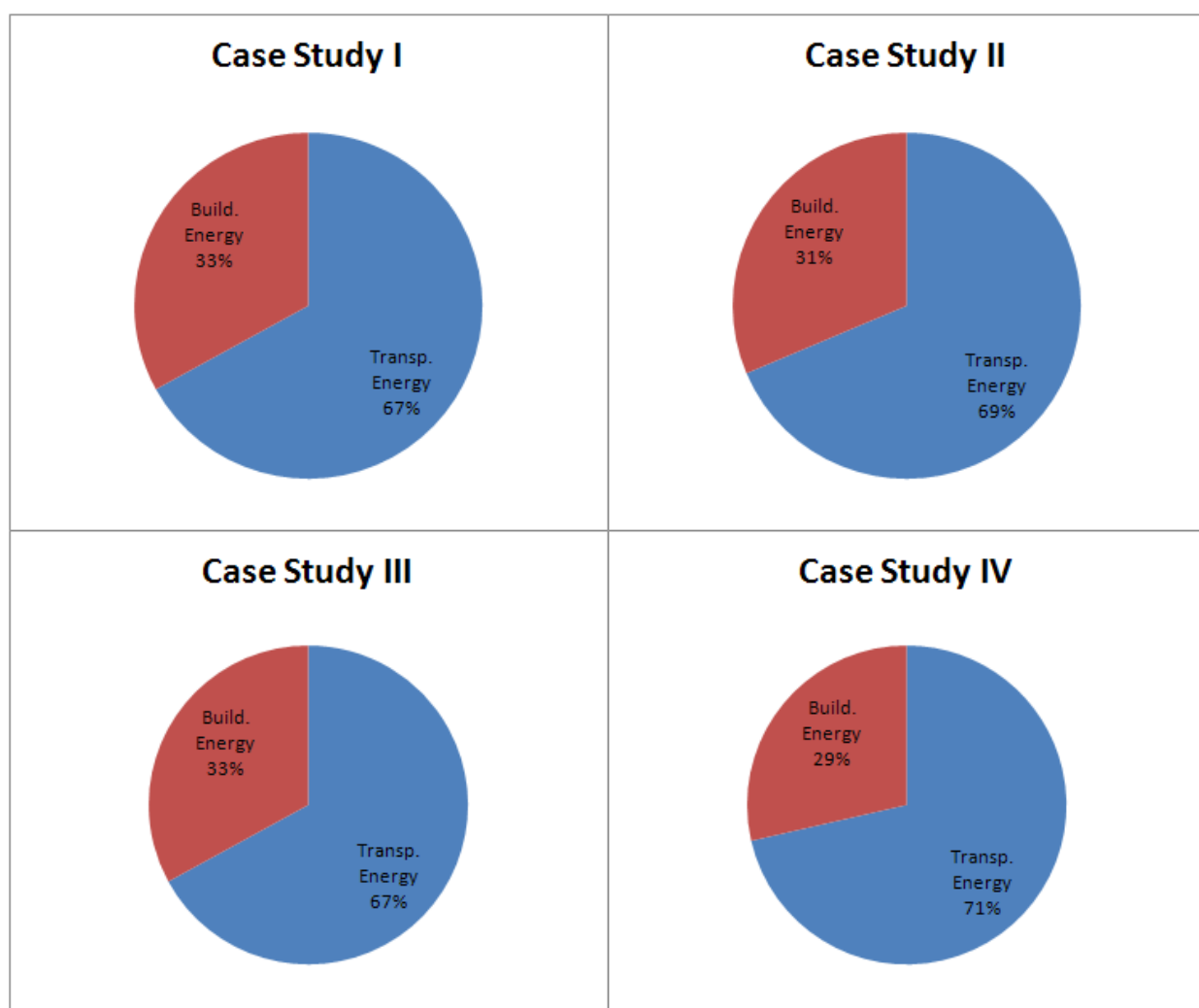


Figure 128: Relative proportion of direct plus upstream (primary) energy consumption of building and transportation systems.

The component contributions of site and upstream energy consumption for both the transportation and building energy systems are illustrated in Figure 129 below. Figure 129 shows

that the ratio of direct (site) to upstream energy consumption for the transportation systems is roughly the inverse of the same ratio for the building systems. Given the predominance of electric utility energy in office building systems and of gasoline fuels in private automobile transportation systems, the proportions shown in Figure 129 are likely representative of many office building/sites in North America. However, it should be stressed that the purpose of the framework is not to produce generalizable results, but rather to quantify building/site-specific estimates of performance. Nevertheless, it is interesting to note that the total difference in transportation energy consumption between the best performing (Case Study II) and worst performing site (Case Study I) is almost as great as the total energy consumption for the best performing building (Case Study II).

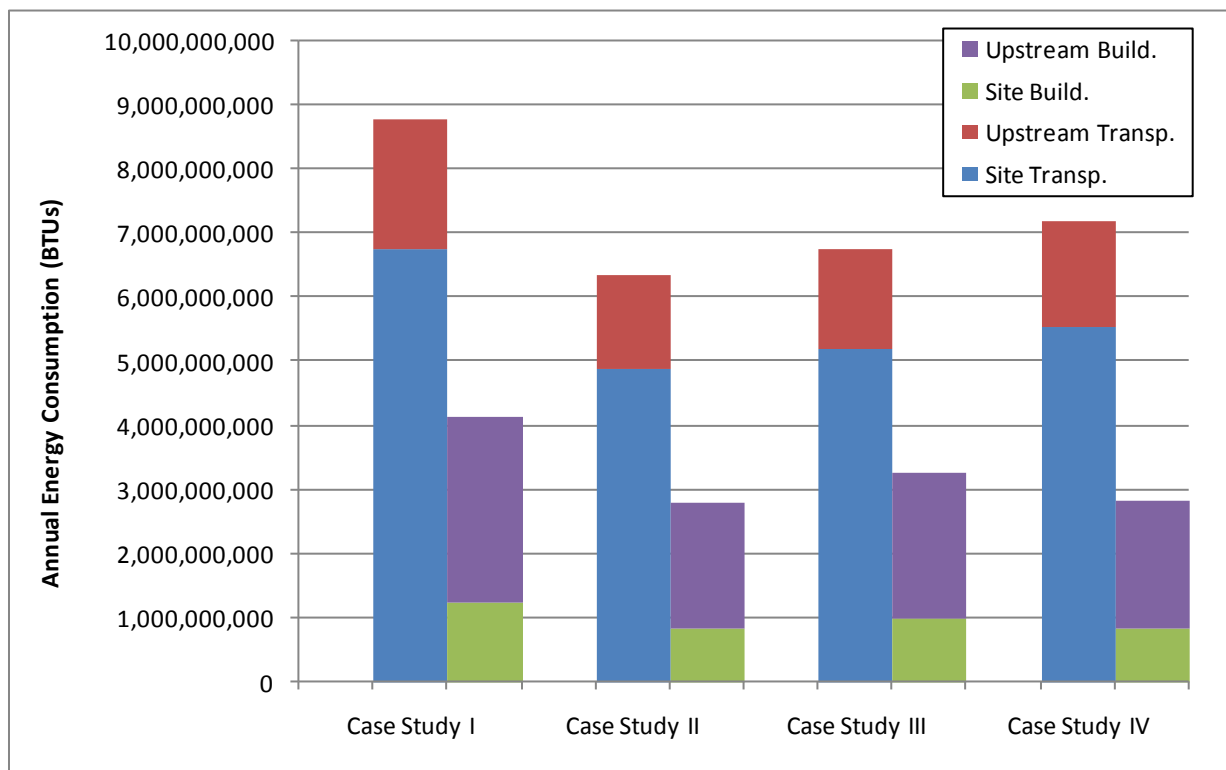


Figure 129: Annual building and transportation energy consumption (site and upstream).

In terms of GHG emissions, the relative proportion between the building systems and transportation systems is very similar to the proportions for primary energy consumption. Figure 130 and Figure 131 below show the relative proportion of GHG emissions of building and transportation systems for direct and primary emissions, respectively. This similarity exists because the most “direct” measure of electric utility emissions is the Scope 2 emissions. Thus, what is considered to be “direct” in GHG emission accounting is considered to be “primary” or “upstream” in energy consumption accounting. The similarities between the energy consumption pie charts and GHG emission pie charts can largely be explained by the fact that the majority of all energy supplied to the building and transportation systems are from GHG-intensive fuel sources. If more renewable and less carbon-intensive fuel/energy sources were utilized, either on-site or in the utility power mix, then the GHG emissions performance of the buildings/sites would become less correlated with the energy consumption performance.

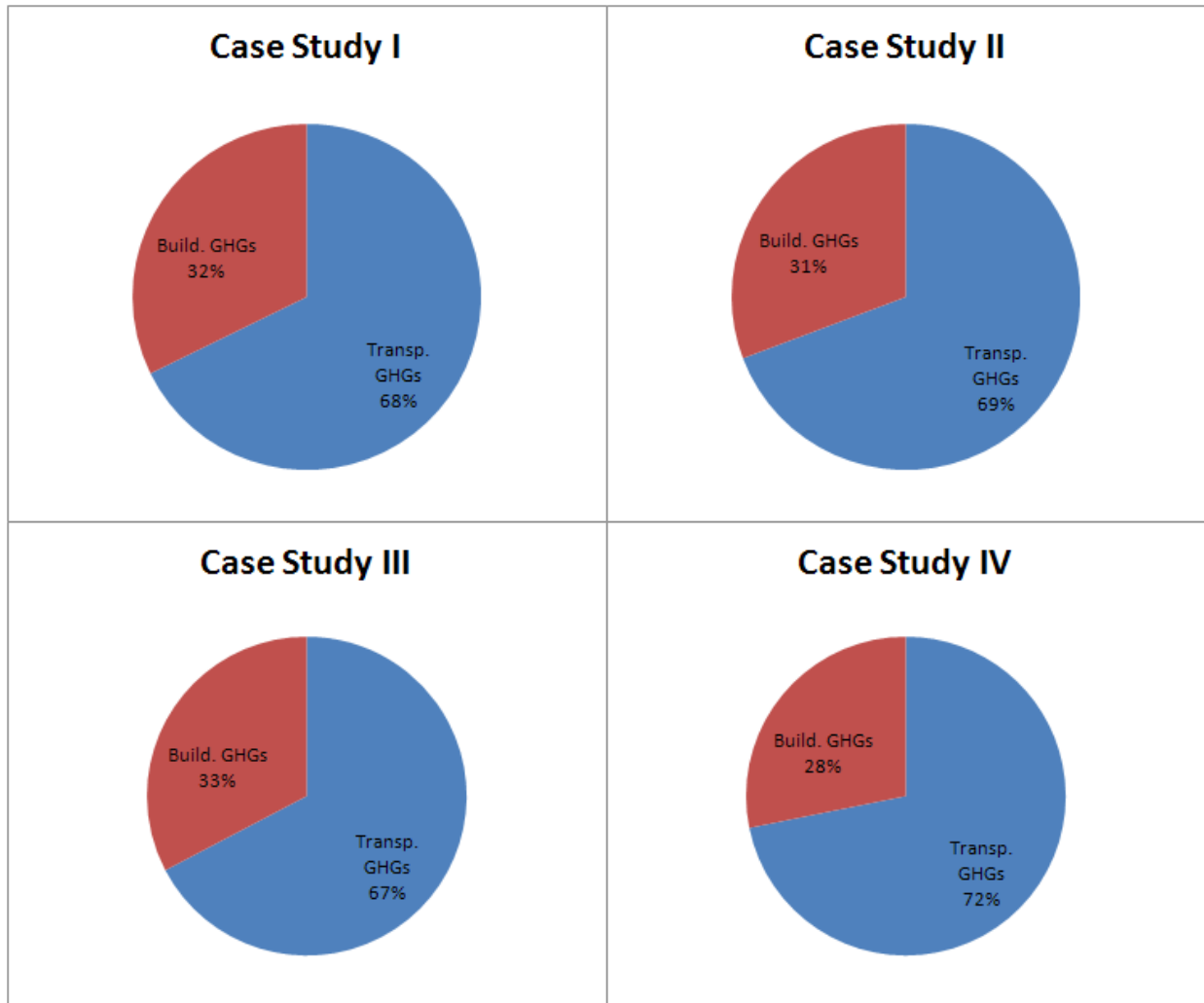


Figure 130: Relative proportion of direct GHG emissions of building and transportation systems (Scope 1 and 2).

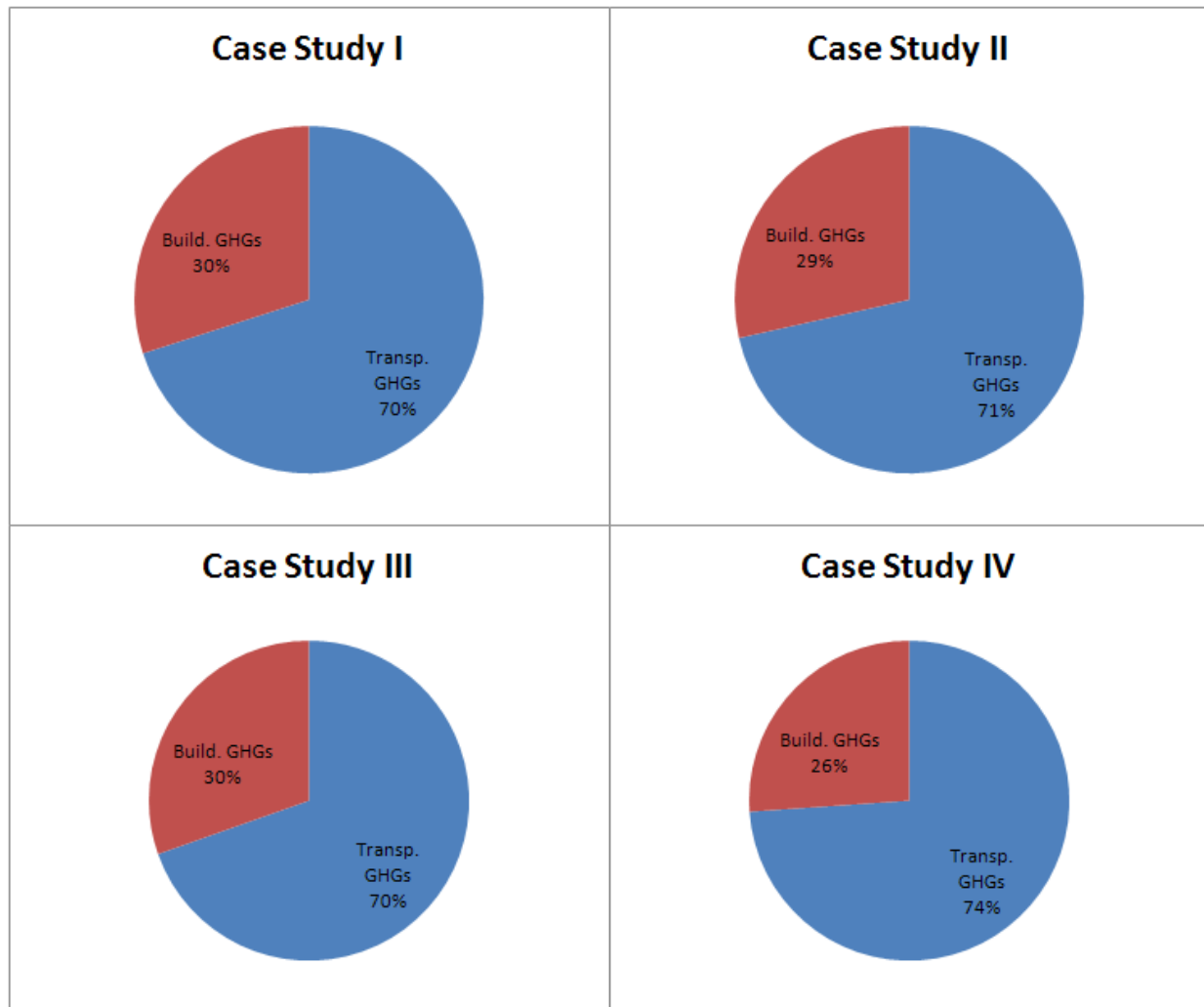


Figure 131: Relative proportion of direct plus upstream (primary) GHG emissions of building and transportation systems (Scope 1, 2, and 3).

The relative contribution of direct and indirect GHG emissions from the transportation and building systems for each of the case studies is shown in Figure 132 below. The higher proportion of upstream emissions for the transportation energy systems is yet another factor contributing to the dominance of transportation systems in a whole-building evaluation of GHG emissions performance.

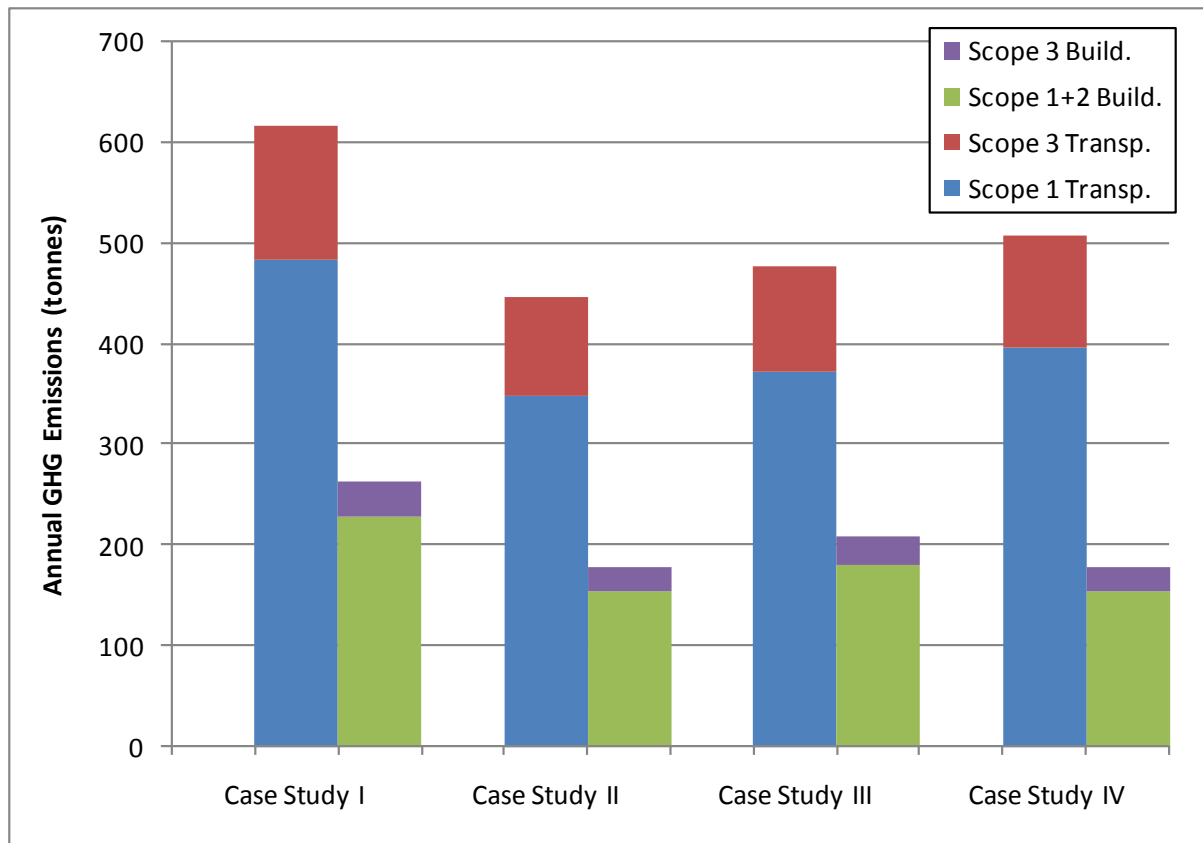


Figure 132: Annual building and transportation GHG emissions (Scope 1, 2, and 3).

The relative combined transportation and building energy consumption of the case study buildings/sites is perhaps best illustrated by the distributions of estimated energy consumption. Figure 133 below shows the combined transportation and building site energy consumption for the initial building Monte Carlo analysis. The transportation component of the combined estimates does not include NHB trips nor the impact of the proposed travel demand management strategies. The transportation and building energy consumption distributions were combined by sampling from the PDFs of each of the distributions (see Appendix E). The initial building Monte Carlo analysis for Case Study I and Case Study III produced a high degree of skew (see Sections 7.1.2.3 and 7.1.4.3). This skew is evident but less pronounced in Figure 133. One important insight from the figure below that was not apparent in the individual building case

study analyses of Chapter 7 is that the skew in Case Study I and Case Study III has no impact on determining the best performing site. Therefore, combining the transportation and building energy consumption distributions early in the analysis process can help to reduce the time and effort expended to collect more precise input data and to run additional Monte Carlo simulations. The combined transportation and building site energy consumption for the revised building Monte Carlo analysis is shown in Figure 134.

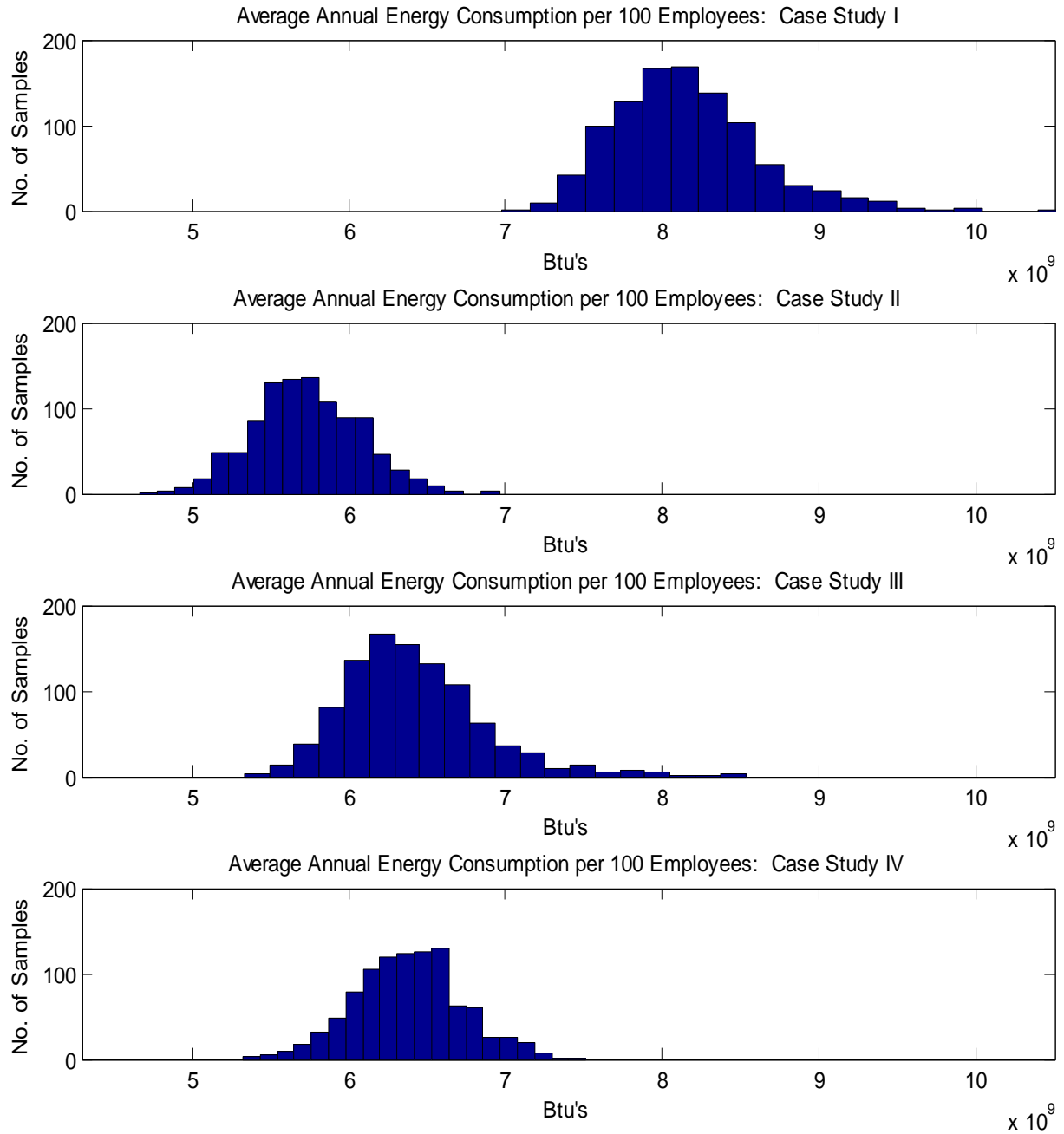


Figure 133: Combined transportation and building site energy consumption per 100 employees for initial building Monte Carlo analysis.

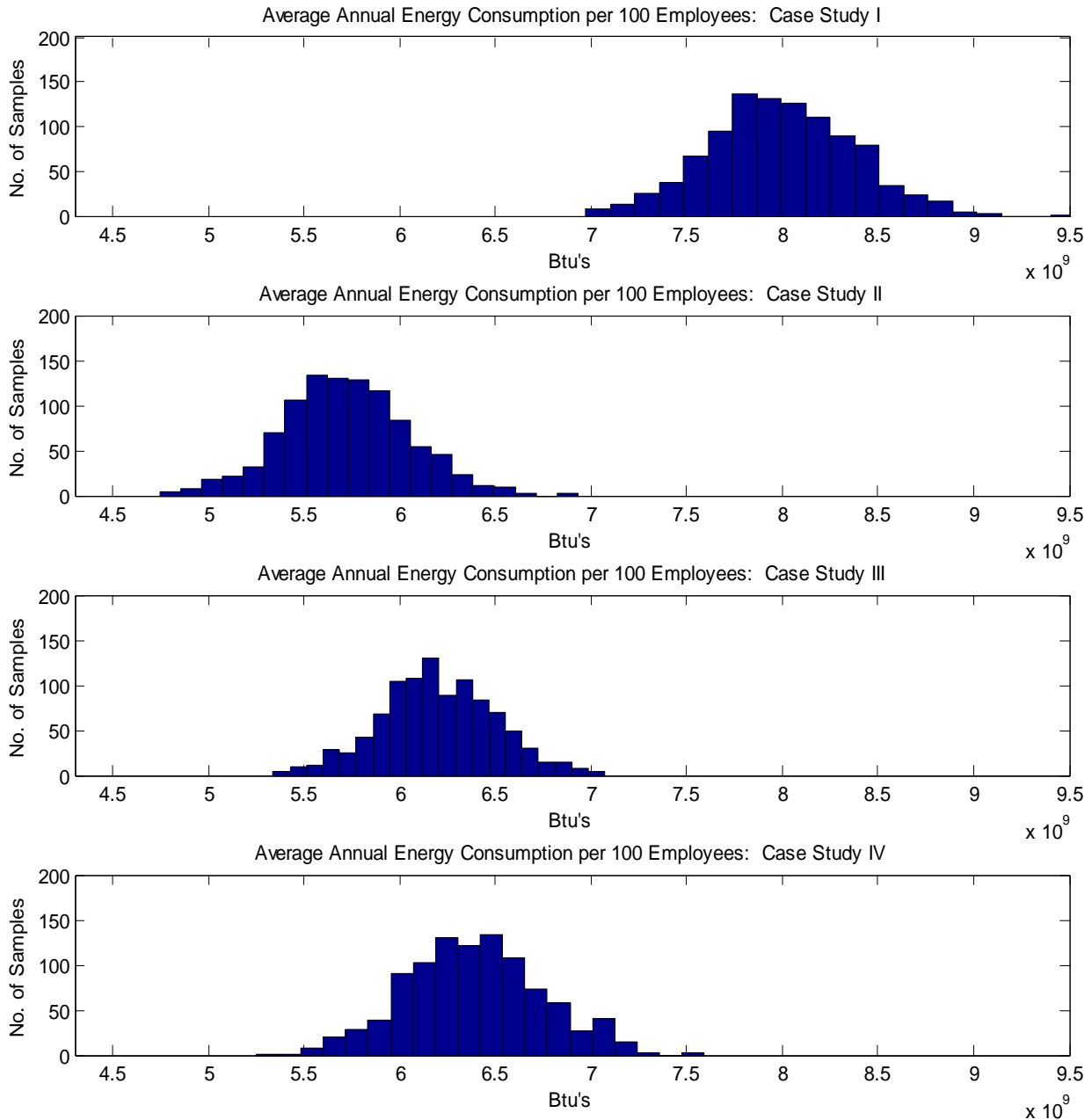


Figure 134: Combined transportation and building site energy consumption per 100 employees for revised building Monte Carlo analysis.

The combined *primary* energy estimates shown in Figure 135 below indicate a similar relative rank in performance. The relative performance of TAZ IV is slightly improved in Figure 135 due to the superior building energy performance of this case study and the lower ratio of

upstream to direct energy consumption for the building energy systems relative to the transportation energy systems. Nevertheless, Case Study II remains as the overall best performing site.

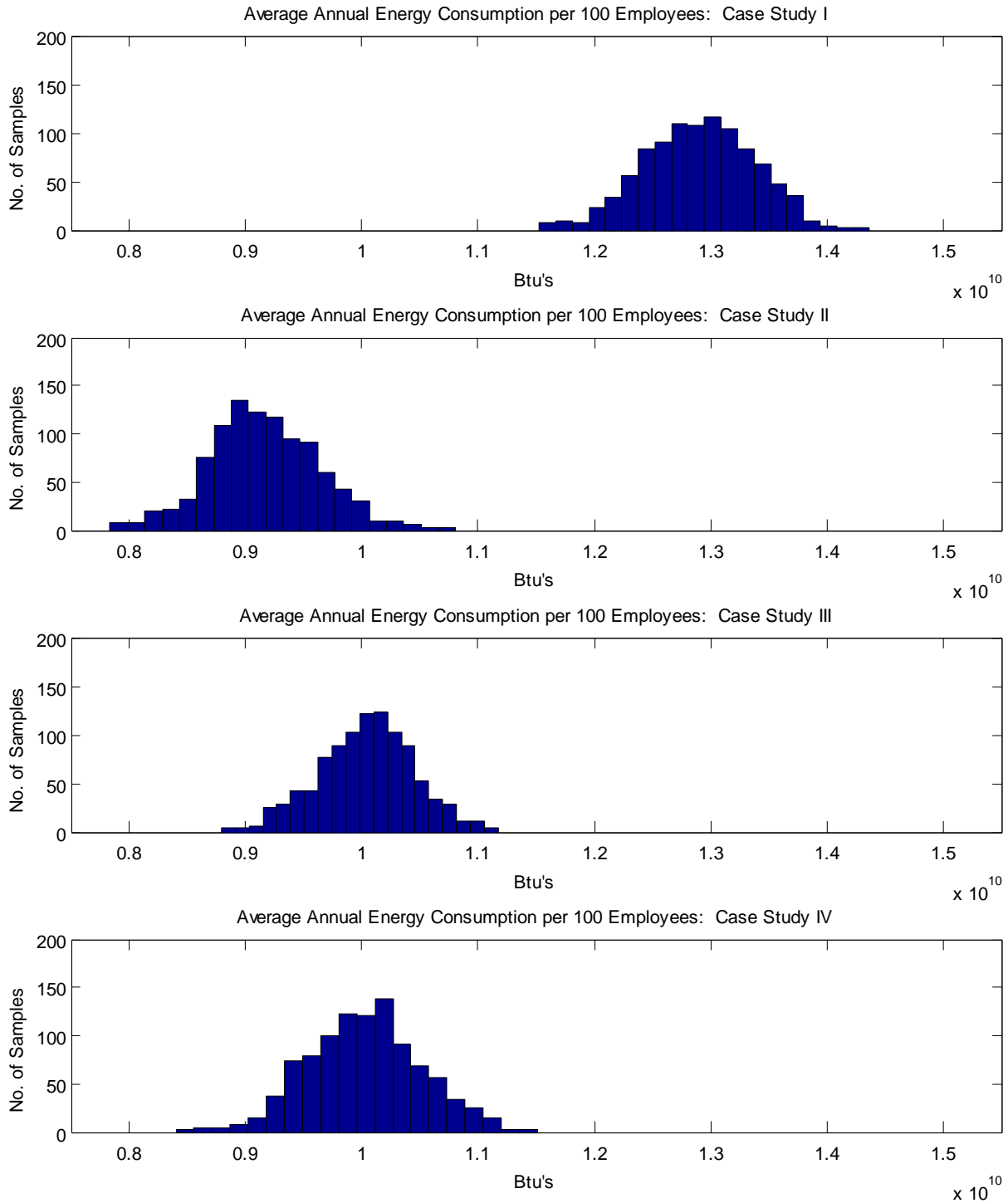


Figure 135: Combined transportation and building primary energy consumption per 100 employees for revised building Monte Carlo analysis.

In terms of GHG emissions, the distributions for each of the case studies are very similar to the energy estimates. Figure 136 below shows the combined transportation and building primary GHG emissions for each of the case studies.

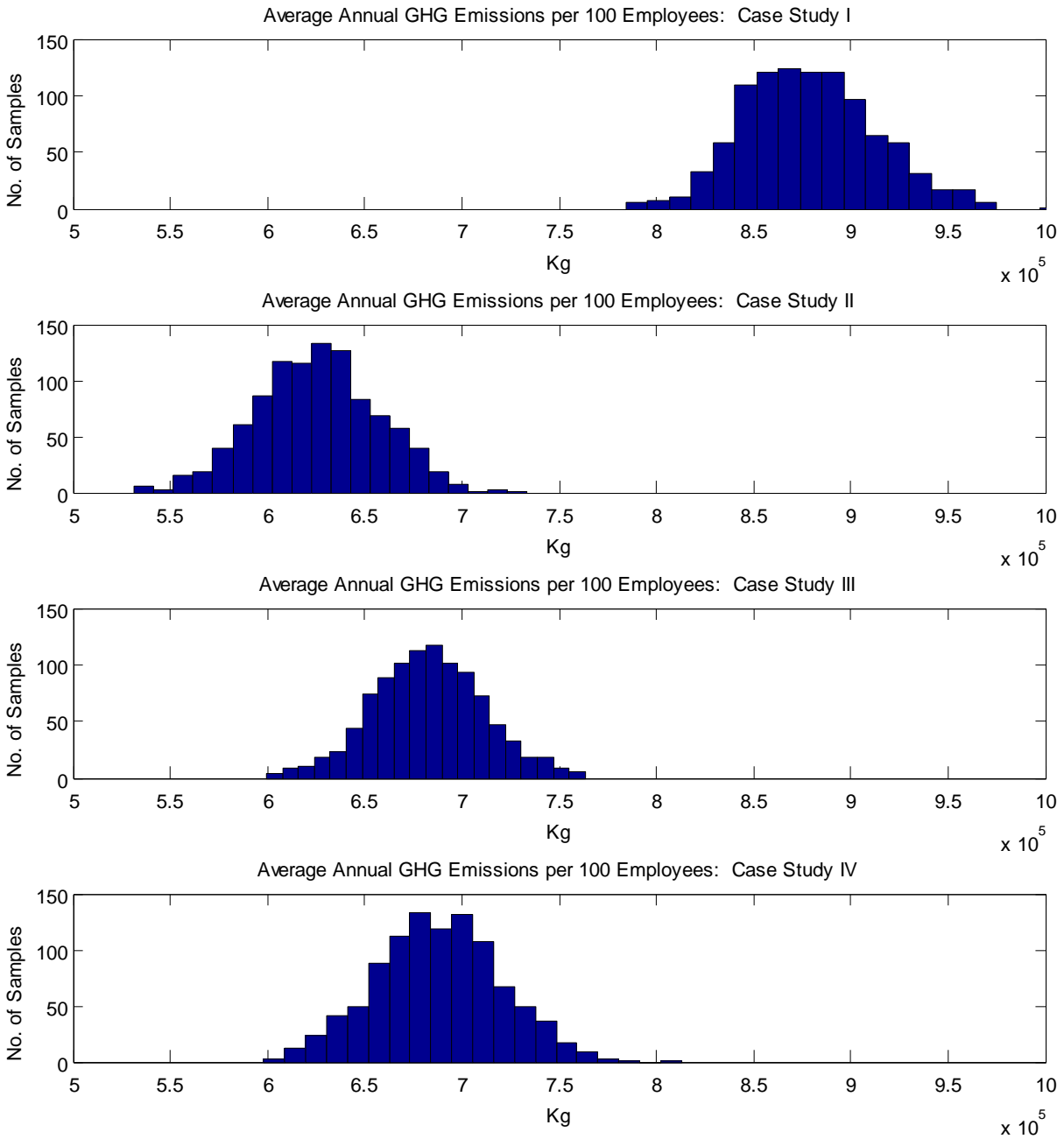


Figure 136: Combined transportation and building primary GHG emissions per 100 employees for revised building Monte Carlo analysis.

8.2.6.1. Probabilities of Relative Performance

The developed framework is intended to help office location decision-makers assess the relative energy/emissions performance of alternative buildings/sites under uncertainty. From the Monte Carlo simulation outputs of transportation and building energy consumption, it is possible to calculate the probabilities of relative performance. The Monte Carlo output histograms may be converted to probability distribution functions (PDFs) through a mathematical process known as kernel density estimation or kernel smoothing. The kernel density function in MATLAB was used to convert the combined energy consumption histograms into a smooth PDF. Figure 133 shows the PDFs of the estimated annual combined transportation and building energy consumption for Case Studies II and III. The overlap of the PDFs indicates the possibility of higher energy consumption for Case Study II, even though Case Study II has the lowest mean energy consumption. Thus, a decision-maker may wish to know the probability of achieving energy savings from one building/site alternative relative to another.

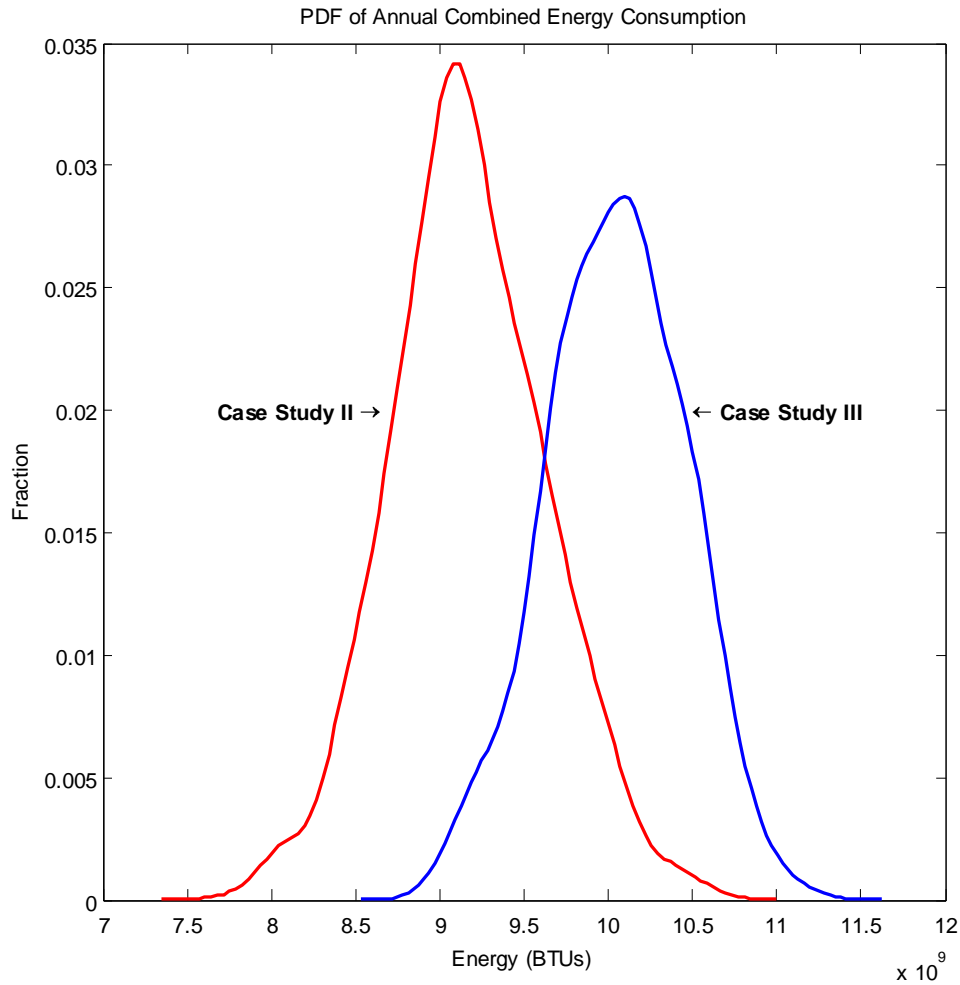


Figure 137: Probability distribution functions of estimated annual combined transportation and building energy consumption for Case Study II and Case Study III.

The probability of Case Study II saving energy relative to Case Study III may be calculated from the PDFs of estimated annual energy consumption. Appendix E contains the MATLAB code used to combine the transportation and building energy consumption distributions, and to calculate the probability of energy savings. Each of the PDFs are discretized into 100 intervals by the kernel smoothing function. In the nested loops following the use of the kernel smoothing function, the discrete differences in energy consumption between the two

curves are taken, with the probability of each difference calculated as the product of the independent probabilities. The probabilities are then added together for each of 100 bins of estimated energy savings (negative energy consumption). The result is a PDF of energy savings between two building/site alternatives. Figure 138 below shows the cumulative distribution function (CDF) of estimated annual combined transportation and building energy consumption saved for Case Study II relative to Case Study III. The probability of saving more than 0 Btu's of energy is 92 percent. The probability of saving the mean difference in combined energy consumption (873,400,000 Btu's) is 53 percent.

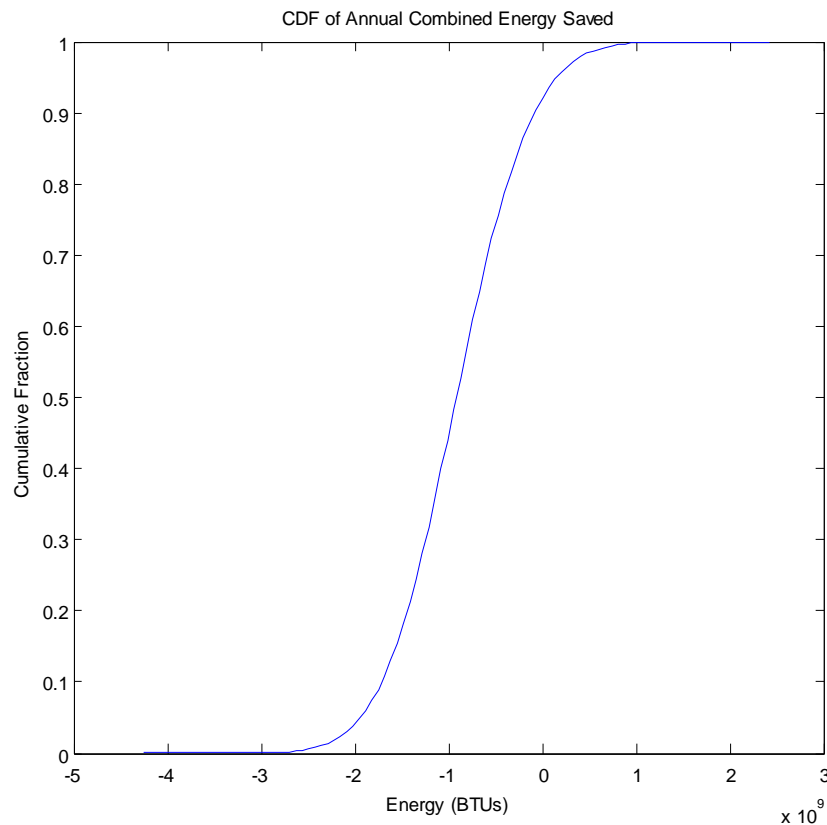


Figure 138: Cumulative distribution function of estimated annual combined transportation and building energy consumption saved for Case Study II relative to Case Study III.

8.2.6.2. Impact of Scale

The scale of a building/site (i.e. number of employees, square footage of work space) will undoubtedly impact the estimated total energy consumption, and perhaps also the normalized performance. In this evaluation framework, the scale of a building/site is accounted for by the user's selection of comparable building/site alternatives – comparable in terms of both size and service. The scale of building/site alternatives may present unique building and transportation efficiencies for larger facilities or larger employee populations (e.g. on-site cogeneration or renewable energy plants, employer-based vanpool programs, etc.). From a policy/implementation perspective, building/site scale plays a role in the number of site selection decisions taking place in the marketplace (i.e. frequent small-scale scenarios and less-frequent large scale scenarios), and the degree of impact for each of those decisions. These issues of scale may be investigated through market studies of site selection decisions and by applying the framework to smaller and larger scale developments.

One impact of scale explored in this section is the impact on the uncertainty of transportation system estimates. In the transportation system calculation procedures, one of the most important parameters influencing estimated energy consumption and GHG emissions is the average trip distance. The trip distances are estimated through a process of sampling trip origins from the regional travel demand model trip tables. The dispersion of the estimated trips distances and the concomitant energy and emissions estimates is sensitive to the number of origins sampled. Assuming that the trip distribution model of a regional travel demand model is a reasonable representation of the average commute shed to a given location, as the number of trips sampled from a trip origin PDF increases, the average trip distance for the sample will

approach the average trip distance of the population (i.e. the trip table). As the sample mean approaches the population mean, the variance of sample means decreases for each run in an iterative Monte Carlo simulation, thereby decreasing the dispersion in the simulation results. The number of origins sampled is of course dependent upon the number of employees commuting to/from the commercial office location. Thus, as the number of employees increases for a given set of location alternatives, one would expect the dispersion and subsequent overlap of energy/emission estimates for each of the alternatives to decrease. To test this relationship, the HBW transportation energy calculation script was run for 300 employees in each of the case study TAZs. Figure 139 shows the HBW average annual SOV + HOV + D2T energy consumption per 300 employees for each of the case study TAZs. By comparing Figure 139 to the result estimated for 100 employees in Figure 120, one can see that the overlap in the estimated distributions is reduced for the 300 employee scenario.

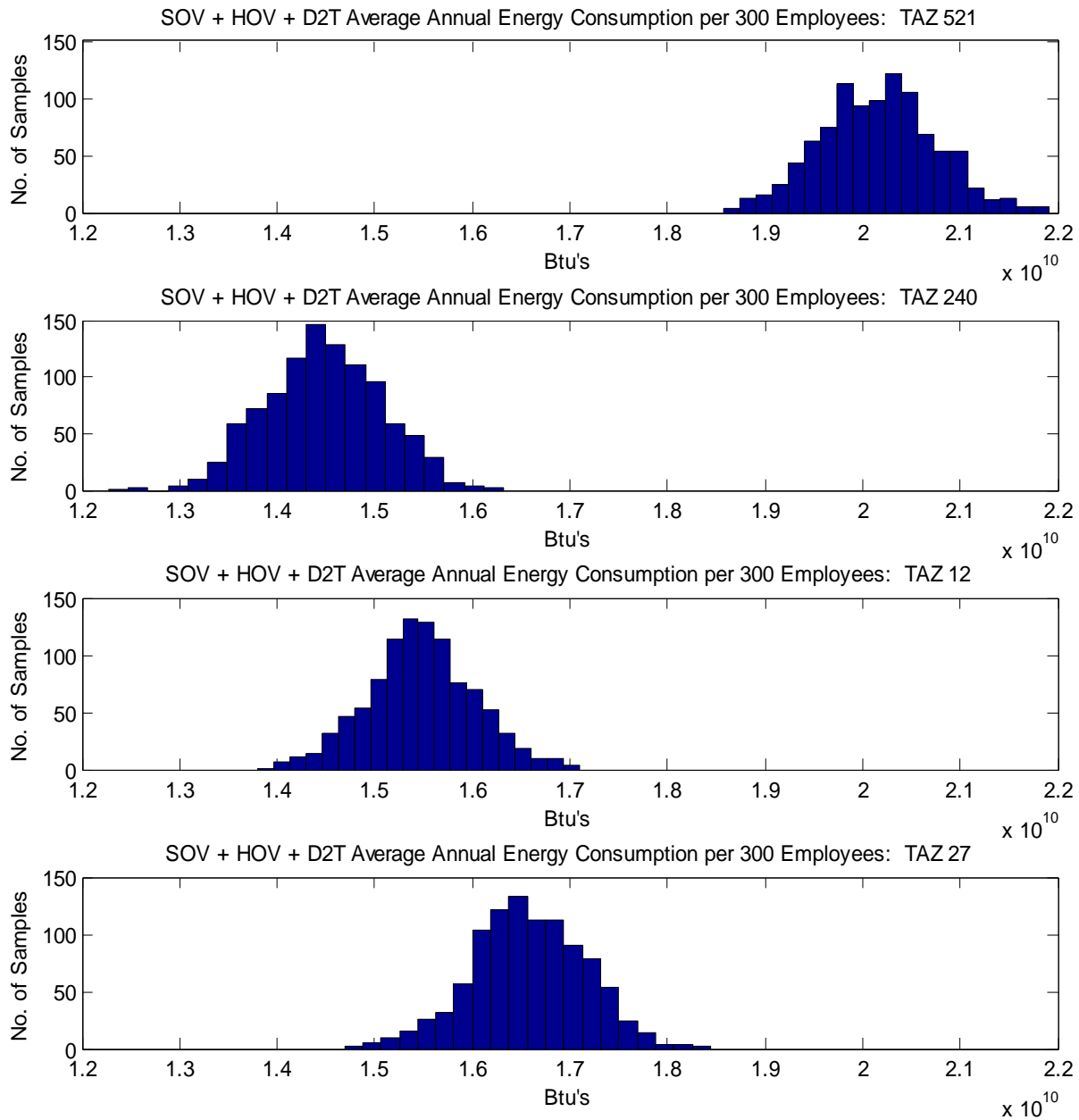


Figure 139: HBW average annual SOV + HOV + drive-to-transit energy consumption per 300 employees for case study TAZs.

The reduction in dispersion for higher employee populations is explained mathematically by the definitions of standard deviation and the coefficient of variation, shown below by Equation 22 and Equation 23, respectively:

Equation 22

$$s = \sqrt{\frac{1}{N-1} \sum_{i=1}^N (x_i - \bar{x})^2}$$

where: s = Sample standard deviation
 N = Number of samples (observations)
 x_i = Value of the i^{th} observation
 \bar{x} = Mean of observations

Equation 23

$$C_v = \frac{s}{\bar{x}}$$

where: C_v = Coefficient of variation

Increasing the number of observations, N , will have the effect of increasing both the numerator and denominator of Equation 22. It should be noted that the standard deviation of concern is not the standard deviation of a sample of n employees, but rather the standard deviation of the average observations (e.g. average energy consumption) for the Monte Carlo simulation runs. If the standard deviation decreases relative to the mean, then the coefficient of variation will decrease. In the case of increasing the number of employees from 100 to 300 in Monte Carlo simulations of 1,000 runs, the coefficient of variation for the estimated HBW transportation energy consumption decreases by approximately 40 percent. The decrease in dispersion for higher numbers of employees effectively increases the probability that the relative difference in energy consumption (between the estimated means of site alternatives) will occur.

The higher dispersion for Monte Carlo Simulations of fewer employees is essentially a matter of sampling error. Based on this relationship between the number of employees and the dispersion of estimated energy consumption, at some minimum number of employees the overlapping area of a pair of PDFs would become large enough to preclude a sufficiently confident determination of the relative energy performance.

CHAPTER 9

CONCLUSION

Realization of a more sustainable built environment that meets the challenges of climate change mitigation and energy conservation will require greater efficiencies in transportation and building systems. While the deployment of new technologies will hopefully provide much of the efficiency gains needed, significant gains in efficiency must still be leveraged from the efficient utilization of new and existing transportation and building systems. This building/site evaluation framework can help to improve the efficient utilization of transportation and building systems by helping commercial building occupants satisfy their space and access needs with the most efficient transportation and building infrastructure available in the marketplace. The application of the evaluation framework to case studies of commercial office development provides insight into the opportunities for more efficiently utilizing transportation and building systems in the built environment – specifically, that a tenant’s whole-building energy consumption and GHG emissions are sensitive to building/site location, and that site-related transportation is a major component of overall performance.

The developed calculation framework contributes a novel, trip attraction-centered, performance-based approach for estimating potential, baseline work-trip energy consumption of office location alternatives. The application of the developed framework shows how region-specific modeling resources may be leveraged to evaluate spatial variations in transportation energy efficiency. Although regional travel demand model data introduces unspecified errors (i.e. uncalibrated values) in sub-regional travel activity, the travel demand model data more directly supports present and future year estimates of travel activity than do data from historical

surveys. Importantly, the sampling process incorporated into the calculation framework supports an explicit accounting of input parameter uncertainty and the propagation of error to estimated outputs.

From a building energy consumption and GHG emissions perspective, the developed framework provides an approach for evaluating existing building infrastructure. The approach is focused on minimizing energy consumption by identifying which existing building alternative offers the lowest baseline energy and/or emissions. In their current form, green building rating systems account for existing building baseline energy consumption only after a site has been selected. The selection and development of buildings/sites with a lower baseline of energy consumption and GHG emissions represent a new opportunity for improving the efficient utilization of building and transportation infrastructure in the built environment.

In the developed framework, the process of combining building performance with transportation performance speaks to the potential synergies of efficient transportation and building systems. For example, in dense urban development areas (CBDs) characterized by multi-tenant office towers and high capacity public transit service, the whole-building energy performance of a commercial office building/site could be enhanced by both the architectural impacts of the setting (e.g. reduced envelope-to-floor area ratio, and higher efficiency high-capacity heating and cooling systems, including district heating and cooling) and the transportation impacts of the setting (e.g. higher public transit mode share and greater potential for mode shift through parking pricing). Synergies may also exist in a suburban context, such as a higher potential for onsite, solar PV power generation coupled with shorter travel access to/from commuter bedroom communities. Acknowledgement of such synergies is important for the development and delivery of policies designed to improve the efficient utilization and

development of commercial buildings/sites (see Section 9.1). In instances where such synergies do not exist, the framework's whole-building evaluation perspective may help to inform the creation of cost/benefit sharing mechanisms addressing tradeoffs between building system and transportation system performance.

The potential impact of the commercial building/site evaluation framework can be enhanced not only by the policy opportunities discussed in the following section, but also by a larger evaluation framework that extends beyond the decision-point of building/site selection. Opportunities for improving the whole-building energy and emissions performance of a building site exist as a continuum throughout the life cycle of a building/site. Notable opportunities include building design, major renovations, minor retrofits, TDM program implementation, building commissioning, and building retro-commissioning. As the AEC industries move toward a building performance paradigm that incorporates regular monitoring of performance (e.g. the City of New York's Local Law 87), the opportunities for evaluating, managing, and improving whole-building energy performance will likely increase.

9.1. Policy Opportunities for Encouraging the Selection of Efficient Buildings/Sites

The framework represents an effort to operationalize performance-based, energy consumption assessments of location choice from the perspective of office location decision-makers. This perspective departs from the predominant macro-level perspective of traditional transportation and land-use planning, yet it utilizes regional transportation and land-use modeling resources. "Green building" ratings systems aimed at assessing location efficiency and sustainability have formalized the micro-level perspective of energy conservation through location choice (e.g. sustainable site transportation credits), but have so far lacked a supporting,

performance-based framework for evaluating the transportation energy consumption of development sites before they are occupied. The research presented in this dissertation provides a working framework for quantifying potential transportation access energy consumption and baseline building energy consumption of office location alternatives.

By itself, the commercial building/site evaluation framework is likely not a sufficiently compelling instrument for influencing the selection of more efficient buildings or sites. Energy and emissions efficiency through location choice may be of interest to a location decision maker; however, minimization of energy consumption and GHG emissions will very likely compete with other important considerations for location choice. Although the purpose of this research is not to model the process or criteria for office firm location choice, it should be recognized that the influence of building/site energy and emissions performance information on location decisions would be made more relevant or impactful if the information were integrated with policy mechanisms that can help to influence the selection of more efficient buildings/sites.

To encourage the selection of more efficient buildings/sites, three primary types of policy mechanisms may be leveraged: development regulations, financial incentives/disincentives, and green building rating systems.

9.1.1. Development Regulations

Development regulations are particularly important for removing barriers to more efficient use of transportation networks. Commercial development in most all urbanized areas in North America is regulated by land-use and zoning laws. These laws/regulations may prevent commercial development (e.g. office space) in locations that enable more efficient work-trip patterns on a regional transportation network. The transportation procedures of the transportation

system evaluation framework can help to identify zones within a region that are potentially the most location-efficient and for which new or revised commercial zoning laws can help to accommodate efficient utilization of transportation infrastructure.

One particular development regulation process that can help to encourage the development of more efficient commercial sites is the review of TIAs for DRIs (see Section 2.6). The processes involved in the permitting of major developments could utilize the evaluation framework presented in this dissertation to quantify the transportation energy impacts. The quantified impacts could then be compared to a regional minimum benchmark of performance. The scale of development would play an important role in the evaluation process (see Section 8.2.6.2). As with traditional DRIs, only developments meeting a minimum size criterion would fall under the review of DRI regulations. Larger DRIs are likely to have more opportunities for mixed use internal trip capture and TDM ridesharing efficiencies, which can add complexity to the evaluation.

9.1.2. Financial Incentives/Disincentives

Financial incentives/disincentives are another major category of policy mechanisms for encouraging the selection of efficient buildings/sites. As has been mentioned previously, this dissertation does not attempt to model commercial office firm location choice; however, it is fair to say that financial cost is a substantial consideration in selecting a preferred location alternative. Therefore, financial incentives/disincentives from public agencies concerned with energy conservation and GHG emission mitigation may help to influence commercial office location decisions that minimize the marginal increases in energy consumption and GHG emissions arising from the utilization of building and transportation system infrastructure. The

location efficient mortgage model of residential location efficiency and financing (see Section 2.5.1.2) could be applied to commercial office development in two ways through the use of the evaluation framework's transportation and building system calculation procedures. One way is simply to help finance buildings/sites that are more costly than less efficient alternatives, and that meet a minimum energy (or emissions) performance target. The energy cost savings could then be used to payback the capital financing. Another option for incentivizing/financing the selection of efficient buildings/sites is to allow a transfer of cost savings between the transportation and building systems. This process follows the model of residential location efficient mortgages; however, it is complicated by the fact that the building costs and transportation costs are the responsibility of separate agents. It is highly unlikely that the transfer of commuter cost savings from employees to an office building owner/leasee would be tenable. If, however, the potential reduction in transportation energy/emissions is supported by a public agenda for transportation efficiency, then the use of public funds may help to indirectly transfer some of the cost savings between the transportation and building systems.

Justification of the use of public grants, loans, credits, fees, or taxes requires a performance evaluation perspective that extends beyond the building/site alternative choice set considered by a location decision maker. That is to say, the best performing alternative among a decision maker's choice set may not be sufficiently efficient to warrant the use of public resources. Regional benchmarks of performance (e.g. mean or N^{th} percentile performance) should be developed and used to determine the eligibility of building/site alternatives for financial incentives or disincentives. As has been shown in this dissertation, such benchmarks may be derived from the evaluation framework's transportation calculation procedures, and from building performance databases and standards (e.g. CBECS database and ASHRAE Standard

100-2006). The overall goal of the financial incentives/disincentives discussed here is to allow the market to become more efficient by removing the financial (typically principal agent first cost) barriers to lower lifecycle cost, energy, and emissions.

9.1.3. Green Building Rating Systems

Green building rating systems, such as LEED, represent a unique opportunity for operationalizing building/site efficiency for entities that value green/sustainable commercial developments. Green building rating systems have helped to transform the building marketplace by changing not only the way in which buildings are designed and constructed (e.g. integrative design and high performance systems), but also by capturing economic externalities of the AEC industries (e.g. material waste, water conservation, alternative transportation access, etc.) into the market value of certified buildings. With respect to transportation system efficiency, green building rating system criteria related to sustainable site selection can help to encourage the selection and development of locations with superior transportation energy and emissions performance. The transportation system evaluation framework of this dissertation can provide a performance-based evaluation of location alternatives, thereby improving upon the prescriptive site criteria that may not be aligned with the selection of the most efficient location alternatives (see Section 1.3.3).

With respect to building energy and emissions performance, the evaluation framework could improve upon the current paradigm of building energy efficiency evaluation in the LEED rating system by accounting for existing, baseline building performance in a site selection decision. In the current LEED rating system, building energy performance points are awarded by percent reductions relative to a code minimum (in the case of new construction) or existing

building baseline (see discussion in Section 4.2.4.3). Estimation and selection of the most efficient baseline building can help to achieve greater energy performance, not only for the use of existing building fit-outs, but also for major renovations that may further improve upon the existing building performance. The evaluation framework offers enhanced capability for evaluating whole-building energy performance as it relates to the selection of an efficient building/site, but the complexity of the framework's calculation procedures presents a workload that exceeds contemporary capacities for building/site analysis in the AE industry. Simplification of the modeling methods would help to make the evaluation framework more amenable to current green building rating systems and the AE professionals that utilize them.

9.2. Limitations of the Evaluation Framework

Relative to existing evaluation frameworks for buildings/sites, this dissertation research contributes an enhanced framework for estimating building/site energy consumption and GHG emissions performance. However, the data, methodology, and capabilities of the framework are not without limitations. As is mentioned in the previous section, the complexity of the calculation procedures, particularly for the building energy systems, is such that utilization of the framework requires a level of analytical effort that is most likely beyond the available resources typically budgeted for building performance assessment. Developing building energy models for multiple buildings, each of which accounts for input parameter uncertainty, is a very time consuming task given available building energy modeling resources. That is not to say that the building system evaluation framework cannot be incorporated into industry practices. Purpose-built energy simulation software for estimating the energy consumption of commercial buildings under uncertainty could help to alleviate the amount of time necessary to analyze the energy and

emissions performance of multiple building alternatives (see following section). The perimeter/core thermal zoning used in the building energy modeling represents an attempt to simplify the calculations, but the tradeoff is the introduction of un-specified error into the energy estimates (see discussion in Section 7.1.2.1).

One of the more significant limitations of the transportation system data and calculations is the fact that the interzonal travel activity in travel demand models are not calibrated for each zone. The trip attraction models may not reflect actual trip distances, which in the context of the Atlanta, GA metropolitan region are the strongest predictors of transportation energy consumption for demographic groups with high automobile ownership and household income. Another limitation of the transportation calculations is the estimation of site-specific NHB trip frequencies based on “area type” averages in the model data. These aggregate measures of average NHB trip frequency do not appear to account for the unique development characteristics at and adjacent to a commercial office site that may encourage NHB trips and/or encourage non-motorized mode shares for NHB trips. This limitation extends from the fact that 4-step travel demand models do not adequately account for non-motorized trips or trip chaining. Fortunately, NHB trips and non-motorized trips constitute only a fraction of total work PMT to/from most commercial office sites. Another important limitation of the transportation energy calculations is the estimation of vehicle fuel efficiency from average speeds on the network. The average speed and efficiency data do not account for the impact of vehicle acceleration cycles and roadway grades on vehicle energy consumption.

9.3. Opportunities for Future Research

In the process of developing and applying the building/site energy and GHG evaluation framework, future research needs and opportunities have been identified in several areas. First, application of the calculation framework to the contexts of other metropolitan regions, particularly those with higher utilization of alternative transportation modes and different climate zones, could help to gain insights into the types of commercial buildings/sites that are potentially the most energy efficient. Each transportation, land-use, and building stock context will yield unique results, but wider application of the framework to a variety of contexts may yield generalizable characteristics of efficient buildings/sites. Such generalizable findings may help to simplify the calculation procedures down to a subset of predictors, such as TAZ average SOV trip distance, average SOV mode share, average trip speed, office lighting power density, and envelope U-value. In applying the building energy framework in this dissertation, many more uncertain parameters were included than were found to be significant in the sensitivity analyses. For the transportation calculations in each of the case studies, the transportation energy performance was correlated with each site's average SOV trip distance. This relationship is particular to the demographic profile selected for the case studies – the majority of the employees are categorized within the highest stratification of household income and automobile ownership. For other market segments with lower household income and automobile ownership, other predictors such as alternative mode share will likely have a higher correlation with transportation energy/emissions performance. Further research into the main input parameters with the greatest effect on estimated energy consumption could help to reduce the complexity of the building energy modeling procedures. The complexity of the framework calculations could be substantially reduced by eliminating the Monte Carlo simulation procedures; however, such a

modification would eliminate the capability for quantifying the probability associated with energy/emissions savings between alternatives.

For the transportation energy system estimates, an important need and opportunity for future research is the calibration of travel demand model interzonal trip patterns (notably trip distances). Since the zone-specific work trip data utilized in this framework is synthetically produced from a gravity model of trip distribution and a nested logit model of mode choice, it could be helpful to validate the zone-specific trip table data through employee surveys of commute trip behavior, post site selection. A single employer survey could help to verify that the range of calculation outputs for a given location captures an observed result. Many employer surveys would be necessary to validate that the estimated distribution of calculation outputs is representative of the population of employees within a given zone. It is unfortunately unlikely that employee survey data collection will ever feasibly support a complete validation of estimated location-specific commute energy consumption, given the necessary level of detail (home address, demographics, trip frequency, mode choice, vehicle type, travel distance, and travel time) and participation (near 100 percent). Such survey data is rarely ever available, even for researchers or managers of employer-based travel demand management programs. Given the limitations of available travel behavior data, arguably a more productive focus for future research in commercial office location efficiency is the development of uncertainty quantification and visualization tools that help office location decision makers and policy makers better understand the energy conservation potential of office location alternatives, so that location-dependent energy conservation opportunities may be effectively identified and exploited.

Finally, the incorporation of vehicle-specific fuel economy curves coupled with data on commute vehicle ownership by home-location would help to better define the range of

uncertainty in SOV energy consumption. Additional data would be needed on vehicle time-space trajectories on network links to more accurately estimate energy consumption during individual trips. Additionally, consideration of roadway grades in the calculation framework may reveal that grades, in some network contexts, are a significant parameter influencing relative energy consumption by location.

APPENDIX A: MATLAB TRANSPORTATION SCRIPTS

Script: “Load_Var_HBW”

```
1 %This script loads the travel demand model data and reads mode shift or trip reduction inputs.
2
3 clc
4 clear
5
6 strat_status = input('Do you have stratified employment data? (Enter "1" for NO, or "2" for YES)');
7 strat = []; % Initializes empty stratification array.
8 if strat_status == 2
9     s_num = input('How many stratification do you have? ');
10    for i = 1:s_num
11        strat(i) = input('Enter the stratification number: ');
12    end;
13 else
14     strat = 5;
15 end;
16
17 % HIDE ONLY FOR PRELIM / REGIONAL CALCS!!!!
18 %
19 disp(['Do you wish to enter trip reduction targets? (1 for "NO", 2 for "Yes")'])
20 TR_yn = input('');
21 if TR_yn == 2
22     disp(['Are you using the Appendix A look-up tables in the FHWA TDM Manual? (1 for "NO", 2 for "YES")'])
23     FHWA_TDM_yn = input('');
24 end;
25 disp(['Do you wish to enter mode shift targets? (1 for "NO", 2 for "YES")'])
26 MS_yn = input('');
27 disp(['How many TAZs will be attracting trips?'])
28 num_of_taz = input(''); %User input of number of TAZs.
29 for i = 1:num_of_taz
30     disp(['Enter the TAZ# attracting trips: (',num2str(i),' of ',num2str(num_of_taz),')'])
31     taz(i) = input(''); %User input of site TAZ.
32     if TR_yn == 2
33         disp(['Enter the target percent trip reduction (SOV) for TAZ ',num2str(taz(i))])
34         TR_taz(i) = input('')/100; %User input of target trip reduction for TAZ.
35         if FHWA_TDM_yn == 2
36             disp(['Enter the CP + VP Program Level for TAZ ',num2str(taz(i))])
37             PL_CPVP_taz(i) = input('') + 1; %User input of CP + VP Program Level for TAZ. Plus 1 to avoid zero value.
38             disp(['Enter the Transit Program Level for TAZ ',num2str(taz(i))])
39             PL_transit_taz(i) = input('') + 1; %User input of Transit Program Level for TAZ. Plus 1 to avoid zero value.
40         end;
41     end;
42     if MS_yn == 2
43         disp(['Enter the target percent increase in HOV mode share for TAZ ',num2str(taz(i))])
44         MS_HOV_taz(i) = input('')/100; %User input of target increase in HOV mode share for TAZ.
45         disp(['Enter the target percent increase in transit mode share for TAZ ',num2str(taz(i))])
46         MS_transit_taz(i) = input('')/100; %User input of target increase in transit mode share for TAZ.
47     end;
48 end;
49 %}
50
51 direct = '\\sebwinrsrv2.ce.gatech.edu\Students$bweig3\Profile\Desktop\Dissertation\ARC_MAT\';
52 directory = '\\sebwinrsrv2.ce.gatech.edu\Students$bweig3\Profile\Desktop\Dissertation\ARC_MAT\4_29_11\';
53 directory_2 = '\\sebwinrsrv2.ce.gatech.
edu\Students$bweig3\Profile\Desktop\Dissertation\ARC_MAT\6_20_11\';
54
55 % UN-HIDE ONLY FOR / REGIONAL CALCS!!!! Trip reduction and mode
56 % shift calcs are disabled for regional calcs.
57 %}
58 data = load(strcat(direct,'TAZ_Calc_list.mat'));
59 taz = data.data;
60 clear('data');
61 num_of_taz = length(taz);
62 TR_yn = 1;
63 MS_yn = 1;
64 %}
65
66 dist_pc(1) = load(strcat(directory,'AMPK10HWY_SKM_dist.mat')); %Highway congested distances, in miles.
```

```

67 dist_pc(2) = load(strcat(directory_2,'SOVFFM10_SKM_dist.mat')); %SOV un-congested distances, in hundredths of a ✓
mile.
68 time_pc(1) = load(strcat(directory,'AMPK10HWY_SKM_time.mat')); %Highway congested time, in minutes. With ✓
terminal and intrazonal time.
69 time_pc(2) = load(strcat(directory_2,'SOVFFM10_SKM_time.mat')); %Highway SOV un-congested time, in ✓
hundredths of minutes. With terminal or intrazonal time.
70 dist_drive_transit(1) = load(strcat(directory,'AUTOLOC_ALL_SKM_dist.mat')); %Drive to local transit total distance, ✓
in hundredths of a mile
71 dist_drive_transit(2) = load(strcat(directory,'AUTOPRE_ALL_SKM_dist.mat')); %Drive to premium transit total ✓
distance, in hundredths of a mile
72 dist_drive_transit(3) = load(strcat(directory_2,'OFFAUTLOC_ALL_SKM_dist.mat')); %Drive to local transit total ✓
distance, in hundredths of a mile, un-congested.
73 dist_drive_transit(4) = load(strcat(directory_2,'OFFAUTPRE_ALL_SKM_dist.mat')); %Drive to premium transit total ✓
distance, in hundredths of a mile, un-congested.
74 time_drive_transit(1) = load(strcat(directory,'AUTOLOC_ALL_SKM_drivetime.mat')); %Drive to local transit drive ✓
time, in hundredths of minutes
75 time_drive_transit(2) = load(strcat(directory,'AUTOPRE_ALL_SKM_drivetime.mat')); %Drive to premium transit ✓
drive time, in hundredths of minutes
76 time_drive_transit(3) = load(strcat(directory_2,'OFFAUTLOC_ALL_SKM_drivetime.mat')); %Drive to local transit ✓
drive time, in hundredths of minutes, un-congested.
77 time_drive_transit(4) = load(strcat(directory_2,'OFFAUTPRE_ALL_SKM_drivetime.mat')); %Drive to premium transit ✓
drive time, in hundredths of minutes, un-congested.
78 dist_transit(1) = load(strcat(directory,'AUTOLOC_ALL_SKM_trndist.mat')); %Drive to local transit (transit) distance, ✓
in hundredths of a mile
79 dist_transit(2) = load(strcat(directory,'AUTOPRE_ALL_SKM_trndist.mat')); %Drive to premium transit (transit) ✓
distance, in hundredths of a mile
80 dist_transit(3) = load(strcat(directory,'WLKLOC_ALL_SKM_trndist.mat')); %Walk to local transit (transit) distance, ✓
in hundredths of a mile
81 dist_transit(4) = load(strcat(directory,'WLKPRE_ALL_SKM_trndist.mat')); %Walk to premium transit (transit) ✓
distance, in hundredths of a mile
82 dist_transit(5) = load(strcat(directory_2,'OFFAUTLOC_ALL_SKM_trndist.mat')); %Drive to local transit (transit) ✓
distance, in hundredths of a mile, un-congested.
83 dist_transit(6) = load(strcat(directory_2,'OFFAUTPRE_ALL_SKM_trndist.mat')); %Drive to premium transit (transit) ✓
distance, in hundredths of a mile, un-congested.
84 time_transit(1) = load(strcat(directory,'AUTOLOC_ALL_SKM_trntime.mat')); %Drive to local transit (transit) time, in ✓
hundredths of minutes
85 time_transit(2) = load(strcat(directory,'AUTOPRE_ALL_SKM_trntime.mat')); %Drive to premium transit (transit) ✓
time, in hundredths of minutes
86 time_transit(3) = load(strcat(directory,'WLKLOC_ALL_SKM_trntime.mat')); %Walk to local transit (transit) time, in ✓
hundredths of minutes
87 time_transit(4) = load(strcat(directory,'WLKPRE_ALL_SKM_trntime.mat')); %Walk to premium transit (transit) time, ✓
hundredths of in minutes
88 time_transit(5) = load(strcat(directory_2,'OFFAUTLOC_ALL_SKM_trntime.mat')); %Drive to local transit (transit) ✓
time, in hundredths of minutes, un-congested.
89 time_transit(6) = load(strcat(directory_2,'OFFAUTPRE_ALL_SKM_trntime.mat')); %Drive to premium transit ✓
(transit) time, in hundredths of minutes, un-congested.
90
91 TAZ_Non_Moto = load(strcat(direct,'TAZ_Non_Moto.mat')); % Non motorized mode share from CTPP.
92
93 %remove taz number from first column.
94 for i = 1:length(dist_pc)
95     dist_pc(i).M(:,1) = [];
96     time_pc(i).M(:,1) = [];
97 end
98 %dist_sov.M(:,1) = [];
99 for i = 1:length(dist_drive_transit)
100     dist_drive_transit(i).M(:,1) = [];
101     time_drive_transit(i).M(:,1) = [];
102 end
103 for i = 1:length(dist_transit)
104     dist_transit(i).M(:,1) = [];
105     time_transit(i).M(:,1) = [];
106 end
107
108
109 %Convert hundredths of miles to miles, hundredths of a minute to minutes.
110 for i = 2

```

```

111 dist_pc(i).M = dist_pc(i).M / 100;
112 time_pc(i).M = time_pc(i).M / 100;
113 end;
114 for i = 1:4
115     dist_drive_transit(i).M = dist_drive_transit(i).M / 100;
116     dist_transit(i).M = dist_transit(i).M / 100;
117     time_drive_transit(i).M = time_drive_transit(i).M / 100;
118     time_transit(i).M = time_transit(i).M / 100;
119 end;
120 for i = 5:6
121     dist_transit(i).M = dist_transit(i).M / 100;
122     time_transit(i).M = time_transit(i).M / 100;
123 end;
124
125 % Load stratified trip data.
126 if strat_status == 2
127     %s_num = input('How many stratification do you have?');
128     for i = 1:s_num
129         if strat(i) == 1
130             Load_Var_HBW_S1;
131         elseif strat(i) == 2
132             Load_Var_HBW_S2;
133         elseif strat(i) == 3
134             Load_Var_HBW_S3;
135         elseif strat(i) == 4
136             Load_Var_HBW_S4;
137         end;
138     end;
139 end;
140
141

```

Script: "Load_Var_HBW_S1"

```
1 %This script loads the stratified travel demand model trip data.
2
3 %clear('trips_mode')
4 clear('trips_mode_str1')
5
6 directory = '\\sebwinsrv2.ce.gatech.edu\Students$bweigel3\Profile\Desktop\Dissertation\ARC_MAT\4_29_11\';
7
8 %Import trips by mode.
9 trips_mode_str1(1) = load(strcat(directory,'HBWSOV_MTT_strat1.mat'));
10 trips_mode_str1(2) = load(strcat(directory,'HBWHOV_MTT_hov2strat1.mat'));
11 trips_mode_str1(3) = load(strcat(directory,'HBWHOV_MTT_hov3strat1.mat'));
12 trips_mode_str1(4) = load(strcat(directory,'HBWHOV_MTT_hov4strat1.mat'));
13 trips_mode_str1(5) = load(strcat(directory,'HBWTRN_MTT_W2Bstrat1.mat'));
14 trips_mode_str1(6) = load(strcat(directory,'HBWTRN_MTT_W2Rstrat1.mat'));
15 trips_mode_str1(7) = load(strcat(directory,'HBWTRN_MTT_D2Bstrat1.mat'));
16 trips_mode_str1(8) = load(strcat(directory,'HBWTRN_MTT_D2Rstrat1.mat'));
17
18 p_trips_str1_temp = load(strcat(directory,'HBW_PTT_strat1.mat'));
19 p_trips_str1_temp.M(:,1) = [];
20
21 mode_input_count = length(trips_mode_str1);
22
23 for i = 1:mode_input_count
24     trips_mode_str1(i).M(:,1) = []; %Remove taz number from first column.
25 end;
26
27 %Reduce tables down to selected TAZs.
28 d = 8;
29 for k = 1:d
30     trips_mode_str1(k).M = trips_mode_str1(k).M(:,taz);
31 end;
32 p_trips_str1_temp.M = p_trips_str1_temp.M(:,taz);
33
34 p_trips(1) = p_trips_str1_temp; % Replaces stratified person trips table with modified version (fractional non-
motorized trips removed).
35 clear('p_trips_str1_temp')
```

Script: “Transp_Calcs_HBW”

```
1 %This script calculates the HBW trip outputs.
2
3 Output.test_count = zeros(1,num_of_taz);
4 Output.test_count2 = zeros(1,num_of_taz);
5 Output.test_count3 = zeros(1,num_of_taz);
6
7 %
8 clear('num_emp','trip_rate','num_trips','str');
9 clear('Test_HOV_diff','Test_Transit_diff','Test_HOV_mult','Test_Transit_mult','Test_pct_diff');
10
11 freq_MF = 253; % Number of times per year that weekday trip patterns occur.
12 freq_Sa = 52; % Number of times per year that Saturday trip pattern occurs.
13 freq_Ho = 60; % Number of times per year that Sunday/Holiday trip pattern occurs.
14
15 i_loop = 1000; %Number of iterations for random samples of the origins.
16
17 s_max = max(strat);
18 num_emp = zeros(max(strat),1);
19 if strat_status == 2
20     for i = 1:s_num
21         disp(['Enter the # of employees in stratification ',num2str(strat(i)),': '])
22         num_emp(strat(i),1) = input(''); %User input of # of employees in each stratification.
23     end;
24 end;
25
26 ltm = 8; %Number of modes in trip tables.
27 ts = 2027; %Number of rows in trip tables.
28
29 % Initialize summary outputs.
30
31 Output.MC_sum = zeros(i_loop,ltm+1);
32 Output.Trips_sum = zeros(i_loop,ltm);
33 Output.VMT_sum = zeros(i_loop,ltm+2,num_of_taz);
34 Output.Time_sum = zeros(i_loop,ltm+2);
35 Output.Speed_sum = zeros(i_loop,ltm+2);
36 Output.Energy_sum = zeros(i_loop,ltm+2,num_of_taz);
37 Output.Energy_PP_sum = zeros(i_loop,ltm+2);
38 Output.Energy_PVMT_sum = zeros(i_loop,ltm+2,num_of_taz);
39 Output.GHG_sum = zeros(i_loop,ltm+2,num_of_taz);
40 Output.GHG_PP_sum = zeros(i_loop,ltm+2);
41 Output.GHG_PVMT_sum = zeros(i_loop,ltm+2,num_of_taz);
42 Output.GHG_Total_sum = zeros(i_loop,num_of_taz);
43 Output.Energy_Total_sum = zeros(i_loop,num_of_taz);
44 Output.Dist_per_trip_avg = zeros(i_loop,ltm+2,num_of_taz);
45 Output.MC_pct = zeros(i_loop,ltm+1,num_of_taz);
46 Output.VMT_AVG = zeros(ltm+2,num_of_taz);
47 Output.VMT_STD = zeros(ltm+2,num_of_taz);
48 Output.VMT_CoV = zeros(ltm+2,num_of_taz);
49 Output.Time_AVG = zeros(ltm+2,num_of_taz);
50 Output.Time_STD = zeros(ltm+2,num_of_taz);
51 Output.Time_CoV = zeros(ltm+2,num_of_taz);
52 Output.Speed_AVG = zeros(ltm+2,num_of_taz);
53 Output.Speed_STD = zeros(ltm+2,num_of_taz);
54 Output.Speed_CoV = zeros(ltm+2,num_of_taz);
55 Output.Trip_Dist_AVG = zeros(ltm+2,num_of_taz);
56 Output.Trip_Dist_STD = zeros(ltm+2,num_of_taz);
57 Output.Trip_Dist_CoV = zeros(ltm+2,num_of_taz);
58 Output.Energy_AVG = zeros(ltm+2,num_of_taz);
59 Output.Energy_STD = zeros(ltm+2,num_of_taz);
60 Output.Energy_CoV = zeros(ltm+2,num_of_taz);
61 Output.Energy_PP_AVG = zeros(ltm+2,num_of_taz);
62 Output.Energy_PP_STD = zeros(ltm+2,num_of_taz);
63 Output.Energy_PP_CoV = zeros(ltm+2,num_of_taz);
64 Output.Energy_PVMT_AVG = zeros(ltm+2,num_of_taz);
65 Output.Energy_PVMT_STD = zeros(ltm+2,num_of_taz);
66 Output.Energy_PVMT_CoV = zeros(ltm+2,num_of_taz);
67 Output.Energy_Total_AVG = zeros(num_of_taz);
```

```

68 Output.Energy_Total_STD = zeros(num_of_taz);
69 Output.Energy_Total_CoV = zeros(num_of_taz);
70 Output.GHG_AVG = zeros(ltm+2,num_of_taz);
71 Output.GHG_STD = zeros(ltm+2,num_of_taz);
72 Output.GHG_CoV = zeros(ltm+2,num_of_taz);
73 Output.GHG_PP_AVG = zeros(ltm+2,num_of_taz);
74 Output.GHG_PP_STD = zeros(ltm+2,num_of_taz);
75 Output.GHG_PP_CoV = zeros(ltm+2,num_of_taz);
76 Output.GHG_PVMT_AVG = zeros(ltm+2,num_of_taz);
77 Output.GHG_PVMT_STD = zeros(ltm+2,num_of_taz);
78 Output.GHG_PVMT_CoV = zeros(ltm+2,num_of_taz);
79 Output.GHG_Total_AVG = zeros(num_of_taz);
80 Output.GHG_Total_STD = zeros(num_of_taz);
81 Output.GHG_Total_CoV = zeros(num_of_taz);
82 Output.Trips_AVG = zeros(ltm+2,num_of_taz);
83 Output.Trips_STD = zeros(ltm+2,num_of_taz);
84 Output.MC_AVG = zeros(ltm+1,num_of_taz);
85 Output.MC_STD = zeros(ltm+1,num_of_taz);
86 non_moto_pct = zeros(num_of_taz,max(strat));
87 num_emp_taz = zeros(num_of_taz,max(strat));
88
89 Output.short_trips_ped = zeros(1,num_of_taz);
90 Output.short_trips_ped_pct = zeros(1,num_of_taz);
91 Output.short_trips_bike = zeros(1,num_of_taz);
92 Output.short_trips_bike_pct = zeros(1,num_of_taz);
93
94 trips_MF_I_P = zeros(1,4);
95 trips_MF_O_P = zeros(1,4);
96 trips_MF_I_NP = zeros(1,4);
97 trips_MF_O_NP = zeros(1,4);
98 trips_Sa_I_P = zeros(1,4);
99 trips_Sa_O_P = zeros(1,4);
100 trips_Sa_I_NP = zeros(1,4);
101 trips_Sa_O_NP = zeros(1,4);
102 trips_Ho_I_NP = zeros(1,4);
103 trips_Ho_O_NP = zeros(1,4);
104
105 pct_diff = zeros(num_of_taz,1);
106 MS_HOV_mult = zeros(num_of_taz,1);
107 MS_Transit_mult = zeros(num_of_taz,1);
108 HOV_ratio = zeros(num_of_taz,1);
109 Transit_ratio = zeros(num_of_taz,1);
110 MS_mult_const = zeros(num_of_taz,1);
111
112 %Loop calculations for each of the TAZs being considered.
113 for x = 1:num_of_taz
114     % Incorporate non-motorized mode share data from CTPP.
115     if strat_status == 2
116         for i = 1:s_num
117             s = strat(i);
118             non_moto_pct(x,s) = TAZ_Non_Moto.TAZ_Non_Moto(taz(x),4);
119             num_emp_taz(x,s) = round(num_emp(s)*(1 - non_moto_pct(x,s)));
120         end;
121     end;
122
123 %Period trips based on office occupancy schedule.
124 if strat_status == 2
125     for i = 1:s_num
126         s = strat(i);
127         trips_MF_I_P(1,s) = round(num_emp_taz(x,s) * 0.95);
128         trips_MF_O_P(1,s) = round(num_emp_taz(x,s) * 0.85);
129         trips_MF_I_NP(1,s) = round(num_emp_taz(x,s) * 0);
130         trips_MF_O_NP(1,s) = round(num_emp_taz(x,s) * 0.10);
131         trips_Sa_I_P(1,s) = round(num_emp_taz(x,s) * 0);
132         trips_Sa_O_P(1,s) = round(num_emp_taz(x,s) * 0.30);
133         trips_Sa_I_NP(1,s) = round(num_emp_taz(x,s) * 0.30);
134         trips_Sa_O_NP(1,s) = round(num_emp_taz(x,s) * 0.0);

```

```

135     trips_Ho_I_NP(1,s) = round(num_emp_taz(x,s) * 0.05);
136     trips_Ho_O_NP(1,s) = round(num_emp_taz(x,s) * 0.05);
137     end;
138 end;
139 % Total number of trips in each period, before accounting for frequency of periods.
140 base_trips = (sum(trips_MF_I_P) + sum(trips_MF_O_P) + sum(trips_MF_I_NP) + sum(trips_MF_O_NP) + sum(
141 (trips_Sa_I_P) + sum(trips_Sa_O_P) + sum(trips_Sa_I_NP) + sum(trips_Sa_O_NP) + sum(trips_Ho_I_NP) + sum(
142 (trips_Ho_O_NP));
143 % Calculate frequency of trips by period type: Inbound-peak, Outbound-peak, Inbound-non-peak, Outbound-non-
144 peak.
145 freq_adjust = zeros(1,16);
146 if strat_status == 2
147     for s = 1:4
148         freq_adjust(1+(4*(s-1))) = ((freq_MF * trips_MF_I_P(s)) + (freq_Sa * trips_Sa_I_P(s))) / (trips_MF_I_P(s)
149 + trips_Sa_I_P(s)); % I_P
150         if isnan(freq_adjust(1+(4*(s-1)))) == 1
151             freq_adjust(1+(4*(s-1))) = 0;
152         end;
153         freq_adjust(2+(4*(s-1))) = ((freq_MF * trips_MF_O_P(s)) + (freq_Sa * trips_Sa_O_P(s))) / (trips_MF_O_P
154 (s) + trips_Sa_O_P(s)); % O_P
155         if isnan(freq_adjust(2+(4*(s-1)))) == 1
156             freq_adjust(2+(4*(s-1))) = 0;
157         end;
158         freq_adjust(3+(4*(s-1))) = ((freq_MF * trips_MF_I_NP(s)) + (freq_Sa * trips_Sa_I_NP(s)) + (freq_Ho *
159 trips_Ho_I_NP(s))) / (trips_MF_I_NP(s) + trips_Sa_I_NP(s) + trips_Ho_I_NP(s)); % I_NP
160         if isnan(freq_adjust(3+(4*(s-1)))) == 1
161             freq_adjust(3+(4*(s-1))) = 0;
162         end;
163         freq_adjust(4+(4*(s-1))) = ((freq_MF * trips_MF_O_NP(s)) + (freq_Sa * trips_Sa_O_NP(s)) + (freq_Ho *
164 trips_Ho_O_NP(s))) / (trips_MF_O_NP(s) + trips_Sa_O_NP(s) + trips_Ho_O_NP(s)); % O_NP
165         if isnan(freq_adjust(4+(4*(s-1)))) == 1
166             freq_adjust(4+(4*(s-1))) = 0;
167         end;
168     end;
169 end;
170 p_trips_all_TAZ_tot = zeros(1,s_max);
171 for i = 1:s_num
172     s = strat(i);
173     p_trips_all_TAZ_tot(s) = sum(p_trips(s).M(:,x)); %Based on TDM trip tables (gravity model).
174 end;
175 %create trips PDF from O/D matrix.
176 trip_OD_TAZ_pdf = zeros(4,ts);
177 for i = 1:ts
178     for j = 1:s_num
179         s = strat(j);
180         trip_OD_TAZ_pdf(s,i) = p_trips(s).M(i,x)/p_trips_all_TAZ_tot(s); %Based on TDM trip tables (gravity model).
181     end;
182 end;
183 %Sum of modal trips from each origin for TAZ.
184 for i = 1:s_num
185     s = strat(i);
186     trips_mode_tot(s).m = zeros(ts,1); %Initialize variable.
187     mc_OD_TAZ_pdf(s).m = zeros(ts,ltm);
188 end;
189 for l = 1:s_num
190     s = strat(l);
191     % Total the number of trips taken by each mode for each stratification.
192     for i = 1:ts
193         for j = 1:ltm
194             if s == 5
195                 trips_mode_tot(s).m(i) = trips_mode_tot(s).m(i) + trips_mode(j).M(i,x);
196             elseif s == 1

```



```

195     trips_mode_tot(s).m(i) = trips_mode_tot(s).m(i) + trips_mode_str1(j).M(i,x);
196 elseif s == 2
197     trips_mode_tot(s).m(i) = trips_mode_tot(s).m(i) + trips_mode_str2(j).M(i,x);
198 elseif s == 3
199     trips_mode_tot(s).m(i) = trips_mode_tot(s).m(i) + trips_mode_str3(j).M(i,x);
200 elseif s == 4
201     trips_mode_tot(s).m(i) = trips_mode_tot(s).m(i) + trips_mode_str4(j).M(i,x);
202 end;
203 end;
204 %create PDF of mode choice for each origin producing trips attracted to TAZ.
205 for j = 1:ltm
206     if trips_mode_tot(s).m(i) > 0 %Prevents dividing by 0.
207         if s == 5
208             mc_OD_TAZ_pdf(s).m(i,j) = trips_mode(j).M(i,x) / trips_mode_tot(s).m(i);
209         elseif s == 1
210             mc_OD_TAZ_pdf(s).m(i,j) = trips_mode_str1(j).M(i,x) / trips_mode_tot(s).m(i);
211         elseif s == 2
212             mc_OD_TAZ_pdf(s).m(i,j) = trips_mode_str2(j).M(i,x) / trips_mode_tot(s).m(i);
213         elseif s == 3
214             mc_OD_TAZ_pdf(s).m(i,j) = trips_mode_str3(j).M(i,x) / trips_mode_tot(s).m(i);
215         elseif s == 4
216             mc_OD_TAZ_pdf(s).m(i,j) = trips_mode_str4(j).M(i,x) / trips_mode_tot(s).m(i);
217         end;
218     else
219         mc_OD_TAZ_pdf(s).m(i,j) = 0;
220     end;
221 end;
222 end;
223
224 end;
225
226 %Create PDF of mode choice for origins that do not have trips according to gravity model (mc_OD_TAZ_pdf(s).m
227 (i,j) = 0). Assume this trips are HOV trips.
228 for i = 1:s_num
229     s = strat(i);
230     mc_OD_TAZ_tot(s).m = zeros(1,4);
231     if s == 5
232         for j = 2:4
233             mc_OD_TAZ_tot(s).m(1,j) = sum(trips_mode(j).M(:,x));
234         end;
235     elseif s == 1
236         for j = 2:4
237             mc_OD_TAZ_tot(s).m(1,j) = sum(trips_mode_str1(j).M(:,x));
238         end;
239     elseif s == 2
240         for j = 2:4
241             mc_OD_TAZ_tot(s).m(1,j) = sum(trips_mode_str2(j).M(:,x));
242         end;
243     elseif s == 3
244         for j = 2:4
245             mc_OD_TAZ_tot(s).m(1,j) = sum(trips_mode_str3(j).M(:,x));
246         end;
247     elseif s == 4
248         for j = 2:4
249             mc_OD_TAZ_tot(s).m(1,j) = sum(trips_mode_str4(j).M(:,x));
250         end;
251     end;
252 end;
253 for i = 1:s_num
254     s = strat(i);
255     mc_OD_TAZ_pdf_NG(s).m = zeros(1,ltm);
256     for j = 2:4 %Include only SOV, HOV2, HOV3, HOV4 for mode choice.
257         mc_OD_TAZ_pdf_NG(s).m(1,j) = mc_OD_TAZ_tot(s).m(1,j)/sum(mc_OD_TAZ_tot(s).m(1,1:4));
258         if isnan(mc_OD_TAZ_pdf_NG(s).m(1,j)) == 1
259             mc_OD_TAZ_pdf_NG(s).m(1,j) = 0.001;
260             Output.test_count3 = Output.test_count3 + 1; % Counts the number of times that non-gravity MC PDF is
261             undefined.

```

```

260     end;
261     end;
262 end;
263
264 % Initialize values for mode shift and trip reduction variables.
265 m = 0;
266 pct_diff(x) = 100;
267 MS_HOV_mult(x) = 1;
268 MS_Transit_mult(x) = 1;
269 HOV_ratio(x) = 1;
270 Transit_ratio(x) = 1;
271 MS_mult_const(x) = 1;
272 while (pct_diff(x) >= 0.5) || (pct_diff(x) <= -0.5); % Was -1 to 1.
273     m = m+1;
274     if MS_HOV_mult(x) < 0
275         MS_HOV_mult(x) = (1 / HOV_ratio(x)) * 0.75;
276     elseif MS_HOV_mult(x) < 1
277         HOV_ratio(x) = 1;
278     end;
279     if MS_Transit_mult(x) < 0
280         MS_Transit_mult(x) = (1 / Transit_ratio(x)) * 0.75;
281     elseif MS_Transit_mult(x) < 1
282         Transit_ratio(x) = 1;
283     end;
284
285     for l = 1:s_num
286         s = strat(l);
287         for i = 1:ts
288             for j = 2:4
289                 mc_OD_TAZ_pdf(s).m(i,j) = mc_OD_TAZ_pdf(s).m(i,j) * MS_HOV_mult(x) * HOV_ratio(x);
290             end;
291             for j = 5:8
292                 mc_OD_TAZ_pdf(s).m(i,j) = mc_OD_TAZ_pdf(s).m(i,j) * MS_Transit_mult(x) * Transit_ratio(x);
293             end;
294         end;
295     end;
296
297     for i = 1:i_loop
298         VMT_per_OD = zeros(base_trips,ltm+2);
299         Time_per_OD = zeros(base_trips,ltm+2);
300         Speed_per_OD = zeros(base_trips,ltm+2);
301         Fuel_per_OD = zeros(base_trips,ltm+2);
302         Energy_per_OD = zeros(base_trips,ltm+2);
303         GHG_per_OD = zeros(base_trips,ltm+2);
304         OD_Count = 0; %Counts the number of times where an origin produces > 0 trips.
305         clear OD_samp;
306         clear('OD_samp_MF_I_P','OD_samp_MF_O_P','OD_samp_MF_I_NP','OD_samp_MF_O_NP');
307         clear('OD_samp_Sa_I_P','OD_samp_Sa_O_P','OD_samp_Sa_I_NP','OD_samp_Sa_O_NP');
308         clear('OD_samp_Ho_I_NP','OD_samp_Ho_O_NP');
309         for j = 1:s_num
310             s = strat(j);
311             c = num_emp_taz(x,s);
312             OD_samp(s).m = randsample(ts,c,true,trip_OD_TAZ_pdf(s,:)); %This picks the TAZ origins.
313
314             % Sample from selected origins, the scheduled subsets of trips (peak vs. non-peak)
315             OD_samp_MF_I_P(s).m = randsample(OD_samp(s).m,trips_MF_I_P(s));
316             OD_samp_MF_O_P(s).m = randsample(OD_samp(s).m,trips_MF_O_P(s));
317             OD_samp_MF_I_NP(s).m = randsample(OD_samp(s).m,trips_MF_I_NP(s));
318             OD_samp_MF_O_NP(s).m = randsample(OD_samp(s).m,trips_MF_O_NP(s));
319
320             OD_samp_Sa_I_P(s).m = randsample(OD_samp(s).m,trips_Sa_I_P(s));
321             OD_samp_Sa_O_P(s).m = randsample(OD_samp(s).m,trips_Sa_O_P(s));
322             OD_samp_Sa_I_NP(s).m = randsample(OD_samp(s).m,trips_Sa_I_NP(s));
323             OD_samp_Sa_O_NP(s).m = randsample(OD_samp(s).m,trips_Sa_O_NP(s));
324
325             OD_samp_Ho_I_NP(s).m = randsample(OD_samp(s).m,trips_Ho_I_NP(s));
326             OD_samp_Ho_O_NP(s).m = randsample(OD_samp(s).m,trips_Ho_O_NP(s));

```

```

327     end;
328
329     % Aggregate peak trips and non-peak trips.
330     clear agg;
331     for s = 1:s_max
332         agg(1+(4*(s-1))).OD_SAMP = vertcat(OD_samp_MF_I_P(s).m, OD_samp_Sa_I_P(s).m); % I_P
333         agg(2+(4*(s-1))).OD_SAMP = vertcat(OD_samp_MF_O_P(s).m, OD_samp_Sa_O_P(s).m); % O_P
334         agg(3+(4*(s-1))).OD_SAMP = vertcat(OD_samp_MF_I_NP(s).m, OD_samp_Sa_I_NP(s).m, ✓
OD_samp_Ho_I_NP(s).m); % I_NP
335         agg(4+(4*(s-1))).OD_SAMP = vertcat(OD_samp_MF_O_NP(s).m, OD_samp_Sa_O_NP(s).m, ✓
OD_samp_Ho_O_NP(s).m); % O_NP
336     end;
337
338     lod = base_trips;
339     loop_mc_count_OD_trips = zeros(lod,ltm); %Initialize variable. This variable stores the total number of trips ✓
attracted for each mode.
340
341     max_g = 4*s_max;
342     for g = 1:max_g % Loop through aggregated OD samples, max 4 trip types for each of the 4 market segments ✓
(16 iterations).
343         lagg = length(agg(g).OD_SAMP);
344         if sum(agg(g).OD_SAMP) > 0
345             for h = 1:lagg
346                 j = agg(g).OD_SAMP(h);
347                 if (g == 1) || (g == 5) || (g == 9) || (g == 13) % I_P
348                     s = ((g - 1) / 4) + 1;
349                     row = j;
350                     col = taz(x);
351                     SOV_d = 1; SOV_t = 1; HOV_d = 1; HOV_t = 1; W2B_d = 3; W2B_t = 3; W2R_d = 4; W2R_t = 4; ✓
D2B_d = 1; D2B_t = 1; D2R_d = 2; D2R_t = 2; D2B_dr_d = 1; D2B_dr_t = 1; D2R_dr_d = 2; D2R_dr_t = 2;
352                     elseif (g == 2) || (g == 6) || (g == 10) || (g == 14) % O_P
353                         s = ((g - 2) / 4) + 1;
354                         row = taz(x);
355                         col = j;
356                         SOV_d = 1; SOV_t = 1; HOV_d = 1; HOV_t = 1; W2B_d = 3; W2B_t = 3; W2R_d = 4; W2R_t = 4; ✓
D2B_d = 1; D2B_t = 1; D2R_d = 2; D2R_t = 2; D2B_dr_d = 1; D2B_dr_t = 1; D2R_dr_d = 2; D2R_dr_t = 2;
357                     elseif (g == 3) || (g == 7) || (g == 11) || (g == 15) % I_NP
358                         s = ((g - 3) / 4) + 1;
359                         row = j;
360                         col = taz(x);
361                         SOV_d = 2; SOV_t = 2; HOV_d = 2; HOV_t = 2; W2B_d = 3; W2B_t = 3; W2R_d = 4; W2R_t = 4; ✓
D2B_d = 5; D2B_t = 5; D2R_d = 6; D2R_t = 6; D2B_dr_d = 3; D2B_dr_t = 3; D2R_dr_d = 4; D2R_dr_t = 4;
362                     elseif (g == 4) || (g == 8) || (g == 12) || (g == 16) % O_NP
363                         s = ((g - 4) / 4) + 1;
364                         row = taz(x);
365                         col = j;
366                         SOV_d = 2; SOV_t = 2; HOV_d = 2; HOV_t = 2; W2B_d = 3; W2B_t = 3; W2R_d = 4; W2R_t = 4; ✓
D2B_d = 5; D2B_t = 5; D2R_d = 6; D2R_t = 6; D2B_dr_d = 3; D2B_dr_t = 3; D2R_dr_d = 4; D2R_dr_t = 4;
367                     end;
368
369                     OD_Count = OD_Count + 1; %Index for each of the trips between origin and destination.
370                     %Random sample of mode choice.
371                     if sum(mc_OD_TAZ_pdf(s).m(j,:)) == 0 %Check if there is a person trip taken, but none of the 8 ✓
modes selected (HOV2)
372                         mc_samp = randsample(ltm,1,true,mc_OD_TAZ_pdf_NG(s).m(1,:)); %Random sample of modes ✓
from the producing TAZ (only SOV, HOV2, HOV3, and HOV4).
373                         Output.test_count(1,x) = Output.test_count(1,x) + 1; %Counts the number of times that the a ✓
person trips is taken but no mode indicated in MC tables.
374                     else
375                         mc_samp = randsample(ltm,1,true,mc_OD_TAZ_pdf(s).m(j,:)); %Random sample of modes from ✓
the producing TAZ.
376                         Output.test_count2(1,x) = Output.test_count2(1,x) + 1; %Counts the number of times that a ✓
person trip is taken with a mode indicated.
377                     end;
378                     %Initialize variables
379                     mc_samp_OD = zeros(1,ltm);
380                     for p = 1:ltm

```

```

381         if mc_samp == p
382             mc_samp_OD(1,p) = 1;
383             loop_mc_count_OD_trips(OD_Count,p) = loop_mc_count_OD_trips(OD_Count,p) + freq_adjust(g);
384         else
385             mc_samp_OD(1,p) = 0;
386         end;
387     end;
388     %Count trips that are within bike/ped distance.
389     if dist_pc(1).M(taz(x),j) <= 1
390         Output.short_trips_ped(x) = Output.short_trips_ped(x) + freq_adjust(g);
391     end;
392     if dist_pc(1).M(taz(x),j) <= 3
393         Output.short_trips_bike(x) = Output.short_trips_bike(x) + freq_adjust(g);
394     end;
395     %Calculate the VMT for each mode in this sample.
396     for p = 1:(ltn + 2)
397         if p == 1 % SOV
398             VMT_per_OD(OD_Count,p) = freq_adjust(g) * mc_samp_OD(1,p) * (dist_pc(SOV_d).M(row,col));
399             Time_per_OD(OD_Count,p) = freq_adjust(g) * mc_samp_OD(1,p) * (time_pc(SOV_t).M(row,col));
400             %Calculates the travel time. SOV
401             Speed_per_OD(OD_Count,p) = VMT_per_OD(OD_Count,p) / (Time_per_OD(OD_Count,p) / 60);
402             if isnan(Speed_per_OD(OD_Count,p)) == 1
403                 Speed_per_OD(OD_Count,p) = 0; %Changes NaN values to 0.
404             end;
405             Fuel_per_OD(OD_Count,p) = VMT_per_OD(OD_Count,p) * (0.1823381+(-0.0082321*Speed_per_OD(OD_Count,p)^2)+(-0.0000088419*Speed_per_OD(OD_Count,p)^3)); % 20 mpg as a place holder!!!! =0.1823381+(-0.0082321*C4)+(0.00015265*C4^2)+(-0.0000088419*C4^3)
406             Energy_per_OD(OD_Count,p) = Fuel_per_OD(OD_Count,p) * 124238; %Btu's, TCR GRP Table 13.1 gasoline 5.218 MMBtu/barrel.
407             GHG_per_OD(OD_Count,p) = 8.81*Fuel_per_OD(OD_Count,p) + (0.015*310 + 0.0105*21)*VMT_per_OD(OD_Count,p)/1000; % TCR GRP Table 13.1 gasoline 8.81 kg CO2 / gal, Table 13.3 EPA Tier 1 0.015 g N2O / mile and 0.0105 g CH4 / mile.
408         elseif (p >= 2) && (p <= 4) % HOV
409             VMT_per_OD(OD_Count,p) = freq_adjust(g) * mc_samp_OD(1,p) * (dist_pc(HOV_d).M(row,col));
410             Time_per_OD(OD_Count,p) = freq_adjust(g) * mc_samp_OD(1,p) * (time_pc(HOV_t).M(row,col));
411             Speed_per_OD(OD_Count,p) = VMT_per_OD(OD_Count,p) / (Time_per_OD(OD_Count,p) / 60);
412             if isnan(Speed_per_OD(OD_Count,p)) == 1
413                 Speed_per_OD(OD_Count,p) = 0; %Changes NaN values to 0.
414             end;
415             Fuel_per_OD(OD_Count,p) = VMT_per_OD(OD_Count,p) * (0.1823381+(-0.0082321*Speed_per_OD(OD_Count,p)^2)+(-0.0000088419*Speed_per_OD(OD_Count,p)^3)); % 20 mpg as a place holder!!!!
416             Energy_per_OD(OD_Count,p) = Fuel_per_OD(OD_Count,p) * 124238; %Btu's, TCR GRP Table 13.1 gasoline 5.218 MMBtu/barrel.
417             GHG_per_OD(OD_Count,p) = 8.81*Fuel_per_OD(OD_Count,p) + (0.015*310 + 0.0105*21)*VMT_per_OD(OD_Count,p)/1000; % TCR GRP Table 13.1 gasoline 8.81 kg CO2 / gal, Table 13.3 EPA Tier 1 0.015 g N2O / mile and 0.0105 g CH4 / mile.
418         elseif p == 5 % W2B
419             VMT_per_OD(OD_Count,p) = freq_adjust(g) * mc_samp_OD(1,p) * (dist_transit(W2B_d).M(row,col));
420             Time_per_OD(OD_Count,p) = freq_adjust(g) * mc_samp_OD(1,p) * (time_transit(W2B_t).M(row,col));
421             Speed_per_OD(OD_Count,p) = VMT_per_OD(OD_Count,p) / (Time_per_OD(OD_Count,p) / 60);
422             if isnan(Speed_per_OD(OD_Count,p)) == 1
423                 Speed_per_OD(OD_Count,p) = 0; %Changes NaN values to 0.
424             end;
425             Energy_per_OD(OD_Count,p) = VMT_per_OD(OD_Count,p) * 4398; %Btu's, NTD Tables 17 and 19, 4398 Btu's/Pax-mi.
426             GHG_per_OD(OD_Count,p) = VMT_per_OD(OD_Count,p) * 0.36; % 0.36 kg CO2e / pax-mile, from Thesis.
427         elseif p == 6 % W2R
428             VMT_per_OD(OD_Count,p) = freq_adjust(g) * mc_samp_OD(1,p) * (dist_transit(W2R_d).M(row,col));

```

```

col)); %Calculates the transit PMT. W2R
428 Time_per_OD(OD_Count,p) = freq_adjust(g) * mc_samp_OD(1,p) * (time_transit(W2R_t).M(row,
col)); %Calculates the transit travel time. W2R
429 Speed_per_OD(OD_Count,p) = VMT_per_OD(OD_Count,p) / (Time_per_OD(OD_Count,p) / 60);
430 if isnan(Speed_per_OD(OD_Count,p)) == 1
431 Speed_per_OD(OD_Count,p) = 0; %Changes NaN values to 0.
432 end;
433 Energy_per_OD(OD_Count,p) = VMT_per_OD(OD_Count,p) * 641.6 / 0.4706; %Btu's, NTD Tables
17 and 19, 641.6 Btu's/Pax-mi. eGRID2007 GA: 990630472.5878 MMBtu heat input, 136617442.03 MWh output ==>
0.4706 combustion energy efficiency
434 GHG_per_OD(OD_Count,p) = VMT_per_OD(OD_Count,p) * 0.10; % 0.10 kg CO2e / pax-mile, from
Thesis.
435 elseif p == 7 % D2B
436 VMT_per_OD(OD_Count,p) = freq_adjust(g) * mc_samp_OD(1,p) * (dist_transit(D2B_d).M(row,
col)); %Calculates the transit vehicle PMT. D2B
437 Time_per_OD(OD_Count,p) = freq_adjust(g) * mc_samp_OD(1,p) * (time_transit(D2B_d).M(row,
col)); %Calculates the transit vehicle travel time. D2B
438 Speed_per_OD(OD_Count,p) = VMT_per_OD(OD_Count,p) / (Time_per_OD(OD_Count,p) / 60);
439 if isnan(Speed_per_OD(OD_Count,p)) == 1
440 Speed_per_OD(OD_Count,p) = 0; %Changes NaN values to 0.
441 end;
442 Energy_per_OD(OD_Count,p) = VMT_per_OD(OD_Count,p) * 4398; %Btu's, NTD Tables 17 and
19, 4398 Btu's/Pax-mi.
443 GHG_per_OD(OD_Count,p) = VMT_per_OD(OD_Count,p) * 0.36; % 0.36 kg CO2e / pax-mile, from
Thesis.
444 elseif p == 8 % D2R
445 VMT_per_OD(OD_Count,p) = freq_adjust(g) * mc_samp_OD(1,p) * (dist_transit(D2R_d).M(row,
col)); %Calculates the transit vehicle PMT. D2R
446 Time_per_OD(OD_Count,p) = freq_adjust(g) * mc_samp_OD(1,p) * (time_transit(D2R_t).M(row,
col)); %Calculates the transit vehicle travel time. D2R
447 Speed_per_OD(OD_Count,p) = VMT_per_OD(OD_Count,p) / (Time_per_OD(OD_Count,p) / 60);
448 if isnan(Speed_per_OD(OD_Count,p)) == 1
449 Speed_per_OD(OD_Count,p) = 0; %Changes NaN values to 0.
450 end;
451 Energy_per_OD(OD_Count,p) = VMT_per_OD(OD_Count,p) * 641.6 / 0.4706; %Btu's, NTD Tables
17 and 19, 641.6 Btu's/Pax-mi. eGRID2007 GA: 990630472.5878 MMBtu heat input, 136617442.03 MWh output ==>
0.4706 combustion energy efficiency
452 GHG_per_OD(OD_Count,p) = VMT_per_OD(OD_Count,p) * 0.10; % 0.10 kg CO2e / pax-mile, from
Thesis.
453 elseif p == 9 % Driving D2B + D2R. Was mode 10.
454 VMT_per_OD(OD_Count,p) = freq_adjust(g) * 1*((mc_samp_OD(1,7) * (dist_drive_transit
(D2B_dr_d).M(j,taz(x)) - dist_transit(D2B_d).M(j,taz(x)))) + (mc_samp_OD(1,8) * (dist_drive_transit(D2R_dr_d).M(j,
taz(x)) - dist_transit(D2R_d).M(j,taz(x)))));
455 %Calculates the drive to transit driving VMT. D2B + D2R.
456 Time_per_OD(OD_Count,p) = freq_adjust(g) * 1*((mc_samp_OD(1,7) * time_drive_transit
(D2B_dr_t).M(j,taz(x)) + (mc_samp_OD(1,8) * time_drive_transit(D2R_dr_t).M(j,taz(x)))));
457 %Calculates the drive to transit driving time. D2B + D2R.
458 Speed_per_OD(OD_Count,p) = VMT_per_OD(OD_Count,p) / (Time_per_OD(OD_Count,p) / 60);
459 if isnan(Speed_per_OD(OD_Count,p)) == 1
460 Speed_per_OD(OD_Count,p) = 0; %Changes NaN values to 0.
461 end;
462 Fuel_per_OD(OD_Count,p) = VMT_per_OD(OD_Count,p) * (0.1823381+(-0.0082321
*Speed_per_OD(OD_Count,p))+(0.00015265*Speed_per_OD(OD_Count,p)^2)+(-0.00000088419*Speed_per_OD
(OD_Count,p)^3)); % 20 mpg as a place holder!!!!
463 Energy_per_OD(OD_Count,p) = Fuel_per_OD(OD_Count,p) * 124238; %Btu's, TCR GRP Table
13.1 gasoline 5.218 MMBtu/barrel.
464 GHG_per_OD(OD_Count,p) = 8.81*Fuel_per_OD(OD_Count,p) + (0.015*310 + 0.0105*21)
*VMT_per_OD(OD_Count,p)/1000; % TCR GRP Table 13.1 gasoline 8.81 kg CO2 / gal, Table 13.3 EPA Tier 1 0.015 g N2O
/ mile and 0.0105 g CH4 / mile.
465 elseif p == 10 % SOV All. Was mode 11
466 VMT_per_OD(OD_Count,p) = VMT_per_OD(OD_Count,1) + VMT_per_OD(OD_Count,9); % Total
VMT from SOV and Drive 2 Transit.
467 Time_per_OD(OD_Count,p) = Time_per_OD(OD_Count,1) + Time_per_OD(OD_Count,9); % Total
Time from SOV and Drive 2 Transit.
468 Speed_per_OD(OD_Count,p) = VMT_per_OD(OD_Count,p) / (Time_per_OD(OD_Count,p) / 60);
469 if isnan(Speed_per_OD(OD_Count,p)) == 1
470 Speed_per_OD(OD_Count,p) = 0; %Changes NaN values to 0.

```

```

471         end;
472         Fuel_per_OD(OD_Count,p) = Fuel_per_OD(OD_Count,1) + Fuel_per_OD(OD_Count,9);
473         Energy_per_OD(OD_Count,p) = Energy_per_OD(OD_Count,1) + Energy_per_OD(OD_Count,9);
474         GHG_per_OD(OD_Count,p) = GHG_per_OD(OD_Count,1) + GHG_per_OD(OD_Count,9);
475     end;
476 end;
477 end
478 end;
479 end;
480
481 for p = 1:(Itm + 2) %Summarize VMT and MC for the i-loop.
482     Output.VMT_sum(i,p,x) = sum(VMT_per_OD(:,p)); %Total of VMT from each origin, indexed by i-loop ✓
iteration, for each mode and each attracting TAZ.
483     Output.Time_sum(i,p) = sum(Time_per_OD(:,p)); %Total of travel time from each origin, indexed by i-loop ✓
iteration, for each mode and each attracting TAZ.
484     Output.Speed_sum(i,p) = sum(VMT_per_OD(:,p)) / (sum(Time_per_OD(:,p)) / 60); %Total average travel ✓
speed from each origin, indexed by i-loop iteration, for each mode and each attracting TAZ.
485     Output.Energy_sum(i,p,x) = sum(Energy_per_OD(:,p));
486     Output.Energy_PP_sum(i,p) = Output.Energy_sum(i,p,x) / num_emp(s);
487     Output.Energy_PVMT_sum(i,p,x) = Output.Energy_sum(i,p,x) / Output.VMT_sum(i,p,x);
488     Output.GHG_sum(i,p,x) = sum(GHG_per_OD(:,p));
489     Output.GHG_PP_sum(i,p) = Output.GHG_sum(i,p,x) / num_emp(s);
490     Output.GHG_PVMT_sum(i,p,x) = Output.GHG_sum(i,p,x) / Output.VMT_sum(i,p,x);
491     if p <= Itm
492         Output.MC_sum(i,p) = sum(loop_mc_count_OD_trips(:,p)); %Total number of trips from origins indexed ✓
by i-loop iteration, for each mode and each attracting TAZ.
493         Output.Trips_sum(i,p) = sum(loop_mc_count_OD_trips(:,p)); %Average number of trips from origins ✓
indexed by i-loop iteration, for each mode and each attracting TAZ.
494         Output.Dist_per_trip_avg(i,p,x) = sum(VMT_per_OD(:,p)) / (sum(loop_mc_count_OD_trips(:,p))); % ✓
Averaged trip distance from origins indexed by i-loop iteration, for each mode and each attracting TAZ.
495         if p >= 2 && p <= 4
496             Output.Dist_per_trip_avg(i,p,x) = (sum(VMT_per_OD(:,p))*p) / (sum(loop_mc_count_OD_trips(:,p))); ✓
%Averaged trip distance from origins indexed by i-loop iteration, for each mode and each attracting TAZ.
497         end;
498         elseif p == 9
499             Output.Dist_per_trip_avg(i,p,x) = sum(VMT_per_OD(:,p)) / ((sum(loop_mc_count_OD_trips(:,7)) + sum ✓
(loop_mc_count_OD_trips(:,8)))); %Average distance driven for drive to transit trips.
500         elseif p == 10
501             Output.Dist_per_trip_avg(i,p,x) = (sum(VMT_per_OD(:,p))) / (sum(loop_mc_count_OD_trips(:,1)) + ✓
sum(loop_mc_count_OD_trips(:,7)) + sum(loop_mc_count_OD_trips(:,8))); %Average distance driven for drive to ✓
transit trips.
502         end;
503         if isnan(Output.Energy_PVMT_sum(i,p,x)) == 1
504             Output.Energy_PVMT_sum(i,p,x) = 0; %Changes NaN values to 0.
505         end;
506         if isnan(Output.GHG_PVMT_sum(i,p,x)) == 1
507             Output.GHG_PVMT_sum(i,p,x) = 0; %Changes NaN values to 0.
508         end;
509     end;
510     Output.GHG_Total_sum(i,x) = sum(Output.GHG_sum(i,1:9,x));
511     Output.Energy_Total_sum(i,x) = sum(Output.Energy_sum(i,1:9,x));
512     disp(['TAZ ', num2str(x), ' of ', num2str(num_of_taz)])
513     disp(['Completed sample i-loop ', num2str(i), ' of ', num2str(i_loop)])
514 end;
515 for i = 1:i_loop
516     for p = 1:(Itm+1)
517         Output.MC_pct(i,p,x) = (Output.MC_sum(i,p) / sum(Output.MC_sum(i,:))) * (1 - non_moto_pct(x)); % ✓
Mode choice percent, based on total number of trips from origins, indexed by i-loop iteration.
518         if p == (Itm+1)
519             Output.MC_pct(i,p,x) = non_moto_pct(x);
520         end;
521     end;
522 end;
523
524 %Store mean, standard deviation, and covariance of outputs by mode.
525 for p = 1:(Itm + 2)
526     Output.VMT_AVG(p,x) = mean(Output.VMT_sum(:,p,x));

```

```

527 Output.VMT_STD(p,x) = std(Output.VMT_sum(:,p,x));
528 Output.VMT_CoV(p,x) = Output.VMT_STD(p,x) / Output.VMT_AVG(p,x);
529 Output.Time_AVG(p,x) = mean(Output.Time_sum(:,p));
530 Output.Time_STD(p,x) = std(Output.Time_sum(:,p));
531 Output.Time_CoV(p,x) = Output.Time_STD(p,x) / Output.Time_AVG(p,x);
532 Output.Speed_AVG(p,x) = nanmean(Output.Speed_sum(:,p)); %Ignores NaN values.
533 Output.Speed_STD(p,x) = nanstd(Output.Speed_sum(:,p)); %Ignores NaN values.
534 Output.Speed_CoV(p,x) = Output.Speed_STD(p,x) / Output.Speed_AVG(p,x);
535 Output.Trip_Dist_AVG(p,x) = nanmean(Output.Dist_per_trip_avg(:,p,x)); %Ignores NaN values.
536 Output.Trip_Dist_STD(p,x) = nanstd(Output.Dist_per_trip_avg(:,p,x)); %Ignores NaN values.
537 Output.Trip_Dist_CoV(p,x) = Output.Trip_Dist_STD(p,x) / Output.Trip_Dist_AVG(p,x);
538 Output.Energy_AVG(p,x) = mean(Output.Energy_sum(:,p,x));
539 Output.Energy_STD(p,x) = std(Output.Energy_sum(:,p,x));
540 Output.Energy_CoV(p,x) = Output.Energy_STD(p,x) / Output.Energy_AVG(p,x);
541 Output.Energy_PP_AVG(p,x) = mean(Output.Energy_PP_sum(:,p));
542 Output.Energy_PP_STD(p,x) = std(Output.Energy_PP_sum(:,p));
543 Output.Energy_PP_CoV(p,x) = Output.Energy_PP_STD(p,x) / Output.Energy_PP_AVG(p,x);
544 Output.Energy_PVMT_AVG(p,x) = mean(Output.Energy_PVMT_sum(:,p,x));
545 Output.Energy_PVMT_STD(p,x) = std(Output.Energy_PVMT_sum(:,p,x));
546 Output.Energy_PVMT_CoV(p,x) = Output.Energy_PVMT_STD(p,x) / Output.Energy_PVMT_AVG(p,x);
547 Output.GHG_AVG(p,x) = mean(Output.GHG_sum(:,p,x));
548 Output.GHG_STD(p,x) = std(Output.GHG_sum(:,p,x));
549 Output.GHG_CoV(p,x) = Output.GHG_STD(p,x) / Output.GHG_AVG(p,x);
550 Output.GHG_PP_AVG(p,x) = mean(Output.GHG_PP_sum(:,p));
551 Output.GHG_PP_STD(p,x) = std(Output.GHG_PP_sum(:,p));
552 Output.GHG_PP_CoV(p,x) = Output.GHG_PP_STD(p,x) / Output.GHG_PP_AVG(p,x);
553 Output.GHG_PVMT_AVG(p,x) = mean(Output.GHG_PVMT_sum(:,p,x));
554 Output.GHG_PVMT_STD(p,x) = std(Output.GHG_PVMT_sum(:,p,x));
555 Output.GHG_PVMT_CoV(p,x) = Output.GHG_PVMT_STD(p,x) / Output.GHG_PVMT_AVG(p,x);
556 Output.Energy_Total_AVG(x) = mean(Output.Energy_Total_sum(:,x));
557 Output.Energy_Total_STD(x) = std(Output.Energy_Total_sum(:,x));
558 Output.Energy_Total_CoV(x) = Output.Energy_Total_STD(x) / Output.Energy_Total_AVG(x);
559 Output.GHG_Total_AVG(x) = mean(Output.GHG_Total_sum(:,x));
560 Output.GHG_Total_STD(x) = std(Output.GHG_Total_sum(:,x));
561 Output.GHG_Total_CoV(x) = Output.GHG_Total_STD(x) / Output.GHG_Total_AVG(x);
562
563 if p <= Itm
564     Output.Trips_AVG(p,x) = mean(Output.Trips_sum(:,p));
565     Output.Trips_STD(p,x) = std(Output.Trips_sum(:,p));
566     Output.MC_AVG(p,x) = mean(Output.MC_pct(:,p,x));
567     Output.MC_STD(p,x) = std(Output.MC_pct(:,p,x));
568 elseif p == 9
569     Output.MC_AVG(p,x) = mean(Output.MC_pct(:,p,x));
570     Output.MC_STD(p,x) = std(Output.MC_pct(:,p,x));
571 end;
572 end;
573 if m == 1 % Store initial values before trip reduction or mode shift.
574     VT_initial(x) = Output.Trips_AVG(1,x) + Output.Trips_AVG(2,x)/2 + Output.Trips_AVG(3,x)/3 + Output.↵
Trips_AVG(4,x)/4;
575
576 if TR_yn == 2
577     VT_target(x) = VT_initial(x) * (1 - TR_taz(x));
578 end;
579
580 MC_initial(:,x) = Output.MC_AVG(:,x);
581
582 if MS_yn == 2
583     MC_HOV_target(x) = (sum(MC_initial(2:4,x)) + (MS_HOV_taz(x)));
584     MC_Transit_target(x) = (sum(MC_initial(5:8,x)) + (MS_transit_taz(x)));
585 end;
586
587 VMT_initial(:,x) = Output.VMT_AVG(:,x);
588 Energy_initial(:,x) = Output.Energy_AVG(:,x);
589 Trip_Dist_initial(:,x) = Output.Trip_Dist_AVG(:,x);
590 end;
591
592 if TR_yn == 2

```

```

593     VT_actual(x) = Output.Trips_AVG(1,x) + Output.Trips_AVG(2,x)/2 + Output.Trips_AVG(3,x)/3 + Output.✓
Trips_AVG(4,x)/4;
594     pct_diff(x) = (TR_taz(x) - ((VT_initial(x) - VT_actual(x)) / VT_initial(x))) * 100;
595     MS_HOV_mult(x) = 1 + (((VT_actual(x) - VT_target(x)) / (VT_initial(x) - VT_target(x))) * MS_mult_const✓
(x));
596     MS_Transit_mult(x) = MS_HOV_mult(x);
597
598     if PL_CPVP_taz(x) == PL_transit_taz(x)
599         HOV_ratio(x) = 1;
600         Transit_ratio(x) = 1;
601     else;
602         HOV_ratio(x) = PL_CPVP_taz(x)/(PL_CPVP_taz(x) + PL_transit_taz(x));
603         Transit_ratio(x) = 1 - HOV_ratio(x);
604         Transit_ratio(x) = 1 + Transit_ratio(x);
605         HOV_ratio(x) = 1 + HOV_ratio(x);
606     end;
607
608     if (PL_CPVP_taz(x) == 1) && (PL_transit_taz(x) ~ 1)
609         MS_HOV_mult(x) = 1;
610         HOV_ratio(x) = 1;
611     elseif (PL_CPVP_taz(x) ~ 1) && (PL_transit_taz(x) == 1)
612         MS_Transit_mult(x) = 1;
613         Transit_ratio(x) = 1;
614     end;
615     MS_mult_const(x) = 0.25;
616 end;
617
618 if MS_yn == 2
619
620     MC_HOV_pct_diff(x) = (MS_HOV_taz(x) - (sum(Output.MC_AVG(2:4,x)) - sum(MC_initial(2:4,x)))) * 100;
621
622     if MS_HOV_taz(x) == 0
623         MS_HOV_mult(x) = 1 + ((MC_HOV_target(x) - sum(Output.MC_AVG(2:4,x))) * MS_mult_const(x));
624     else
625         MS_HOV_mult(x) = 1 + (((MC_HOV_target(x) - sum(Output.MC_AVG(2:4,x))) / abs(MC_HOV_target(x) - ✓
sum(MC_initial(2:4,x)))) * MS_mult_const(x));
626     end;
627
628     MC_Transit_pct_diff(x) = (MS_transit_taz(x) - (sum(Output.MC_AVG(5:8,x)) - sum(MC_initial(5:8,x)))) * ✓
100;
629
630     if MS_transit_taz(x) == 0
631         MS_Transit_mult(x) = 1 + ((MC_Transit_target(x) - sum(Output.MC_AVG(5:8,x))) * MS_mult_const(x));
632     else
633         MS_Transit_mult(x) = 1 + (((MC_Transit_target(x) - sum(Output.MC_AVG(5:8,x))) / abs ✓
(MC_Transit_target(x) - sum(MC_initial(5:8,x)))) * MS_mult_const(x));
634     end;
635
636     if abs(MC_HOV_pct_diff(x)) > abs(MC_Transit_pct_diff(x))
637         pct_diff(x) = MC_HOV_pct_diff(x);
638     else
639         pct_diff(x) = MC_Transit_pct_diff(x);
640     end;
641
642     MS_mult_const(x) = 1;
643
644     Test_HOV_diff(m,x) = MC_HOV_pct_diff(x);
645     Test_Transit_diff(m,x) = MC_Transit_pct_diff(x);
646
647 end;
648
649 Test_pct_diff(m,x) = pct_diff(x);
650 Test_HOV_mult(m,x) = MS_HOV_mult(x);
651 Test_Transit_mult(m,x) = MS_Transit_mult(x);
652
653 if TR_yn == 1 && MS_yn == 1
654     pct_diff(x) = 0;

```



```

655     end;
656
657 end;
658 end;
659 Output.num_of_taz = num_of_taz;
660 Output.taz = taz;
661 % Store mode shift variables in Output.
662 Output.ms_MC_initial = MC_initial;
663 Output.ms_pct_diff = pct_diff;
664 Output.ms_Test_pct_diff = Test_pct_diff;
665 Output.ms_Test_HOV_mult = Test_HOV_mult;
666 Output.ms_Test_Transit_mult = Test_Transit_mult;
667 Output.ms_VMT_initial = VMT_initial;
668 Output.ms_Energy_initial = Energy_initial;
669 Output.ms_Trip_Dist_initial = Trip_Dist_initial;
670 Output.ms_VT_initial = VT_initial;
671 if TR_yn == 2
672     Output.ms_VT_target = VT_target;
673     Output.ms_PL_CPVP_taz = PL_CPVP_taz;
674     Output.ms_PL_transit_taz = PL_transit_taz;
675     Output.ms_HOV_ratio = HOV_ratio;
676     Output.ms_Transit_ratio = Transit_ratio;
677 end;
678 if MS_yn == 2
679     Output.ms_MC_HOV_target = MC_HOV_target;
680     Output.ms_MC_Transit_target = MC_Transit_target;
681 end;
682
683 % Calculate percentage of person trips (which according to TDM are all motorized) that are attracted from origins ✓
    within non-motorized range.
684 for x = 1:num_of_taz
685     Output.short_trips_ped_pct(x) = Output.short_trips_ped(x) / (freq_adjust(g) * OD_Count * i_loop);
686     Output.short_trips_bike_pct(x) = Output.short_trips_bike(x) / (freq_adjust(g) * OD_Count * i_loop);
687 end;

```

APPENDIX B: BUILDING ENERGY SIMULATION INPUTS

Table B - 1: Building Energy Simulation Input Values with Uncertainty (Case Study I)

	#	Variable	Variable Description	Units	Value	Min	Max	Notes
Space								
Occupancy								
	--	--	Occupancy Schedule					COMMON
	--	Occ_SFPer _Off	Office Occupancy Area/Person	SF	250	--	--	Adjusted so that total occupancy is consistent
	--	Occ_SFPer _Conf	Conference Occupancy Area/Person	SF	50	--	--	Adjusted so that total occupancy is consistent
	--	Occ_Heat_ Total	Total Heat Gain	Btu/h- per	450	--	--	COMMON
	--	Occ_Heat_ Sens	Sensible Heat Gain	Btu/h- per	250	--	--	COMMON
	--	Occ_Heat_ Lat	Latent Heat Gain	Btu/h- per	200	--	--	COMMON
Lighting								
	--	--	Lighting Schedule	NA	--	--	--	COMMON
	--	--	Lighting Type	NA	Sus Fluor	--	--	COMMON
	1	LPD_Off	Lighting Power Density Office	W/SF	1.6	1	1.8	Based on DOE Ref. Bldg.
	2	LPD_Conf	Lighting Power Density Conference	W/SF	1.5	1	1.8	
	3	LPD_Lob	Lighting Power Density Lobby	W/SF	1.5	1	2	
	4	LPD_Tlt	Lighting Power Density Toilet	W/SF	1	0.8	1.2	
	5	LPD_Str	Lighting Power Density Stairs	W/SF	0.5	0.4	0.6	
	6	Lt_Rad_F	Radiant Fraction	NA	0.67	0.3	0.9	
Equipment								
	--	EPD_Off	Equipment Power Density Office	W/SF	0.96	--	--	Total watts consistent between case studies.
	--	EPD_Lob	Equipment Power Density Lobby	W/SF	0.25	--	--	COMMON

Table B – 1 (continued)

	#	Variable	Variable Description	Units	Value	Min	Max	Notes
	Internal Mass							
	--	--	Floor Weight	lb/SF	--	--	--	Autocalculate
	--	--	Furniture Weight	lb/SF	2	--	--	COMMON
	--	--	Furniture Fraction	NA	0.2	--	--	COMMON
	Infiltration							
	--	--	Infiltration Schedule	NA	--	--	--	COMMON
	7	Infil_EW	Infiltration Flow East West	AC/hr	0.98	0.49	1.47	Based on DOE Ref. Bldg., - 50% to + 50%
	8	Infil_NS	Infiltration Flow North South	AC/hr	1.03	0.515	1.55	Based on DOE Ref. Bldg., - 50% to + 50%
	--	--	Infiltration Core	AC/hr	0	--	--	Based on DOE Ref. Bldg.
	Wall / Floor							
	Daylighting/Shading/Other							
	9	Gnd_Ref	Ground Reflectance	NA	0.2	0.08	0.32	
	10	Out_Emiss	Outside Emissivity	NA	0.9	0.1	0.9	
	11	In_SAbs_W	Inside Solar Absorptance Wall	NA	0.5	0.2	0.9	
	12	In_Vref_W	Inside Visible Reflectance Wall	NA	0.5	0.2	0.9	= 1 - absorptance
	Windows							
	Basic Specifications							
	13	Frm_Width	Frame Width	ft	0.11	0.083 33	0.208 3	
	14	Frm_Cond	Frame Conductance	Btu/h-SF-degF	2.781	1.63	3.01	1.63 to 3.01 in ASHRAE Fund. 2009, Ch 15, Table1
	15	Frm_Abs	Frame Absorptance	NA	0.7	0.2	0.9	
	16	Shade_Sch	Shading Schedule	NA	0.75	0.4	0.9	ASHRAE Fund. 2009, Ch 15, Table 13
	--	--	Conductance Schedule	NA	1	--	--	COMMON
	--	--	Max Solar Schedule	Btu/h-SF	50	--	--	COMMON
	17	VT_Sch	Visible Transmittance Schedule	NA	0.23	0.14	0.35	
	--	--	Open Shade Schedule	NA	0.5	--	--	COMMON
	--	--	Sun Control Probability	NA	0.8	--	--	COMMON
	--	--	Glare Control Probability	NA	0.8	--	--	COMMON

Table B – 1 (continued)

	#	Variable	Variable Description	Units	Value	Min	Max	Notes
	--	--	Inside Visible Reflectance	NA	0.25	--	--	COMMON
Construction								
	18	Const_Abs_Ewall	Absorptance Exterior Wall	NA	0.8	0.5	0.9	Wood. Extreme values are 0.1 to 0.95
	--	Const_SR_Ewall	Surface Roughness Exterior Wall	NA	4	--	--	Code word only. Wood
	19	Const_Abs_Roof	Absorptance Roof	NA	0.7	0.6	0.8	Gray Roof. Extreme values are 0.1 to 0.95
	--	Const_SR_Roof	Surface Roughness Roof	NA	3	--	--	Code word only
Materials (Ewall Const layers)								
	20	Face1_Thk	Wood 2in Thickness	ft	0.167	0.083	0.333	DOE Ref. Bldg.
	21	Face1_Con d	Wood 2in Conductivity	Btu/h-ft-degF	0.063 6	0.04	0.1	DOE Ref. Bldg. ASHRAE Fund. 2009, Ch 26, Table 4
	22	Face1_Den s	Wood 2in Density	lb/CF	34	15	50	DOE Ref. Bldg. ASHRAE Fund. 2009, Ch 26, Table 4
	23	Face1_SpH	Wood 2in Specific Heat	Btu/lb-degF	0.289	0.24	0.33	DOE Ref. Bldg. ASHRAE Fund. 2009, Ch 26, Table 4
	24	Wall_Insul 1_Thk	Wall Assembly Insulation Thickness	ft	0.167	0.066	0.333	DOE Ref. Bldg.
	25	Wall_Insul 1_Con d	Wall Assembly Conductivity	Btu/h-ft-degF	0.028 3	0.017	0.417	DOE Ref. Bldg. ASHRAE Fund. 2009, Ch 26, Table 4
	26	Wall_Insul 1_Dens	Wall Assembly Density	lb/CF	16.52	10	20	DOE Ref. Bldg. ASHRAE Fund. 2009, Ch 26, Table 4
	27	Wall_Insul 1_SpH	Wall Assembly Specific Heat	Btu/lb-degF	0.2	0.14	0.35	DOE Ref. Bldg. ASHRAE Fund. 2009, Ch 26, Table 4

Table B – 1 (continued)

	#	Variable	Variable Description	Units	Value	Min	Max	Notes
	28	Roof_Blt_Thk	Roof Assembly 4in Thickness	ft	0.353	0.25	0.4167	DOE Ref. Bldg.
	29	Roof_Blt_Conduct	Roof Assembly 4in Conductivity	Btu/h-ft-degF	0.0283	0.025	0.035	DOE Ref. Bldg. ASHRAE Fund. 2009, Ch 26, Table 4
	30	Roof_Blt_Dens	Roof Assembly 4in Density	lb/CF	16.54	10	23	DOE Ref. Bldg. ASHRAE Fund. 2009, Ch 26, Table 4
	31	Roof_Blt_SpH	Roof Assembly 4in Specific Heat	Btu/lb-degF	0.2	0.14	0.2	DOE Ref. Bldg. ASHRAE Fund. 2009, Ch 26, Table 4
	32	Gflr_Conc_Thk	Conc HW 140lb 6in Thickness	ft	0.5	0.333	0.5	DOE Ref. Bldg.
	33	Gflr_Conc_Conduct	Conc HW 140lb 6in Conductivity	Btu/h-ft-degF	1	0.275	1.667	DOE Ref. Bldg. ASHRAE Fund. 2009, Ch 26, Table 4
	34	Gflr_Conc_Dens	Conc HW 140lb 6in Density	lb/CF	140	80	150	DOE Ref. Bldg. ASHRAE Fund. 2009, Ch 26, Table 4
	35	Gflr_Conc_SpH	Conc HW 140lb 6in Specific Heat	Btu/lb-degF	0.2	0.19	0.24	DOE Ref. Bldg. ASHRAE Fund. 2009, Ch 26, Table 4
Glass Types								
	36	Glaz1_SC	Glazing Shading Coefficient	NA	0.29	0.2	0.6	DOE Ref. Bldg.
	37	Glaz1_Conduct	Glazing Glass Conductance	Btu/h-SF-degF	0.72	0.5	0.8	DOE Ref. Bldg. ASHRAE Fund. 2009, Ch 15, Table 4
	38	Glaz1_VT	Glazing Visible Transmittance	NA	0.53	0.35	0.68	DOE Ref. Bldg. ASHRAE Fund. 2009, Ch 15, Table 10
	39	Glaz1_Out_Emiss	Glazing Outside Emissivity	NA	0.1	0.05	0.2	DOE Ref. Bldg. ASHRAE Fund. 2009, Ch 15, Table 4

Table B – 1 (continued)

	#	Variable	Variable Description	Units	Value	Min	Max	Notes
Air Side HVAC (VAV Systems)								
Basic								
	--	Max_Humid	Maximum Humidity	%	50	--	--	
Fans								
	40	SFan_Sp	Supply Fan Static	in. wg	3.5	2.5	4.5	
	41	SFan_Tot_Eff	Supply Fan Total Efficiency	NA	0.63	0.5	0.75	
	42	SFan_Mec_Eff	Supply Fan Mechanical Efficiency	NA	0.72	0.5	0.8	
	43	RFan_Sp	Return Fan Static	in. wg	1.17	1	2	
	44	RFan_Tot_Eff	Return Fan Total Efficiency	NA	0.63	0.5	0.75	
	45	Fan_MinFlow	Min Flow Ratio	NA	0.3	0.2	0.5	
Cooling								
	--	Cool_Coil_BF	Coil Design Bypass Factor	0.037		--	--	COMMON
	46	Cool_Cntl_Rng	Cool Control Range	degF	4	3	6	
	47	Cool_EIR	Cool Electric Input Ratio	NA	0.357 1	0.334 6	0.379 2	DOE Ref. Bldg., ASHRAE 90.1
	48	AHU_Cap_R	Air Handler Sizing Ratio	NA	1.15	1	1.2	
	49	CRS_Sup_at_Low	Max Cooling Reset Temp	degF	65	60	65	
	--	CRS_Sup_at_High	Min Cooling Reset Temp	degF	55	--	--	COMMON
	50	CRS_MinFlow	Minimum Reset Flow	NA	0.66	0.3	0.66	
Heating								
	51	Heat_MaxT	Zone Entering Max Supply Temp	degF	95	85	120	
	52	Heat_DT	Reheat Delta T	degF	30	20	40	
	53	Heat_Pre_T	Preheat T	degF	58	40	65	
	54	Heat_HIR	Heat Input Ratio	NA	1.240 7	1.2	1.35	DOE Ref. Bldg.
Zones								
	55	OA_PerPerson_Off	OA Flow/Person	cfm	20	10	20	IMC

Table B – 1 (continued)

	#	Variable	Variable Description	Units	Value	Min	Max	Notes
	56	OA_PerPerson_Conf	OA Flow/Person	cfm	10	10	15	IMC
	57	Exh_CFM	Exhaust Air Flow	cfm	300	200	400	6 urinals / WC
	58	Exh_Sp	Exhaust Static Pressure	in. wg	0.3	0.2	0.5	
	59	Exh_Tot_Eff	Exhaust Total Efficiency	NA	0.4	0.4	0.7	
	60	Tstat_ThRng	Throttle Range	degF	2	1	3	
	61	Hmax_Flow	Hmax Flow Ratio	NA	0.5	0.4	0.6	
Domestic Hot Water								
	62	DHW_Temp	Design HW Temp	degF	135	110	140	
	63	DHW_CircTime	Avg Circ Time	minutes	1.5	1	5	
	64	DHW_PipeHead	Pipe Head	ft	21.6	15	25	
	65	DHW_Load_single	Process Load_single	gpm	0.3	0.15	0.5	
	66	DHW_Loss_DT	Supply Loss DT	degF	7.5	5	10	
	67	DHW_HIR	Heat Input Ratio	NA	1.28	1.2	1.35	DOE Ref. Bldg.
Exterior Lighting								
Parking								
	68	Park_Light	Parking Load	kW	8.756	7	10	Based on DOE Ref. Bldg.
Conveyances								
Elevator								
	69	Elev	Elevator Load	kW	14.61	7.305	21.915	Based on DOE Ref. Bldg.

Table B - 2: Building Energy Simulation Input Values with Uncertainty (Case Study II)

	#	Variable	Variable Description	Units	Value	Min	Max	Notes
Space								
	Occupancy							
	--	--	Occupancy Schedule					COMMON
	--	Occ_SFPer _Off	Office Occupancy Area/Person	SF	250	--	--	Adjusted so that total occupancy is consistent
	--	Occ_SFPer _Conf	Conference Occupancy Area/Person	SF	50	--	--	Adjusted so that total occupancy is consistent
	--	Occ_Heat_T otal	Total Heat Gain	Btu/h-per	450	--	--	COMMON
	--	Occ_Heat_S ens	Sensible Heat Gain	Btu/h-per	250	--	--	COMMON
	--	Occ_Heat_L at	Latent Heat Gain	Btu/h-per	200	--	--	COMMON
	Lighting							
	--	--	Lighting Schedule	NA	--	--	--	COMMON
	--	--	Lighting Type	NA	Sus Fluor	--	--	COMMON
	1	LPD_Off	Lighting Power Density Office	W/SF	0.65	0.6	1.1	LEED Submittal Data, ASHRAE 90.1
	2	LPD_Conf	Lighting Power Density Conference	W/SF	0.9	0.9	1.3	LEED Submittal Data, ASHRAE 90.1
	3	LPD_Lob	Lighting Power Density Lobby	W/SF	1.5	1	2	ASHRAE 90.1
	4	LPD_Tlt	Lighting Power Density Toilet	W/SF	0.9	0.7	0.9	LEED Submittal Data, ASHRAE 90.1

Table B – 2 (continued)

	#	Variable	Variable Description	Units	Value	Min	Max	Notes
	5	LPD_Str	Lighting Power Density Stairs	W/SF	0.41	0.4	0.6	LEED Submittal Data, ASHRAE 90.1
	6	Lt_Rad_F	Radiant Fraction	NA	0.67	0.3	0.9	
Equipment								
	--	EPD_Off	Equipment Power Density Office	W/SF	0.96	--	--	Total watts consistent between case studies.
	--	EPD_Lob	Equipment Power Density Lobby	W/SF	0.25	--	--	COMMON
Internal Mass								
	--	--	Floor Weight	lb/SF	--	--	--	Autocalculate
	--	--	Furniture Weight	lb/SF	2	--	--	COMMON
	--	--	Furniture Fraction	NA	0.2	--	--	COMMON
Infiltration								
	--	--	Infiltration Schedule	NA	--	--	--	COMMON
	7	Infil_E	Infiltration Flow East	cfm/SF	0.0335	0.01675	0.067	Based on eQUEST defaults, - 50% to + 100%
	8	Infil_NSW	Infiltration Flow North South West	cfm/SF	0.029	0.0145	0.058	Based on eQUEST defaults, - 50% to + 100%
	--	--	Infiltration Core	cfm/SF	0.001	--	--	Based on eQUEST defaults
Wall / Floor								
Daylighting/Shading/Other								
	9	Gnd_Ref	Ground Reflectance	NA	0.2	0.08	0.32	
	10	Out_Emiss	Outside Emissivity	NA	0.9	0.1	0.9	
	11	In_SAbs_W	Inside Solar Absorptance Wall	NA	0.5	0.2	0.9	
	12	In_SAbs_F	Inside Solar Absorptance Floor	NA	0.8	0.5	0.9	

Table B – 2 (continued)

	#	Variable	Variable Description	Units	Value	Min	Max	Notes
	13	In_Vref_W	Inside Visible Reflectance Wall	NA	0.5	0.2	0.9	= 1 - absorptance
Windows								
Basic Specifications								
	14	Frm_Width	Frame Width	ft	0.11	0.0833	0.2083	
	15	Frm_Cond	Frame Conductance	Btu/h-SF-degF	1.691	1.63	3.01	1.63 to 3.01 in ASHRAE Fund. 2009, Ch 15, Table1
	16	Frm_Abs	Frame Absorptance	NA	0.7	0.2	0.9	
	17	Shade_Sch	Shading Schedule	NA	0.75	0.4	0.9	ASHRAE Fund. 2009, Ch 15, Table 13
	--	--	Conductance Schedule	NA	1	--	--	COMMON
	--	--	Max Solar Schedule	Btu/h-SF	50	--	--	COMMON
	18	VT_Sch	Visible Transmittance Schedule	NA	0.23	0.14	0.35	
	--	--	Open Shade Schedule	NA	0.5	--	--	COMMON
	--	--	Sun Control Probability	NA	0.8	--	--	COMMON
	--	--	Glare Control Probability	NA	0.8	--	--	COMMON
	--	--	Inside Visible Reflectance	NA	0.25	--	--	COMMON
Construction								
	23	Const_Abs_Ewall	Absorptance Exterior Wall	NA	0.6	0.5	0.8	Stucco. Extreme values are 0.1 to 0.95
	--	Const_SR_E wall	Surface Roughness Exterior Wall	NA	1	--	--	Code word only. Stucco
	24	Const_Abs_Roof	Absorptance Roof	NA	0.3	0.2	0.4	White Roof. Extreme values are 0.1 to 0.95
	--	Const_SR_Roof	Surface Roughness Roof	NA	1	--	--	Code word only

Table B – 2 (continued)

	#	Variable	Variable Description	Units	Value	Min	Max	Notes
Materials (Ewall Const layers)								
	25	Face1_Thk	Stucco 1in Thickness	ft	0.083	0.063	0.0833	LEED Submittal Data
	26	Face1_Con	Stucco 1in Conductivity	Btu/h-ft-degF	0.4167	0.375	0.8083	ASHRAE Fund. 2009, Ch 26, Table 4
	27	Face1_Dens	Stucco 1in Density	lb/CF	116	80	120	ASHRAE Fund. 2009, Ch 26, Table 4
	28	Face1_SpH	Stucco 1in Specific Heat	Btu/lb-degF	0.2	0.19	0.21	ASHRAE Fund. 2009, Ch 26, Table 4
	29	Insul_Bd1_Thk	Insul Bd 2in Thickness	ft	0.167	0.0833	0.25	LEED Submittal Data
	30	Insul_Bd1_Con	Insul Bd 2in Conductivity	Btu/h-ft-degF	0.025	0.0083	0.0475	ASHRAE Fund. 2009, Ch 26, Table 4
	31	Insul_Bd1_Dens	Insul Bd 2in Density	lb/CF	18	2	27	ASHRAE Fund. 2009, Ch 26, Table 4
	32	Insul_Bd1_SpH	Insul Bd 2in Specific Heat	Btu/lb-degF	0.2	0.14	0.35	ASHRAE Fund. 2009, Ch 26, Table 4
	33	Wall_Insul1_Thk	Mineral Wool Batt (Effect. R-7) Thickness	ft	0.188	0.167	0.25	LEED Submittal Data
	34	Wall_Insul1_Con	Mineral Wool Batt (Effect. R-7) Conductivity	Btu/h-ft-degF	0.025	0.01	0.025	ASHRAE Fund. 2009, Ch 26, Table 4
	35	Wall_Insul1_Dens	Mineral Wool Batt (Effect. R-7) Density	lb/CF	0.6	0.4	3	ASHRAE Fund. 2009, Ch 26, Table 4

Table B – 2 (continued)

	#	Variable	Variable Description	Units	Value	Min	Max	Notes
	36	Wall_Insul1_SpH	Mineral Wool Batt (Effect. R-7) Specific Heat	Btu/lb-degF	0.2	0.19	0.21	ASHRAE Fund. 2009, Ch 26, Table 4
	37	Roof_Insul1_Thk	Polyisocyanurate 4in Thickness	ft	0.333	0.25	0.4167	LEED Submittal Data
	38	Roof_Insul1_Cond	Polyisocyanurate 4in Conductivity	Btu/h-ft-degF	0.0117	0.01	0.0158	ASHRAE Fund. 2009, Ch 26, Table 4
	39	Roof_Insul1_Dens	Polyisocyanurate 4in Density	lb/CF	2	1.6	4	ASHRAE Fund. 2009, Ch 26, Table 4
	40	Roof_Insul1_SpH	Polyisocyanurate 4in Specific Heat	Btu/lb-degF	0.35	0.22	0.4	ASHRAE Fund. 2009, Ch 26, Table 4
	41	Gflr_Conc_Thk	Conc HW 140lb 6in Thickness	ft	0.5	0.333	0.5	
	42	Gflr_Conc_Cond	Conc HW 140lb 6in Conductivity	Btu/h-ft-degF	1	0.275	1.667	ASHRAE Fund. 2009, Ch 26, Table 4
	43	Gflr_Conc_Dens	Conc HW 140lb 6in Density	lb/CF	140	80	150	ASHRAE Fund. 2009, Ch 26, Table 4
	44	Gflr_Conc_SpH	Conc HW 140lb 6in Specific Heat	Btu/lb-degF	0.2	0.19	0.24	ASHRAE Fund. 2009, Ch 26, Table 4
Glass Types								
	19	Glaz1_SC	Guardian SN 68 Shading Coefficient	NA	0.39	0.28	0.6	Guardian SN 68 Cutsheet
	20	Glaz1_Cond	Guardian SN 68 Glass Conductance	Btu/h-SF-degF	0.29	0.29	0.5	Guardian SN 68 Cutsheet. ASHRAE Fund. 2009, Ch 15, Table 4

Table B – 2 (continued)

	#	Variable	Variable Description	Units	Value	Min	Max	Notes
	21	Glaz1_VT	Guardian SN 68 Visible Transmittance	NA	49	0.35	0.68	Guardian SN 68 Cutsheet
	22	Glaz1_Out_Emiss	Guardian SN 68 Outside Emissivity	NA	0.1	0.05	0.2	ASHRAE Fund. 2009, Ch 15, Table 4
Air Side HVAC (VAV Systems)								
Basic								
	--	Max_Humid	Maximum Humidity	%	50	--	--	
Fans								
	45	SFan_Sp	Supply Fan Static	in. wg	3.5	2.5	4.5	
	46	SFan_Tot_Eff	Supply Fan Total Efficiency	NA	0.63	0.5	0.75	
	47	SFan_Mec_Eff	Supply Fan Mechanical Efficiency	NA	0.72	0.5	0.8	
	48	RFan_Sp	Return Fan Static	in. wg	1.17	1	2	
	49	RFan_Tot_Eff	Return Fan Total Efficiency	NA	0.63	0.5	0.75	
	50	Fan_MinFlow	Min Flow Ratio	NA	0.3	0.2	0.5	
Outdoor Air Enthalpy Control								
	50	Econ_Enthalpy	Enthalpy High Limit	Btu/lb	30	28	32	ASHRAE 90.1 Table 6.5.1.1.3B
Cooling								
	--	Cool_Coil_BF	Coil Design Bypass Factor	0.037		--	--	COMMON
	52	Cool_Cntl_Rng	Cool Control Range	degF	4	3	6	
	53	Cool_EIR	Cool Electric Input Ratio	NA	0.3346	0.3103	0.3792	LEED Submittal Data, ASHRAE 90.1
	54	AHU_Cap_R	Air Handler Sizing Ratio	NA	1.15	1	1.2	
	55	CRS_Sup_at_Low	Max Cooling Reset Temp	degF	65	60	65	
	--	CRS_Sup_at_High	Min Cooling Reset Temp	degF	55	--	--	COMMON
	56	CRS_MinFlow	Minimum Reset Flow	NA	0.66	0.3	0.66	

Table B – 2 (continued)

	#	Variable	Variable Description	Units	Value	Min	Max	Notes
Heating								
	57	Heat_MaxT	Zone Entering Max Supply Temp	degF	95	85	120	
	--	Heat_DT	Reheat Delta T	degF	30	--	--	
Zones								
	58	OA_PerPers_Off	OA Flow/Person	cfm	10	5	15	IMC: 5 cfm/pers and 50 pers / 1000 SF. For 215 SF per person:
	59	OA_PerPers_Conf	OA Flow/Person	cfm	10	5	15	
	60	Exh_CFM	Exhaust Air Flow	cfm	300	200	400	
	61	Exh_Sp	Exhaust Static Pressure	in. wg	0.3	0.2	0.5	
	62	Exh_Tot_Eff	Exhaust Total Efficiency	NA	0.4	0.4	0.7	
	63	Tstat_ThRng	Throttle Range	degF	2	1	3	
	64	Hmax_Flow	Hmax Flow Ratio	NA	0.5	0.4	0.6	
Domestic Hot Water								
	65	DHW_Temp	Design HW Temp	degF	135	110	140	
	66	DHW_CircTime	Avg Circ Time	minutes	1.5	1	5	
	67	DHW_PipeHead	Pipe Head	ft	21.6	15	25	
	68	DHW_Load_single	Process Load_single	gpm	0.3	0.15	0.5	
	69	DHW_Loss_DT	Supply Loss DT	degF	10	5	20	
	70	DHW_EIR	Electric Input Ratio	NA	1.124	1.1	1.2	LEED Submittal Data
Exterior Lighting								
Parking								
	72	Park_Light	Parking Load	kW	2.8	2.5	3	LEED Submittal Data
Conveyances								
Elevator								
	73	Elev	Elevator Load	kW	14.61	7.305	21.915	LEED Submittal Data
Shading								
Trees								
	71	Tree_Trans	Tree Solar Transmittance	NA	0.5	0.1	0.9	

Table B - 3: Building Energy Simulation Input Values with Uncertainty (Case Study III)

	#	Variable	Variable Description	Units	Value	Min	Max	Notes
Site Data								
	Terrain							
	1	Shld_Coeff	Shielding Coeff.	NA	0.24	0.3	1	
	--	TP1	Terrain Parameter 1	NA	0.85	0.47	1	
	--	TP2	Terrain Parameter 2	NA	0.2	0.1	0.35	Varies inversely with terrain parameter 1
Space								
	Occupancy							
	--	--	Occupancy Schedule					COMMON
	--	Occ_SF_Pers_Off	Office Occupancy Area/Person	SF	242	--	--	Adjusted so that total occupancy is consistent
		Occ_SF_Pers_Conf	Conference Occupancy Area/Person	SF	50	--	--	Adjusted so that total occupancy is consistent
	--	Occ_Heat_Total	Total Heat Gain	Btu/h-per	450			COMMON
	--	Occ_Heat_Sens	Sensible Heat Gain	Btu/h-per	250			COMMON
	--	Occ_Heat_Lat	Latent Heat Gain	Btu/h-per	200			COMMON
	Lighting							
	--	--	Lighting Schedule					COMMON
	--	COMMON	Lighting Type	NA	Sus Fluor			
	2	LPD_Off	Lighting Power Density Office	W/SF	1.5	1	1.8	Based on DOE Ref. Bldg.
	3	LPD_Conf	Lighting Power Density Conference	W/SF	1.2	1	1.8	
	4	LPD_Lob	Lighting Power Density Lobby	W/SF	1.7	1	2	
	5	LPD_Tlt	Lighting Power Density Toilet	W/SF	1	0.8	1.2	
	6	LPD_Str	Lighting Power Density Stairs	W/SF	0.5	0.4	0.6	
	7	Lt_Rad_F	Radiant Fraction	NA	0.67	0.3	0.9	

Table B – 3 (continued)

	#	Variable	Variable Description	Units	Value	Min	Max	Notes
Equipment								
	--	EPD_Off	Equipment Power Density Office	W/SF	1			Total watts consistent between case studies.
	--	EPD_Lob	Equipment Power Density Lobby	W/SF	0.25			COMMON
Internal Mass								
	--	--	Floor Weight	lb/SF				Autocalculate
	--	--	Furniture Weight	lb/SF	2			COMMON
	--	--	Furniture Fraction	NA	0.2			COMMON
Infiltration								
	--	--	Infiltration Schedule	NA				COMMON
	8	Infil_EW	Infiltration Flow East West	AC/hr	0.95	0.475	1.425	Based on DOE Ref. Bldg., - 50% to + 50%
	9	Infil_NS	Infiltration Flow North South	AC/hr	0.98	0.49	1.47	Based on DOE Ref. Bldg., - 50% to + 50%
	--	--	Infiltration Core	AC/hr	0	--	--	Based on DOE Ref. Bldg.
	10	Infil_PM	Infiltration Flow Plenum Mid-Floors	AC/hr	0.28	0.14	0.42	Based on DOE Ref. Bldg., - 50% to + 50%
	11	Infil_PT	Infiltration Flow Plenum Top-Floor	AC/hr	3.63	1.815	5.45	Based on DOE Ref. Bldg., - 50% to + 50%
Wall / Floor								
Daylighting/Shading/Other								
	12	Gnd_Ref	Ground Reflectance	NA	0.2	0.08	0.32	
	--	--	Sky Form Factor					Autocalculate
	--	--	Ground Form Factor					Autocalculate
	13	Out_Emiss	Outside Emissivity	NA	0.9	0.1	0.9	
	14	In_SAbs_W	Inside Solar Absorptance Wall	NA	0.5	0.2	0.9	

Table B – 3 (continued)

	#	Variable	Variable Description	Units	Value	Min	Max	Notes
	15	In_SAbs_F	Inside Solar Absorptance Floor	NA	0.8	0.5	0.9	
	16	In_Vref_W	Inside Visible Reflectance Wall	NA	0.5	0.2	0.9	
	17	In_Vref_F	Inside Visible Reflectance Floor	NA	0.8	0.5	0.9	
Windows								
	Basic Specifications							
	18	Frm_Width	Frame Width	ft	0.11	0.083 33	0.20 83	1 to 2.5 inches
	19	Frm_Cond	Frame Conductance	Btu/h-SF-degF	1.691	1.63	3.01	ASHRAE Fund. 2009, Ch 15, Table1
	20	Frm_Abs	Frame Absorptance	NA	0.7	0.2	0.9	
	21	Shade_Sch	Shading Schedule	NA	0.75	0.4	0.9	ASHRAE Fund. 2009, Ch 15, Table 13
	--	--	Conductance Schedule	NA	1			COMMON
	--	--	Max Solar Schedule	Btu/h-SF	50			COMMON
	22	VT_Sch	Visible Transmittance Schedule	NA	0.23	0.14	0.35	
	--	--	Open Shade Schedule	NA	0.5			COMMON
	--	--	Sun Control Probability	NA	0.8	0	1	COMMON
	--	--	Glare Control Probability	NA	0.8	0	1	COMMON
	--	--	Inside Visible Reflectance	NA	0.25			COMMON
Construction								
	23	Const_Abs_Ewall	Absorptance Exterior Wall	NA	0.8	0.6	0.9	Based on DOE Ref. Bldg. Extreme values are 0.1 to 0.95
	--	--	Surface Roughness Exterior Wall	NA	6			Code word only
	24	Const_Abs_Roof	Absorptance Roof	NA	0.7	0.2	0.88	Based on DOE Ref. Bldg., Gray Roof. Extreme values are 0.1 to 0.95
	--	--	Surface Roughness Roof	NA	3			Code word only

Table B – 3 (continued)

	#	Variable	Variable Description	Units	Value	Min	Max	Notes
	Materials (Ewall Const layers)							
	25	Face1_Thk	Stucco 1in Thickness	ft	0.083	0.06225	0.10375	
	26	Face1_Conduct	Stucco 1in Conductivity	Btu/h-ft-degF	0.4	0.375	0.8083	DOE Ref. Bldg. ASHRAE Fund. 2009, Ch 26, Table 4
	27	Face1_Dens	Stucco 1in Density	lb/CF	116	80	120	DOE Ref. Bldg. ASHRAE Fund. 2009, Ch 26, Table 4
	28	Face1_SpH	Stucco 1in Specific Heat	Btu/lb-degF	0.2	0.15	0.25	DOE Ref. Bldg. ASHRAE Fund. 2009, Ch 26, Table 4
	29	Wall_Conc_Thk	Wall Concrete 8in Thickness	ft	0.667	0.50025	0.83375	
	30	Wall_Conc_Conduct	Wall Concrete 8in Conductivity	Btu/h-ft-degF	0.7576	0.5833	1.667	DOE Ref. Bldg. ASHRAE Fund. 2009, Ch 26, Table 4
	31	Wall_Conc_Dens	Wall Concrete 8in Density	lb/CF	140	130	150	DOE Ref. Bldg. ASHRAE Fund. 2009, Ch 26, Table 4
	32	Wall_Conc_SpH	Wall Concrete 8in Specific Heat	Btu/lb-degF	0.2	0.15	0.25	DOE Ref. Bldg. ASHRAE Fund. 2009, Ch 26, Table 4
	33	Wall_Insul1_Thk	Wall Assembly Insulation Thickness	ft	0.167	0.066	0.333	DOE Ref. Bldg.
	34	Wall_Insul1_Conduct	Wall Assembly Conductivity	Btu/h-ft-degF	0.0283	0.017	0.417	DOE Ref. Bldg. ASHRAE Fund. 2009, Ch 26, Table 4
	35	Wall_Insul1_Dens	Wall Assembly Density	lb/CF	16.52	10	20	DOE Ref. Bldg. ASHRAE Fund. 2009, Ch 26, Table 4
	36	Wall_Insul1_SpH	Wall Assembly Specific Heat	Btu/lb-degF	0.2	0.14	0.35	DOE Ref. Bldg. ASHRAE Fund. 2009, Ch 26, Table 4

Table B – 3 (continued)

	#	Variable	Variable Description	Units	Value	Min	Max	Notes
	37	Roof_Blt_Thk	Roof Assembly 4in Thickness	ft	0.353	0.25	0.4167	DOE Ref. Bldg.
	38	Roof_Blt_Cond	Roof Assembly 4in Conductivity	Btu/h-ft-degF	0.0283	0.025	0.035	DOE Ref. Bldg. ASHRAE Fund. 2009, Ch 26, Table 4
	39	Roof_Blt_Dens	Roof Assembly 4in Density	lb/CF	16.54	10	23	DOE Ref. Bldg. ASHRAE Fund. 2009, Ch 26, Table 4
	40	Roof_Blt_SpH	Roof Assembly 4in Specific Heat	Btu/lb-degF	0.2	0.14	0.2	DOE Ref. Bldg. ASHRAE Fund. 2009, Ch 26, Table 4
	41	Gflr_Conc_Thk	Conc HW 140lb 6in Thickness	ft	0.5	0.333	0.5	DOE Ref. Bldg.
	42	Gflr_Conc_Cond	Conc HW 140lb 6in Conductivity	Btu/h-ft-degF	1	0.275	1.667	DOE Ref. Bldg. ASHRAE Fund. 2009, Ch 26, Table 4
	43	Gflr_Conc_Dens	Conc HW 140lb 6in Density	lb/CF	140	80	150	DOE Ref. Bldg. ASHRAE Fund. 2009, Ch 26, Table 4
	44	Gflr_Conc_SpH	Conc HW 140lb 6in Specific Heat	Btu/lb-degF	0.2	0.19	0.24	DOE Ref. Bldg. ASHRAE Fund. 2009, Ch 26, Table 4
Glass Types								
	45	Glaz1_SC	Glazing Shading Coefficient	NA	0.29	0.2	0.6	DOE Ref. Bldg.
	46	Glaz1_Con d	Glazing Glass Conductance	Btu/h-SF-degF	0.72	0.5	0.8	DOE Ref. Bldg. ASHRAE Fund. 2009, Ch 15, Table 4
	47	Glaz1_VT	Glazing Visible Transmittance	NA	0.53	0.35	0.68	DOE Ref. Bldg. ASHRAE Fund. 2009, Ch 15, Table 10
	48	Glaz1_Out_Emiss	Glazing Outside Emissivity	NA	0.1	0.05	0.2	DOE Ref. Bldg. ASHRAE Fund. 2009, Ch 15, Table 4

Table B – 3 (continued)

	#	Variable	Variable Description	Units	Value	Min	Max	Notes
Air Side HVAC (VAV Systems)								
Basic								
	49	Max_Humid	Maximum Humidity	%	50	40	60	
Fans								
	50	SFan_Sp	Supply Fan Static	in. wg	3.5	2.5	4.5	
	51	SFan_Tot_Eff	Supply Fan Total Efficiency	NA	0.63	0.5	0.75	
	52	SFan_Mec_Eff	Supply Fan Mechanical Efficiency	NA	0.72	0.5	0.8	
	53	RFan_Sp	Return Fan Static	in. wg	1.17	1	2	
	54	RFan_Tot_Eff	Return Fan Total Efficiency	NA	0.63	0.5	0.75	
	55	Fan_MinFlow	Min Flow Ratio	NA	0.3	0.2	0.5	
Cooling								
	--	Cool_Coil_BF	Coil Design Bypass Factor	NA	0.037			COMMON
	56	Cool_Cntl_Rng	Cool Control Range	degF	4	3	6	
	57	AHU_Cap_R	Air Handler Sizing Ratio	NA	1.15	1	1.2	
	58	CRS_Sup_at_Low	Max Cooling Reset Temp	degF	65	60	65	
	--	CRS_Sup_at_High	Min Cooling Reset Temp	degF	55			Unchanged
	59	CRS_MinFlow	Minimum Reset Flow	NA	0.66	0.3	0.66	
Heating								
	60	Heat_Max_T	Zone Entering Max Supply Temp	degF	95	85	120	
	61	Heat_DT	Reheat Delta T	degF	30	20	50	
	62	Heat_Pre_T	Preheat T	degF	58	40	65	
	63	Heat_HIR	Heat Input Ratio	NA	1.2407	1.2	1.35	DOE Ref. Bldg.
Zones								
	64	OA_PerPers_Off	OA Flow/Person	cfm	20	10	20	IMC
	65	OA_PerPers_Conf	OA Flow/Person	cfm	10	10	15	IMC
	66	OA_PerSF	OA Flow/Area	cfm/SF	0.3	0.25	0.35	

Table B – 3 (continued)

	#	Variable	Variable Description	Units	Value	Min	Max	Notes
	67	Exh_CFM	Exhaust Air Flow	cfm	600	500	750	6 urinals / WC
	68	Exh_Sp	Exhaust Static Pressure	in. wg	0.3	0.2	0.5	
	69	Exh_Tot_Eff	Exhaust Total Efficiency	NA	0.4	0.4	0.7	
	70	Tstat_ThRng	Throttle Range	degF	2	1	3	
	71	Hmax_Flow	Hmax Flow Ratio	NA	0.5	0.4	0.6	
Water Side HVAC								
Chilled Water Loop								
	72	CHW_DT	Loop Design DT	degF	10	8	14	Vary inversely
	--	CHW_T	Design CHW Temp	degF	44	40	46	Vary inversely
	73	CHW_Circ Time	Avg Circ Time	minutes	1.5	1.5	15	
	74	CHW_Pipe Head	Pipe Head	ft	21.6	15	50	
	75	CHW_Head_SRng	Head Setpoint Range	ft	2	1	4	
	76	CHW_FlowRes	Loop Flow Reset	NA	0.7	0.5	0.8	
	77	CHW_Loop_SRng	Loop Setpoint Range	degF	2	0.05	3	
	78	CHW_Max Res_T	Max Reset Temp	degF	65	60	65	
	79	CHW_Min Res_T	Min Reset Temp	degF	40	40	44	
Chillers								
	80	Chill_EIR	Electric Input Ratio	NA	0.192	0.17	0.2	DOE Ref. Bldg.
	81	Chill_Min R	Minimum Ratio	NA	0.1	0.1	0.3	
	82	Chill_Min Con_T	Minimum Condenser Temp	degF	70	60	70	
	83	Chill_Head	Chiller Head	ft	20	10	30	
	84	Chill_Con Head	Condenser Head	ft	20	10	30	
	85	Chill_Start up_t	Start-up Time	h	0.04	0.0167	0.0833	
	86	Chill_Standby_t	Standby Time	h	0.025	0.0167	0.0833	
	87	Chill_Cap_R	Chiller Capacity Ratio	NA	1.2	1	1.5	

Table B – 3 (continued)

	#	Variable	Variable Description	Units	Value	Min	Max	Notes
CHW pump								
	88	CHWP_Mot_Eff	Motor Efficiency	NA	0.8	0.6	0.95	
	89	CHWP_Mech_Eff	Mech Efficiency	NA	0.77	0.8	0.8	
	90	CHWP_Min_Spd	Minimum Speed	NA	0.4	0.3	0.5	
Condenser Water Loop								
	91	CW_DT	Loop Design DT	degF	10	8	14	Vary inversely
	--	CW_T	Design CW Temp	degF	88	84	90	Vary inversely
	92	CW_Circ Time	Avg Circ Time	minutes	1.5	1	2	
	93	CW_Pipe Head	Pipe Head	ft	21.6	15	50	
	94	CW_Head_SRng	Head Setpoint Range	ft	2	1	4	
	95	CW_Loop_SRng	Loop Setpoint Range	degF	2	0.05	3	
	96	CW_Max_Res_T	Max Reset Temp	degF	95	85	95	
	--	CW_Min_Res_T	Min Reset Temp	degF	70	60	70	Interlocked with Minimum Condenser Temp
CW Pumps								
	97	CWP_Mot_Eff	Motor Efficiency	NA	0.8	0.6	0.95	
	98	CWP_Mech_Eff	Mech Efficiency	NA	0.77	0.8	0.8	
Cooling Towers								
	99	CT_Fan_EIR	Fan Electric Input Ratio	NA	0.0226	0.0105	0.05	
	100	CT_FanOffFlow	Fan Off Flow	NA	0.01	0	0.05	
	101	CT_Head	Head	ft	10	5	20	
	102	CT_StaticHead	Static Head	ft	10	5	20	
	103	CT_Capacity_R	Cooling Tower Capacity Ratio	NA	1.2	1	1.5	
Domestic Hot Water								
	104	DHW_HIR	Heat Input Ratio	NA	1.28	1.2	1.35	DOE Ref. Bldg.
	105	DHW_Temp	Design HW Temp	degF	135	110	140	

Table B – 3 (continued)

	#	Variable	Variable Description	Units	Value	Min	Max	Notes
	106	DHW_Circ Time	Avg Circ Time	minutes	1.5	1	5	
	107	DHW_PipeHead	Pipe Head	ft	21.6	15	25	
	108	DHW_Load	Process Load	gpm	4.41	2	6	Based on 1 gal/pers./day, ASHRAE Std. 90.1
	109	DHW_Load_single	Process Load_single	gpm	0.3	0.15	0.5	Based on 1 gal/pers./day, ASHRAE Std. 90.1
	110	DHW_Loss_DT	Supply Loss DT	degF	10	5	10	
Exterior Lighting								
	Parking							
	111	Park_Light	Parking Load	kW	11.84	7.5	15	
	112	Door_Light	Doorways Load	kW	1.69	1	3	
Conveyances								
	Elevator							
	113	Elev	Elevator Load	kW	111.2	55.6	166.8	

Table B - 4: Building Energy Simulation Input Values with Uncertainty (Case Study IV)

	#	Variable	Variable Description	Units	Value	Min	Max	Notes
Site Data								
	Terrain							
	1	Shld_Coeff	Shielding Coeff.	NA	0.24	0.3	1	
	--	TP1	Terrain Parameter 1	NA	0.85	0.47	1	
	--	TP2	Terrain Parameter 2	NA	0.2	0.1	0.35	Varies inversely with terrain parameter 1
Space								
	Occupancy							
	--	--	Occupancy Schedule					COMMON
	--	Occ_SFPer _Off	Office Occupancy Area/Person	SF	242	--	--	Adjusted so that total occupancy is consistent
		Occ_SFPer _Conf	Conference Occupancy Area/Person	SF	50	--	--	Adjusted so that total occupancy is consistent
	--	Occ_Heat_T otal	Total Heat Gain	Btu/h- per	450			COMMON
	--	Occ_Heat_S ens	Sensible Heat Gain	Btu/h- per	250			COMMON
	--	Occ_Heat_L at	Latent Heat Gain	Btu/h- per	200			COMMON
	Lighting							
	--	--	Lighting Schedule					COMMON
	--	COMMON	Lighting Type	NA	Sus Fluor			
	2	LPD_Off	Lighting Power Density Office	W/SF	1	0.9	1.1	ASHRAE Std. 90.1
	138	LPD_Lob	Lighting Power Density Lobby	W/SF	1.5	1	2	ASHRAE Std. 90.1
	3	LPD_Tlt	Lighting Power Density Toilet	W/SF	0.8	0.7	0.9	ASHRAE Std. 90.1
	4	LPD_Str	Lighting Power Density Stairs	W/SF	0.5	0.4	0.6	ASHRAE Std. 90.1
	134	LPD_Conf	Lighting Power Density Conference	W/SF	1.2	0.9	1.3	ASHRAE Std. 90.1
	5	Lt_Rad_F	Radiant Fraction	NA	0.67	0.3	0.9	

Table B – 4 (continued)

	#	Variable	Variable Description	Units	Value	Min	Max	Notes
Daylighting								
	6	DL_kW_F	KW Fraction	NA	1	0	1	
	7	DL_MinP_F	Min Power Fraction	NA	0.3	0.1	0.5	
	8	DL_MinL_F	Min Light Fraction	NA	0.3	0.1	0.5	
	9	DL_Setpoint	Set Point	fc	50	20	500	Range indicated in LEED NC
	10	DL_MaxGlare	Max Glare		22	15	30	
	11	DL_ViewAz	View Azimuth	deg	180	90	270	
Equipment								
	--	EPD_Off	Equipment Power Density Office	W/SF	1			Total watts consistent between case studies.
	--	EPD_Lob	Equipment Power Density Lobby	W/SF	0.25			COMMON
Internal Mass								
	--	--	Floor Weight	lb/SF				Autocalculate
	--	--	Furniture Weight	lb/SF	2			COMMON
	--	--	Furniture Fraction	NA	0.2			COMMON
Infiltration								
	--	--	Infiltration Schedule	NA				COMMON
	12	Infil_E	Infiltration Flow East	cfm/SF	0.0335	0.01675	0.05025	Based on eQUEST defaults, ± 50 percent
	13	Infil_NSW	Infiltration Flow North South West	cfm/SF	0.029	0.0145	0.0435	Based on eQUEST defaults, ± 50 percent

Table B – 4 (continued)

	#	Variable	Variable Description	Units	Value	Min	Max	Notes
Wall / Floor								
Daylighting/Shading/Other								
	14	Gnd_Ref	Ground Reflectance	NA	0.2	0.08	0.32	
	--	--	Sky Form Factor					Autocalculate
	--	--	Ground Form Factor					Autocalculate
	15	Out_Emiss	Outside Emissivity	NA	0.9	0.1	0.9	
	16	In_SAbs_W	Inside Solar Absorptance Wall	NA	0.5	0.2	0.9	
	17	In_SAbs_F	Inside Solar Absorptance Floor	NA	0.8	0.5	0.9	
	18	In_Vref_W	Inside Visible Reflectance Wall	NA	0.5	0.2	0.9	
	19	In_Vref_F	Inside Visible Reflectance Floor	NA	0.8	0.5	0.9	
Windows								
Basic Specifications								
	20	Frm_Width	Frame Width	ft	0.11	0.0833	0.2083	
	21	Frm_Cond	Frame Conductance	Btu/h-SF-degF	1.691	1.63	3.01	1.63 to 3.01 in ASHRAE Fund. 2009, Ch 15, Table1
	22	Frm_Abs	Frame Absorptance	NA	0.7	0.2	0.9	
	23	Shade_Sch	Shading Schedule	NA	0.75	0.4	0.9	ASHRAE Fund. 2009, Ch 15, Table 13
	--	--	Conductance Schedule	NA	1			COMMON
	--	--	Max Solar Schedule	Btu/h-SF	50			COMMON
	24	VT_Sch	Visible Transmittance Schedule	NA	0.23	0.14	0.35	
	--	--	Open Shade Schedule	NA	0.5			COMMON
	--	--	Sun Control Probability	NA	0.8	0	1	COMMON
	--	--	Glare Control Probability	NA	0.8	0	1	COMMON
	--	--	Inside Visible Reflectance	NA	0.25			COMMON

Table B – 4 (continued)

	#	Variable	Variable Description	Units	Value	Min	Max	Notes
Construction								
	25	Const_Abs_Ewall	Absorptance Exterior Wall	NA	0.6	0.6	0.9	Extreme values are 0.1 to 0.95
	--	--	Surface Roughness Exterior Wall	NA	6			Code word only
	26	Const_Abs_Roof	Absorptance Roof	NA	0.25	0.2	0.88	Extreme values are 0.1 to 0.95
	--	--	Surface Roughness Roof	NA	1			Code word only
Materials (Ewall Const layers)								
	27	Insul_Bd1_Thk	Insul Bd 3/4in Thickness	ft	0.063	0.041 7	0.08 33	
	28	Insul_Bd1_Conduct	Insul Bd 3/4in Conductivity	Btu/h-ft-degF	0.031 6	0.008 3	0.04 75	ASHRAE Fund. 2009, Ch 26, Table 4
	29	Insul_Bd1_Density	Insul Bd 3/4in Density	lb/CF	18	2	27	ASHRAE Fund. 2009, Ch 26, Table 4
	30	Insul_Bd1_SpH	Insul Bd 3/4in Specific Heat	Btu/lb-degF	0.31	0.14	0.35	ASHRAE Fund. 2009, Ch 26, Table 4
	31	Spand1_Conduct	1/4in Spandrel Glass Conductivity	Btu/h-ft-degF	0.59	0.11	0.6	ASHRAE Fund. 2009, Ch 15, Table 4, Note 2
	32	Spand1_Density	1/4in Spandrel Glass Density	lb/CF	172	100	200	
	33	Spand1_SpH	1/4in Spandrel Glass Specific Heat	Btu/lb-degF	0.2	0.1	0.3	
	34	Ewall_M2_Rval	Ewall Cons Mat 2 (0.91) R-Value	h-SF-degF/Btu	0.91	0	5	
			(Ewall_Cons_Lay_Granite)					
	35	Trzz_Thk	Tarrazzo 1in (TZ01) Thickness	ft	0.083	0.063	0.08 33	
	36	Trzz_Conduct	Tarrazzo 1in (TZ01) Conductivity	Btu/h-ft-degF	1.041 6	0.666 6	2.5	ASHRAE Fund. 2009, Ch 26, Table 4
	37	Trzz_Density	Tarrazzo 1in (TZ01) Density	lb/CF	140	100	180	ASHRAE Fund. 2009, Ch 26, Table 4

Table B – 4 (continued)

	#	Variable	Variable Description	Units	Value	Min	Max	Notes
	38	Trzz_SpH	Tarrazzo 1in (TZ01) Specific Heat	Btu/lb-degF	0.2	0.19	0.21	ASHRAE Fund. 2009, Ch 26, Table 4
			(Roof Cons Layers)					
	39	Roof_Blt_Thk	Blt-Up Roof 3/8in (BR01) Thickness	ft	0.031	0.0208	0.04167	
	40	Roof_Blt_Cond	Blt-Up Roof 3/8in (BR01) Conductivity	Btu/h-ft-degF	0.0939	0.09	0.3	
	41	Roof_Blt_Dens	Blt-Up Roof 3/8in (BR01) Density	lb/CF	70	50	90	
	42	Roof_Blt_SpH	Blt-Up Roof 3/8in (BR01) Specific Heat	Btu/lb-degF	0.35	0.25	0.45	
	43	Roof_Insul_Thk	Polyurethane 3in (IN46) Thickness	ft	0.25	0.25	0.5	ASHRAE Fund. 2009, Ch 26, Table 4
	44	Roof_Insul_Con d	Polyurethane 3in (IN46) Conductivity	Btu/h-ft-degF	0.0133	0.01	0.025	ASHRAE Fund. 2009, Ch 26, Table 4
	45	Roof_Insul_De ns	Polyurethane 3in (IN46) Density	lb/CF	1.5	0.4	3	ASHRAE Fund. 2009, Ch 26, Table 4
	46	Roof_Insul_Sp H	Polyurethane 3in (IN46) Specific Heat	Btu/lb-degF	0.38	0.35	0.4	ASHRAE Fund. 2009, Ch 26, Table 4
	47	Roof_Conc_Thk	Conc HW 140 lb 4in (CC03) Thickness	ft	0.333	0.25	0.4167	
	48	Roof_Conc_Co nd	Conc HW 140 lb 4in (CC03) Conductivity	Btu/h-ft-degF	0.7576	0.275	1.667	ASHRAE Fund. 2009, Ch 26, Table 4
	49	Roof_Conc_De ns	Conc HW 140 lb 4in (CC03) Density	lb/CF	140	80	150	ASHRAE Fund. 2009, Ch 26, Table 4
	50	Roof_Conc_Sp H	Conc HW 140 lb 4in (CC03) Specific Heat	Btu/lb-degF	0.2	0.19	0.24	ASHRAE Fund. 2009, Ch 26, Table 4
			(GfIr Cons Layers)					
	51	Uflr_M1_Rval	Uflr Cons Mat 1 (10.47) R-Value	h-SF-degF/Btu	10.47	10	25	
	52	Gflr_Conc_Thk	Conc HW 140lb 4in (HF-C5) Thickness	ft	0.333	0.25	0.4167	
	53	Roof_Conc_Co nd	Conc HW 140lb 4in (HF-C5) Conductivity	Btu/h-ft-degF	1	0.275	1.667	ASHRAE Fund. 2009, Ch 26, Table 4

Table B – 4 (continued)

	#	Variable	Variable Description	Units	Value	Min	Max	Notes
	54	Gflr_Conc_Dens	Conc HW 140lb 4in (HF-C5) Density	lb/CF	140	80	150	ASHRAE Fund. 2009, Ch 26, Table 4
	55	Gflr_Conc_SpH	Conc HW 140lb 4in (HF-C5) Specific Heat	Btu/lb -degF	0.2	0.19	0.24	ASHRAE Fund. 2009, Ch 26, Table 4
Glass Types								
	56	Glaz1_SC	Viracon_VRE1_59 Shading Coefficient	NA	0.39	0.28	0.6	ASHRAE Fund. 2009, Ch 15, Table 4, and ASHRAE 90.1 Climate zone 3A
	57	Glaz1_Cond	Viracon_VRE1_59 Glass Conductance	Btu/h-SF-degF	0.32	0.3	0.5	ASHRAE Fund. 2009, Ch 15, Table 4
	58	Glaz1_VT	Viracon_VRE1_59 Visible Transmittance	NA	0.53	0.45	0.76	ASHRAE Fund. 2009, Ch 15, Table 4
	59	Glaz1_Out_Emiss	Viracon_VRE1_59 Outside Emissivity	NA	0.1	0.05	0.2	ASHRAE Fund. 2009, Ch 15, Table 4
	60	Glaz2_SC	Viracon_VE1_2M Shading Coefficient	NA	0.44	0.28	0.6	ASHRAE Fund. 2009, Ch 15, Table 4, and ASHRAE 90.1 Climate zone 3A
	61	Glaz2_Cond	Viracon_VE1_2M Glass Conductance	Btu/h-SF-degF	0.31	0.3	0.5	ASHRAE Fund. 2009, Ch 15, Table 4
	62	Glaz2_VT	Viracon_VE1_2M Visible Transmittance	NA	0.7	0.45	0.76	ASHRAE Fund. 2009, Ch 15, Table 4
	63	Glaz2_Out_Emiss	Viracon_VE1_2M Outside Emissivity	NA	0.1	0.05	0.2	ASHRAE Fund. 2009, Ch 15, Table 4
Air Side HVAC (VAV Systems)								
Basic								
	64	Max_Humid	Maximum Humidity	%	50	40	60	
Fans								
	65	SFan_Sp	Supply Fan Static	in. wg	3.5	2.5	4.5	

Table B – 4 (continued)

	#	Variable	Variable Description	Units	Value	Min	Max	Notes
	66	SFan_Tot_Eff	Supply Fan Total Efficiency	NA	0.63	0.5	0.75	
	67	SFan_Mec_Eff	Supply Fan Mechanical Efficiency	NA	0.72	0.5	0.8	
	68	RFan_Sp	Return Fan Static	in. wg	1.17	1	2	
	69	RFan_Tot_Eff	Return Fan Total Efficiency	NA	0.63	0.5	0.75	
	70	Fan_MinFlow	Min Flow Ratio	NA	0.3	0.2	0.5	
Outdoor Air Enthalpy Control								
	71	Econ_Enthalpy	Enthalpy High Limit	Btu/lb	30	28	32	ASHRAE 90.1 Table 6.5.1.1.3B
Enthalpy Wheel								
	72	OA_Purge	OSA Increase for Purge	NA	0	0	0.2	
	73	HX_Eff_Sens	HX Effectiveness Sensible	NA	0.75	0.5	0.85	ASHRAE HVAC Systems & Equipment, Ch 25, Table 2
	74	HX_Eff_Lat	HX Effectiveness Latent	NA	0.75	0.5	0.85	ASHRAE HVAC Systems & Equipment, Ch 25, Table 2
	75	HX_FilmR_Sens	HX Air Film Resistance Sensible	NA	0.7	0.5	0.9	
	76	HX_FilmR_Lat	HX Air Film Resistance Latent	NA	0.7	0.5	0.9	
	--	HX_FilmR_E_Sens	Air Film Resist Exp Sensible	NA	0.5			Unchanged
	--	HX_FilmR_E_Lat	Air Film Resist Exp Latent	NA	0.4			Unchanged
	77	HX_Air_H_Setp	Make-up Air Heat Setpoint	degF	65	60	85	
	78	HX_Air_C_Setp	Make-up Air Cool Setpoint	degF	55	50	65	
	79	HX_Power	HX Power	kW/cfm	0.000085	0.00004	0.00012	
	80	HX_Fan_Eff	ERV Fan Efficiency	NA	0.6	0.5	0.75	
	--	HX_Fan_Mot_Eff	Fan Motor Efficiency	NA	Standard			
Cooling								
	--	--	Coil Design Bypass Factor	NA	0.037			COMMON

Table B – 4 (continued)

	#	Variable	Variable Description	Units	Value	Min	Max	Notes
	81	Cool_Cntl_Rng	Cool Control Range	degF	4	3	6	
	82	CRS_Sup_at_Low	Max Cooling Reset Temp	degF	65	60	65	
	--	CRS_Sup_at_High	Min Cooling Reset Temp	degF	55			Unchanged
	83	CRS_MinFlow	Minimum Reset Flow	NA	0.66	0.3	0.66	
	Heating							
	84	Heat_MaxT	Zone Entering Max Supply Temp	degF	95	85	120	
	85	Heat_DT	Reheat Delta T	degF	30	20	50	
	Zones							
	86	OA_PerPers_Off	OA Flow/Person	cfm	10	5	15	
	135	OA_PerPers_Conf	OA Flow/Person	cfm	10	5	15	
	87	OA_PerSF	OA Flow/Area	cfm/SF	0.3	0.25	0.35	
	88	Exh_CFM	Exhaust Air Flow	cfm	600	500	750	
	89	Exh_Sp	Exhaust Static Pressure	in. wg	0.3	0.2	0.5	
	90	Exh_Tot_Eff	Exhaust Total Efficiency	NA	0.4	0.4	0.7	
	91	Tstat_ThRng	Throttle Range	degF	2	1	3	
	92	Hmax_Flow	Hmax Flow Ratio	NA	0.5	0.4	0.6	
Water Side HVAC								
	Chilled Water Loop							
	93	CHW_DT	Loop Design DT	degF	10	8	14	Vary inversely
	--	CHW_T	Design CHW Temp	degF	44	40	46	Vary inversely
	94	CHW_CircTime	Avg Circ Time	minutes	1.5	1.5	15	
	95	CHW_PipeHead	Pipe Head	ft	21.6	15	50	
	96	CHW_Head_SRng	Head Setpoint Range	ft	2	1	4	
	97	CHW_FlowRes	Loop Flow Reset	NA	0.7	0.5	0.8	
	98	CHW_Loop_SRng	Loop Setpoint Range	degF	2	0.05	3	
	99	CHW_MaxRes_T	Max Reset Temp	degF	65	60	65	
	100	CHW_MinRes_T	Min Reset Temp	degF	40	40	44	

Table B – 4 (continued)

	#	Variable	Variable Description	Units	Value	Min	Max	Notes
Chillers								
	101	Chill_EIR	Electric Input Ratio	NA	0.1639	0.15	0.18	
	102	Chill_MinR	Minimum Ratio	NA	0.1	0.1	0.3	
	103	Chill_MinCon_T	Minimum Condenser Temp	degF	70	50	70	
	104	Chill_Head	Chiller Head	ft	20	10	30	
	105	Chill_ConHead	Condenser Head	ft	20	10	30	
	106	Chill_Startup_t	Start-up Time	h	0.047	0.0167	0.0833	
	107	Chill_Standby_t	Standby Time	h	0.0257	0.0167	0.0833	
	108	Chill_Econ_Eff	Water Economizer HX Effectiveness	NA	0.8	0.5	0.95	
	136	Chill_Cap_R	Chiller Capacity Ratio	NA	1.2	1	1.5	
CHW pump								
	109	CHWP_Mot_Eff	Motor Efficiency	NA	0.8	0.6	0.95	
	110	CHWP_Mech_Eff	Mech Efficiency	NA	0.77	0.8	0.8	
	111	CHWP_Min_Speed	Minimum Speed	NA	0.4	0.3	0.5	
Condenser Water Loop								
	112	CW_DT	Loop Design DT	degF	10	8	14	Vary inversely
	--	CW_T	Design CW Temp	degF	88	84	90	Vary inversely
	113	CW_CircTime	Avg Circ Time	minutes	1.5	1	2	
	114	CW_PipeHead	Pipe Head	ft	21.6	15	50	
	115	CW_Head_SRng	Head Setpoint Range	ft	2	1	4	
	116	CW_Loop_SRng	Loop Setpoint Range	degF	2	0.05	3	
	117	CW_MaxReset_T	Max Reset Temp	degF	95	85	95	
	--	CW_MinReset_T	Min Reset Temp	degF	70	50	70	Interlocked with Minimum Condenser Temp

Table B – 4 (continued)

	#	Variable	Variable Description	Units	Value	Min	Max	Notes
CW Pumps								
	118	CWP_Mot_Eff	Motor Efficiency	NA	0.8	0.6	0.95	
	119	CWP_Mech_Eff	Mech Efficiency	NA	0.77	0.8	0.8	
Cooling Towers								
	120	CT_Fan_EIR	Fan Electric Input Ratio	NA	0.0226	0.0105	0.05	
	121	CT_FanOffFlow	Fan Off Flow	NA	0.01	0	0.05	
	122	CT_Head	Head	ft	10	5	20	
	123	CT_StaticHead	Static Head	ft	10	5	20	
	137	CT_Capacity_Ratio	Cooling Tower Capacity Ratio	NA	1.2	1	1.5	
Domestic Hot Water								
	124	DHW_Temp	Design HW Temp	degF	135	110	140	
	125	DHW_CircTime	Avg Circ Time	minutes	1.5	1	5	
	126	DHW_PipeHead	Pipe Head	ft	21.6	15	25	
	127	DHW_Load	Process Load	gpm	6.51	3	10	
	128	DHW_Load_single	Process Load_single	gpm	0.3	0.15	0.5	
	129	DHW_Loss_DT	Supply Loss DT	degF	10	5	10	
Exterior Lighting								
Parking								
	130	Park_Light	Parking Load	kW	11.84	7.5	15	
	131	Sign_Light	Signage Load	kW	17	8	22	
	132	Door_Light	Doorways Load	kW	1.69	1	3	
Conveyances								
Elevator								
	133	Elev	Elevator Load	kW	229.2	114.6	343.8	

APPENDIX C: MORRIS METHOD MATLAB SCRIPT

```
% -----
% This script generates a file called MorrisExperiment.csv which specifies
% the runs for a Method of Morris screening experiment. To use this
% script, please do the following:

% 1.  REQUIRED FILES
% Have the following files in your working directory in Matlab:
% - generate_experiment.m (this script)
% - morris_experiment.m

% 2.  EDIT CODE FOR YOUR FACTORS
% Adapt the script for the number of factors that you are analyzing.
% - Specify your factors the comments following Line 23.
% - Specify lower bounds for your factors in Line 31.
% - Specify upper bounds for your factors in Line 32.
% - Specify the number of random observations in Line 40.
% -----

% -----
% SPECIFY FACTORS
% -----

% -----edit-below-----
% x = [Factor1,...,Factork]
% Factor1 ranges from a to b                                --> [a, b]
% ...
% Factork ranges from c to d                                --> [c, d]
% -----edit-above-----

% -----edit-below-----
% xlb = [ ]; %Read from MorrisReadVariables.m file
% xub = [ ]; %Read from MorrisReadVariables.m file
% -----edit-above-----

% -----
% SPECIFY NUMBER OF RANDOM OBSERVATIONS
% -----

% -----edit-below-----
r = 20; % the number of random observations
% -----edit-above-----

k = length(xlb); % the number of factors
e = morris_experiment(k,r,xlb,xub);
csvwrite('MorrisExperiment.csv',e)
% -----
```

Source: Dr. Chris Paredis

```

function X = morris_experiment(k, r, xlb, xub, seed);

% Meaning of the variables:
% we use the same variable names as in the paper
% k = number of input factors
% p = grid_level (should be even)
% r = the number of effects that one wants to sample
% lb = optional lower bound on the x values
% ub = optional upper bound ont the x values
% seed = optional random number generator seed

m = k+1; % number of experiments per batch
n = m*r; % total number of experiments

% pick p to be something large so that it is unlikely that
% the same grid point will be sampled twice
p = r*10000;
delta = p/(2*(p-1));

% check for lower and upper bounds
if nargin < 4
    xlb = zeros(1,k);
    xub = ones(1,k);
end

% seed the random number generator
if nargin==5
    rand('state',seed);
else
    rand('state',sum(100*clock));
end

% %define sampling matrix of the form
% B = [0 0 0 0;
%       1 0 0 0;
%       1 1 0 0;
%       1 1 1 0;
%       1 1 1 1];
J = ones(m,k);
B = tril(J,-1);

X = zeros(n,k);
for i=1:r
    Dstar = diag(floor(rand(k,1)*2)*2-ones(k,1));
    xstar = floor(rand(1,k)*p/2)/(p-1);
    Btemp = ones(m,1)*xstar+delta/2*((2*B-J)*Dstar+J);
    Bstar = Btemp(:,randperm(k));
    X((i-1)*m+1:i*m,:) = ones(m,1)*xlb+ones(m,1)*(xub-xlb).*Bstar;
end

return;
Source: Dr. Chris Paredis

```

APPENDIX D: ARC TRAVEL DEMAND MODEL FILES

Table D - 1: ARC Travel Demand Model HBW Mode Choice Tables

HBW	Stratification	Trips File	Tab	Trips MAT File
SOV	All	MCHBW.MTT	5	MCHBW_MTT_sov.mat
	Strat1	HBWSOV.MTT	1	HBWSOV_MTT_strat1.mat
	Strat2	HBWSOV.MTT	2	HBWSOV_MTT_strat2.mat
	Strat3	HBWSOV.MTT	3	HBWSOV_MTT_strat3.mat
	Strat4	HBWSOV.MTT	4	HBWSOV_MTT_strat4.mat
HOV2	All	MCHBW.MTT	6	MCHBW_MTT_hov2.mat
	Strat1	HBWHOV.MTT	1	HBWHOV_MTT_hov2strat1.mat
	Strat2	HBWHOV.MTT	2	HBWHOV_MTT_hov2strat2.mat
	Strat3	HBWHOV.MTT	3	HBWHOV_MTT_hov2strat3.mat
	Strat4	HBWHOV.MTT	4	HBWHOV_MTT_hov2strat4.mat
HOV3	All	MCHBW.MTT	7	MCHBW_MTT_hov3.mat
	Strat1	HBWHOV.MTT	5	HBWHOV_MTT_hov3strat1.mat
	Strat2	HBWHOV.MTT	6	HBWHOV_MTT_hov3strat2.mat
	Strat3	HBWHOV.MTT	7	HBWHOV_MTT_hov3strat3.mat
	Strat4	HBWHOV.MTT	8	HBWHOV_MTT_hov3strat4.mat
HOV4	All	MCHBW.MTT	8	MCHBW_MTT_hov4.mat
	Strat1	HBWHOV.MTT	9	HBWHOV_MTT_hov4strat1.mat
	Strat2	HBWHOV.MTT	10	HBWHOV_MTT_hov4strat2.mat
	Strat3	HBWHOV.MTT	11	HBWHOV_MTT_hov4strat3.mat
	Strat4	HBWHOV.MTT	12	HBWHOV_MTT_hov4strat4.mat
D2B	All	MCHBW.MTT	3	MCHBW_MTT_D2B.mat
	Strat1	HBWTRN.MTT	9	HBWTRN_MTT_D2Bstrat1.mat
	Strat2	HBWTRN.MTT	10	HBWTRN_MTT_D2Bstrat2.mat
	Strat3	HBWTRN.MTT	11	HBWTRN_MTT_D2Bstrat3.mat
	Strat4	HBWTRN.MTT	12	HBWTRN_MTT_D2Bstrat4.mat
D2R	All	MCHBW.MTT	4	MCHBW_MTT_D2R.mat
	Strat1	HBWTRN.MTT	13	HBWTRN_MTT_D2Rstrat1.mat
	Strat2	HBWTRN.MTT	14	HBWTRN_MTT_D2Rstrat2.mat
	Strat3	HBWTRN.MTT	15	HBWTRN_MTT_D2Rstrat3.mat
	Strat4	HBWTRN.MTT	16	HBWTRN_MTT_D2Rstrat4.mat
W2B	All	MCHBW.MTT	1	MCHBW_MTT_W2B.mat
	Strat1	HBWTRN.MTT	1	HBWTRN_MTT_W2Bstrat1.mat
	Strat2	HBWTRN.MTT	2	HBWTRN_MTT_W2Bstrat2.mat
	Strat3	HBWTRN.MTT	3	HBWTRN_MTT_W2Bstrat3.mat
	Strat4	HBWTRN.MTT	4	HBWTRN_MTT_W2Bstrat4.mat

Table D – 1 (continued)

HBW	Stratification	Trips File	Tab	Trips MAT File
W2R	All	MCHBW.MTT	2	MCHBW_MTT_W2R.mat
	Strat1	HBWTRN.MTT	5	HBWTRN_MTT_W2Rstrat1.mat
	Strat2	HBWTRN.MTT	6	HBWTRN_MTT_W2Rstrat2.mat
	Strat3	HBWTRN.MTT	7	HBWTRN_MTT_W2Rstrat3.mat
	Strat4	HBWTRN.MTT	8	HBWTRN_MTT_W2Rstrat4.mat
ALL				
	Strat1	HBW.PTT	1	HBW_PTT_strat1.mat
	Strat2	HBW.PTT	2	HBW_PTT_strat2.mat
	Strat3	HBW.PTT	3	HBW_PTT_strat3.mat
	Strat4	HBW.PTT	4	HBW_PTT_strat4.mat

Table D - 2: ARC Travel Demand Model NHB Mode Choice Tables

NHB	Stratification	Trips File	Tab	Trips MAT File
SOV	All	MCNHB.MTT	5	MCNHB_MTT_sov.mat
	Strat1	NHBISOV.MTT	1	NHBISOV_MTT_strat1.mat
	Strat2	NHBISOV.MTT	2	NHBISOV_MTT_strat2.mat
	Strat3	NHBISOV.MTT	3	NHBISOV_MTT_strat3.mat
	Strat4	NHBISOV.MTT	4	NHBISOV_MTT_strat4.mat
HOV2	All	MCNHB.MTT	6	MCNHB_MTT_hov2.mat
	Strat1	NHBHOV.MTT	1	NHBHOV_MTT_hov2strat1.mat
	Strat2	NHBHOV.MTT	2	NHBHOV_MTT_hov2strat2.mat
	Strat3	NHBHOV.MTT	3	NHBHOV_MTT_hov2strat3.mat
	Strat4	NHBHOV.MTT	4	NHBHOV_MTT_hov2strat4.mat
HOV3	All	MCNHB.MTT	7	MCNHB_MTT_hov3.mat
	Strat1	NHBHOV.MTT	5	NHBHOV_MTT_hov3strat1.mat
	Strat2	NHBHOV.MTT	6	NHBHOV_MTT_hov3strat2.mat
	Strat3	NHBHOV.MTT	7	NHBHOV_MTT_hov3strat3.mat
	Strat4	NHBHOV.MTT	8	NHBHOV_MTT_hov3strat4.mat
HOV4	All	MCNHB.MTT	8	MCNHB_MTT_hov4.mat
	Strat1	NHBHOV.MTT	9	NHBHOV_MTT_hov4strat1.mat
	Strat2	NHBHOV.MTT	10	NHBHOV_MTT_hov4strat2.mat
	Strat3	NHBHOV.MTT	11	NHBHOV_MTT_hov4strat3.mat
	Strat4	NHBHOV.MTT	12	NHBHOV_MTT_hov4strat4.mat
D2B	All	MCNHB.MTT	3	MCNHB_MTT_D2B.mat
	Strat1	NHBTRN.MTT	9	NHBTRN_MTT_D2Bstrat1.mat
	Strat2	NHBTRN.MTT	10	NHBTRN_MTT_D2Bstrat2.mat
	Strat3	NHBTRN.MTT	11	NHBTRN_MTT_D2Bstrat3.mat
	Strat4	NHBTRN.MTT	12	NHBTRN_MTT_D2Bstrat4.mat
D2R	All	MCNHB.MTT	4	MCNHB_MTT_D2R.mat
	Strat1	NHBTRN.MTT	13	NHBTRN_MTT_D2Rstrat1.mat
	Strat2	NHBTRN.MTT	14	NHBTRN_MTT_D2Rstrat2.mat
	Strat3	NHBTRN.MTT	15	NHBTRN_MTT_D2Rstrat3.mat
	Strat4	NHBTRN.MTT	16	NHBTRN_MTT_D2Rstrat4.mat
W2B	All	MCNHB.MTT	1	MCNHB_MTT_W2B.mat
	Strat1	NHBTRN.MTT	1	NHBTRN_MTT_W2Bstrat1.mat
	Strat2	NHBTRN.MTT	2	NHBTRN_MTT_W2Bstrat2.mat
	Strat3	NHBTRN.MTT	3	NHBTRN_MTT_W2Bstrat3.mat
	Strat4	NHBTRN.MTT	4	NHBTRN_MTT_W2Bstrat4.mat

Table D – 2 (continued)

NHB	Stratification	Trips File	Tab	Trips MAT File
W2R	All	MCNHB.MTT	2	MCNHB_MTT_W2R.mat
	Strat1	NHBTRN.MTT	5	NHBTRN_MTT_W2Rstrat1.mat
	Strat2	NHBTRN.MTT	6	NHBTRN_MTT_W2Rstrat2.mat
	Strat3	NHBTRN.MTT	7	NHBTRN_MTT_W2Rstrat3.mat
	Strat4	NHBTRN.MTT	8	NHBTRN_MTT_W2Rstrat4.mat
ALL				
	Strat1	NHB.PTT	1	NHB_PTT_strat1.mat
	Strat2	NHB.PTT	2	NHB_PTT_strat2.mat
	Strat3	NHB.PTT	3	NHB_PTT_strat3.mat
	Strat4	NHB.PTT	4	NHB_PTT_strat4.mat

Table D - 3: ARC Travel Demand Model Distance Tables

	Distance File	Tab	Distance MAT File	Description
Highway (SOV)	AMPK10HWY.SKM	2	AMPK10HWY_SKM_dist.mat	Highway congested distance in miles
	SOVFFM10.SKM	2	SOVFFM10_SKM_dist.mat	SOV un-congested distance in hundredths of a mile
D2B	AUTOLOC_ALL.SKM	20	AUTOLOC_ALL_SKM_dist.mat	Drive to local transit, total congested distance in hundredths of a mile
	AUTOLOC_ALL.SKM	21	AUTOLOC_ALL_SKM_trndist.mat	Drive to local transit, transit vehicle congested distance in hundredths of a mile
	OFFAUTLOC_ALL.SKM	20	OFFAUTLOC_ALL_SKM_dist.mat	Drive to local transit, total un-congested distance in hundredths of a mile
	OFFAUTLOC_ALL.SKM	21	OFFAUTLOC_ALL_SKM_trndist.mat	Drive to local transit, transit vehicle un-congested distance in hundredths of a mile
D2R	AUTOPRE_ALL.SKM	20	AUTOPRE_ALL_SKM_dist.mat	Drive to premium transit, total congested distance in hundredths of a mile
	AUTOPRE_ALL.SKM	21	AUTOPRE_ALL_SKM_trndist.mat	Drive to premium transit, transit vehicle congested distance in hundredths of a mile
	OFFAUTPRE_ALL.SKM	20	OFFAUTPRE_ALL_SKM_dist.mat	Drive to premium transit, total un-congested distance in hundredths of a mile
	OFFAUTPRE_ALL.SKM	21	OFFAUTPRE_ALL_SKM_trndist.mat	Drive to premium transit, transit vehicle un-congested distance in hundredths of a mile

Table D – 3 (continued)

	Distance File	Tab	Distance MAT File	Description
W2B	WLKLOC_ALL.SKM	20	WLKLOC_ALL_SKM_dist.mat	Walk to local transit, total congested distance in hundredths of a mile
	WLKLOC_ALL.SKM	21	WLKLOC_ALL_SKM_trndist.mat	Walk to local transit, transit vehicle congested distance in hundredths of a mile
	OFFLOC_ALL.SKM	20	OFFLOC_ALL_SKM_dist.mat	Walk to local transit, total un-congested distance in hundredths of a mile
	OFFLOC_ALL.SKM	21	OFFLOC_ALL_SKM_trndist.mat	Walk to local transit, transit vehicle un-congested distance in hundredths of a mile
W2R	WLKPRE_ALL.SKM	20	WLKPRE_ALL_SKM_dist.mat	Walk to premium transit, total congested distance in hundredths of a mile
	WLKPRE_ALL.SKM	21	WLKPRE_ALL_SKM_trndist.mat	Walk to premium transit, transit vehicle congested distance in hundredths of a mile
	OFFPRE_ALL.SKM	20	OFFPRE_ALL_SKM_dist.mat	Walk to premium transit, total un-congested distance in hundredths of a mile
	OFFPRE_ALL.SKM	21	OFFPRE_ALL_SKM_trndist.mat	Walk to premium transit, transit vehicle un-congested distance in hundredths of a mile

Table D - 4: ARC Travel Demand Model Travel Time Tables

	Time File	Tab	Time MAT File	Description
Highway (SOV)	AMPK10HWY.SKM	3	AMPK10HWY_SKM_time.mat	Highway congested travel time, with terminal and intrazonal time, in minutes
	SOVFFM10.SKM	3	SOVFFM10_SKM_time.mat	SOV un-congested travel time, with terminal and intrazonal time, in hundredths of a minute
D2B	AUTOLOC_ALL.SKM	2	AUTOLOC_ALL_SKM_drivetime.mat	Drive to local transit, total congested time in hundredths of a minute
	AUTOLOC_ALL.SKM	19	AUTOLOC_ALL_SKM_trntime.mat	Drive to local transit, transit vehicle congested time in hundredths of a minute
	OFFAUTLOC_ALL.SKM	2	OFFAUTLOC_ALL_SKM_drivetime.mat	Drive to local transit, total un-congested time in hundredths of a minute
	OFFAUTLOC_ALL.SKM	19	OFFAUTLOC_ALL_SKM_trntime.mat	Drive to local transit, transit vehicle un-congested time in hundredths of a minute
D2R	AUTOPRE_ALL.SKM	2	AUTOPRE_ALL_SKM_drivetime.mat	Drive to premium transit, total congested time in hundredths of a minute
	AUTOPRE_ALL.SKM	19	AUTOPRE_ALL_SKM_trntime.mat	Drive to premium transit, transit vehicle congested time in hundredths of a minute
	OFFAUTPRE_ALL.SKM	2	OFFAUTPRE_ALL_SKM_drivetime.mat	Drive to premium transit, total un-congested time in hundredths of a minute
	OFFAUTPRE_ALL.SKM	19	OFFAUTPRE_ALL_SKM_trntime.mat	Drive to premium transit, transit vehicle un-congested time in hundredths of a minute

Table D – 4 (continued)

	Time File	Tab	Time MAT File	Description
W2B	WLKLOC_ALL.SKM	1	WLKLOC_ALL_SKM_walktime.mat	Walk to local transit, total congested time in hundreths of a minute
	WLKLOC_ALL.SKM	19	WLKLOC_ALL_SKM_trntime.mat	Walk to local transit, transit vehicle congested time in hundredths of a minute
	OFFLOC_ALL.SKM	1	OFFLOC_ALL_SKM_walktime.mat	Walk to local transit, total un-congested time in hundreths of a minute
	OFFLOC_ALL.SKM	19	OFFLOC_ALL_SKM_trntime.mat	Walk to local transit, transit vehicle un-congested time in hundredths of a minute
W2R	WLKPRE_ALL.SKM	1	WLKPRE_ALL_SKM_walktime.mat	Walk to premium transit, total congested time in hundreths of a minute
	WLKPRE_ALL.SKM	19	WLKPRE_ALL_SKM_trntime.mat	Walk to premium transit, transit vehicle congested time in hundredths of a minute
	OFFPRE_ALL.SKM	1	OFFPRE_ALL_SKM_walktime.mat	Walk to premium transit, total un-congested time in hundreths of a minute
	OFFPRE_ALL.SKM	19	OFFPRE_ALL_SKM_trntime.mat	Walk to premium transit, transit vehicle un-congested time in hundredths of a minute

APPENDIX E: MATLAB COMBINED ENERGY SCRIPTS

```

energy_transp = zeros(1000,4);
energy_transp(1:1000,3) =
Output.Energy_sum(:,10,10)+Output.Energy_sum(:,2,10)+Output.Energy_sum(:,3,10)
)+Output.Energy_sum(:,4,10); % TAZ 12
energy_transp(1:1000,4) =
Output.Energy_sum(:,10,21)+Output.Energy_sum(:,2,21)+Output.Energy_sum(:,3,21)
)+Output.Energy_sum(:,4,21); % TAZ 27
energy_transp(1:1000,2) =
Output.Energy_sum(:,10,120)+Output.Energy_sum(:,2,120)+Output.Energy_sum(:,3,
120)+Output.Energy_sum(:,4,120); % TAZ 240
energy_transp(1:1000,1) =
Output.Energy_sum(:,10,222)+Output.Energy_sum(:,2,222)+Output.Energy_sum(:,3,
222)+Output.Energy_sum(:,4,222); % TAZ 521

energy_transp = energy_transp*1.3; %Convert Site to Primary

energy_bldg = zeros(1000,4);
[xls_num,xls_string]=xlsread(strcat(directory,'Case_Study_I_MonteCarlo_result
s_revised.xls'),1);
energy_bldg(1:1000,1) = (xls_num(1:1000,27)*3412.14*3.364 +
xls_num(1:1000,28)*1000000*1.092); %Revised Primary
[xls_num,xls_string]=xlsread(strcat(directory,'Case_Study_II_MonteCarloResul
ts.xls'),1);
energy_bldg(1:1000,2) = (xls_num(1:1000,27)*1000000*3.364); %Original
Primary
[xls_num,xls_string]=xlsread(strcat(directory,'Case_Study_III_MonteCarlo_resu
lts_2.xls'),1);
energy_bldg(1:1000,3) = (xls_num(1:1000,39)*3412.14*3.364 +
xls_num(1:1000,40)*1000000*1.092); %Revised Primary
[xls_num,xls_string]=xlsread(strcat(directory,'Case_Study_IV_MonteCarlo_resu
lts138.xls'),1);
energy_bldg(1:1000,4) = (xls_num(1:1000,45)*3412.14*3.364); %Original
Primary

Energy_Total = zeros(1000,4);

bins = 100;

energy_t_avg = zeros(bins,3,4);
energy_b_avg = zeros(bins,3,4);
for i = 1:4
    min_val_t = min(energy_transp(:,i));
    min_val_b = min(energy_bldg(:,i));
    max_val_t = max(energy_transp(:,i));
    max_val_b = max(energy_bldg(:,i));
    bin_width_t = range(energy_transp(:,i))/bins;
    bin_width_b = range(energy_bldg(:,i))/bins;
    for j = 1:bins
        energy_t_avg(j,1,i) = min_val_t + (j-1)*bin_width_t +
0.5*bin_width_t;
        energy_b_avg(j,1,i) = min_val_b + (j-1)*bin_width_b +
0.5*bin_width_b;
    end
end

```

```

        for k = 1:1000
            if (energy_transp(k,i) >= (min_val_t + (j-1)*bin_width_t)) &&
                (energy_transp(k,i) <= (min_val_t + j*bin_width_t))
                energy_t_avg(j,2,i) = energy_t_avg(j,2,i) + 1;
            end;
            if (energy_bldg(k,i) >= (min_val_b + (j-1)*bin_width_b)) &&
                (energy_bldg(k,i) <= (min_val_b + j*bin_width_b))
                energy_b_avg(j,2,i) = energy_b_avg(j,2,i) + 1;
            end;
        end;
    end;
end;

for i = 1:4
    for j = 1:bins
        energy_t_avg(j,3,i) = energy_t_avg(j,2,i) / sum(energy_t_avg(:,2,i));
        energy_b_avg(j,3,i) = energy_b_avg(j,2,i) / sum(energy_b_avg(:,2,i));
    end;
end;

for i = 1:4
    for j = 1:1000
        Energy_Total(j,i) =
            randsample(energy_t_avg(:,1,i),1,true,energy_t_avg(:,3,i)) +
            randsample(energy_b_avg(:,1,i),1,true,energy_b_avg(:,3,i));
    end;
end;

[f,a] = ksdensity(Energy_Total(:,2)); %Empirical PDF of Case Study II
[g,b] = ksdensity(Energy_Total(:,3)); %Empirical PDF of Case Study III

f=f.*(1/sum(f)); %Scales ksdensity up to a cumulative sum of 1.
g=g.*(1/sum(g));

Energy_diff_prob = zeros(10000,2); %Sized by 100 x 100.
counter = 0;
for i = 1:100
    for j = 1:100
        counter = counter + 1;
        Energy_diff_prob(counter,1) = a(i)-b(j);
        Energy_diff_prob(counter,2) = f(i).*g(j); % f is greater than g.
    end;
end;

min_val = min(Energy_diff_prob(:,1));
max_val = max(Energy_diff_prob(:,1));
bin_width = (max_val - min_val)/100;
En_diff_bin = zeros(100,2);
for i = 1:100
    En_diff_bin(i,1) = min_val + (i-1)*bin_width + 0.5*bin_width;
    for j = 1:10000
        if (Energy_diff_prob(j,1) > (min_val+(i-1)*bin_width)) &&
            (Energy_diff_prob(j,1) <= (min_val+i*bin_width))
            En_diff_bin(i,2) = En_diff_bin(i,2) + Energy_diff_prob(j,2);
        end;
    end;
end;

```

```

    end;
end;

ProbSave = interp1(En_diff_bin(:,1),cumsum(En_diff_bin(:,2)),0); %The
probability of saving 0 or greater.
ProbNoSave = 1 - ProbSave;
MeanEnergy1 = mean(Energy_Total(:,2));
MeanEnergy2 = mean(Energy_Total(:,3));
DiffMeanEnergy = MeanEnergy1 - MeanEnergy2;
ProbSaveMean =
interp1(En_diff_bin(:,1),cumsum(En_diff_bin(:,2)),DiffMeanEnergy);
%Probability of saving the difference in means

```

REFERENCES

1. Junnila, S. and A. Horvath. Life-Cycle Environmental Effects of an Office Building. In *Journal of Infrastructure Systems*, Vol. 9, No. 4, 2003, pp. 157 - 166.
2. Norman, J., H. MacLean, and C. Kennedy. Comparing High and Low Residential Density: Life-Cycle Analysis of Energy Use and Greenhouse Gas Emissions. In *Journal of Urban Planning and Development*, Vol. 132, No. 1, 2006, pp. 10-21.
3. Oak Ridge National Laboratory, *Transportation Energy Data Book*, Ed. 29. Department of Energy, Washington, D.C., 2010.
4. National Energy Technology Laboratory, *2010 Buildings Energy Data Book*. Department of Energy, Washington, D.C., 2011.
5. U.S. Energy Information Administration, *Emissions of Greenhouse Gases in the United States 2008*. DOE/EIA-0573(2008), Department of Energy, Washington, D.C., 2009. www.eia.doe.gov/oiaf/1605/ggrpt/
6. U.S. Energy Information Administration, *Emissions of Greenhouse Gases in the United States 2007*. DOE/EIA-0573(2007), Department of Energy, Washington, D.C., 2007. www.eia.doe.gov/oiaf/1605/ggrpt/
7. Brown, M., F. Southworth, and T. Stovall. *Towards a Climate-Friendly Built Environment*. Pew Center on Global Climate Change, Washington, D.C., 2005.
8. Cambridge Systematics, Inc., *Moving Cooler: An Analysis of Transportation Strategies for Reducing Greenhouse Gas Emissions*. Urban Land Institute, Washington, D.C., 2009.
9. Ewing, R., et al. *Growing Cooler: Evidence on Urban Development and Climate Change*. Urban Land Institute, Washington, D.C., 2007.
10. Transportation Research Board, *Driving and the Built Environment: The Effects of Compact Development on Motorized Travel, Energy Use, and CO₂ Emissions*. Special Report 298, The National Research Council of the National Academies, Washington, D.C., 2010.
11. Congressional Budget Office, *Public Spending on Transportation and Water Infrastructure*. Congress of the United States, Washington, D.C., 2010.
12. Wilson, A. and R. Navaro. Driving to Green Buildings: The Transportation Energy Intensity of Buildings. In *Environmental Building News*, No. September, 2007.
13. U.S. Green Building Council, *LEED 2009 for New Construction and Major Renovations*. Washington, D.C., 2008.

14. U.S. Green Building Council, *LEED 2009 for Commercial Interiors*. Washington, D.C., 2008.
15. U.S. Green Building Council, *LEED 2009 for Core and Shell Development*. Washington, D.C., 2008.
16. U.S. Green Building Council, *LEED 2009 for Neighborhood Development*. Washington, D.C., 2009.
17. International Initiative for a Sustainable Built Environment, *An Overview of SBTool September 2007 Release*. Ottawa, ON, 2007.
18. Green Building Initiative, *Green Globes New Construction Module*. 2009.
19. U.S. Green Building Council, *LEED 2009 for Existing Buildings Operations and Maintenance*. Washington, D.C., 2008.
20. Thomas, M. and S. Edwards. *Transport and Buildings: Reducing the Environmental Impact*. BRE Global Limited, Watford, U.K., 2000.
21. R.S. Parfett & Associates Inc., *Development of a Commuter Traffic Generation Module for the Green Buildings Tool*. Prepared for the Green Buildings Tool Initiative, Natural Resources Canada, Ottawa, ON, 2001.
22. BRE Global Limited, *BREEAM Offices 2008*. Scheme Document SD 5055, Watford, UK, 2010.
23. ENERGY Star. *Target Finder*. U.S. Department of Energy and U.S. Environmental Protection Agency.
http://www.energystar.gov/index.cfm?c=new_bldg_design.bus_target_finder. Accessed July 14, 2010.
24. ENERGY Star. *Portfolio Manager Overview*. U.S. Department of Energy and U.S. Environmental Protection Agency.
http://www.energystar.gov/index.cfm?c=evaluate_performance.bus_portfoliomanager. Accessed July 14, 2010.
25. ASHRAE, *Energy Standard for Buildings Except Low-Rise Residential Buildings*. ANSI/ASHRAE/IESNA Standard 90.1-2010, American Society of Heating Refrigerating and Air-Conditioning Engineers, Inc., Atlanta, GA, 2010.
26. ASHRAE, *Standard for the Design of High-Performance Green Buildings*. ANSI/ASHRAE/USGBC/IES Standard 189.1-2009, American Society of Heating Refrigerating and Air-Conditioning Engineers, Inc., Atlanta, GA, 2009.

27. Peterson, K. and H. Crowther. Building EUIs. In *High Performing Buildings: A magazine of the American Society of Heating, Refrigerating and Air-Conditioning Engineers, Inc.*, No. Summer, 2010, pp. 40-50.
28. ASHRAE, *Standard Methods of Measuring, Expressing and Comparing Building Energy Performance*. ANSI/ASHRAE Standard 105-2007, American Society of Heating Refrigerating and Air-Conditioning Engineers, Inc., Atlanta, GA, 2007.
29. ASHRAE, *Energy Standard for Buildings Except Low-Rise Residential Buildings*. ANSI/ASHRAE/IESNA Standard 90.1-2004, American Society of Heating Refrigerating and Air-Conditioning Engineers, Inc., Atlanta, GA, 2004.
30. American National Standards Institute, *Environmental management - Life cycle assessment - Principles and framework*. ANSI/ISO 14040 - 1997, 1997.
31. American Institute of Architects, *AIA Guide to Building Life Cycle Assessment in Practice*. Washington, D.C., 2010.
32. Fabre, G. *The Low-Carbon Buildings Standard 2010*. Lulu Enterprises, Inc., 2009.
33. Building Energy Software Tools Directory. *DOE-2*. U.S. Department of Energy. http://apps1.eere.energy.gov/buildings/tools_directory/software.cfm/ID=34/pagename=alpha_list. Accessed August 1, 2010.
34. Oxizidis, S., A. Dudek, and N. Aquilina. Typical Weather Years and the Effect of Urban Microclimate on the Energy Behaviour of Buildings and HVAC Systems. In *Advances in Building Energy Research*, Vol. 1, 2007, pp. 89-103.
35. *Green Footstep*. Rocky Mountain Institute. <http://greenfootstep.org/>. Accessed August 16, 2010.
36. *URBEMIS Environmental Management Software v9.2.4*. Rimpo and Associates Inc. <http://www.urbemis.com/>. Accessed August 6, 2010.
37. *Transportation Energy Intensity TEI Calculator, Beta*. Center for Neighborhood Technology. <http://tei.cnt.org/index.php>. Accessed July 15, 2011.
38. Institute of Transportation Engineers, *Trip Generation*. Washington, D.C., 2008.
39. Institute of Transportation Engineers, *Transportation Impact Analysis for Site Development*. Washington, D.C., 2005.
40. Institute of Transportation Engineers, *Transportation Planning Handbook*. Washington, D.C., 2009.

41. Georgia Regional Transportation Authority, *GRTA DRI Review Package Technical Guidelines*. Atlanta, GA, 2008.
http://www.grta.org/dri/PDF_files/FINAL_Technical_Guidelines_04_09_2008.pdf
42. *Commuter Model v2.0*. U.S. Environmental Protection Agency.
http://www.epa.gov/oms/stateresources/policy/pag_transp.htm. Accessed August 16, 2010.
43. *ARC Travel Demand Model*. Atlanta Regional Commission.
<http://www.atlantaregional.com/transportation/travel-demand-model>. Accessed August 1, 2010.
44. Transportation Research Board, *Metropolitan Travel Forecasting: Current Practice and Future Direction*. Special Report 288, The National Research Council of the National Academies, Washington, D.C., 2007.
45. Badoe, D. and E. Miller. Transportation-land-use interactions: empirical findings in North America, and their implications for modeling. In *Transportation Research Part D: Transport and Environment*, Vol. 5, No. 4, 2000, pp. 235-263.
46. Newman, P. and J. Kenworthy. *Cities and Automobile Dependence: An International Sourcebook*. Gower Publishing, Farnham, UK, 1989.
47. Hagler Bailly, Inc. *Transportation and Environmental Analysis of the Atlantic Steel Development Proposal*. Prepared for the U.S. Environmental Protection Agency, Washington, D.C., 1999.
48. Boussauw, K. and F. Witlox. Introducing a commute-energy performance index for Flanders. In *Transportation Research Part A: Policy and Practice*, Vol. 43, No. 5, 2009, pp. 580-591.
49. Cervero, R. *America's Suburban Centers*. Unwin Hyman, Inc., Winchester, MA, 1989.
50. Mindali, O., A. Raveh, and I. Salomon. Urban density and energy consumption: a new look at old statistics. In *Transportation Research Part A: Policy and Practice*, Vol. 38, No. 2, 2004, pp. 143-162.
51. Holtzclaw, J., et al. Location Efficiency: Neighborhood and Socioeconomic Characteristics Determine Auto Ownership and Use - Studies in Chicago, Los Angeles and San Francisco. In *Transportation Planning and Technology*, Vol. 25, No. 2002, pp. 1-27.
52. Kennedy, C., J. Cuddihy, and J. Engel-Yan. The Changing Metabolism of Cities. In *Journal of Industrial Ecology*, Vol. 11, No. 2, 2007, pp. 43-59.

53. Decker, E., et al. Energy and Material Flow Through the Urban Ecosystem. In *Annual Review of Energy and the Environment* Vol. 25, 2000, pp. 685-740.
54. Green Building Initiative, *Green Building Assessment Protocol for Commercial Buildings*. ANSI/GBI 01-2010, 2010.
55. U.S. Department of Energy, *ENERGY STAR Performance Ratings Technical Methodology for Office, Bank/Financial Institutions, and Courthouse*. Washington, D.C., 2007.
56. Barley, D., et al. National Renewable Energy Laboratory, *Procedure for Measuring and Reporting Commercial Building Energy Performance*. NREL/TP-550-38601, U.S. Department of Energy, Washington, D.C., 2005.
57. ASHRAE Pressroom. *What is Energy Use Intensity? ASHRAE Seeks to Define, Educate*. American Society of Heating, Refrigerating, and Air-Conditioning Engineers, Inc. <http://www.ashrae.org/pressroom/detail/what-is-energy-use-intensity>. Accessed December 28, 2011.
58. Williamson, T., E. Erell, and V. Soebarto. "Assessing the Error from Failure to Account for Urban Microclimate in Computer Simulation of Building Energy Performance". Presented at *Eleventh International IBPSA Conference*, Glasgow, Scotland. 2009.
59. Akbari, H. Lawrence Berkeley National Laboratory, *Energy Savings Potential and Air Quality Benefits of Urban Heat Island Mitigation*. U.S. Department of Energy, 2005.
60. Williamson, T. and E. Erell. "Thermal Performance Simulation and the Urban Microclimate: Measurements and Prediction". Presented at *Seventh International IBPSA Conference*, Rio de Janeiro, Brazil. 2009.
61. Elgar, I., B. Farooq, and E. Miller. Modeling Location Decisions of Office Firms: Introducing Anchor Points and Constructing Choice Sets in the Model System. In *Transportation Research Record: Journal of the Transportation Research Board*, No. 2133, 2009, pp. 56-63.
62. Elgar, I. and E. Miller. How Office Firms Conduct Their Location Search Process: An Analysis of a Survey from the Greater Toronto Area. In *International Regional Science Review*, Vol. 33, No. 1, 2010, pp. 60 - 85.
63. U.S. Environmental Protection Agency, *Smart Growth: A Guide to Developing and Implementing Greenhouse Gas Reduction Programs (Draft)*. Washington, D.C., 2010.
64. Smart Growth. *Atlantic Station (Atlantic Steel Site Redevelopment Project)*. U.S. Department of Energy. http://www.epa.gov/dced/topics/atlantic_steel.htm. Accessed May 1, 2010.

65. U.S. Environmental Protection Agency, *Measuring the Air Quality and Transportation Impacts of Infill Development*. EPA 231-R-07-001, Washington, D.C., 2007.
66. California Legislative Counsel, *California Senate Bill 375*. Sacramento, CA, 2008.
67. Green Star Environmental Plan. *Atlantic Station: 2008 Project XL Report*. Atlantic Station. http://www.atlanticstation.com/concept_green_projectXL08.php. Accessed May 1, 2010.
68. Burer, M., D. Goldstein, and J. Holtzclaw. *Location Efficiency as the Missing Piece of the Energy Puzzle: How Smart Growth Can Unlock Trillion Dollar Consumer Cost Savings*. 2003.
69. Atlanta Regional Commission. *Developments of Regional Impact*. <http://www.atlantaregional.com/land-use/developments-of-regional-impact>. Accessed July 29, 2010.
70. USGBC. "Transportation Energy Intensity Calculator Project". Center for Neighborhood Technology. Webinar presented on July 26, 2011.
71. The Climate Registry. *General Reporting Protocol*. Version 1.1. <http://www.theclimateregistry.org/downloads/GRP.pdf>. Accessed July 7, 2009.
72. The Greenhouse Gas Protocol. *Corporate Accounting and Reporting Standard*. World Resources Institute. <http://www.ghgprotocol.org/standards/corporate-standard>. Accessed July 7, 2009.
73. ICLEI. *Local Governments Operations Protocol*. Version 1.0. <http://www.icleiusa.org/programs/climate/ghg-protocol>. Accessed July 7, 2009.
74. The California Climate Action Registry. *The General Reporting Protocol*. Version 3.1. <http://www.climateregistry.org/>. Accessed July 7, 2009.
75. Phillips, E. and D. Pugh. *How to Get a PhD*. Open University Press, New York, NY, 2000.
76. U.S. Energy Information Administration. *Commercial Buildings Energy Consumption Survey (CBECS)*. <http://www.eia.doe.gov/emeu/cbecs/>. Accessed July 14, 2010.
77. ASHRAE, *User's Manual for ANSI/ASHRAE/IESNA Standard 90.1-2007*. American Society of Heating Refrigerating and Air-Conditioning Engineers, Inc., Atlanta, GA, 2007.
78. Weigel, B. "Development of a Commercial Building Site Selection Framework for Minimizing Greenhouse Gas Emissions and Energy Consumption". Presented at *World Sustainable Building Conference*, Helsinki, FI. 2011.

79. Elgar, I. and E. Miller. Conceptual Model of Location of Small Office Firms. In *Transportation Research Record: Journal of the Transportation Research Board*, No. 1977, 2006, pp. 190-196.
80. Elgar, I., E. Miller, and K. Habib. Office Decisions to Change Location. In *Transportation Research Record: Journal of the Transportation Research Board*, No. 2077, 2008, pp. 175-181.
81. Abraham, J. E. and J. D. Hunt. Firm Location in the MEPLAN Model of Sacramento. In *Transportation Research Record: Journal of the Transportation Research Board*, No. 1685, 1999, pp. 187 - 198.
82. Nguyen, Y. and K. Sano. Location Choice Model for Logistic Firms with Consideration of Spatial Effects. In *Transportation Research Record: Journal of the Transportation Research Board*, No. 2168, 2010, pp. 17-23.
83. Nguyen, Y., et al. "Firm Relocation Patterns Incorporating Spatial Interactions". Presented at *90th Annual Meeting of the Transportation Research Board*, Washington, D.C. 2011.
84. Maoh, H. and P. Kanaroglou. Intrametropolitan Location of Business Establishments. In *Transportation Research Record: Journal of the Transportation Research Board*, No. 2133, 2009, pp. 33-45.
85. Manzato, G., et al. "Matching Office Firms Types and Location Characteristics: An Exploratory Analysis Using Bayesian Classifier Networks". Presented at *89th Annual Meeting of the Transportation Research Board*, Washington, D.C. 2010.
86. United Nations Framework Conference on Climate Change. *Kyoto Protocol*. United Nations. http://unfccc.int/kyoto_protocol/items/2830.php. Accessed June 8, 2010.
87. American Public Transportation Association, *Recommended Practice for Quantifying Greenhouse Gas Emissions from Transit*. APTA CC-RP-001-09, Washington, D.C., 2009.
http://www.apta.com/resources/hottopics/Documents/apta_climate_change_recommended_practice_final_august_14.pdf
88. Hodges, T. *Public Transportation's Role in Responding to Climate Change*. Federal Transit Administration, Washington D.C., 2009.
<http://www.fta.dot.gov/documents/PublicTransportationsRoleInRespondingToClimateChange.pdf>
89. Buildings Energy Data Book. *CBECS*. U.S. Department of Energy. <http://buildingsdatabook.eren.doe.gov/CBECS.aspx>. Accessed December 12, 2011.

90. JCGM, *Evaluation of Measurement Data - Guide to the Expression of Uncertainty in Measurement*. JCGM 100:2008, Joint Committee for Guides in Metrology, Sèvres Cedex, FR, 2008.
91. Taylor, B. and C. Kuyatt. *Guidelines for Evaluating and Expressing the Uncertainty of NIST Measurement Results*. NIST Technical Note 1297, National Institute of Standards and Technology, Gaithersburg, MD, 1994.
92. JCGM, *Evaluation of Measurement Data - Supplement 1 to the "Guide to the Expression of Uncertainty in Measurement" - Propagation of distributions using a Monte Carlo method*. JCGM 101:2008, Joint Committee for Guides in Metrology, Sèvres Cedex, FR, 2008.
93. ASHRAE, *Proposed Revision of Standard ASHRAE/IESNA Standard 100-2006*. American Society of Heating Refrigerating and Air-Conditioning Engineers, Inc., Atlanta, GA, 2011.
94. National Energy Technology Laboratory, *2008 Buildings Energy Data Book*. Department of Energy, Washington, D.C., 2009.
95. Deru, M. and P. Torcellini. National Renewable Energy Laboratory, *Source Energy and Emission Factors for Energy Use in Buildings*. NREL/TP-550-38617, U.S. Department of Energy, Washington, D.C., 2007.
96. Huang, J. and J. Broderick. "A Bottom-Up Engineering Estimate of the Aggregate Heating and Cooling Loads of the Entire U.S. Building Stock". Presented at *2000 ACEEE Summer Study on Energy Efficiency in Buildings*, Pacific Grove, CA. 2000.
97. Heat Island Effect. *Measuring Heat Islands*. U.S. Environmental Protection Agency. <http://www.epa.gov/heatisland/about/measuring.htm>. Accessed January 9, 2012, 2012.
98. Santamouris, M., et al. On the Impact of Urban Climate on the Energy Consumption of Buildings. In *Solar Energy*, Vol. 70, No. 3, 2001, pp. 201-216.
99. Givoni, B. *Climate Considerations in Building and Urban Design*. John Wiley & Sons, Inc., New York, NY, 2006.
100. Wilcox, S. and W. Marion. National Renewable Energy Laboratory, *Users Manual for TMY3 Data Sets*. NREL/TP-581-43156, U.S. Department of Energy, Washington, D.C., 2008.
101. Malkin, S. Autodesk Green Building Studio, *Weather Data for Building Energy Analysis*. 2008.

102. Metonorm Software. *Meteonorm Dataset*. Meteotest. <http://meteonorm.com/products/meteonorm-dataset/>. Accessed January 9, 2012.
103. Gowri, K., D. Winiarski, and R. Jamagin. Pacific Northwest National Laboratory, *Infiltration Modeling Guidelines for Commercial Building Energy Analysis*. PNNL-18898, U.S. Department of Energy, Washington, D.C., 2009.
104. Emmerich, S., T. McDowell, and W. Anis. National Institute of Standards and Technology, *Investigation of the Impact of Commercial Building Envelope Airtightness on HVAC Energy Use*. NISTIR 7238, U.S. Department of Commerce, Washington, D.C., 2005.
105. COMNET, *Commercial Buildings Energy Modeling Guidelines and Procedures*. RESNET Publication 2010-001, Commercial Energy Services Network, Oceanside, CA, 2010.
106. Autodesk Labs. *Project Vasari*. <http://labs.autodesk.com/utilities/vasari/>. Accessed January 6, 2012.
107. *eQUEST v3.64*. James J. Hirsch & Associates. <http://doe2.com/equest/>. Accessed August 1, 2010.
108. *EnergyPlus v7.0.0*. U.S. Department of Energy. <http://apps1.eere.energy.gov/buildings/energyplus/>. Accessed January 9, 2012.
109. Simergy Partnerships. *Visualizing EnergyPlus: A New Partnership*. U.S. Department of Energy. <http://eetd.lbl.gov/bt/simergy/partnerships.html>. Accessed January 9, 2012.
110. *ModelCenter 10.0*. Phoenix Integration, Inc. http://www.phoenix-int.com/software/phx_modelcenter.php. Accessed January 9, 2012.
111. Huang, J. and E. Franconi. Lawrence Berkeley National Laboratory, *Commercial Heating and Cooling Loads Component Analysis*. LBL-37208, U.S. Department of Energy, Washington, D.C., 1999.
112. ASHRAE, *Energy Conservation in Existing Buildings*. ANSI/ASHRAE/IESNA Standard 100-2006, American Society of Heating Refrigerating and Air-Conditioning Engineers, Inc., Atlanta, GA, 2006.
113. ASHRAE, *Proposed Revision of Standard 100-2006, Energy Conservation in Existing Buildings*. ANSI/ASHRAE/IESNA Standard 100-2006R, American Society of Heating Refrigerating and Air-Conditioning Engineers, Inc., Atlanta, GA, 2011.
114. Deru, M., et al. National Renewable Energy Laboratory, *U.S. Department of Energy Commercial Reference Building Models of the National Building Stock*. NREL/TP-5500-46861, U.S. Department of Energy, Washington, D.C., 2011.

115. Huang, J., et al. "Using EnergyPlus for California Title-24 Compliance Calculations". Presented at *Second National IBPSA-USA Conference*, Cambridge, MA. 2006.
116. ASHRAE, *Procedures for Commercial Building Energy Audits*. American Society of Heating Refrigerating and Air-Conditioning Engineers, Inc., Atlanta, GA, 2004.
117. McKay, M., R. Beckman, and W. Conover. A Comparison of Three Methods for Selecting Values of Input Variables in the Analysis of Output from a Computer Code. In *Technometrics*, Vol. 42, No. 1, February 2000, pp. 55 - 61.
118. Morris, M. Factorial Sampling Plans for Preliminary Computational Experiments. In *Technometrics*, Vol. 33, No. 2, May 1991, pp. 161 - 174.
119. eGRID2007. *The Emissions & Generation Resource Integrated Database*. U.S. Environmental Protection Agency. <http://www.epa.gov/cleanenergy/energy-resources/egrid/index.html>. Accessed July 7, 2009.
120. Weigel, B. Development of a Calculator for Estimation and Management of Greenhouse Gas Emissions from Public Transit Agency Operations. Masters Thesis, Civil & Environmental Engineering, Georgia Institute of Technology, Atlanta, GA, 2010.
121. Weigel, B. *Public Transit GHG Emissions Management Calculator v1b Beta*. Georgia Institute of Technology UTC. <http://www.prism.gatech.edu/~bweigel3/>. Accessed September 24, 2011.
122. Cambridge Systematics, Inc., *Enhancing the American Community Survey Data as a Source for Home-to-Work Flows*. NCHRP 8-36, Task 81, Transportation Research Board, Washington, D.C., 2009.
123. Census Transportation Planning Products. Federal Highway Administration. http://www.fhwa.dot.gov/planning/census_issues/ctpp/. Accessed May 27, 2011.
124. U.S. Census Bureau. *LED OnTheMap*. Version 3. <http://lehdmap3.did.census.gov/themap3/>. Accessed September 11, 2009.
125. U.S. Environmental Protection Agency, *Technical Guidance on the Use of MOVES2010 for Emission Inventory Preparation in State Implementation Plans and Transportation Conformity*. EPA 420-B-10-023, Washington, D.C., 2010.
126. U.S. Environmental Protection Agency, *Motor Vehicle Emission Simulator (MOVES): User Guide for MOVES2010a*. EPA 420-B-10-036, Washington, D.C., 2010.
127. Kuzmyak, J., J. Evans, and R. Pratt. *Traveler Response to Transportation System Changes: Chapter 19 - Employer and Institutional TDM Strategies*. TCRP Report 95,

- Transportation Research Board, Washington, D.C., 2010. http://onlinepubs.trb.org/onlinepubs/tcrp/tcrp_rpt_95c19.pdf
128. Shoup, D. *The High Cost of Free Parking*. American Planning Association, Chicago, IL, 2011.
 129. Hess, D. Effect of Free Parking on Commuter Mode Choice: Evidence from Travel Diary Data. In *Transportation Research Record: Journal of the Transportation Research Board*, No. 1753, 2001, pp. 35 - 42.
 130. Kuzmyak, J., et al. *Traveler Response to Transportation System Changes: Chapter 18 - Parking Management and Supply*. TCRP Report 95, Transportation Research Board, Washington, D.C., 2003. http://onlinepubs.trb.org/onlinepubs/tcrp/tcrp_rpt_95c18.pdf
 131. Guensler, R. "Increasing Vehicle Occupancy in the United States". Presented at *L'Avenir Des Deplacements en Ville*, Laboratoire d'Economie des Transports, Lyon, France. 1998.
 132. Murakami, E. Federal Highway Administration. Personal communication. Census Transportation Planning Products, Part 2, Table 2. Received May 27, 2011.
 133. Cervero, R. and K. Kockelman. Travel Demand and the 3Ds: Density, Diversity, and Design. In *Transportation Research Part D: Transport and Environment*, Vol. 2, No. 3, 1997, pp. 199-219.
 134. Kuzmyak, J., et al. *Traveler Response to Transportation System Changes: Chapter 15 - Land Use and Site Design*. TCRP Report 95, Transportation Research Board, Washington, D.C., 2003. http://onlinepubs.trb.org/onlinepubs/tcrp/tcrp_rpt_95c15.pdf
 135. Bochner, B., et al. *Enhancing Internal Trip Capture Estimation for Mixed-Use Developments*. NCRP Report 684, Transportation Research Board, Washington, D.C., 2011. http://onlinepubs.trb.org/onlinepubs/nchrp/nchrp_rpt_684.pdf
 136. Bachman, W., et al. Research Needs for Determining Spatially Resolved Subfleet Characteristics. In *Transportation Research Record: Journal of the Transportation Research Board*, No. 1625, 1998, pp. 139-146.
 137. National Center for Transit Research Center for Urban Transportation Research, *Worksite Trip Reduction Model and Manual*. BC-137-41, Tampa, FL, 2004.
 138. Federal Highway Administration, *A Guidance Manual for Implementing Effective Employer-based Travel Demand Management Programs*. Washington, D.C., 1993.
 139. U.S. Environmental Protection Agency, *Procedures Manual for the COMMUTER Model v2.0*. EPA 420-B-05-018, Washington, D.C., 2005.

140. U.S. Environmental Protection Agency, *COMMUTER Model v2.0 Coefficients*. EPA 420-B-05-019, Washington, D.C., 2005.
141. California Department of Transportation, *Technical Supplement to User's Guide, Volume2: Transportation Management Systems (TMS), Operational Improvements, Pavement Rehabilitation, and Economic Value Updates*. Sacramento, CA, 2004.
142. Spasovic, L. *Alternative Performance Measures for Evaluation of Congestion - Congestion Analysis Model Update and Maintenance*. FHWA-NJ-2007-006, National Center for Transportation and Industrial Productivity, Newark, NJ, 2008.
143. Guensler, R. and M. Rodgers. Georgia Institute of Technology. Personal communication. Commute Vehicle Fleet Efficiency. Received April 7, 2011.
144. Bureau of Transportation Statistics. *National Transportation Statistics*. U.S. Department of Transportation. http://www.bts.gov/publications/national_transportation_statistics/. Accessed January 19, 2012.
145. National Transit Database. Federal Transit Administration. <http://www.ntdprogram.gov/ntdprogram/data.htm>. Accessed October 15, 2010.
146. Boriboonsomsin, B. and M. Barth. Impacts of Road Grade on Fuel Consumption and Carbon Dioxide Emissions Evidenced by Use of Advanced Navigation Systems. In *Transportation Research Record: Journal of the Transportation Research Board*, No. 2139, 2009, pp. 21 - 30.
147. *The Greenhouse Gases, Regulated Emissions, and Energy Use in Transportation (GREET) V1.8c.0 Fuel-Cycle Model*. U.S. Department of Energy, Argonne National Laboratory. http://www.transportation.anl.gov/modeling_simulation/GREET/index.html. Accessed June 18, 2009.
148. Federal Highway Administration, *Congestion: Who is Traveling in the Peak?* U.S. Department of Transportation, Washington, D.C., August 2007. <http://nhts.ornl.gov/briefs/Congestion%20-%20Peak%20Travelers.pdf>
149. COMNET, *Commercial Buildings Energy Modeling Guidelines and Procedures - Appendix C*. RESNET Publication 2010-001, Commercial Energy Services Network, Oceanside, CA, 2010.